

Fibroblasts, Androgen Signalling

And

Oesophageal Adenocarcinoma

by

Helen Palethorpe

B Med Pharm Sc (Hons), B Lab Med, Dip Biomed Sc

A thesis by publication submitted for the degree of
Doctor of Philosophy

Discipline of Surgery, School of Medicine
Faculty of Health Science
The University of Adelaide

July 2017

TABLE OF CONTENTS

TABLE OF CONTENTS	i
ABSTRACT	v
DECLARATION	vii
ACKNOWLEDGEMENTS	ix
ABBREVIATIONS	x
CHAPTER 1: INTRODUCTION	1
1.1 Thesis overview	3
1.2 Oesophageal adenocarcinoma.....	3
1.3 A role for androgens in the biology of oesophageal adenocarcinoma.....	4
1.3.1 <i>Androgens</i>	6
1.3.2 <i>The androgen receptor</i>	7
1.3.3 <i>Androgen receptor function and androgen signalling</i>	7
1.3.4 <i>The role of androgens and the androgen receptor in cancer cells</i>	8
1.3.5 <i>Androgen receptor expression and androgen signalling in oesophageal cancers</i>	10
1.4 Fibroblasts in cancer	11
1.4.1 <i>The tumour stroma</i>	12
1.4.2 <i>Normal fibroblasts</i>	12
1.4.3 <i>Cancer-associated fibroblasts</i>	13
1.4.4 <i>The extracellular matrix in cancer</i>	14

1.4.5	<i>DNA methylation</i>	15
1.5	The crosstalk between fibroblasts and epithelial cancer cells	17
1.5.1	<i>Co-culture techniques used to assess fibroblast-epithelial cancer cell crosstalk</i>	17
1.5.2	<i>The significance of myofibroblast androgen receptor in prostate cancer</i>	18
1.5.3	<i>The effect of fibroblasts on androgen signalling in oesophageal adenocarcinoma..</i>	19
1.6	Aims of the study.....	20
CHAPTER 2: FIBROBLASTS DERIVED FROM OESOPHAGEAL ADENOCARCINOMA DIFFER IN DNA METHYLATION PROFILE FROM NORMAL OESOPHAGEAL FIBROBLASTS		
		21
CHAPTER 3: STROMAL ANDROGEN RECEPTOR REGULATES THE COMPOSITION OF THE MICROENVIRONMENT TO INFLUENCE PROSTATE CANCER OUTCOME		
		35
CHAPTER 4: MYOFIBROBLAST ANDROGEN RECEPTOR EXPRESSION DETERMINES CELL SURVIVAL IN CO-CULTURES OF MYOFIBROBLASTS AND PROSTATE CANCER CELLS IN VITRO		
		69
CHAPTER 5: ANDROGEN RECEPTOR AND ANDROGEN-RESPONSIVE GENE FKBP5 ARE INDEPENDENT PROGNOSTIC INDICATORS FOR ESOPHAGEAL ADENOCARCINOMA		
		101
CHAPTER 6: ANDROGEN SIGNALLING IN ESOPHAGEAL ADENOCARCINOMA CELL LINES IN VITRO.....		
		127
CHAPTER 7: CONCLUSIONS		
		163
APPENDIX A: SUPPLEMENTARY TABLES.....		
		171

APPENDIX B: ABSTRACTS PRESENTED/PUBLISHED293

B1: The effect of androgen receptor expression in fibroblasts co-cultured with prostate cancer cells.....295

B2: Myofibroblast androgen receptor expression regulates direct and indirect interactions between myofibroblast and prostate cancer cells *in vitro*297

B3: Fibroblast androgen receptor expression regulates fibroblast and prostate cancer cell interactions *in vitro*299

B4: Expression of androgen receptor and the androgen receptor responsive gene FKBP5 in oesophageal adenocarcinoma300

B5: Androgen receptor pathway as a prognostic indicator in esophageal adenocarcinoma302

B6: Myofibroblast androgen receptor expression modifies direct and indirect interactions between myofibroblasts and prostate cancer cells *in vitro*304

B7: Expression of androgen receptor and the androgen-responsive gene FKBP5 are independent prognostic indicators for oesophageal adenocarcinoma.....306

B8: Myofibroblast androgen receptor expression modifies direct and indirect interactions between myofibroblasts and prostate cancer cells *in vitro*308

B9: Myofibroblast androgen receptor expression modifies direct and indirect interactions between myofibroblasts and prostate cancer cells *in vitro*310

B10: Developing an *in vitro* model to investigate the role of androgen signalling in oesophageal adenocarcinoma312

B11: The effect of fibroblasts on androgen signalling in oesophageal adenocarcinoma cell lines *in vitro*314

APPENDIX C: PRESENTATIONS & AWARDS.....315

Conference & community presentations	317
Awards.....	318
REFERENCES	319

ABSTRACT

Fibroblasts and androgen signalling can influence the biology of cancer. In this thesis their role has been explored in oesophageal adenocarcinoma (OAC), and in prostate cancer. In both cancers there is a need for biomarkers to guide patient management, and more effective treatments to reduce patient morbidity and mortality.

Oesophageal adenocarcinoma (OAC) has a dismal course, with a five-year survival of around 15%. Its incidence has increased rapidly in Western countries over the last four decades. The cancer cells are embedded in a stroma of cells, predominantly fibroblasts, and extracellular matrix. The cancer-associated (myo)fibroblasts (CAFs) differ phenotypically from normal fibroblasts. This thesis documents differences in the genome-wide DNA methylation profiles of primary fibroblasts derived from normal oesophageal mucosa and from OAC tissue, consistent with a role for DNA methylation in establishing and maintaining the CAF phenotype.

Interactions between these fibroblasts and OAC cells were to be investigated in direct or indirect co-culture, to differentiate effects due to juxtacrine (cell-cell or cell-extracellular matrix) or paracrine (soluble factors) signalling. Whilst unsuccessfully attempting to immortalise the oesophageal fibroblasts, proof of concept experiments were undertaken using co-cultures of prostate myofibroblasts and cancer cells.

This permitted the investigation of the effect of androgen receptor (AR) expression in the myofibroblasts on their interactions with prostate cancer cells. This study was clinically relevant since a reduction in stromal AR expression is associated with a poorer prognosis in prostate cancer. The results suggest that AR-expressing myofibroblasts inhibit prostate cancer progression through paracrine signals that slow proliferation and induce apoptosis in the cancer cells, and that myofibroblasts lacking AR permit prostate cancer progression by undergoing apoptosis in response to juxtacrine signals from the cancer cells.

Around 85% of OAC is diagnosed in males, for reasons unknown. A role for androgens was therefore explored. The AR was expressed in 97% of OAC patients in a large cohort, and appeared functional in the majority of these based on its nuclear localisation and expression of the androgen-responsive gene FK506-binding protein 5 (FKBP5). Nuclear AR and FKBP5

expression were independently associated with decreased survival. Following on from this, the effects of androgen signalling were studied in OAC cell lines stably transduced with AR. Cell proliferation and gene expression were altered, and could be modified by the concentration of the androgen and the presence of fibroblasts in co-culture. This was the first reported study of the effect of androgen signalling in OAC cell lines in vitro, with results consistent with a role for androgen signalling in this disease.

This thesis provides new insight into the role of androgens and fibroblasts in the regulation of OAC and prostate cancer. The prognostic significance of AR expression and signalling in both cancers is highlighted, and the in vitro studies suggest novel mechanisms by which the microenvironment may contribute to the biology of these cancers. This research reveals areas of investigation that could lead to the identification of clinically useful biomarkers, and the development of novel treatments.

DECLARATION

I certify that this work contains no material which has been accepted for the award of any other degree or diploma in my name, in any university or other tertiary institution and, to the best of my knowledge and belief, contains no material previously published or written by another person, except where due reference has been made in the text. In addition, I certify that no part of this work will, in the future, be used in a submission in my name, for any other degree or diploma in any university or other tertiary institution without the prior approval of the University of Adelaide and where applicable, any partner institution responsible for the joint award of this degree.

I give consent to this copy of my thesis when deposited in the University Library, being made available for loan and photocopying, subject to the provisions of the Copyright Act 1968.

I acknowledge that copyright of published works contained within this thesis resides with the copyright holder(s) of those works.

1. Smith, E[#], **Palethorpe, HM[#]**, Hayden, A, Young, JP, Drew, PA & Underwood, TJ. Fibroblasts derived from oesophageal adenocarcinoma differ in DNA methylation profile from normal oesophageal fibroblasts. *Scientific Reports*. 2017; 7: 3368. Copyright © 2017, Smith et al., Macmillan Publishers Limited.
2. Leach, DA, Need, EF, Toivanen R, Trotta, AP, **Palethorpe HM**, Tamblyn DJ, Kopsaftis, T, England, GM, Smith E, Drew, PA, Pinnock, CB, Lee, P, Holst, J, Risbridger, GP, Chopra, S, DeFranco, DB, Taylor, RA, Buchanan, G. Stromal androgen receptor regulates the composition of the microenvironment to influence prostate cancer outcome. *Oncotarget*. 2015; 6(18): 16135-16150. Copyright © 2017, Impact Journals.
3. **Palethorpe, HM**, Leach, DA, Evdokiou, A, Need, EF, Smith, E & Drew, PA. Myofibroblast androgen receptor expression determines cell survival in co-cultures of myofibroblasts and prostate cancer cells in vitro. Submitted to *Molecular Cancer*, 2017.
4. Smith, E[#], **Palethorpe, HM[#]**, Ruszkiewicz, AR, Edwards, SE, Leach, DA, Underwood, TJ, Need, EF & Drew, PA. Androgen receptor and androgen-responsive gene FKBP5 are independent prognostic indicators for esophageal adenocarcinoma. *Digestive Diseases*

and Sciences. 2016; 61(2): 433-443. Copyright © 2015, Springer Science + Business Media, New York.

5. **Palethorpe, HM**, Smith, E & Drew, PA. Androgen signalling in esophageal adenocarcinoma cell lines in vitro. Submitted to *Digestive Diseases and Sciences*, 2017.

Authors contributed equally

I also give permission for the digital version of my thesis to be made available on the web, via the University's digital research repository, the Library Search and also through web search engines, unless permission has been granted by the University to restrict access for a period of time.

I acknowledge the support I have received for my research through the provision of an Australian Government Research Training Program Scholarship.

Helen Palethorpe

26th July 2017

ACKNOWLEDGEMENTS

I am grateful for this opportunity to acknowledge all those who have made this thesis possible.

Firstly, I thank my supervisors Dr Paul Drew and Dr Eric Smith. The knowledge and guidance you provided was invaluable throughout my candidature and I can't thank you both enough for your continued support and encouragement.

I thank the University of Adelaide for providing the opportunity to undertake this project, and the Basil Hetzel Institute for Translational Health Research for being the fantastic facility that it is, as well as the staff and students there for encouragement during times of need. I thank The Hospital Research Foundation for generous financial support.

Finally, I thank my family and friends, especially my Mum, Dad, brother Mark, and my four nephews, William, James, Thomas and Matthew. I would have given up long ago without your support and encouragement. I am eternally grateful to you all for seeing me through this journey and for instilling values of hard work and perseverance. I love you.

ABBREVIATIONS

ADT	androgen deprivation therapy
AR	androgen receptor
ARE	androgen response element
ARG	androgen-responsive gene
ARKO	androgen receptor knockout
α SMA	alpha-smooth muscle actin
BMI	body mass index
BO	Barrett's oesophagus
CAF	cancer-associated fibroblast
CIC	cancer initiating cell
CpG	cytosine-phosphate-guanine
CRC	colorectal cancer
CSC	cancer stem cell
DBD	DNA-binding domain
DHEA	dehydroepiandrosterone
DHEAS	dehydroepiandrosterone sulfate
DHT	dihydrotestosterone
ECM	extracellular matrix
EMT	epithelial-mesenchymal transition
FAP	fibroblast activation protein
FKBP5	FK506 binding protein 5
GFP	green fluorescent protein
GORD	gastro-oesophageal reflux disease
GR	glucocorticoid receptor
HCC	hepatocellular carcinoma

Hsp90	heat shock protein 90
LBD	ligand-binding domain
NDF	normal oesophageal mucosa-derived fibroblast
NFF	neonatal foreskin fibroblast
NTD	N-terminal domain
MMP	matrix metalloproteinase
MR	mineralocorticoid receptor
OAC	oesophageal adenocarcinoma
OR	oestrogen receptor
OSCC	oesophageal squamous cell carcinoma
PDGFR β	platelet-derived growth factor receptor beta
PG-40	chondroitin sulfate proteoglycan
PR	progesterone receptor
RFP	red fluorescent protein
SGC	scirrhous-type gastric carcinoma
TDF	tumour-derived fibroblast from OAC
TGF- β	transforming growth factor beta

CHAPTER 1: INTRODUCTION

1.1 Thesis overview

This thesis describes research that predominantly focuses on two aspects of cancer cell biology, the role of fibroblasts, and of androgen signalling, in oesophageal adenocarcinoma (OAC) and prostate cancer. The possibility that changes in DNA methylation may be at least in part responsible for the phenotypic changes characteristic of cancer-associated fibroblasts (CAFs) was investigated. A system for the direct co-culture of fibroblasts and tumour cells was established. This permitted the visualisation and measurement of the effect of juxtacrine (cell-cell or cell-extracellular matrix contact) or paracrine (soluble factors) signalling on the behaviour of each of the cells. The prognostic significance of the expression of the androgen receptor (AR) and the androgen-responsive gene (ARG) FK506-binding protein 5 (FKBP5) in OAC tissues was determined, and the effect of androgen signalling on the behaviours of AR-expressing OAC cell lines was assessed *in vitro*.

1.2 Oesophageal adenocarcinoma

Oesophageal adenocarcinoma (OAC) is a malignant tumour that develops from glandular epithelium in the lower third of the oesophagus, or at the gastro-oesophageal junction (Lerut et al. 2004, DiMaio et al. 2012, Lepage et al. 2013). It typically affects older, overweight, white males (Bodelon et al. 2011, Cooper & Trudgill 2012, Lepage et al. 2013), and its incidence has increased rapidly in Western countries over the last four decades (Bodelon et al. 2011, Chen et al. 2012, Edgren et al. 2013, Hur et al. 2013, Lepage et al. 2013). It has a dismal prognosis, with a five-year survival of around 15% (Whiteman et al. 2008, Thrift & Whiteman 2012, Edgren et al. 2013, Lagergren & Lagergren 2013, Domper Arnal et al. 2015). The cancer is often detected late, because it can remain symptomless until at an advanced stage. Approximately 75% of patients are unsuitable for surgery at the time of diagnosis, and, for those who undergo surgery, the recurrence rate is high (Kim et al. 2010, Lagergren & Lagergren 2013, Gregson et al. 2016). Increased understanding of the biology of this cancer may lead to the discovery of better biomarkers for early detection and management, or more effective treatments.

The major risk factors for OAC are gastro-oesophageal reflux disease (GORD), Barrett's oesophagus (BO), and obesity (Rutegard et al. 2011, Nordenstedt et al. 2012). The risk of OAC is strongly associated with the frequency and duration of GORD, being five-fold higher in patients experiencing symptoms of reflux at least weekly (Lagergren et al. 1999, Anderson et al. 2007, Xie & Lagergren 2016b). GORD is also the principal risk factor for BO, the

pre-malignant tissue from which OAC is generally believed to originate (Anderson et al. 2007, Kendall et al. 2013, Zhang et al. 2014). In BO the normal oesophageal squamous epithelium is replaced by a metaplastic columnar epithelium (Derakhshan et al. 2009, Chai & Jamal 2012, Kendall et al. 2013, Lagergren & Lagergren 2013, Spechler & Souza 2014, Domper Arnal et al. 2015). This is thought to be a protective epithelial response to repeated damage from GORD (Anderson et al. 2007, Spechler & Souza 2014). Only a small percentage of GORD patients develop BO, and only 0.2-0.7% of patients with BO progress to OAC per year (Gregson et al. 2016).

Obesity, the other major risk factor for OAC, can be estimated by the body mass index (BMI) or measures of body fat distribution (Lagergren & Lagergren 2013). BMI is a crude estimate of obesity, as it does not allow for differences in body composition or where the fat is distributed (Lagergren 2011). Adverse outcomes from obesity are more related to properties of visceral fat than subcutaneous fat (Matsuzawa 2008, Kendall et al. 2013, Tchernof & Despres 2013). Visceral fat is commonly estimated by the waist circumference or waist:hip ratio. Both obesity and abdominal obesity with a normal BMI are associated with an increased risk of BO and OAC (Corley et al. 2008, Whiteman et al. 2008, O'Doherty et al. 2012, Kendall et al. 2013, Domper Arnal et al. 2015). Overall obesity, measured by BMI, is a risk factor for OAC independent of acid reflux or smoking (Whiteman et al. 2008), and abdominal obesity is a risk factor for BO or OAC independent of BMI or GORD (Corley et al. 2008, Lagergren 2011, Kendall et al. 2013, Cook et al. 2015a).

1.3 A role for androgens in the biology of oesophageal adenocarcinoma

Many studies have reported that OAC occurs more frequently in males, with a male:female ratio in the range of 7-10:1 (Rutegard et al. 2011, Nordenstedt et al. 2012). This predominance cannot be explained by abnormal male:female ratios in GORD, BO or obesity (Corley et al. 2008, Chandanos & Lagergren 2009, Lagergren 2011, Cooper & Trudgill 2012, Lu & Lagergren 2012, Kendall et al. 2013, Menon et al. 2014). GORD occurs equally in males and females in population controls and in BO cases (Chandanos & Lagergren 2009, Kendall et al. 2013), and, although BO shows a male predominance, it is much lower than for OAC, at only 2-4:1 (Awan et al. 2007, Nordenstedt et al. 2012, Kendall et al. 2013). Increased BMI is equally prevalent in males and females. Whilst males have a higher incidence of abdominal obesity or excess visceral fat than females, this is considered insufficient to account for the very high male:female ratio in OAC (Corley et al. 2008, Kendall et al. 2013, Cook et al. 2015b). Other factors must therefore contribute to this higher

incidence in males (Anderson et al. 2007). Epidemiological studies suggest that the observed differences in incidence between males and females can be explained by a 20-year and 17-year delay in the development of BO and OAC respectively in females (Chandanos & Lagergren 2009, Derakhshan et al. 2009, Lagergren & Lagergren 2013). The gender difference in the incidence of OAC suggests a role for sex hormones, since their levels change over the lifetime and differ between the sexes.

For example, oestrogen and progesterone production decrease abruptly with menopause in women. This correlates with the higher incidence of OAC in older females and suggests oestrogen may protect from OAC (Rutegard et al. 2011, Mathieu et al. 2014). However existing studies supporting a role for oestrogen are limited. There have been few reports of oestrogen receptor expression in BO and OAC tissues (Akgun et al. 2002, Tiffin et al. 2003, Liu et al. 2004, Kalayarasan et al. 2008), and studies investigating the effect of exogenous oestrogens and reproductive factors on the incidence of OAC in women are conflicting (Andersson et al. 1991, Curtis et al. 1996, Matsuyama et al. 2000, Lagergren & Jansson 2005, Chandanos et al. 2006, Lindblad et al. 2006, Anderson et al. 2007, Chandanos & Lagergren 2009, Derakhshan et al. 2009, Green et al. 2012a, Green et al. 2012b, Lagergren & Lagergren 2013, Lagergren et al. 2014, Menon et al. 2014, Xie & Lagergren 2016b, Xie & Lagergren 2016a).

The studies reported in this thesis focused on the potential role of androgens in OAC, mainly because a preliminary review of the literature indicated that this possibility had not been well studied. Unlike the abrupt decline in oestrogen levels in menopausal women, men do not experience abrupt changes in androgen levels with age (Muller et al. 2003b, Rutegard et al. 2011). Instead there is a steady decline in testosterone production throughout life in adult men, decreasing as little as 1-3% per year, beginning around the age of 35-40 years (Muller et al. 2003a, Rutegard et al. 2011, Horstman et al. 2012). Although women have much lower testosterone levels than men, their testosterone production also declines with age (Sukocheva et al. 2015), however the bioavailability of testosterone increases in women and decreases in men. This is consistent with the incidence of OAC after 80 years of age, which declines in males yet continues to increase in females (Morley 2001, Morley & Perry 2003, Mathieu et al. 2014).

1.3.1 Androgens

Androgens are hormones with roles in a wide range of developmental and physiological processes, including the development and maintenance of the male reproductive system and secondary sexual characteristics (Lonergan & Tindall 2011, Davey & Grossmann 2016). They also regulate skeletal muscle growth, bone formation, fat distribution, and sexual function (Gao et al. 2005). Additionally, androgens act as precursors for the production and synthesis of oestrogen and are important for the maturation of ovarian follicles in women (Horstman et al. 2012).

Androgens are synthesised from cholesterol, mainly in the adrenal cortex, testes, and ovaries (Sukocheva et al. 2015). Testosterone and its more active metabolite dihydrotestosterone (DHT) are the major endogenous androgens. DHT is produced by the reduction of testosterone by the enzyme 5-alpha reductase, which is produced in many tissues, but in highest concentration in the prostate gland, skin, brain, and liver. For this reason, tissue levels of DHT do not necessarily mimic serum levels of DHT or testosterone, and can differ between tissues depending on which isoform of the reductase enzyme is present and its concentration (Yassin & Saad 2007, Yamashita et al. 2009, Page et al. 2011). DHT is more biologically active than testosterone, with a 2-fold higher affinity for the receptor (Gao et al. 2005, Munoz et al. 2015). There are other androgens of adrenal origin which bind with a low affinity compared to testosterone and DHT. They include androstenedione, dehydroepiandrosterone (DHEA), and DHEA sulfate (DHEAS) (Munoz et al. 2015, Sukocheva et al. 2015). The circulating concentration of androgens is 20- to 25-fold lower in women compared to men (Horstman et al. 2012). The predominant androgens in the circulation are testosterone in men, and androstenedione and testosterone in women (Yialamas & Hayes 2003).

Androgens mediate their effects predominantly through activation of the androgen receptor (AR) (Matsumoto et al. 2013, Davey & Grossmann 2016). Their ability to activate the AR depends on whether they are free or bound. Approximately 60% of circulating testosterone is bound with low affinity to albumin, 40% is bound tightly to sex hormone binding globulin and 1-2% is free (Yialamas & Hayes 2003, Gao et al. 2005). Both free and albumin-bound testosterone is bioavailable to the tissues, however only free testosterone is able to activate the AR (Sukocheva et al. 2015).

1.3.2 The androgen receptor

The AR is a ligand-dependent nuclear transcription factor (Matsumoto et al. 2013). It is a member of the steroid hormone nuclear receptor family (Shukla et al. 2016), the others being the oestrogen receptor (OR), progesterone receptor (PR), glucocorticoid receptor (GR), and mineralocorticoid receptor (MR) (Davey & Grossmann 2016). The AR gene is located on the X chromosome, and encodes a 110 kDa protein, 919 amino acids in length (Gao et al. 2005, Tan et al. 2015). There are three major functional domains; a poorly conserved N-terminal domain (NTD), a highly conserved DNA-binding domain (DBD), and a moderately conserved C-terminal ligand-binding domain (LBD) (Gao et al. 2005), each of which is important for receptor function.

The AR is distributed widely throughout normal human tissues but is predominantly expressed in the prostate, skeletal muscle, liver, and central nervous system (CNS) (Sukocheva et al. 2015, Tan et al. 2015). The expression of AR is moderate to high in the reproductive tissues of both females and males (Bennett et al. 2010), with the prostate, adrenal gland, and epididymis having the highest (Gao et al. 2005). It is also expressed, at lower levels, in fetal and adult non-genital tissues, including the brain, skin, kidney, thyroid, intestine, thymus, fat, bone, and all vasculature structures (Bennett et al. 2010).

1.3.3 Androgen receptor function and androgen signalling

In its unbound state, AR resides primarily in the cell cytoplasm, typically associated with molecular chaperones such as heat shock protein 90 (Hsp90) (Smith & Toft 2008, Lonergan & Tindall 2011). Upon the binding of androgens, such as testosterone or DHT, the AR undergoes conformational change, dissociation from the chaperone proteins and translocation into the nucleus (Gao et al. 2005, Lonergan & Tindall 2011, Tan et al. 2015, Davey & Grossmann 2016). There, AR dimerises and binds to androgen response elements (ARE) within the genome where it regulates the transcription of androgen-responsive genes (ARGs) (Thornton & Kelley 1998, Gao et al. 2005, Tan et al. 2015, Davey & Grossmann 2016, Shukla et al. 2016). The transcriptional activity of androgen-bound AR is modified by the availability of androgen and the relative availabilities of a number of pioneer, coactivator or corepressor proteins, which are recruited by the AR-ARE complex (Lonergan & Tindall 2011, Chang et al. 2013, Davey & Grossmann 2016, Shukla et al. 2016, Leach & Buchanan 2017). In this manner specific ARGs that encode proteins and noncoding RNAs are up or down regulated by androgen signalling via the AR (Matsumoto et al. 2013).

The nuclear translocation of AR and changes in the expression of ARGs are markers of functional androgen signalling, and can be measured at the protein and transcript level respectively. A classical and commonly measured ARG is FK506 binding protein 5 (FKBP5). It is commonly measured to identify functional androgen signalling in a tissue of interest (Pei et al. 2009, Li et al. 2011, Leach et al. 2017). In this thesis, the nuclear localisation of AR and the change in transcript abundance of FKBP5 and other ARGs were used as measures of functional androgen signalling in OAC tissues and cell lines.

1.3.4 The role of androgens and the androgen receptor in cancer cells

Androgen signalling in the cancer cells of a tumour has been implicated in the development and progression of a number of carcinomas, including prostate, bladder, colon, and liver (Chang et al. 2014, Munoz et al. 2015). The role of androgen signalling has been most thoroughly researched in prostate cancer, in which it plays a central role (Munoz et al. 2015). Prostate cancer is the second most common cancer in men worldwide, and a significant cause of morbidity and mortality (Singh et al. 2014, Torre et al. 2015, Torre et al. 2016, Leach & Buchanan 2017). The prostate is comprised of an epithelium of secretory luminal cells outlined with basal cells, and a surrounding stroma of fibroblasts and smooth muscle cells (Singh & Lee 2013). The prostatic epithelial stem cells give rise to cells that differentiate into basal, intermediate, and luminal epithelial cells (Niu et al. 2010). The AR is expressed in the epithelial and stromal cells of the prostate (Singh & Lee 2013, Singh et al. 2014), and this is necessary for the development and maintenance of the normal prostate as well as the development and progression of prostate cancer (Minamiguchi et al. 2003, Cunha et al. 2004, Cano et al. 2007, Lonergan & Tindall 2011, Munoz et al. 2015, Shukla et al. 2016).

Studies have shown that the AR and androgen signalling in prostate epithelial cancer cells can have opposing roles, either promoting or suppressing tumour progression (Chang et al. 2013). It is reported that the differential effects of epithelial AR may depend in part on whether the disease is in an early or late stage, and which epithelial cell type, luminal or basal, expresses the AR (Chang et al. 2013, Matsumoto et al. 2013, Munoz et al. 2015). For instance, clinically, the expression of AR is generally lower in prostate cancer compared to normal prostate and in metastatic compared to primary disease (Li et al. 2004), however higher levels of AR in the prostate cancer cells are associated with a higher degree of malignancy, more advanced disease progression and poor biochemical recurrence-free survival (Henshall et al. 2001, Li et al. 2004, Ricciardelli et al. 2005). In transgenic mouse models of prostate cancer, AR knockin and knockout experiments showed that AR in prostatic epithelial cells was

associated with the development of prostate cancer (Han et al. 2005, Zhu et al. 2011), and promoted the survival of luminal epithelial cells (Niu et al. 2008a), whereas it suppressed the proliferation of basal and intermediate epithelial cells and suppressed prostate cancer metastasis (Gingrich et al. 1997, Niu et al. 2008a, Niu et al. 2008b). In vitro studies in prostate cancer cell lines are also consistent with the differential effect of epithelial AR. For instance, AR expression in PC3 cells suppressed their proliferation and metastasis (Garcia-Arenas et al. 1995, Heisler et al. 1997, Litvinov et al. 2004, Litvinov et al. 2006, Niu et al. 2008a), whilst it stimulated or suppressed the proliferation of LNCaP (Olea et al. 1990, Kokontis et al. 1998, Eder et al. 2000), CWR22Rv1 (Niu et al. 2008a), and PC346C (Marques et al. 2005) cells (Niu et al. 2010).

Whilst the evidence for a role for androgens is strongest in prostate cancer, there is also evidence for its role in the biology of other cancers. Bladder cancer is 3-4 times more common in males than females (Kakehi et al. 2010, Chang et al. 2013, Li et al. 2017, Siegel et al. 2017b). Mice with knockout of AR, either total knockout or only in the urothelial cells, had a lower incidence of carcinogen induced bladder cancer compared to their wild-type littermates (Miyamoto et al. 2007, Hsu et al. 2013), and androgens have been shown to promote the growth of human AR-expressing bladder cancer cell lines, both in mouse xenografts (Miyamoto et al. 2007) and in vitro (Li et al. 2017).

The incidence of primary liver cancer is 2-4 times higher in males than in females (Nordenstedt et al. 2010, Siegel et al. 2017b). Hepatocellular carcinoma (HCC) accounts for approximately 90% of all primary liver cancers (Nordenstedt et al. 2010). The development of carcinogen-induced HCC was suppressed in AR knockout (ARKO) mice, leading the authors to conclude that functional androgen signalling was a key factor in its development (Ma et al. 2008). In vitro, knockin of AR in human HCC cell lines resulted in increased proliferation, decreased apoptosis, and increased anchorage-independent growth independently of androgen, whilst therapeutic targeting of AR, through either knockdown or anti-androgen therapy, suppressed proliferation, and enhanced apoptosis (Ma et al. 2008).

The incidence of colorectal cancer (CRC) is higher in males across all age groups (Majek et al. 2013, Purim et al. 2013, Siegel et al. 2017a). Tumour incidence was reduced in castrated males, but not in females who received exogenous hormone replacement of progestin and 17-beta-estradiol following ovariectomy. This suggests that androgens promote CRC, and that oestrogens are not protective (Amos-Landgraf et al. 2014).

1.3.5 Androgen receptor expression and androgen signalling in oesophageal cancers

There are very few studies on AR expression or androgen signalling in oesophageal cancer. Of these, the majority relate to oesophageal squamous cell carcinoma (OSCC). OSCC is 3 times more common in males than females, a lower ratio than for OAC. The higher incidence in males has been generally attributed to higher tobacco usage and heavier alcohol consumption (Mathieu et al. 2014, Xie & Lagergren 2016a, Xie & Lagergren 2016b), but several studies suggest a potential role for AR and androgens.

In terms of AR expression in human OSCC tissues, one study showed expression in 3 of 14 cases (Tihan et al. 2001). Another study showed no AR expression in all of 10 cases, but 2 of 10 human OSCC xenografts implanted into nude mice expressed AR (Yamashita et al. 1989). Neither study mentioned the location of the AR. In vivo, the incidence of chemically induced OSCC was higher in intact male rats compared to castrated rats and was completely suppressed in castrated rats treated with oestrogen. This research is difficult to interpret however as there was no assessment of AR expression in the cancer cells (Kobayashi 1985). In vitro, testosterone stimulated, and oestrogen inhibited, the growth of an AR-expressing human OSCC cell line, KSE-1, but not an AR-negative human OSCC cell line, KSE-2 (Matsuoka et al. 1987), yet when the cell lines were implanted into intact mice, the administration of DHT did not alter the growth rate of either cell line (Ueo et al. 1990).

In terms of AR expression in cancer tissues from OAC patients, studies are limited and, as for OSCC, conflicting. One reported AR staining in 1 of 10 patients with no mention of where the AR was located (Tiffin et al. 2003). A second detected expression in the cancer epithelial cells of 5 of 11 patients with no expression in the stroma (Tihan et al. 2001). A third study observed no expression in the cancer epithelial cells but did detect expression in the stroma of 13 of 18 patients (Awan et al. 2007).

Several studies have reported that serum testosterone levels are higher in men with BO and OAC compared to normal age-matched controls (Awan et al. 2007, Cook et al. 2015b). This suggests a role for androgens however studies of patients on anti-androgen therapy are inconsistent. A Swedish study hypothesised that if hormonal factors explained the male predominance then treatment that increased oestrogen and/or lowered testosterone would reduce the risk of OAC. They assessed prostate cancer patients who received prolonged treatment with anti-androgens, typically oestrogens, and showed no reduction in the risk of

OAC, suggesting no role for either oestrogen or testosterone in the aetiology of this cancer (Lagergren & Nyren 1998). Another study reported a reduced risk of OAC in patients with primary prostate cancer treated with androgen-deprivation therapy (ADT), suggesting either ADT, or its effect of lowering androgens, was protective. However, the possibility that there were risk factors associated with prostate cancer which were negatively associated with OAC, or that the risk of OAC was reduced as a result of lifestyle changes made following a prostate cancer diagnosis, could not be excluded (Cooper et al. 2009, Cooper & Trudgill 2012).

It is not possible to draw definitive conclusions on a role for AR in OAC from these reported studies. The patient cohorts used were underpowered and the results conflicting. Functional androgen signalling, as opposed to AR expression, was not assessed. This led to two studies reported in this thesis. The prognostic significance of functional androgen signalling in OAC was assessed in a large patient cohort (Chapter 5). The effect of androgen signalling on the behaviours of OAC cells was explored in vitro using OAC cell lines stably transduced with AR (Chapter 6). These are the most comprehensive in vivo and in vitro studies of the role of androgens and AR signalling in OAC reported to date.

1.4 Fibroblasts in cancer

The influence of stromal fibroblasts on the biology of OAC and prostate cancer was investigated. Initially, the intention was to study cell interactions in co-cultures of oesophageal fibroblasts and OAC cancer cells, comparing fibroblasts derived from normal oesophageal mucosa (NDFs) to tumour-derived fibroblasts from OAC (TDFs), however the isolation of fibroblasts from patient tissues proved challenging. Only 22 lines were ultimately available - most proliferated very slowly, and many ceased to divide beyond around 10 subdivisions. Sufficient cells were harvested from early subcultures to permit a comparison of the DNA methylation profiles of NDFs and TDFs (Chapter 2). For co-culture experiments, the oesophageal fibroblasts were to be stably transduced with red fluorescent protein (RFP) to differentiate them from OAC cell lines, which had been stably transduced with green fluorescent protein (GFP). To undertake a long-term project studying these cells, it was clear that the fibroblasts needed to be immortalised.

The attempts to immortalise the oesophageal fibroblasts were unsuccessful, very time consuming, and, after 18 months, were abandoned. During this time, the feasibility of the proposed co-culture experiments was determined in pilot studies using immortalised prostate myofibroblasts labelled with RFP and the prostate cancer cell line, PC3, labelled with GFP.

Since stromal fibroblasts normally express AR early in prostate cancer, and subsequent loss of AR expression in the cancer-associated stroma is associated with a poorer prognosis (Leach et al. 2017), two myofibroblast lines were used, one AR negative, PShTert, and a subline stably transduced with AR, PShTert-AR. This was an attempt to study the effect of myofibroblast AR on the myofibroblast-prostate cancer cell interaction (Chapters 3 and 4). Since using primary oesophageal fibroblast lines was impractical, and attempts to generate immortalised lines had failed, non-oesophageal fibroblast lines were used to investigate the effect of fibroblasts on androgen signalling in OAC cells (Chapter 6).

1.4.1 The tumour stroma

An epithelial tumour is comprised of two compartments, the tumour epithelial cells and the stroma within which the tumour cells exist (Turley et al. 2015, Kalluri 2016). The tumour stroma includes fibroblasts of multiple phenotypes, particularly myofibroblasts and cancer-associated fibroblasts (CAFs), immune and inflammatory cells, blood and lymph vessels, nerves, neuroendocrine cells, and adipose cells, and the extracellular matrix (ECM) the stromal cells produce (Mbeunkui & Johann 2009, Balkwill et al. 2012, Chen et al. 2015). As well as providing physical support, there is a bi-directional crosstalk between the tumour stroma and the malignant cells, by which one compartment influences the behaviour and structure of the other. In this manner, the stromal cells can influence most or all aspects of tumour development, including growth, metastasis, and chemoresistance (Quail & Joyce 2013, Turley et al. 2015, Gascard & Tlsty 2016).

1.4.2 Normal fibroblasts

Fibroblasts are the major cell type in the normal stroma and are found ubiquitously throughout the body (Flavell et al. 2008, Phan 2008, Iacopino et al. 2012, Mao et al. 2013). Identifying features include their spindle-shaped morphology, ability to adhere to plastic, and their lack of epithelial, vascular and leukocyte lineage markers (Flavell et al. 2008, Franco et al. 2010). Fibroblasts play the major role in the production and remodelling of the ECM. They also create an environment that supports the normal functioning of neighbouring epithelial and endothelial cells, and help to regulate immune and inflammatory responses through the production of chemokines and cytokines (Jordana et al. 1994, Flavell et al. 2008).

1.4.3 Cancer-associated fibroblasts

Normally fibroblasts are quiescent, and are present in the stroma in relatively low numbers. In response to a range of stimuli they can undergo a process of activation, and are then referred to as activated fibroblasts or myofibroblasts (Worthley et al. 2010, Kalluri 2016). This response was first observed in wound healing and later in acute and chronic inflammation and tissue fibrosis (Kalluri 2016). Activated fibroblasts differ from quiescent tissue fibroblasts phenotypically and functionally, including their rate of proliferation and migration, level of metabolic activity, and production of growth factors and extracellular matrix. Some markers can help to differentiate between quiescent and activated fibroblasts, such as α -smooth muscle actin (α SMA), platelet-derived growth factor receptor beta (PDGFR β), and fibroblast activation protein (FAP) (Mao et al. 2013, Kalluri 2016). However no marker is specific for fibroblasts or their state of activation, and activated fibroblasts may not necessarily express all of the possible markers at the same time (Ohlund et al. 2014, Kalluri 2016). It is feasible that fibroblasts may be able to differentiate into distinct functional subsets with a range of activities, similar to T lymphocyte differentiation (Kalluri 2016).

Fibroblasts within the tumour stroma are commonly activated and are referred to as cancer-associated fibroblasts (CAFs) (Lin et al. 2016). These are a major component of the tumour stroma (Allen & Louise Jones 2011, Mao et al. 2013, Narunsky et al. 2014). They are reported to arise variously from resident fibroblasts, smooth muscle cells, myoepithelial cells or mesenchymal stem cells, or local endothelial or epithelial cells (Balkwill et al. 2012, Mao et al. 2013, De Wever et al. 2014, Narunsky et al. 2014, Ohlund et al. 2014). Fibroblasts can modify or change the fate of premalignant or malignant cells (Ohlund et al. 2014). Compared to quiescent fibroblasts, which typically suppress carcinogenesis (Dumont et al. 2013, Chen et al. 2015, Kalluri 2016), CAFs may suppress (Ozdemir et al. 2014, Rhim et al. 2014) or promote tumour development and progression (Dumont et al. 2013, Narunsky et al. 2014, Ohlund et al. 2014, Klemm & Joyce 2015, Kalluri 2016). This may reflect functional heterogeneity within the CAF population, with activated fibroblasts differentiating into distinct subsets of CAFs, or it may reflect the same subset having different functions depending on the context of the specific tumour stroma (Kalluri 2016).

In terms of the tumour-promoting ability of CAFs, in vitro and tissue recombinant studies have shown that CAFs, but not normal fibroblasts, can induce tumorigenesis in initiated prostate epithelial cells (Olumi et al. 1999) and can promote the growth, invasion, and metastasis of malignant cells from a range of cancers (Orimo et al. 2005, Gaggioli et al. 2007,

Karnoub et al. 2007, Giannoni et al. 2011, Goetz et al. 2011, Sanz-Moreno et al. 2011, Calon et al. 2012, Dumont et al. 2013, Mao et al. 2013). The CAFs have the potential to secrete cytokines and other immunomodulatory signalling molecules that can modify local immune responses. They can upregulate local inflammation and create a microenvironment that supports tumour growth and angiogenesis, which would be particularly relevant early in the development of a cancer (Ohlund et al. 2014). They can also promote local immunosuppression, which may permit a tumour to flourish (Kalluri 2016). Clinically, the increased expression of CAF specific markers is associated with a poor prognosis in a number of tumours, including colorectal (Henry et al. 2007, Tsujino et al. 2007), breast (Yamashita et al. 2012), and head and neck cancers (Marsh et al. 2011).

In relation to OAC, the chronic injury and inflammation associated with GORD and BO is believed to activate fibroblasts, resulting in increased local levels of free radicals, cytokines, and inflammatory enzymes. These result in intracellular damage in the epithelial cells and the creation of a tissue microenvironment that promotes the development of OAC (Mbeunkui & Johann 2009, Rieder et al. 2010, Worthley et al. 2010, Taddei et al. 2014, Verbeek et al. 2014, Lin et al. 2016, Wang et al. 2016). Within the developed OAC, the CAFs can enhance OAC cell growth, angiogenesis (Nie et al. 2014), invasion, and resistance to chemotherapy (Hayden et al. 2012, Underwood et al. 2015), with higher expression of CAF-specific markers in OAC tissues a predictor of poor survival (Underwood et al. 2015).

1.4.4 The extracellular matrix in cancer

The extracellular matrix (ECM) surrounds and supports the cells of solid tissues (Frantz et al. 2010, Bonnans et al. 2014). Specific ECM components include fibrous proteins, such as collagens, elastins, laminins, and fibronectins, as well as proteoglycans and hyaluronans that form a hydrated gel (Frantz et al. 2010, Peddareddigari et al. 2010, Rubashkin et al. 2014). Each tissue has a unique ECM composition and topology (Frantz et al. 2010, Lu et al. 2012, Hubmacher & Apte 2013). The ECM has several functional roles. It provides cells with structural and mechanical support and serves as a reservoir for cytokines and growth factors. The ECM proteins act as ligands for cell receptors, particularly integrins, thereby influencing cellular functions such as adhesion, migration, proliferation, apoptosis, survival, and differentiation (Peddareddigari et al. 2010, Lu et al. 2011, Bonnans et al. 2014, Narunsky et al. 2014, Ohlund et al. 2014, Klemm & Joyce 2015, Sever & Brugge 2015).

The functional properties of the ECM are determined by the composition and organisation of the matrix components. This is regulated by ECM remodelling, a continuous process whereby matrix components are synthesised, secreted, modified, and enzymatically degraded (Cox & Erler 2011). Degradation of the ECM involves protease enzymes secreted mainly by stromal cells or localised on the cell surface, particularly matrix metalloproteinases (MMPs) (Mbeunkui & Johann 2009, Peddareddigari et al. 2010, Lu et al. 2011, Lu et al. 2012, Bonnans et al. 2014). These ECM dynamics must be tightly regulated to ensure tissue homeostasis (Bergamaschi et al. 2008, Frantz et al. 2010, Allen & Louise Jones 2011, Cox & Erler 2011, Lu et al. 2012, Bonnans et al. 2014).

In cancer, ECM dynamics and structure are dysregulated (Franco et al. 2010, Allen & Louise Jones 2011, Kim et al. 2011, Lu et al. 2011, Balkwill et al. 2012, Lu et al. 2012, Bonnans et al. 2014, Narunsky et al. 2014, Klemm & Joyce 2015). Compared to normal tissue, tumours are stiffer as a result of increased ECM deposition and modification by CAFs. The modifications include the increased crosslinking of the collagen and elastin fibres by lysyl oxidases secreted from the stromal cells, stiffening the tumour further (Frantz et al. 2010, Allen & Louise Jones 2011, Balkwill et al. 2012, Narunsky et al. 2014). This promotes cancer cell migration and integrin signalling pathways, which enhance tumour progression (Egeblad et al. 2010, Allen & Louise Jones 2011, Sever & Brugge 2015). Elevated expression of lysyl oxidases has been correlated with metastasis and decreased survival in mouse models of cancer and in cancer patients (Erler & Giaccia 2006). Additionally, there is upregulation of proteinase synthesis and secretion leading to aberrant remodelling of ECM proteins (Peddareddigari et al. 2010, Allen & Louise Jones 2011, Sever & Brugge 2015). The MMPs degrade the ECM, which releases chemokines, and growth and angiogenic factors, thereby facilitating tumour growth and metastasis (Balkwill et al. 2012). The expression of MMPs is involved in the progression from BO to OAC (Salmela et al. 2001, Grimm et al. 2010), and is associated with tumour stage in OSCC (Gu et al. 2005, Zhang et al. 2014). In prostate cancer, the expression of genes encoding certain ECM proteins and ECM degrading enzymes has prognostic significance, and breast cancer patients can be subclassified into distinct groups with distinct clinical outcomes based on differences in the ECM gene profile of the cancer tissue (Bacac et al. 2006, Bergamaschi et al. 2008).

1.4.5 DNA methylation

Several studies have shown that the phenotypic characteristics of CAFs are preserved during subculture. A plausible explanation is that at least some of the CAF characteristics are

maintained as a result of epigenetic modifications such as DNA methylation (Hu et al. 2005, Madar et al. 2013, Albregues et al. 2015). In DNA methylation there is the covalent addition of a methyl group (CH₃) to, most commonly, the cytosine residue of a cytosine-phosphate-guanine (CpG) dinucleotide (Jones & Takai 2001, Lim & Maher 2010). Many of the CpG dinucleotides are concentrated in short stretches of DNA termed CpG islands. The transcription start site of 70% of all human gene promoters, and also many enhancers, are closely associated with CpG islands (Sharma et al. 2010, Dawson & Kouzarides 2012, Zeisberg & Zeisberg 2013, Wagner et al. 2014). In normal cells these are typically unmethylated. Methylation in these regions inhibits transcription and results in partial or complete silencing of the associated genes (Zeisberg & Zeisberg 2013).

Studies investigating DNA methylation in cancer have mainly focused on changes in the malignant epithelial cells with little attention being given to the fibroblasts (Gonda et al. 2010, Vizoso et al. 2015). The few studies that have looked suggest that there are DNA methylation changes in fibroblasts and that these could play a role in the altered phenotype of CAFs compared to normal fibroblasts. In prostate cancer, three genes important for prostate cancer carcinogenesis showed high DNA methylation in the cancer-associated stroma compared to normal stroma (Hanson et al. 2006). The treatment of dermal fibroblasts with transforming growth factor beta (TGF- β) resulted in the induction of a sustained pro-invasive phenotype which required DNA methylation for its maintenance, and CAFs isolated from head and neck, lung or breast cancer cultured with DNA methylation inhibitors lost this phenotype (Albregues et al. 2015). In colorectal cancer, chondroitin sulfate proteoglycan (PG-40) expression was associated with ECM alterations that supported tumour growth and invasion and was enhanced in neoplastic stroma, but not normal stroma. This enhanced expression was due to a hypomethylation of the PG-40 gene in the neoplastic stromal cells (Adany et al. 1990, Adany & Iozzo 1990, Adany & Iozzo 1991). Differences in DNA methylation profiles between normal fibroblasts and CAFs have been reported in breast (Hu et al. 2005), gastric (Jiang et al. 2008), and colorectal (Mrazek et al. 2014) cancers.

The research reported in chapter 2 compared the genome-wide DNA methylation profiles of fibroblasts derived from normal oesophageal mucosa (NDFs) and tumour-derived fibroblasts from OAC (TDFs) using the Illumina 450K platform. At the time the experiments were undertaken there were no reports of the assessment of genome-wide DNA methylation in CAFs from any cancer, using the Illumina 450K platform. However, during the preparation of the manuscript, Vizoso et al. published a comparison of the DNA methylation between

normal fibroblasts and CAFs in non-small cell lung cancer using this methodology (Vizoso et al. 2015).

1.5 The crosstalk between fibroblasts and epithelial cancer cells

Neighbouring cells can communicate with each other by either juxtacrine or paracrine signalling. Juxtacrine signalling occurs via cell-to-cell or cell-to-ECM interactions and requires close contact. Paracrine signalling occurs via the diffusion of soluble molecules, such as growth factors, chemokines, and cytokines, or soluble subcellular organelles including microvesicles and exosomes (Fang & Declerck 2013). Most studies of local cell signalling in cancer have concentrated on paracrine signalling. However there is increasing evidence to suggest that juxtacrine signalling, particularly between CAFs and cancer cells, is very important (Yamaguchi et al. 2014). This may induce effects in either cell type to promote cancer progression. In relation to the cancer cells, *in vitro* studies have shown that direct cell-cell contact with CAFs enhanced cancer cell proliferation and invasion in lung and breast cancer (Camp et al. 2011, Otomo et al. 2014) and promoted cancer cell invasion via remodelling of the ECM (Krtolica et al. 2001, Gaggioli et al. 2007, Yamaguchi et al. 2014). In non-small cell lung cancer, CAFs enhanced EMT and motility more strongly via direct rather than indirect interactions (Choe et al. 2013), and in scirrhous-type gastric carcinoma (SGC), SGC-associated fibroblasts required direct contact with SGC cells for the marked fibroblast proliferation that is associated with rapid progression and a poor prognosis (Semba et al. 2009). Direct interactions have also been shown to be important in the stemness, or capacity for self-renewal and differentiation, of cancer stem cells/cancer-initiating cells (CSCs/CICs). This was mediated by direct contact with the CD44 molecule on the CAF surface (Kinugasa et al. 2014). The research presented in this thesis therefore investigated direct interactions between fibroblasts and epithelial cancer cells, both cell-cell and cell-ECM, since they are a relevant but rarely studied cellular interaction.

1.5.1 Co-culture techniques used to assess fibroblast-epithelial cancer cell crosstalk

Paracrine signalling can be studied *in vitro* using indirect co-culture systems, the most common of which is the transwell chamber. One cell type is seeded into the lower chamber, the other into an insert with a permeable base. Signalling molecules can diffuse between the two cell types through the pores of the insert. Another technique to investigate paracrine signalling is to culture one cell type for a period, harvest the culture medium, and then add

this conditioned medium, containing any secreted signalling molecules, to a monoculture of the target cell (Miki et al. 2012).

Juxtacrine signalling can be studied in vitro using direct co-culture systems, in which two or more cell types are seeded into the same well, allowing cell-cell and cell-ECM contact. Direct co-culture has the potential to mimic more closely the in vivo environment than indirect co-culture (Miki et al. 2012), however direct interactions have been less commonly investigated in vitro predominantly due to the difficulty of visualising the different cell types or sorting them for downstream analyses. In the direct co-culture experiments described in this thesis the fibroblasts were seeded and allowed to form a monoculture over 48 hours, after which a smaller number of cancer cells were overlaid. The two cell types were distinguished by labelling them with different intracellular fluorescent dyes.

Another difficulty with direct co-cultures is that it is not possible to prevent paracrine signalling, which would permit the study of juxtacrine signalling in isolation. It is therefore common to study direct (paracrine and juxtacrine signalling) and indirect (paracrine signalling) co-cultures in the same experiment as a way of attempting to distinguish juxtacrine from paracrine signalling.

A modified form of direct co-culture permits the investigation of cell-ECM interactions. A confluent monolayer of one cell type is grown. The cells are subsequently stripped away using mild detergents or chelating agents, leaving a layer of matrix. A suspension of the target cells can then be seeded onto this matrix layer and its effect on variables such as growth or motility can be measured.

Co-cultures were used in two studies in this thesis. The first examined the influence of AR signalling in the fibroblasts on the interactions between prostate cancer cells and fibroblasts (Chapters 3 and 4). The second study examined the influence of fibroblasts on the response of AR-expressing OAC cell lines to androgen (Chapter 6).

1.5.2 The significance of myofibroblast androgen receptor in prostate cancer

During the development and progression of prostate cancer there is a required, complex and bidirectional cross talk between the stromal fibroblasts and the epithelial cells (Wen et al. 2015, Leach & Buchanan 2017), both of which can express the AR. The initial development and the early stages of the progression of prostate cancer are dependent on AR expressed by

the stromal cells (Cunha 1994, Hayward et al. 1997, Cunha et al. 2003, Cunha et al. 2004, Niu et al. 2010, Singh et al. 2014, Wen et al. 2015). However, as the disease further progresses there can be a significant decrease in the expression of AR in the stroma. Such a decrease is associated with an increased risk of biochemical relapse and poorer prognosis (Mohler et al. 1996, Olapade-Olaopa et al. 1999, Henshall et al. 2001, Ricciardelli et al. 2005, Li et al. 2008, Wikstrom et al. 2009, Leach et al. 2015, Leach et al. 2017).

The reason for the association between loss of stromal AR and poor outcome is not understood. Indeed there are many experimental studies suggesting the opposite should apply, that the loss of stromal AR should be associated with the suppression of prostate tumorigenesis, and that stromal AR should promote prostate cancer progression, malignant transformation, and metastasis. Some of these studies have been undertaken in vivo, using AR knockout mouse models and tissue recombinants, and some in vitro, using indirect methods to assess paracrine signalling (Niu et al. 2008a, Niu et al. 2008b, Niu et al. 2010, Lai et al. 2012, Ricke et al. 2012, Yu et al. 2012, Yu et al. 2013). However none have assessed the contribution of juxtacrine signalling in vitro. The research presented in this thesis therefore determined the effect of myofibroblast AR in prostate cancer specifically in relation to juxtacrine signalling, utilising both direct and indirect co-cultures with myofibroblasts (AR-expressing and AR-negative) and prostate cancer cell line, PC3 (Chapter 4). Juxtacrine signalling mediated by cell-ECM interactions was also investigated by growing PC3 cells in direct contact with ECM produced by AR-expressing myofibroblasts treated with or without androgen (Chapter 3).

1.5.3 The effect of fibroblasts on androgen signalling in oesophageal adenocarcinoma

There have been extensive studies investigating how AR can modify the behaviours of cancer cells (none using OAC cells) (Castoria et al. 2003, Cunha et al. 2003, Compagno et al. 2007, Niu et al. 2008a, Niu et al. 2008b, Niu et al. 2010) and fibroblasts (Castoria et al. 2003, Cunha et al. 2003, Li et al. 2008, Niu et al. 2008a, Niu et al. 2008b, Niu et al. 2010, Tanner et al. 2011, Lai et al. 2012, Ricke et al. 2012, Yu et al. 2013). There are very few studies examining whether fibroblasts can modify the response to androgen in an AR-expressing cancer cell (Culig et al. 1994, Blanchere et al. 1998, Cano et al. 2007, Eder et al. 2016). Research reported in this thesis investigated the ability of fibroblasts to modify the androgen response of an AR-expressing OAC cell line (Chapter 6). Normal foreskin fibroblasts (NFFs)

and PShTert myofibroblasts were used in place of oesophageal fibroblasts, since attempts to immortalise the primary cells had failed.

1.6 Aims of the study

The research presented in this thesis addressed three specific aims:

1. To compare the DNA methylation profiles of normal oesophageal fibroblasts and tumour-derived fibroblasts from OAC (Chapter 2)
2. To establish a direct co-culture system for the study of juxtacrine and/or paracrine signalling between fibroblasts and cancer cells in vitro (Chapters 3 and 4)
3. To investigate the expression of functional AR and its utility as a biomarker in OAC, and the effect of androgen signalling on the behaviour of AR-expressing OAC cell lines in vitro (Chapters 5 and 6)

**CHAPTER 2: FIBROBLASTS DERIVED FROM
OESOPHAGEAL ADENOCARCINOMA DIFFER IN DNA
METHYLATION PROFILE FROM NORMAL
OESOPHAGEAL FIBROBLASTS**

Eric Smith^{1,2,†,*}, Helen M. Palethorpe^{1,†}, Annette L. Hayden³, Joanne P. Young^{1,2}, Timothy J. Underwood^{3,‡}, Paul A. Drew^{1,4,‡}

¹Discipline of Surgical Specialities, Adelaide Medical School, Faculty of Health Sciences,
The University of Adelaide, SA 5000, Australia.

²Department of Haematology and Oncology, The Queen Elizabeth Hospital, Woodville, SA
5011, Australia.

³Cancer Sciences Unit, Somers Cancer Research Building, University of Southampton,
Southampton General Hospital, Tremona Road, Southampton, SO16 6YD, UK.

⁴School of Nursing and Midwifery, Flinders University, PO Box 2100, Adelaide, SA 5001,
Australia.

†These authors contributed equally.

‡These authors contributed equally.

Scientific Reports 2017; 7(1): 3368

Statement of Authorship

Title of Paper	Fibroblasts derived from oesophageal adenocarcinoma differ in DNA methylation profile from normal oesophageal fibroblasts
Publication Status	Published
Publication Details	Smith E, Palethorpe HM , Hayden AL, Young JP, Underwood TJ, Drew PA: Fibroblasts derived from oesophageal adenocarcinoma differ in DNA methylation profile from normal oesophageal fibroblasts . Submitted to <i>Scientific Reports</i> 2017.

Principal Author

Name of Principal Author (Candidate)	Helen M Palethorpe		
Contribution to the Paper	Conceived and designed the experiments, performed the experiments, analysed the data and wrote the manuscript.		
Overall percentage (%)	40%		
Certification:	This paper reports on original research I conducted during the period of my Higher Degree by Research candidature and is not subject to any obligations or contractual agreements with a third party that would constrain its inclusion in this thesis. I am the primary author of this paper.		
Signature		Date	08/12/16

Co-Author Contributions

By signing the Statement of Authorship, each author certifies that:

- i. the candidate's stated contribution to the publication is accurate (as detailed above);
- ii. permission is granted for the candidate to include the publication in the thesis; and
- iii. the sum of all co-author contributions is equal to 100% less the candidate's stated contribution.

Name of Co-Author	Eric Smith		
Contribution to the Paper	Conceived and designed the experiments, performed the experiments, analysed the data and wrote the manuscript.		
Signature		Date	08/12/16

Name of Co-Author	Annette L. Hayden		
Contribution to the Paper	Isolation and phenotyping of fibroblasts		
Signature		Date	11/05/17

Name of Co-Author	Joanne P. Young		
Contribution to the Paper	Provided critical evaluation of the manuscript		
Signature		Date	03/05/17

Name of Co-Author	Timothy J. Underwood		
Contribution to the Paper	Tissue collection, and provided critical evaluation of the manuscript		
Signature		Date	11/05/17

Name of Co-Author	Paul A. Drew		
Contribution to the Paper	Conceived and designed the experiments, analysed the data, wrote the manuscript.		
Signature		Date	08/12/16

SCIENTIFIC REPORTS

OPEN

Fibroblasts derived from oesophageal adenocarcinoma differ in DNA methylation profile from normal oesophageal fibroblasts

Eric Smith^{1,2}, Helen M. Palethorpe¹, Annette L. Hayden³, Joanne P. Young^{1,2}, Timothy J. Underwood³ & Paul A. Drew^{1,4}

Received: 29 November 2016
Accepted: 2 May 2017
Published online: 13 June 2017

Oesophageal adenocarcinoma (OAC) is increasing in incidence and has a poor prognosis. Tumour derived fibroblasts (TDFs) differ functionally from normal fibroblasts (NDFs), and play a pivotal role in cancer. Many of the differences persist through subculture. We measured the DNA methylation profiles of 10 TDFs from OAC with 12 NDF from normal oesophageal mucosa using Infinium HumanMethylation450 Beadchips and found they differed in multidimensional scaling analysis. We identified 4,856 differentially methylated CpGs (DMCs, adjusted $p < 0.01$ and absolute difference in average β -value > 0.15), of which 3,243 (66.8%) were hypomethylated in TDFs compared to NDFs. Hypermethylated DMCs were enriched at transcription start sites (TSSs) and in CpG islands, and depleted in transcriptional enhancers. Gene ontology analysis of genes with DMCs at TSSs revealed an enrichment of genes involved in development, morphogenesis, migration, adhesion, regulation of processes and response to stimuli. Alpha-smooth muscle actin (α -SMA) is a marker of activated fibroblasts and a poor prognostic indicator in OAC. Hypomethylated DMCs were observed at the TSS of transcript variant 2 of α -SMA, which correlated with an increase in α -SMA protein expression. These data suggest that DNA methylation may contribute to the maintenance of the TDF phenotype.

Oesophageal adenocarcinoma (OAC), which has increased rapidly in incidence in the Western world over recent decades¹, has a five year survival rate of about 15%². Most patients are unsuitable for treatment with curative intent. The major risk factors include gastro-oesophageal reflux disease and obesity, which lead to the premalignant condition, Barrett's oesophagus, the only described precursor lesion for OAC. A deeper understanding of the mechanisms that regulate the development and progression of OAC may lead to improvements in early diagnosis and treatment.

An emerging body of evidence demonstrates that fibroblasts play a significant role in the development and progression of solid tumours (reviewed in ref. 3). Within a cancer they are a phenotypically heterogeneous population of cells, distinct from the fibroblasts found in normal tissue, and are referred to as activated, cancer associated, or tumour derived fibroblasts (reviewed in ref. 4). These have been shown to promote tumour growth, facilitate tumour cell invasion, migration and metastasis, promote therapeutic drug resistance and act to prevent immune cell infiltration. Expression signatures that characterise these fibroblasts are associated with poor survival outcomes in many solid tumour types including OAC^{5–10}.

A number of studies have reported that many of the phenotypic characteristics of tumour derived fibroblasts (TDFs) are maintained in culture^{11,12}. This is consistent with at least some of the phenotypic alterations being maintained by epigenetic mechanisms such as DNA methylation^{13–15}, which involves the covalent addition of a methyl group to, most commonly, the cytosine residue of a cytosine-phosphate-guanine (CpG) dinucleotide.

¹Discipline of Surgical Specialities, Adelaide Medical School, Faculty of Health Sciences, The University of Adelaide, South Australia, 5000, Australia. ²Department of Haematology and Oncology, The Queen Elizabeth Hospital, Woodville, South Australia, 5011, Australia. ³Cancer Sciences Unit, Somers Cancer Research Building, University of Southampton, Southampton General Hospital, Tremona Road, Southampton, SO16 6YD, UK. ⁴School of Nursing and Midwifery, Flinders University, PO Box 2100, Adelaide, South Australia, 5001, Australia. Eric Smith and Helen M. Palethorpe contributed equally to this work. Timothy J. Underwood and Paul A. Drew jointly supervised this work. Correspondence and requests for materials should be addressed to E.S. (email: eric.smith@adelaide.edu.au)

Regions of the genome with a relatively high density of CpGs, CpG islands, and their flanking shores and shelves are associated with 60–70% of all human genes¹⁶. Methylation at the transcription start site (TSS) or within the body of genes is frequently associated with the silencing of transcription, and methylation of transcriptional enhancers may also affect gene transcription¹⁷. Aberrant methylation in intergenic regions has been associated with genomic instability or global silencing of large chromatin domains. Whilst genome-wide DNA methylation profiles of many tumour types, including OAC^{18–22}, have been ascertained, these studies have been conducted using whole tissue samples or cancer cell lines. There are reports of the genome-wide DNA methylation profiles of TDFs in breast¹³, gastric²³, colorectal¹⁴, and non-small cell lung carcinoma¹⁵, but none in OAC.

The aim of this study was to compare the genome-wide DNA methylation profiles of low-passage primary TDFs from patients with OAC to fibroblasts derived from macroscopically normal oesophageal squamous mucosa. We show that the TDFs have a DNA methylation profile which distinguishes them from most NDFs. Differentially methylated CpGs were observed at TSSs of genes which have a known role in cancer development and progression, suggesting that the TDF phenotype may be regulated, at least in part, by epigenetic mechanisms.

Results

Tumour derived fibroblasts were aberrantly methylated. Twenty-two primary fibroblast lines were established from resected specimens of 16 patients with oesophageal cancer (Supplementary Table S1). There were 10 TDFs and 12 NDFs, which included six patient matched fibroblast pairs. The median age of the patients was 65 years (range 57 to 82). There was not a significant difference in the age of the patients from whom the TDFs and NDFs were established. There were 13 males and three females. Five patients were treated with surgery alone, and 11 received a combination of neoadjuvant chemotherapy and surgery.

The genome-wide DNA methylation profile of the fibroblasts was measured using the Infinium HumanMethylation450 Beadchip. Unsupervised pairwise multidimensional scaling was performed using the β -values for all 408,329 probes included in the analysis (Fig. 1a). The distribution of the TDFs differed from NDFs. The NDFs formed a tight cluster, with two outliers. In contrast, the TDFs were more widely dispersed. The coefficient of variation (CV) for the median β -values of each fibroblast was 7.6% for the NDFs and 10.2% for the TDFs, but the variance of median β -values of each fibroblast was not significantly different ($p = 0.1836$). Comparing methylation in the TDFs and NDFs, there were 4,856 DMCs, of which 3,243 (66.8%) were hypomethylated and 1,613 (33.2%) hypermethylated. Hierarchical clustering of these 4,856 DMCs revealed that the fibroblasts formed two major clusters, with 10 of the 12 NDF clustering together, the remaining two NDF (N.181 and N.217) within the TDF cluster (Fig. 1b).

Differentially methylated CpGs and functional genomic regions. We analysed the distribution of the DMCs between the functional genomic regions. The probes were allocated as TSS1500, TSS200, 5'UTR, 1st exon, gene body or 3'UTR according to the Illumina probe annotation²⁴. Many probes are annotated to more than one genomic region since a locus may be within more than one gene, or more than one variant of a gene, so that the sum of the loci in genomic locations is greater than the number of probes analysed. Probes which were not annotated to a gene region were categorised as intergenic. The results in Table 1 show the proportion of all CpGs analysed and DMCs in each of these regions. There was a significant difference in the distribution of the DMCs across the functional genomic locations compared to that of all the cytosines analysed (Chi square test for proportions: $p < 0.0001$). The most significant differences were a depletion around the TSS, particularly the TSS200 (3.6% of DMCs compared to 11.6% of all analysed) and the first exon (2.2% v 7.2%), and an enrichment in the intergenic region (32.0% v 19.5%). Overall there were significantly fewer differentially methylated cytosines associated with the promoter region (defined as TSS1500, TSS200, 5'UTR and 1st Exon; 27.9% versus 46.1%). There were no significant differences in the distribution of DMCs within the annotated microRNAs or lncRNAs. The proportion of hypomethylated and hypermethylated DMCs differed between the gene regions (Table 2). Hypermethylated DMCs were more frequent in the TSS200 and 3'UTR, and less in the gene body and intergenic regions.

Differentially methylated CpGs and CpG islands. CpG islands are important genomic regulatory elements that are defined by a high density of CpGs relative to entire genome. The regions 2 kilobases either side of an island are defined as shores, the 2 kilobase regions flanking the shores are defined as shelves²⁴, and here we define the remainder of the genome as open seas. The distribution of DMCs in the context of CpG islands is shown in Table 1. Of all the CpGs for analysis, 65.7% were in islands, shores or shelves, compared to 44.3% of the DMCs. Within the CpG islands DMCs were significantly depleted (9.3% v 32.7% of all analysed cytosines), but there was no significant difference in the distribution of DMCs in the shores or shelves. There was a significantly greater proportion of DMCs in the open seas (55.7% v 34.3%). There was significant enrichment of hypermethylated DMCs in CpG islands and adjacent shores, and depletion in shelves and open seas (Table 2).

We then determined if there were a difference in the distribution of DMCs between CpG islands that overlap annotated genes and those located in the intergenic regions. An island was classified as intragenic if any of its CpGs were in an annotated gene region (that is, within the TSS1500 to 3'UTR regions). Of the DMCs within CpG islands, a significantly greater proportion were in islands in the intergenic regions (34.2% v 13.8% of all CpGs, odds ratio (OR) 3.276, 95% confidence interval (CI) 2.696–3.981, $p < 0.0001$), and lesser in islands which overlapped genes (31.8% v 70.0%, $p < 0.0001$). The proportion of hypermethylated DMCs within CpG islands did not significantly vary between intergenic and intragenic CpG islands (62.1% and 54.8% respectively, OR 1.389, 95% CI 0.9096–1.998, $p = 0.1647$).

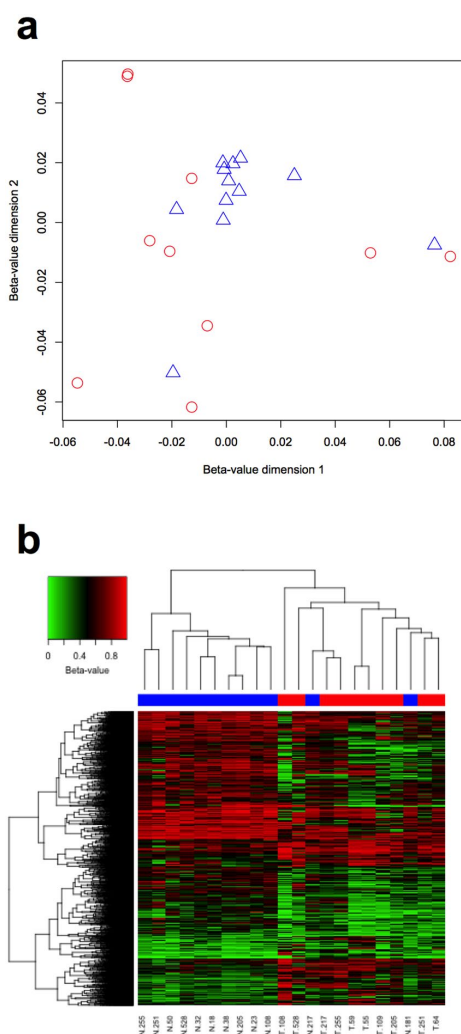


Figure 1. Genome-wide DNA methylation profiles of TDFs and NDFs. **(a)** Multidimensional scaling performed using the β -values for all 408,329 probes for NDFs (blue triangles) and TDFs (red circles). **(b)** Hierarchical clustering using the 4,856 DMC for NDFs (blue) and TDFs (red).

Differentially methylated CpGs and enhancer regions. Next, we investigated the distribution of DMCs between enhancer and non-enhancer regions. Of the total of 408,329 CpGs for analysis, 90,996 (22.3%) were in enhancer regions. The DMCs were significantly enriched in enhancer (46.3% of DMCs compared to 22.3% of all analysed, $p < 0.0001$) compared to non-enhancer regions (53.7% v 77.7%) (Table 1). The proportion of hypermethylated DMCs was significantly lower in enhancer compared to non-enhancer regions (Table 2; $p < 0.0001$). Further analysis of the DMCs in enhancers revealed that they were enriched in the intergenic compared to intragenic regions (57.9% versus 40.1% respectively, OR 2.058, 95% CI 1.825–2.320, $p < 0.0001$). The proportion of hypermethylated DMCs in enhancers was greater in those in intragenic compared to intergenic regions (31.9% and 23.7% respectively, OR 1.507, 95% CI 1.248–1.919, $p < 0.0001$). The proportion of hypermethylated DMCs in non-enhancer regions was greater in the intragenic compared to intergenic regions (39.1% and 32.9% respectively, OR 1.310, 95% CI 1.093–1.570, $p = 0.0040$).

Methylation of ACTA2 correlated with decreased α -SMA protein expression. To ascertain the potential functional significance of the observed DMC, we conducted gene ontology enrichment analyses using genes that had one or more DMCs located within 1,500 bases of their TSS. Of the 4,856 DMCs, 1,354 (27.9%) were located within 1,500 bases of a TSS, representing 1,145 unique Entrez Gene IDs. Of these, 743 (64.9%) were hypomethylated in TDFs, and 402 (35.1%) were hypermethylated. Hypermethylated DMCs were observed

	DMC (%)	All CpGs Analysed (%)	OR (95% CI)	p-value
Gene Regions				
Total ^a	5,302	479,691		
TSS1500	682 (12.9%)	73,530 (15.3%)	0.8137 (0.7505–0.8822)	<0.0001
TSS200	192 (3.6%)	55,640 (11.6%)	0.2839 (0.2457–0.3280)	<0.0001
5'UTR	488 (9.2%)	57,408 (12.0%)	0.7435 (0.6771–0.8164)	<0.0001
1 st Exon	117 (2.2%)	34,391 (7.2%)	0.2898 (0.2415–0.3482)	<0.0001
Gene body	1,954 (36.9%)	148,809 (31.0%)	1.302 (1.231–1.377)	<0.0001
3'UTR	173 (3.3%)	16,571 (3.5%)	0.9421 (0.8089–1.097)	0.4652
Intragenic	1,686 (32.0%)	93,342 (19.5%)	1.947 (1.837–2.064)	<0.0001
microRNA	33 (0.6%)	2,331 (0.5%)	0.9995 (0.7114–1.404)	>0.999
lncRNA	4 (0.08%)	429 (0.01%)	0.658 (0.2562–1.675)	0.5835
CpG Island Regions				
Total	4,856	408,329		
CGI	453 (9.3%)	133,415 (32.7%)	0.2093 (0.1900–0.2306)	<0.0001
Shores	1,208 (24.9%)	97,243 (23.8%)	1.060 (0.9929–1.132)	0.0836
Shelves	488 (10.0%)	37,691 (9.2%)	1.100 (1.001–1.209)	0.0502
Open sea	2,707 (55.7%)	139,980 (34.3%)	2.443 (2.307–2.586)	<0.0001
Enhancer Regions				
Non-enhancer	2,608 (53.7%)	317,333 (77.7%)		
Enhancer	2,248 (46.3%)	90,996 (22.3%)	3.057 (2.888–3.246)	<0.0001

Table 1. The proportion of all CpGs analysed and differentially methylated cytosines (DMC) in each annotated region. ^aProbes may annotate to more than one gene region.

about the TSS of genes predominantly involved in development, morphogenesis and migration, whilst genes with hypomethylated DMCs were involved in regulation of processes, response to stimuli, development and adhesion (Supplementary Table S2).

A gene which featured in several enriched biological processes was ACTA2. Multiple alternatively spliced variants of ACTA2 have been reported, and they each encode the same protein, alpha-smooth muscle actin (α -SMA). Variant 2 varies from the other variants by an alternate TSS (Fig. 2a). We observed that the region about the TSS for transcript variant 2 was hypomethylated in TDFs compared to NDFs (Fig. 2a and b). In contrast, the β -values for the probes about the TSS of variant 1 and 3 varied little between TDFs and NDFs, and were relatively low (β -value < 0.15). Sufficient material was available from three patient matched fibroblast pairs to analyse the expression of α -SMA by western immunoblot. The results confirmed that α -SMA was elevated in these TDFs compared to the NDFs (Fig. 2c and d). Methylation about the TSS of variant 2, but not variant 1 and 3, inversely correlated with α -SMA protein expression (Fig. 2e), suggesting that the low α -SMA expression observed in cultured oesophageal NDFs was associated with DNA methylation about the TSS of variant 2.

Discussion

This is the first study to compare the genome-wide DNA methylation profiles of oesophageal NDFs to OAC TDFs using the high resolution Infinium HumanMethylation450 BeadChip. Multidimensional scaling analysis of all probes analysed showed that, with respect to DNA methylation, the NDFs clustered tightly apart from two outliers, whereas the TDFs were markedly heterogeneous. Hierarchical clustering using the 4,856 DMCs demonstrated that the TDFs grouped differently to the NDFs. Detailed examination of the genomic locations of the DMCs revealed significant regional variation in DNA methylation between the two fibroblast groups. In TDFs, the DMCs were depleted about the transcription start sites and in CpG islands and enriched in gene bodies, open seas and in enhancers. The DMCs were observed in the TSSs of genes which have a known role in cancer development and progression. Methylation was significantly decreased at the TSS of variant 2 of α -SMA, which correlated with an increase in α -SMA protein expression.

Previous studies have investigated DNA methylation profiles of TDFs in breast¹³, gastric²³, colorectal¹⁴, and non-small cell lung carcinoma¹⁵. Consistent with our findings, these studies demonstrated differences in DNA methylation between TDF and NDFs, with general DNA hypomethylation and concomitant focal hypermethylation observed in TDFs compared to NDFs. Only one used the Infinium HumanMethylation450 BeadChip¹⁵, and reported a strikingly similar distribution of DMCs across the functional genomic regions, including the depletion about TSSs and CpG islands, and the enrichment in gene bodies and open seas. In addition, we report the novel observation of differential methylation in transcriptional enhancers. Multiple enhancers may cooperate to finely tune the expression of a single transcript, and integrate extracellular signals with intracellular cell fate information to generate cell type-specific transcriptional responses²⁵. Together, these results suggest that differences in DNA methylation, through their role in regulation of gene expression, contribute to the alterations in fibroblast phenotypes observed in cancer.

The results from the multidimensional scaling of all CpGs analysed and the hierarchical clustering of DMCs showed that the DNA methylation profiles of the TDFs were markedly more heterogeneous than the NDFs. The primary function of fibroblasts is to establish, maintain, and modify connective tissue²⁶. They are a heterogeneous

	Hypermethylated (%)	Hypomethylated (%)	Total	OR (95% CI)	p-value
Total	1,613 (33.2%)	3,243 (66.8%)	4,856		
Gene Regions					
TSS1500	237 (34.8%)	445 (65.2%)	682	1.083 (0.9133–1.284)	0.3823
TSS200	86 (44.8%)	106 (55.2%)	192	16.78 (13.59–20.72)	<0.0001
5'UTR	166 (34.0%)	322 (66.0%)	488	1.041 (0.8540–1.268)	0.7302
1 st Exon	39 (33.3%)	78 (66.7%)	117	1.005 (0.6813–1.484)	0.9424
Gene body	705 (36.1%)	1,249 (63.9%)	1,954	0.7294 (0.6510–0.8173)	<0.0001
3'UTR	77 (44.5%)	96 (55.5%)	173	1.643 (1.210–2.232)	0.0018
Intragenic	468 (27.6%)	1,228 (72.4%)	1,696	0.6707 (0.5896–0.7629)	<0.0001
CpG Island Regions					
CGI	270 (59.6%)	183 (40.3%)	453	1.954 (1.790–2.134)	<0.0001
Shores	489 (40.5%)	719 (59.5%)	1,208	1.314 (1.208–1.429)	<0.0001
Shelves	138 (28.3%)	350 (71.7%)	488	0.8374 (0.7227–0.9703)	<0.0001
Open sea	716 (26.4%)	1,991 (73.6%)	2,707	0.6337 (0.5848–0.6866)	<0.0001
Enhancer Regions					
Non-enhancer	976 (37.4%)	1,632 (62.6%)	2,608		
Enhancer	637 (28.3%)	1,611 (71.7%)	2,248	0.6612 (0.5856–0.7464)	<0.0001

Table 2. The percentage of hypermethylated or hypomethylated differentially methylated cytosines (DMC) in each of the annotated region.

population of cells, particularly in disease. The origin of TDFs can be from resident fibroblasts, as well as infiltrating cells, including epithelial, endothelial, and bone marrow-derived mesenchymal stem cells²⁷ and fibrocytes^{15, 28}. They can exist in differing states of activation and functional potential^{29–31}. It is therefore highly likely that primary cultures of TDFs contain differing proportions of fibroblast subpopulations. The heterogeneity of their DNA methylation profiles most likely reflects the heterogeneity of their origins and functions in cancer.

Expression of α -SMA is commonly used as a marker for TDFs, and is associated with poor prognosis in a range of cancers, including OAC^{10, 31}, oesophageal squamous cell carcinoma³², colorectal⁶, breast³³, and head and neck cancers³⁴. In humans, the α -SMA protein is encoded by the ACTA2 gene, and transcript variant 2 varies from 1 and 3 by an alternate TSS, with the entire first exon of each variant being a 5'UTR. We observed the novel finding that DNA methylation about the TSS of variant 2 inversely correlated with α -SMA protein expression. This raises the possibility that methylation of this region may be of functional significance in repressing α -SMA expression in oesophageal fibroblasts. In rat lung fibroblasts, myofibroblasts, and alveolar epithelial type cells, methylation of the ACTA2 promoter inversely correlated with expression³⁵. In addition, inhibition of DNMT activity led to significant induction of α -SMA expression, while ectopic expression of DNMTs suppressed its expression, suggesting that DNA methylation plays a key role in the regulation of α -SMA gene expression during myofibroblast differentiation³⁵. Further experiments confirming the functional significance of the observed methylation are warranted, considering the prognostic significance of α -SMA expression.

It is possible that neoadjuvant chemotherapy might have altered the DNA methylation profiles in either of the normal or cancer associated fibroblasts. To the best of our knowledge, there are no studies that demonstrate this in fibroblasts, although several reports suggest that this may occur in cancer cells^{36, 37}. Future studies to compare the DNA methylation of fibroblasts before and after chemotherapy would require the harvesting of sufficient fibroblasts from the small amount of tissue obtainable by biopsy.

In conclusion, we compared the genome-wide DNA methylation profiles of 10 TDFs from oesophageal adenocarcinoma tumour tissues with 12 NDFs from macroscopically normal oesophageal mucosa using Infinium HumanMethylation450 Beadchips. The genome-wide DNA methylation profile of TDFs differed significantly from that of NDFs. The focal distribution of the DMCs about the transcription start sites and within CpG islands and transcriptional enhancers may, by the regulation of gene expression, contribute to the establishment and maintenance of the TDF phenotype *in vitro* and *in vivo*.

Methods

Research Ethics. All methods were carried out in accordance with relevant guidelines and regulations.

All experimental protocols were approved by the Southampton and South West Hampshire Research Ethics Committee (09/H0504/66). Informed consent was obtained from all subjects.

Primary human oesophageal fibroblasts. Primary human oesophageal fibroblast lines were established as described previously³⁸. Briefly, macroscopically normal squamous mucosa and tumour tissues were sampled from resection specimens and transported in Hank's balanced salt solution (Invitrogen, Carlsbad, CA, USA). Tissues were washed twice in Dulbecco's phosphate buffered saline (DPBS; Invitrogen), placed in fresh DPBS supplemented with 250 ng/ml amphotericin B (Invitrogen), and diced into 2 mm³ pieces. Single fragments of tissue were then placed into individual wells of six-well plates, and cultured at 37 °C in a humidified atmosphere with 10% CO₂. The fibroblast culture medium was composed of Dulbecco's modified Eagle's medium (Invitrogen) supplemented with 10% (v/v) fetal bovine serum (Autogen Bioclear UK Ltd, Wiltshire, UK or Sigma-Aldrich, St Louis, MO, USA), 100 units/ml penicillin, 100 µg/ml streptomycin, 250 ng/ml amphotericin B and 292 µg/ml

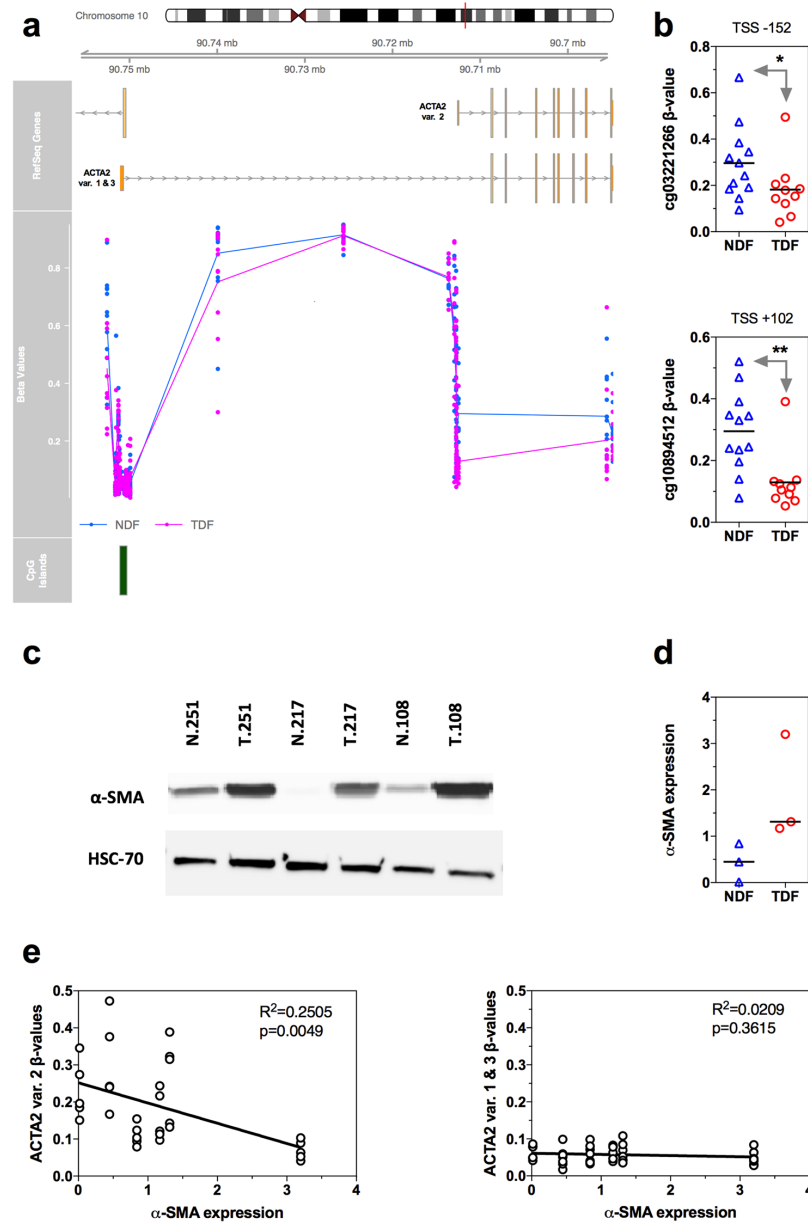


Figure 2. DNA methylation and expression of α -SMA (ACTA2). (a) The relative location of ACTA2 splice variants, individual β -values for all NDFs (blue circles) and TDFs (pink circles), and CpG islands. The lines for the β -values represent the average β -value for the NDF and TDF groups. (b) The β -values for all individual NDF and TDF samples for the probes cg03221266 and cg10894512 located at positions -152 bp or $+102$ bp respectively of the TSS of ACTA2 variant 2. *Benjamini-Hochberg adjusted $p = 8.55 \times 10^{-9}$, **Benjamini-Hochberg adjusted $p = 2.46 \times 10^{-19}$. (c) Western immunoblot for α -SMA and the loading control HSC-70 for the three available patient matched pairs of NDFs (N.251, N.217 and N.108) and TDFs (T.251, T.217 and T.108). (d) Quantification of α -SMA protein expression for the three patient matched pairs. (e) Correlation between α -SMA protein expression and β -values for the probes about ACTA2 TSS of the splice variants for the three patient matched pairs.

L-glutamine (Invitrogen). The primary fibroblasts were expanded by subculturing in fibroblast medium, on tissue culture treated plastic, at 37 °C in a humidified atmosphere with 5% CO₂. The phenotype of *ex-vivo* fibroblasts was confirmed as vimentin-positive, cytokeratin-negative, CD31-negative and desmin-negative, as described previously³⁸.

Genome-wide DNA methylation profiling. Genomic DNA was isolated from the primary fibroblasts at the earliest subculture that sufficient cells were available. The DNA was isolated using either the DNeasy Blood and Tissue Kit (Qiagen, Hilden, Germany) or Trizol (Invitrogen), and concentrated, if required, using the phenol chloroform ethanol precipitation method. The DNA (500–2000 ng) was bisulphite modified with the EZ DNA Methylation-Gold Kit (Zymo Research, Irvine, CA, USA), as described previously^{39,40}. The bisulphite-modified DNA was hybridized onto Infinium HumanMethylation450 BeadChips following the Illumina Infinium HD Methylation protocol, and scanned using an Illumina HiScan SQ scanner (Illumina, San Diego, CA, USA), as described previously⁴¹.

Raw fluorescence intensity values were normalised using the GenomeStudio Methylation Module (v1.8.5; Illumina), with background subtraction and normalisation to internal controls. Normalised intensities were used to calculate β -values. The β -value represents the percentage of the cytosines at that locus which were methylated, and ranges from 0 (no methylation) to 1 (complete methylation). The average β -value at each locus was calculated for the NDF and TDF groups.

Probes were excluded from the analysis if they did not target a cytosine within a CpG, or if they were known to align to a single nucleotide polymorphism (SNP) or to multiple locations⁴², or if its target cytosine was two or fewer nucleotides from a known SNP for which the SNP had a minor allele frequency above 0.05⁴³, or if the detection p value, which defines the chance that the target signal was not distinguishable from background, was greater than 0.01 in any sample, or if the bead count was less than three. Probes on the X and Y chromosomes were also excluded.

Differentially methylated CpGs (DMCs) between the TDF and NDF groups were determined using the Illumina Custom Model in the GenomeStudio Methylation Module with false discovery rate (FDR) adjustment. The software calculates a p value for the significance of the difference in β -values between the groups for each locus, corrected for multiple testing using the Benjamini-Hochberg FDR adjustment. A CpG was considered to be differentially methylated if $p < 0.01$ and the absolute difference in the average β -values of each group was >0.15 . A DMC was defined to be hypermethylated if the average β -value for the TDFs was greater than the NDFs, and hypomethylated if the average β -value for the TDFs was less than the NDFs. The allocation of DMCs into gene regions, CpG islands, and enhancer regions was determined from the Illumina GenomeStudio probe annotation²⁴.

Gene ontology enrichment analysis of differentially methylated CpGs. The DMCs were aligned to the TSS of the nearest transcript using the FDb. Infinium Methylation. hg 19 annotation package (v2.2.0) in R (v3.3.0). Transcripts with one or more DMCs located within 1,500 bases up- or down-stream of its TSS were selected. The transcripts were converted to Entrez Gene IDs, and gene ontology enrichment analysis on all, hypomethylated, and hypermethylated DMC was performed using the clusterProfiler R package (v2.4.3)⁴⁴.

Western immunoblot for alpha-smooth muscle actin (α -SMA). Measurement of specific protein expression by western immunoblots was performed as previously described¹⁰. Briefly, adherent fibroblasts were washed with DPBS, detached by trypsin digestion and pelleted by centrifugation. Pelleted cells were lysed with 50 μ l RIPA buffer (0.75 M NaCl, 5% NP40, 2.5% deoxycholic acid, 0.5% SDS, 0.25 M Tris, pH 8.0) for 15 minutes at 4 °C, and clarified by centrifugation at $8000 \times g$ for 5 min. Protein was quantified by Bradford protein assay, and 20 μ g was resolved using sodium dodecyl sulfate-polyacrylamide gel electrophoresis, transferred to Hybond-ECL membranes (GE Healthcare Life Sciences, Buckinghamshire, UK). Membranes were immunostained using mouse monoclonal anti- α -SMA (M085129-2, Dako) and mouse monoclonal anti-HSC-70 (sc-7298, Santa Cruz, USA). Immunoreactivity was detected using horseradish peroxidase-labelled secondary antibody, and visualised with SuperSignal West Pico Chemiluminescent Substrate (Thermo Scientific Pierce, Waltham, MA, USA) using a ChemiDoc-It Imager (UVP, Upland, CA, USA). The intensity of the α -SMA and the HSC-70 bands were determined using ImageJ (v1.47). The α -SMA expression was calculated as the ratio of the intensity of α -SMA divided by the intensity of HSC-70.

Statistical analysis. Pairwise multidimensional scaling was conducted using the LIMMA R package (v3.18.5). The equality of the fibroblast group variances was compared using the median centred Levene test in the car R package (v2.1-2). The proportion of DMCs in gene regions, CpG islands, or enhancer regions and the proportion of hypomethylated and hypermethylated DMC in each of these regions was analysed with the Chi-squared test with Yates correction, using Prism 6.0 h for Macintosh (GraphPad Software, San Diego, CA, USA). A two-tailed $p < 0.05$ was considered statistically significant.

References

1. Esophageal cancer: epidemiology, pathogenesis and prevention. *Nat Clin Pract Gastroenterol Hepatol* 5, 517–526, doi:[10.1038/npgasthep1223](https://doi.org/10.1038/npgasthep1223) (2008).
2. Lagergren, J. & Mattsson, F. Diverging trends in recent population-based survival rates in oesophageal and gastric cancer. *PLoS One* 7, e41352, doi:[10.1371/journal.pone.0041352](https://doi.org/10.1371/journal.pone.0041352) (2012).
3. Ohlund, D., Elyada, E. & Tuveson, D. Fibroblast heterogeneity in the cancer wound. *J Exp Med* 211, 1503–1523, doi:[10.1084/jem.20140692](https://doi.org/10.1084/jem.20140692) (2014).
4. Hu, M. & Polyak, K. Microenvironmental regulation of cancer development. *Curr Opin Genet Dev* 18, 27–34, doi:[10.1016/j.gde.2007.12.006](https://doi.org/10.1016/j.gde.2007.12.006) (2008).

5. Surowiak, P. *et al.* Occurrence of stromal myofibroblasts in the invasive ductal breast cancer tissue is an unfavourable prognostic factor. *Anticancer Res* **27**, 2917–2924 (2007).
6. Tsujino, T. *et al.* Stromal myofibroblasts predict disease recurrence for colorectal cancer. *Clin Cancer Res* **13**, 2082–2090, doi:10.1158/1078-0432.CCR-06-2191 (2007).
7. Saadi, A. *et al.* Stromal genes discriminate preinvasive from invasive disease, predict outcome, and highlight inflammatory pathways in digestive cancers. *Proc Natl Acad Sci USA* **107**, 2177–2182, doi:10.1073/pnas.0909797107 (2010).
8. Wu, Y. *et al.* Comprehensive genomic meta-analysis identifies intra-tumoural stroma as a predictor of survival in patients with gastric cancer. *Gut* **62**, 1100–1111, doi:10.1136/gutjnl-2011-301373 (2013).
9. De Monte, L. *et al.* Intratumor T helper type 2 cell infiltrate correlates with cancer-associated fibroblast thymic stromal lymphopoietin production and reduced survival in pancreatic cancer. *J Exp Med* **208**, 469–478, doi:10.1084/jem.20101876 (2011).
10. Underwood, T. J. *et al.* Cancer-associated fibroblasts predict poor outcome and promote periostin-dependent invasion in oesophageal adenocarcinoma. *J Pathol* **235**, 466–477, doi:10.1002/path.4467 (2015).
11. Madar, S., Goldstein, I. & Rotter, V. 'Cancer associated fibroblasts'—more than meets the eye. *Trends Mol Med* **19**, 447–453, doi:10.1016/j.molmed.2013.05.004 (2013).
12. Leach, D. A. *et al.* Stromal androgen receptor regulates the composition of the microenvironment to influence prostate cancer outcome. *Oncotarget* **6**, 16135–16150, doi:10.18632/oncotarget.3873 (2015).
13. Hu, M. *et al.* Distinct epigenetic changes in the stromal cells of breast cancers. *Nat Genet* **37**, 899–905, doi:10.1038/ng1596 (2005).
14. Mrazek, A. A. *et al.* Colorectal Cancer-Associated Fibroblasts are Genotypically Distinct. *Curr Cancer Ther Rev* **10**, 97–218, doi:10.2174/157339471002141124123103 (2014).
15. Vizoso, M. *et al.* Aberrant DNA methylation in non-small cell lung cancer-associated fibroblasts. *Carcinogenesis* **36**, 1453–1463, doi:10.1093/carcin/bgv146 (2015).
16. Illingworth, R. S. & Bird, A. P. CpG islands—'a rough guide'. *FEBS Lett* **583**, 1713–1720, doi:10.1016/j.febslet.2009.04.012 (2009).
17. Aran, D., Sabato, S. & Hellman, A. DNA methylation of distal regulatory sites characterizes dysregulation of cancer genes. *Genome Biol* **14**, R21, doi:10.1186/gb-2013-14-3-r21 (2013).
18. Gaur, P., Hunt, C. R. & Pandita, T. K. Emerging therapeutic targets in esophageal adenocarcinoma. *Oncotarget* **7**, 48644–48655, doi:10.18632/oncotarget.8777 (2016).
19. Zhai, R. *et al.* Genome-wide DNA methylation profiling of cell-free serum DNA in esophageal adenocarcinoma and Barrett esophagus. *Neoplasia* **14**, 29–33 (2012).
20. Krause, L. *et al.* Identification of the CIMP-like subtype and aberrant methylation of members of the chromosomal segregation and spindle assembly pathways in esophageal adenocarcinoma. *Carcinogenesis* **37**, 356–365, doi:10.1093/carcin/bgw018 (2016).
21. Kaz, A. M. *et al.* Global DNA methylation patterns in Barrett's esophagus, dysplastic Barrett's, and esophageal adenocarcinoma are associated with BMI, gender, and tobacco use. *Clin Epigenetics* **8**, 111, doi:10.1186/s13148-016-0273-7 (2016).
22. Kaz, A. M. *et al.* DNA methylation profiling in Barrett's esophagus and esophageal adenocarcinoma reveals unique methylation signatures and molecular subclasses. *Epigenetics* **6**, 1403–1412, doi:10.4161/epi.6.12.18199 (2011).
23. Jiang, L. *et al.* Global hypomethylation of genomic DNA in cancer-associated myofibroblasts. *Cancer Res* **68**, 9900–9908, doi:10.1158/0008-5472.CAN-08-1319 (2008).
24. Bibikova, M. *et al.* High density DNA methylation array with single CpG site resolution. *Genomics* **98**, 288–295, doi:10.1016/j.ygeno.2011.07.007 (2011).
25. Sur, I. & Taipale, J. The role of enhancers in cancer. *Nat Rev Cancer* **16**, 483–493, doi:10.1038/nrc.2016.62 (2016).
26. Sorrell, J. M. & Caplan, A. I. Fibroblasts—a diverse population at the center of it all. *Int Rev Cell Mol Biol* **276**, 161–214, doi:10.1016/S1937-6448(09)76004-6 (2009).
27. Sorrell, J. M., Baber, M. A. & Caplan, A. I. Influence of adult mesenchymal stem cells on *in vitro* vascular formation. *Tissue Eng Part A* **15**, 1751–1761, doi:10.1089/ten.tea.2008.0254 (2009).
28. Chesney, J., Bacher, M., Bender, A. & Bucala, R. The peripheral blood fibrocyte is a potent antigen-presenting cell capable of priming naive T cells *in situ*. *Proc Natl Acad Sci USA* **94**, 6307–6312 (1997).
29. Augsten, M. Cancer-associated fibroblasts as another polarized cell type of the tumor microenvironment. *Front Oncol* **4**, 62, doi:10.3389/fonc.2014.00062 (2014).
30. Herrera, M. *et al.* Functional heterogeneity of cancer-associated fibroblasts from human colon tumors shows specific prognostic gene expression signature. *Clin Cancer Res* **19**, 5914–5926, doi:10.1158/1078-0432.CCR-13-0694 (2013).
31. Hanley, C. J. *et al.* A subset of myofibroblastic cancer-associated fibroblasts regulate collagen fiber elongation, which is prognostic in multiple cancers. *Oncotarget* **7**, 6159–6174, doi:10.18632/oncotarget.6740 (2016).
32. Cheng, Y. *et al.* Cancer-associated fibroblasts are associated with poor prognosis in esophageal squamous cell carcinoma after surgery. *Int J Clin Exp Med* **8**, 1896–1903 (2015).
33. Yamashita, M. *et al.* Role of stromal myofibroblasts in invasive breast cancer: stromal expression of alpha-smooth muscle actin correlates with worse clinical outcome. *Breast Cancer* **19**, 170–176, doi:10.1007/s12282-010-0234-5 (2012).
34. Marsh, D. *et al.* Stromal features are predictive of disease mortality in oral cancer patients. *J Pathol* **223**, 470–481, doi:10.1002/path.2830 (2011).
35. Hu, B., Gharraee-Kermani, M., Wu, Z. & Phan, S. H. Epigenetic regulation of myofibroblast differentiation by DNA methylation. *Am J Pathol* **177**, 21–28, doi:10.2353/ajpath.2010.090999 (2010).
36. Toyota, M. *et al.* Cancer epigenomics: implications of DNA methylation in personalized cancer therapy. *Cancer Sci* **100**, 787–791, doi:10.1111/j.1349-7006.2009.01095.x (2009).
37. Avraham, A. *et al.* Serum DNA methylation for monitoring response to neoadjuvant chemotherapy in breast cancer patients. *International journal of cancer* **131**, E1166–1172, doi:10.1002/ijc.27526 (2012).
38. Underwood, T. J. *et al.* A comparison of primary oesophageal squamous epithelial cells with HET-1A in organotypic culture. *Biol Cell* **102**, 635–644, doi:10.1042/BC20100071 (2010).
39. Smith, E., Ruszkiewicz, A. R., Jamieson, G. G. & Drew, P. A. IGFBP7 is associated with poor prognosis in oesophageal adenocarcinoma and is regulated by promoter DNA methylation. *Br J Cancer* **110**, 775–782, doi:10.1038/bjc.2013.783 (2014).
40. Smith, E. *et al.* The effect of long-term control of reflux by fundoplication on aberrant deoxyribonucleic acid methylation in patients with Barrett esophagus. *Ann Surg* **252**, 63–69, doi:10.1097/SLA.0b013e3181e4181c (2010).
41. Lim, Y. Y. *et al.* Epigenetic modulation of the miR-200 family is associated with transition to a breast cancer stem-cell-like state. *J Cell Sci* **126**, 2256–2266, doi:10.1242/jcs.122275 (2013).
42. Nordlund, J. *et al.* Genome-wide signatures of differential DNA methylation in pediatric acute lymphoblastic leukemia. *Genome Biol* **14**, r105, doi:10.1186/gb-2013-14-9-r105 (2013).
43. Chen, Y. A. *et al.* Discovery of cross-reactive probes and polymorphic CpGs in the Illumina Infinium HumanMethylation450 microarray. *Epigenetics* **8**, 203–209, doi:10.4161/epi.23470 (2013).
44. Yu, G., Wang, L. G., Han, Y. & He, Q. Y. ClusterProfiler: an R package for comparing biological themes among gene clusters. *OMICS* **16**, 284–287, doi:10.1089/omi.2011.0118 (2012).

Acknowledgements

T.J.U. is funded by a Clinician Scientist Award from the UK Medical Research Council. We thank the staff in the University of Southampton ECMC Tissue Bank, in particular Kathy Potter.

Author Contributions

E.S., P.A.D. and T.J.U. conceived and directed the project. E.S., H.M.P., A.H., J.P.Y., P.A.D. and T.J.U. wrote the manuscript. Each author listed on this manuscript has seen and approved this submission and takes full responsibility for the manuscript.

Additional Information

Supplementary information accompanies this paper at doi:[10.1038/s41598-017-03501-6](https://doi.org/10.1038/s41598-017-03501-6)

Competing Interests: The authors declare that they have no competing interests.

Publisher's note: Springer Nature remains neutral with regard to jurisdictional claims in published maps and institutional affiliations.



Open Access This article is licensed under a Creative Commons Attribution 4.0 International License, which permits use, sharing, adaptation, distribution and reproduction in any medium or format, as long as you give appropriate credit to the original author(s) and the source, provide a link to the Creative Commons license, and indicate if changes were made. The images or other third party material in this article are included in the article's Creative Commons license, unless indicated otherwise in a credit line to the material. If material is not included in the article's Creative Commons license and your intended use is not permitted by statutory regulation or exceeds the permitted use, you will need to obtain permission directly from the copyright holder. To view a copy of this license, visit <http://creativecommons.org/licenses/by/4.0/>.

© The Author(s) 2017

Refer to Appendix A for Supplementary Tables 1 and 2.

**CHAPTER 3: STROMAL ANDROGEN RECEPTOR
REGULATES THE COMPOSITION OF THE
MICROENVIRONMENT TO INFLUENCE PROSTATE
CANCER OUTCOME**

Damien A. Leach¹, Eleanor F. Need¹, Roxanne Toivanen², Andrew P. Trotta¹, Helen M. Palethorpe¹, David J. Tamblyn³, Tina Kopsaftis³, Georgina M. England⁴, Eric Smith¹, Paul A. Drew^{1,5}, Carole B. Pinnock³, Peng Lee⁶, Jeff Holst^{7,8}, Gail P. Risbridger², Samarth Chopra^{3,9}, Donald B. DeFranco¹⁰, Renea A. Taylor^{2,11} & Grant Buchanan¹

¹The Basil Hetzel Institute for Translational Health Research, University of Adelaide, SA, Australia;

²Department of Anatomy and Development, Monash University, VIC, Australia;

³Urology Unit, Repatriation General Hospital, SA, Australia;

⁴Department of Surgical Pathology, SA Pathology at Flinders Medical Centre, Bedford Park, SA, Australia;

⁵School of Nursing and Midwifery, Flinders University, Bedford Park, SA, Australia;

⁶Department of Pathology and Urology, New York University, NY, USA;

⁷Origins of Cancer Laboratory, Centenary Institute, NSW, Australia;

⁸Sydney Medical School, University of Sydney, NSW, Australia;

⁹Department of Urology, St Vincent's Hospital Sydney and Garvan Institute, NSW, Australia;

¹⁰Department of Pharmacology and Chemical Biology, University of Pittsburgh, PA, USA;

¹¹Department of Physiology, Monash University, VIC, Australia.

Oncotarget 2015; 6(18): 16135-16150

Statement of Authorship

Title of Paper	Stromal androgen receptor regulates the composition of the microenvironment to influence prostate cancer outcome
Publication Status	Published
Publication Details	Leach DA, Need EF, Toivanen R, Trotta AP, Palethorpe HM , Tamblyn DJ, Kopsaftis T, England GM, Smith E, Drew PA, Pinnock CB, Lee P, Holst J, Risbridger GP, Chopra S, DeFranco DB, Taylor RA, Buchanan G: Stromal androgen receptor regulates the composition of the microenvironment to influence prostate cancer outcome. <i>Oncotarget</i> 2015, 6(18).

Principal Author

Name of Principal Author (Candidate)	Helen M Palethorpe		
Contribution to the Paper	Conceived, designed and performed one aspect of the manuscript pertaining to PC3 cell migration over 3D matrices, acquired images for analysis and analysed the data relating to the experiment. Additionally evaluated the manuscript.		
Overall percentage (%)	5%		
Certification:	This paper reports on original research I conducted during the period of my Higher Degree by Research candidature and is not subject to any obligations or contractual agreements with a third party that would constrain its inclusion in this thesis. I am the primary author of this paper.		
Signature		Date	20/10/15

Co-Author Contributions

By signing the Statement of Authorship, each author certifies that:

- iv. the candidate's stated contribution to the publication is accurate (as detailed above);
- v. permission is granted for the candidate to include the publication in the thesis; and
- vi. the sum of all co-author contributions is equal to 100% less the candidate's stated contribution.

Name of Co-Author	Damien A. Leach		
Contribution to the Paper	Responsible for developing and integrating project, Oversaw design and development of tissue microarray. Undertook cohort immunohistochemistry and analysis, performed all cell based studies, including transient luciferase assays, RNA microarray, RT-qPCR, CHIP, adhesion and trypsinisation assays, cell proliferation assays, protein silencing, and western blotting. Generated and perfected new methodology/assays. Data analysis and figure generation, analysis of all experiments (except animal work), and data interpretation. Wrote manuscript.		
Signature		Date	20/10/15

Name of Co-Author	Eleanor F. Need		
Contribution to the Paper	Supervised work. Contributed to planning of research and article, and provided critical evaluation.		
Signature		Date	20/10/15

Name of Co-Author	Roxanne Toivanen		
Contribution to the Paper	Performed and analysed <i>in vivo</i> mice studies.		
Signature		Date	14/10/15

Please cut and paste additional co-author panels here as required.

Name of Co-Author	Andrew P. Trotta		
Contribution to the Paper	Contributed to planning of article and provided critical evaluation.		
Signature		Date	13/10/15

Name of Co-Author	David J. Tamblyn		
Contribution to the Paper	Facilitated design and delivery of archived human tissue samples for 64 patient cohort.		
Signature		Date	14/10/15

Name of Co-Author	Tina Kopsaftis		
Contribution to the Paper	Identified and supplied clinical data for the 64 patient clinical cohort.		
Signature		Date	13/10/15

Name of Co-Author	Georgina M. England		
Contribution to the Paper	Performed pathological categorization and annotation of human samples in the 64 patient clinical cohort.		
Signature		Date	13/10/15

Name of Co-Author	Eric Smith		
Contribution to the Paper	Conceived and designed the migration experiment, analysed the data, and provided critical evaluation of the manuscript.		
Signature		Date	14/10/16

Name of Co-Author	Paul A. Drew		
Contribution to the Paper	Conceived and designed the migration experiment, analysed the data, and provided critical evaluation of the manuscript.		
Signature		Date	14/10/16

Name of Co-Author	Carole B. Pinnock		
Contribution to the Paper	Facilitated design and delivery of archived human tissue samples for 64 patient cohort, contributed to conceptual development.		
Signature		Date	13/10/15

Name of Co-Author	Peng Lee		
Contribution to the Paper	Generated human prostatic PShTert/PShTert-AR fibroblast cells.		
Signature		Date	27/10/15

Name of Co-Author	Jeff Holst		
Contribution to the Paper	Manuscript evaluation, editing and data interpretation.		
Signature		Date	13/10/16

APPROVALS
RESEARCH GROUP / NON RESEARCH

Comments:

Name of Co-Author	Gail P. Risbridge Signature: (Research Group Head or Manager) Date:		
Contribution to the Paper	Contributed to the design and provision of in vivo studies (Figure 2) and		
Signature		Date	10/15

FUNDING

RESEARCH GRANT NON RESEARCH HONARARY APPOINTMENT

Personnel Budget Awarded: \$:

Period of Grant: From: To:

Budget Compliance:

Comments:

.....
ce Manager/ COO) Date:

H & SAFETY

Safety Induction required before starting
 Safety Induction already completed

Name of Co-Author	Sama Signature: (WHS & Operations Manager) Date:		
Contribution to the Paper	Facilitated design and delivery of tissue samples, contributed to conceptual development and undertook manuscript evaluation.		
Signature		Date	28/10/15

CHIEF OPERATING OFFICER OR DELEGATED OFFICER

.....
pleted Form to Human Resources, Level 5

Name of Co-Author	Donald B. DeFranco		
Contribution to the Paper	Contributed to conceptual development, supplied WPMY-1 and PShTert cells, and undertook critical evaluation of the manuscript.		
Signature		Date	29/10/15

Name of Co-Author	Renea A. Taylor		
Contribution to the Paper	Contributed to conceptual development, contributed to <i>in vivo</i> studies (Figure 2) and provision of CAF NPF fibroblasts (Figure 6).		
Signature		Date	13/10/15

Name of Co-Author	Grant Buchanan		
Contribution to the Paper	Overall conceptual development, supervision and design review, data interpretation, and critical evaluation of the manuscript.		
Signature		Date	15/10/15

Stromal androgen receptor regulates the composition of the microenvironment to influence prostate cancer outcome

Damien A. Leach¹, Eleanor F. Need¹, Roxanne Toivanen², Andrew P. Trotta¹, Helen M. Palenthorpe¹, David J. Tamblyn³, Tina Kopsaftis³, Georgina M. England⁴, Eric Smith¹, Paul A. Drew^{1,5}, Carole B. Pinnock³, Peng Lee⁶, Jeff Holst^{7,8}, Gail P. Risbridger², Samarth Chopra^{3,9}, Donald B. DeFranco¹⁰, Renea A. Taylor^{2,11} and Grant Buchanan¹

¹ The Basil Hetzel Institute for Translational Health Research, University of Adelaide, SA, Australia

² Department of Anatomy and Development, Monash University, VIC, Australia

³ Urology Unit, Repatriation General Hospital, SA, Australia

⁴ Department of Surgical Pathology, SA Pathology at Flinders Medical Centre, Bedford Park, SA, Australia

⁵ School of Nursing and Midwifery, Flinders University, Bedford Park, SA, Australia

⁶ Department of Pathology and Urology, New York University, NY, USA

⁷ Origins of Cancer Laboratory, Centenary Institute, NSW, Australia

⁸ Sydney Medical School, University of Sydney, NSW, Australia

⁹ Department of Urology, St Vincent's Hospital, Sydney and Garvan Institute

¹⁰ Department of Pharmacology and Chemical Biology, University of Pittsburgh, PA, USA

¹¹ Department of Physiology, Monash University, VIC, Australia

Correspondence to: Grant Buchanan, **email:** grant.buchanan@adelaide.edu.au

Renea Taylor, **email:** renea.taylor@monash.edu

Keywords: prostate cancer, androgen receptor, stroma, fibroblasts, extracellular matrix

Received: December 04, 2014

Accepted: April 02, 2015

Published: April 19, 2015

This is an open-access article distributed under the terms of the Creative Commons Attribution License, which permits unrestricted use, distribution, and reproduction in any medium, provided the original author and source are credited.

ABSTRACT

Androgen receptor (AR) signaling in stromal cells is important in prostate cancer, yet the mechanisms underpinning stromal AR contribution to disease development and progression remain unclear. Using patient-matched benign and malignant prostate samples, we show a significant association between low AR levels in cancer associated stroma and increased prostate cancer-related death at one, three and five years post-dignosis, and in tissue recombination models with primary prostate cancer cells that low stromal AR decreases castration-induced apoptosis. AR-regulation was found to be different in primary human fibroblasts isolated from adjacent to cancerous and non-cancerous prostate epithelia, and to represent altered activation of myofibroblast pathways involved in cell cycle, adhesion, migration, and the extracellular matrix (ECM). Without AR signaling, the fibroblast-derived ECM loses the capacity to promote attachment of both myofibroblasts and cancer cells, is less able to prevent cell-matrix disruption, and is less likely to impede cancer cell invasion. AR signaling in prostate cancer stroma appears therefore to alter patient outcome by maintaining an ECM microenvironment inhibitory to cancer cell invasion. This paper provides comprehensive insight into AR signaling in the non-epithelial prostate microenvironment, and a resource from which the prognostic and therapeutic implications of stromal AR levels can be further explored.

INTRODUCTION

Prostate cancer causes more than 28,000 deaths each year in the United States [1]. Critically, 10-33% of clinically localized cancers treated by surgery will eventually progress, indicative of undetected pre-existing metastatic disease [2, 3]. Although epithelial differentiation scored by Gleason pathology at diagnosis aids in prognosis and management, it is imprecise in prediction of sub-clinical metastases or low grade tumors at risk of rapid progression. Recent studies of various solid tumors suggest that the stromal microenvironment may yield additional diagnostic information and novel avenues for therapeutic intervention [4-7].

Prostate development and homeostasis requires bidirectional signaling between epithelial cells and stromal constituents, including fibroblast and smooth muscle cells, vasculature, soluble factors and extracellular matrix (ECM) proteins. This signaling is disrupted in cancer [8-10], where the stroma becomes disorganized, normal non-malignant prostatic fibroblasts (NPFs) are replaced by activated cancer-associated fibroblasts (CAFs), and the composition of the ECM is altered [11-14]. Compared to NPFs, CAFs exhibit increased proliferation and migratory behavior [15], induce malignancy in non-tumorigenic prostate epithelial cells [16-18], and provoke tumor progression via secretion of signaling factors [19-22]. Moreover, genomic-level studies have identified prognostic CAF-specific gene signatures in digestive, non-small cell lung, breast and prostate cancers [4, 23-25].

In the adult prostate, activation of epithelial androgen receptor (AR) by testosterone (T) and 5 α -dihydrotestosterone (DHT) is necessary for cell survival and regulation of seminal fluid proteins including prostate specific antigen (PSA) [26], which is used clinically for tumour detection and monitoring. Although targeting androgens through ablation is therefore an effective initial treatment strategy for advanced cancer, most recur by refractory reactivation of epithelial AR [27-29]. In prostate development however, it is the stromal AR that is necessary for establishment of normal prostatic architecture, and for epithelial differentiation and function [30]. Decreased stromal AR expression in cancer has been associated with tumor resistance to androgen deprivation [31], and with relapse and progression following radical prostatectomy [25, 32, 33]. Currently however, we do not know how decreased stromal AR contributes to prostate cancer progression, or indeed how androgen action differs between prostate stromal and epithelial cells.

In this study, we compared AR levels in epithelial and stromal compartments of patient-matched benign and malignant prostate tissue, and demonstrate an association between low stromal AR levels and death from prostate cancer at one, three and five years post diagnosis. This is the first time that stromal AR changes have been shown to be specific to the immediate cancer

microenvironment and not due to differences between patients, and are related to adjacent malignant but not benign regions of the same prostate. We further show that androgen signaling in human prostatic myofibroblasts induces a microenvironment inhibitory to the movement and invasion of tumor cells, primarily by altering ECM composition. This protective AR-mediated phenotype in prostate cancer-associated stroma has implications for understanding the early stages of cancer progression, and for the use of androgen withdrawal in the absence of surgical management.

RESULTS

Association of AR levels in epithelium and stroma of benign and malignant prostate tissue with clinical parameters

The relationship between prostate cancer outcome and AR levels in stroma and epithelium was investigated by AR immunohistochemistry on 64 patient-matched BPH and prostate cancer samples in patients of median age 87 years (Fig. 1A). Similar to a previous report [33], the median intensity of AR staining was lower in stroma than in epithelia (Fig 1A, B). Median AR levels were similar in malignant and benign epithelia, but were lower in cancer-associated compared to benign stroma ($p=4.1 \times 10^{-8}$, Fig. 1B, Table 1A). Consistent with established clinical associations, patients with higher Gleason score had a greater extent of disease, higher serum PSA levels, and were more likely to have died from their disease at censure. Additionally, a positive association between serum PSA levels was observed for AR content in cancer epithelia ($p=0.004$), but not with the other AR measures (Supplementary Fig. S1A-D). Higher Gleason score was associated with a higher median AR level in cancer epithelia ($p<0.05$) and lower AR in cancer-associated stroma ($p<0.05$; Fig.1C, Table 1A). Previous studies have reported an association between low stromal AR levels and biochemical recurrence [25, 32-34]. Here we assessed stromal and epithelial AR levels in paired BPH and cancer samples from the same patients, allowing discrimination of changes specific to cancer stroma from those related to an individual patient or prostate. Critically, we observed that low AR levels in cancer stroma, but not BPH stroma, were associated with prostate cancer related death ($p=0.02$; Table 1A) at censure, which was a minimum five years post initial diagnosis. The level of AR in cancer or BPH epithelia was not associated with outcome. We next dichotomized the cohort by median AR level in cancer epithelia or cancer stroma. High epithelial AR levels was associated with the extent of disease, Gleason score and serum PSA ($p<0.05$), but not with outcome (Table 1B). Conversely, low AR in cancer

Table 1: AR levels in epithelia and stroma of prostate cancer and patient-matched benign regions.

A.		all (n=64) [®]	Gleason ≤7 (n=24) [®]	Gleason >7 (n=39)	p value [#]	PCa Death NO=(n=38) [®]	YES (n=26)	p value [#]
age		87 (60-100)	86 (67-97)	88 (60-100)	ns	86 (67-98)	88 (60-100)	ns
% Prostate cancer		50 (10-100)	22 (10-88)	80 (10-100)	<0.0001	30 (10-100)	78 (12-99)	0.0051
Gleason score		8 (4-10)				7 (4-10)	9 (7-10)	0.0002
PSA (ng/ml)		16.5 (0.5-8300)	6 (0.5-174)	26 (1-8300)	0.0011	14.3 (0.5-174)	18.4 (0.9-8300)	ns
PCa death		26	3	23	0.0001^{&}			
PCa-epithelia	AR score	6.50 (0.67-8.83)	5.57 (3.43-7.57)	6.36 (0.67-8.83)	0.0179	6.50 (3.42-8.14)	6.36 (0.67-8.83)	ns
PCa-stroma		2.10 (0-5.15)	2.67 (0-4.86)	1.71 (0.07-5.13)	0.0262	2.21 (0-4.86)	1.33 (0.21-5.15)	0.028
BPH-epithelia		5.89 (3.17-8.14)	6.33 (3.75-8.14)	5.86 (3.17-7.4)	ns	6.30 (3.17-8.14)	5.86 (3.75-7.40)	ns
BPH-stroma		4.14 (0.71-6.00)	4.75 (2.27-6)	3.77 (0.71-5.57)	0.0155	4.00 (0.71-6.00)	4.5 (1.07-5.57)	ns
B.		all (n=64) [®]	AR Low PCa-Ep * (n=28)	AR High PCa-Ep (n=29)	p value [#]	AR Low PCa-St * (n=29)	AR High PCa-St (n=28)	p value [#]
age		87 (60-100)	88 (71-100)	84 (60-94)	0.0115	88 (71-100)	85 (60-95)	ns
% Prostate cancer		50 (10-100)	25 (10-100)	80 (10-100)	0.0021	80 (12-100)	33 (10-99)	0.046
Gleason score		8 (4-10)	7 (4-10)	9 (6-10)	0.0139	9 (5-10)	7 (4-10)	ns
PSA (ng/ml)		16.5 (0.5-8300)	8 (0.5-174)	25 (2-8300)	0.0161	17 (1-2617)	16 (1-8300)	ns
PCa death		24	13	11	ns ^{&}	16	8	0.0245^{&}
PCa-epithelia	AR score	6.50 (0.67-8.83)				6.50 (0.67-8.83)	6.36 (3.34-7.69)	ns
PCa-stroma		2.10 (0-5.15)	2.07 (0-5.15)	2.10 (0.07-4.86)	ns			
BPH-epithelia		5.89 (3.17-8.14)	5.86 (3.75-8.00)	6.15 (3.75-8.14)	ns	5.89 (3.75-7.43)	5.86 (3.86-8.14)	ns
BPH-stroma		4.14 (0.71-6.00)	4.50-1.50-6.00)	3.42 (0.71-5.79)	ns	4.17 (0.71-6.00)	4.00 (1.17-5.71)	ns
PCa specific survival		1-yr survival rate				88%	65%	
		3-yr survival rate				68%	45%	
		5-yr survival rate				56%	30%	

[®] Data for age, percent cancer in sample (% prostate cancer), Gleason score, PSA and AR staining score are presented as median (range), and for prostate cancer related death as absolute numbers

[®] Gleason score and Prostate cancer (PCa) death status available at censure for 63/64 patients

* Samples dichotomized about the median AR score

[#] Two-tailed Mann-Whitney U test unless otherwise indicated

[&] Barnard's Exact test

stroma was associated with more extensive disease, and a greater risk of prostate cancer-related death ($p < 0.05$, Table 1B). At the time of censure, the median prostate cancer specific survival for patients with low stromal AR was 622 days, which was significantly less than patients with high stromal AR expression at 2528 days ($p = 0.013$). Finally, we observed lower 1, 3, and 5 year prostate cancer specific survival in patients with low stromal AR (30% at 5 years) compared to high stromal AR (56% at 5 years; Table 1B). Despite AR in epithelial cells being more related to clinical parameters of histologically aggressive disease, our data suggest the intriguing possibility that AR in fibroblasts plays a more critical role in protecting against prostate cancer progression. Moreover, AR level in BPH stroma from the same patients was not associated with progression, supporting the existence of pathological cancer associated stroma in prostate cancer.

Myofibroblast AR expression modulates patient cancer cell response to castration in a tissue recombination model

To investigate the role of stromal AR in cancer, we utilized *in vivo* tissue recombination [35]. Human prostate cancer tissues obtained from four patients with moderate (Gleason 7) tumors were combined as heterotypic recombinants with AR positive human prostate PShTert-AR myofibroblasts or AR negative PShTert-ctrl and sub-renal grafted into immunodeficient NOD-SCID mice. Human cancer cells combined with both PShTert-AR and PShTert-ctrls formed phenotypically similar ductal structures that stained positive for the human-specific epithelial marker p63/CK8.18 (Fig. 2A). The survival of cancer foci, detected as p63+/CK8.18+, was similar in grafts from the four patients with PShTert-AR (65%, 11/17) and PShTert-ctrl (56%, 13/23) lines. As expected, a significantly lower proportion of stroma in the grafts containing PShTert-ctrl myofibroblasts expressed AR ($p < 0.01$; Supplementary Fig. 1E), with residual stromal AR expression arising from mouse-derived stroma. Castration resulted in significantly reduced tumor cell

proliferation in both PShTert-AR ($p < 0.01$; Fig. 2B) and PShTert-ctrl myofibroblast ($p < 0.001$; Fig. 2B) grafts, a reduction in cancer p63/CK8.18⁺ foci (Fig. 2C), and a higher percentage of apoptotic cancer cells (caspase-3 positive; $p < 0.001$; Fig. 2D). More importantly, there was significantly less cancer cell apoptosis in grafts with PShTert-ctrl cells in comparison to grafts with PShTert-AR cells ($p < 0.05$; Fig. 2D). This latter result suggests that low stromal AR reduces apoptosis of primary cancer cells in response to androgen deprivation *in vivo*.

Transcription activity, gene regulation, chromatin targeting and proliferation of prostate epithelial and myofibroblast cells diverge in response to androgens

We next sought to define the molecular actions of AR in PShTert-AR myofibroblasts, and to contrast those

from androgen responses of prostate cancer epithelial C4-2B cells. These lines have a comparable levels of AR protein (Fig. 3A), and both have a functional AR signaling pathway as demonstrated by increased FKBP5 protein levels and probasin reporter (PB3) transactivation in response to DHT (Fig. 3A, Supplementary Fig. S2A). These responses are AR specific, and could be blocked by the AR antagonist, BIC (Fig. 3A, Supplementary Fig. S2A). Transcriptional reporter assays suggest however, that the DHT response of AR is 10-fold less sensitive in myofibroblasts than in epithelia (Supplementary Fig. S2B), and is not due to technical limitations such as reporter level (Supplementary Fig. S2C). Furthermore, only classical androgen agonists (DHT and T) and medroxyprogesterone acetate (MPA) could produce a transcriptional response in PShTert-AR cells (Supplementary Fig. S2D), compared with the expected broader ligand responses in C4-2B cells (Supplementary Fig. S2E). Nevertheless, the ability of the AR to stimulate a panel of AR-targeted reporters

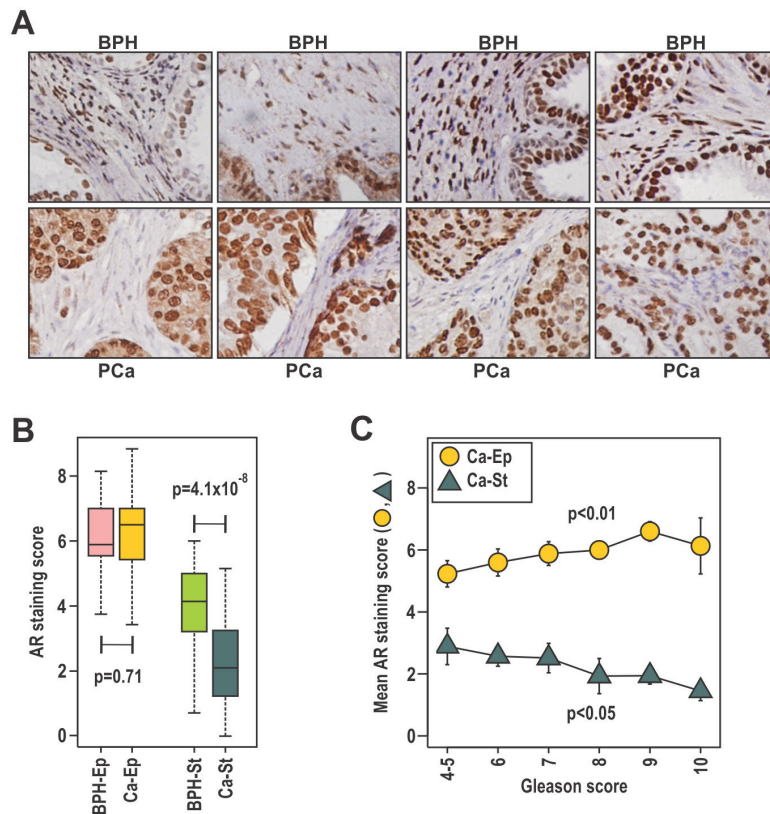


Figure 1: The expression of stromal AR is related to clinical parameters and outcomes of prostate cancer. A-C. Patient-matched duplicate cores of BPH and cancer were immunostained with anti-AR antibody. Samples were scored by two independent researchers, using a scale of high (3), moderate (2), low (1) intensity or absent (0) immunostaining in the epithelia and stroma and averaged between the duplicate samples and scorers. **B.** Scores were evaluated in relation to disease state for stroma (St) and epithelia (Ep) and compared using the Wilcoxon Rank-Sum test. **C.** Mean AR score \pm SEM for both the cancer stroma (Ca-St) and epithelia (Ca-Ep) was calculated for each Gleason grade.

was consistent between PShTert-AR and C4-2B cells (Supplementary Fig. S2F).

In order to more precisely define the transcriptional role for AR in PShTert-AR cells, we performed expression microarray analysis, identifying 2615 DHT regulated genes in PShTert-AR myfibroblasts and 1000 in C4-2B epithelial cells (>0.5 log₂ fold change). Importantly, only 254 of those regulated genes were common between the two cell lines, and half of those (127/254) were regulated in the opposite direction (Fig. 3B). RT-qPCR analysis of an independent sample set confirmed the uniquely regulated (Fig. 3C-D) and similarly regulated (Fig. 3E) responses to DHT in each cell line. The AR-specific nature of myfibroblast responses was confirmed by their absence in PShTert-ctrl cells (Supplementary Fig. S3). ChIP analysis of well-characterized androgen target genes suggests that divergent AR occupancy of promoters/enhancers is

responsible for the cell-specific regulation by DHT (Fig. 3F-H), consistent with a contemporary understanding of AR chromatin targeting [36]. We next applied pathway analysis to the top 1000 regulated genes in each cell line, which in PShTert-AR cells comprised 390 upregulated and 610 downregulated genes, and in C4-2B cells 648 upregulated and 352 downregulated genes. DHT-treated myfibroblasts were enriched in adhesion and ECM organization, but depleted in cell cycle and migration (Supplementary Table 2). In contrast, DHT in C4-2B cells drives processes of lipid and fatty acid synthesis and migration, and depletion of apoptosis (Supplementary Table 2). Importantly, a considerable number of pathways were regulated in opposite directions by DHT in epithelial and myfibroblast cells, despite limited commonality in regulated genes (Fig. 3B; Supplementary Table 2). Consistent with the divergent gene responses, DHT

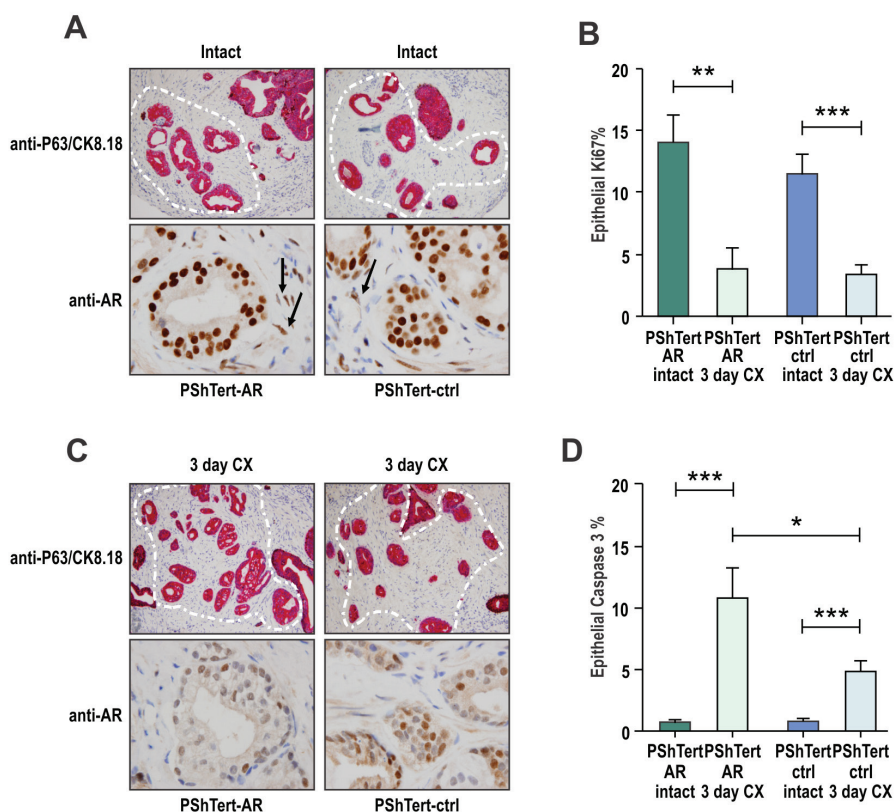


Figure 2: Loss of myfibroblast AR protects cancerous prostatic epithelia from castration induced apoptosis. Tissue recombination of patient prostate cancer tissues co-grafted with either PShTert-AR or PShTert-ctrl myfibroblasts into immune-deficient host mice. After 8 weeks, host mice were castrated for a further three days. **A.** Human tissue was identified by dual immunostaining of basal cell marker p63 (brown stain) and epithelial marker CK8/18 (pink stain); cancer foci were p63-CK8/18⁺ highlighted by white outline. AR levels were assessed in samples immunostained with anti-AR antibody. **B.** Epithelial proliferation was determined by the percentage of cells immunostained for anti-Ki-67. **C.** Human cancer tissue grafts from castrated mice was assessed for CK8/18, p63 and AR as described in (A). **D.** Epithelial cell death was measured through cleaved caspase-3 immunostaining and percent positive cells counted (*, p<0.05, **, p<0.01, ***, p<0.001, Student's T-test).

stimulated C4-2B cells to proliferate as previously reported [37] ($p < 0.05$; Fig. 4A), but inhibited PShTert-AR growth in a dose-dependent manner ($p < 0.001$, Fig. 4B). Cell death did not vary significantly between treatments in C4-2Bs over the 6 day period, but was significantly altered by all doses of DHT in PShTert-AR cells at days 3 and 4 ($p < 0.05$; 5-20% of viable cells; Supplementary Fig. S4). Importantly, BIC reversed these effects, confirming AR mediation of the divergent growth responses (Fig. 4A, B; right panels).

One mediator of the anti-proliferative effect of androgen in myofibroblasts may be the fibroblast-specific androgen regulated *F-box protein 32* (*FBXO32*) gene product. *FBXO32* is a member of the family of DNA-ligensing proteins that regulates progression from G1 phase by inhibiting cyclin D1 [38]. To determine whether *FBXO32* could regulate proliferation in AR expressing myofibroblasts, we used siRNA knockdown (Fig. 4C).

FBXO32 depletion partially reversed the inhibitory effect of DHT on myofibroblast cell growth over the course of a five day period ($p < 0.05$; Fig. 4D). Together, the above results demonstrate that AR in epithelial and myofibroblast lineages plays distinct roles, one of which is to direct divergent proliferative responses to DHT.

AR action in myofibroblasts promotes epithelial cancer proliferation

We next considered whether AR activity in myofibroblasts could affect epithelial growth. Conditioned media was collected from PShTert-AR and PShTert-ctrl myofibroblasts treated with or without DHT. Compared to vehicle, media from DHT treated AR positive myofibroblasts increased C4-2B and PC-3 proliferation by 1.64 and 2.72 fold respectively ($p < 0.05$, Fig. 4E, F).

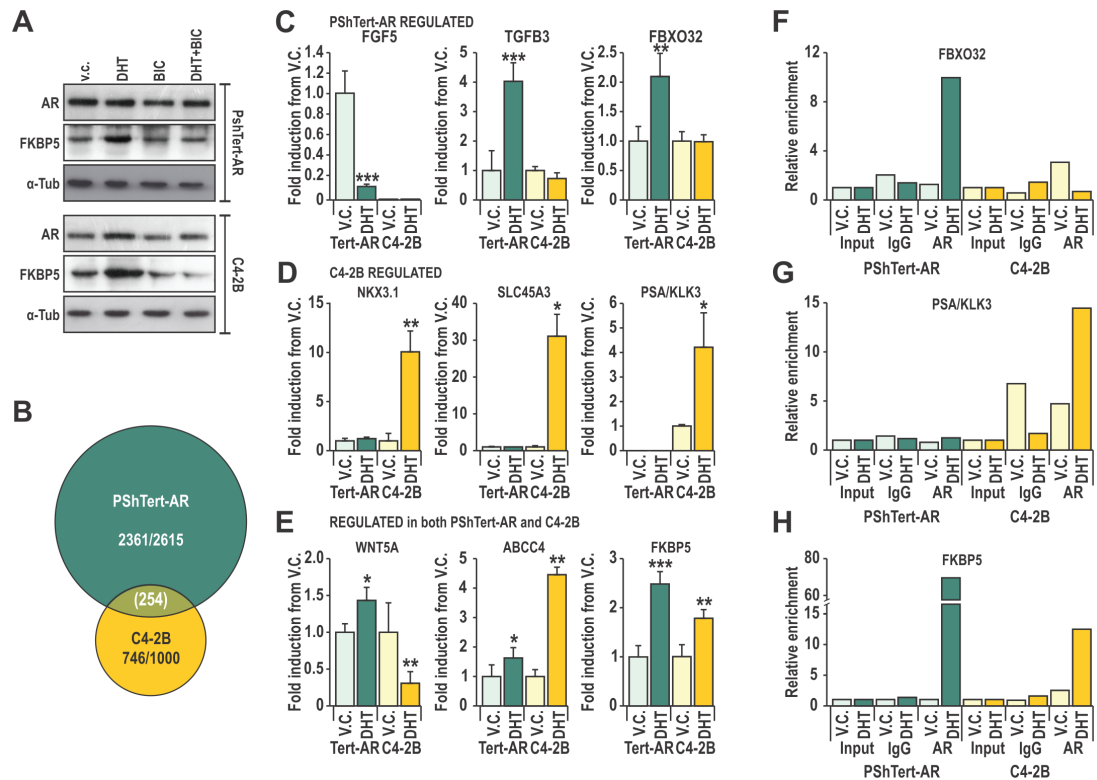


Figure 3: Cell specificity of AR action may be mediated by interactions of AR with DNA. A. Lysates from C4-2B and PShTert-AR cells treated with or without 10 nM DHT and 10 μ M bicalutamide (BIC) were probed for AR and FKBP5. B. Affymetrix 1.0st Gene Array of 10 nM DHT or vehicle control (V.C.) treated PShTert-AR or C4-2B cells, presented as a Venn-diagram of genes with > 0.5 \log_2 fold change in expression between treatments. C-E. Microarray was validated via RT-qPCR of independent samples produced under the same conditions. Data is represented as mean + SEM of triplicate biological replicates (V.C. vs DHT * $p < 0.05$, ** $p < 0.01$, *** $p < 0.001$ Student's T-test). F-H. Chromatin immunoprecipitation (ChIP) was performed on C4-2B and PShTert-AR cells treated with 10 nM DHT or vehicle, and immunoprecipitated with anti-AR N20 or nonspecific IgG antibody. ChIP samples were quantified by RT-qPCR and mean percent input for each binding region in the proximity of (F) *FBXO32*, (G) *PSA* and (H) *FKBP5* was normalized to a non-specific binding region.

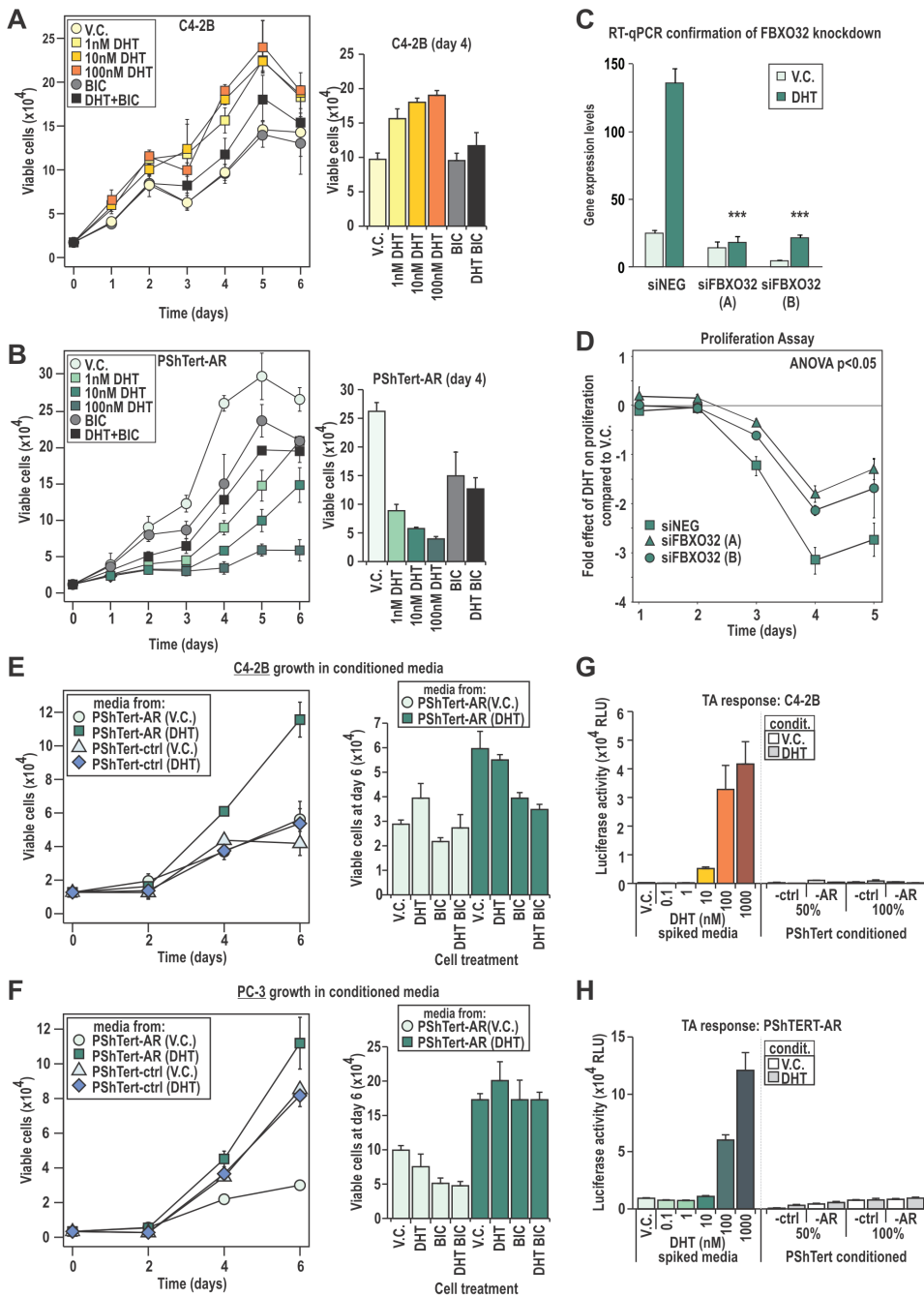


Figure 4: C4-2B and PShTert-AR cells have different proliferative responses to DHT. A-B. Proliferative response of C4-2B and PShTert-AR cells to 10 nM DHT was measured daily via Trypan blue exclusion assays. C,D. The androgen mediated gene and DNA-licensing factor, FBXO32, was silenced via siRNA (C) and the effect on PShTert-AR growth in response to 10 nM DHT was measured via Trypan blue exclusion assay (D). E,F. The effect of conditioned media from PShTert-AR and PShTert-ctrl on C4-2B and PC-3 cells was measured as in A. Data represents the mean number of viable cells in triplicate wells \pm SEM. G,H. The presence of DHT in the conditioned media was assessed via transactivation assays performed on C4-2B (G) and PShTert-AR (H) cells. Data presented as mean relative light units (RLU) \pm SEM of six independently transfected wells.

Media from DHT treated AR negative myofibroblasts did not alter the proliferative response of either epithelial line. The addition of DHT to vehicle conditioned media from PShTert-AR cells enhanced proliferation of C4-2B but not AR negative PC-3 cells, an effect reversed by co-treatment with BIC (Fig. 4E, F). In contrast, DHT supplementation had no effect on the higher proliferation seen with DHT stimulated myofibroblast conditioned media (Fig. 4E, F). Residual DHT from the conditioning process was not responsible for these effects, as high-sensitivity transcriptional reporter assays did not reveal any androgen activity in conditioned media (Fig. 4G, H).

It appears likely from these studies that DHT stimulation of AR positive myofibroblasts produces secreted, soluble factors that are pro-proliferative to epithelial cells.

AR action in prostate myofibroblast cells controls adherence of myofibroblast cells

As pathways involving adhesion were highly enriched in DHT treated myofibroblasts, we next assessed whether this translated to altered attachment. Treatment with DHT had no effect on trypsinization of C4-2B cells or PShTert-ctrl cells, but increased retention of PShTert-

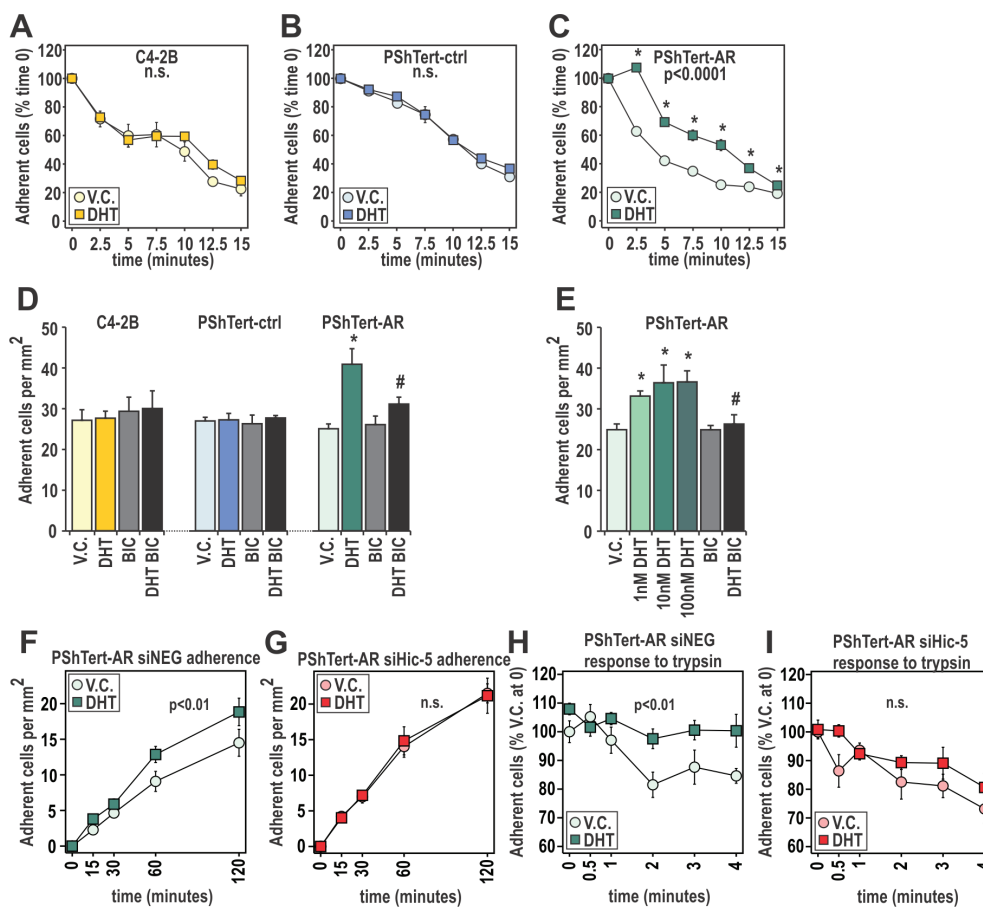


Figure 5: DHT has pro-adherent effects on fast and long term adherence of myofibroblast cells. A-C. The quantity of C4-2B, PShTert-ctrl, and PShTert-AR cells, treated with 10 nM DHT or equivalent vehicle (V.C.), remaining after trypsinization over 15 min was measured using crystal violet staining. Presented as mean \pm SEM of six technical replicates, and representative of three independent experiments. D, E. Adherence was measured by manually counting the number of 10 nM DHT, V.C. or 10 μ M bicalutamide (BIC) treated C4-2B, PShTert-ctrl, and PShTert-AR cells adhering after 30 min. Data is presented as mean \pm SEM of four samples and is representative of three independent experiments. (* $p < 0.05$ V.C. vs DHT, # $p < 0.05$ DHT vs DHT+BIC Student's T-test). F, G. PShTert-AR cells transfected with siRNA against Hic-5 or scrambled control were assayed for adherence as described in D but measured over a 2 h period. Data is presented as mean \pm SEM of four replicates and representative of three independent experiments. H-I. Hic-5 contribution to androgen-mediated attachment was assayed as described in A-C. For all time course adherence data, significance ($p < 0.05$) was determined by one-way ANOVA.

AR cells by $25.1 \pm 3.6\%$ to $44.7 \pm 1.8\%$ ($p < 0.0001$, Fig. 5A-C). This response was DHT dose dependent and reversible by BIC ($p < 0.05$; Supplementary Fig. S5), thus demonstrating AR involvement. Furthermore, DHT treatment significantly increased attachment of PShTert-AR cells by 33-44% at 30 min in a dose-dependent manner, suggestive of an additional non-genomic effect ($p < 0.05$, Fig. 5D, E). This response was measurable for 4 h and could be reversed by BIC (Fig. 5D), but did not occur with either C4-2B or PShTert-ctrl cells.

We recently reported that hydrogen peroxide-inducible gene 5 (*Hic-5/TGFB111*), a predominantly fibroblast-specific AR coregulator and a component of the focal adhesion (FA) complex, plays an important role in AR-mediated activity in myofibroblasts [39-41]. To assess whether *Hic-5* might be involved in DHT/AR-mediated adherence, we utilized siRNA knockdown in PShTert-AR cells (Supplementary Fig. S6). Compared to negative siRNA control, depletion of *Hic-5* abolished the effect of DHT on myofibroblast adherence (Fig. 5F, G). Similarly, *Hic-5* knockdown eliminated the positive effect of DHT pretreatment on myofibroblast attachment (Fig. 5 H, I). AR however retained the capacity to regulate FKBP5 expression when *Hic-5* was depleted, implying that decreased adherence was not due to absolute loss of AR activity (Supplementary Fig. S6). Together, these results suggest an active role for AR in myofibroblast attachment, mediated via cellular interactions with a known AR coregulator.

AR action in prostate myofibroblasts alters the ECM to increase cancer cell attachment and decrease cancer cell migration and invasion

As we had observed increased attachment and altered expression of ECM components with DHT treatment in the myofibroblast cells (Supplementary Table 2), we next measured adherence of epithelial cells to the myofibroblast-deposited matrix. PC-3 attachment to matrix generated by DHT treated PShTert-AR cells was increased $31 \pm 12\%$ over matrix from vehicle treated cells, and could be inhibited by BIC ($p < 0.05$, Fig. 6A). In contrast, PC-3 adhesion to matrix from PShTert-ctrl cells was unaffected by ligand (Fig. 6A). Similarly, PC-3 migration over ECM generated by DHT treated PShTert-AR cells was significantly less than migration over ECM produced under vehicle control treatment after 7 ($22 \pm 3\%$ vs $30 \pm 3.5\%$) and 11 ($1 \pm 1.3\%$ vs $7 \pm 2.4\%$) hours ($p < 0.05$, Fig 6B, Supplementary Fig. S7). As previously reported, cancer cell migration was significantly faster over ECM than cancer cell migration over plastic alone [42]. We next assessed the adherence of cancer cells to a myofibroblast conditioned 3D-ECM as previously described [43]. Consistent with the above results, a significant increase in C4-2B attachment (Fig. 6C) and proliferation (Fig.

6D) was only observed in gelatin conditioned by DHT-treated PShTert-AR cells, but not with gelatin conditioned by vehicle-treated PShTert-AR cells, or with vehicle- or DHT-treated PShTert-ctrl line (Fig. 6C, D). We also identified a significant decrease in invasion of the cancer cells through DHT-treated PShTert-AR gelatin matrix in comparison to matrix conditioned by vehicle treated PShTert-AR or DHT-treated PShTert-ctrl cells (Fig. 6E).

Candidate RT-qPCR analysis confirmed DHT upregulation of ECM proteins with adhesive properties (i.e. *COL1A1*, *COL3A1*, *COL4A6*, and *FN1*), and inhibition of ECM degrading enzymes (i.e. MMP1; Fig. 6F). Using ELISA, dose dependent DHT regulation of Collagen 1 protein was confirmed ($p < 0.05$; Fig. 6G). Significantly, in a set of human patient cancer-adjacent, BPH, and normal fibroblasts (CAF, BAF, and NPF respectively) we observed increased expression of *FBXO32* and *COL4A6* genes when treated with DHT in CAFs and BAFs only ($p < 0.05$, Fig. 6H), and a marked decrease in expression of *MMP1* expression in all three cell types ($p < 0.05$, Fig. 6I). Collectively, the above results suggest that stromal/fibroblast AR may act to alter the composition of the ECM, resulting in a pro-adhesive, anti-migratory matrix.

DISCUSSION

Extensive analyses of cancerous epithelia have failed to significantly improve prediction of pre-existing prostate metastases or subsequent progression [44]. However, it has been known for over a decade that the level of stromal AR is inversely related to Gleason score, response to therapy, metastasis and subsequent biochemical relapse [25, 31-34]. This is the first study to associate decreased stromal AR levels with increased prostate cancer-related death, even in the context of older patients with significant disease burden at the time of diagnosis and initial management. Importantly, this now establishes that there is no maximum age at which stromal AR content cannot provide additional prognostic information. Conversely, since Gleason score in our cohort was found to be related to traditional tumor characteristics of poor prognosis, such as serum PSA, cancer-related death and epithelial AR content, the stromal AR results are likely reflective of what also happens in younger patients. In addition to confirming a protective role for stromal AR against prostate cancer progression, our data suggest that analysis of stromal AR levels and/or function may provide useful information regarding tumor aggressiveness and/or early metastasis, and could guide clinical decision making in younger and older men alike. This is particularly important in the latter group where there is a pervasive belief that older men are more likely to die with prostate cancer than from it.

Metastasis of solid tumors is accomplished by either proteolytic migration, involving secretion of ECM

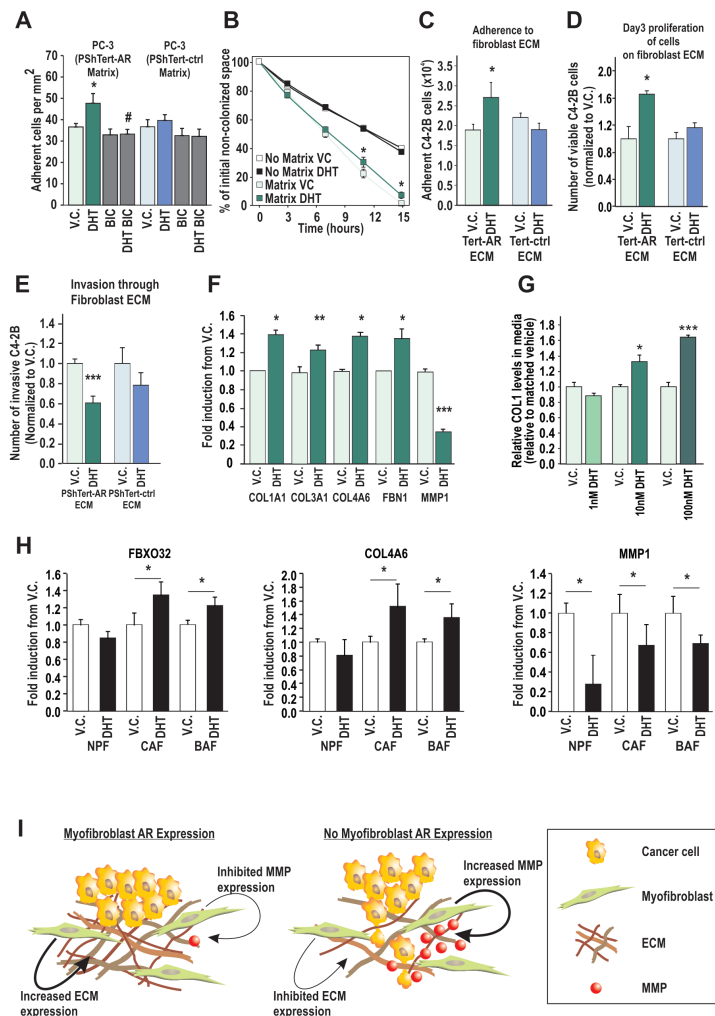


Figure 6: AR in cancer associated fibroblasts and model of AR action in prostate stroma. A. PC-3 attachment to ECM deposited by PShTert-ctrl and PShTert-AR cells treated with or without 10 nM DHT ± 10 μM BIC was measured as described in Fig. 5D. Data presented as mean adherence per mm² of four wells ± SEM. (* p<0.05 vehicle control (V.C.) vs DHT, # p<0.05 DHT vs DHT+BIC Student T-test). B. Migration of PC-3 cells over matrices created from V.C. or DHT treated PShTert-AR myofibroblasts was assessed by measuring the area of the cell-free gap over a 15 hour time period and calculated as a percentage of time point 0. Data represents mean ± SEM of three replicates. C-E. PShTert-AR or PShTert-ctrl cells were grown to confluence on a gelatin layer and allowed to deposit a 3D-ECM for 8 d following 10 nM DHT or V.C. treatment before myofibroblast removal. C. Adherence of 5 × 10⁴ C4-2B cells to the 3D-matrices was determined after an hour. Data is presented as mean ± SEM of four replicates and is representative of three independent experiments. D. The effect of the 3D-matrices on epithelial proliferation was determined via Trypan blue exclusion assay. Data is presented as mean ± SEM of four replicates and is representative of three independent experiments. E. Invasion of calcein-labeled C4-2B cells through the myofibroblast 3D-matrices was determined via a modified Boyden chamber technique. Data is presented as mean ± SEM of six samples and is representative of three independent experiments. F. RT-qPCR analysis for expression of selected ECM genes in PShTert-AR cells. Data represents the mean + SEM from triplicate biological replicates. G. ELISA analysis of collagen-1 (COL1) levels in conditioned media from DHT treated PShTert-AR cells. Data is presented as the mean + SEM from six replicates representative of two independent experiments. H. RT-qPCR gene analysis in human patient cancer associated fibroblasts (CAF), BPH associated fibroblasts (BAF), and normal prostatic fibroblasts (NPFs), isolated and treated with either V.C. or 100 nM DHT. Data represents the mean of technical triplicates (± SEM) from N=1 for each cell type (in all panels * p<0.05, ***p<0.001, Student's T-test). I. Model of AR action in prostate myofibroblasts. The AR signaling in myofibroblasts causes increased production of ECM components and inhibition of MMP enzymes. When AR signaling in myofibroblasts is lost, decreased expression of ECM components and enhanced MMP expression create an environment which decreases cancer cell attachment and increases cancer cell invasion.

degrading enzymes to create space into which cells move, and/or amoeboid (non-proteolytic) squeezing of cells through the ECM. The amount and arrangement of ECM fibers, enzymes, and ECM pore size are capable of altering each type of migration, and have been implicated in malignant disease [45-47], and studies of malignant ovarian and breast cancers have identified defects in matrix protein cross-linking that render ECM more susceptible to proteolytic degradation [48, 49]. We show here that AR action in myofibroblasts leads to decreased expression of enzymes involved in ECM digestion and increased expression of key components of the ECM, both in our model cell line and primary patient fibroblasts. These results are supported by our findings that AR positive myofibroblasts produce a more adhesive ECM when treated with DHT, which inhibits migration and provides a less invasive environment for prostate cancer cells. Further work will be required to distinguish the role of androgen regulation of matrix degrading proteases. Collectively, our data suggest that fibroblast AR may play a key role in regulating cell attachment, and in organization of the ECM, and that a loss of stromal AR creates a passive ECM environment that is less adhesive for cancer epithelia and more conducive for metastatic spread (Fig. 6H). We predict that defining the precise contribution that AR makes to ECM composition may inform on early disease spread and therefore overall patient outcome.

It appears from our results and those of others that stromal AR may also promote prostate cancer proliferation, as suggested here by the production of an unidentified soluble mediator, and/or ECM-bound growth factor [50-52]. On the surface, this appears at odds with clinical data demonstrating an association between low stromal AR and death from prostate cancer. Given decreased stromal AR expression throughout progression however [13, 50, 53, 54], or as shown here with increasing Gleason score, these two findings may not be as paradoxical as might be thought. Indeed, stromal AR may be pro-proliferative in early prostate cancer; exogenous tumors in mice grow larger when associated with AR sensitive stroma [55], and are inhibited by stroma lacking AR [50]. Conversely *in vivo* knockdown of stromal AR was found to be more effective at inhibiting tumor growth in early stages of progression rather than at later stages [50, 56]. In this study, there was no difference between take rate or cellular morphology of human tumors grafted with either AR positive or AR negative myofibroblasts. Instead, we found in grafts containing AR positive myofibroblasts that cancer cells exhibit increased apoptosis following castration. Collectively, these findings suggest that stromal AR can play a pro-proliferative, pro-adhesive and/or anti-migratory role in prostate cancer. It is entirely possible that stromal AR is pro-tumorigenic in very early stage disease, but prevents metastasis of evolving epithelial cancer cells by altering the composition and permissiveness of the ECM.

In conclusion, this manuscript is the first to show that unique androgen/AR transcriptional responses in prostate myofibroblasts play an important role in stromal-mediated alterations to the ECM and microenvironment. Clinically, it will be important to determine the key factors affected by a loss of stromal AR that may influence patient outcome and could be exploited by targeted therapies. The precise composition of the ECM may be one such key mediator of epithelial cancer cell invasiveness and thus indicative of patient outcome, tumor aggressiveness and treatment response.

MATERIALS AND METHODS

Clinical cohorts

The South Australia Prostate Cancer Clinical Outcomes Collaborative (SA-PCCOC; <http://www.sapccoc.com/>) tracks men diagnosed with prostate cancer in the South Australian public health system. Using the SA-PCCOC database, we identified 66 sequential patients whom underwent TURP for symptomatic relief of BPH urinary obstruction at the Repatriation General Hospital (RGH; Daws Park, South Australia) between 2000 and 2007, in which there was (i) a first diagnosis of prostate cancer on histological Gleason grading, (ii) cancer comprising >5% of the specimen, and (iii) sufficient areas of BPH and cancer in each sample from which multiple cores could be obtained. Areas of BPH and cancer were identified by H&E staining and mapped onto paraffin embedded material by a pathologist. Duplicate five mm cores of BPH and cancer from each individual were then used to generate tissue microarrays. Clinical data relating to each patient was acquired from the SA-PCCOC database. Sample and data acquisition was performed according to protocols approved by the Flinders Medical Centre and RGH Ethics Committees (Protocol #042/10).

Immunohistochemistry was performed with the AR N-20 antisera (Santa Cruz Biotechnology) and, detected using the LSAB+ System-HRP kit (Dako Laboratories, CA, USA). Staining was scored additively by two researchers in three independent fields from 0 (no staining) to 3 (very intense staining), yielding sample scores of 0-9 in epithelial and stromal compartments of both cancer and BPH. No stromal compartment achieved very intense staining. The mean sample score from the two researchers yielded the AR staining intensity score. Differences in staining intensity, Gleason Score, serum PSA and percent prostate cancer were assessed using two-tailed Mann-Whitney U tests. In samples dichotomized by median AR level, differences in prostate cancer-specific death were assessed using Barnard's Exact test. Significance was set at $p < 0.05$.

Human tissue was obtained from consented patients

in accordance with Human Ethics Research Approvals 34306 at Epworth Hospital, 03-14-04-08 at Cabrini Hospital and RMO 2006/61082004000145 at Monash University, and processed as previously published [18]. Briefly, tissue from patients with BPH or Gleason score 7 prostate cancers were extracted from TURP and radical prostatectomy specimens respectively. Primary fibroblasts, representing CAFs, BAFs and NPFs were isolated from patient specimens, cultured in RPMI with 5% FCS and 100nM testosterone or equivalent vehicle (ethanol), and assessed *in vitro* between passages 3-6. The integrity of primary fibroblast cultures was confirmed *in vitro* by growth properties, immunological markers and RNA expression, and their tumorigenic potential *in vivo* using tissue recombination with BPH-1 cells.

Cell lines

For *in vitro* experiments C4-2B [57] and PC-3 (ATCC, VA, USA) prostate cancer epithelial cells, telomerase immortalized human prostate stromal myofibroblast cells expressing AR (PShTertAR) or matched empty vector control (PShTert-ctrl) [31], and WMPY human prostate fibroblasts expressing Hic-5 or scrambled shRNA [58] were used. All cell lines were authenticated via Short Tandem Repeat testing in 2014, completed at CellBank Australia (NSW, Australia). In experimental conditions cells were incubated in stripped medium (Phenol Red Free-RPMI 1640 with 5% dextran coated (DCC) FBS) supplemented with 10 nM DHT or vehicle, or 10 μ M bicalutamide (BIC). For conditioned media, confluent PShTert-AR and PShTert-ctrl cells were incubated in stripped medium (Phenol Red Free-RPMI 1640 with 5% dextran coated (DCC) FBS) supplemented with 10 nM DHT or vehicle. Media was collected at 6, 12, 18, 24, 36, or 48 h after initial treatment, centrifuged to remove debris, filtered and frozen, and subsequently used neat for transactivation assays or at a 1:1 dilution with fresh stripped media for other cell studies.

Transactivation assays

Transactivation studies were performed as described previously [59] using Lipofectamine 2000™ (Life Technologies, CA, USA) or LTX-plus (Life Technologies) for transfection of luciferase constructs. Following transfection, cells were treated with 0.1-1000 nM of steroids or equivalent vehicle (ethanol) control for 22 h. Results are presented as mean (\pm SEM) of six independently transfected wells.

Chromatin immunoprecipitation (ChIP)

ChIP was performed as described previously [59], using semi-confluent PShTert-AR or C4-2B cells were treated for 4 hours with 10nM DHT or vehicle. Cells were then formaldehyde fixed and sonicated to produce 300-1500 bp fragments. Lysates were pre-cleared with yeast tRNA and protein G sepharose, and immunoprecipitated overnight with 4 μ g of AR N-20 (Santa Cruz Biotechnology) or rabbit IgG (Santa Cruz Biotechnology) antiserum. Protein-DNA complexes were eluted from the beads, digested with proteinase K and was DNA purified by phenol-chloroform extraction. Resulting DNA samples were assessed by RT-qPCR in triplicate, with primers listed in Supplementary Table 1. Data was calculated as percent input and normalized to non-specific control (NC2). Results are representative of three independent experiments.

ELISA

ELISA was used to measure collagen 1 levels in media collected from confluent PShTert-AR myofibroblasts treated with 50 μ g/ml ascorbic acid (Sigma-Aldrich, NSW, Australia) and either DHT, vehicle control and or BIC. Media collected from six independent treated confluent cells was plated into 96-well Maxisorp (Nunc, Simga Aldrich) plates and incubated overnight at 4°C. Plates were washed in PBS supplemented with 0.1% Tween (PBST), blocked in 2.5% BSA and washed in PBST, plates were probed with rabbit anti-collagen type 1 antibody (0.25 μ g/ml, Rockland Immunochemistry, PA, USA) for 3 h and detected via a europium-tagged anti-rabbit secondary antibody. The concentration of collagen was subsequently fluorescently detected using 340 nm excitation/615 nm emission spectra.

Tissue recombination

Renal capsule tissue recombination grafting of PShTert-AR or PShTert-ctrl cells with pieces of patient-derived primary human prostate cancer tissue into NOD-SCID mice was performed and analyzed as previously described [18, 35, 60]. Briefly, PShTert-AR or PShTert-ctrl cells (2.5×10^5) were combined with 2 mm X 2 mm X 1 mm pieces of patient-derived primary human prostate cancer tissue in 30 μ l of collagen/RPMI 1640 + 5% FBS with 0.1% penicillin-streptomycin for 24 h, and grafted under the renal capsule of NOD-SCID mice for 8 weeks. Mice were castrated, and grafts allowed to grow for an additional 3 days before being removed, paraffin-embedded and sectioned. Immunohistochemistry for Ki-67 (Sigma-Aldrich), caspase-3 (Sigma-Aldrich), and AR (Sigma-Aldrich) was performed.

Microarrays

RNA extracted from cells treated with either DHT or vehicle using the RNeasy Kit (Qiagen, Melbourne, Australia), was analyzed using Affymetrix 1.0st Gene Arrays. Data was Bioinformatically analyzed using either in R using Gene Ontology categories, or in R or using DAVID Bioinformatics Resources <http://david.abcc.ncifcrf.gov/home.jsp> (46, 47).

Quantitative real-time PCR (RT-qPCR)

cDNA created from sample RNA was analyzed via RT-qPCR as previously described [61], using SYBR Green (Biorad) and primer pairs detailed in Supplementary Table 1. Data is presented relative to *GAPDH*, *PPIA*, and *mRPL19* as per GeNorm (<http://medgen.ugent.be/~jvdesomp/genorm/#introduction>).

Immunoblot

Protein lysates in RIPA buffer were prepared as previously described [59] and immunostained with anti-AR (N20, Santa Cruz Biotechnology), anti-FKBP5 (H100, Santa Cruz Biotechnology), anti-alpha tubulin (05-829, Millipore, Bedford, MA), or anti-β-actin (A1978, Sigma-Aldrich).

Proliferation, adhesion and motility

Proliferative response of PShTert-AR or C4-2B cells to DHT and or BIC was measured in quadruplicate via Trypan blue exclusion. Adhesion of PShTert-AR, PShTert-ctrl, or C4-2B cells was measured using an adhesion assay as described previously [62]. Briefly, 5×10^4 PShTert-AR, PShTert-ctrl, or C4-2B cells were added to 24-well plates containing treatment media and left to adhere for 15-240 min at 37°C. Media was removed and cells were washed with PBS before manual counting. Cellular attachment (trypsinization resistance) was measured using a crystal violet assay adapted from a previous study [62]. Briefly, PShTert-AR or C4-2B cells were plated in stripped media (5×10^4 cells/well in 96 well plates) overnight and treated with 1-100 nM DHT ± 10 μM BIC or equivalent vehicle control for 16 h. Cells were washed with PBS and incubated with trypsin for 2.5 - 15 min. Cells were washed, ethanol fixed and stained with 1% crystal violet solution. Dye was eluted from cells with 10% glacial acetic acid and the concentration measured at an absorbance of 595 nm. Motility and invasion was tested described previously [63], using calcein labelled C4-2B cells were applied to modified Boyden chambers (ChemoTx, Neuro Probe). Calcein AM was measured in the bottom wells using a FLUOstar OPTIMA plate reader at 480 nm excitation and

520 nm emission wavelengths.

Conditioned matrix

Matrices produced from confluent fibroblasts treated with 50 μg/ml ascorbic acid and 10 nM DHT or vehicle or 10 μM BIC, were decellularized with EDTA and used in adhesion assays (above) and trypsinization assays adapted from previous descriptions [62].

3D-matrices

3D-matrices were produced from DHT or vehicle treated fibroblasts seeded into gelatin coated wells as previously described [43]. After decellularization with extraction buffer containing PBS, 0.28% ammonium hydroxide (Sigma-Aldrich), and 0.5% Triton-X (Sigma-Aldrich), the remaining 3D-matrix was used for adherence, proliferation, invasion, and motility/gap closure assays.

When the cells had grown to 100% confluence, media was replaced with stripped media supplemented with 50 μg/ml ascorbic acid and 10 nM DHT or equivalent vehicle control. Treatment was repeated every 48 h. After 8 days, myofibroblasts were removed via an extraction buffer containing PBS, 0.28% ammonium hydroxide (Sigma-Aldrich), and 0.5% Triton-X (Sigma-Aldrich). Remaining 3D matrix was gently washed in PBS prior to adherence, proliferation and invasion assays.

For cancer cell gap closure assays, into each well, sterile silicon culture-inserts (Ibidi 80209) were positioned into wells containing 3-D matrices, and PC3 cells (3.5×10^4 cells per chamber) in stripped medium were aliquoted. Following 16h by incubation, Ibidi inserts were removed, leaving a 500 μm cell-free gap. Migration of PC3 cells across the gap was monitored for 0, 3, 7, 11, and 15 h time-points, using a Zeiss Axio Observer.Z1 with HBO 100 microscope illuminating system (Zeiss, Göttingen, Germany). Migration was measuring as cell-free gap-closure using AxioVision Rel 4.8 software, and analysed with the MRI Wound Healing Tool (ImageJ software, version 1.47v).

ACKNOWLEDGMENTS

The authors would like to acknowledge the South Australian Prostate Cancer Clinical Outcomes Collaborative in cohort assembly and clinical data collation. Drs Claudine Bonder, Carmella Ricciardelli, and Margaret Centenera provided methodological assistance, Aleksandra Ochnik assisted in TMA construction, and Melissa Papagiris in fresh patient tissues collection through the Australian Prostate Cancer Bioresource.

CONFLICTS OF INTEREST

The authors disclose no potential conflicts of interest.

GRANT SUPPORT

This work was funded by the Prostate Cancer Foundation of Australia (GB, PG2210; RT, PG0810), Foundation Daw Park (SC, GG, CBP), seed funding from the Freemasons Foundation Centre for Men's Health (GB), the US Department of Defense Prostate Cancer Research Program (PL, PC080010), National Health and Medical Research Council of Australia (RT, ID:606492), the National Institutes of Health (PL, 1U01CA149556-01), and Cancer Australia (GB, EFN, & RT, APP1032970). DAL holds an Australian Postgraduate Award, EFN holds an Early Career Fellowship from The Hospital Research Foundation, JH holds a National Breast Cancer Foundation Fellowship.

Editorial note

This paper has been accepted based in part on peer-review conducted by another journal and the authors' response and revisions as well as expedited peer-review in *Oncotarget*.

REFERENCES

1. American Cancer Society I. (2012). Cancer Facts & Figures 2012. American Cancer Society).
2. Amling CL, Blute ML, Bergstralh EJ, Seay TM, Slezak J and Zincke H. Long-term hazard of progression after radical prostatectomy for clinically localized prostate cancer: continued risk of biochemical failure after 5 years. *J Urol*. 2000; 164:101-105.
3. Freedland SJ, Humphreys EB, Mangold LA, Eisenberger M, Dorey FJ, Walsh PC and Partin AW. Risk of prostate cancer-specific mortality following biochemical recurrence after radical prostatectomy. *JAMA*. 2005; 294:433-439.
4. Saadi A, Shannon NB, Lao-Sirieix P, O'Donovan M, Walker E, Clemons NJ, Hardwick JS, Zhang C, Das M, Save V, Novelli M, Balkwill F and Fitzgerald RC. Stromal genes discriminate preinvasive from invasive disease, predict outcome, and highlight inflammatory pathways in digestive cancers. *Proc Natl Acad Sci U S A*. 2010; 107:2177-2182.
5. Ma XJ, Dahiya S, Richardson E, Erlander M and Sgroi DC. Gene expression profiling of the tumor microenvironment during breast cancer progression. *Breast Cancer Res*. 2009; 11:R7.
6. Brennen WN, Rosen DM, Wang H, Isaacs JT and Denmeade SR. Targeting carcinoma-associated fibroblasts within the tumor stroma with a fibroblast activation protein-activated prodrug. *J Natl Cancer Inst*. 2012; 104:1320-1334.
7. Hanson JA, Gillespie JW, Grover A, Tangrea MA, Chuaqui RF, Emmert-Buck MR, Tangrea JA, Libutti SK, Linehan WM and Woodson KG. Gene promoter methylation in prostate tumor-associated stromal cells. *J Natl Cancer Inst*. 2006; 98:255-261.
8. Cunha GR, Donjacour AA, Cooke PS, Mee S, Bigsby RM, Higgins SJ and Sugimura Y. The endocrinology and developmental biology of the prostate. *Endocr Rev*. 1987; 8:338-362.
9. Chung LW, Anderson NG, Neubauer BL, Cunha GR, Thompson TC and Rocco AK. Tissue interactions in prostate development: roles of sex steroids. *Prog Clin Biol Res*. 1981; 75A:177-203.
10. Thompson TC, Cunha GR, Shannon JM and Chung LW. Androgen-induced biochemical responses in epithelium lacking androgen receptors: characterization of androgen receptors in the mesenchymal derivative of urogenital sinus. *J Steroid Biochem*. 1986; 25:627-634.
11. Barron DA and Rowley DR. The reactive stroma microenvironment and prostate cancer progression. *Endocr Relat Cancer*. 2012; 19:R187-204.
12. Clark AK, Taubenberger AV, Taylor RA, Niranjana B, Chea ZY, Zotenko E, Sieh S, Pedersen JS, Norden S, Frydenberg M, Grummet JP, Pook DW, Stirzaker C, Clark SJ, Lawrence MG, Ellem SJ, et al. A bioengineered microenvironment to quantitatively measure the tumorigenic properties of cancer-associated fibroblasts in human prostate cancer. *Biomaterials*. 2013; 34:4777-4785.
13. Cunha GR, Rieke W, Thomson A, Marker PC, Risbridger G, Hayward SW, Wang YZ, Donjacour AA and Kurita T. Hormonal, cellular, and molecular regulation of normal and neoplastic prostatic development. *J Steroid Biochem Mol Biol*. 2004; 92:221-236.
14. Tuxhorn JA, Ayala GE, Smith MJ, Smith VC, Dang TD and Rowley DR. Reactive stroma in human prostate cancer: induction of myofibroblast phenotype and extracellular matrix remodeling. *Clin Cancer Res*. 2002; 8:2912-2923.
15. Schor SL, Schor AM and Rushton G. Fibroblasts from cancer patients display a mixture of both foetal and adult-like phenotypic characteristics. *J Cell Sci*. 1988; 90:401-407.
16. Olumi AF, Grossfeld GD, Hayward SW, Carroll PR, Tlsty TD and Cunha GR. Carcinoma-associated fibroblasts direct tumor progression of initiated human prostatic epithelium. *Cancer Res*. 1999; 59:5002-5011.
17. Franco OE, Jiang M, Strand DW, Peacock J, Fernandez S, Jackson RS, 2nd, Revelo MP, Bhowmick NA and Hayward SW. Altered TGF-beta signaling in a subpopulation of human stromal cells promotes prostatic carcinogenesis. *Cancer Res*. 2011; 71:1272-1281.
18. Taylor RA, Toivanen R, Frydenberg M, Pedersen J, Harewood L, Australian Prostate Cancer B, Collins AT,

- Maitland NJ and Risbridger GP. Human epithelial basal cells are cells of origin of prostate cancer, independent of CD133 status. *Stem Cells*. 2012; 30:1087-1096.
19. Bhowmick NA, Neilson EG and Moses HL. Stromal fibroblasts in cancer initiation and progression. *Nature*. 2004; 432:332-337.
 20. Bhowmick NA, Chytil A, Plieth D, Gorska AE, Dumont N, Shappell S, Washington MK, Neilson EG and Moses HL. TGF-beta signaling in fibroblasts modulates the oncogenic potential of adjacent epithelia. *Science*. 2004; 303:848-851.
 21. Ao M, Franco OE, Park D, Raman D, Williams K and Hayward SW. Cross-talk between paracrine-acting cytokine and chemokine pathways promotes malignancy in benign human prostatic epithelium. *Cancer Res*. 2007; 67:4244-4253.
 22. Joesting MS, Perrin S, Elenbaas B, Fawell SE, Rubin JS, Franco OE, Hayward SW, Cunha GR and Marker PC. Identification of SFRP1 as a candidate mediator of stromal-to-epithelial signaling in prostate cancer. *Cancer Res*. 2005; 65:10423-10430.
 23. Navab R, Strumpf D, Bandarchi B, Zhu CQ, Pintilie M, Ramnarine VR, Ibrahimov E, Radulovich N, Leung L, Barczyk M, Panchal D, To C, Yun JJ, Der S, Shepherd FA, Jurisica I, et al. Prognostic gene-expression signature of carcinoma-associated fibroblasts in non-small cell lung cancer. *Proc Natl Acad Sci U S A*. 2011; 108:7160-7165.
 24. Planche A, Bacac M, Provero P, Fusco C, Delorenzi M, Stehle JC and Stamenkovic I. Identification of prognostic molecular features in the reactive stroma of human breast and prostate cancer. *PLoS One*. 2011; 6:e18640.
 25. Wikstrom P, Marusic J, Stattin P and Bergh A. Low Stroma Androgen Receptor Level in Normal and Tumor Prostate Tissue Is Related to Poor Outcome in Prostate Cancer Patients. *Prostate*. 2009; 69:799-809.
 26. Cunha GR, Chung LW, Shannon JM, Taguchi O and Fujii H. Hormone-induced morphogenesis and growth: role of mesenchymal-epithelial interactions. *Recent Prog Horm Res*. 1983; 39:559-598.
 27. Scher HI, Buchanan G, Gerald W, Butler LM and Tilley WD. Targeting the androgen receptor: improving outcomes for castration-resistant prostate cancer. *Endocr Relat Cancer*. 2004; 11:459-476.
 28. Tindall DJ and Rittmaster RS. The rationale for inhibiting 5alpha-reductase isoenzymes in the prevention and treatment of prostate cancer. *J Urol*. 2008; 179:1235-1242.
 29. Feldman BJ and Feldman D. The development of androgen-independent prostate cancer. *Nat Rev Cancer*. 2001; 1:34-45.
 30. Cunha GR and Donjacour A. Stromal-epithelial interactions in normal and abnormal prostatic development. *Prog Clin Biol Res*. 1987; 239:251-272.
 31. Li Y, Li CX, Ye H, Chen F, Melamed J, Peng Y, Liu J, Wang Z, Tsou HC, Wei J, Walden P, Garabedian MJ and Lee P. Decrease in stromal androgen receptor associates with androgen-independent disease and promotes prostate cancer cell proliferation and invasion. *J Cell Mol Med*. 2008; 12:2790-2798.
 32. Ricciardelli C, Choong CS, Buchanan G, Vivekanandan S, Neufing P, Stahl J, Marshall VR, Horsfall DJ and Tilley WD. Androgen receptor levels in prostate cancer epithelial and peritumoral stromal cells identify non-organ confined disease. *Prostate*. 2005; 63:19-28.
 33. Henshall SM, Quinn DI, Lee CS, Head DR, Golovsky D, Brenner PC, Delprado W, Stricker PD, Grygiel JJ and Sutherland RL. Altered expression of androgen receptor in the malignant epithelium and adjacent stroma is associated with early relapse in prostate cancer. *Cancer Res*. 2001; 61:423-427.
 34. Olapade-Olaopa EO, MacKay EH, Taub NA, Sandhu DP, Terry TR and Habib FK. Malignant transformation of human prostatic epithelium is associated with the loss of androgen receptor immunoreactivity in the surrounding stroma. *Clin Cancer Res*. 1999; 5:569-576.
 35. Lawrence MG, Taylor RA, Toivanen R, Pedersen J, Norden S, Pook DW, Frydenberg M, Papargiris MM, Niranjan B, Richards MG, Wang H, Collins AT, Maitland NJ and Risbridger GP. A preclinical xenograft model of prostate cancer using human tumors. *Nat Protoc*. 2013; 8:836-848.
 36. Shang Y and Brown M. Molecular determinants for the tissue specificity of SERMs. *Science*. 2002; 295:2465-2468.
 37. Gregory CW, Johnson RT, Jr., Mohler JL, French FS and Wilson EM. Androgen receptor stabilization in recurrent prostate cancer is associated with hypersensitivity to low androgen. *Cancer Res*. 2001; 61:2892-2898.
 38. Santra MK, Wajapeyee N and Green MR. F-box protein FBXO31 mediates cyclin D1 degradation to induce G1 arrest after DNA damage. *Nature*. 2009; 459:722-725.
 39. Heitzer MD and DeFranco DB. Hic-5/ARA55, a LIM domain-containing nuclear receptor coactivator expressed in prostate stromal cells. *Cancer Res*. 2006; 66:7326-7333.
 40. Matsuya M, Sasaki H, Aoto H, Mitaka T, Nagura K, Ohba T, Ishino M, Takahashi S, Suzuki R and Sasaki T. Cell adhesion kinase beta forms a complex with a new member, Hic-5, of proteins localized at focal adhesions. *J Biol Chem*. 1998; 273:1003-1014.
 41. Leach DA, Need EF, Trotta AP, Grubisha MJ, DeFranco DB and Buchanan G. Hic-5 influences genomic and non-genomic actions of the androgen receptor in prostate myofibroblasts. *Mol Cell Endocrinol*. 2014; 384:185-199.
 42. Palumbo A, Jr., Ferreira LB, Reis de Souza PA, Oliveira FL, Pontes B, Viana NB, Machado DE, Palmero CY, Alves LM, Gimba ER and Nasciutti LE. Extracellular matrix secreted by reactive stroma is a main inducer of pro-tumorigenic features on LNCaP prostate cancer cells. *Cancer Lett*. 2012; 321:55-64.
 43. Castello-Cros R and Cukierman E. Stromagenesis during tumorigenesis: characterization of tumor-associated fibroblasts and stroma-derived 3D matrices. *Methods Mol*

- Biol. 2009; 522:275-305.
44. Sutcliffe P, Hummel S, Simpson E, Young T, Rees A, Wilkinson A, Hamdy F, Clarke N and Staffurth J. Use of classical and novel biomarkers as prognostic risk factors for localised prostate cancer: a systematic review. *Health Technol Assess.* 2009; 13:iii, xi-xiii 1-219.
 45. Ehrbar M, Sala A, Lienemann P, Ranga A, Mosiewicz K, Bittermann A, Rizzi SC, Weber FE and Lutolf MP. Elucidating the role of matrix stiffness in 3D cell migration and remodeling. *Biophys J.* 2011; 100:284-293.
 46. Peyton SR and Putnam AJ. Extracellular matrix rigidity governs smooth muscle cell motility in a biphasic fashion. *J Cell Physiol.* 2005; 204:198-209.
 47. Levental KR, Yu H, Kass L, Lakins JN, Egeblad M, Erler JT, Fong SF, Csiszar K, Giaccia A, Weninger W, Yamauchi M, Gasser DL and Weaver VM. Matrix crosslinking forces tumor progression by enhancing integrin signaling. *Cell.* 2009; 139:891-906.
 48. Kauppila S, Bode MK, Stenback F, Risteli L and Risteli J. Cross-linked telopeptides of type I and III collagens in malignant ovarian tumours in vivo. *Br J Cancer.* 1999; 81:654-661.
 49. Kauppila S, Stenback F, Risteli J, Jukkola A and Risteli L. Aberrant type I and type III collagen gene expression in human breast cancer in vivo. *J Pathol.* 1998; 186:262-268.
 50. Niu Y, Altuwajri S, Lai KP, Wu CT, Ricke WA, Messing EM, Yao J, Yeh S and Chang C. Androgen receptor is a tumor suppressor and proliferator in prostate cancer. *Proc Natl Acad Sci U S A.* 2008; 105:12182-12187.
 51. Shigemura K, Isotani S, Wang R, Fujisawa M, Gotoh A, Marshall FF, Zhou HE and Chung LW. Soluble factors derived from stroma activated androgen receptor phosphorylation in human prostate LNCaP cells: roles of ERK/MAP kinase. *Prostate.* 2009; 69:949-955.
 52. Tanner MJ, Welliver RC, Jr., Chen M, Shtutman M, Godoy A, Smith G, Mian BM and Buttyan R. Effects of androgen receptor and androgen on gene expression in prostate stromal fibroblasts and paracrine signaling to prostate cancer cells. *PLoS One.* 2011; 6:e16027.
 53. Lai KP, Yamashita S, Huang CK, Yeh S and Chang C. Loss of stromal androgen receptor leads to suppressed prostate tumorigenesis via modulation of pro-inflammatory cytokines/chemokines. *EMBO Mol Med.* 2012; 4:791-807.
 54. Ricke EA, Williams K, Lee YF, Couto S, Wang Y, Hayward SW, Cunha GR and Ricke WA. Androgen hormone action in prostatic carcinogenesis: stromal androgen receptors mediate prostate cancer progression, malignant transformation and metastasis. *Carcinogenesis.* 2012;33:1391-1398.
 55. Marques RB, Erkens-Schulze S, de Ridder CM, Hermans KG, Waltering K, Visakorpi T, Trapman J, Romijn JC, van Weerden WM and Jenster G. Androgen receptor modifications in prostate cancer cells upon long-term androgen ablation and antiandrogen treatment. *Int J Cancer.* 2005; 117:221-229.
 56. Niu Y, Altuwajri S, Yeh S, Lai KP, Yu S, Chuang KH, Huang SP, Lardy H and Chang C. Targeting the stromal androgen receptor in primary prostate tumors at earlier stages. *Proc Natl Acad Sci U S A.* 2008; 105(34):12188-12193.
 57. Wu HC, Hsieh JT, Gleave ME, Brown NM, Pathak S and Chung LW. Derivation of androgen-independent human LNCaP prostatic cancer cell sublines: role of bone stromal cells. *Int J Cancer.* 1994; 57:406-412.
 58. Heitzer MD and DeFranco DB. Mechanism of action of Hic-5/androgen receptor activator 55, a LIM domain-containing nuclear receptor coactivator. *Mol Endocrinol.* 2006; 20:56-64.
 59. Need EF, Scher HI, Peters AA, Moore NL, Cheong A, Ryan CJ, Wittert GA, Marshall VR, Tilley WD and Buchanan G. A novel androgen receptor amino terminal region reveals two classes of amino/carboxyl interaction-deficient variants with divergent capacity to activate responsive sites in chromatin. *Endocrinology.* 2009; 150:2674-2682.
 60. Toivanen R, Berman DM, Wang H, Pedersen J, Frydenberg M, Meeker AK, Ellem SJ, Risbridger GP and Taylor RA. Brief report: a bioassay to identify primary human prostate cancer repopulating cells. *Stem Cells.* 2011; 29:1310-1314.
 61. Trotta AP, Need EF, Butler LM, Selth LA, O'Loughlin MA, Coetzee GA, Tilley WD and Buchanan G. Subdomain structure of the co-chaperone SGTA and activity of its androgen receptor client. *J Mol Endocrinol.* 2012; 49:57-68.
 62. Humphries MJ. Cell adhesion assays. *Methods Mol Biol.* 2009; 522:203-210.
 63. Ween MP, Hummitzsch K, Rodgers RJ, Oehler MK and Ricciardelli C. Versican induces a pro-metastatic ovarian cancer cell behavior which can be inhibited by small hyaluronan oligosaccharides. *Clin Exp Metastasis.* 2011; 28:113-125.

Stromal androgen receptor regulates the composition of the microenvironment to influence prostate cancer outcome

Supplementary Material

Supplementary Table 1: PCR Primers

Use [@]	Gene [%]	Direction	Sequence [*]	Refs [#]
Q	GAPDH	forward	GTCATGGGTGTGAACCATGAGA	(11)
		reverse	GGTCATGAGTCCTTCCACGATAC	
Q	PSA	forward	GGCAGCATTGAACCAGAGGAG	(11)
		reverse	GCATGAACCTTGGTCACCTTCTG	
Q	FKBP5	forward	ATTATCCGGAGAACCAAACG	
		reverse	CAAACATCCTTCCACCACAG	
Q	ABCC4	forward	CCCCGTGGGAGCAGGGAAGT	
		reverse	CCGAGAACACCCAGGGCTGC	
Q	WNT5A	forward	AAGGAGTTCGTGGACGCCCG	
		reverse	GCAGGCCACATCAGCCAGGT	
Q	SLC45A3	forward	GCCTCCCTCTACCACCGGGA	
		reverse	GCCTGGCAGGAAGCTGGTCA	
Q	NKX3-1	forward	CCGAGACGCTGGCAGAGACC	
		reverse	GTGGGAGAAGGCAGCTCGGG	
Q	FBXO32	forward	CCCTTCAGCTCTGCAAACACTGTC	
		reverse	CTCCAGTCAGCAGGGGGACC	
Q	TGFB3	forward	GGCCCTTGCCCATACCTCCG	
		reverse	AGCAAGGCGAGGCAGATGCT	
Q	FGF5	forward	CGGATGGCAAAGTCAATGGATCC	
		reverse	CGCTCCCTGAACTTGCAGTCAT	
Q	PPIA	forward	GCATACGGGTCCTGGCAT	
		reverse	ACATGCTTGCCATCCAACC	
Q	MRPL19	forward	TGCCAGTGGAAAATCAGCCA	
		reverse	CAAAGCAAATCTCGACACCTTG	
Q	FBN1	forward	CTCCTGGAAGTTTTGTGTACCTGC	
		reverse	GGGCTGTTCTTGACAGACTCCATTA	
Q	COL1A1	forward	AGGGCTCCAACGAGATCGAGATCCG	
		reverse	TACAGGAAGCAGACAGGGCCAACGTCG	
Q	COL3A1	forward	AGCTGGCTACTTCTCGCTCTGCTT	
		reverse	CGCATAGGACTGACCAAGATGGG	
Q	COL4A6	forward	AGGACTGCAGTGGGAGCTGTCAGT	
		reverse	AGGACCTGTTGGGCCTTGAATTC	
Q	MMP1	forward	GACGTTCCAAAATCCTGTCCAG	
		reverse	GGTAGAAGGGATTTGTGCGCATGT	
C	NC2	forward	GTGAGTGCCCAAGTTAGAGCATCTA	(12)
		reverse	GGAACCAAGTGGGTCTTGAAGTG	
C	FKBP5	forward	GCTCTGACTTATTGTTCTTACTGCC	(13)
		reverse	TTGCTGTCAGCACATCGAGTTCA	
C	PSA	forward	GCCTGGATCTGAGAGATATCATC	(11)
		reverse	ACACCTTTTTTTTTCTGGATTGTTG	
C	FBXO32	forward	GGCTCTCCAGCCGTGCATGA	
		reverse	AGCAGGTGTGCACGTCCCTC	

@ Primers used in either RT-QPCR (Q) or ChIP (C)

% Gene primer raised against

* Sequence primer raised against

Reference for primers used, were applicable

Supplementary Table 2: Androgens enrich different cell functional pathways in fibroblasts compared to epithelial cells

Category name [®]	PshTERT-AR			C4-2B		
	Fold Enrichment [%]	p value [#]	No. of Genes* examples	Fold Enrichment [%]	p value [#]	No. of Genes* examples
GO.0007155~cell adhesion	+ 1.83	0.004	36 CLDN7, ARHGAP6, PTK2B, LYVE1	NR -	-	0 -
GO.0007156~homophilic cell adhesion	+ 3.39	0.5E-04	9 PCDH8, CADM1, PCDH2, PCDH9	- 1.78	0.30	5 PCDH2, CELSR1, CDH3, CDH6
GO.0005578~proteinaceous extracellular matrix	+ 3.06	5.0E-05	19 LOX, WNT5A, LUM, COL3A1	NR 0.00	-	0 -
GO.0005583~fibrillar collagen	+ 1.06	0.03	3 LUM, COL3A1, COL5A2	NR 0.00	-	0 -
GO.0032963~collagen metabolic process	+ 5.80	0.03	4 HIF1A, COL3A1, ADAMTS3, ADAMTS2	NR 0.00	-	0 -
GO.0042981~regulation of apoptosis	+ 1.78	0.05	29 IER3, TRAIIP, BIRC5, TGFB3	- 1.63	0.0128	28 BLACF1, NFKB1, BARD1, TP53INP1
GO.0001568~blood vessel development	- 0.91	0.736	6 ARHGAP22, VEGFC, MYOCD, JUN	+ 2.18	0.0125	14 VEGFA, THBS1, ANGPT2, ZMIZ1
GO.0022403~cell cycle phase	- 8.35	7.82E-75	96 CDKN1A, PPP3CA, CCNG1, PPP1CB	NR -	-	0 -
GO.0000278~mitotic cell cycle	- 7.80	9.31E-39	96 CDKN1A, PPP3CA, CCNG1, PPP1CB	NR -	-	0 -
GO.0040017~positive regulation of locomotion	- 2.45	0.044	8 PLD1, PDGFRB, THBS1, SCG2	+ 3.8	0.01	10 IL8, JUB, LAMB1, ITGA
GO.0040017~positive regulation of cell motion	- 2.45	0.04	8 PTK2B, BCL6, JAK2, THBS1	+ 1.8	0.01	10 LYN, JUB, LAMB1, ITGA
GO.0051726~regulation of cell cycle	- 4.90	4.35E-22	54 KNTC1, MYC, CDK1, JUN	NR -	-	0 -
GO.0000087~M phase of mitotic cell cycle	- 13.52	6.18E-68	79 CDK2, KIF2C, NCAPD3, CDCA8	+ 0.68	0.94	4 MPHOSPH9, MAP9, CDC26, NCAPD3
GO.0010740~positive regulation of protein kinase cascade	NR 0.00	-	0 -	+ 3.65	0.00003	16 HIPK2, TICAM2, TGM2, KCNKG
GO.0009967~positive regulation of signal transduction	NR 0.00	-	0 -	+ 2.58	0.0003	20 GOLT1B, TAOK3, PCK2, HIPK2

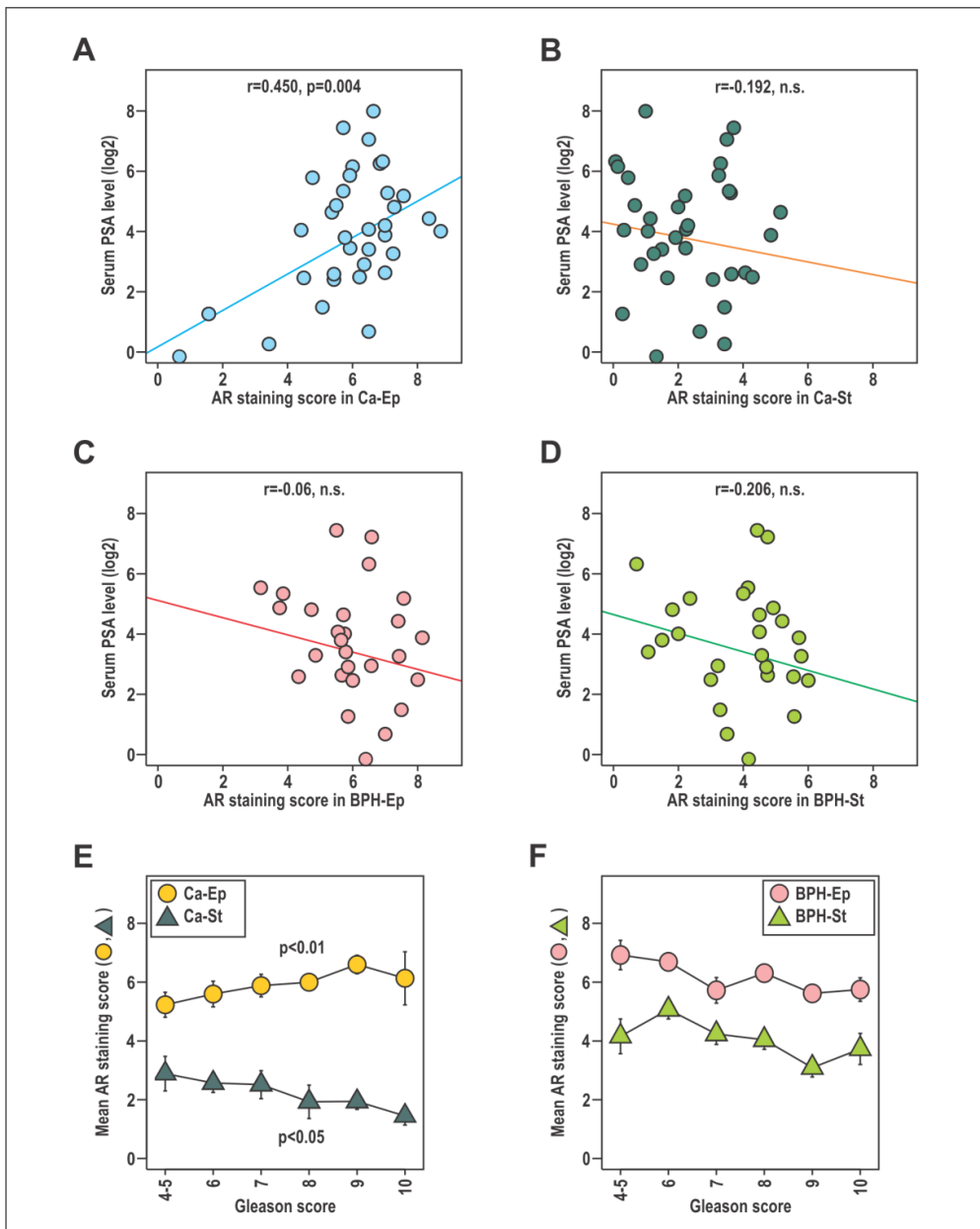
@ Functional pathway analysis of the top up and down genes regulated by androgen in C4-2B and PShTert-AR cells.

% Fold change in functional pathway enrichment or depletion

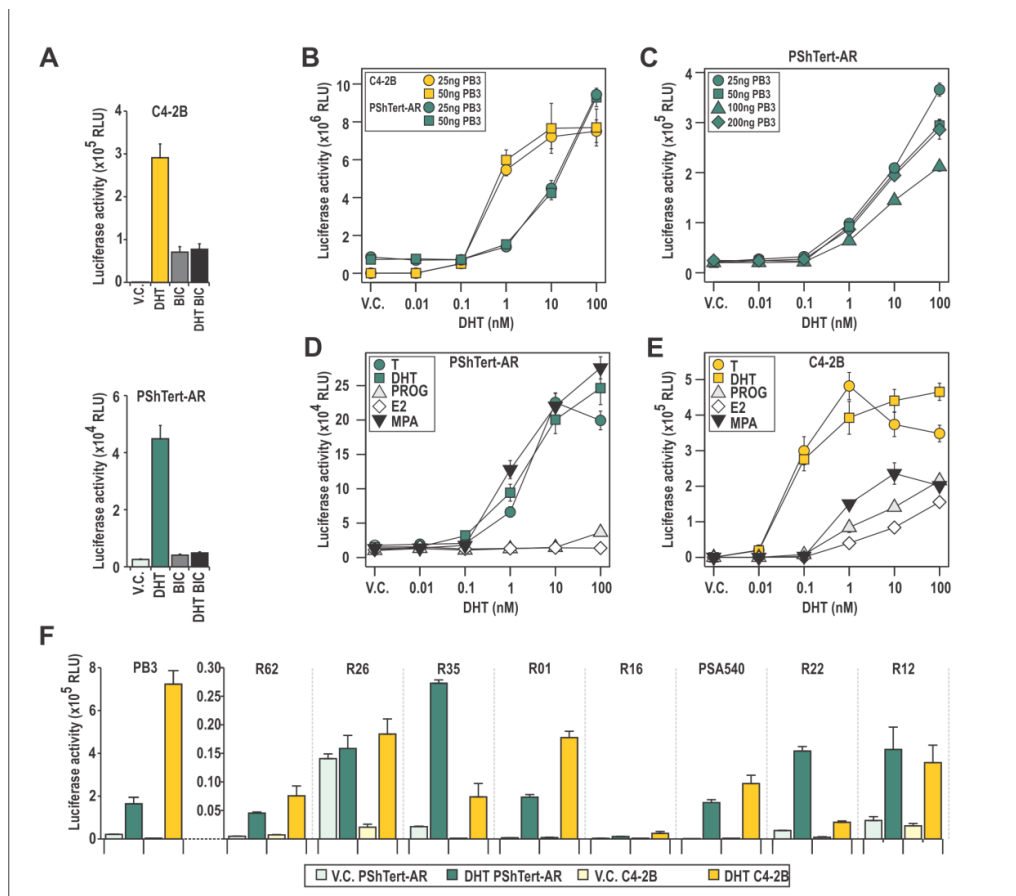
* Number of regulated genes in each category out of the 1000 genes initially inputted from each cell type

Modified Fisher Exact P-Value score

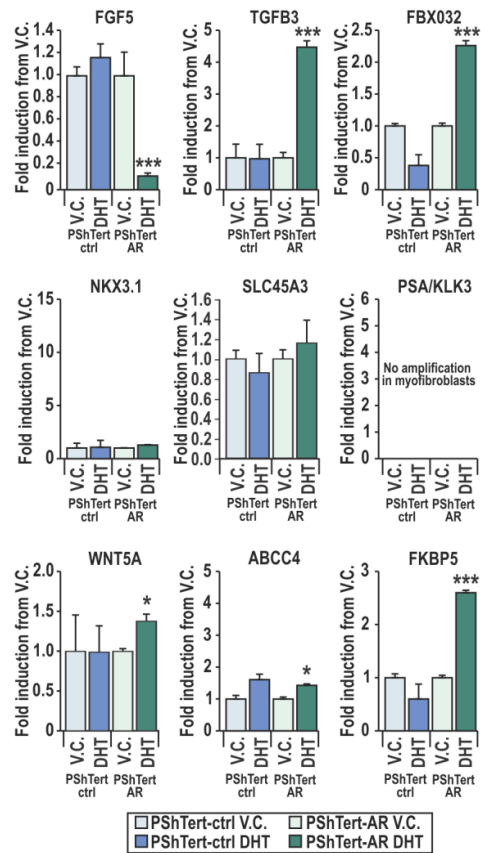
NR = not regulated. +/- represents direction of regulation



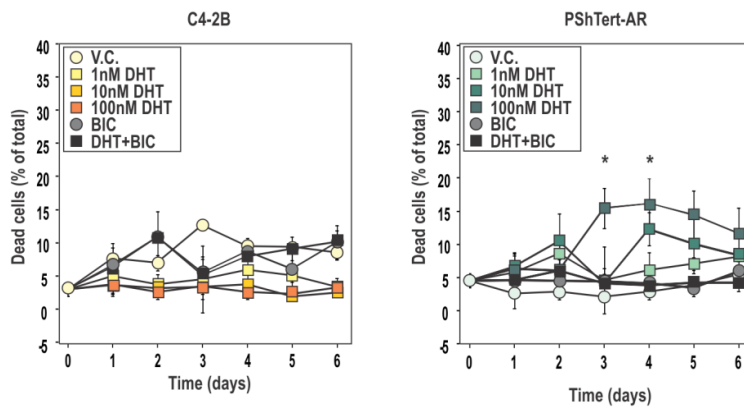
Supplementary Figure S1: Stromal and epithelial AR in relation to Gleason grade and serum PSA. **A-D.** The average AR score from each compartment in benign or cancerous state were analyzed in relation to serum PSA. **E.** Mean AR scores for stromal (St) and epithelial (Ep) compartments in patient BPH samples (stained overnight with anti-AR N20) were analyzed in relation to Gleason grade of the matched cancer sample.



Supplementary Figure S2: Fibroblast and epithelial androgen signaling in response to reporter concentration and different ligands. **A**. C4-2B and PShTert-AR cells were transfected with probasin reporter (PB3) and treated with 10 nM vehicle or DHT in the presence or absence of bicalutamide (BIC). **B-C**. C4-2B and PShTert-AR cells were transfected with 25-200 ng of PB3 reporter vector and treated with 0-100 nM DHT as described in materials and methods. Data represents mean \pm SEM of six independently transfected wells. **D,E**. PShTert-AR (**D**) and C4-2B (**E**) cells were transfected with 25 ng probasin reporter (PB3) and treated with 0-100 nM testosterone (T), dihydrotestosterone (DHT), progesterone (PROG), estradiol (E2), and medroxyprogesterone acetate (MPA). **F**. C4-2B and PShTert-AR cells were transfected with a variety of AR reporter constructs as described in (4, 12, 14), and stimulated with 10 nM DHT. Data represents mean \pm SEM relative light units (RLU) of six independently transfected wells.

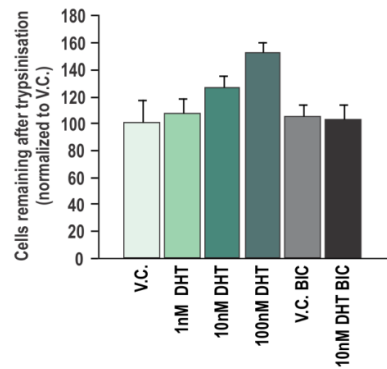


Supplementary Figure S3: Microarray validation. Triplicate RNA samples from 10 nM DHT or vehicle treated PShTert-ctrl or PShTert-AR cells were pooled and analyzed via RT-qPCR. Data represents mean + SEM of triplicate biological replicates measured in duplicate PCR samples. Significance between DHT and V.C. treatments was calculated via Student's T-test; * $p < 0.05$, ** $p < 0.01$, *** $p < 0.001$.

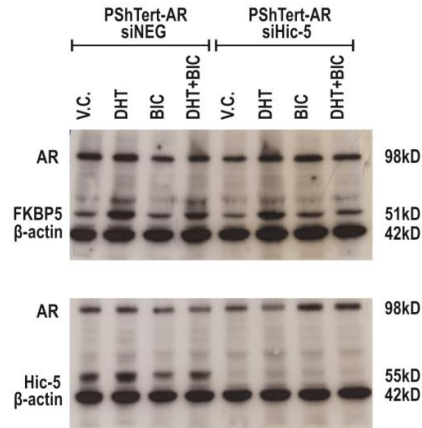


Supplementary Figure S4: Cell death in response to androgen treatment.

PShTert-AR or C4-2B cells (1.5×10^3 cells/well in 24 well plates) were treated with 0.1-100 nM DHT, and/or 10 μ M bicalutamide (BIC), or equivalent vehicle control. Dead cells were analyzed as previously described (15), and are presented as the mean \pm SEM of the percentage of total cells.

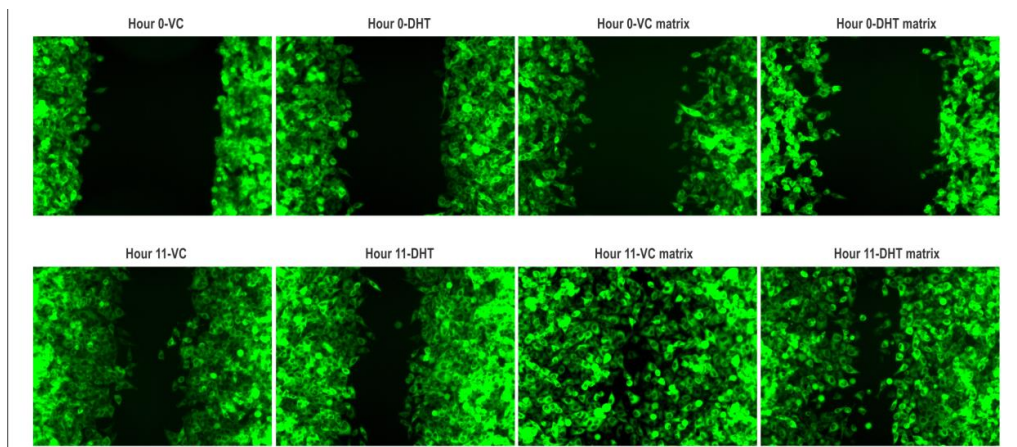


Supplementary Figure S5: PShTert-AR cells (1×10^4 cells/well in 96 well plates) were treated with 0.1-100 nM DHT, and/or 10 μ M bicalutamide (BIC), or equivalent vehicle control. Cells were treated with trypsin for 5 minutes, and remaining attached cells were stained with crystal violet. Data represents mean \pm SEM absorbance of six independently transfected wells and is presented as the percentage of vehicle control.



Supplementary Figure S6: Hic-5 silencing alters Hic-5 protein levels but does not affect AR transactivation of FKBP5

Lysates from PShTert-AR cells transfected with siRNA against Hic-5 or control siRNA were treated with 10 nM DHT or equivalent vehicle control (V.C.) and 10 μM bicalutamide (BIC). Lysates were prepared as described in materials and methods, and were probed using anti-AR N-20 (Santa Cruz Biotechnology), anti-FKBP5 H100 (Santa Cruz Biotechnology), and anti-Hic-5 611165 (BD Transduction Laboratories, USA). Anti-β-Actin (Millipore, Bedford, MA) was used as a loading control.



Supplementary Figure S7: PC-3 gap closure across PShTert-AR derived matrix. PC-3 cells expressing GFP were seeded onto matrices created by PShTert-AR treated with or without DHT, or non-matrix controls. Using an Ibidi chamber a 500um space was created in the PC-3 monolayer. The closure of this gap was measured over a 15 hour period.

References cited

1. Wu HC, Hsieh JT, Gleave ME, Brown NM, Pathak S, Chung LW. Derivation of androgen-independent human LNCaP prostatic cancer cell sublines: role of bone stromal cells. *Int J Cancer*. 1994 May 1;57(3):406-12. PubMed PMID: 8169003. Epub 1994/05/01. eng.
2. Li Y, Li CX, Ye H, Chen F, Melamed J, Peng Y, et al. Decrease in stromal androgen receptor associates with androgen-independent disease and promotes prostate cancer cell proliferation and invasion. *J Cell Mol Med*. 2008 Dec;12(6B):2790-8. PubMed PMID: 18266956. Epub 2008/02/13. eng.
3. Heitzer MD, DeFranco DB. Mechanism of action of Hic-5/androgen receptor activator 55, a LIM domain-containing nuclear receptor coactivator. *Mol Endocrinol*. 2006 Jan;20(1):56-64. PubMed PMID: 16141357. Epub 2005/09/06. eng.
4. Need EF, Scher HI, Peters AA, Moore NL, Cheong A, Ryan CJ, et al. A novel androgen receptor amino terminal region reveals two classes of amino/carboxyl interaction-deficient variants with divergent capacity to activate responsive sites in chromatin. *Endocrinology*. 2009 Jun;150(6):2674-82. PubMed PMID: 19282387. Pubmed Central PMCID: 2689802. Epub 2009/03/14. eng.
5. Taylor RA, Toivanen R, Frydenberg M, Pedersen J, Harewood L, Australian Prostate Cancer B, et al. Human epithelial basal cells are cells of origin of prostate cancer,

- independent of CD133 status. *Stem Cells*. 2012 Jun;30(6):1087-96. PubMed PMID: 22593016. Epub 2012/05/18. eng.
6. Lawrence MG, Taylor RA, Toivanen R, Pedersen J, Norden S, Pook DW, et al. A preclinical xenograft model of prostate cancer using human tumors. *Nat Protoc*. 2013 Apr 4;8(5):836-48. PubMed PMID: 23558784. Epub 2013/04/06. eng.
 7. Toivanen R, Berman DM, Wang H, Pedersen J, Frydenberg M, Meeker AK, et al. Brief report: a bioassay to identify primary human prostate cancer repopulating cells. *Stem Cells*. 2011 Aug;29(8):1310-4. PubMed PMID: 21674698. Epub 2011/06/16. eng.
 8. Trotta AP, Need EF, Butler LM, Selth LA, O'Loughlin MA, Coetzee GA, et al. Subdomain structure of the co-chaperone SGTA and activity of its androgen receptor client. *J Mol Endocrinol*. 2012 Oct;49(2):57-68. PubMed PMID: 22693264. Epub 2012/06/14. eng.
 9. Humphries MJ. Cell adhesion assays. *Methods Mol Biol*. 2009;522:203-10. PubMed PMID: 19247616. Epub 2009/02/28. eng.
 10. Castello-Cros R, Cukierman E. Stromagenesis during tumorigenesis: characterization of tumor-associated fibroblasts and stroma-derived 3D matrices. *Methods Mol Biol*. 2009;522:275-305. PubMed PMID: 19247611. Pubmed Central PMCID: 2670062. Epub 2009/02/28. eng.
 11. Jia L, Kim J, Shen H, Clark PE, Tilley WD, Coetzee GA. Androgen receptor activity at the prostate specific antigen locus: steroidal and non-steroidal mechanisms. *Mol Cancer Res*. 2003 Mar;1(5):385-92. PubMed PMID: 12651911. Epub 2003/03/26. eng.
 12. Jia L, Berman BP, Jariwala U, Yan X, Cogan JP, Walters A, et al. Genomic androgen receptor-occupied regions with different functions, defined by histone acetylation, coregulators and transcriptional capacity. *PLoS One*. 2008;3(11):e3645. PubMed PMID: 18997859. Pubmed Central PMCID: 2577007. Epub 2008/11/11. eng.
 13. Denny WB, Prapapanich V, Smith DF, Scammell JG. Structure-function analysis of squirrel monkey FK506-binding protein 51, a potent inhibitor of glucocorticoid receptor activity. *Endocrinology*. 2005 Jul;146(7):3194-201. PubMed PMID: 15802496. Epub 2005/04/02. eng.
 14. Buchanan G, Ricciardelli C, Harris JM, Prescott J, Yu ZC, Jia L, et al. Control of androgen receptor signaling in prostate cancer by the cochaperone small glutamine rich tetratricopeptide repeat containing protein alpha. *Cancer Res*. 2007 Oct 15;67(20):10087-96. PubMed PMID: 17942943. Epub 2007/10/19. eng.
 15. Marrocco DL, Tilley WD, Bianco-Miotto T, Evdokiou A, Scher HI, Rifkind RA, et al. Suberoylanilide hydroxamic acid (vorinostat) represses androgen receptor expression and acts synergistically with an androgen receptor antagonist to inhibit prostate cancer cell proliferation. *Mol Cancer Ther*. 2007 Jan;6(1):51-60. PubMed PMID: 17218635. Epub 2007/01/16. eng.

**CHAPTER 4: MYOFIBROBLAST ANDROGEN RECEPTOR
EXPRESSION DETERMINES CELL SURVIVAL IN CO-
CULTURES OF MYOFIBROBLASTS AND PROSTATE
CANCER CELLS IN VITRO**

Helen M Palethorpe¹, Damien A Leach¹, Eleanor F Need¹, Paul A Drew^{1,2*}, Eric Smith^{1,3*}

¹Discipline of Surgical Specialities, The University of Adelaide, Basil Hetzel Institute for Translational Health Research, The Queen Elizabeth Hospital, The University of Adelaide, 28 Woodville Road, Woodville South, SA 5011, Australia;

²School of Nursing and Midwifery, Flinders University, PO Box 2100, Adelaide, SA 5001, Australia;

³Department of Medical Oncology, Basil Hetzel Institute for Translational Health Research, The Queen Elizabeth Hospital, 28 Woodville Rd, Woodville South, SA 5011, Australia.

*Equal contributors

Molecular Cancer 2017; submitted paper

Statement of Authorship

Title of Paper	Myofibroblast androgen receptor expression determines cell survival in co-cultures of myofibroblasts and prostate cancer cells in vitro
Publication Status	Submitted for publication
Publication Details	Palethorpe HM , Leach DL, Need EF, Drew PA, Smith E: Myofibroblast androgen receptor expression determines cell survival in co-cultures of myofibroblasts and prostate cancer cells in vitro . Submitted to <i>Molecular Cancer</i> 2017.

Principal Author

Name of Principal Author (Candidate)	Helen M Palethorpe		
Contribution to the Paper	Conceived and designed the experiments, performed the experiments, analysed the data and wrote the manuscript.		
Overall percentage (%)	80%		
Certification:	This paper reports on original research I conducted during the period of my Higher Degree by Research candidature and is not subject to any obligations or contractual agreements with a third party that would constrain its inclusion in this thesis. I am the primary author of this paper.		
Signature		Date	01/03/17

Co-Author Contributions

By signing the Statement of Authorship, each author certifies that:

- i. the candidate's stated contribution to the publication is accurate (as detailed above);
- ii. permission is granted for the candidate to include the publication in the thesis; and
- iii. the sum of all co-author contributions is equal to 100% less the candidate's stated contribution.

Name of Co-Author	Damien A. Leach		
Contribution to the Paper	Participated in the analysis of results and provided critical evaluation of the manuscript.		
Signature		Date	10/07/2017

Name of Co-Author	Eleanor F. Need		
Contribution to the Paper	Participated in the analysis of results and provided critical evaluation of the manuscript.		
Signature		Date	09/07/2017

Name of Co-Author	Paul A. Drew		
Contribution to the Paper	Conceived and designed the experiments, analysed the data, wrote the manuscript.		
Signature		Date	01/03/17

Name of Co-Author	Eric Smith		
Contribution to the Paper	Conceived and designed the experiments, analysed the data, wrote the manuscript.		
Signature		Date	01/03/17

ABSTRACT

Background

Fibroblasts express the androgen receptor (AR) in the normal prostate and early during prostate cancer development. We have previously shown that loss of AR expression in prostate cancer-associated fibroblasts is a poor prognostic indicator. Here we investigated the outcomes of direct and indirect co-cultures of immortalised AR-positive (PShTert-AR) or AR-negative (PShTert) myofibroblasts and the prostate cancer cell line, PC3.

Methods

To differentiate the cells, prostate myofibroblasts were stably transduced with red fluorescent protein and the prostate cancer cell line, PC3, with green fluorescent protein. The PC3 cells were co-cultured with myofibroblasts in direct co-culture or in transwells (indirect co-culture), or were grown in myofibroblast conditioned culture medium (CCM). To determine the effect of androgen receptor signalling, cultures were supplemented with the AR ligand, 5 α -dihydrotestosterone (DHT), or vehicle, with or without bicalutamide. Outcome measures included cell morphology, counts, proliferation, cell cycle analysis and apoptosis.

Results

There was a significant reduction in PC3 cell counts following direct and indirect co-culture with PShTert-AR myofibroblasts compared to PShTert myofibroblasts ($P < 0.0001$). Microscopically, in direct co-culture, the PC3 cells were lost with the PShTert-AR myofibroblasts, whereas with the PShTert they formed cohesive rafts of cells and there was total loss of the underlying and adjacent myofibroblasts. The PShTert-AR myofibroblasts induced PC3 cell apoptosis by paracrine signalling, and PC3 cells induced PShTert myofibroblast apoptosis by juxtacrine signalling. The addition of DHT to cultures moderated, but did not prevent, the effects of the PShTert-AR myofibroblasts, and did not alter the effect of the PShTert myofibroblasts.

Conclusions

These results suggest, at least in part, an explanation for the clinical observation that a reduction in stromal AR expression is associated with a poorer outcome, and a mechanism by which the stroma may inhibit or promote prostate cancer progression.

Keywords

Prostate cancer - Tumour-stroma crosstalk - Direct co-culture - Androgen receptor - PShTert-AR myofibroblast - PShTert myofibroblast - PC3 cell

BACKGROUND

Androgens are essential for the normal development of the prostate, and, in the adult, are required for prostate epithelial cell survival and function. In the early phases of prostate development the androgen receptor (AR) is expressed exclusively in mesenchymal cells, which in turn regulate epithelial cell growth and differentiation, and thereby prostate size [1]. In the adult prostate, AR is expressed in both stromal and epithelial compartments [2, 3]. Here androgens help maintain stromal smooth muscle and epithelial differentiation and function via reciprocal stromal-epithelial cell interactions [2].

Androgens and AR also play a pivotal role in the development and progression of prostate cancer. The majority of studies investigating the role of AR in prostate cancer have focused on its function in the malignant epithelial cells, however it is becoming increasingly apparent that androgen signalling in the stroma influences cancer development and progression.

The stroma of the normal prostate is comprised predominantly of smooth muscle cells, with a small number of fibroblasts and myofibroblasts. In prostate cancer, the myofibroblast, or cancer-associated fibroblast (CAF), is the predominant stromal cell type and influences the growth, invasiveness and metastasis of cancer cells [4-6]. The AR is strongly expressed in the stroma in early prostate cancer, but may be decreased in areas surrounding cancerous tissue, especially in androgen-independent cancer [7, 8], and this can be associated with early relapse [3]. We have shown a significant association between low AR levels in cancer-associated stroma and increased prostate cancer-related death at 1, 3, and 5 years post-diagnosis [5, 6]. High epithelial AR levels were associated with higher Gleason score and higher serum PSA levels, but not with outcome, whilst, in contrast, low stromal AR levels were associated with more extensive disease, and a greater risk of prostate cancer-related death [5]. Whilst this indicates that AR expression in the prostate stroma is an important prognostic biomarker [9-12], how AR influences cancer progression is unclear.

Fibroblasts have the potential to influence the behaviour of epithelial cells via soluble or non-soluble factors. Soluble factors, such as growth factors, are typically studied using indirect

co-culture systems, such as transwell chambers, or conditioned culture medium (CCM). Insoluble factors, which include matrix or cell membrane molecules, are studied in direct co-cultures, usually where the epithelial cells are added onto established stromal cell monolayers. Studying the behaviour of cells in direct co-cultures is challenging because it is difficult to distinguish and analyse each cell type separately.

We have overcome this limitation by stably transducing red fluorescent protein (RFP) into stromal myofibroblasts, and green fluorescent protein (GFP) into epithelial cancer cells, allowing monitoring or measuring by fluorescence microscopy or flow cytometry. In this study we have co-cultured the prostate cancer cell line PC3 with two sublines of a telomerase immortalized human prostate stromal myofibroblast cell line, one stably transduced with AR, the other with empty vector and not expressing AR, to determine the effect of myofibroblast AR expression on myofibroblast-prostate cancer cell interactions in vitro.

METHODS

Cell lines and cell culture

The prostate cancer cell lines PC3, LNCaP, C4-2B and DU145 were maintained in complete RPMI consisting of RPMI 1640 (Life Technologies, Grand Island, NY, USA) supplemented with 10% fetal bovine serum (FBS; Sigma-Aldrich, St Louis, MO, USA), 200 U/ml penicillin and 200 µg/ml streptomycin (Life Technologies). Telomerase immortalised human prostate stromal myofibroblasts stably transduced with AR (PShTert-AR) or empty vector (PShTert) [5, 7] were maintained in DMEM (Life Technologies) supplemented with 10% FBS, 200 U/ml penicillin and 200 µg/ml streptomycin. The AR status of the cell lines was confirmed by western blotting. All cells were cultured at 37°C with 5% CO₂ in air.

Fluorescent labelling of cell lines

The PC3 and LNCaP cells were stably transduced with the triple reporter gene construct SFG-NES-TGL to express green fluorescent protein (GFP) as described previously [13]. The C4-2B and DU145 cells were labelled using the CellTrace Violet (CTV) Cell Proliferation Kit according to the manufacturer's protocol (Life Technologies). The PShTert-AR and PShTert myofibroblasts were stably transduced with the SFG-RFP/Rluc construct to express red fluorescent protein (RFP) [14].

Direct/indirect co-cultures and confrontation assays

RFP-labelled myofibroblasts were cultured for 24 h in phenol red free RPMI 1640 containing L-glutamine (Life Technologies), supplemented with 10% dextran-coated charcoal-stripped FBS (Equitech-Bio, Inc., Kerrville, TX, USA), 200 U/ml penicillin and 200 µg/ml streptomycin (stripped medium), then seeded in stripped medium into six-well plates (BD Biosciences, San Jose, CA, USA), or dishes with imprinted cell relocation grid (µ-Dish 35mm, Grid-500; Ibidi, Martinsried, Germany), and incubated for 48 h. Labelled prostate cancer cells resuspended in stripped medium were either seeded onto the myofibroblast monolayer for direct co-culture, or onto polyester membrane inserts, with 0.4 µm pores (Corning Inc. Life Sciences, Tewksbury, MA, USA), placed in wells of myofibroblast monolayers for indirect co-culture. The medium was replaced with fresh, stripped medium on day 3 of co-culture. To test the effect of androgen on the cultures, either vehicle (0.1% ethanol), 10 nM 5 α -dihydrotestosterone (DHT; Sigma-Aldrich), 10 µM bicalutamide (Bic; Sigma-Aldrich), or 10 nM DHT and 10 µM Bic were added at the time that the myofibroblasts were seeded into wells (day -2), on the addition of the PC3 cells (day 0), and on day 3 of co-culture. Confrontation assays between myofibroblasts and PC3 cells were prepared by seeding the cells in separate chambers (500 µM apart) of the Ibidi Culture-Insert 2 well positioned in an Ibidi µ-Dish 35 mm (3.5 x 10⁴ cells per well). Cells were left to adhere for 16 h under standard culture conditions. Culture inserts were carefully removed and the cells washed with DPBS 3 times followed by replacement with stripped medium. The interface where the two cell types met as they proliferated and migrated was monitored by time-lapse fluorescence microscopy.

Morphological evaluation

Cell morphology was assessed daily by fluorescence microscopy using an Axio Observer.Z1 with HBO 100 illuminator and AxioVision Rel 4.8 software (Carl Zeiss Microscopy GmbH, Jena, Germany). High-power images were acquired using a LSM 700 confocal microscope with Zen software (Zeiss).

Cell counts

Cells were washed with Dulbecco's phosphate buffered saline (DPBS; Life Technologies), incubated with 0.25% trypsin-EDTA (Life Technologies), and resuspended in stripped medium. Cells were centrifuged at 300 x g for 5 min, and resuspended in DPBS. Fluorescently labelled cells were counted using a haemocytometer under fluorescence microscopy.

Preparation of myofibroblast conditioned culture medium

RFP-labelled PShTert-AR or PShTert myofibroblasts were cultured for 24 h in stripped medium, and then seeded into flasks in stripped medium at 7.2×10^6 cells per 175 cm^2 . Conditioned culture medium (CCM) was collected and replaced with fresh, stripped medium every 2 days for 6 days.

Cell proliferation

GFP-labelled PC3 cells were labelled using the CTV Proliferation Kit, seeded in stripped medium at 2.5×10^4 cells per well in six-well plates, and incubated for 5 h until the cells were adherent. The medium was replaced with freshly prepared myofibroblast CCM every 2 days for up to 6 days. Cells were harvested every day for 6 days, washed, and resuspended in DPBS. Cell counts were performed and the CTV fluorescence intensity was determined using a FACSCanto II flow cytometer (BD Biosciences, Franklin Lakes, NJ, USA). Cell doublets were excluded by doublet discrimination, based on non-linearity of forward scatter and side scatter area versus height plots. Proliferation was quantitated by dye dilution.

Cell cycle analysis

GFP-labelled PC3 cells were seeded in stripped medium at 5×10^5 cells per well in six-well plates, and incubated for 24 h. The medium was replaced with freshly prepared myofibroblast CCM every 2 days for 6 days. Cells were harvested every day for 6 days, washed, resuspended in DPBS, and fixed with a final concentration of 70% ice cold ethanol. Next, cells were pelleted, rehydrated with 0.25% Triton X-100 in DPBS, and stained for 2 h with $25 \mu\text{g/ml}$ propidium iodide in DPBS containing $40 \mu\text{g/ml}$ RNase A. Cells were analysed using a FACS Canto II flow cytometer, with doublets excluded. Cells in G0/G1 and G2/M were calculated as the percentage of total cells (i.e., total events minus subG1 events). The subG1 population was calculated as the percentage of total events.

Investigating caspase-3/7 activity and cell death pathways

To measure apoptosis induced by myofibroblast CCM, unlabelled PC3 cells were seeded at 2.86×10^3 cells per well in μ -Plate 96-well plates (Ibidi) and cultured overnight. The medium was replaced with either stripped medium or fresh CCM supplemented with $1 \mu\text{M}$ CellEvent Caspase-3/7 Green Detection Reagent (Life Technologies).

To measure apoptosis in direct co-cultures, RFP-labelled PShTert myofibroblasts in stripped medium were seeded at 1.1×10^4 cells per well in μ -Plate 96-well plates and cultured for 2 days. Next, 1.43×10^3 GFP-labelled PC3 cells per well in stripped medium supplemented

with 1 μ M CellEvent Caspase-3/7 Green Detection Reagent were added directly onto the myofibroblast monolayer. Cells treated with 200 nM actinomycin D (Sigma-Aldrich) were used as a positive control. Cells were monitored for 5 days using a LSM 700 confocal microscope. The mean percentage of apoptotic cells was determined from two high-power fields of view. To measure the effect of caspase inhibition, PShTert myofibroblasts (4×10^5) were seeded for 48 h and then overlaid with medium containing either no cells or PC3 cells (5×10^3), and supplemented with either vehicle (0.1% dimethyl sulfoxide; Sigma-Aldrich), a pan-caspase inhibitor (PCI; Z-VAD-FMK; 20 μ M; Calbiochem Merck, Darmstadt, Germany), or a caspase-8 inhibitor (C8I; Z-IETD-FMK; 20 μ M; R&D Systems, Minneapolis, MN, USA). Actinomycin D (200 nM) was used with the pan-caspase inhibitor as a positive control. The medium was replaced on day 3 and the cells counted on day 6.

Data analysis

All graphs and statistical analyses were generated using GraphPad Prism version 6.0d (GraphPad software Inc., San Diego, CA). Unless otherwise indicated, groups were compared using student *t*-tests, and differences were considered significant when *P*-values were ≤ 0.05 .

RESULTS

The fate of PC3 cells in co-culture depended on myofibroblast AR status

The growth of the PC3 cells in direct co-culture with myofibroblasts was compared to that of cells in monoculture. After 6 days in monoculture the majority of PC3 cells were polygonal in shape, with distinct cell borders and minimal variation in size or shape. A fine perinuclear granulation was visible by phase contrast microscopy throughout the culture period. The PC3 cells were arranged singly or in small discohesive clusters on days 1 and 2, and then expanded in number to form cell aggregates, which ultimately coalesced into a cohesive sheet with well-defined cell borders by day 6 (Fig. 1a).

The PC3 cells in direct co-culture with PShTert-AR myofibroblasts were enlarged and pleomorphic within 24 hours, compared to the cells grown in monoculture. They formed short cytoplasmic extensions, which lengthened and narrowed by day 2 to 3, and failed to form the cohesive aggregates observed in monoculture. There was prominent cellular and nuclear shrinkage from day 2, followed by cell disintegration, leaving remnants of adherent

extensions and cell fragments either attached to the well or free in the growth media (Fig. 1b and 2a).

The PC3 cells grown in direct co-culture with PShTert myofibroblasts showed increased perinuclear granulation, together with cytoplasmic accumulation of numerous large, coarse granules from day 1. Short cytoplasmic extensions were observed from day 2 and these progressively narrowed and lengthened from days 3 to 6 as the cells proliferated. The number of PC3 cells increased rapidly, forming interconnected smallish rafts with clearing of the PShTert myofibroblasts immediately beneath. By day 6 the PC3 cells had formed large cohesive rafts of cells in the centre of the well (Fig. 1c and 2b).

The fate of myofibroblasts in co-culture depended on their AR status

The PShTert-AR myofibroblasts grown in direct co-culture with the PC3 cells retained the morphological features seen in monoculture. By 48 h after seeding they were irregular in size and shape with a dense cytoplasm, and formed wide, cohesive bands of randomly orientated cells with occasional spaces between the bands (Fig. 1b, day 0). This appearance did not change throughout the period of co-culture.

The PShTert myofibroblasts grown in direct co-culture with the PC3 cells retained the morphological features seen in monoculture in areas where there were no PC3 cells. There they grew as a relatively complete and uniform monolayer of narrow cells with clearly defined edges (Fig. 1c, day 0). However, in areas underlying or immediately adjacent to PC3 cells, the PShTert myofibroblasts, over days, became condensed, elongated, irregularly shaped, and eventually disappeared. As the population of PC3 cells expanded, the numbers of PShTert myofibroblasts decreased significantly (Fig. 1c and 2b). The density and morphology of myofibroblasts remote from the PC3 cells appeared similar to that of cells in monoculture.

In confrontation assays the myofibroblasts and PC3 cells were separated by a 500- μ M gap at the time of seeding. The cells proliferated and migrated during culture, and the interactions were observed where the two cell fronts met. The fates of the cells in this assay were similar to those seen in direct co-cultures. For the PC3 cells and PShTert-AR myofibroblasts the gap closed relatively slowly, and where the migrating fronts met the morphology of the PC3 cells altered and their number reduced with time (Supplementary Fig. S1a). With PC3 cells and PShTert myofibroblasts the gap closed more rapidly. After 96 h, the PC3 cells had formed a distinct and much denser border of cells at the boundary of the two cell fronts, and appeared

to invade through and clear the PShTert myofibroblasts. Where there were no PC3 cells, the PShTerts retained their morphology as observed in monoculture (Supplementary Fig. S1b).

PShTert-AR myofibroblasts induced PC3 cell apoptosis by paracrine signalling

To determine the role of juxtacrine and paracrine signalling on the changes in cell growth observed, we compared the cell counts in the direct co-cultures to indirect co-cultures in transwell chambers. The results in Fig. 3 show that after 6 days there were approximately 15-fold fewer PC3 cells following direct (Fig. 3a) and indirect (Fig. 3b) co-culture with PShTert-AR myofibroblasts compared to PShTert myofibroblasts. The PC3 cells in indirect co-culture were similar in morphology to those in direct co-culture.

We then investigated the effect of altering the seeding ratios of the two types of cells in the co-cultures to determine if this would influence the outcomes. Seeding a constant number of PC3 cells against decreasing numbers of myofibroblasts, revealed an inverse relationship between the number of PShTert-AR myofibroblasts seeded and the number of PC3 cells after 6 days of culture, but a direct relationship between the PShTert myofibroblasts and PC3 cells (Fig. 3c). Increasing the number of PC3 cells seeded to a constant number of myofibroblasts did not alter the inhibitory effect of the PShTert-AR or the pro-proliferative effect of the PShTert myofibroblasts on the PC3 cell counts (Fig. 3d). Thus, the ratio of myofibroblasts to PC3 cells influenced the degree, but not the nature, of the interactions between the co-cultured cells.

The results from the indirect co-culture experiments suggested that soluble factors from the PShTert-AR myofibroblasts were associated with the reduction in PC3 cell counts. We confirmed that the addition of PShTert-AR CCM to PC3 monocultures resulted in a significant reduction in PC3 cell numbers from day 3 onwards compared to cells grown in PShTert CCM (Fig. 4a). The PC3 cells cultured with CCM from the myofibroblasts showed similar changes in cell morphology to those seen in co-cultures. These results showed that paracrine factors from the myofibroblasts were at least in part responsible for the changes observed in the PC3 cell morphology and number in co-culture.

We investigated the mechanism for the reduction in PC3 cell numbers. There was a significant reduction in the rate of PC3 cell proliferation following treatment with CCM from PShTert-AR myofibroblasts, as evidenced by a reduction in the rate of dilution of CellTrace Violet fluorescence, evident from day 2 (Fig. 4b). This was accompanied by an alteration in the cell cycle kinetics. There was an increase in the percentage of cells in G0/G1 from day 1

(Fig. 4c), followed by a significant increase in subG1 events from day 4 onwards (Fig. 4d). The latter was associated with a marked increase in the percentage of caspase-3/7 positive apoptotic cells (Fig. 5). Together, these results show that CCM from the PShTert-AR myofibroblasts reduced PC3 cell numbers through inhibition of proliferation and induction of apoptosis.

PC3 cells induced apoptosis in PShTert myofibroblasts by juxtacrine signalling

Next we investigated the destruction of the PShTert myofibroblasts in direct co-culture with PC3 cells. There was a significant reduction in total PShTert myofibroblast counts in direct (Fig. 6a), but not indirect (Fig. 6b) co-culture, apparent microscopically from day 3. The number of surviving PShTert myofibroblasts in direct co-cultures with PC3 cells was inversely proportional to the PC3 cell seeding density (Fig. 6c).

Apoptosis was assessed as a mechanism for PShTert loss. Microscopically, only the PShTert myofibroblasts in close proximity to PC3 cells were positive for caspase-3/7 activation (Supplementary Fig. S2), suggesting the PShTerts were undergoing apoptosis in response to juxtacrine signals from PC3 cells. The loss of PShTerts in direct co-culture could be blocked almost completely by a pan-caspase inhibitor (PCI) and completely by a caspase-8 inhibitor (C8I) (Fig. 6d), providing further evidence that apoptosis was the mechanism involved.

To determine if our observations were specific to PC3 cells, we set up direct co-cultures of myofibroblasts (4×10^5 cells per well) and LNCaP, C4-2B or DU145 prostate cancer cell lines (5×10^3 cells per well). There was a significant reduction in the cell count of each of these prostate lines when co-cultured with PShTert-AR myofibroblasts (Fig. 7a). Whilst there was not a significant reduction in the total counts (Fig. 7b), there was an obvious focal destruction of the PShTert myofibroblasts in the immediate proximity of the cancer cells for each of these cell lines (Fig. 8).

DHT reduced PShTert-AR counts and this increased PC3 counts in co-culture

The results in Fig. 9 show the effect of activation of the AR signalling pathway on the outcome of co-culture. The addition of the AR ligand DHT to co-cultures with PShTert-AR myofibroblasts resulted in a significant 4-fold increase in the number of PC3 cells in both direct (Fig. 9a) and indirect (Fig. 9b) co-cultures. This increase in PC3 cell counts was abrogated by bicalutamide in indirect co-culture (Fig. 9c), confirming that DHT was acting through the AR signalling pathway in the myofibroblasts. DHT had no significant effect on PC3 cell counts in direct (Fig. 9a) or indirect (Fig. 9b) co-culture with PShTert

myofibroblasts, consistent with the lack of AR in both cell types. The addition of DHT to myofibroblast monocultures resulted in a reduction in the number of PShTert-AR myofibroblasts over the period of culture, but no change in the number of PShTert myofibroblasts, as reported in a previous study [5]. In direct co-cultures with DHT there was also a significant reduction in the number of PShTert-AR myofibroblasts but not of PShTert myofibroblasts (Fig. 9d). The focal destruction of the PShTert myofibroblasts observed adjacent to PC3 cells in direct co-cultures was not altered by the DHT. The higher recovery of PC3 cells with PShTert-AR in the presence of DHT, together with the results in Fig. 3c, which show an inverse relationship between PShTert-AR and PC3 numbers in co-cultures, suggest that the increase in PC3 cell numbers is a result of a DHT induced decrease in the number of PShTert-AR myofibroblasts.

DISCUSSION

Androgen receptor (AR) expression in stromal fibroblasts is required for the development and maintenance of the normal prostate, and for the development of prostate cancer, yet interestingly stromal AR expression is frequently reduced in prostate cancer, with associated poor clinical outcomes [5]. Previously, we showed in a cohort of 64 patients that low AR expression is significantly associated with prostate cancer-related death at 1, 3, and 5 years post-diagnosis [5]. Others have also reported that the progressive loss of stromal AR correlates with progression of the disease, high-risk clinical parameters and/or poor outcome [3, 8, 15-18]. Why poor outcome is associated with the loss of stromal AR is unknown [6].

Here we provide new insights, with the first comprehensive in vitro study of the effect of AR expression in prostate myofibroblasts on the outcomes of direct and indirect co-culture with prostate cancer cells. We used hTERT immortalised myofibroblasts transduced with either AR (PShTert-AR), or empty vector (PShTert), in co-culture with an AR-negative prostate cancer cell line PC3, so that we could isolate the effect of AR expression to the myofibroblast alone. Firstly, we observed a reduction in PC3 cell counts following direct or indirect co-culture with PShTert-AR myofibroblasts, compared to PShTert myofibroblasts, and showed that this effect was consistent across three other prostate cancer cell lines. There was an inverse relationship between the numbers of PC3 cells recovered and the numbers of PShTert-AR myofibroblasts seeded. These effects were due to paracrine signals from the PShTert-AR myofibroblasts, which slowed the proliferation of the PC3 cells, with arrest at G0/G1, and increased their apoptosis. Secondly, we report the novel finding that direct but not indirect

co-culture with PC3 cells significantly reduced the numbers of PShTert myofibroblasts, with apoptosis mediated by juxtacrine signalling between the two cell types. The morphological changes and apoptosis were detected exclusively in PShTert myofibroblasts in contact with PC3 cells. In a confrontation assay the PShTert myofibroblasts promoted the migration and invasion of PC3 cells. Thirdly, we found that DHT reduced the proliferation of the PShTert-AR myofibroblasts, and as a result of their reduced number, the number of PC3 cells increased. The PShTert-AR myofibroblasts therefore contained and killed the cancer cells, in contrast to the PShTert myofibroblasts, which did not exert any noticeable inhibitory control and were destroyed.

Whilst a number of studies have investigated the interaction between fibroblasts and cancer cells in co-culture in vitro, most have compared different fibroblasts, such as normal versus cancer-associated, or different epithelial cells, such as normal versus malignant [19-28]. Few studies have investigated the effect of AR expression or signalling in prostate cancer myofibroblasts. The major difficulty is that while myofibroblasts are the major cell type in the prostate cancer stroma, and they express AR, primary human prostate myofibroblasts, within several passages in vitro, generally lose AR expression or do not express it at levels adequate to show androgen-dependent changes in gene expression [29].

One way to overcome this limitation is to stably transduce immortalised human prostate myofibroblasts with AR. This has been done previously using WPMY myofibroblasts transduced with either AR (WPMY-AR) or empty vector (WPMY-Vec), with conditioned medium from DHT-treated WPMY-AR cells significantly increasing the growth of LNCaP prostate cancer cells, compared to conditioned medium from WPMY-Vec cells [29]. However in this study the role of myofibroblast AR was investigated in the context of paracrine signalling alone. We explored both paracrine and juxtacrine effects using hTERT immortalised human prostate myofibroblasts, transduced with AR or empty vector. To our knowledge, ours is the first in vitro investigation of juxtacrine signalling in prostate cancer in the context of myofibroblast AR.

The hTERT myofibroblasts we used are representative of cancer-associated fibroblasts and the PShTert-AR line has been shown to have a similar AR binding profile, and gene regulation, as primary fibroblasts and in vivo stroma [30]. Tissue recombination studies using these cell lines have produced results consistent with our in vitro findings. Nude male mice were co-injected subcutaneously with PC3 cells and either PShTert-AR or PShTert myofibroblasts, with tumour growth reduced by PShTert-AR and promoted by PShTert [7].

Similarly, using immunodeficient NOD-SCID mice sub-renally grafted with human-derived primary prostate cancer tissue, and either PShTert-AR or PShTert myofibroblasts, we found that grafts with PShTert-AR showed significantly more apoptosis in the cancer cells than grafts with PShTert, in castrated mice [5]. Here we extend these two *in vivo* studies further by investigating the mechanistic basis for these observations.

We have shown that paracrine signalling by AR expressing myofibroblasts slowed PC3 proliferation, and induced apoptosis *in vitro*. The death of cancer cells caused by fibroblasts has been reported by others, but not in the context of myofibroblast AR. In prostate cancer, conditioned culture medium, from bone marrow stromal cells, decreased the proliferation of and induced apoptosis in LNCaP and C4-2B, but not PC3 cells [31], CAFs induced apoptosis in gastric cancer cells [32], and human mesenchymal stem/stromal cells (hMSCs) and CAFs, activated to express tumour necrosis factor (TNF)-alpha-related apoptosis-inducing ligand (TRAIL), induced apoptosis in breast cancer cells [33, 34]. Conversely, a number of other studies have reported that normal fibroblasts and/or CAFs inhibit cancer cell apoptosis [35-37]. None of the aforementioned studies indicated fibroblast AR status.

Additionally, our results show that juxtacrine signalling was responsible for the destruction of the AR-negative myofibroblasts by apoptosis, and this allowed the PC3 cells to grow. The inability of these myofibroblasts to control the expansion of the cancer cells may explain why an AR-negative stroma is associated with more advanced prostate cancer. Several studies report observations consistent with ours, but not in the context of stromal AR. Normal human fibroblasts, in direct co-culture with prostate cancer cell lines PC3 and DU145, formed islands around the cancer cells early on and were eventually overtaken and almost completely destroyed by the growing cancer cells [28]. This arrangement of fibroblasts around tumour cells has also been described previously in direct co-cultures with HeLa cells [38], and in direct co-cultures of normal or malignant prostate epithelial cells with prostatic stromal cells from malignant tissue, where the epithelial cells displaced and grew within the stromal cells rather than growing on top [25, 37]. Breast cancer cells have been reported to release soluble factors that induced apoptosis in human bone marrow stromal cells *in vitro* [39], and lung fibroblasts were reduced in number, with evidence of apoptosis, following 3D co-culture with non-small cell lung cancer cell lines [40]. Another study reported that CAFs formed stromal islands in co-culture spheroids with prostate cancer cells, and were lost over time, with less than 10% remaining by day 8. The authors suggested juxtacrine interactions were involved but did not investigate the mechanisms, and, although they mentioned the CAFs were AR-negative, they did not explore whether similar effects occurred with AR-positive CAFs [41].

Here, we have confirmed that juxtacrine interactions were responsible for the loss of the AR-negative myofibroblasts, through the induction of apoptosis, with no loss of myofibroblasts that expressed AR.

Interestingly, the differential effects of myofibroblasts stably transduced with AR compared to those transduced with empty vector, occurred in the absence of ligand. The experiments were performed in stripped media which has no, or a very low, concentration of androgen. This suggests the expression of AR, in itself, can have significant biological effects independent of ligand binding. Several studies support this conclusion. The stable transduction of AR into WPMY human prostate myofibroblasts significantly altered their gene expression pattern compared to those transduced with empty vector, in the absence of DHT [29]. Knockdown of AR by siRNA in an AR-positive cancer-associated fibroblast line produced significant differences in the expression of several growth factor genes, and the proliferation and migration of PC3 cells in transwell co-cultures [42], and the transfection of human AR into AR-deficient mouse Sertoli cells significantly altered the expression of 672 genes in the absence of androgen stimulation [43]. These two studies did not specify whether stripped medium was used. Together, these studies provide strong evidence that there are ligand independent effects from AR expression in prostate cancer myofibroblasts.

CONCLUSIONS

Relatively little is known regarding the functional effects of AR expression in prostate myofibroblasts. We have shown that the outcome of co-culturing prostate myofibroblasts and the PC3 cell line differs depending on whether the myofibroblast expresses AR or not, and involves paracrine and juxtacrine signalling. Our findings suggest AR-expressing myofibroblasts inhibit prostate cancer progression through paracrine signals that slow proliferation and induce apoptosis in the cancer cells, and that myofibroblasts lacking AR permit prostate cancer progression by undergoing apoptosis in response to juxtacrine signals from the cancer cells. This is consistent with our published findings that a loss of stromal AR is associated with reduced survival in prostate cancer. Understanding the regulation and function of AR expression in stromal myofibroblasts may lead to the development of novel treatments that modify prostate cancer progression.

Abbreviations

AR: Androgen receptor **BIC:** Bicalutamide **CAF:** Cancer-associated fibroblast **CCM:** Conditioned culture medium **DHT:** 5 α -dihydrotestosterone
FBS: Fetal bovine serum **DPBS:** Dulbecco's phosphate buffered saline **GFP:** Green fluorescent protein **RFP:** Red fluorescent protein

REFERENCES

1. Cunha GR. Mesenchymal-epithelial interactions: past, present, and future. *Differentiation*. 2008;76(6):578-586.
2. Cunha GR, et al. Hormonal, cellular, and molecular regulation of normal and neoplastic prostatic development. *J Steroid Biochem Mol Biol*. 2004;92(4):221-236.
3. Henshall SM, et al. Altered expression of androgen receptor in the malignant epithelium and adjacent stroma is associated with early relapse in prostate cancer. *Cancer Res*. 2001;61(2):423-427.
4. Marsh T, Pietras K, McAllister SS. Fibroblasts as architects of cancer pathogenesis. *Biochim Biophys Acta*. 2013;1832(7):1070-1078.
5. Leach DA, et al. Stromal androgen receptor regulates the composition of the microenvironment to influence prostate cancer outcome. *Oncotarget*. 2015;6(18):16135-16150.
6. Leach DA, Buchanan G. Stromal Androgen Receptor in Prostate Cancer Development and Progression. *Cancers (Basel)*. 2017;9(1).
7. Li Y, et al. Decrease in stromal androgen receptor associates with androgen-independent disease and promotes prostate cancer cell proliferation and invasion. *J Cell Mol Med*. 2008;12(6B):2790-2798.
8. Olapade-Olaopa EO, et al. Malignant transformation of human prostatic epithelium is associated with the loss of androgen receptor immunoreactivity in the surrounding stroma. *Clin Cancer Res*. 1999;5(3):569-576.
9. Saito S, et al. Stromal fibroblasts are predictors of disease-related mortality in esophageal squamous cell carcinoma. *Oncol Rep*. 2014;32(1):348-354.
10. Finak G, et al. Stromal gene expression predicts clinical outcome in breast cancer. *Nat Med*. 2008;14(5):518-527.
11. Navab R, et al. Prognostic gene-expression signature of carcinoma-associated fibroblasts in non-small cell lung cancer. *Proc Natl Acad Sci U S A*. 2011;108(17):7160-7165.

12. Saadi A, et al. Stromal genes discriminate preinvasive from invasive disease, predict outcome, and highlight inflammatory pathways in digestive cancers. *Proc Natl Acad Sci U S A*. 2010;107(5):2177-2182.
13. Zinonos I, et al. Apomab, a fully human agonistic antibody to DR5, exhibits potent antitumor activity against primary and metastatic breast cancer. *Mol Cancer Ther*. 2009;8(10):2969-2980.
14. Dobrenkov K, et al. Monitoring the efficacy of adoptively transferred prostate cancer-targeted human T lymphocytes with PET and bioluminescence imaging. *J Nucl Med*. 2008;49(7):1162-1170.
15. Li R, et al. High level of androgen receptor is associated with aggressive clinicopathologic features and decreased biochemical recurrence-free survival in prostate: cancer patients treated with radical prostatectomy. *Am J Surg Pathol*. 2004;28(7):928-934.
16. Ricciardelli C, et al. Elevated levels of HER-2/neu and androgen receptor in clinically localized prostate cancer identifies metastatic potential. *Prostate*. 2008;68(8):830-838.
17. Singh M, Lee P. Expression and Function of Stromal Androgen Receptor in Prostate Cancer. 2013.
18. Wikstrom P, Marusic J, Stattin P, Bergh A. Low stroma androgen receptor level in normal and tumor prostate tissue is related to poor outcome in prostate cancer patients. *Prostate*. 2009;69(8):799-809.
19. Dong-Le Bourhis X, et al. Effect of stromal and epithelial cells derived from normal and tumorous breast tissue on the proliferation of human breast cancer cell lines in co-culture. *Int J Cancer*. 1997;71(1):42-48.
20. Camps JL, et al. Fibroblast-mediated acceleration of human epithelial tumor growth in vivo. *Proc Natl Acad Sci U S A*. 1990;87(1):75-79.
21. Cornil I, et al. Fibroblast cell interactions with human melanoma cells affect tumor cell growth as a function of tumor progression. *Proc Natl Acad Sci U S A*. 1991;88(14):6028-6032.
22. Kabalin JN, Peehl DM, Stamey TA. Clonal growth of human prostatic epithelial cells is stimulated by fibroblasts. *Prostate*. 1989;14(3):251-263.
23. Kooistra A, Romijn JC, Schroder FH. Stromal inhibition of epithelial cell growth in the prostate; overview of an experimental study. *Urol Res*. 1997;25 Suppl 2S97-105.
24. Degeorges A, et al. Stromal cells from human benign prostate hyperplasia produce a growth-inhibitory factor for LNCaP prostate cancer cells, identified as interleukin-6. *Int J Cancer*. 1996;68(2):207-214.

25. Lang SH, Stower M, Maitland NJ. In vitro modelling of epithelial and stromal interactions in non-malignant and malignant prostates. *Br J Cancer*. 2000;82(4):990-997.
26. Flaberg E, et al. High-throughput live-cell imaging reveals differential inhibition of tumor cell proliferation by human fibroblasts. *Int J Cancer*. 2011;128(12):2793-2802.
27. Flaberg E, et al. The architecture of fibroblast monolayers of different origin differentially influences tumor cell growth. *Int J Cancer*. 2012;131(10):2274-2283.
28. Iacopino F, Angelucci C, Sica G. Interactions between normal human fibroblasts and human prostate cancer cells in a co-culture system. *Anticancer Res*. 2012;32(5):1579-1588.
29. Tanner MJ, et al. Effects of androgen receptor and androgen on gene expression in prostate stromal fibroblasts and paracrine signaling to prostate cancer cells. *PLoS One*. 2011;6(1):e16027.
30. Leach DA, et al. Cell-lineage specificity and role of AP-1 in the prostate fibroblast androgen receptor cisome. *Mol Cell Endocrinol*. 2017;439:261-272.
31. Zhang C, et al. Paracrine factors produced by bone marrow stromal cells induce apoptosis and neuroendocrine differentiation in prostate cancer cells. *Prostate*. 2011;71(2):157-167.
32. Itoh G, et al. Cancer-associated fibroblasts induce cancer cell apoptosis that regulates invasion mode of tumours. *Oncogene*. 2017.
33. Lee RH, Yoon N, Reneau JC, Prockop DJ. Preactivation of human MSCs with TNF-alpha enhances tumor-suppressive activity. *Cell Stem Cell*. 2012;11(6):825-835.
34. Yoon N, et al. Activated human mesenchymal stem/stromal cells suppress metastatic features of MDA-MB-231 cells by secreting IFN-beta. *Cell Death Dis*. 2016;7:e2191.
35. Wang M, et al. The primary growth of laryngeal squamous cell carcinoma cells in vitro is effectively supported by paired cancer-associated fibroblasts alone. *Tumour Biol*. 2017;39(5):1010428317705512.
36. Olumi AF, Dazin P, Tlsty TD. A novel coculture technique demonstrates that normal human prostatic fibroblasts contribute to tumor formation of LNCaP cells by retarding cell death. *Cancer Res*. 1998;58(20):4525-4530.
37. Olumi AF, et al. Carcinoma-associated fibroblasts direct tumor progression of initiated human prostatic epithelium. *Cancer Res*. 1999;59(19):5002-5011.
38. Delinassios JG. Fibroblasts against cancer cells in vitro. *Anticancer Res*. 1987;7(5B):1005-1010.
39. Fromiguet O, et al. Breast cancer cells release factors that induced apoptosis in human bone marrow stromal cells. *J Bone Miner Res*. 2001;16(9):1600-1610.

40. Amann A, et al. Development of an innovative 3D cell culture system to study tumour--stroma interactions in non-small cell lung cancer cells. *PLoS One*. 2014;9(3):e92511.
41. Eder T, et al. Cancer-Associated Fibroblasts Modify the Response of Prostate Cancer Cells to Androgen and Anti-Androgens in Three-Dimensional Spheroid Culture. *Int J Mol Sci*. 2016;17(9).
42. Yu S, et al. Androgen receptor in human prostate cancer-associated fibroblasts promotes prostate cancer epithelial cell growth and invasion. *Med Oncol*. 2013;30(3):674.
43. Fietz D, et al. Transfection of Sertoli cells with androgen receptor alters gene expression without androgen stimulation. *BMC Mol Biol*. 2015;1623.

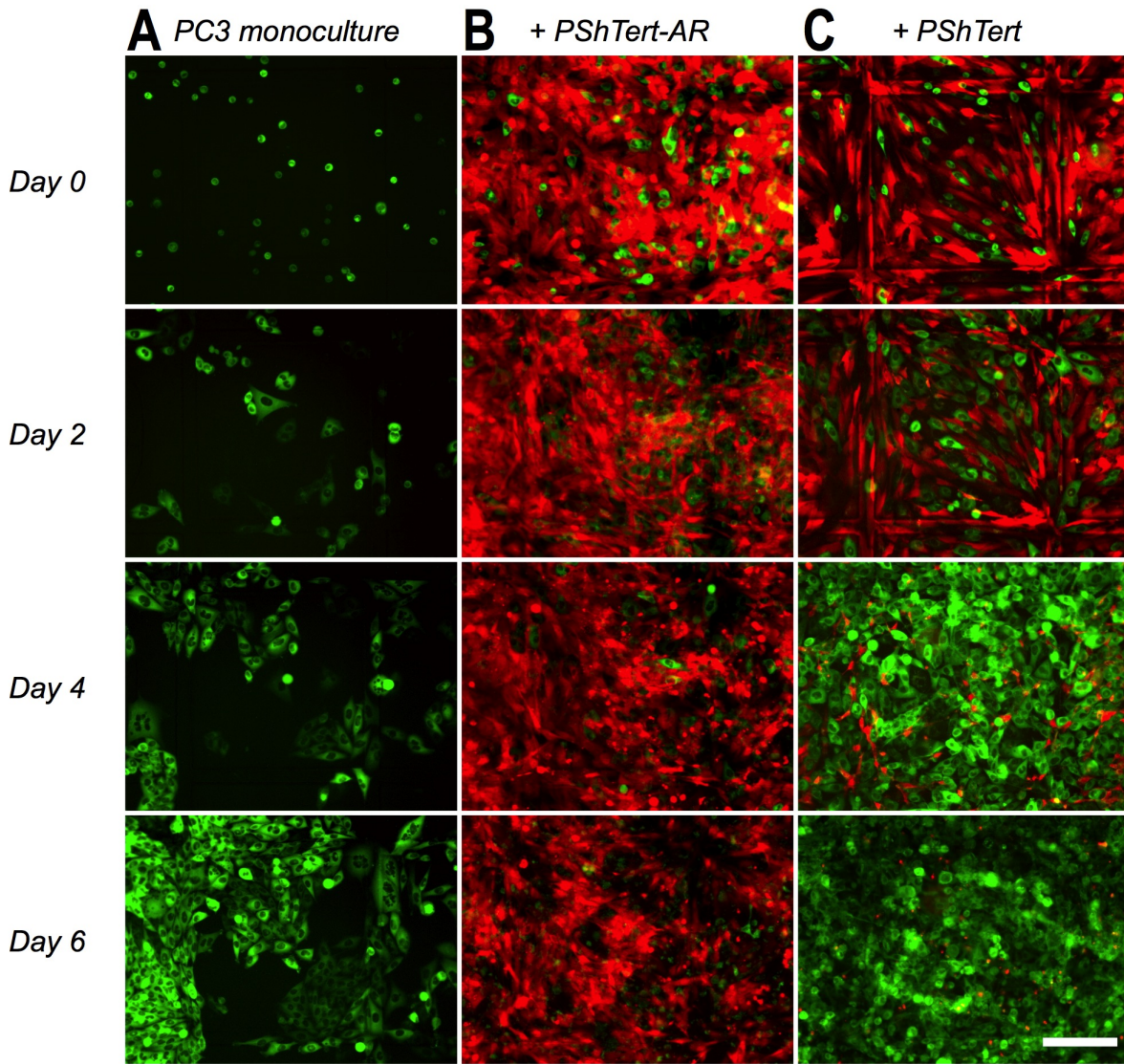


Figure 1. PC3 cells in monoculture and direct co-culture with myofibroblasts. PC3 cells (GFP-labelled; 5×10^3) were added to culture dishes with imprinted relocation grid (Ibidi) either in **a** monoculture or direct co-culture with 1.5×10^5 RFP-labelled **b** PShTert-AR, or **c** PShTert myofibroblasts. Original magnification 100 x. Scale bar 200 μ M.

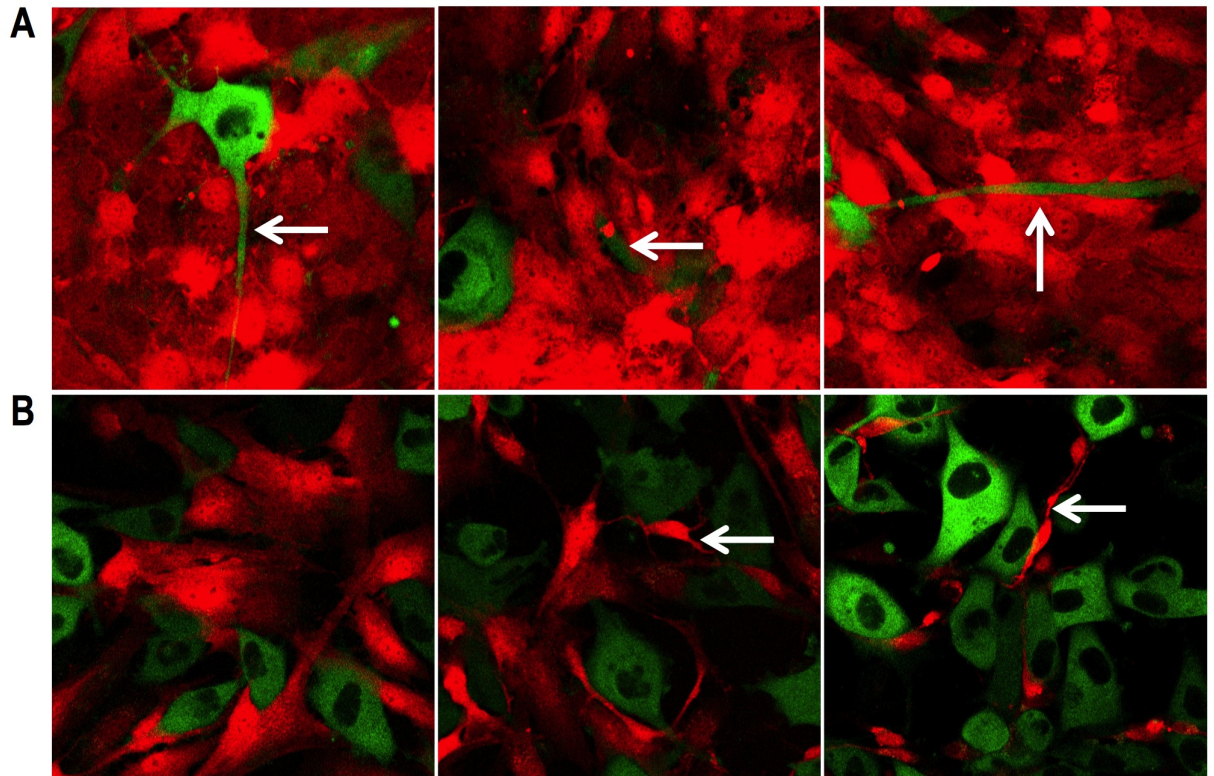


Figure 2. Specific morphological changes. **a** Changes in PC3 cells directly co-cultured with PShTert-AR myofibroblasts. Arrows show extensions of the cytoplasm (left), cell disintegration (centre) and remnants of adherent extensions (right). **b** Progressive destruction of PShTert myofibroblasts directly co-cultured with PC3 cells.

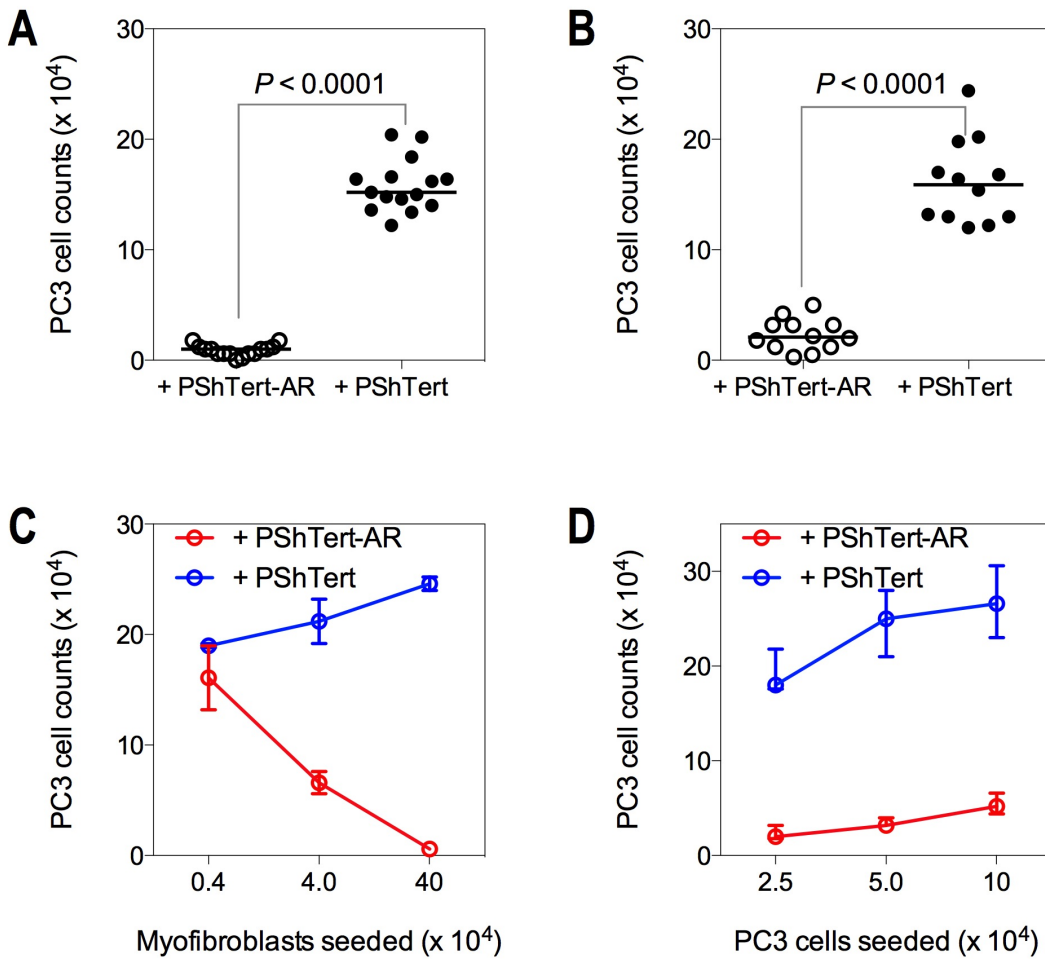


Figure 3. PC3 cell counts on day 6 of direct and indirect co-culture. PC3 cells (5×10^3) were either **a** directly or **b** indirectly co-cultured with PShTert-AR or PShTert myofibroblasts (4×10^5). Medians of independent experiments shown; $n = 15$ (direct), $n = 12$ (indirect). P -values determined by Mann-Whitney U-test. **c** PC3 cells (5×10^3) were directly co-cultured against decreasing numbers of myofibroblasts. **d** Increasing numbers of PC3 cells were directly co-cultured against a constant seeding density of myofibroblasts (4×10^5). Medians with range shown of a single experiment performed in triplicate.

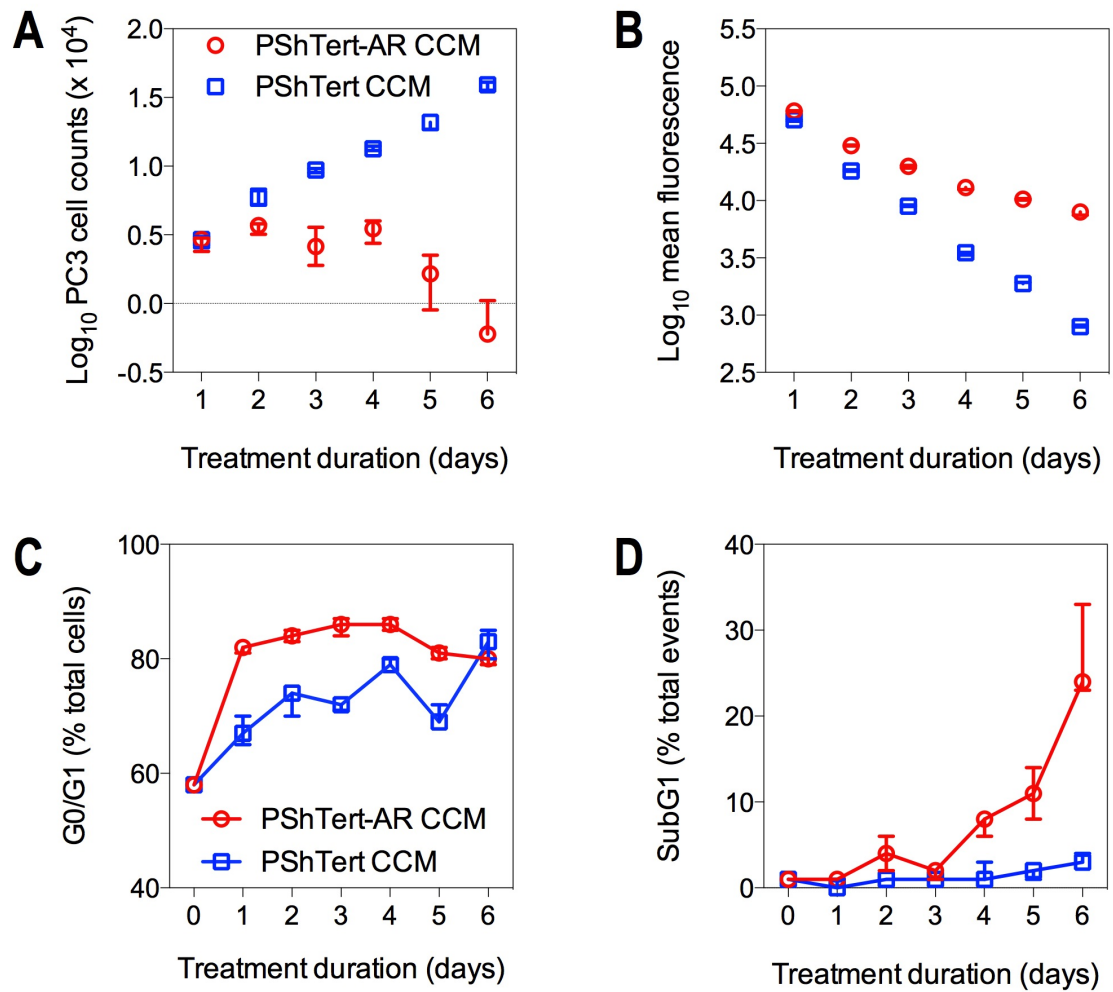


Figure 4. The effect of myofibroblast CCM on cell counts, proliferation and cell cycle. PC3 cells (2.5×10^4) were treated for 6 days with PShTert-AR or PShTert CCM replaced every 48 h. PC3 cells were **a** counted and **b** CellTrace violet fluorescence intensity measured daily. For cell cycle analysis, PC3 cells (5×10^5) were treated with myofibroblast CCM every 48 h for 6 days. Cells were harvested and stained (25 $\mu\text{g/ml}$ propidium iodide in DPBS containing 40 $\mu\text{g/ml}$ RNase A) daily. **c** The percentage of total cells in G0/G1 of the cell cycle. **d** The percentage of total events in subG1. Data is the median and range of a single reproducible experiment.

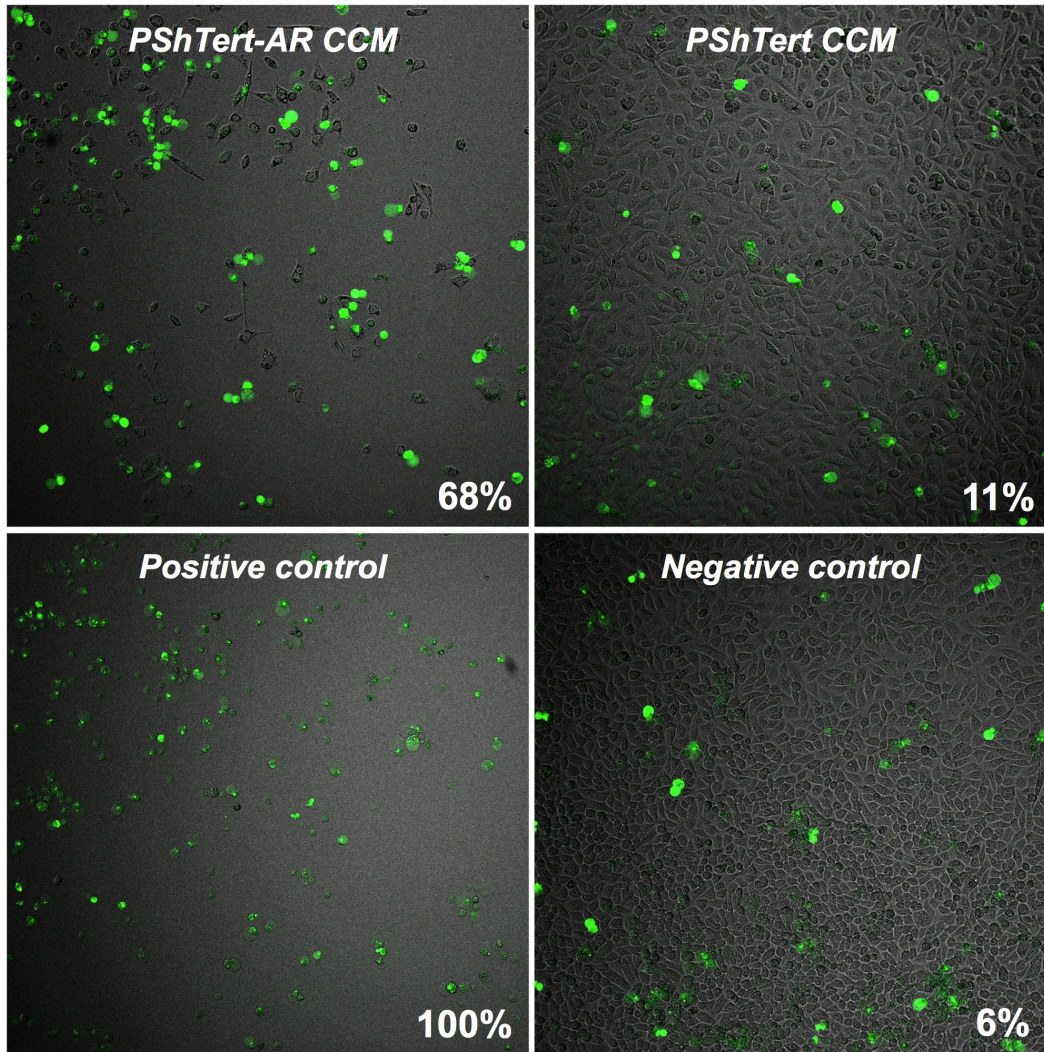


Figure 5. The effect of myofibroblast CCM on caspase-3/7 activity in PC3 cells. Unlabelled PC3 cells (2.86×10^3) were seeded overnight in μ -Plate 96-well plates (Ibidi) and treated with either PShTert-AR or PShTert CCM supplemented with CellEvent dye ($1 \mu\text{M}$). A positive control of PC3 cells treated with actinomycin D (200 nM) for 24 h, and a negative control of PC3 cells in normal stripped medium, were also prepared with the inclusion of CellEvent. Cells were observed for 96 h in real-time to detect the formation of a green fluorescence, indicative of activated caspase-3/7.

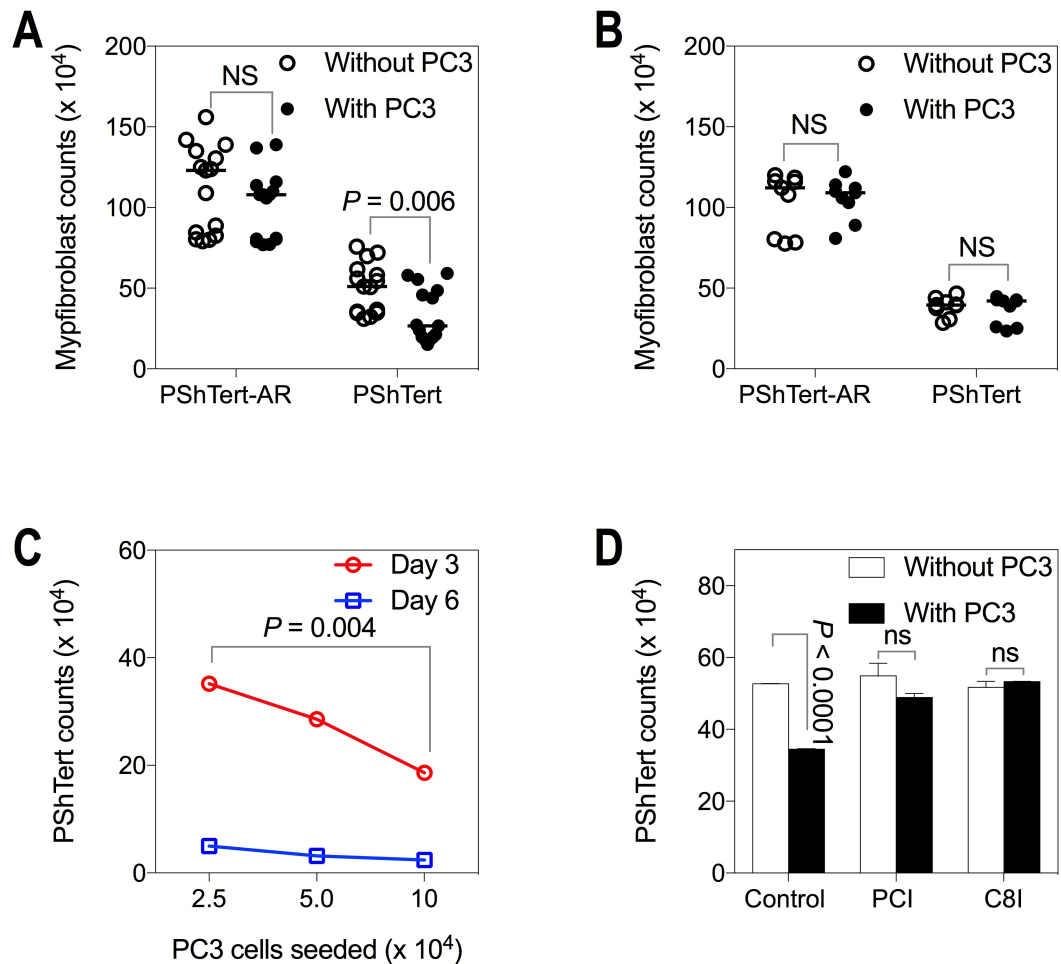


Figure 6. Myofibroblast counts in co-culture with PC3 cells. Myofibroblast cell counts following 6 days of **a** direct and **b** indirect co-culture with PC3 cells compared to monoculture without PC3 cells. Medians of independent experiments shown; $n = 15$ (direct), $n = 9$ (indirect). P -values determined by Mann-Whitney U-test. **c** PShTert myofibroblast counts following 3 and 6 days of direct co-culture with PC3 cells of increasing seeding density. Medians and range from a single reproducible experiment. P -values calculated by unpaired, parametric Student's t -test. **d** The effect of pan-caspase (PCI), and caspase-8 (C8I) inhibitors on PShTert myofibroblast counts in monoculture and direct co-culture with PC3 cells for 6 days. Medians and range of independent experiments; $n = 2$. P -values calculated by unpaired, parametric Student's t -test.

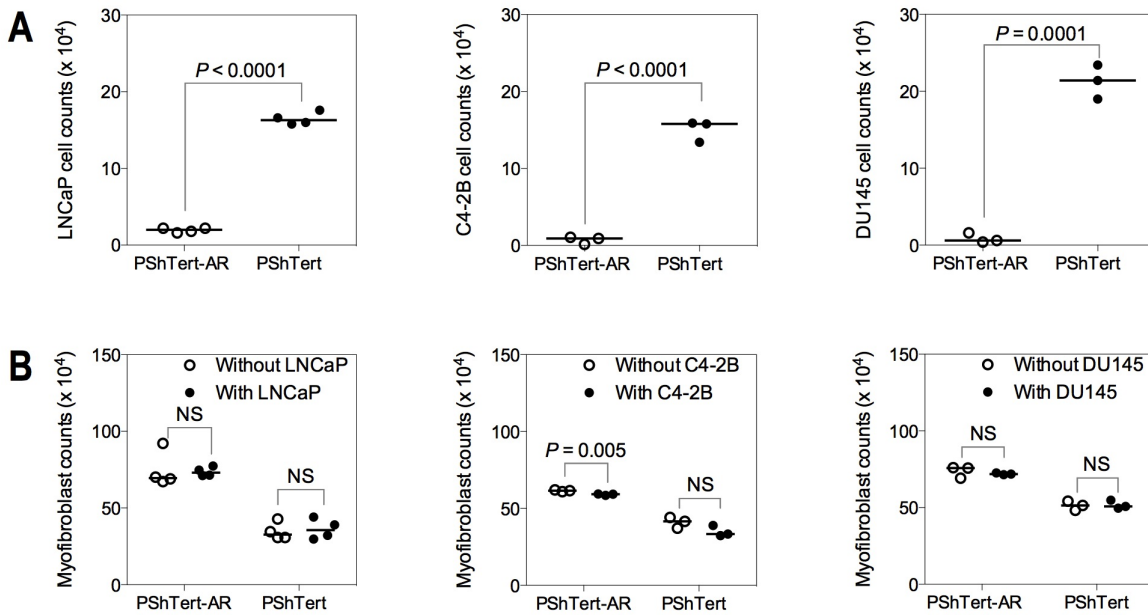


Figure 7. Cell counts after 6 days of direct co-culture between myofibroblasts and other prostate cancer cell lines. PShTert myofibroblasts (4×10^5) were directly co-cultured with, either LNCaP, C4-2B, or DU145 prostate cancer cell lines (5×10^3) with cells harvested and counted on day 6. Cell counts for **a** prostate cancer cell lines and **b** myofibroblasts in monoculture and direct co-culture. Medians presented from a reproducible experiment. *P*-values calculated by unpaired, parametric Student's *t*-test.

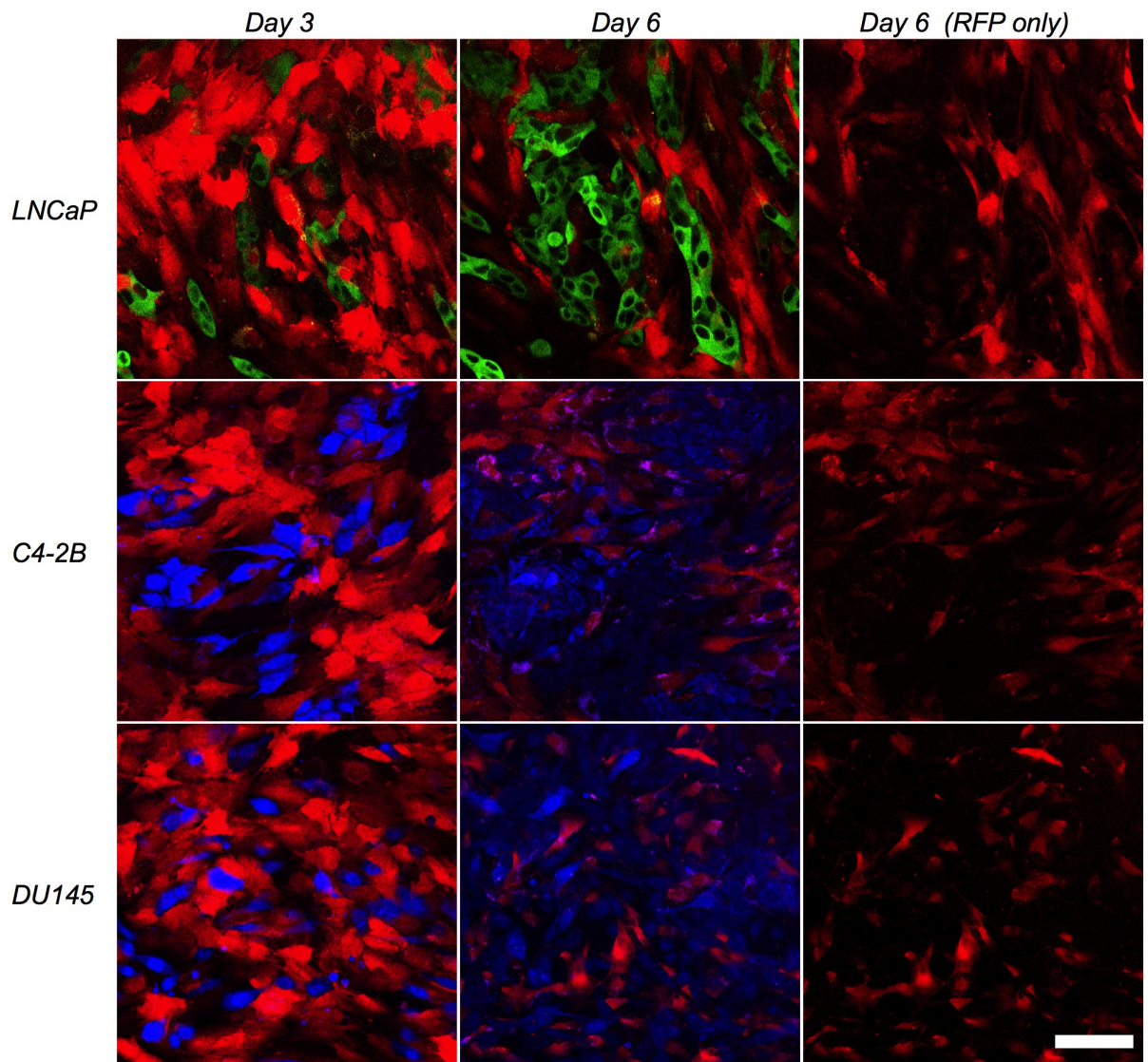


Figure 8. Morphology of PShTert myofibroblasts in direct co-culture with other prostate cancer cell lines. PShTert myofibroblasts (red) were directly co-cultured with GFP-labelled LNCaP (green), or CellTrace Violet-labelled C4-2B, or DU145 prostate cancer cell lines (blue), with images captured on the LSM 700 in real-time for 6 days. Images represent morphology of PShTerts on day 3 and 6 of direct co-culture. Images on far right show the red channel (RFP) only for the day 6 images to show the morphological changes in PShTert myofibroblasts. Magnification 200 x. Scale bar 75 μ M.

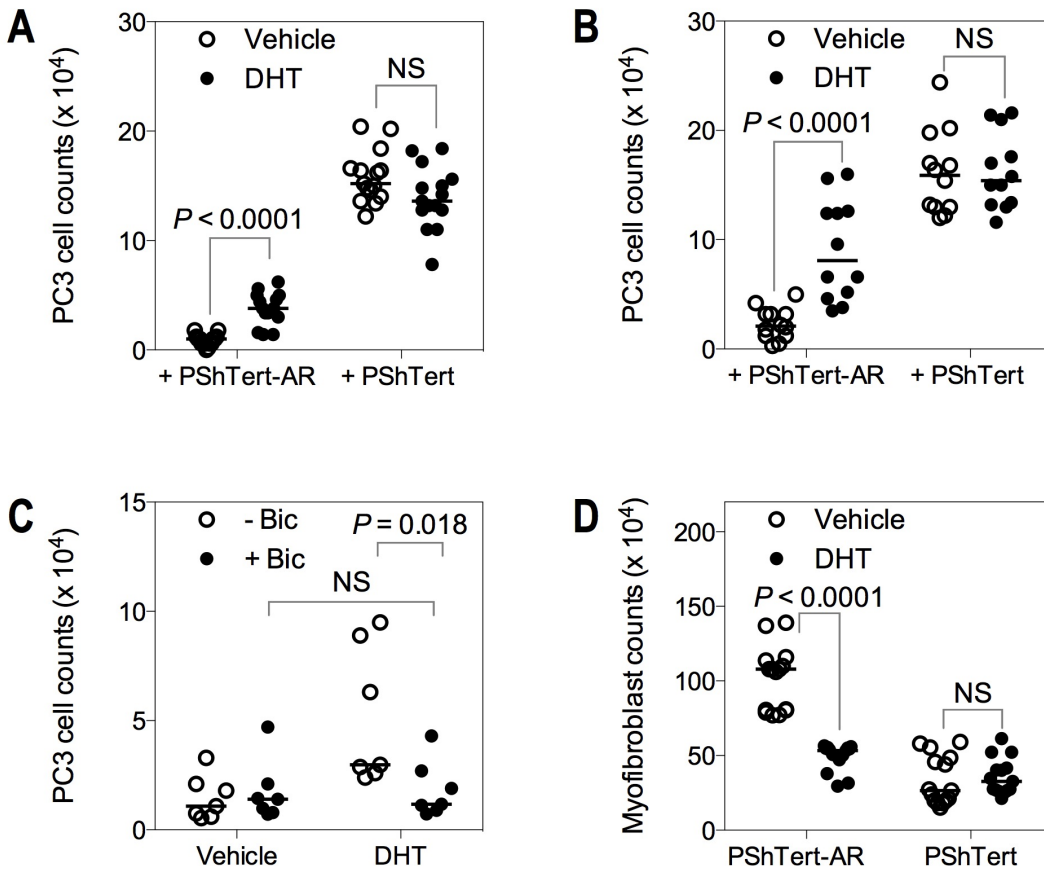
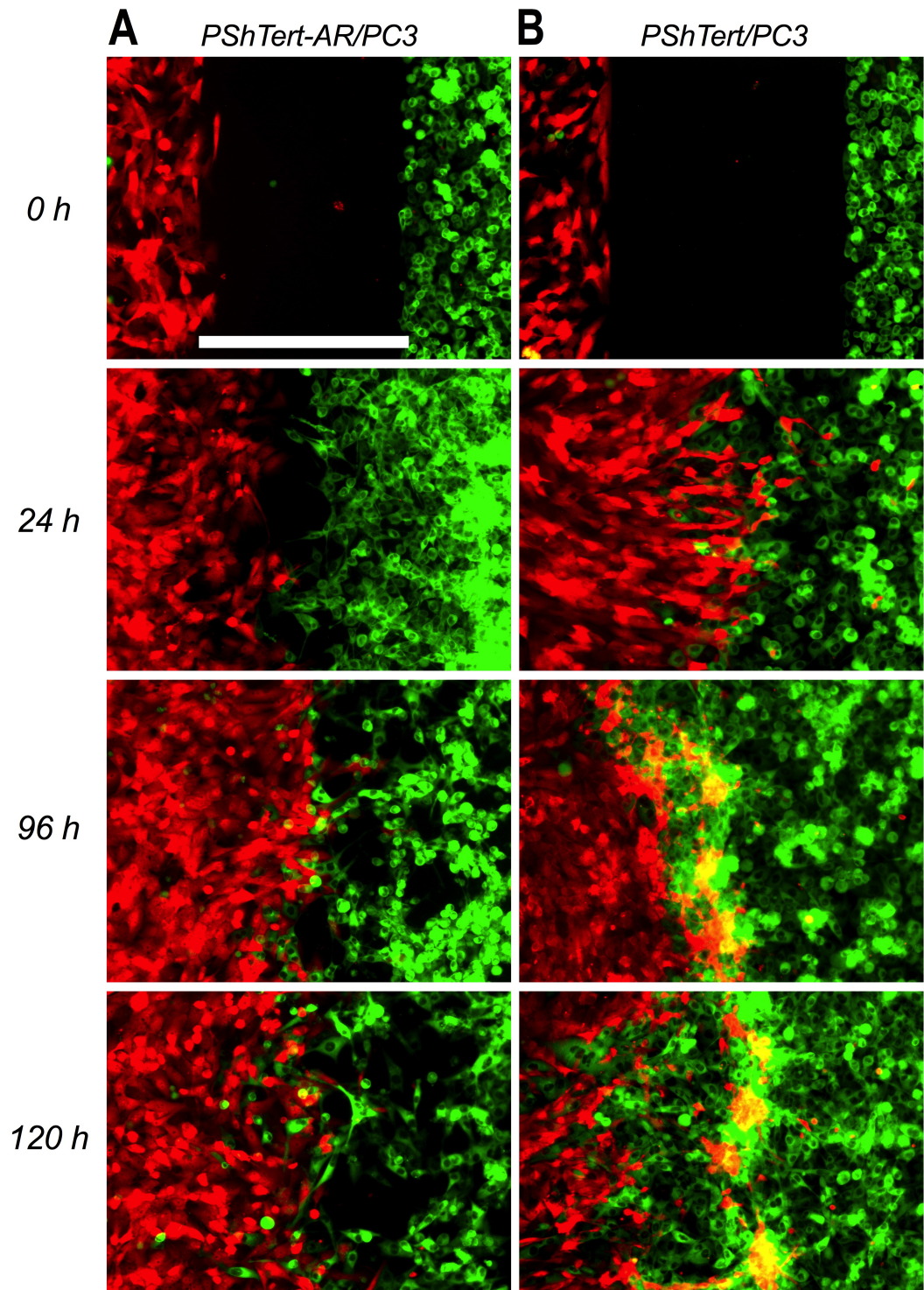
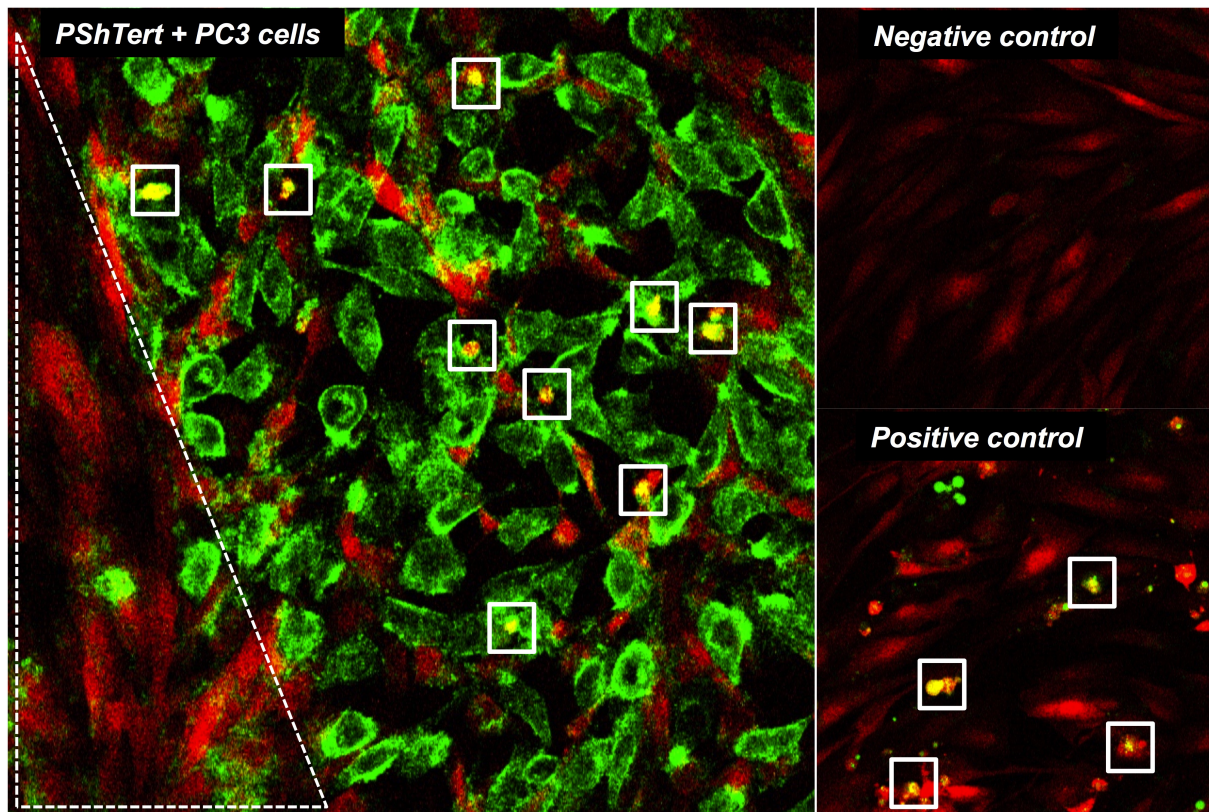


Figure 9. The effect of DHT on PC3 cell and myofibroblast counts in co-culture. The effect of DHT on PC3 cell counts on day 6 of both **a** direct and **b** indirect co-culture with myofibroblasts. **c** Abrogation of the effect of DHT on PC3 cells indirectly co-cultured with PShTert-AR myofibroblasts by bicalutamide ($n = 7$). **d** The effect of DHT on myofibroblast counts (direct co-culture shown). Median values of multiple, independent experiments: **a** $n = 15$; **b** $n = 12$; **c** $n = 7$; and **d** $n = 15$. P -values calculated by Mann-Whitney U-test.



Supplementary Figure S1. Confrontation assay between PShTert-AR or PShTert myofibroblasts and PC3 cells. PC3 cells and myofibroblasts were seeded in separate wells of an Ibidi Culture-Insert 2 well (3.5×10^4 cells per well) and left to adhere. Culture inserts were removed, cells washed and medium replaced (0 h). Images of the 500- μ M gap were captured at 0, 24, 96, and 120 h to monitor movement of the two cell fronts. Original magnification 100 x. Scale bar 500 μ M.



Supplementary Figure S2. Caspase-3/7 activation in PShTert myofibroblasts in direct contact with PC3 cells. PShTert myofibroblasts (1.1×10^4) were directly co-cultured with PC3 cells (1.43×10^3) in normal medium supplemented with CellEvent ($1 \mu\text{M}$). Cells were monitored in real-time for 96 h. Caspase-3/7 was activated only in PShTert myofibroblasts in contact with PC3 cells (squares). The area of PShTert myofibroblasts devoid of PC3 cells (dotted line) showed no evidence of caspase-3/7 activation. PShTert myofibroblasts treated with normal stripped medium or medium supplemented with actinomycin D (200 nM), both with CellEvent, were used as negative and positive controls respectively.

**CHAPTER 5: ANDROGEN RECEPTOR AND ANDROGEN-
RESPONSIVE GENE FKBP5 ARE INDEPENDENT
PROGNOSTIC INDICATORS FOR ESOPHAGEAL
ADENOCARCINOMA**

Eric Smith^{1*}, Helen M. Palethorpe^{1*}, Andrew R. Ruszkiewicz², Suzanne Edwards³, Damien A. Leach⁴, Tim J. Underwood, Eleanor F. Need, Paul A. Drew

¹Solid Cancer Regulation Group, Discipline of Surgery, Basil Hetzel Institute for Translational Health Research, The Queen Elizabeth Hospital, The University of Adelaide, 28 Woodville Rd, Woodville South, SA 5011, Australia;

²Gastroenterology Research Laboratory, SA Pathology, Frome Road, Adelaide, SA 5000, Australia;

³Data Management and Analysis Centre, Royal Adelaide Hospital, The University of Adelaide, North Terrace, Adelaide, SA 5005, Australia;

⁴Cancer Biology Group, Discipline of Surgery, Basil Hetzel Institute for Translational Health Research, The Queen Elizabeth Hospital, The University of Adelaide, 28 Woodville Rd, Woodville South, SA 5011, Australia;

⁵Cancer Sciences Unit, Somers Cancer Research Building, Southampton General Hospital, University of Southampton, Tremona Road, Southampton SO16 6YD, UK;

⁶Breast Biology and Cancer Unit, Discipline of Surgery, Basil Hetzel Institute for Translational Health Research, The Queen Elizabeth Hospital, The University of Adelaide, 28 Woodville Rd, Woodville South, SA 5011, Australia;

⁷School of Nursing and Midwifery, Flinders University, PO Box 2100, Adelaide, SA 5001, Australia.

*Equal contributors

Digestive Diseases and Sciences 2016; 61(2): 433-443

Statement of Authorship

Title of Paper	Androgen receptor and androgen-responsive gene FKBP5 are independent prognostic indicators for esophageal adenocarcinoma
Publication Status	Published
Publication Details	Smith E, Palethorpe HM , Ruszkiewicz AR, Edwards S, Leach DA, Underwood TJ, Need EF, Drew PA: Androgen receptor and androgen-responsive gene FKBP5 are independent prognostic indicators for esophageal adenocarcinoma. <i>Digestive Diseases and Sciences</i> 2016, 61, 433-443.

Principal Author

Name of Principal Author (Candidate)	Helen M Palethorpe		
Contribution to the Paper	Conceived and designed the experiments, performed the experiments, analysed the data and wrote the manuscript.		
Overall percentage (%)	40%		
Certification:	This paper reports on original research I conducted during the period of my Higher Degree by Research candidature and is not subject to any obligations or contractual agreements with a third party that would constrain its inclusion in this thesis. I am the primary author of this paper.		
Signature		Date	1/12/15

Co-Author Contributions

By signing the Statement of Authorship, each author certifies that:

- i. the candidate's stated contribution to the publication is accurate (as detailed above);
- ii. permission is granted for the candidate to include the publication in the thesis; and
- iii. the sum of all co-author contributions is equal to 100% less the candidate's stated contribution.

Name of Co-Author	Eric Smith		
Contribution to the Paper	Conceived and designed the experiments, performed the experiments, analysed immunohistochemistry, analysed the data and wrote the manuscript.		
Signature		Date	13/10/16

Name of Co-Author	Andrew R. Ruskiewicz		
Contribution to the Paper	Analysed histopathology and immunohistochemistry, analysed the data, and contributed to the writing of the manuscript.		
Signature		Date	5/10/16

Name of Co-Author	Suzanne Edwards		
Contribution to the Paper	Analysed the data and contributed to the writing of the manuscript.		
Signature		Date	5/10/16


Name of Co-Author	Damien A. Leach		
Contribution to the Paper	Analysed the data and contributed to the writing of the manuscript.		
Signature		Date	1/12/15

Name of Co-Author	Tim J. Underwood		
Contribution to the Paper	Analysed the data and contributed to the writing of the manuscript.		
Signature		Date	4/10/16

Name of Co-Author	Eleanor F. Need		
Contribution to the Paper	Analysed the data and contributed to the writing of the manuscript.		
Signature		Date	1/12/15

Name of Co-Author	Paul A. Drew		
Contribution to the Paper	Conceived and designed the experiments, analysed the data, wrote the manuscript.		
Signature		Date	14/10/16

Androgen Receptor and Androgen-Responsive Gene FKBP5 Are Independent Prognostic Indicators for Esophageal Adenocarcinoma

Eric Smith¹  · Helen M. Palethorpe¹ · Andrew R. Ruskiewicz² · Suzanne Edwards³ · Damien A. Leach⁴ · Tim J. Underwood⁵ · Eleanor F. Need⁶ · Paul A. Drew^{1,7}

Received: 14 June 2015 / Accepted: 28 September 2015 / Published online: 14 October 2015
© Springer Science+Business Media New York 2015

Abstract

Background Esophageal adenocarcinoma is a male-dominant disease, but the role of androgens is unclear.

Aims To examine the expression and clinical correlates of the androgen receptor (AR) and the androgen-responsive gene FK506-binding protein 5 (FKBP5) in esophageal adenocarcinoma.

Methods Expression of AR and FKBP5 was determined by immunohistochemistry. The effect of the AR ligand 5 α -dihydrotestosterone (DHT) on the expression of a panel of androgen-responsive genes was measured in AR-positive and AR-negative esophageal adenocarcinoma cell lines. Correlations in expression between androgen-responsive

genes were analyzed in an independent cohort of esophageal adenocarcinoma tissues.

Results There was AR staining in 75 of 77 cases (97 %), and FKBP5 staining in 49 (64 %), all of which had nuclear AR. Nuclear AR with FKBP5 expression was associated with decreased median survival (451 vs. 2800 days) and was an independent prognostic indicator (HR 2.894, 95 % CI 1.396–6.002, $p = 0.0043$) in multivariable Cox proportional hazards models. DHT induced a significant increase in expression of the androgen-responsive genes FKBP5, HMOX1, FBXO32, VEGFA, WNT5A, and KLK3 only in AR-positive cells in vitro. Significant correlations in expression were observed between these androgen-responsive genes in an independent cohort of esophageal adenocarcinoma tissues.

Conclusion Nuclear AR and expression of FKBP5 is associated with decreased survival in esophageal adenocarcinoma.

Eric Smith and Helen M. Palethorpe have contributed equally to this work.

Electronic supplementary material The online version of this article (doi:10.1007/s10620-015-3909-0) contains supplementary material, which is available to authorized users.

✉ Eric Smith
eric.smith@adelaide.edu.au

¹ Solid Cancer Regulation Group, Discipline of Surgery, Basil Hetzel Institute for Translational Health Research, The Queen Elizabeth Hospital, The University of Adelaide, 28 Woodville Rd, Woodville South, SA 5011, Australia

² Gastroenterology Research Laboratory, SA Pathology, Frome Road, Adelaide, SA 5000, Australia

³ Data Management and Analysis Centre, Royal Adelaide Hospital, The University of Adelaide, North Terrace, Adelaide, SA 5005, Australia

⁴ Cancer Biology Group, Discipline of Surgery, Basil Hetzel Institute for Translational Health Research, The Queen Elizabeth Hospital, The University of Adelaide, 28 Woodville Rd, Woodville South, SA 5011, Australia

⁵ Cancer Sciences Unit, Somers Cancer Research Building, Southampton General Hospital, University of Southampton, Tremona Road, Southampton SO16 6YD, UK

⁶ Breast Biology and Cancer Unit, Discipline of Surgery, Basil Hetzel Institute for Translational Health Research, The Queen Elizabeth Hospital, The University of Adelaide, 28 Woodville Rd, Woodville South, SA 5011, Australia

⁷ School of Nursing and Midwifery, Flinders University, PO Box 2100, Adelaide, SA 5001, Australia

Keywords Adenocarcinoma of the esophagus · Androgen receptors · FK506-binding protein 5 · Steroids · Prognosis

Background

Esophageal adenocarcinoma (EAC) is a dismal disease with a relative 5-year survival rate of 14 % [1]. Its incidence has increased more rapidly than any other cancer over the last four decades in the West, but most markedly in males [2–4]. The major risk factors are gastroesophageal reflux disease and obesity, leading to the only described precursor lesion for the cancer, Barrett's esophagus (BE). The reported ratio of males to females ranges from 7–10 to 1 [4]. This ratio is highest in younger patients and lower in older patients [4], which is in part accounted for by an approximately 20-year delay in onset in females for BE [5] and EAC [6].

The high ratio of males with this cancer, and the change in the ratio with age, suggests a role for the sex steroid hormones: Their concentrations differ between males and females and change over the lifespan. Serum estrogen and progesterone levels cycle about a relatively high mean in the adult female and drop abruptly at menopause. Serum androgen levels are high in young adult males and decline progressively throughout adulthood. However, evidence that these hormones play a role in EAC is limited. The male dominance could be, at least partly, explained by a protective effect of estrogens in females which is lost after menopause. Estrogen receptors have been reported in esophageal tissue [7, 8], and there are reports which suggest that estrogen is inhibitory to EAC cell lines [9].

Alternatively, androgens could be involved in the biology of this cancer. There have been relatively few studies of androgens or androgen receptor (AR) signalling in EAC. Serum androgens have been reported to be elevated in both BE [10] and EAC [11]. Three previous studies investigated AR protein expression in EAC, but they examined relatively small patient cohorts, produced conflicting results, did not examine whether AR was functional, and reported no associations with survival [8, 11, 12]. Two epidemiological reports support a role for androgens. Prostate cancer patients given anti-androgen therapy had a statistically significant 30 % risk reduction for EAC [13], and gastroesophageal cancer was positively associated with a family history of prostate cancer [14].

The androgen signalling cascade is activated by androgens, particularly testosterone and its metabolite 5 α -dihydrotestosterone (DHT), which binds to the AR in the cytoplasm. The activated AR translocates to the nucleus and binds to androgen response elements in the genome. This binding may then result in the up- or down-regulation of transcription of androgen-responsive genes, such as

FK506-binding protein 5 (FKBP5) [15–17], heme oxygenase 1 (HMOX1) [18], F-box protein 32 (FBXO32) [19], wingless-type MMTV integration site family, member 5A (WNT5A) [20], vascular endothelial growth factor A (VEGFA) [21], and kallikrein-related peptidase 3 (KLK3) [22]. The actual genes whose expression is altered are influenced by the interaction of AR and various co-regulators and are tissue and context dependent. FKBP5 expression is often used as an indicator of functional AR signalling, as in prostate cancer studies where it reflects better than any other AR target gene androgen levels after either short-term or long-term androgen deprivation therapy [23].

Given the conflicting data on AR expression in EAC, and the lack of information as to whether, when present, it is functional, the specific aim of this study was to investigate AR expression and signalling in EAC. Associations between expression of AR and FKBP5 and clinicopathological parameters, including overall survival, were examined using multivariable Cox proportional hazards models to adjust for confounding parameters. The effect of DHT on the expression of androgen-responsive genes was assessed in AR-negative and AR-positive esophageal cancer cell lines. Correlations between the expression levels of putative androgen-responsive genes were assessed using tissues from an independent cohort of patients with BE and EAC.

Materials and Methods

Tissue Microarrays and Immunohistochemistry

Specificity of all antibodies was confirmed by Western immunoblot, which included both positive and negative controls. Each antibody labeled a single band at the expected molecular weight. Antibodies then were optimized with control tissue blocks before application to the tissue microarrays. A tissue microarray composed of one or more representative cores from 77 cases of EAC was constructed as previously described [24]. None of the patients had been given preoperative chemotherapy or radiotherapy. Sequential 4- μ m sections were mounted on polylysine-coated slides, dewaxed, and rehydrated. Antigen retrieval was performed by heating the sections for 5 min in 10 mmol/L citrate buffer (pH 6) in a microwave pressure cooker. After cooling to room temperature, sections were immunostained using an Autostainer Plus (Dako, Glostrup, Denmark). Sections were incubated for 60 min with either 1:50 rabbit anti-human AR (clone N-20, raised against the first 20 amino acids of the N terminus of AR) polyclonal IgG (Santa Cruz Biotechnology Inc., Santa Cruz, CA, USA) or 1:400 rabbit anti-human FKBP5

(FKBP51, clone H-100) polyclonal IgG (Santa Cruz Biotechnology Inc.). Slides were then incubated with MACH 4 Universal Horseradish Peroxidase-Polymer (Biocare Medical, Concord, CA, USA). Liquid 3,3-diaminobenzidine (Dako) was used as the chromogen, and sections were counterstained with Meyer's hematoxylin. The staining was scored by an experienced gastrointestinal pathologist (ARR) and ES. Expression of AR was scored separately in the cytoplasm and the nucleus as positive (present in ≥ 5 % of the tumor epithelial cells) or negative. Expression of FKBP5 was scored as positive (present in ≥ 5 % tumor epithelial cells) or negative.

Cell Lines

The EAC cell lines OE33, OE19, and JH-EsoAd1 were maintained in RPMI-1640, and FLO-1 in DMEM, supplemented with 10 % fetal bovine serum, 4 mmol/L L-glutamine, 200 U/mL penicillin, and 200 μ g/mL streptomycin. The esophageal squamous cell line TE7 was similarly maintained in RPMI-1640 plus supplements. All cells were incubated at 37 °C with 5 % CO₂ in air.

Stable Transduction of Cell Lines with Androgen Receptor

The AR gene was amplified from the expression vector pCMV-AR3.1 using Gateway cloning-compatible primers (Supplementary Table S1) and transferred into pLV411 plasmid using the Gateway cloning system, as previously described [25]. Stably transduced cells were selected using two rounds of fluorescence activated cell sorting for green fluorescent protein. The mock-transduced OE33 and AR-expressing cell line (OE33-AR) were maintained in phenol red-free media supplemented with 10 % dextran-coated charcoal-stripped fetal bovine serum, 4 mmol/L L-glutamine, 200 U/mL penicillin, and 200 μ g/mL streptomycin (stripped medium).

In Vitro Transactivation Assay

Cells were seeded at 15,000 cells per well in 96-well plates in stripped medium and incubated for 24 h. Cells were transiently transfected with either 50 ng of the synthetic minimal androgen-responsive luciferase probasin-driven promoter tk81-PB3 (PB3-luc) or 50 ng of PB3-luc and 2.5 ng of the androgen receptor expression vector pCMV-AR3.1 (AR) and incubated for 4 h, as previously described [26]. Cells were treated with either vehicle (V; 0.1 % ethanol), 10 nmol/L DHT, 10 mmol/L of the anti-androgen bicalutamide (B), or 10 nmol/L DHT and 10 mmol/L B (DHT + B) in stripped medium and incubated for 16–20 h. Cells were lysed and luciferase activity was

measured using a FLUOstar Optima (BMG Labtech, Ortenberg, Germany). Whole-cell lysates from six replicate wells were pooled and analyzed for protein expression by Western immunoblot.

Western Immunoblot Analysis

Cells were seeded at 2×10^5 cells per well in six-well plates in stripped medium and incubated for 72 h. Cells were treated with either V or 10 nmol/L DHT for 16 h. Whole-cell lysates were prepared, and 15 μ g of protein was resolved by denaturing electrophoresis on 4–15 % Mini-Protean TGX precast polyacrylamide gels (Bio-Rad Laboratories, Hercules, CA), transferred to Hybond-C membrane (Amersham Biosciences, Castle Hill, NSW, Australia), and immunostained using 1:10,000 rabbit anti-human AR (N-20) polyclonal IgG, 1:4000 rabbit anti-human FKBP5 (H-100) polyclonal IgG, and 1:5000 mouse anti-human β -actin (clone AC-15) polyclonal IgG1 (Sigma-Aldrich, St Louis, MO). Immunoreactivity was detected using the appropriate horseradish peroxidase-conjugated IgG and visualized using enhanced chemiluminescence (Amersham).

Measurement of Gene Expression by Quantitative Real-Time Reverse-Transcription PCR

Cells were seeded in stripped medium at 5×10^5 cells per well in six-well plates and incubated for 24 h. Cells were treated with either V or 10 nmol/L DHT in stripped medium and incubated for 4, 8, or 24 h. Total RNA was isolated using the RNeasy Mini Kit with on-column DNase I digestion (Qiagen, Hilden, Germany). Total RNA (1 μ g) was reverse-transcribed using the iScript cDNA Synthesis Kit (Bio-Rad Laboratories) in a final volume of 20 μ L. Gene expression was determined using iQ SYBR Green Supermix (Bio-Rad Laboratories) in a final volume of 10 μ L, containing 0.1 μ L of cDNA and a final concentration of 0.2 μ mol/L of each forward and reverse primer (Supplementary Table S1). Triplicate reactions were performed using a CFX (Bio-Rad Laboratories) at 95 °C for 3 min, then 40 cycles of 95 °C for 15 s, 60 °C for 15 s, and 72 °C for 30 s, followed by a final extension of 72 °C for 1 min. The products were melted to confirm specificity. Normalized fold expression ($\Delta\Delta$ Cq) was calculated using β -actin (ATCB) and glyceraldehyde-3-phosphate dehydrogenase (GAPDH) as reference genes using the CFX software.

Statistical Analysis

The statistical software used was SAS 9.3 (SAS Institute Inc., Cary, NC, USA) and Prism 6.0d for Macintosh

(GraphPad Software, San Diego CA, USA; www.graphpad.com). Hazard ratios (HR), 95 % confidence intervals (CI), and p values were calculated from univariate and multivariable Cox proportional hazards models. The proportional hazards assumption was found to be upheld for each univariate and multivariable regression. Initially, each confounder that had a significant HR in univariate analysis ($p < 0.1$) was included in the multivariable model with the predictor being AR nuclear localization or FKBP5 expression or AR nuclear localization and FKBP5. However, there were too few observations to account for the 10 covariates. Therefore, backwards stepwise elimination was performed. The confounder with the highest p value was eliminated, one at a time, until the final most parsimonious model had all confounders with $p < 0.05$ or $p < 0.2$ depending on the model. Normalized fold expression data were compared using unpaired t test. Correlations between androgen-responsive genes in esophageal tissues were determined using linear regression. All statistics were considered significant when the two-tailed $p < 0.05$.

Results

Expression of AR and FKBP5 in Esophageal Adenocarcinoma Tissues

The protein expression of AR and FKBP5 was investigated by immunohistochemistry in resection tissue from 77 cases of EAC (Fig. 1). Low-to-medium-intensity staining of AR in tumor epithelial cells was observed in 75 of the 77 cases (97.4 %). Nuclear localization was observed in 70 cases (90.9 %). There was nuclear only staining in seven cases (9.1 %), cytoplasmic only in five (6.5 %), and both nuclear and cytoplasmic in 63 (81.8 %).

Low-to-high-intensity staining of FKBP5 in tumor epithelial cells was observed in 49 cases (63.6 %). All of the FKBP5 positive cases also had nuclear localization of AR. Of the 28 cases that did not express FKBP5, 21 had nuclear localization of AR and seven did not. There was a significant association between FKBP5 expression and AR nuclear localization ($p = 0.0005$). These data suggest that in primary EAC epithelial cells, nuclear localization of the AR is necessary but not sufficient for FKBP5 expression.

Clinical Significance of AR and FKBP5 in Esophageal Adenocarcinoma

To determine the clinical significance of the expression of AR and FKBP5, we examined associations with clinicopathological data which was available for 76 of the cases. The median age of these patients at surgery was 64 years (range 36–81), the median follow-up time was 865 days

(range 37–4661), and the 5-year overall survival rate was 36.7 %.

Nuclear localization of AR was significantly associated with the presence of BE (Supplementary Table S2; $p = 0.0009$). It was detected in all tissues from patients who had coexisting BE, but only 76.7 % of tissues from patients without BE. There was no significant difference in AR staining for patient age or gender. Patients with nuclear AR had a median overall survival of 671 days compared to 1321 days for those without (Fig. 2a).

Similarly, the expression of FKBP5 was more prevalent in patients with BE observable on endoscopy or in the resection specimen (Supplementary Table S2; $p = 0.0495$). Patients with FKBP5 expression had a median overall survival of 451 days compared to 1338 days for those that were FKBP5-negative (Fig. 2b). For those patients who were FKBP5-negative but had nuclear AR (nuc AR+/FKBP5–), the median overall survival was 2800 days (Fig. 2c).

To investigate the difference between hazards of dying, univariate and multivariable Cox proportional hazards models were used. In univariate models, neither AR nuclear localization nor FKBP5 expression was associated with a significant difference in risk of death (Supplementary Table S3). In multivariable models when adjusting for confounders, AR nuclear localization (HR 3.290, 95 % CI 1.125–9.620, $p = 0.0296$) and FKBP5 expression (HR 3.043, 95 % CI 1.417–6.531, $p = 0.0043$) were associated with a significant increase in risk of death (Supplementary Table S3). For the subset of patients who had AR nuclear localization, FKBP5 expression was not associated with a significant difference in risk of death in the univariate model (Table 1; HR 1.829, 95 % CI 0.904–3.701, $p = 0.0930$). However, in the multivariable model, after adjusting for confounders, patients who had AR nuclear localization and FKBP5 expression had 2.9 times the hazard of dying (Table 1; HR 2.894, 95 % CI 1.396–6.002, $p = 0.0043$).

AR and FKBP5 in Esophageal Cancer Cell Lines

The expression of AR and FKBP5 protein was measured in esophageal cancer cell lines (Fig. 3a). AR was not detected, nor induced by DHT, in OE33, OE19, JH-EsoAd1, FLO-1, or TE7. FKBP5 expression was low in OE33, OE19, JH-EsoAd1, and TE7, higher in FLO-1, and not upregulated by DHT in any of these cell lines.

Functional AR activity was not measured by transactivation assay in cell lines which were transiently transfected just with the synthetic minimal androgen-responsive luciferase probasin-driven promoter tk81-PB3 (PB3-luc; Fig. 3b, c). No luciferase activity was induced over a broad concentration range of DHT (0.01–1000 nmol/L) in OE33 or

Fig. 1 AR and FKBP5 are expressed in human esophageal adenocarcinoma. Representative images of AR and FKBP5 immunohistochemistry. Tissue which is AR negative and FKBP5 negative (a, b). Tissue which is nuclear AR positive and FKBP5 negative (c, d). Tissue which is nuclear AR-positive and FKBP5-positive (e, f)

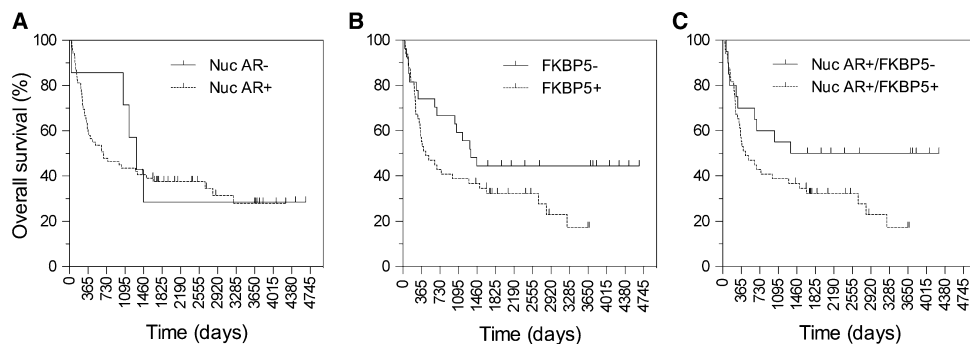
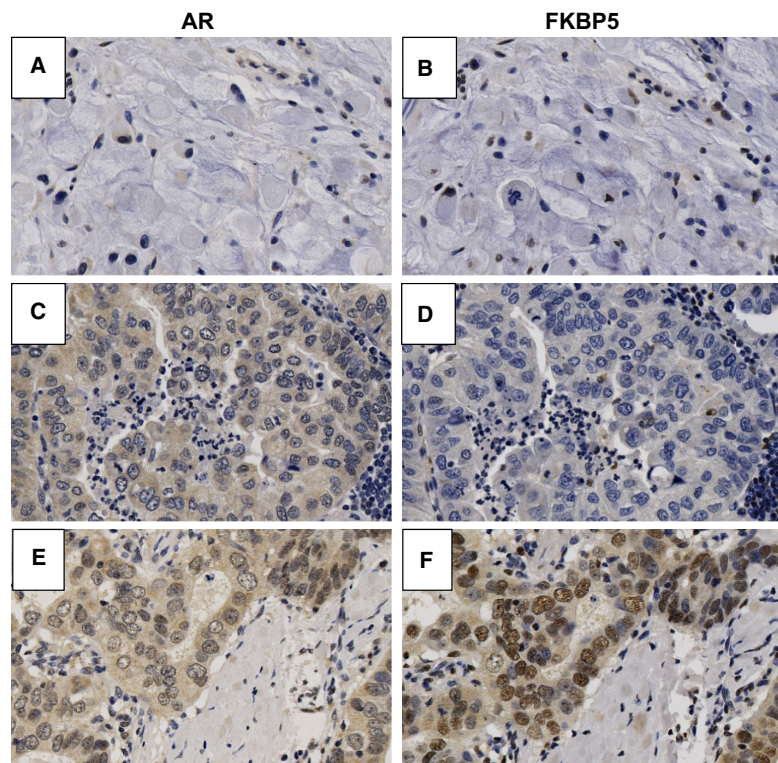


Fig. 2 AR and FKBP5 protein expression associate with survival. Kaplan–Meier analysis of overall survival of patients with esophageal adenocarcinoma with expression measured by immunohistochemistry. **a** nuclear AR negative (Nuc AR–; $n = 7$) or nuclear AR

positive (Nuc AR+; $n = 69$). **b** FKBP5 negative (FKBP5–; $n = 27$) or FKBP5 positive (FKBP5+; $n = 49$). **c** Nuclear AR positive and FKBP5 negative (Nuc AR+/FKBP5–; $n = 20$) or nuclear AR positive and FKBP5 positive (Nuc AR+/FKBP5+; $n = 49$)

at 10 nmol/L in OE19, JH-EsoAd1, and FLO-1. However, transient co-transfection of both the AR expression vector pCMV-AR3.1 (AR) and the PB3-luc resulted in DHT-induced luciferase expression (Fig. 3b, c). Expression of AR in these transiently co-transfected cells was confirmed by Western immunoblots (data not shown). Luciferase activity

was dependent on the concentration of DHT and was blocked by the anti-androgen bicalutamide. These results show that although functional AR was not expressed in the cell lines, they were competent for AR signalling.

In order to examine the effect of AR signalling, we stably transduced OE33 cells with AR, designating them

Table 1 Univariate and multivariable analysis of associations between clinicopathological parameters and overall survival in nuclear AR-positive tumors

	<i>n</i>	Median overall survival (days)	5-year overall survival (%)	Univariate		Multivariable	
				HR (95 % CI)	<i>p</i> value	HR (95 % CI)	<i>p</i> value
FKBP5 expression							
Negative	20	2800	50	1		1	
Positive	49	451	32.3	1.829 (0.904–3.701)	0.093	2.894 (1.396–6.002)	0.0043
Barrett's esophagus							
Absent	23	352	13	1		1	
Present	46	1581	49.7	0.388 (0.215–0.701)	0.0017	0.486 (0.260–0.910)	0.0240
Gender							
Female	10	476	20	1			
Male	59	976	40.5	0.596 (0.286–1.241)	0.1666		
Age at surgery ^a	69	671	37.5	1.038 (1.003–1.073)	0.0308		
Tumor length ^a	69	671	37.5	1.014 (1.002–1.025)	0.0149		
Primary tumor (T)							
T1a	6	3162	100	1		1	
T1b	11	2072	81.8	2.055 (0.214–19.778)	0.5330 ^b	1.530 (0.157–14.872)	0.7140 ^b
T2	9	1438	55.6	5.804 (0.672–50.115)	0.1098	4.599 (0.531–39.852)	0.1661
T3	32	459	18.8	10.258 (1.377–76.344)	0.0231	8.842 (1.158–67.492)	0.0356
T4a/b	11	160	0	35.258 (4.357–285.328)	0.0008	34.712 (4.190–287.563)	0.0010
Regional lymph node (N)							
N0	29	1760	65.3	1			
N1	14	650	35.7	2.246 (0.966–5.223)	0.0602 ^b		
N2	17	337	11.8	4.766 (2.147–10.577)	0.0001		
N3	9	252	0	8.157 (3.209–20.735)	<0.0001		
Grade of differentiation							
Well/moderate	19	2136	73.7	1			
Poor/undifferentiated	49	363	22.1	3.630 (1.609–8.188)	0.0019		
Circumferential resection margin							
Negative	37	1711	59.1	1			
Positive	32	279	12.5	3.355 (1.835–6.134)	<0.0001		
Vascular invasion							
Negative	15	2674	86.2	1			
Positive	48	358	20.6	6.702 (2.336–19.227)	0.0004		
Perineural invasion							
Negative	23	2136	69.6	1			
Positive	34	312	14.1	4.141 (1.921–8.930)	0.0003		

^a This predictor is continuous variable^b Global $p < 0.0001$

OE33-AR. Expression of AR was confirmed by Western immunoblot (Fig. 3a), and AR function was confirmed by transactivation assay (Fig. 3d). Treatment with DHT did not alter FKBP5 mRNA expression in the untransduced, AR-negative, OE33 cells (Fig. 3e), but did induce a time-dependent increase in OE33-AR (Fig. 3f). Furthermore, the abundance of FKBP5 protein steady-state levels in the OE33-AR cells was increased by DHT (Fig. 3a).

Androgen-Responsive Genes in AR-Positive Cell Line and Esophageal Tissues

To further explore the effect of functional AR in cell lines, we measured the effect of DHT on the expression of a panel of putative, clinically relevant androgen-responsive genes. Androgen-responsive genes have not been defined in EAC, so we measured expression of genes known to be androgen responsive in other tissues and cell lines. DHT

significantly increased the expression of HMOX1 (23-fold), FBXO32 (19-fold), WNT5A (fourfold), and VEGFA (threefold), and induced the expression of KLK3 in the AR-positive OE33-AR, but not in the AR-negative OE33 (Fig. 4).

To determine whether this panel of androgen-responsive genes was also altered in an independent cohort of esophageal tissues, we looked for correlations between the genes in a publicly available transcriptional microarray dataset [27]. There were significant correlations between FKBP5 and each of the genes in the panel in EAC (Fig. 5). In contrast, there was no significant correlation in esophageal squamous mucosa (SQ), and the only correlations in BE were observed for FBXO32 and KLK3.

Discussion

We observed AR protein expression in tumor epithelial cells in 75 of 77 patients with EAC. There was nuclear localization in 91 % of these. The androgen-responsive gene FKBP5 was expressed in 64 % of these tissues, but only in those which also had nuclear localization of AR. Expression of either AR or FKBP5 was associated with decreased overall survival by multivariable analysis. We created an AR-positive EAC cell line, OE33-AR, by stably transducing the gene for AR into the AR-negative OE33. We found that DHT induced a time-dependent increase in FKBP5 expression in the OE33-AR cells, but not the AR-negative OE33. Also, DHT increased expression of the androgen-responsive genes HMOX1, FBXO32, WNT5A, VEGFA, and KLK3. Correlations between the expressions of these androgen-responsive genes were observed in an independent cohort of EAC tissues, consistent with functional AR being expressed in EAC.

Ours is the largest cohort to date used to investigate AR protein expression in EAC. Three previous studies of AR expression in EAC have produced conflicting results. Focal staining was reported in one of 20 patients [8], in the tumor epithelial cells in five of 11 patients with no stromal expression [12], and in the stroma in 13 of 18 patients with no expression in the tumor epithelial cells [11]. In contrast, we observed a significantly higher incidence of AR expression and nuclear localization in EAC tumor epithelial cells than the previous reports. There are several possible explanations for the discrepancy. There may be differences in the sensitivity of the staining methods or reporting thresholds, particularly as the abundance of AR in EAC is relatively low compared to, for example, prostate or breast cancer. Two of the studies used a different antibody to ours [11, 12], and although these two studies used the same antibody, one reported no staining of AR in the tumor epithelial cells and the other staining in 45 % of

cases. Variability of positivity and staining intensity between studies is not unusual. AR is expressed across a wide range of cancers, but for most cancers, just as with EAC, the published rates of expression vary widely, for reasons that are not clear [28].

To determine whether the AR signalling pathway was functional in EAC, we stained for the androgen-responsive gene FKBP5. Expression was only found in a subset of tumors which had nuclear localization of AR, suggesting that AR activation was required, but not sufficient, for FKBP5 expression. This was consistent with our cell line data, where DHT did not alter FKBP5 expression in the AR-negative EAC cell lines, but did in the AR-positive cell line, OE33-AR.

One explanation for our survival data is that the expression of FKBP5 is a marker of a functional AR signalling pathway which alters the expression of one or more genes which then reduce overall survival. In the nuclear AR-positive, FKBP5-negative cells, the AR pathway might not be functional, or is regulating different androgen-responsive genes from those in the FKBP5-positive tissues. This is consistent with recent studies which show that AR signalling is not a simple ligand-receptor bound to specific DNA receptor element model. Rather AR, like other steroid receptors, derives cell-specific transcription activity from interactions with various co-regulators and DNA-binding proteins that regulate receptor binding and lineage-specific chromatin organization [29]. Alternatively, FKBP5 itself may influence survival, but in our tissues it is only expressed in cells with a functional AR signalling pathway, while in other contexts it may be expressed as a result of progesterin or glucocorticoid signalling.

Overexpression of FKBP5 has been reported in a range of solid tumors [30], including melanoma [31], glioma [32], colon [33], and prostate [34–37]. FKBP5 can inhibit apoptosis and promote cell proliferation in normal, pre-malignant, and malignant tissues. In melanoma, expression correlated with tumor aggressiveness and was maximal in metastatic lesions [31] and in glioma expression correlated with stage and overall patient survival [32]. In contrast, down-regulation of FKBP5 has been reported in pancreatic cancer, and decreased expression resulted in hyperphosphorylation of Akt and decreased cell death following genotoxic stress in cell lines [38]. These reports do not detail the AR status of the cancer tissues. Thus, FKBP5 may either be acting as a surrogate marker of a particular AR activated set of genes, or it may be the responsible gene itself.

None of the four common EAC cell lines we examined expressed AR. Lack of AR expression in cultured cell lines does not mean that the receptor was not present in the primary tissue from which the cell line was derived. Protein expression of steroid receptors, such as AR, present in

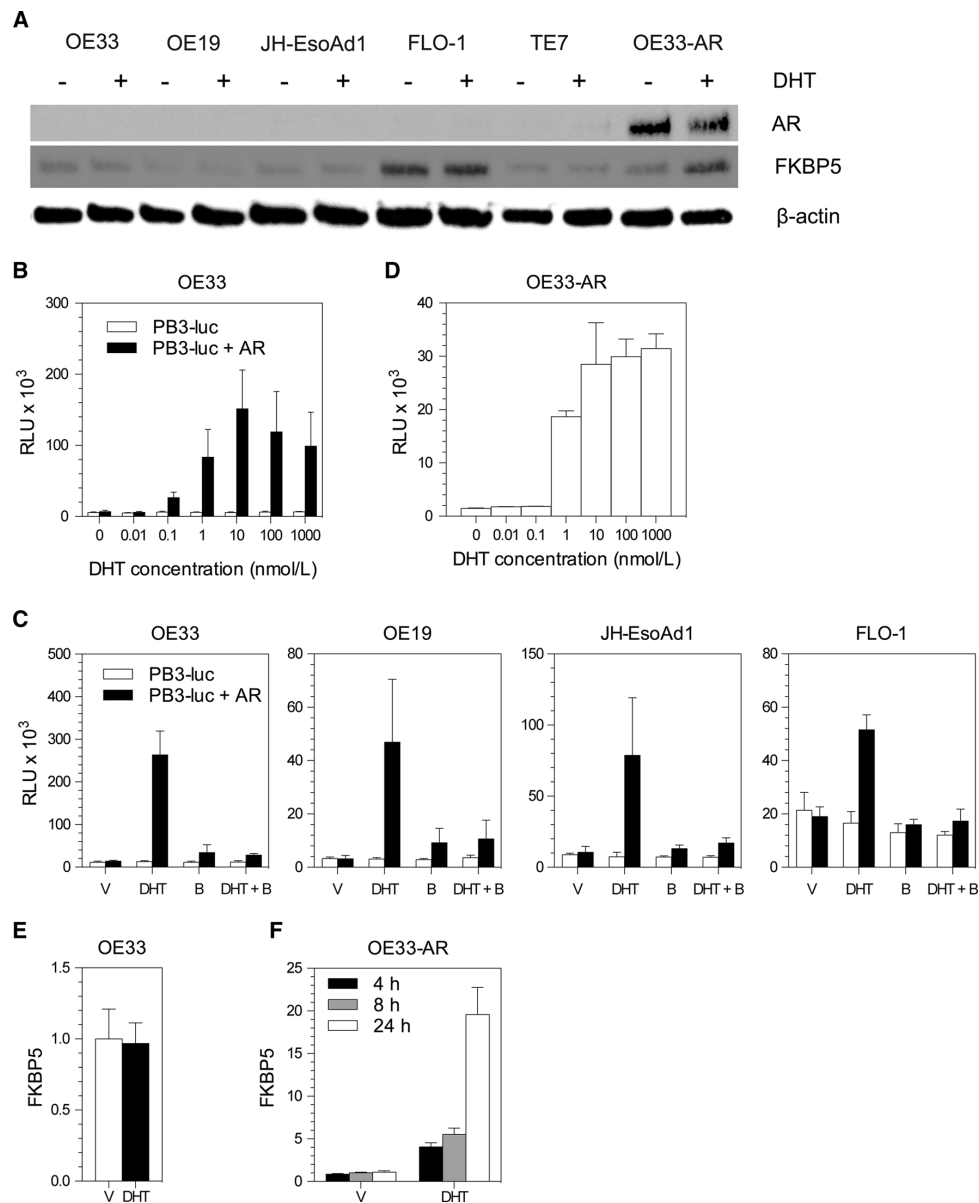


Fig. 3 Functional expression of androgen receptor in human esophageal cancer cell lines. **a** Western immunoblot for AR and FKBP5 expression in esophageal adenocarcinoma (OE33, OE19, JH-EsoAd1 and FLO-1) and squamous cell carcinoma (TE7) cell lines following 16-h treatment with either 0.1 % ethanol vehicle (-) or 10 nmol/L DHT (+). **b** Transactivation assay for OE33 transfected with either synthetic androgen-responsive probasin-driven luciferase reporter (PB3-luc) alone or together the androgen receptor expression vector pCMV-AR3.1 (PB3-luc + AR), and treated with 0–1000 nmol/L DHT. **c** Transactivation assay for cell lines transfected with either PB3-luc or PB3-luc + AR and treated with either

0.1 % ethanol vehicle (V), 10 nmol/L DHT, 10 nmol/L anti-androgen bicalutamide (**b**), or 10 nmol/L DHT and 10 nmol/L bicalutamide (DHT + B). **d** Transactivation assay for OE33-AR transfected with PB3-luc and treated with 0–1000 nmol/L DHT. Data for all transactivation assays are the mean relative luminescence units (RLU) \pm standard deviation of six replicates. **e** Normalized fold FKBP5 expression for OE33 treated with either V or 10 nmol/L DHT for 24 h. **f** Normalized fold FKBP5 expression for OE33-AR treated with either V or 10 nmol/L DHT for 4, 8, or 24 h. Data for FKBP5 normalized fold expression are the mean \pm standard deviation of triplicate reactions for three biological replicates

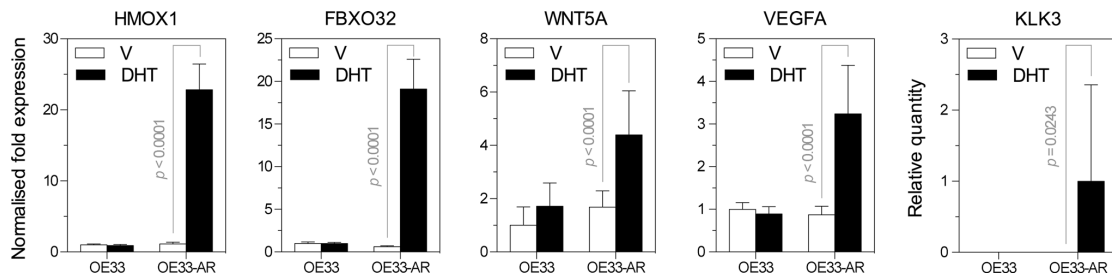


Fig. 4 Expression of androgen-responsive genes in human esophageal cancer cell lines. Normalized fold expression or relative quantity for OE33 or OE33-AR treated with either V or 10 nmol/L DHT for 24 h. Data for normalized fold expression or relative quantity are the mean \pm standard deviation of triplicate reactions for three biological replicates

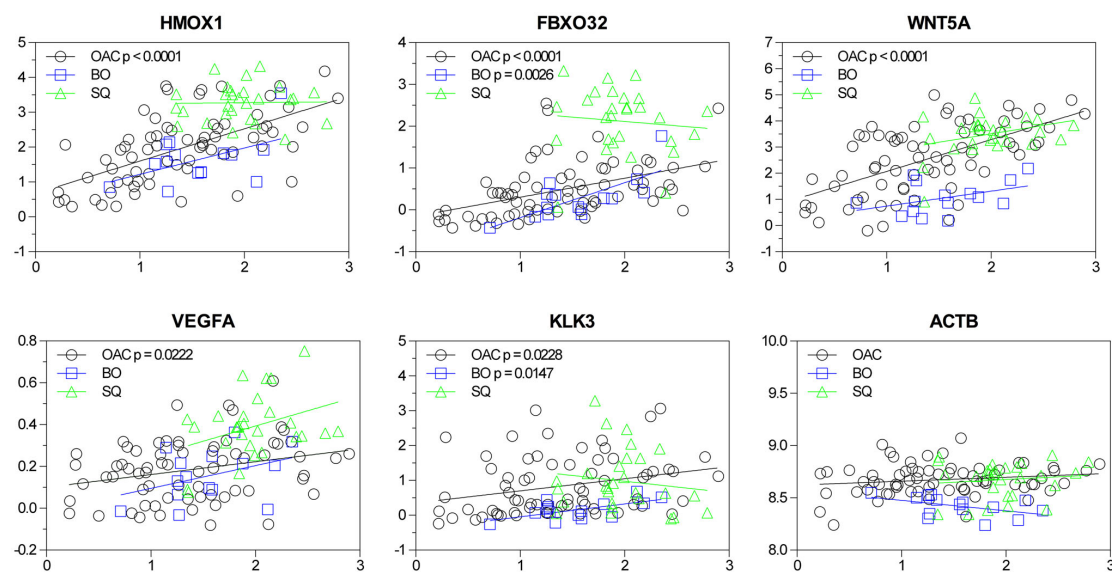


Fig. 5 Androgen-responsive genes are expressed in esophageal tissues. Correlations of \log_2 median-centered intensities for FKBP5 (x-axis) versus either HMOX1, FBXO32, WNT5A, VEGFA, KLK3, or ACTB (y-axis) for EAC, SQ, or BE tissues

cells of the primary tissue are frequently lost from the cells following culture, by mechanisms that are not clearly understood [39, 40]. However, these esophageal cell lines expressed the necessary co-regulators for AR signalling, as they exhibited AR transactivation activity following either transient transfection or stable transduction with the AR gene. We further showed that FKBP5, HMOX1, FBXO32, WNT5A, VEGFA, and KLK3 were androgen-responsive genes in the OE33-AR cell line following treatment with DHT.

This is the largest study of AR expression in EAC, and it shows that in most patients tumor epithelial cells express AR. This is the first study to show AR to be functional in the majority, but not all, cases of EAC, as defined by

nuclear localization and expression of the androgen-responsive gene FKBP5. Significantly, it was sufficiently powered to show that AR and the androgen-responsive gene FKBP5 were independently associated with decreased overall survival. The correlation between nuclear localization of AR and expression of FKBP5 in our cohort of EACs and the correlations between the expressions of androgen-responsive genes in an independent cohort of patients, suggest that AR is functional in at least the majority of tumors. It further suggests that AR, FKBP5, or other androgen-responsive genes influence survival. These findings raise the possibility of novel therapeutic options for EAC, such as the use of drugs which target AR signalling, or the androgen-responsive genes.

Acknowledgments The authors would like to thank Mr. Bill Panagopoulos for technical assistance and provision of PCR primers.

Compliance with ethical standards

Conflict of interest The authors declare that they have no conflict of interest.

References

- Lagergren J, Mattsson F. Diverging trends in recent population-based survival rates in oesophageal and gastric cancer. *PLoS One*. 2012;7:e41352.
- Lord RV, Law MG, Ward RL, Giles GG, Thomas RJ, Thursfield V. Rising incidence of oesophageal adenocarcinoma in men in Australia. *J Gastroenterol Hepatol*. 1998;13:356–362.
- Dodaran MS, Silcocks PB, Logan RFA. Continuing rise in incidence of oesophageal adenocarcinoma in England and Wales. *Gut*. 2001;48:110.
- Rutegard M, Lagergren P, Nordenstedt H, Lagergren J. Oesophageal adenocarcinoma: the new epidemic in men? *Maturitas*. 2011;69:244–248.
- van Soest EM, Siersema PD, Dieleman JP, Sturkenboom MC, Kuipers EJ. Age and sex distribution of the incidence of Barrett's esophagus found in a Dutch primary care population. *Am J Gastroenterol*. 2005;100:2599–2600.
- Derakhshan MH, Liptrot S, Paul J, Brown IL, Morrison D, McColl KE. Oesophageal and gastric intestinal-type adenocarcinomas show the same male predominance due to a 17 year delayed development in females. *Gut*. 2009;58:16–23.
- Akgun H, Lechago J, Younes M. Estrogen receptor-beta is expressed in Barrett's metaplasia and associated adenocarcinoma of the esophagus. *Anticancer Res*. 2002;22:1459–1461.
- Tiffin N, Suvarna SK, Trudgill NJ, Riley SA. Sex hormone receptor immunohistochemistry staining in Barrett's oesophagus and adenocarcinoma. *Histopathology*. 2003;42:95–96.
- Sukocheva OA, Wee C, Ansar A, Hussey DJ, Watson DI. Effect of estrogen on growth and apoptosis in esophageal adenocarcinoma cells. *Dis Esophagus*. 2013;26:628–635.
- Cook MB, Wood SN, Cash BD, et al. Association between circulating levels of sex steroid hormones and Barrett's esophagus in men: a case-control analysis. *Clin Gastroenterol Hepatol*. 2015;13:673–682.
- Awan AK, Iftikhar SY, Morris TM, et al. Androgen receptors may act in a paracrine manner to regulate oesophageal adenocarcinoma growth. *Eur J Surg Oncol*. 2007;33:561–568.
- Tihan T, Harmon JW, Wan X, et al. Evidence of androgen receptor expression in squamous and adenocarcinoma of the esophagus. *Anticancer Res*. 2001;21:3107–3114.
- Cooper SC, Croft S, Day R, Thomson CS, Trudgill NJ. Patients with prostate cancer are less likely to develop oesophageal adenocarcinoma: could androgens have a role in the aetiology of oesophageal adenocarcinoma? *Cancer Causes Control*. 2009;20:1363–1368.
- Jiang X, Tseng CC, Bernstein L, Wu AH. Family history of cancer and gastroesophageal disorders and risk of esophageal and gastric adenocarcinomas: a case-control study. *BMC Cancer*. 2014;14:60.
- Magee JA, Chang LW, Stormo GD, Milbrandt J. Direct, androgen receptor-mediated regulation of the FKBP5 gene via a distal enhancer element. *Endocrinology*. 2006;147:590–598.
- Makkonen H, Kauhanen M, Paakinaho V, Jaaskelainen T, Palmimo JJ. Long-range activation of FKBP51 transcription by the androgen receptor via distal intronic enhancers. *Nucleic Acids Res*. 2009;37:4135–4148.
- Nelson PS, Clegg N, Arnold H, et al. The program of androgen-responsive genes in neoplastic prostate epithelium. *Proc Natl Acad Sci USA*. 2002;99:11890–11895.
- Kwack MH, Sung YK, Chung EJ, et al. Dihydrotestosterone-inducible dickkopf 1 from balding dermal papilla cells causes apoptosis in follicular keratinocytes. *J Invest Dermatol*. 2008;128:262–269.
- Leach DA, Need EF, Trotta AP, Grubisha MJ, DeFranco DB, Buchanan G. Hic-5 influences genomic and non-genomic actions of the androgen receptor in prostate myofibroblasts. *Mol Cell Endocrinol*. 2014;384:185–199.
- Leach DA, Need EF, Toivanen R, et al. Stromal androgen receptor regulates the composition of the microenvironment to influence prostate cancer outcome. *Oncotarget*. 2015;6:16135–16150.
- Eisermann K, Broderick CJ, Bazarov A, Moazam MM, Fraizer GC. Androgen up-regulates vascular endothelial growth factor expression in prostate cancer cells via an Sp1 binding site. *Mol Cancer*. 2013;12:7.
- Wang G, Jones SJ, Marra MA, Sadar MD. Identification of genes targeted by the androgen and PKA signaling pathways in prostate cancer cells. *Oncogene*. 2006;25:7311–7323.
- Mostaghel EA, Page ST, Lin DW, et al. Intraprostatic androgens and androgen-regulated gene expression persist after testosterone suppression: therapeutic implications for castration-resistant prostate cancer. *Cancer Res*. 2007;67:5033–5041.
- Smith E, Ruzsiewicz AR, Jamieson GG, Drew PA. IGF1BP7 is associated with poor prognosis in oesophageal adenocarcinoma and is regulated by promoter DNA methylation. *Br J Cancer*. 2014;110:775–782.
- Barry SC, Harder B, Brzezinski M, Flint LY, Seppen J, Osborne WR. Lentivirus vectors encoding both central polypurine tract and posttranscriptional regulatory element provide enhanced transduction and transgene expression. *Hum Gene Ther*. 2001;12:1103–1108.
- Need EF, Scher HI, Peters AA, et al. A novel androgen receptor amino terminal region reveals two classes of amino/carboxyl interaction-deficient variants with divergent capacity to activate responsive sites in chromatin. *Endocrinology*. 2009;150:2674–2682.
- Kim SM, Park YY, Park ES, et al. Prognostic biomarkers for esophageal adenocarcinoma identified by analysis of tumor transcriptome. *PLoS One*. 2010;5:e15074.
- Munoz J, Wheler JJ, Kurzrock R. Androgen receptors beyond prostate cancer: an old marker as a new target. *Oncotarget*. 2015;6:592–603.
- Chang C, Lee SO, Yeh S, Chang TM. Androgen receptor (AR) differential roles in hormone-related tumors including prostate, bladder, kidney, lung, breast and liver. *Oncogene*. 2014;33:3225–3234.
- Staibano S, Mascolo M, Ilardi G, Siano M, De Rosa G. Immunohistochemical analysis of FKBP51 in human cancers. *Curr Opin Pharmacol*. 2011;11:338–347.
- Romano S, Staibano S, Greco A, et al. FK506 binding protein 51 positively regulates melanoma stemness and metastatic potential. *Cell Death Dis*. 2013;4:e578.
- Jiang W, Cazacu S, Xiang C, et al. FK506 binding protein mediates glioma cell growth and sensitivity to rapamycin treatment by regulating NF-kappaB signaling pathway. *Neoplasia*. 2008;10:235–243.
- Mukaide H, Adachi Y, Taketani S, et al. FKBP51 expressed by both normal epithelial cells and adenocarcinoma of colon suppresses proliferation of colorectal adenocarcinoma. *Cancer Invest*. 2008;26:385–390.
- Periyasamy S, Hinds T Jr, Shemshedini L, Shou W, Sanchez ER. FKBP51 and Cyp40 are positive regulators of androgen-

- dependent prostate cancer cell growth and the targets of FK506 and cyclosporin A. *Oncogene*. 2010;29:1691–1701.
35. Romano S, D'Angelillo A, Staibano S, Ilardi G, Romano MF. FK506-binding protein 51 is a possible novel tumoral marker. *Cell Death Dis*. 2010;1:e55.
 36. Amler LC, Agus DB, LeDuc C, et al. Dysregulated expression of androgen-responsive and nonresponsive genes in the androgen-independent prostate cancer xenograft model CWR22-R1. *Cancer Res*. 2000;60:6134–6141.
 37. Velasco AM, Gillis KA, Li Y, et al. Identification and validation of novel androgen-regulated genes in prostate cancer. *Endocrinology*. 2004;145:3913–3924.
 38. Pei H, Li L, Fridley BL, et al. FKBP51 affects cancer cell response to chemotherapy by negatively regulating Akt. *Cancer Cell*. 2009;16:259–266.
 39. Ronnov-Jessen L, Petersen OW, Bissell MJ. Cellular changes involved in conversion of normal to malignant breast: importance of the stromal reaction. *Physiol Rev*. 1996;76:69–125.
 40. Peehl DM. Primary cell cultures as models of prostate cancer development. *Endocr Relat Cancer*. 2005;12:19–47.

Supplementary Table S1. Primers used in this study

Gene	Sequence
AR F	GGGGACAAGTTTGTACAAAAAAGCAGGCTACCA TGGAAAGTGCAGTTAGGGGCTGGGAA
AR R	GGGGACCACCTTTGTACAAAGAAAGCTGGGTTCACTGGGTGGGAAATAGA
FKBP5 F	ATTATCCGGGAGAACCAACG
FKBP5 R	CAAAACATCCTTCCACCACAG
HMOX1 F	ACCCAGGCAGAGAA TGCTGAGTT
HMOX1 R	CCTCCTCCAGGGCCACATAGATG
FBXO32 F	CCCTTCAGCTCTGCAAAACACTGTC
FBXO32 R	CTCCAGTCAGCAGGGGGACC
WNT5A F	AAGGAGTTCGTGGACGCCCG
WNT5A R	GCAGGCCACATCAGCCAGGT
VEGFA F	TGCAGATTATGCCGGATCAAACC
VEGFA R	TGCATTACAGATTGTGTGTGTAG
KLK3 F	GGCAGCATTGAACCAGAGGAG
KLK3 R	GCATGAACTTGGTCACCTTCTG
ATCB F	CATCCGCAAAGACCTGTACG

ATCB R	AGTACTTGCGCTCAGGAGG
GAPDH F	GTCA TGGGTGTGAACCATGAGA
GAPDH R	GGTCATGAGTCCCTCCACGATAC

Supplementary Table S2. Association between AR and FKBP5 expression and clinicopathological parameters

	Total	Nuclear AR		p value ^a	FKBP5		p value ^a
		negative	positive		negative	positive	
Total	76	7 (9.2%)	69 (90.8%)	-	27 (35.5%)	49 (64.5%)	-
Gender							
Female	11	1 (9.1%)	10 (90.9%)		3 (27.3%)	8 (72.7%)	
Male	65	6 (9.2%)	59 (90.8%)	1.0000	24 (36.9%)	41 (63.1%)	0.7368
Age, median (years)^b	76	64	64	0.8777	64	64	0.9634
Age							
<64 years	35	3 (8.6%)	32 (91.4%)		11 (31.4%)	24 (68.6%)	
≥64 years	41	4 (9.8%)	37 (90.2%)	1.0000	16 (39.0%)	25 (61.0%)	0.6313
Barrett's esophagus							
Absent	30	7 (23.3%)	23 (76.7%)		15 (50.0%)	15 (50.0%)	
Present	46	0 (0%)	46 (100%)	0.0009	12 (26.1%)	34 (73.9%)	0.0495
Tumor length, median (mm)^b	76	40	40	0.5874	40	40	0.2922
Primary tumor (T-Stage)							
T1a	6	0 (0%)	6 (100%)		2 (33.3%)	4 (66.7%)	

T1b	11	0 (0%)	11 (100%)		2 (18.2%)	9 (81.8%)	
T2	10	1 (10.0%)	9 (90.0%)		2 (20.0%)	8 (80.0%)	
T3	37	5 (13.5%)	32 (86.5%)		15 (40.5%)	22 (59.5%)	
T4a/b	12	1 (8.3%)	11 (91.7%)	0.6335	6 (50.0%)	6 (50.0%)	0.4042
Regional lymph node (N-Stage)^c							
N0	30	1 (3.3%)	29 (96.7%)		9 (30.0%)	21 (70.0%)	
N1	17	3 (17.6%)	14 (82.4%)		9 (52.9%)	8 (47.1%)	
N2	17	0 (0%)	17 (100%)		3 (17.6%)	14 (82.4%)	
N3	12	3 (25.0%)	9 (75.0%)	0.0463	6 (50.0%)	6 (50.0%)	0.1059
Grade of differentiation							
Well/Moderate	21	2 (9.5%)	19 (90.5%)		9 (42.9%)	12 (57.1%)	
Poor/Undifferentiated	54	5 (9.3%)	49 (90.7%)	1.0000	18 (33.3%)	36 (66.7%)	0.5928
Unknown ^d	1	0 (0%)	1 (100%)		0 (0%)	1 (100%)	
Circumferential resection margin							
Negative	39	2 (5.1%)	37 (94.9%)		10 (25.6%)	29 (74.4%)	
Positive	37	5 (13.5%)	32 (86.5%)	0.2562	17 (45.9%)	20 (54.1%)	0.0932
Vascular invasion							

Negative	15	0 (0%)	15 (100%)		5 (33.3%)	10 (66.7%)	
Positive	55	7 (12.7%)	48 (87.3%)	0.3326	21 (38.2%)	34 (61.8%)	1.0000
Unknown ^d	6	0 (0%)	6 (100%)		1 (16.7%)	5 (83.3%)	
Perineural invasion							
Negative	24	1 (4.2%)	23 (95.8%)		7 (29.2%)	17 (70.8%)	
Positive	39	5 (12.8%)	34 (87.1%)	0.3937	16 (41.0%)	23 (59.0%)	0.4240
Unknown ^d	13	1 (7.7%)	12 (92.3%)		4 (30.8%)	9 (69.2%)	

- a. *p* value calculated using Fisher's exact test unless otherwise stated.
- b. *p* value calculated using Mann Whitney test.
- c. *p* value calculated using Chi-square test.
- d. Unknown not included in statistical analysis.

Absent	30	569.5	16.7	1		1		1	
Present	46	1581	49.7	0.472 (0.271 - 0.821)	0.0079	0.612 (0.305 - 1.226)	0.166	0.608 (0.313 - 1.184)	0.1436
Gender									
Female	11	627	18.2	1					
Male	65	1056	39.8	0.589 (0.294 - 1.182)	0.1366				
Age at surgery^a	76	865	36.7	1.038 (1.006 - 1.071)	0.0204	1.047 (1.013 - 1.082)	0.0069	1.033 (0.997 - 1.070)	0.0699
Tumor length^a	76	865	36.7	1.013 (1.002 - 1.024)	0.0235				
Primary tumor (T)									
T1a	6	3162	100	1				1	
T1b	11	2072	81.8	2.023 (0.210 - 19.457)	0.542			1.240 (0.121 - 12.692)	0.8562 ^c
T2	10	1606.5	50	6.055 (0.725 - 50.588)	0.0964			4.416 (0.514 - 37.961)	0.176

Resection margin																				
Negative	39	1711	58.6	1																
Positive	37	299	13.5	3.144 (1.767 - 5.597)																
Vascular invasion																				
Negative	15	2674	86.2	1																
Positive	55	451	21.5	6.022 (2.135 - 16.982)																0.0053
Perineural invasion																				
Negative	24	2104	66.7	1																
Positive	39	865	17.3	3.160 (1.535 - 6.506)																0.0018

a. p value calculated as a continuous variable

b. Global $p = 0.0025$

c. Global $p = 0.0237$

d. Global $p = 0.1129$

CHAPTER 6: ANDROGEN SIGNALLING IN ESOPHAGEAL ADENOCARCINOMA CELL LINES IN VITRO

Helen M. Palethorpe¹, Paul A. Drew^{1,2}, Eric Smith^{1,3}

¹ Solid Cancer Regulation Group, Discipline of Surgery, Basil Hetzel Institute for Translational Health Research, The Queen Elizabeth Hospital, The University of Adelaide, 28 Woodville Rd, Woodville South, SA 5011, Australia;

² School of Nursing and Midwifery, Flinders University, PO Box 2100, Adelaide, SA 5001, Australia;

³ Department of Medical Oncology, Basil Hetzel Institute for Translational Health Research, The Queen Elizabeth Hospital, 28 Woodville Rd, Woodville South, SA 5011, Australia.

Digestive Diseases and Sciences 2017; submitted paper

Statement of Authorship

Title of Paper	Androgen signalling in esophageal adenocarcinoma cell lines in vitro
Publication Status	Submitted for publication
Publication Details	Palethorpe HM , Drew PA, Smith E: Androgen signalling in esophageal adenocarcinoma cell lines in vitro . Submitted to <i>Digestive Diseases and Sciences</i> 2017.

Principal Author

Name of Principal Author (Candidate)	Helen M Palethorpe		
Contribution to the Paper	Conceived and designed the experiments, performed the experiments, analysed the data and wrote the manuscript.		
Overall percentage (%)	80%		
Certification:	This paper reports on original research I conducted during the period of my Higher Degree by Research candidature and is not subject to any obligations or contractual agreements with a third party that would constrain its inclusion in this thesis. I am the primary author of this paper.		
Signature		Date	1/03/17

Co-Author Contributions

By signing the Statement of Authorship, each author certifies that:

- i. the candidate's stated contribution to the publication is accurate (as detailed above);
- ii. permission is granted for the candidate to include the publication in the thesis; and
- iii. the sum of all co-author contributions is equal to 100% less the candidate's stated contribution.

Name of Co-Author	Paul A. Drew		
Contribution to the Paper	Conceived and designed the experiments, analysed the data, wrote the manuscript.		
Signature		Date	1/03/17

Name of Co-Author	Eric Smith		
Contribution to the Paper	Conceived and designed the experiments, performed one of the experiments, analysed the data and wrote the manuscript.		
Signature		Date	1/03/17

ABSTRACT

Background

We showed previously that nuclear localisation of the androgen receptor (AR) and expression of the androgen-responsive gene FK506-binding protein 5 (FKBP5) in esophageal adenocarcinoma (EAC) tissues were associated with decreased patient survival, suggesting a role for androgens in this cancer.

Aim

To investigate the effect of the AR ligand 5 α -dihydrotestosterone (DHT) on AR-expressing EAC cell lines in vitro.

Methods and Results

In tissue resection specimens from EAC patients, FKBP5 expression was positively associated with Ki-67 expression. We stably transduced AR into three AR-negative EAC cell lines, OE33, JH-EsoAd1 and OE19, to investigate androgen signalling in vitro. Growth was inhibited by 1 nM or 10 nM DHT, concentrations most commonly used to study AR signalling, whilst at DHT concentrations near the IC50 there was both cell growth and expression of androgen-responsive genes. OE33-AR cells in direct co-culture with PShTert myofibroblasts grew with 10 nM DHT and the expression of androgen-responsive genes was maintained as in monoculture.

Conclusions

This is the first study to show that EAC cell lines respond to androgen in vitro. Lower DHT concentrations or a permissive microenvironment permitted proliferation and expression of androgen-responsive genes, consistent with tissue observations. These findings are consistent with a role for androgen signalling in EAC.

Keywords

Esophageal adenocarcinoma, androgen receptor, fibroblast, FKBP5, dihydrotestosterone, direct co-culture, in vitro

Abbreviations

ACTB, actin beta; CTV, CellTrace violet; DHT, 5 α -dihydrotestosterone; EAC, esophageal adenocarcinoma; E2F1, E2F transcription factor 1; FBXO32, F-box protein 32; FKBP5, FK506-binding protein 5; GFP, green fluorescent protein; HMOX1, heme oxygenase 1; IC50, half maximal inhibitory concentration; NDRG1, N-myc downstream regulated 1; NFF, neonatal foreskin fibroblast; qRT-PCR, quantitative reverse transcription polymerase chain reaction; RFP, red fluorescent protein; SA- β -gal, senescence-associated beta-galactosidase; SD, standard deviation; TERT, telomerase reverse transcriptase; TMA, tissue microarray.

INTRODUCTION

The incidence of esophageal adenocarcinoma (EAC) has increased rapidly over recent decades in Western countries [1-5]. It has a dismal prognosis, with around 65 % of patients unsuitable for surgery at the time of diagnosis and an overall five-year survival rate of less than 15 % [6, 7]. The major risk factors for EAC are gastro-esophageal reflux disease and obesity, leading to the only described precursor lesion for this cancer, Barrett's esophagus. This cancer has one of the highest male:female ratios of cancers of non-reproductive organs, ranging from 7-10 to 1 [1, 2, 4, 6, 8-11], significantly higher than for the major risk factors. The gender difference appears to result from an approximate 20-year delay in onset in females of Barrett's esophagus [12] and EAC [13]. These observations are consistent with a role for the sex steroid hormones, with their concentrations differing between males and females, and changing over the lifespan.

The most important sex hormones in males are the androgens, and the most predominant androgen is testosterone. Testosterone passes through the cell membrane and into the cytoplasm where it, or its more physiologically effective metabolite 5 α -dihydrotestosterone (DHT), binds to and activates the androgen receptor (AR). Activated AR translocates from the cytoplasm into the nucleus and binds to androgen response elements in the genome, influencing the transcription of androgen-responsive genes. The nature of the response can be modified by the relative abundance of multiple co-regulators (both co-activators and co-repressors) [14].

We previously reported the immunostaining of EAC tissues for AR and the androgen-responsive gene FKBP5-binding protein 5 (FKBP5) [15]. We detected AR in the cancer cells of 75 of 77 cases, and in 70 it was nuclear. The expression of FKBP5 was observed in 64 % of cases, and only when the AR was nuclear. There was a significant association between nuclear AR and FKBP5 expression and decreased survival.

Given the association between AR localisation, FKBP5 expression and poor survival, we sought suitable cell lines to investigate the effect of androgen signalling on the behaviours of EAC cells. All available cell lines were AR negative, probably due to loss of AR expression during the establishment of cell lines from tissues [15]. We therefore stably transduced three EAC cell lines with AR, and in this study we have investigated factors that affect their growth and gene expression in response to androgen.

METHODS

Immunohistochemistry for Ki-67 and FKBP5

Tissue microarrays (TMAs) composed of one or more representative cores of EAC were constructed as described previously [16]. Sequential sections consisting of cores from 74 cases were immunostained for FKBP5 [15] and Ki-67 [17]. Cores were scored as the percent of epithelial cells that expressed FKBP5 or Ki-67 as follows: 0, negative; 1, <5 % (rare); 2, < 25 %; 3, >25 % <75 %; 4, >75 %. The median score for FKBP5 and Ki-67 (Ki-67 index) was determined for multiple cores from each case.

Cell culture

The EAC cell lines OE33, JH-EsoAd1 and OE19 were stably transduced with AR and green fluorescent protein (GFP), or with GFP only [15]. At least six single-cell clones were established from each AR-transduced cell line, and the clone expressing the lowest amount of AR, as determined by western immunoblot, was used for all experiments unless otherwise stated. The cell lines expressing AR and GFP are referred to as OE33-AR, JH-AR and OE19-AR respectively. The EAC cell lines were maintained in androgen depleted growth medium (stripped medium) consisting of phenol red-free RPMI-1640 containing L-glutamine (Life Technologies, Eugene, OR, USA), supplemented with 10 % dextran charcoal stripped fetal bovine serum (Equitech-Bio, Inc., Kerrville, TX, USA), 200 U/mL penicillin and 200 µg/mL streptomycin (Life Technologies). Stripped medium was used for experiments unless stated otherwise.

The PShTert myofibroblasts [18, 19] were stably transduced with the SFG-RFP/Rluc construct to express red fluorescent protein (RFP) [20]. Neonatal foreskin fibroblasts (NFF) and PShTert myofibroblasts were used between passages 10 and 20. Fibroblasts were maintained in DMEM containing L-glutamine (Life Technologies), supplemented with 10 % foetal bovine serum (FBS; Sigma-Aldrich, St Louis, MO, USA), 200 U/ml penicillin and 200 µg/ml streptomycin (Life Technologies).

Direct co-culture

The NFFs and PShTert myofibroblasts were cultured in stripped medium overnight, seeded at 4×10^5 cells per well into six-well plates (BD Biosciences, Franklin Lakes, NJ, USA), and then incubated for 48 h to form confluent monolayers. Next, OE33-ARs were seeded at 1×10^5 cells per well either in monoculture or in direct co-culture with the fibroblasts. The following day (day 0), and every 48 h thereafter, the medium was replaced with stripped

medium supplemented with vehicle (0 nM DHT; 0.1 % ethanol) or 10 nM DHT. Cells were harvested on day 6 of treatment, unless stated otherwise.

Translocation of androgen receptor

To establish direct co-cultures fibroblasts were cultured in stripped medium overnight, then seeded at 8×10^4 fibroblasts per well in eight-well Lab-Tek Chamber Slides (Thermo Fisher Scientific, Rochester, NY, USA), and incubated for 48 h. Next, OE33-ARs (2×10^4 cells per well) were added to the wells, followed by overnight incubation. The medium, supplemented with vehicle or 10 nM DHT (day 0), was replaced then and every 48 h for 6 days.

Following treatment, the cells were washed in Dulbecco's phosphate buffered saline (DPBS), fixed in methanol on ice for 5 min, and air-dried. The cells were blocked with 10 % normal goat serum (Dako, Glostrup, Denmark) in DPBS for 20 min, and labelled with rabbit anti-human AR polyclonal IgG (clone N-20; 1 $\mu\text{g}/\text{mL}$ in 1.5 % goat serum; Santa Cruz Biotech Inc., Santa Cruz, CA, USA) for 1 h, followed by incubation with Alexa Fluor 568 goat anti-rabbit IgG (2 $\mu\text{g}/\text{mL}$ in 1.5 % goat serum; Molecular Probes by Life Technologies) for 45 min. Nuclei were stained with 1 $\mu\text{g}/\text{mL}$ 4', 6-diamidino-2-phenylindole dihydrochloride (DAPI; Sigma-Aldrich) in DPBS for 15 min. Slides were mounted in fluorescent mounting medium (Dako) and stored at 4 °C in darkness. Images were captured using a Zeiss LSM 700 Confocal microscope.

Cell proliferation

To measure cell proliferation, 1×10^3 cells per well were seeded in 96-well plates and cultured for 48 h. The cells were then treated with either vehicle or various concentrations of DHT for 6 to 12 days, depending on the cell line. The cells were next fixed in 10 % neutral buffered formalin for 30 min, stained for 10 min with 1 % crystal violet (Sigma-Aldrich) in 2 % ethanol, washed eight times in distilled water, and then air dried overnight. The crystal violet was eluted using 10 % acetic acid and gentle rotation of the plates. The absorbance of the eluent was measured at 595 nM using a FLUOstar Optima microplate reader (BMG Labtech, Ortenberg, Germany). To determine whether growth inhibition with DHT was mediated via AR, OE33-ARs were seeded into six-well plates (1×10^5 cells per well) and cultured for 48 h. The cells were treated for 6 days with 10 nM DHT and either vehicle (0.15 % dimethyl sulfoxide; Sigma-Aldrich) or 15 μM enzalutamide (MedChem Express, Princeton, NJ, USA).

Cell division of OE33-AR was measured by dye dilution, using CellTrace Violet (CTV; Life Technologies). Cells were seeded in six-well plates (3×10^4 cells per well) and incubated for 24 h. Wells for time 0 were then fixed in 4 % paraformaldehyde. In the other wells the medium was replaced daily, supplemented with either vehicle or DHT at around the half maximal inhibitory concentration (IC₅₀; 0.06 and 0.1 nM), or 10 nM. Other wells were fixed with 4 % paraformaldehyde 1, 3 or 5 days following. The amount of CTV in the cells was measured using a FACSCanto II (BD Biosciences) with BD FACSDiva software. Cell doublets were excluded by doublet discrimination, based on non-linearity of forward scatter and side scatter area versus height plots. Cells were gated based on GFP-positivity, and the median CTV intensity of this population determined using FlowJo software version 8.8.7 (Ashland, OR, USA).

Quantitative real-time reverse-transcription PCR (qRT-PCR)

Total RNA was isolated from cells using TRIzol, and 1 µg was reverse-transcribed using the iScript cDNA Synthesis Kit (Bio-Rad Laboratories, Hercules, CA, USA) in a final reaction volume of 20 µL. Gene expression was determined by quantitative real-time reverse-transcription polymerase chain reaction (qRT-PCR) using iQ SYBR Green Supermix (Bio-Rad Laboratories) in a final reaction volume of 10 µL, containing 0.1 µL of cDNA and a final concentration of 0.2 µM of each forward and reverse primer (Supplementary Table S1). Reactions were performed using a CFX96 (Bio-Rad Laboratories) at 95 °C for 3 min, then 40 cycles of 95 °C for 15 s, 60 °C for 15 s, and 72 °C for 30 s, followed by a final extension of 72 °C for 1 min. Products were melted to confirm specificity. Normalized fold expression was calculated using ACTB as the reference gene.

Cell cycle analysis

OE33-ARs were seeded at 1×10^5 cells per well in stripped medium in six-well plates, and incubated for 24 h. The medium was then replaced daily, supplemented either with vehicle or 0.06, 0.1 or 10 nM DHT. Wells were harvested at 0, 24, 48 or 72 h. The cells were washed, resuspended in DPBS, and fixed with a final concentration of 70 % ice-cold ethanol. The cells were pelleted, resuspended with 0.25 % Triton X-100 (Sigma-Aldrich) in DPBS, and incubated for 2 h with 25 µg/ml propidium iodide (Sigma-Aldrich) and 40 µg/ml bovine pancreas ribonuclease A (Sigma-Aldrich) in DPBS. The DNA content of single cells was measured using a FACSCanto II. The percentages of cells in each cell cycle phase and in subG1 were calculated using BD FACSDiva software.

Confocal microscopy

To assess morphology, OE33-AR (1.72×10^3), JH-AR (5.73×10^3) or OE19-AR (5.73×10^3) cells were seeded into 96 well μ -plates (Ibidi, Martinsried, Germany) in stripped medium supplemented with either vehicle or 10 nM DHT replaced daily for 3 days. For direct co-cultures, NFFs were labelled using the CellTrace Violet (CTV) Cell Proliferation Kit according to the manufacturer's protocol (Life Technologies). Fibroblasts were seeded at 1.14×10^4 per well and OE33-ARs were seeded overnight at 1.43×10^3 cells per well, either in monoculture or overlying fibroblasts followed by treatment with vehicle or 10 nM DHT for 6 days, with medium replaced every 48 h. Images were captured using a Zeiss LSM 700 Confocal microscope with Zen2012 SP1 (black edition) software version 8.1.

Senescence-associated beta-galactosidase assay

Cells were seeded in 24-well plates at 2×10^3 cells per well for OE33 and OE33-AR and 3×10^3 cells per well for JH-AR and OE19-AR, followed by 48 h incubation. The culture medium was then replaced daily with fresh medium supplemented with vehicle or DHT (IC50s and 10 nM). On days 0, 1, 3 and 5 for OE33 and OE33-AR, and 0, 4, 6 and 8 for JH-AR and OE19-AR, wells were stained with the Senescence Cells Histochemical Staining Kit (Sigma-Aldrich). The percentage of senescence-associated beta-galactosidase (SA- β -gal) positive cells was calculated from a count of 200 cells.

Statistics

The statistical software used was Prism 6.0d for Macintosh (GraphPad Software, San Diego, CA, USA). Proliferation dose response curves were fitted, and the IC50 determined, by nonlinear regression analysis. Data is the mean \pm SD of a single experiment reproduced in triplicate with *p*-values determined by parametric unpaired student's *t*-test assuming equal standard deviations (SD), unless stated otherwise. Differences were considered significant when the two-tailed *p*-value was ≤ 0.05 .

RESULTS

EAC tissues with a high percentage of FKBP5 positive cells had a high proliferation index

Previously we reported that the expression of FKBP5, a surrogate marker for androgen signalling, was associated with reduced survival in EAC [15]. To determine the relationship between AR signalling and tumour growth *in vivo*, we measured the percentage of FKBP5

positive cells and the Ki-67 proliferation index in EAC resection specimens. The results in Fig. 1 show that the proliferation index was significantly higher in those tissues with higher FKBP5 expression ($p = 0.0002$).

DHT inhibited proliferation of AR-expressing EAC cell lines in vitro

Expression of AR protein was confirmed in the three EAC cell lines stably transduced with AR, OE33-AR, JH-AR and OE19-AR, by western immunoblot (Supplementary Fig. S1a) and immunocytochemistry (Supplementary Fig. S1b). In the absence of DHT, AR immunoreactivity was seen by confocal microscopy to be moderate in the cytoplasm and mild to moderate in the nucleus. Exposure to 10 nM DHT induced complete nuclear localisation of the AR, confirming that the transduced AR was functionally responsive to androgen.

In the AR-negative cell lines, exposure to DHT at concentrations up to 100 nM did not significantly alter proliferation (data not shown). The dose response curves for each of the AR-expressing lines, given a single dose of DHT at the start of culture, are shown in Fig. 2a. The concentration of DHT used in most reported studies of AR signalling in vitro is 10 nM, which completely inhibited proliferation of OE33-AR and JH-AR, and almost completely of OE19-AR. The IC₅₀s were 0.09, 0.26 and 1.3 nM for OE33-AR, JH-AR and OE19-AR respectively. To determine if the differences in the DHT dose response curves between the cell lines were due to the amount of AR expressed, we compared, within each of the transduced lines, clones with the highest and lowest expression of AR, and found no significant differences in the DHT dose response curves (data not shown). We also observed the same or similar dose response for the uncloned OE33-AR. The addition of the AR antagonist enzalutamide (15 μ M) completely blocked the growth inhibition of the AR-expressing cells induced by 10 nM DHT, confirming that the anti-proliferative effect was mediated by the AR ($p < 0.0001$) (Fig. 2b).

For subsequent experiments we used two concentrations of DHT near the IC₅₀ (0.06 and 0.1 nM for OE33-AR, 0.25 and 0.5 nM for JH-AR, and 0.5 and 1.0 nM for OE19-AR), as well as 10 nM. We next examined the possibility that proliferation may differ with daily replenishment of DHT compared to a single treatment at the start of the culture. The results in Fig. 3a show the DHT dose response curves for OE33-AR. These were similar whether the DHT was given as a single treatment or daily in fresh medium, with IC₅₀s of 0.08 and 0.06 nM respectively.

DHT induced androgen responsive gene expression in AR-expressing cell lines

In preliminary studies we found that cell lines cultured with a single dose of 10 nM DHT expressed high levels of the androgen-responsive gene FKBP5, even though proliferation was inhibited. At lower concentrations of DHT, around the IC50, there was partial inhibition of growth but no, or very low, FKBP5 expression. This appeared to conflict with our immunostains of resection tissues where we frequently measured FKBP5 and Ki-67 expression together.

We therefore compared the effect of a single dose to daily replenishment of DHT on the induction of the androgen-responsive gene FKBP5 in OE33-AR (Fig. 3b). A single dose induced an increase in FKBP5 expression compared to vehicle of 1.2-fold for 0.06 nM DHT ($p = 0.002$), 2.2-fold for 0.1 nM ($p = 0.0004$) and 22-fold for 10 nM ($p = 0.0005$) after 3 days of culture. In contrast, when the DHT was replenished daily, the increase in FKBP5 expression compared to vehicle was 2-fold for 0.06 nM ($p = 0.03$), 4-fold for 0.1 nM ($p < 0.0001$), and 16-fold for 10 nM ($p = 0.0002$). The increases in FKBP5 expression for daily compared to single dosing were significantly greater for 0.06 or 0.1 nM DHT ($p = 0.02$ and $p < 0.0001$ respectively), but not for 10 nM ($p = 0.639$). Daily dosing, which would be expected to more closely mimic in vivo conditions, with concentrations of DHT around the IC50, permitted growth and induced significant expression of FKBP5.

Next, we measured the expression of known androgen-responsive genes in each of the three AR-expressing cell lines at the different concentrations of DHT. We found that the pattern of response was similar between the cell lines, although there were differences in the fold increases (Supplementary Fig. S2).

DHT inhibited cell division and induced cell cycle arrest and cell senescence in AR-expressing cells

To understand better the inhibition of growth, we analysed the effect of DHT on cell division, cell cycle arrest and cell senescence. Cell division in OE33-AR, as measured by the intracellular dilution of CTV, was inhibited after 3 and 5 days of culture (Fig. 4a). The median CTV content at day 0 was 25,724 fluorescence units (FU). After 5 days of treatment with vehicle it was reduced to 535 FU. In contrast, after 5 days of treatment with 0.06, 0.1 and 10 nM DHT the median CTV content was 621 FU, 930 FU and 5,760 FU respectively, indicating that there was less cell division as the concentration of DHT increased.

Next we measured the cell cycle phase distribution by flow cytometry following 3 days of culture. The results are shown in Fig. 4b. There were no significant changes in the proportion of cells in each phase of the cell cycle following treatment with 0.06 nM DHT. Compared to vehicle, there was a 19 % ($p = 0.006$) and 52 % increase ($p = 0.0004$) in the proportion of cells in the G0/G1 phase following treatment with 0.1 and 10 nM DHT respectively, a 34 % ($p = 0.0004$) and 47 % ($p = 0.003$) decrease in cells in the G2/M phase, and no difference and a decrease of 51 % ($p = 0.009$) in the S phase. There was no subG1 population with any of the concentrations, suggesting that DHT did not induce cell death. The expression of E2F1, a transcriptional activator necessary for progression through the G1/S transition, was significantly inhibited with 0.1 nM ($p = 0.0004$) and 10 nM ($p = 0.0002$) of DHT by day 3 of culture (Fig. 4c).

Using time-lapse confocal microscopy we observed that each of the three AR-expressing cell lines underwent extensive morphological changes over 3 days of culture with 10 nM DHT (Fig. 4d). The cells became discohesive, enlarged and flattened, with the appearance of many large cytoplasmic holes. There was no microscopic evidence of extensive cell death. Because these changes were suggestive of senescence, we stained cultures for the senescence marker, senescence-associated beta galactosidase (SA- β -gal). There was a concentration and time dependent increase in the percentage of SA- β -gal stained cells over the duration of culture in each of the three cell lines, which was most pronounced in OE33-AR and least in OE19-AR (Fig. 4e). Together these results demonstrated that DHT inhibited the proliferation of AR-expressing EAC cell lines in vitro by inducing growth arrest and senescence in a dose-dependent manner.

The effect of direct co-culture with fibroblasts

We next explored the possibility that stromal fibroblasts, the major cell population within the tumour microenvironment and known to influence the response of tumour cells to drugs, might modify the response of AR-expressing EAC cells to androgens. Fig. 5a shows the morphology of OE33-AR in monoculture and direct co-culture with NFFs or PShTerts, with vehicle or 10 nM DHT. With vehicle, there was no apparent microscopic difference between OE33-AR grown in monoculture or in direct co-culture with NFFs or PShTerts. They formed numerous clusters of cells with distinct cell borders, polygonal shape and well-defined nuclei. With 10 nM DHT, growth of OE33-AR was inhibited in monoculture and in direct co-culture with NFFs. The cells were enlarged and contained numerous refractile, round bodies devoid of obvious structural content under phase microscopy and lacking GFP under fluorescence microscopy.

In contrast, OE33-AR treated with 10 nM DHT grew when in direct co-culture with PShTert. Their rate of growth and morphology were similar to that seen with vehicle in direct co-culture with PShTert myofibroblasts. On day 6 there was a reduction in the number of OE33-AR cultured with 10 nM DHT, compared to vehicle, of 98 % in monoculture ($p < 0.0001$) and 96 % in direct co-culture with NFFs ($p = 0.0006$), compared to only 33 % in direct co-culture with PShTerts ($p = 0.001$) (Fig. 5b). Increasing the DHT concentration to 100 or 1,000 nM resulted in complete inhibition of proliferation of OE33-AR in direct co-cultures with the PShTert myofibroblasts ($p < 0.0001$) (Supplementary Fig. S3). The addition of enzalutamide to the cultures blocked the DHT mediated inhibition of growth in the monocultures ($p < 0.0001$), but did not alter the outcome of direct co-culture with the PShTert myofibroblasts ($p = 0.544$) (Fig. 5c).

Translocation of AR in direct co-cultures

We investigated if nuclear translocation of AR was altered in OE33-AR in direct co-culture. The results in Fig. 6 show that the OE33-AR treated with vehicle, either in monoculture or direct co-culture, had mild AR immunoreactivity in the cytoplasm and weak immunoreactivity in the nucleus, consistent with a lack of AR activation. With 10 nM DHT, there was complete translocation of AR to the nucleus and no AR in the cytoplasm of OE33-AR in monoculture or direct co-culture with NFFs. In contrast, there was a DHT dose dependent distribution of AR in OE33-AR directly co-cultured with PShTerts. With 10 nM DHT there was moderate immunoreactivity in the nucleus, and mild to moderate immunoreactivity in the cytoplasm. With 100 nM DHT there was complete nuclear translocation in about 50 % of OE33-AR, with mild cytoplasmic and moderate nuclear immunoreactivity in remaining cells, and with 1,000 nM DHT there was complete nuclear translocation in all cells. The finding of both nuclear and cytoplasmic AR in OE33-AR directly co-cultured with PShTerts was similar to our findings in EAC resection samples where AR was expressed in both the nucleus and cytoplasm in the majority of tissues.

DHT induced expression of androgen-responsive genes in co-cultures

We next measured the transcript levels of the androgen-responsive genes FKBP5, HMOX1 (heme oxygenase 1) and NDRG1 (N-myc downstream regulated 1) in OE33-AR with 10 nM DHT in monoculture or direct co-culture. The OE33-ARs (GFP-positive) were sorted from NFFs (GFP-negative) or PShTert myofibroblasts (RFP-positive) in the direct co-cultures. The results in Fig. 7a show that the change in expression induced by DHT, induction or repression, was similar in the monoculture and co-cultures, although the extent of the change varied. FKBP5 was upregulated 27-fold, 39-fold and 58-fold in monoculture, or direct co-

culture with NFFs or PShTerts respectively. HMOX1 was upregulated 1.2-fold, 16-fold and 1.8-fold. NDRG1 was downregulated 11.2-fold, 3-fold and 5.7-fold.

The results in Fig. 7b show the effect of enzalutamide on FKBP5 expression in direct co-cultures of OE33-AR and PShTert with 10 nM DHT. We measured expression in unsorted cells because we had shown that PShTerts expressed very low levels of FKBP5, which did not increase with DHT ($p = 0.238$) (Supplementary Fig. S4). Enzalutamide reduced the expression both in monoculture (10-fold; $p = 0.0002$) and in direct co-culture with PShTerts (17-fold; $p = 0.0003$) indicating that FKBP5 upregulation was mediated through AR. These results indicate that, even in co-culture conditions where DHT did not inhibit proliferation, DHT was functional in regulating the expression of androgen-responsive genes through AR.

DISCUSSION

We have previously reported that nuclear localisation of AR and/or expression of the androgen-responsive gene FKBP5 were associated with decreased survival in EAC, suggesting a role for androgens in this cancer [15]. Here we have extended that study to show that EAC resection tissues with a higher percentage of FKBP5 positive cells also had a higher proliferation index, showing a positive relationship between androgen signalling and cancer cell growth. We have investigated the effects of androgen on the behaviour of AR-expressing EAC cell lines in vitro. The three EAC cell lines that we stably transduced with full length human AR cDNA were responsive to androgen, as shown by DHT induced nuclear localisation of the receptor, and dose dependent changes in cell proliferation, morphology and gene expression. The commonly used concentration of DHT, 10 nM, markedly altered the expression of androgen-responsive genes, but completely inhibited cell proliferation by inducing cell cycle arrest and senescence, which appeared to be inconsistent with our findings in patient tissues of increased proliferation and upregulation of androgen-responsive gene expression. We then found that lower concentrations of DHT around the IC50, allowed proliferation and induced significant, although smaller, changes in the expression of androgen-responsive genes. We also found that in direct co-culture with an immortalised myofibroblast cell line, PShTert, the growth inhibitory effect of 10 nM of DHT was largely nullified, but the effect on expression of androgen-responsive genes was unaltered.

Studies of the effect of androgens on cell proliferation have generated conflicting results. Inhibition of proliferation has been reported often, in normal and cancer cell lines from a

range of tissues, either naturally expressing or transduced with AR [21-36]. No change or an increase in cell proliferation has also been reported [30, 36-39]. Why androgens in some cells increase and in others decrease proliferation is unclear. Many of the reported studies only used a single concentration of DHT, most commonly 10 nM. When dose response studies have been reported, the IC50 for DHT inhibition of proliferation has been of the same order as we measured [25, 26, 29, 36]. Our finding that growth inhibition was associated with cell cycle arrest and the induction of senescence is also consistent with other reports [26, 40-42].

This is the first comprehensive study of the expression of androgen-responsive genes across a range of DHT concentrations, in parallel with measurements of proliferation, in AR-expressing cells that are growth inhibited by DHT. We showed a DHT dose-dependent alteration of the expression of these genes. This could be measured from DHT concentrations around the IC50, significantly lower than the 10 nM most commonly used for in vitro studies [23, 43, 44]. Most reported studies use a single dose of DHT given at the start of the culture period. Single doses around the IC50 resulted in small, but significant, changes in expression of the androgen-responsive genes. Daily replenishment of the DHT increased the magnitude of the gene expression response without significantly altering proliferation. Daily replenishment, compared to a single dose, would be expected to more closely mimic the delivery of hormone in vivo. Our observations that DHT concentrations around the IC50 were sufficient to increase FKBP5 expression and allow proliferation were consistent with the association between FKBP5 and Ki-67 expression we measured in patient EAC resection specimens, which suggests our in vitro findings are clinically relevant.

The tumour microenvironment is an important determinant of the response of cancer cells to molecules such as hormones and drugs [45, 46]. We therefore examined the effect of androgens on our AR-expressing EAC cell lines in direct co-culture with fibroblasts, the primary cellular component of the microenvironment. The PShTert myofibroblast line, an immortalised activated fibroblast line which has properties typical of cancer-associated fibroblasts [18, 19, 47-51], allowed the growth of AR-expressing EAC cells at concentrations of DHT that inhibited the growth of cells in monoculture, without affecting the gene expression changes induced by DHT in monoculture. This suggests that the microenvironment has the potential to modify the response of AR-expressing EAC cells to androgen in vivo.

This is the first study to show a positive association between androgen signalling and cancer cell proliferation in EAC, and that AR-expressing EAC cell lines respond to androgens in

vitro. Proliferation of AR-expressing EAC cells in monoculture was inhibited by higher concentrations of DHT. Our in vitro findings suggest that, in cancer tissues in vivo, AR-expressing EAC cells at lower concentrations of DHT, or in the presence of activated fibroblasts in the microenvironment, would proliferate and DHT would alter the expression of androgen-responsive genes. Our findings are consistent with a role for androgen signalling in EAC.

REFERENCES

1. Chai J, Jamal MM. Esophageal malignancy: a growing concern. *World J Gastroenterol*. 2012;18:6521-6526.
2. Edgren G, Adami HO, Weiderpass E, Nyren O. A global assessment of the oesophageal adenocarcinoma epidemic. *Gut*. 2013;62:1406-1414.
3. Hur C, Miller M, Kong CY, et al. Trends in esophageal adenocarcinoma incidence and mortality. *Cancer*. 2013;119:1149-1158.
4. Lagergren J, Lagergren P. Recent developments in esophageal adenocarcinoma. *CA Cancer J Clin*. 2013;63:232-248.
5. Lepage C, Drouillard A, Jouve JL, Faivre J. Epidemiology and risk factors for oesophageal adenocarcinoma. *Dig Liver Dis*. 2013;45:625-629.
6. Lagergren J, Mattsson F. Diverging trends in recent population-based survival rates in oesophageal and gastric cancer. *PLoS One*. 2012;7:e41352.
7. Oliver SE, Robertson CS, Logan RF. Oesophageal cancer: a population-based study of survival after treatment. *Br J Surg*. 1992;79:1321-1325.
8. Awan AK, Iftikhar SY, Morris TM, et al. Androgen receptors may act in a paracrine manner to regulate oesophageal adenocarcinoma growth. *Eur J Surg Oncol*. 2007;33:561-568.
9. Cooper SC, Trudgill NJ. Subjects with prostate cancer are less likely to develop esophageal cancer: analysis of SEER 9 registries database. *Cancer Causes Control*. 2012;23:819-825.
10. Rutegard M, Lagergren P, Nordenstedt H, Lagergren J. Oesophageal adenocarcinoma: the new epidemic in men? *Maturitas*. 2011;69:244-248.
11. Sukocheva OA, Li B, Due SL, Hussey DJ, Watson DI. Androgens and esophageal cancer: What do we know? *World J Gastroenterol*. 2015;21:6146-6156.

12. van Soest EM, Siersema PD, Dieleman JP, Sturkenboom MC, Kuipers EJ. Age and sex distribution of the incidence of Barrett's esophagus found in a Dutch primary care population. *Am J Gastroenterol*. 2005;100:2599-2600.
13. Derakhshan MH, Liptrot S, Paul J, Brown IL, Morrison D, McColl KE. Oesophageal and gastric intestinal-type adenocarcinomas show the same male predominance due to a 17 year delayed development in females. *Gut*. 2009;58:16-23.
14. Leach DA, Powell SM, Bevan CL. WOMEN IN CANCER THEMATIC REVIEW: New roles for nuclear receptors in prostate cancer. *Endocr Relat Cancer*. 2016;23:T85-T108.
15. Smith E, Palethorpe HM, Ruzkiewicz AR, et al. Androgen Receptor and Androgen-Responsive Gene FKBP5 Are Independent Prognostic Indicators for Esophageal Adenocarcinoma. *Dig Dis Sci*. 2015.
16. Smith E, Ruzkiewicz AR, Jamieson GG, Drew PA. IGFBP7 is associated with poor prognosis in oesophageal adenocarcinoma and is regulated by promoter DNA methylation. *Br J Cancer*. 2014;110:775-782.
17. Abu-Sneineh A, Tam W, Schoeman M, et al. The effects of high-dose esomeprazole on gastric and oesophageal acid exposure and molecular markers in Barrett's oesophagus. *Aliment Pharmacol Ther*. 2010;32:1023-1030.
18. Leach DA, Need EF, Toivanen R, et al. Erratum: Stromal androgen receptor regulates the composition of the microenvironment to influence prostate cancer outcome. *Oncotarget*. 2015;6:36923.
19. Leach DA, Need EF, Toivanen R, et al. Stromal androgen receptor regulates the composition of the microenvironment to influence prostate cancer outcome. *Oncotarget*. 2015;6:16135-16150.
20. Dobrenkov K, Olszewska M, Likar Y, et al. Monitoring the efficacy of adoptively transferred prostate cancer-targeted human T lymphocytes with PET and bioluminescence imaging. *J Nucl Med*. 2008;49:1162-1170.
21. Ortmann J, Prifti S, Bohlmann MK, Rehberger-Schneider S, Strowitzki T, Rabe T. Testosterone and 5 alpha-dihydrotestosterone inhibit in vitro growth of human breast cancer cell lines. *Gynecol Endocrinol*. 2002;16:113-120.
22. Szelei J, Jimenez J, Soto AM, Luizzi MF, Sonnenschein C. Androgen-induced inhibition of proliferation in human breast cancer MCF7 cells transfected with androgen receptor. *Endocrinology*. 1997;138:1406-1412.
23. Kokontis JM, Lin HP, Jiang SS, et al. Androgen suppresses the proliferation of androgen receptor-positive castration-resistant prostate cancer cells via inhibition of Cdk2, CyclinA, and Skp2. *PLoS One*. 2014;9:e109170.

24. Yuan S, Trachtenberg J, Mills GB, Brown TJ, Xu F, Keating A. Androgen-induced inhibition of cell proliferation in an androgen-insensitive prostate cancer cell line (PC-3) transfected with a human androgen receptor complementary DNA. *Cancer Res.* 1993;53:1304-1311.
25. Heisler LE, Evangelou A, Lew AM, Trachtenberg J, Elsholtz HP, Brown TJ. Androgen-dependent cell cycle arrest and apoptotic death in PC-3 prostatic cell cultures expressing a full-length human androgen receptor. *Mol Cell Endocrinol.* 1997;126:59-73.
26. Litvinov IV, Antony L, Dalrymple SL, Becker R, Cheng L, Isaacs JT. PC3, but not DU145, human prostate cancer cells retain the coregulators required for tumor suppressor ability of androgen receptor. *Prostate.* 2006;66:1329-1338.
27. Marcelli M, Haidacher SJ, Plymate SR, Birnbaum RS. Altered growth and insulin-like growth factor-binding protein-3 production in PC3 prostate carcinoma cells stably transfected with a constitutively active androgen receptor complementary deoxyribonucleic acid. *Endocrinology.* 1995;136:1040-1048.
28. Shen R, Sumitomo M, Dai J, et al. Androgen-induced growth inhibition of androgen receptor expressing androgen-independent prostate cancer cells is mediated by increased levels of neutral endopeptidase. *Endocrinology.* 2000;141:1699-1704.
29. Chauhan S, Kunz S, Davis K, et al. Androgen control of cell proliferation and cytoskeletal reorganization in human fibrosarcoma cells: role of RhoB signaling. *J Biol Chem.* 2004;279:937-944.
30. Birrell SN, Bentel JM, Hickey TE, et al. Androgens induce divergent proliferative responses in human breast cancer cell lines. *J Steroid Biochem Mol Biol.* 1995;52:459-467.
31. Macedo LF, Guo Z, Tilghman SL, Sabnis GJ, Qiu Y, Brodie A. Role of androgens on MCF-7 breast cancer cell growth and on the inhibitory effect of letrozole. *Cancer Res.* 2006;66:7775-7782.
32. Rossi R, Franceschetti P, Maestri I, et al. Evidence for androgen receptor gene expression in human thyroid cells and tumours. *J Endocrinol.* 1996;148:77-85.
33. Rossi R, Zatelli MC, Franceschetti P, et al. Inhibitory effect of dihydrotestosterone on human thyroid cell growth. *J Endocrinol.* 1996;151:185-194.
34. Vander Griend DJ, Litvinov IV, Isaacs JT. Conversion of androgen receptor signaling from a growth suppressor in normal prostate epithelial cells to an oncogene in prostate cancer cells involves a gain of function in c-Myc regulation. *Int J Biol Sci.* 2014;10:627-642.

35. Antony L, van der Schoor F, Dalrymple SL, Isaacs JT. Androgen receptor (AR) suppresses normal human prostate epithelial cell proliferation via AR/beta-catenin/TCF-4 complex inhibition of c-MYC transcription. *Prostate*. 2014;74:1118-1131.
36. Whitacre DC, Chauhan S, Davis T, Gordon D, Cress AE, Miesfeld RL. Androgen induction of in vitro prostate cell differentiation. *Cell Growth Differ*. 2002;13:1-11.
37. Yu SQ, Lai KP, Xia SJ, Chang HC, Chang C, Yeh S. The diverse and contrasting effects of using human prostate cancer cell lines to study androgen receptor roles in prostate cancer. *Asian J Androl*. 2009;11:39-48.
38. Zhau HY, Chang SM, Chen BQ, et al. Androgen-repressed phenotype in human prostate cancer. *Proc Natl Acad Sci U S A*. 1996;93:15152-15157.
39. Banu KS, Govindarajulu P, Aruldas MM. Testosterone and estradiol have specific differential modulatory effect on the proliferation of human thyroid papillary and follicular carcinoma cell lines independent of TSH action. *Endocr Pathol*. 2001;12:315-327.
40. Mirochnik Y, Veliceasa D, Williams L, et al. Androgen receptor drives cellular senescence. *PLoS One*. 2012;7:e31052.
41. Roediger J, Hessenkemper W, Bartsch S, et al. Supraphysiological androgen levels induce cellular senescence in human prostate cancer cells through the Src-Akt pathway. *Mol Cancer*. 2014;13:214.
42. Shao C, Wang Y, Yue HH, et al. Biphasic effect of androgens on prostate cancer cells and its correlation with androgen receptor coactivator dopa decarboxylase. *J Androl*. 2007;28:804-812.
43. Rossi R, Zatelli MC, Valentini A, et al. Evidence for androgen receptor gene expression and growth inhibitory effect of dihydrotestosterone on human adrenocortical cells. *J Endocrinol*. 1998;159:373-380.
44. Castoria G, Giovannelli P, Di Donato M, et al. Role of non-genomic androgen signalling in suppressing proliferation of fibroblasts and fibrosarcoma cells. *Cell Death Dis*. 2014;5:e1548.
45. Klemm F, Joyce JA. Microenvironmental regulation of therapeutic response in cancer. *Trends Cell Biol*. 2015;25:198-213.
46. Kalluri R. The biology and function of fibroblasts in cancer. *Nat Rev Cancer*. 2016;16:582-598.
47. Leach DA, Need EF, Trotta AP, Grubisha MJ, DeFranco DB, Buchanan G. Hic-5 influences genomic and non-genomic actions of the androgen receptor in prostate myofibroblasts. *Mol Cell Endocrinol*. 2014;384:185-199.

48. Leach DA, Trotta AP, Need EF, Risbridger GP, Taylor RA, Buchanan G. The prognostic value of stromal FK506-binding protein 1 and androgen receptor in prostate cancer outcome. *Prostate*. 2017;77:185-195.
49. Li Y, Li CX, Ye H, et al. Decrease in stromal androgen receptor associates with androgen-independent disease and promotes prostate cancer cell proliferation and invasion. *J Cell Mol Med*. 2008;12:2790-2798.
50. Lai KP, Huang CK, Fang LY, et al. Targeting stromal androgen receptor suppresses prolactin-driven benign prostatic hyperplasia (BPH). *Mol Endocrinol*. 2013;27:1617-1631.
51. Li Y, Zhang DY, Ren Q, et al. Regulation of a novel androgen receptor target gene, the cyclin B1 gene, through androgen-dependent E2F family member switching. *Mol Cell Biol*. 2012;32:2454-2466.

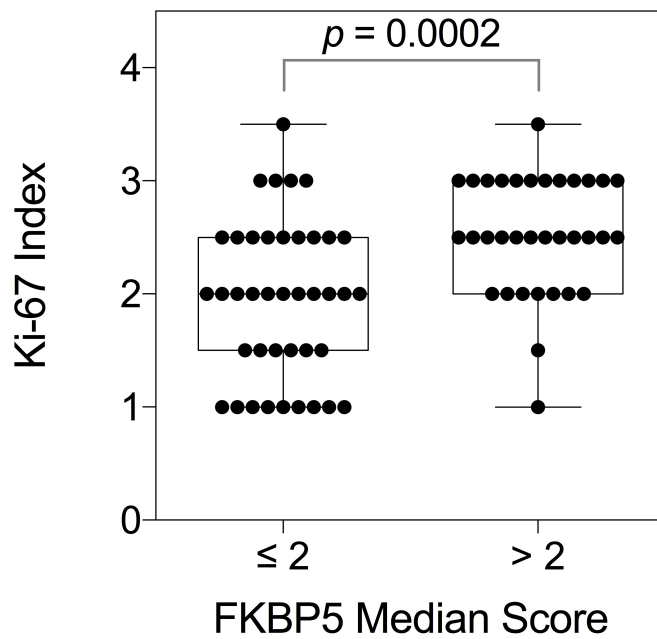


Figure 1. The Ki-67 proliferation indices in EAC resection tissues with low (≤ 2) or high (> 2) FKBP5 expression. Tissue microarrays were immunostained and scored as the percentage of epithelial cells that expressed FKBP5 or Ki-67 as follows: 0, negative; 1, $< 5\%$ (rare); 2, $< 25\%$; 3, $> 25\% < 75\%$; 4, $> 75\%$. Data is the median score of cores from each case. P -value by Mann-Whitney U test.

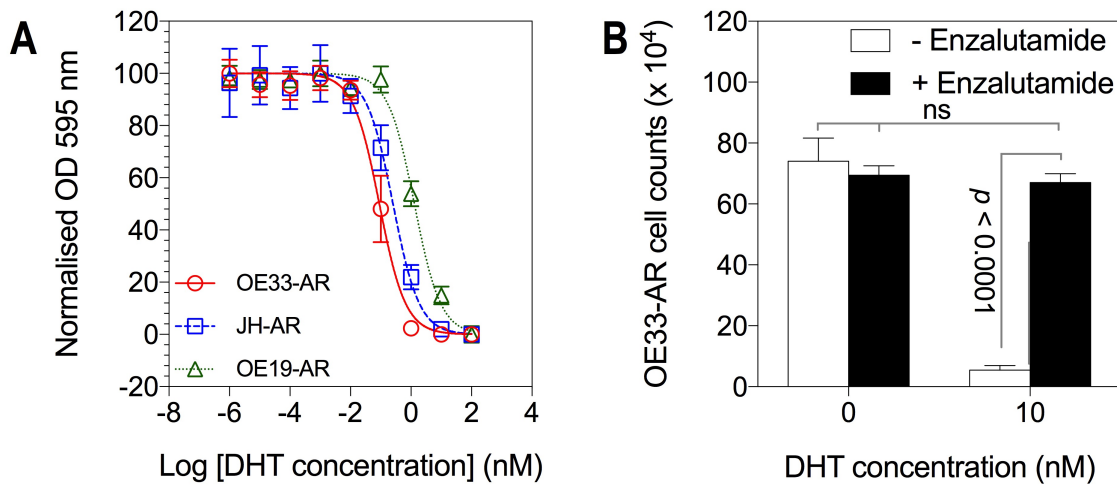


Figure 2. The effect of DHT on the proliferation of AR-expressing EAC cell lines. **a** Dose response curves for the proliferation of AR-expressing EAC cells grown for 6 to 12 days with vehicle or 10-fold serial dilutions of DHT. Proliferation was measured by crystal violet assay. Data are the mean \pm SD of six replicates, and the corresponding nonlinear regression curve, from a representative experiment for each cell line. **b** The effect of enzalutamide (15 μ M) on the proliferation of OE33-AR treated with 10 nM DHT.

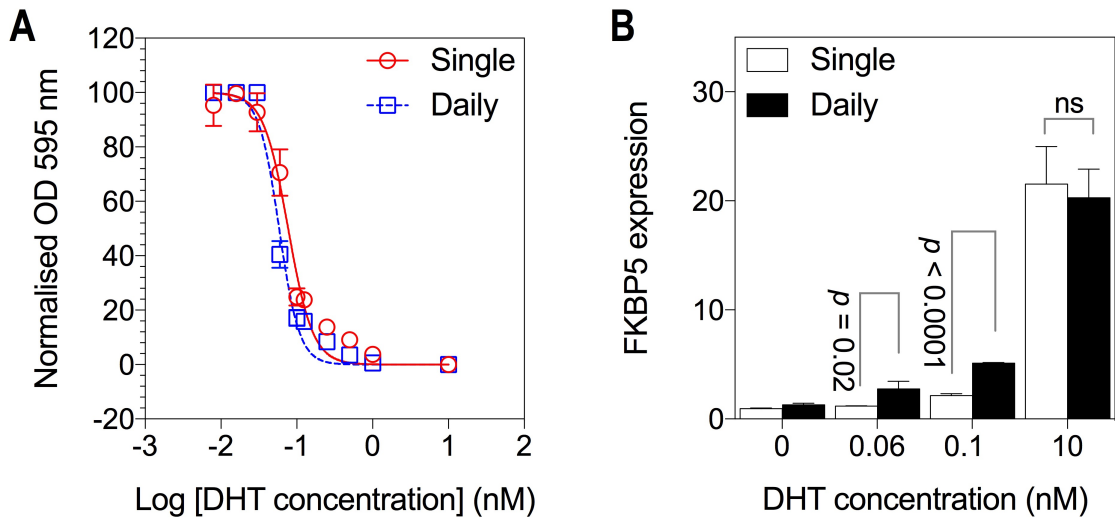


Figure 3. The effect of single compared to daily doses of DHT on OE33-AR growth and FKBP5 expression. **a** Dose response curves for the proliferation of OE33-AR grown for 5 days with vehicle or 2-fold serial dilutions of DHT given as a single dose or replaced daily. Data are the mean \pm SD of six replicates, and the corresponding nonlinear regression curve, from a representative experiment. **b** Normalised fold FKBP5 expression after 3 days culture with a single dose or daily replacement of vehicle or DHT. Data are the mean \pm SD of triplicate reactions for three biological replicates.

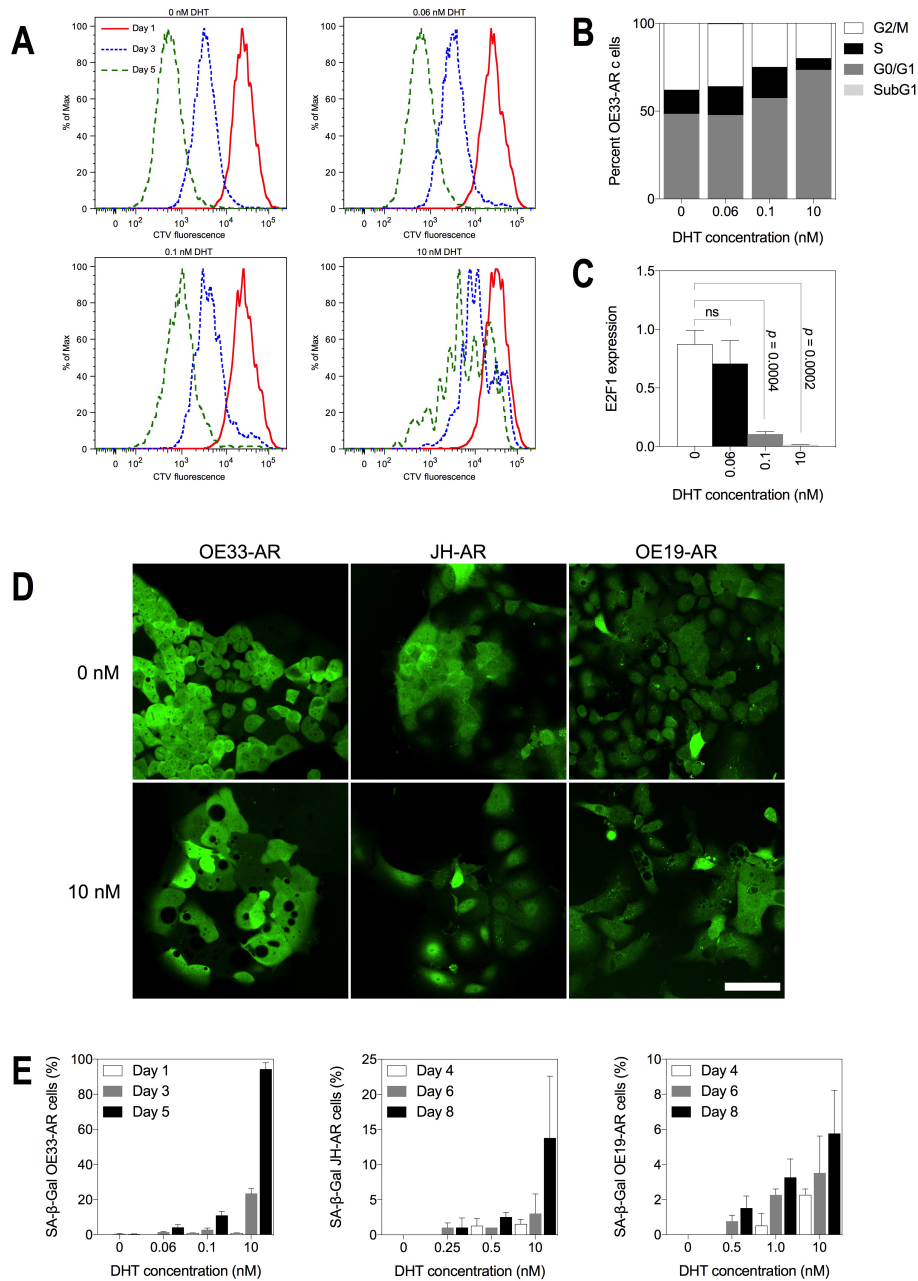


Figure 4. The effect of treatment with vehicle or DHT on cell division, cell cycle stage, morphology and senescence in AR-expressing EAC cells. OE33-ARs were treated with vehicle or DHT at IC50 doses or 10 nM. **a** Division of OE33-AR monitored by CellTrace Violet dye dilution on days 1, 3 and 5 post treatment ($n = 3$). The peaks represent different generations of cells. **b** Cell cycle distribution and **c** normalised E2F1 expression (mean \pm SD) on day 3 following treatment of OE33-AR ($n = 3$). **d** Fluorescent micrographs of OE33-AR, JH-AR and OE19-AR treated for 3 days with vehicle or 10 nM DHT. Scale bar is 75 μ m. **e** Percentage of OE33-AR, JH-AR and OE19-AR positive for senescence-associated beta-galactosidase (SA- β -gal) on various days post treatment with vehicle or DHT. Data are the mean \pm SD of pooled replicate experiments (OE33-AR, $n = 3$; JH-AR and OE19-AR, $n = 2$).

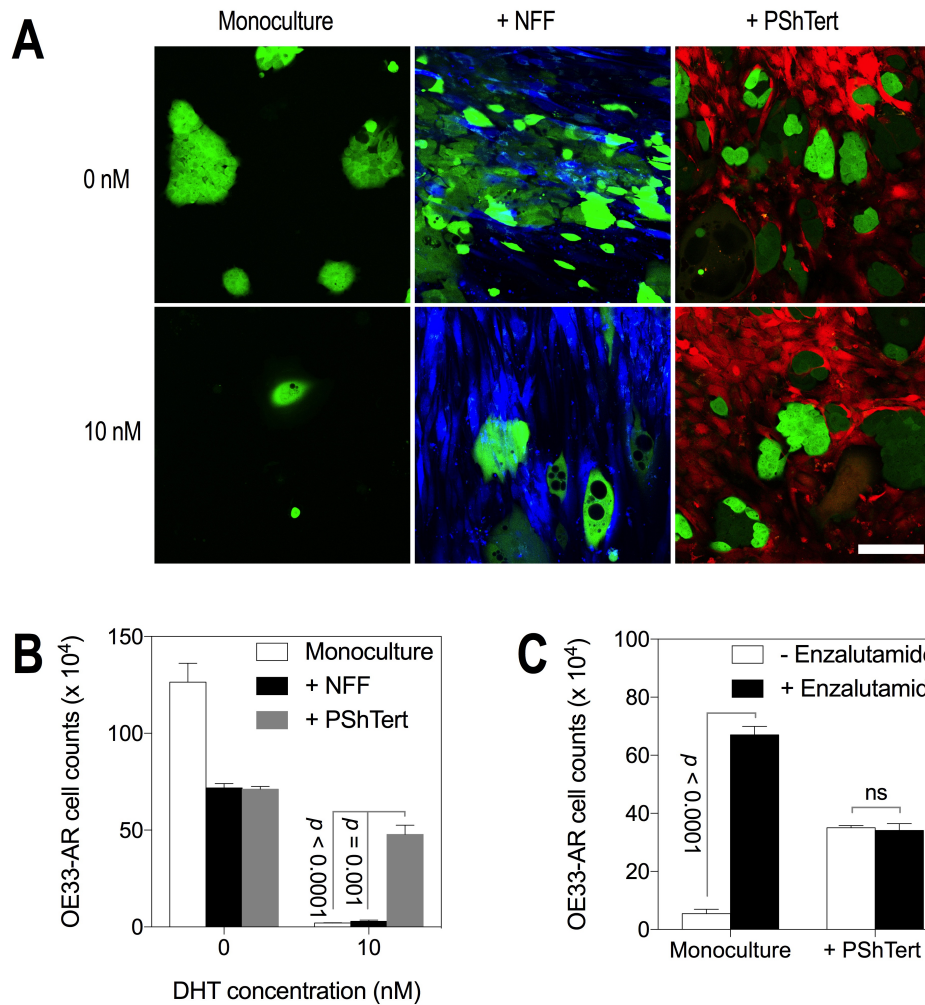


Figure 5. Growth and morphology of OE33-AR in direct co-culture with fibroblasts. **a** Fluorescent micrographs of OE33-AR (green) in monoculture or in direct co-culture with NFFs (blue) or PShTert myofibroblasts (red) treated with vehicle or 10 nM DHT for 6 days, with the medium replaced every 48 h. Scale bar is 75 μ m. **b** Cell counts of OE33-AR grown for 6 days with vehicle or 10 nM DHT in monoculture or direct co-culture with NFFs or PShTert myofibroblasts. **c** Cell counts of OE33-AR grown for 6 days with vehicle or 10 nM DHT, with or without 15 μ M enzalutamide, in monoculture or direct co-culture with PShTert myofibroblasts. Cell count data is the mean \pm SD of three replicates from a representative experiment.

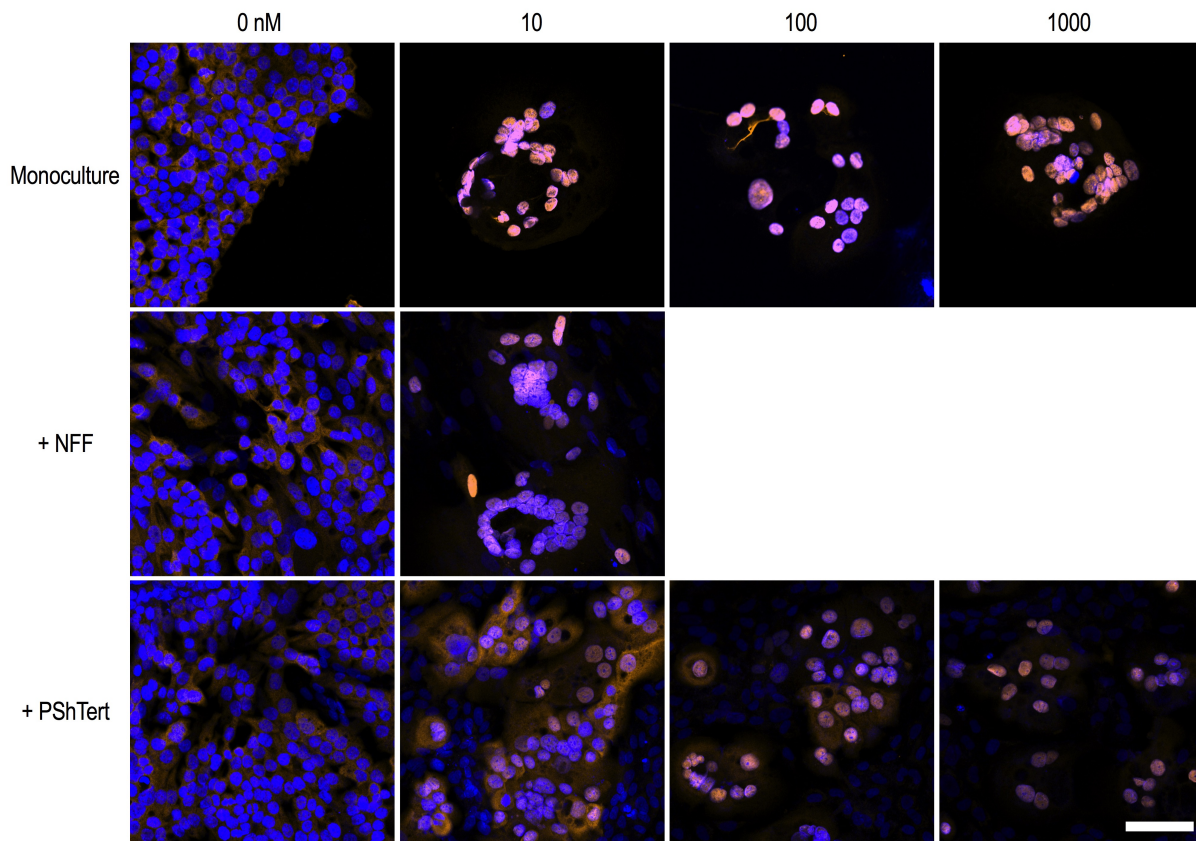


Figure 6. Nuclear translocation of AR induced by DHT in OE33-AR in direct co-culture with fibroblasts. Fluorescent micrographs of OE33-AR grown for 6 days in monoculture or direct co-culture with PShTerts with vehicle or 10, 100 or 1,000 nM DHT, or in direct co-culture with NFFs with vehicle or 10 nM DHT. Cells were labelled with rabbit anti-human AR polyclonal IgG (clone N-20; 1 $\mu\text{g}/\text{mL}$ in 1.5 % goat serum) followed by secondary antibody Alexa Fluor 568 goat anti-rabbit IgG (2 $\mu\text{g}/\text{mL}$ in 1.5 % goat serum) and DAPI (1 $\mu\text{g}/\text{mL}$). Merged channel images were captured using a Zeiss confocal LSM700 microscope. Scale bar is 75 μM .

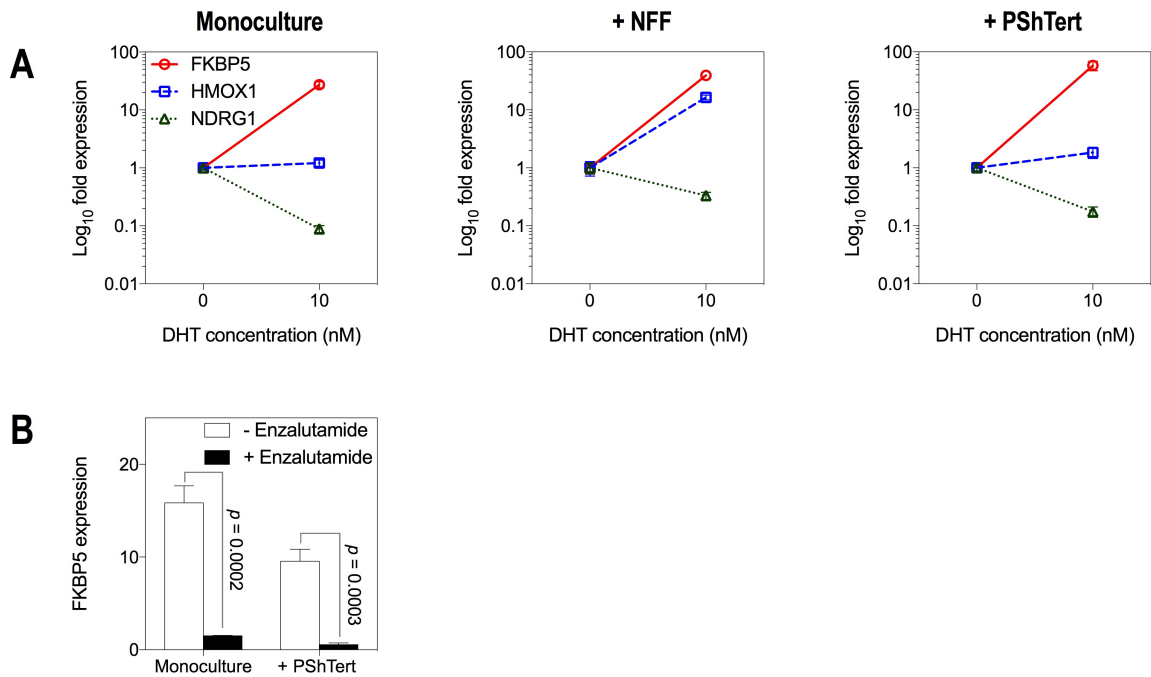


Figure 7. The effect of co-culture with fibroblasts on DHT induced expression of androgen-responsive genes in OE33-AR. **a** The expression of FKBP5, HMOX1 and NDRG1 in OE33-AR grown for 6 days with vehicle or 10 nM DHT in monoculture or direct co-culture with NFFs or PShTert myofibroblasts. Expression was normalised to the reference gene ACTB and graphed relative to expression with vehicle. Data is the mean \pm SD. **b** Expression of FKBP5 in OE33-AR grown for 6 days with vehicle or 10 nM DHT, with or without 15 μ M enzalutamide, in monoculture or direct co-culture with PShTert myofibroblasts.

SUPPLEMENTARY METHODS

Western immunoblot analysis

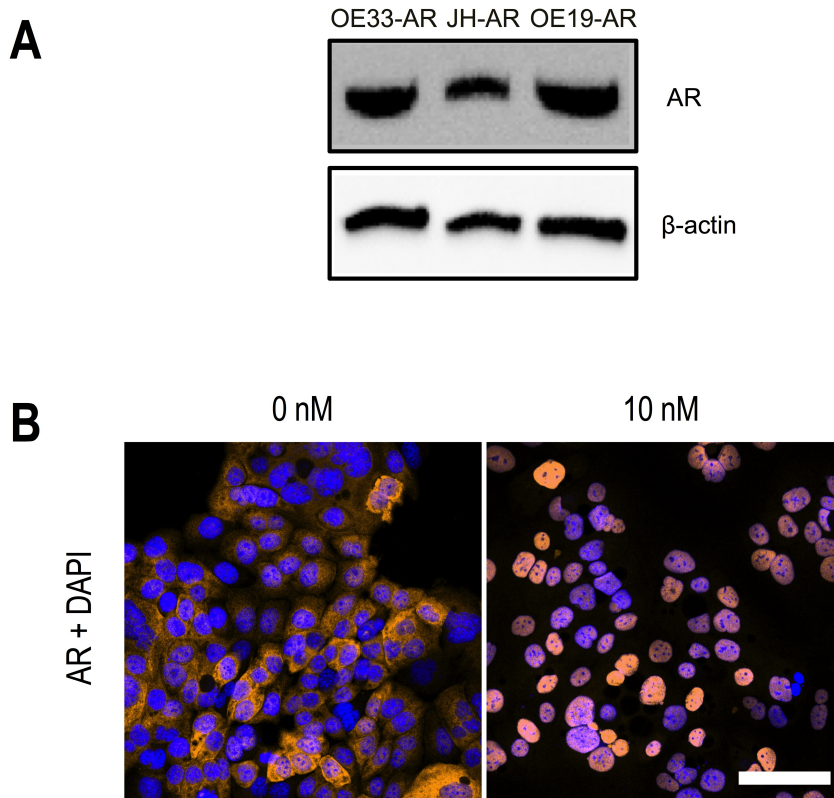
Whole cell lysates were prepared from cells as previously described [1], and 15 µg of protein was resolved by denaturing electrophoresis on 4 – 15 % Mini-PROTEAN TGX precast polyacrylamide gels (Bio-Rad Laboratories, Hercules, CA, USA), followed by transfer to Hybond-C membrane (Amersham Biosciences, Castle Hill, NSW, Australia). Transfers were probed with 1:10,000 rabbit anti-human AR polyclonal IgG (clone N-20; 0.02 µg/mL; Santa Cruz Biotechnology Inc., Santa Cruz, CA, USA) and 1:5,000 mouse anti-human β-actin polyclonal IgG1 (clone AC-15; Sigma-Aldrich, St Louis, MO, USA). Immunoreactivity was detected with the appropriate horseradish peroxidase conjugated immunoglobulin (Dako, Glostrup, Denmark) and visualised by enhanced chemiluminescence (Amersham).

REFERENCE CITED IN SUPPLEMENTARY METHODS

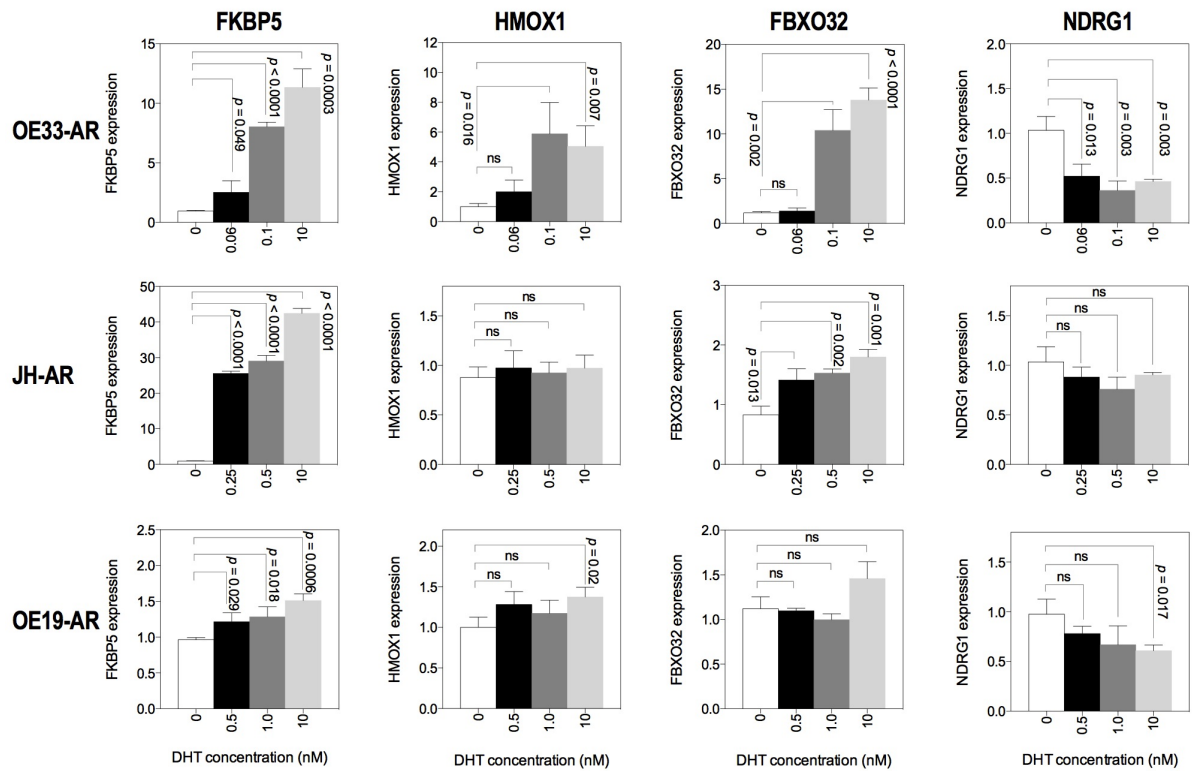
1. Leach DA, Need EF, Toivanen R, et al. Stromal androgen receptor regulates the composition of the microenvironment to influence prostate cancer outcome. *Oncotarget*. 2015;6:16135-16150.

Supplementary Table S1. Primer sequences used in qRT-PCR

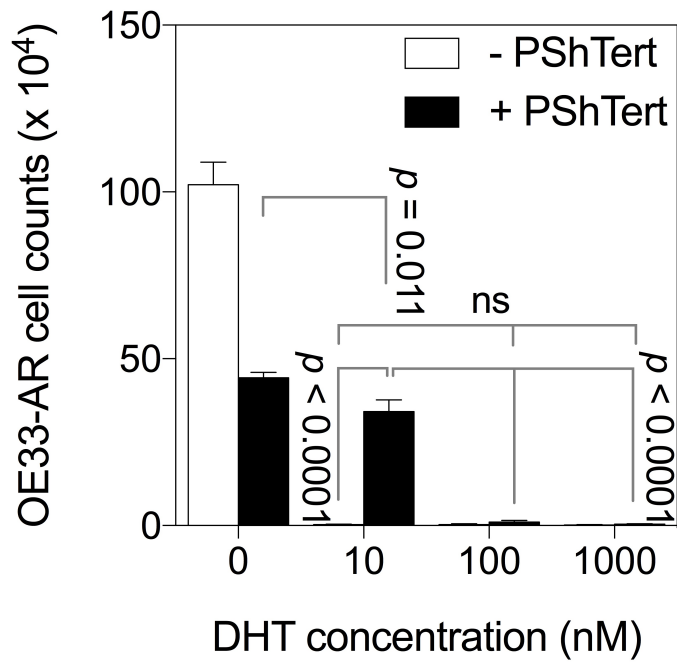
Gene	Forward sequence	Reverse sequence
ACTB	CATCCGCAAAGACCTGTACG	AGTACTTGCGCTCAGGAGG
CCNB1	TCAGGTTGTTGCAGGAGACCATG	CACCAACCAGCTGCAGCATCTT
E2F1	GCAGAGCAGATGGTTATGG	GATCTGAAAGTTCTCCGAAGAG
FBXO32	CCCTTCAGCTCTGCAAACACTGTC	CTCCAGTCAGCAGGGGGACC
FKBP5	ATTATCCGGAGAACCAAACG	CAAACATCCTTCCACCACAG
HMOX1	ACCCAGGCAGAGAATGCTGAGTT	CCTCCTCCAGGGCCACATAGATG
NDRG1	CTGCAAGAGTTTGTATGTCCAGGAG	ACACAGCGTGACGTGAACAGAG



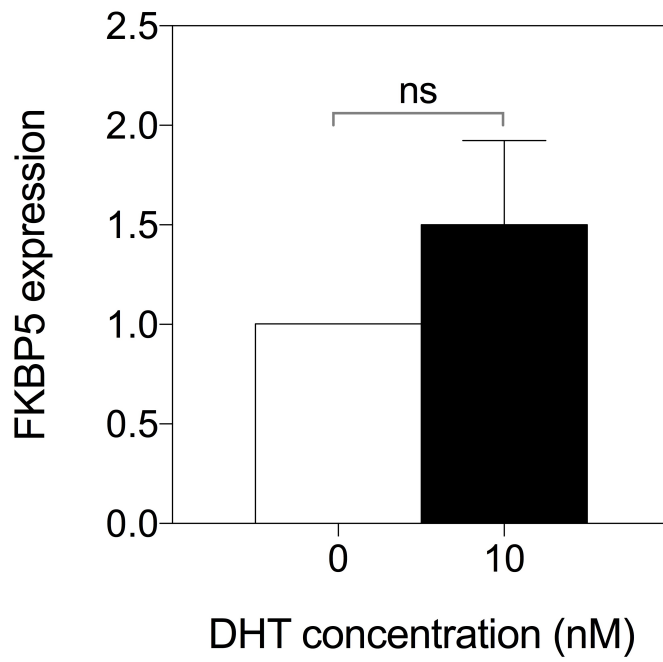
Supplementary Figure S1. AR expression and translocation in AR-expressing EAC cells. **a** Western immunoblot for AR and the housekeeping protein β -actin in OE33-AR, JH-AR and OE19-AR. **b** Fluorescent micrograph of immunostained AR in OE33-AR after treatment for 30 min with vehicle or 10 nM DHT. The merged AR and DAPI channels show the AR distribution relative to the nucleus. Scale bar is 75 μ M.



Supplementary Figure S2. The effect of DHT on the expression of androgen-responsive genes in OE33-AR, JH-AR and OE19-AR. The normalised gene expression was measured after 3 days of treatment with either vehicle or 10 nM DHT. Data is the mean \pm SD from a representative experiment.



Supplementary Figure S3. The effect of increasing DHT concentration on the proliferation of OE33-AR in monoculture or direct co-culture with PShTert myofibroblasts. Cell counts on day 10 of co-culture with vehicle or DHT. Data is the mean \pm SD of three replicates from a representative experiment.



Supplementary Figure S4. FKBP5 expression in PShTerts. Normalised fold FKBP5 expression in PShTert myofibroblasts grown in monoculture for 6 days with vehicle or 10 nM DHT. Data are the mean \pm SD of triplicate reactions for two biological replicates.

CHAPTER 7: CONCLUSIONS

The research presented in this thesis investigated the role of fibroblasts, and the role of the androgen receptor (AR) and androgen signalling, in the progression of oesophageal adenocarcinoma (OAC) and prostate cancer. The major findings related to (1) differences in the genome-wide DNA methylation profiles of primary fibroblasts from normal oesophageal mucosa and tumour-derived fibroblasts from OAC, (2) the effect of AR expression or androgen signalling in myofibroblasts on interactions with prostate cancer cells in vitro, and (3) the effect of AR expression and androgen signalling in OAC in vivo and in vitro.

Differences in the DNA methylation profiles of normal oesophageal fibroblasts and tumour-derived fibroblasts from oesophageal adenocarcinoma

Cancer-associated fibroblasts are normal fibroblasts that are phenotypically altered in response to stimuli from the tumour microenvironment. The phenotype of these cells, when grown in culture, is relatively stable over many subdivisions, suggesting that signals from the tumour microenvironment are not required for its ongoing maintenance. Research presented in this thesis explored the hypothesis that the CAF phenotype is maintained at least in part by changes in DNA methylation.

The findings presented in chapter 2 showed that the DNA methylation profile of fibroblasts derived from OAC tumour tissue differed significantly from that of fibroblasts derived from macroscopically normal oesophageal mucosa. In particular there was a focal distribution of differentially methylated cytosines about the transcription start sites and within CpG islands and transcriptional enhancers. These may, by the regulation of gene expression, contribute to the establishment and maintenance of the CAF phenotype.

This study was limited by a number of technical issues. Establishing cultures of fibroblasts from patient tissues proved to be difficult, so fewer lines were available than planned. Expanding the fibroblast population sufficiently to obtain the large amount of DNA necessary for the analysis was also a challenge. The lines were slow to proliferate and had limited proliferative capacity, with a number of lines ceasing to grow beyond 5-10 subcultures. Additionally, although it was assumed that the fibroblast phenotypes would be stable in culture, this could not be confirmed. The chance or extent of changes induced by in vitro culture was minimised by using cells from the earliest subcultures possible.

The identity of the fibroblast as either normal or tumour-derived was another issue. The fibroblasts were isolated from tissues that were macroscopically considered either normal or tumour, but this could not be verified histologically. Also, populations of fibroblasts,

particularly tumour-derived fibroblasts, are known to be heterogeneous in terms of origin, activation status and functionality. Because of the difficulty in growing cells in vitro it was not realistic to attempt to generate clones. The cultures were therefore almost certainly heterogeneous, which may explain the markedly heterogeneous DNA methylation profiles of the tumour-derived fibroblasts. Immortalisation of the cells with hTERT was attempted, but proved impossible. Lastly, it is not known if neo-adjuvant chemo-radiotherapy, which was given to some patients, might have altered the DNA methylation in the fibroblasts.

Several further studies would build on the reported findings. In the first instance, the results should be validated using another large, independent patient cohort, preferably including more patient-matched pairs of tissues. The DNA methylation profiles could be investigated to determine if there is a fibroblast methylation signature that has prognostic or treatment predictive value. Additionally, the effect of DNA methylation changes on RNA transcript or protein abundance might provide insight into the function of the tumour-associated stroma. In the longer term, understanding the signals which induce fibroblast activation through changes in methylation, or mechanisms which can reverse the induced DNA methylation changes, may lead to the development of novel therapies which can slow or halt cancer progression by modifying the activation and functions of the stroma.

The effect of myofibroblast androgen receptor on myofibroblast-prostate cancer cell interactions

Originally, the intention was to study the interactions between primary oesophageal fibroblasts and AR-expressing OAC cells in direct co-culture. Whilst attempts were being made to immortalise the fibroblasts for these experiments, proof of concept studies of the direct co-culture methods were undertaken using prostate cell lines. There were several reports that a reduction in stromal AR expression is associated with a poorer prognosis in prostate cancer. The opportunity was taken to study the effect of AR expression and androgen signalling in myofibroblasts on the juxtacrine and paracrine interactions between myofibroblasts and prostate cancer cell lines.

Two studies were performed and are reported in Chapters 3 and 4. Decreased stromal AR expression was associated with reduced prostate cancer-related survival across all age groups. Androgen signalling in myofibroblasts in vitro resulted in changes to the extracellular matrix that decreased the migration and invasion of prostate cancer cells. Juxtacrine and paracrine interactions between myofibroblasts and prostate cancer cells affected the behaviours of both cell types in vitro and in vivo, and differed depending on the expression of AR in the

myofibroblasts. Specifically, PShTert-AR myofibroblasts induced apoptosis in and destroyed prostate cancer cells via paracrine signalling whereas the AR-negative PShTert myofibroblasts underwent apoptosis and were destroyed by prostate cancer cells via juxtacrine cell-cell signalling. These were the first in vitro studies of juxtacrine signalling between prostate myofibroblasts and cancer cells in the context of myofibroblast AR. Results were consistent with the clinical finding that a reduction in stromal AR is associated with reduced survival in prostate cancer.

There were a number of potential limitations. Firstly, the only immortalised myofibroblast line available was derived from benign prostatic hyperplasia. Whilst it showed all the characteristics of cancer-associated fibroblasts, which we tested for, it may not have been fully representative of myofibroblasts in prostate cancer. Secondly, the original line was AR negative, so AR was transduced into a subline of this to generate the AR-expressing line. The AR was not under the control of its natural promoter, and was present at increased copy number, either of which could have modified cell behaviour. Thirdly, to ensure the cells were stable and could be maintained for the duration of the study, they were immortalised with hTERT, which may have resulted in unanticipated molecular change. Another potential limitation was the general use of the androgen-insensitive prostate cancer cell line PC3, to interrogate the effect of AR expression in the myofibroblast, without the confounding effect of AR in the cancer cell. Whilst this may have been unrepresentative, since in vivo there is commonly AR expression or signalling in the cancer cells, results with androgen sensitive cancer cell lines were similar to those obtained with PC3 cells, suggesting the findings were valid and generalizable.

Future studies could focus on the molecular details of the juxtacrine and paracrine interactions. This may lead to the discovery of new diagnostic and prognostic biomarkers, or therapeutic targets, against which agonists or antagonists could be directed. Identification of the mechanisms responsible for the loss of stromal AR expression as prostate cancer progresses could facilitate the discovery of novel treatments aimed at reversing this loss, with possible therapeutic benefit.

A potential role for androgen signalling in oesophageal adenocarcinoma

Up to 90% of patients with OAC are reported to be male. The reasons for this male dominance are unknown, but it was hypothesised that androgens and androgen signalling could, at least in part, play a role. When this project began, few studies had examined this

possibility, and of those, the sample sizes were small, the results conflicting, and no attempt had been made to assess whether the AR was functional.

Chapter 5 reports AR expression and functional androgen signalling, as measured by nuclear localisation of AR and expression of the androgen-responsive gene FKBP5, in the largest OAC patient cohort reported to date. There was nuclear localisation of AR in 91% of cases, and FKBP5 expression in two thirds, all of which had nuclear AR. Of clinical significance, nuclear AR and FKBP5 were independently associated with decreased survival.

The major limitation of this study was measurement of the expression of only one androgen-responsive gene. Whilst FKBP5 has been established as a bona fide androgen-responsive gene, investigating the expression of others, and their prognostic significance, could have added to this research.

Extension of this research would include confirming these findings in another large, independent patient cohort. The inclusion of a more comprehensive panel of androgen-responsive genes may lead to a better understanding of the molecular biology of the androgen signalling pathway in OAC cells, and possibly to the discovery of further clinically useful prognostic biomarkers. A proportion of cases expressed nuclear AR yet were FKBP5-negative. These patients survived longer than patients whose OAC was AR+/FKBP5+. Determining the mechanisms responsible for these differences may lead to a better understanding of the biology of this cancer and to therapies based on targeting the AR or FKBP5.

Given that the patient study suggested a role for androgen signalling in OAC, an *in vitro* study was undertaken with OAC cell lines. Since there were no AR-expressing OAC cell lines available, three OAC cell lines were stably transduced with AR to investigate the effect of androgens, AR, and androgen signalling on their behaviour. This *in vitro* study, presented in Chapter 6, showed that AR-expressing OAC cell lines responded to the androgen, DHT, with the inhibition of proliferation and the induction of androgen-responsive genes. The induction of androgen-responsive genes, together with significant proliferation, occurred at concentrations of DHT around the IC₅₀, or in direct co-culture with a myofibroblast line. This was the first study to use AR-expressing OAC cell lines and showed a potential role for androgens in OAC. This could, in part, explain the male predominance of the disease.

There were limitations to the in vitro study. Firstly, OAC cell lines transduced with AR may be unrepresentative of AR-expressing OAC cells in the tissues. For example, the AR was not under the control of its natural promoter and was present at increased copy number. Secondly, the fibroblasts used in the direct co-culture with the OAC cell lines were not of oesophageal origin. The attempts to immortalise primary oesophageal fibroblasts, both from normal oesophageal mucosa and from OAC tumour, were unsuccessful. As alternatives, a normal fibroblast from neonatal foreskin and a prostate myofibroblast line representative of a cancer-associated fibroblast were used, however these may have differed functionally from the equivalent oesophageal cells.

Further research is warranted to increase the understanding of the role of androgens in OAC. The experiments need to be repeated using oesophageal fibroblasts, preferably normal and activated to replace the neonatal foreskin fibroblast and prostate myofibroblast respectively. Little is known about the androgen signalling response in OAC. The androgen-responsive gene profiles of the three AR-expressing OAC cell lines could be defined by sequencing or microarrays and compared to each other or to androgen-responsive prostate cancer cell lines. Ultimately, the cell lines could be used in mouse xenograft studies to study the effect of gene knockout (specifically knockout of AR or androgen-responsive genes such as FKBP5), androgen depletion, or drugs targeting the androgen signalling pathway or androgen-responsive genes.

Overview

The studies described in this thesis relate to the role of fibroblasts and androgen signalling in OAC and prostate cancer, with three novel findings. Firstly, there were significant differences in the DNA methylation profiles of fibroblasts from OAC tumour tissue compared to normal oesophageal mucosa, supporting a role for epigenetic mechanisms in the development and maintenance of the cancer-associated fibroblast phenotype. Secondly, the expression of AR in myofibroblasts modified their juxtacrine and paracrine interactions with prostate cancer cells. This was consistent with the association between reduced stromal AR and increased prostate cancer-related deaths across all age groups, and supports a role for stromal AR in the regulation of tumour growth. Thirdly, an association between androgen signalling and reduced survival in OAC was established, with in vitro studies, using AR-expressing OAC cell lines, consistent with a role for androgen signalling in this disease. The androgen response could be modified by androgen concentration and the presence of a myofibroblast. These studies expand current knowledge of the contribution of fibroblasts and androgen signalling in these two cancers and may lead to the discovery of novel treatments.

APPENDIX A: SUPPLEMENTARY TABLES

Supplementary tables 1 and 2 from manuscript in chapter 2 titled:

Fibroblasts derived from oesophageal adenocarcinoma differ in DNA methylation profile from normal oesophageal fibroblasts.

Eric Smith, Helen M. Palethorpe, Annette L. Hayden, Joanne P. Young, Timothy J. Underwood, Paul A. Drew

Supplementary Table S1

Patient Number	TDF	NDF	Gender	Age	Tumour Type	Tumour Differentiation	Pretreatment T Staging	Pretreatment N Staging	Pretreatment M Staging	Curative Treatment Modality	Radiology Response	Pathological T Staging	Pathological N Staging	Pathological M Staging	Pathological M Staging	Positive Nodes	Total Nodes Counted	Proximal Resection Margin	Distal Resection Margin	Circumferential Resection Margin (CRM)	CRM (mm)	Vascular Invasion	Lymphatic Invasion	Perineural Invasion	Tumour Location
18		N.18	Male	63	AC	G2	T3	N1	M0	Neoadjuvant Chemotherapy + Surgery	Partial Response	T2	N0	M0	M0	0	16	No	No	No	Clear	No	No	No	OGI-S2
23		N.23	Male	65	AC	G3	T3	N1	M0	Neoadjuvant Chemotherapy + Surgery	Complete Response	T2	N0	M0	M0	0	17	No	No	No	1	No	No	No	OGI-S1
32		N.32	Female	68	SCC	G2	T3	N1	M0	Neoadjuvant Chemotherapy + Surgery	Partial Response	T2	N0	M0	M0	0	21	No	No	No	13	Yes	Yes	No	OGI-S1
38		N.38	Male	66	AC	G1	T3	N1	M0	Neoadjuvant Chemotherapy + Surgery	Partial Response	T2	N0	M0	M0	0	17	No	No	No	8	No	No	No	Lower 1/3
50		N.50	Female	57	AC	G2	T3	N0	M0	Neoadjuvant Chemotherapy + Surgery	Partial Response	T3	N3	M0	M0	13	38	No	No	Yes	<1	Yes	No	Yes	Lower 1/3
55		T.55	Male	61	AC	G2	T3	N1	M0	Neoadjuvant Chemotherapy + Surgery	Partial Response	T3	N3	M0	M0	7	18	No	No	No	Clear	Yes	No	No	OGI-S1
64		T.64	Male	70	AC	G3	T3	N0	M0	Neoadjuvant Chemotherapy + Surgery	Partial Response	T1	N0	M0	M0	0	11	No	No	No	9.5	No	No	No	OGI-S1
108		T.108	Male	63	AC	G3	T3	N1	M0	Neoadjuvant Chemotherapy + Surgery	Partial Response	T3	N0	M0	M0	0	22	No	No	No	7	Yes	No	Yes	OGI-S2
109		T.109	Female	73	AC	G3	T3	N1	M0	Surgery only		T3	N1	M0	M0	2	34	No	No	No	1	No	No	No	Lower 1/3
161		N.161	Male	63	AC	G3	T2	N0	M0	Surgery only		T1	N0	M0	M0	0	13	No	No	No	11	No	No	No	OGI-S2
205		T.205	Male	64	AC	G1	T1	N0	M0	Surgery only		T1SHGD	N0	M0	M0	0	28	No	No	No		No	No	No	Lower 1/3
217		T.217	Male	58	AC	G2	T2	N0	M0	Surgery only		T3	N3	M0	M0	15	27	No	No	Yes	1	No	No	No	Lower 1/3
251		T.251	Male	82	AC	G2	T3	N1	M0	Surgery only		T3	N0	M0	M0	0	26	No	No	Yes	<1	No	No	Yes	OGI-S2
255		T.255	Male	64	AC	G3	T3	N1	M0	Neoadjuvant Chemotherapy + Surgery	Partial Response	T3	N0	M0	M0	0	45	No	No	Yes	0	No	No	Yes	OGI-S2
528		T.528	Male	76	AC	G2	T2	N1	M0	Neoadjuvant Chemotherapy + Surgery		T2	N1	M0	M0	2	36	No	No	No		NA	NA	NA	OGI

GO:0009987	cellular process	827/901	13765/17046	2.52E-21	7.52E-18	5.91E-18	AKT3/ABI1/CDH3/ITANK/GNE/ZNF783/CDH9/TSPAN5/COH12/CDH13/SUGP2/MBNL2/KCMB2/CDKN1C/SPEG/CKCK/JCIRG1/MRVL1/TRDN/ABCA9/SPON2/C1D/ZBTB18/TACC2/MTHFS/PDPN/DMRT2/CELF1/CELF2/TBR1/SEPT9/GIB6/HCS1/NPFHR2/ADCY3/PNRC1/TMED10/SLC27A2/LECT1/REK1/HRNPUL1/RPP14/HIBADH/CHG/A/CH3L1/ERLIN2/PSIP1/PKP3/EGLN2/TP53TG1/ATXN2/B46GALT1/PHT2/KIF12/ACOT1/PDAP1/EXOXC3/CHRNA1/CHRNA2/ADPRHL1/CHRNA5/GRINI1/SORCS1/ZBED9/CID/EA/C1QTNF7/ALPK2/PANX3/GALNT15/AP351/CLCA1/CLNS/ANKRD9/MRPL52/FRMB6/CCR1/SLC38A10/SE26/TMFAIP81/CNP/APOA1BP/NEU4/COL9A3/COL11A1/COMP/SC11/MA3K8/ZFP42/ADM/IL13RA/EGFLAM/UBLCP1/HUS1B/OR2A14/CP51/NDUFA56/PXDNI/CRA8P1/ZNF358/TPRM6/MBZ/PARP4/MPTP/FAM101A/B3GLCT/MGAT5/B/ARCDD1/CSTA/KLC3/ZNF738/CTGF/ABCC13/SMYD1/SGOL1/PPM1L/SH3D19/CV8561/CYD1/MBROT1/ADRB3/ESCO2/CY11A1/ZNF782/FTTM1/ADA1/TRPV3/ZNF709/ZNF781/CT/ED4/DOB1/WBP2/NUD/DOOST/RNF168/ZNF366/BHLHA15/COCH/NLRRP6/DIO3/DLGG2/DJMBT1/DNAH6/DNAH8/DNMT3A/ABAT/DPH1/DRD4/DSG3/DTNA/CE1/AGX1/EEF2/EFNA2/EG/FR/EGR3/PATL2/EIF4G1/A2M1/ELK4/TMEM17/EML1/UNC13D/DNAH12/SLC10A4/ENO2/ADCC5/EPHA3/EPHA4/ESR1/ALAS1/PAH/FAT2/SPATA13/FCGR2A/RNF182/PHACTR1/SP8/FGA/FGF10/FHIT/ARN2/RASA3/PPM1E/VASH1/BTBD3/SBNO2/TRAK1/M5RB2/ACIN1/LUMCH1/FOXO1/EXPH5/AKR1B1/SPG20/NFASC/EPB413/FLNB/DFP2A/F/PLEK2/SLC17A5/ADGRF1/RP56K1/PABPC1/GIA3/DNAC2/FGF2/NPTN/GIB2/CUL1/AMPD2/SDCBP2/PDE7B/DK33/CYTH4/GLS2/NPSA4/AMPD3/GPR162/BMP10/ZNF639/GNAS/ZNF311/PIGW/IZUMO1/ZNF844/THM5/GPR26/GPER1/EOGT/DOK7/FFAR2/GRB10/MRPS18B/FLVCR1/GRIK4/ZBTB44/DNAIC15/SCG3/GSTP1/GTF2B/BRF1/TMOD4/GUCY1A3/N/ME7/GPR132/PADI1/GZMA/ANXA2/HAS1/SERPIND1/SOX8/KCNIP2/NRGI/ANXA6/HK1/HLA-B/HLA-DPA1/ANXA13/HLA-E/HLA-F/HLX/HMG21/NR4A1/ACACB/HPCA/APBA2/HOXB3/HOXC4/HOXCS/HOXC6/HOXD3/HRH1/ACA01/HSPA11/HSP90AA1/HSP90AB1/HTR3A/HTR5A/DUPD1/TFAP2E/ID3/ZC3H12D/C/OL28A1/RSPO2/FMNI1/BARHL2/NME9/IGF1/IGF2/CYR61/GPR142/LCE1C/LCE1D/LCE2D/IL1R1/IL1RN/IL6/IL10RA/AOP2/IL11RA/IL12RB2/IL15RA/IL16/FOXK2/AOP5/INHBA/INPP5A/IRF1/AQP9/SL1/ITGA7/ITGB2/ITGB7/ITIH3/ITIH4/IVL/JUP/CDB2/USP50/HILS1/ATP9B/KCNH2/KCNJ9/KCNMB1/KDR/ACAT1/KIF25/PO5/KRT7/KRT15/AMIG03/INSC/HESS/SLC6A17/AFK3/LAMA3/STMN1/OR2A5/LCK/LCP1/MUC21/DLIR/ARHGDI/LGALS9/LHCGR/LLGL1/LMNA/LMO2/RAB19/LOX/LTB1/TBP1/SMAD3/MC2R/MCC/ME1/ME2/MEF2D/M/AP3K1/MEOX1/MEOX2/MF12/MFNG/MGAT1/SCGB2A1/WIT1/LHX8/ASGR1/MOCS1/MOV10/NPZ/PLEKHG7/MTTA/NUDT1/MYH4/MYL2/NUBP1/NDUFB4/DRG1/NEED9/NEU1/ATPIA2/INFATC3/NFY8/NHLH2/NMBR/NOV/NPPC/NRAS/NTF3/OAS2/OPRL1/OR2C1/OR3A2/SLC22A18/P2RY6/PFAFH2/ATP5B/IL2IR/ANO7/PALM/ARHGEF3/PARK2/SPOCK3/UTP11/L/LE1/DDX47/CEND1/PRR16/CHST15/ANGPT4/PDE4C/PCYOX1/PDE7A/C11orf73/SIRT6/PDE6B/ATP8A2/GALNT7/PGAM2/P13/PGIC/PIK3CG/PTX2/PKHDI/PKM/PLA2G2A/PLAG1/SPA17/PLEC/PRKAG3/PML/RIPPL1/RYD6/GRP84/IL20RB/SLC10C1/PNUP/RIPK4/TLR9/TREM1/CYTL1/POMC/SSH1/PON1/RIN2/MOV10L1/POU2AF1/ZDHHC13/APBB1IP/ROB4/MOBA/SLC47A1/SLC29A3/MIS18BP1/WDR33/TRPV6/SMPD3/SLC30A10/CNOT11/CHRNA9/SYBU/PEX26/LIMS2/FRMD4A/VACL4/PARVA/PKAR1B/TTCT17/IIFT12/MCTP2/LMBRD1/CSGALNACT1/PAG1/CSG1/PRKD1/W5B2/MYNN/BIN3/APOB8/MAPK3/MAP2K2/PRKRIR/PROG/MRAP/TRPV5/PRMT8/MASP1/HTRA1/SLAMF8/CDC42SE1/P5MB4/PAK6/ARNTL2/RGMA/PRDM11/TRPC7/LPAR5/PSMD7/SLURP1/ACTR3B/PTGFR/PLEKHG5/TENM2/AD2B/EMN/KLHL14/MARK4/CCAR2/PTPRE/PXN/CREB2/FAM60A/ACTA2/RASGRF2/RFC2/TRIM27/RGR/RGS12/RTT2/EXO44/RPA3/RPL8/RPL29/S100A4/S100A6/BGLAP/SCT/CLL11/CCL17/MRPS14/NPAS3/PARVG/NOD2/STRA6/SERP2/CXCR5/MAP1LC3/B2/ARHGAP9/TRA2B/GZF1/DNAI2/SGK1/MICAL1/CERK1/MEM237/NP533A/BMP4/SLC44A1/ZNF649/SLC8A1/SLC9A3/SLC20A2/BMPR1B/SULT1/BRD9/ZSCANL8/BOX/SOX9/BPI/SRP68/STAT2/STK3/STK10/SUPT6H/BST2/VAMP2/TAF4B/TBP/TCEA1/TCEB2/ZEB1/ACT1/TEAD3/TERF1/TGM2/TCHH/TIMP3/TLR5/TRAPP3/TNFAIP3/TNFRSF1A/TXK
------------	------------------	---------	-------------	----------	----------	----------	---

GO:0044699	single-organism process	770/901	12449/17046	3.78E-20	7.51E-17	5.91E-17	770
<p>AKT3/ABI1/CDH3/ITANK/GNE/CDH9/TPSAN5/CDH12/CDH13/FARP1/KLRIG1/RCAN1/MRVI1/TRDN/ABC9/SPON2/CLD/COG5/ZBTB18/TFAC CZ/MTHFS/PDPN/DMRT2/CELF1/CELF2/TBR1/SEPT9/GUB6/HCS7/NPFER2/ADCY3/TMED10/SLC27A2/LECT1/REB1/ESM1/ADAM29/HIBADH/CHGA/CHI3L1/ERLIN2/PKP3/EGLN2/BA GALT1/PTH2/KF12/ACOTT/PPDAP1/EXOC3/CHRNA1/CHRNA2/CHRNA5/CARD16/GPRIN1/SORCS1/CIDEA/PANX3/GALNT15/AP3S1/CLCA1/FAT3/CLNS/ANKRD9/MRPL52/FRMD6/CC R1/SLC51B/C15orf27/ZG168/SLC38A10/SEZ6/TNFAIP8L1/CNP/APOA10/NEUA/COMPL/SLIT1/GALM/COMP/SLC11/AL1/GALM/PAK48/ZFP42/ADM/AL1RA/EGFLAM/HU5118/ORA2A14/C PS1/NDUFA66/PXDNL/CBAPB1/ZNF358/TRPM6/CR1BBS3/MIB2/PARP4/MPP7/FAM101A/B83GLCT/MGA15B/APCDD1/CSTA/KLC3/CTGF/ABCC13/SMYD1/SGOL1/PPM11/SH3B19/CY B561/CYLD/MBOTAT1/ADRB3/ESCO2/CYP11A1/FTTM1/ADAL1/TRP3/DOB1/WBR2NL/DDOST/ZNF366/BHLH15/COCH/NLRP6/DIO3/DL2/DGZ/SOCH1/DNAH6/DNAH8/DNM13 A/ABAT/DPH1/DRD4/DSG3/DNA/ECEL1/AGXT/EEF2/FENNA2/EGFR/EGR3/EIF4G1/A2M/ELK4/TMEM17/LPH/EMVL1/UNC130/DNAH12/SLC10A4/ENO2/EPHA1/EPHA3/EPH4/ESR1/ ALAS1/F11/FAH/FAT2/SPATA13/FCGR2A/PHACTR1/SP8/FGA/FGF10/FHIT/XRN2/RASA3/PPM1E/VASH1/BTBD3/S8NO2/TRAK1/MISRB2/ACIN1/LIMCH1/FOXO1/FOXO2/FOXO3/EXPH 5/AKR1B1/SPG20/NFASC/EPB41L3/FLNB/DIP2A/FLOT2/MLC1/RHOBTB2/NUPT210/ATP11A/NEDDA41/SYNE1/PSD3/LARP1/PPP1R13B/PUM2/ARRGEF18/RYPB/MORC3/MAPK8IP2/TS SK2/VGLL2/JMTR/FUCA1/SLC37A4/GABBRI1/RASGEF1C/RNF144B/STGGALNAC3/GAK/SAMM50/DFNB31/ALS2C1/PNK4/TFNM4/ACOTT11/RGS22/STEAP2/GAS2/FBXO2/LCE2B/BAT M/6BGT1/GAPDH5/PIEK2/SLC17A5/ADGRF1/RP58K1C1/PABPC1/GIA3/FGF22/NPTN/GIB2/CLUL1/AMPD3/SOCBP2/PDE7B/DNK3/CYTH4/GLS2/VPS4A/AMPD3/GPRL62/DHHD/BMP 10/GNAS1/CRACR2B/PIGW/JZLUMO1/THSM5/GPR26/GPER1/FOG1/TFARP2/GRB10/MRPS18B/FLVCR1/GRK4/DNAIC15/SCG3/GSTP1/TMOD4/GUCY1A3/NNME7/GPRL132/PAD11/GZMA /ANKY2/HAS1/SERPIND1/SOX8/KCNIP2/NRG1/ANKY6/HK1/HLA-B/HLA-DOA/HLA-DPA1/ANKY13/HLA-E/HLA-F/HIX/HMGA1/NR4A1/ACACB/HPC4/APBA2/HOXB3/HOXC4/HOXC5/HOXC6/HOXD3/HRH1/HSD11B1/HSD17B2/ACADL/HSPA1L/HSP90AA1/HSP90AB1/HTR3A/HTR5A/TFAP2E/ID3 /ZC3H12D/COL28A1/RSP02/FMNI1/BARHL2/NME9/IGF1/GF2/CYR61/GPRL142/LCE1C/LCE1D/LL1R1/LILRN/L6/L10RA/AQP2/LL1RA/LL12R2/LL1R2B2/LL1R4/LL1R282/LL1R6/FOXK2/AQP5/JN HBA/INPP5A/IRF1/AQP9/SL1/ITGA7/ITGB2/ITGB7/ITLJ/JUP/CD82/USP50/HLS1/ATP98/KCNH2/KCNJ8/KCNJ9/KCNMB1/KDR/ACAT1/KIF25/PO5/KRT15/AMIGO3/INSC/TOMM20L/ HESS/SLC6A17/RESP18/AFF3/LAMA3/STMN1/ORA25/LCK1CP1/MUC2J/LDIR/ARHGDA1/GALS9/LHCGR/LGL1/LMNA/LMO2/RAB19/LOX1/TB/TBPI/SMAD3/MC2R/MCC/MEI7M EZ/MEF2D/MAP3K1/MEOX1/MEOX2/MF12/MFNG/MGAT1/SCGB2A1/MITF/LHX8/ASGR1/MOCS1/MOVL10/MPZ/PLEKHG7/NUDT1/MTYH4/MY12/NUBP1/NDUFB4/DRG1/NEDD9/NE U1/ATP1A2/NFATC3/NFYB/NHLH2/NMBR/NOV/NPPC/NRAS/NTF3/QAS2/OPRL1/ORB2C1/ORB3A2/SLC22A18/P2RY6/PAFAH2/ATP5B/IL21B/ANOT7/PALM/ARHGEF3/PARK2/SPOCK3/ UTP11L/LEFT1/DDX47/CEND1/PRR16/CHST15/ANGPT4/PDE4C/PCYOXI/PDE7A/CL10F73/SIRTE6/ATP66B/ATP842/GALNT7/PGAM2/PGIC/PK3CG/PTX2/PKHDI1/PKM/PLA2G2A/PLAG L1/SPA17/PLEC/PRKAG3/PML/RIPPLY3/FXYD6/GPR84/IL20RB/SLCO1C1/PNUP/RPK4/TLR9/TREM1/CYTL1/PO/MC/SSH1/POIN1/RIN2/MOVI10.1/ZDHHC13/APBB1P/ROB4/MXR48 /FBLIM1/BNCE2/PALMD/CYP2W1/UPCAT2/BANP/PPP1CB/HERC6/PPP1CC/PWIL2/EIP3/ARHGEF10/PRMT6/GOUPH31/PRM2B/FANC/IMOB1A/SLC47A1/SLC29A3/MIS18BP1/WDR 33/TRPV6/SMPD3/SLC30A10/CNOT11/CHRNA9/SYBU/PEX26/LIMS2/FRMD4A/VAC14/PARVA/PKAR1B/ITTC11/FTI22/ERMARD/MCTP2/LMBRD1/CSGALNACT1/PAG1/CISD1/PKR D1/NSB2/BINS/APOBR/MAPK3/MAP2K2/PKRIR/PROC/MRAP/TRPV5/PRMT8/MASP1/HTRA1/SLAMF8/CDC425E1/PSMB4/PAK6/RGMA/TRPC7/LPARS/PSMD7/SLURP1/ACTR3B/P TGR/PLEKHG5/TEHM2/ERMN/RDH14/METT1L4/MARK4/CCAR2/PTPRE/PXN/FAM60A/ACTA2/RASGRF2/RFC2/TRIM27/RGR/RGS12/RIT2/EXO4/IRP3/RPL8/RPL29/S100A4/S100 A6/BGLAP/SC7/CCL11/CCL17/ABHD4/MRPS14/NPAS3/PARV6/NOD2/TINAGL1/STRAGL1/STRAG2/GZF1/DNAI2/SGK1/MICAL1/CERK/TMEM237/NPS33A/BMP 4/SLC4A1/SLC6A12/SLC8A1/SLC9A3/SLC20A2/BMPRI1B/SLIT1/BOK/SOX9/BPI/SRRP68/STAT2/STK3/STK10/SUPT6H/BST2/VAMP2/TAFA8/TBP/TCEA1/ZEB1/ACTC1/TEAD3/TEB1/TG W2/TCHH/TIMP3/TLE3/TLRS/TRAPP10/TNFAIP3/TNFRSF1A/TNFB/TRAF1/TRAF5/TRPC4/TRPC6/TPR2/M2/PHLDA2/TWIST1/CCR2/TNFRSF4/UCLP1/UPP1/VARS/WNT10B/YWHAG/ZA P70/ZNF7/CAT/CACNA1E/PTP4A1/CACNB2/MOG5/PAX8/CXCR4/IT2D5/RAB7A/CARD14/PDPDF/GDPD3/BCL2L14/LST1/CERS4/TFMEM204/NLRX1/CSPP1/EPHX3/CALD1/FAM188A/G</p>							

GO:0044763	single-organism cellular process	715/901	111314/17046	8.64E-19	1.29E-15	1.01E-15	<p>AKT3/ABI1/CDH3/ITANK/GNE/CDH9/TSAN5/CDH13/FARP1/KLIRG1/RCAN2/KCNMB2/CDKN1C/SPEG/BCDK6/TCIRG1/MRV11/TRDN/ABCA9/SPON2/CLD/ZBTB18/TACC2/MT/HFS/PDPN/CELF1/TBR1/SEPT5/GIB6/HGST/NPFR2/ADCY3/TMED10/SLC27A2/LECT1/REB1/ESM1/HIBADH/CHGA/CHL1/ERLIN2/PKP3/EGLN2/B4GALT7/PTH2/KIF12/ACOT7/PDA/PI/EXOC3/CHRNA1/CHRNA2/CHRNA3/CARD16/GRIN1/SORCS1/CIDEA/PANK3/GALNT15/AP33/CLCA1/CNLS/ANKRD9/MRR52/FRMD6/CCR1/SLC15B/CL150H2/SLC38A10/SE26/TNFAP81/CNIP/APOAI1BP/NEU4/CO19A3/CO11A1/COMP/SCLT1/MAP3K8/ZP42/ADM/IL13RA/EGFLAM1/HUS1B/INDUFA6/PXND/CRABP1/TRPM6/MI2B/PAR4/MPP7/FAM101A/B3GLCT/MGAT5B/APCDD1/CSTA/KLC3/CTGF/ABCC13/SMYD1/SGOL1/PPM1L/SH3D19/CYB561/CYLD/MBOAT1/ADRB3/FESCO2/CYP11A1/FTTM1/ADAL/TRPV3/D/DB1/WBP2/NLDDOST/RNF168/BHLHA15/COCH/NLRP6/DLIG2/DNMT1/DNMT3A/ABAT/DPH1/DRD4/DSG3/DTNA/AGK7/EEF2/EFNA2/EGFR/EGFR3/EIF4G1/A2M/ELK4/TMEM17/EMIL1/UNC13D/DNAH12/SLC10A4/ENO2/EPHA1/EPHA3/EPHA4/ESR1/ALAS1/FAH/FAT2/SPATA13/FCGR2A/PHACTR1/FGA/FGF10/FHT/KNR2/RASA3/PPM1E/VASH1/STBD3/SBNO2/TRAK1/MSRB2/ACIN1/LIMCH1/FOXK1/FOXK2/FOXO1/EXPH5/AKR1B1/SPG20/NFASC/EPH413/FLNB/DIP2A/FLRT2/RHOB1B2/NUP210/ATP11A/NEDD4L/SYNE1/PSD3/LARP1/PPP1R13B/PUM2/ARHGEF18/RYBP/MORC3/MAK8IP2/TSSX2/MTOR/SLC37A4/GABBR1/RA5GF1C/RNF144B/ST6GALNAC3/GAK/SAMM50/DFNB31/ALS2CL/PN/KD/TENM4/ACOT11/RGS22/STEAP2/GAS2/FBXO2/LCE2B/GATM/GBGT1/GAPDH5/PILEK2/SLC17A5/ADGRF1/RPS6K1/PABPC1/GJA3/FGF22/NPTN/GIB2/CLUL1/AMPD2/SDCBP2/P/DE7B/DKX3/CTTH4/SL32/VPS4A/AMPD3/GPR162/BMP10/GNAS/PIGW/ZUW01/THYM5/GPR26/GPER1/EOGT/FFAR2/GRB10/MRPS18B/FLVCR1/GRK4/DNAIC15/SCG3/GSTP1/TM/Od4/GUCY1A3/NME7/GPR132/PAD1/GZMA/ANXA2/HAS1/SOX8/KCNIP2/NRG1/ANXA6/HKI1/HLA-B/HLA-DOA/HLA-DPA1/ANXA13/HLA-E/HLA-F/HIX/HMG1A1/NRA41/ACACB/HPCA/APBA2/HOXB3/HOXD3/HRH1/ACAD1/HSPAL1/HSP90AA1/HSP90AB1/HTR3A/HTR5A/D3/ZC3H12D/COL28A1/RSP02/FMN1/BARHL2/NMES9/GF1/GF2/CYR61/GPR142/LCE1C/LCE1D/LCE2D/LIL1/LIL1R1/LIL1R2/LIL1R3/LIL1R4/AQP2/LIL1R1/LIL1R2/LIL1R3/LIL1R4/LIL1R5/LIL1R6/FOXK2/AQP9/NHBA/INPP5A/IRF1/AQP9/ISL1/ITGA7/ITGB2/ITGB7/IV/LJUP/CD82/USP50/HLS1/ATP9B/KCNH2/KCN8/KCN9/KCNMB1/KDR/ACAT1/KIF25/KRT15/AMIGO3/IN5C/HESS/SLC6A17/LAMA3/STMN1/ORA5/LCK/LCP1/MUC21/LDLR/ARHG/DIA/LGALS9/LHCGR/LGL1/LMNA/RAB19/LOX/ITIB1/ITBP1/SMAD3/MC2R/MCC/MEL/MIEZ/MIEZ2/MA3K1/MEOX1/MEOX2/MEF2/MFNG/MGAT1/SCGB2A1/NITF/LHX8/ASGR1/M/OV10/MPZ/PLEKHG7/NUDT1/AMYH4/MYK2/NUBP1/NDUFBA/NEDD9/NEU1/ATP1A2/NFATC3/NHLH2/NM1B/NOV/NPPC/NRAS/NTF3/OAS2/OPRL1/GRZC1/ORA32/SLC22A18/P2RY/AM2/PIGC/PK3CG/PTX2/PKH1/PKM/PLA2G2A/PLA2G1/SPA17/PLEC/PRKAG3/PML/FOXO6/GPR84/IL20RB/SLCO1C1/PNUP/TL09/TREM1/CYTL1/POMC/SSH1/PONI/RIN2/MOV10/LI/ZDHHC13/APBB1P/ROBO4/MXRAB/FBLIM1/PALMD/CYP2W1/LPCAT2/BANP/PPP1CB/HERC6/PPP1CC/PIWIL2/ELP3/ARHGFE10/PRMT6/GOLPH3/PPP2R2B/FANCI/MOB1A/SL/ACT1/PAG1/CISD1/PRKD1/WSB2/BIN3/APOB/APK3/MAK2K2/PRKRIR/PROC/MRAP/TRPV5/PRMT8/HTRA1/SLANMF8/CDC42SE1/PSMB4/PAK6/RGMA/TRPC7/UPA5/PSMD7/SLU/RP1/ACTR3B/PTGFR/PLEKHG5/TENM2/ERMIN/RDH14/MARK4/CCAR2/PTPRE/PXN/AM60A/ACTA2/RA5GRF2/REF2/TRIM27/AGS12/RTT2/EXOC4/RP3/RPL8/RPL29/S100A4/S/100A6/BGLAP/SCT/CCL11/CCL17/MRPS14/PARG/NOD2/STRA6/SFRP2/CXGR5/ARHGAP9/DNA2/SGK1/MICAL1/CERK/TMEM237/VPS33A/BMP4/SLC4A1/SLC6A12/SLC8A1/SLC9A/3/SLC20A2/BMP1B/SLIT1/BOK/SOX9/BPI/SRP68/STAT2/STK10/SUPT6H/STZ/VAMP2/TA48/7BP/TCAL1/ZEB1/ACTL1/TEAD3/TERF1/TGM2/TCHH/TL5/TLR5/TRAPP10/T/NEAIP3/TNFRSF1A/TNFB/TRAF1/TRAF5/TRPC4/TRPC6/TRPM2/PHLDA2/TWIST1/CCR2/TNFRSF4/UCP1/UPP1/VARS/WNT10B/YWHAF7/AP70/CA7/CACNAIE/PTP4A1/FAAP100/CPEB4/C6orf25/GS/PAX8/CXCR4/FZD5/RAB7A/CARD14/PPDPF/BCL2L14/LST1/CERS4/TMEM204/NLRX1/CSPP1/EPH3/CA1D1/FAM188A/GPR157/ZC3H12A/RAB11/FIP1/FAAP100/CPEB4/C6orf25/COL8A1/EEPD1/CUPTM1L/CALR/COL21A1/UNC93B1/QTRT1/SURP/CNPS/COLO/CAS7/CAP2B/SBHBGR13/SRXT1/HIST1H3A/DYNL1RB2/SLC25A18/SPATA16/ANTXR1/SLA2/MFSD7/C/MAHP/BESP2/ATP13A4/NR0B2/MON1A/CASQ1/HOPX/PARD6G/PARD6B/TBK1/IL1F10/TRIM63/KDM2B/LOXL3/MGAR/CBX2/RAE1/SLC43A1/IFTM1/GAS7/SCIN/CDK10/KMO/R</p>
------------	----------------------------------	---------	--------------	----------	----------	----------	---

GO:0065007	biological regulation	666/901	10343/17046	6.62E-18	7.89E-15	6.21E-15	666
<p>AKT3/ABI1/CDH3/ITANK/ZNF783/TSPAN5/CDH13/MBNL2/FARP1/KLRG1/RCAZC/SPEC7/TCIRG1/MRV1/ITRON/SUNPT2/CID/ZBTB18/PTTRM1/TACC2/PDPN/DMRT2/CELE1/CELE2/TBRI1/GBB6/HCS1/NPFPR2/ADCY3/PNRC1/TMED10/LECT1/REER1/ESM1/HNRNPUL1/CHGA/CHH3L1/EBLN2/PSIP1/EGUN2/ATXN2L/B4GALT7/PTH4/PDAP1/CHRNA1/CHRNA2/CHRNA3/CARD16/SORCS1/ZBED9/GIDEA/A/P351/CLNS1/ANKRD9/FRMO6/CR1/SLC51B/C15orf27/ZG16B/SEZ6/TNFAIP8L1/CNP/COMP/MAP3K8/ZFP42/ADM/IL31RA/VEGFLAM/HUS1B/ORZ2A14/CP51/CRBP1/ZNF358/MB2/MPT7/LD/RAD3/FAM101A/APCD1/CSTA/ZNF738/CTGF/SMDY1/SGOL1/SHD19/CYLD/ADR83/ESCO2/CYP11A1/ZNF781/2/FITM1/TRPV3/ZNF709/ZNF781/CTTED4/DOB1/RNF168/ZNF366/BHLHA15/COCH/NLRP6/DIO3/DL62/DMBT1/DNMT3A/ABAT/DRDA4/DNMA/ECE1/AGXT/EEF2/EFNA2/EGFR/EGR3/PATL2/EIF4G1/JAZM/ELK4/TMEM17/LUNC13D/EPHA1/EPHA3/EPHA4/ESR1/FIT1/SPATA13/FCGR2A/PHACTR1/SP8/FGA/FGF10/FHIT/XRND2/RASA3/PPM1E/VASH1/SBN02/TRAK1/MSRB2/ACIN1/FOXO1/FOXO2/TBCL1/D9B/FOXO1/EXPH5/AKR1B1/SPG20/EPB41L3/GGA3/FLNB/DIP2A/LOTT2/MLC1/TBCL1/D1/RHOBTB2/NUP210/ATP11A/NEDD4L/SYNE1/PSD3/LARP1/PPP1R13B/PUUM2/ARHGFE18/RYB9/MORC3/MAPK8IP2/TSSK2/VGLL2/MTOR/SIC37A4/GABBR1/RA5GEF1/CRNF144B/ZNF549/DHNB31/ALS2C/PNKD/TENM4/ACOT11/RGS22/STEAP2/GAS2/FBXL21/FBXO2/SACS/GAPDH5/PLEK2/ADGRF1/RP56K1/PABPC1/DNAUC2/JFGF2/NPTN/AMPD2/SDCBP2/PDE7B/DK3/CYTH4/GLS2/VPS4A/AMPD3/GPR162/BMP10/ZNF638/GNAS/ZNF311/CRACR2B/ZNF844/GPR26/GPER1/DOK7/FFAR2/GRB10/FLVCR1/GRK4/ZBTB44/DNAIC15/SCG3/GSTP1/GTF2B/BRF1/TMOD4/GUCY1A3/NME7/GPR132/GZM1/ANXA2/HAS1/SERPIND1/SOX8/KCNIP2/NRG1/ANXA9/HKI1/HLA-B/HLA-DQA1/ANXA13/HLA-E/HLA-F/HLX/HMGAI1/NRA41/ACACB/APBAZ/HOXB3/HOXC4/HOXC5/HOXC6/HOXD3/AGFGZ/HRH1/ACAUI/HSPA11/HSP90AA1/HSP90AB1/HTR3A/HTR5A/TFAP2E/ID3/ZC3H12D/COL28A1/RSPO2/FMN1/BAH12/ANNE9/IGF1/IGF2/CYR61/GPR142/IL1R1/IL1RN/IL6/IL10RA/AQP2/IL11RA/IL12RB2/IL15RA/IL16/FOXK2/AOPS/STMN1/ORA5/LCK/LCP1/IDL/ARHGDI4/LGAL/S9/LHCGR/LGLL1/LVMA/LMO2/RAB19/LTB1/TBP1/SMAD3/MC2R/MCC/ME1/ME2/MEF2D/MAP3K1/MEOX1/MEOX2/MF2/MFNG/SCGB2A1/MITF/HX8/MOV10/MIP2/PLEKHG7/MIT1A/MYL2/NUBP1/NEDD9/NEU1/ATP1A2/NEFAT3/NFYB/NHLH2/NMBR/NOV/NPPC/NRAS/NTF3/OAS2/OPRL1/OR2C1/ORA2/P2RY6/PAFAH2/ATP5B/IL21R/ANO7/PALM/ARHG EF3/PARK2/SPOCK3/UTP11/LEF1/DDX47/CEPND1/PRR16/ANGPT4/PD54C/PDE7A/C11orf73/SIR16/PDE6B/TP8A2/PGAM2/P13/P13K3/CG/PITX2/PKHD1/PLA2G2A/PLAGL1/PRKAG3/CB/PPP1CC/PWIL2/EIP3/ARHGFE10/PRMT6/DNAIC17/GOLPH3/ZNF532/PPP2R2B/PANCI/MOBI1/TRPV6/SMPD3/SLC30A10/CNOT11/CHRNA9/SYBU/LIMS2/VACL14/PARVA/PRK AR1B/IFT122/MCTP2/LMBRD1/PAG1/CISD1/PRKD1/WSB2/MYNN/BN3/MAPK3/MAP2K2/PRKRIR/PROCMRAP/PRMT8/MASP1/HTRA1/SLAMF8/CDC42SE1/PSMB4/PAK6/ARNTL2/RGMA/PRDM11/TRPC7/LPAR5/PSMD7/SLURP1/ACTR3B/PTGFR/PLEKHG5/TENM2/GATAD2B/ERMN/RD14/METTL14/MARK4/CCAR2/PTPRE/PXN/CREBZF/FAM60A/ACTA2/RA5G RF2/RFC2/TRIM27/RGR/RGS12/RIT2/RPA3/S100A4/S100A6/BGLAP/SCY/CCL11/CCL17/ABHD4/NPAS3/NOD2/STRA6/SFRP2/CXCR5/ARHGAP9/TRA2B/GZF1/SGK1/MICALL1/TMEM2 37/NPS33A/BMP4/SLC4A1/ZNF649/SLC8A1/SLC9A3/BMPRI1B/SLIT1/BRD9/ZSCAN18/BOK/SOX9/BPI/STAT2/STK310/SUPT16H/BST2/NAMP2/TAF4B/TBP/TCEA1/TCFB2 /ZEB1/ACTC1/TEAD3/TEF1/TGM2/TIMP3/TLF3/TLR5/TNFAIP3/TNFRSF1A/TNXP1/TRAFF5/TRPC4/PHLDA2/TWIST1/CCR2/TNFRSF4/UCP1/VARS/WNT10B/VWHAG/ZA P70/ZNF7/CA7/ZNF124/ZNF177/CACNA1E/PTPA41/CACNB2/PAX8/CXCR4/FZD5/RA7/CAKD14/BCL2L14/LST1/TMEM204/NLRX1/ZNF665/CSPP1/ZC3H14/GPR157/ZNF606/ZC3H 12A/RAB11FIP1/CPEB4/C6orf25/COL18A1/ZNF436/CALR/UNC93B1/SUR1/CA2P2/SH3BGRL3/SCRT1/HIST1H3A/ZNF1344/ZNF397/RORB /CASQ1/HOPX/PARD6B/TTBK1/IL1F10/S/PINK1/TRIM63/KDM2B/LOXL3/MGARP/CBX2/RAE1/FITM1/GAS7/SCIN/CDK10/RUNX1/TP63/RUNX3/SERPINA6/IRS2/ACTN1/CRADD/FAOD /TNFRSF11A/ALDH1A2/SPHK1/BUDD31/CCNA1/SKAP2/LIMD1/TSPAN18/CCR2/IER1/PRC1/STARD13/PIAS2/ZFAND2A/MAP3K6/SYTT1/DB2/ESAM/SLC16A3/CBFAZT2/RSAD2/SMDT 1/AURKB/DAPL1/CD8A/REEP6/TRIP10/ADIPOQ/ARHGAP29/LY86/RAB3D/H2AFY/SMAD5-</p>							

GO:0050789	regulation of biological process	636/901	9837/17046	1.71E-16	1.70E-13	1.33E-13	<p>AKT3/ABI1/CDH3/ITANK/ZNF783/TSPAN5/CDH13/MBNL2/FARP1/KLRG1/RCAN2/KCNMB2/CDKN1C/SPEG/TCIRG1/MRV1/ITRON/SPON2/CID/ZBTB18/PTTRM1/TACC2/PDPV/DMRT2/CELF1/CELF2/TBR1/GBB6/HCS1/NPFPR2/ADCY3/PNRC1/TMED10/LECT1/REER1/ESM1/HNRNPUL1/CHGA/CH13L/EBLN2/PSIP1/EGUN2/ATXN2L/BAGALIT7/PTH2/PDPAPI/CHRNA1/CHRNA2/CHRNA3/CARD16/SORCS1/ZBED9/GDEA/A/P31/ANKRD9/FRMD6/CCR1/US1C5/1B/SEZ6/TNFAIP38/ZFP42/ADM/IL13RA/EGFLAM/HUS1B/ORA2L4/CP51/C/RABP1/ZNF358/MB2/MPP7/LDIRAD3/FAM101A/APCDD1/CSTA/ZNF738/CTGF/SMDY1/SH3D19/CYLD/ADR83/ESCO2/ZNF709/ZNF781/CTE/D4/DBB1/RNF168/ZNF366/BHLHA13/COCH/NLRP6/DIO3/DLGG2/DMBT1/DNMT3A/ABAT/DRD4/DNMT3A/ABAT/EEF2/EFNA2/EGFR/EGR3/PATL2/EF4G1/A2M/ELK4/TMEM17/U/NCL3D/EPHA1/EPHA3/EPHB4/ESR1/F11/SPATA13/FCGR2A/PHACTR1/SP81/SP82/FHIT/XRNB2/RASA3/PPM1E/ASH1/SBNOZ/TRAK1/MSRB2/ACIN1/FOXL1/FOXQ2/TBC1D9B/F/OXO1/EXPH5/AKR1B1/SPG20/EPBA1L3/GGA3/FLNB/DIP2A/FLDT2/MCL1/TBC1D1/RHOBTB2/NUP210/NEDD4/PSD3/LARP1/PPP1R13B/PUM2/ARHGFE18/RYPB/MORC3/MAP8BP2/TSSK2/VGLL2/NTOR1/SLC37A4/GABBR1/RASGEF1C/RNF144B/ZNF549/ALS2CL/PNKD/TENM4/ACOT11/RGS32/GAS3/FBXL21/FBXO2/SACS/GAPDH5/PLEK2/ADGRF1/RPS6K1/PA/BPC1/DNAJC2/FGF22/NFTN/SDCBP2/PDE7B/DK33/CYTH4/GLS2/NP54A/GPR162/BMP10/ZNF638/GNAS/ZNF311/CRACR2B/ZNF844/GPR26/GPER1/DOK7/FFAR2/GRB10/FLVCR1/GRIK4/ZBTB44/DNAJC15/GSTP1/GTF2B/BRE1/TM0D4/GUCY1A3/NME7/GPR132/GZMA/ANXA2/HAS1/SERPIND1/SOX8/KCNIP2/NRG1/ANXA6/HK1/HLA-B/HLA-D0A/HLA-DPA1/ANXA13/HLA-E/HLA-F/HLX/HMGAI1/NR4A1/ACACB/HPCA/APBAZ/HOXB3/HOXC5/HOXC6/HOXD3/AGFG2/HRH1/ACAD/HSPA11/HSP90AA1/HSP90AB1/HTR3A/HTR5A/TFAP2E/ID3/ZC3H12D/C/OI28A1/BSPO2/FMN1/BARHL2/NME9/IGF1/IGF2/CYR61/GPR142/IL1R1/IL1RN/IL6/IL10RA/IL11RA/IL12RB2/IL15RA/IL16/FOXK2/INHBA/RF1/ISL1/ITGA7/ITGB2/ITGB7/ITIH3/ITIH4/IJUP/CD82/USP50/HLS1/KCNH2/KCNJ8/KCNJ9/KDR/KIF25/IPDS/AMIGO3/HESS/AFF3/LAMA3/STWN1/ORA2S/LCK/LCP1/LDIR/ARHGDA/LGAL59/LHCGR/LGL1/LMNA/LMO2/RAB19/LTB/LTBP1/SMAD3/MC2R/MCC/ME1/ME2/MEF2D/MAP3K1/MEOX1/MEOX2/MF2/MFNG/SCGB2A1/MITF/HX8/MOV10/MP2/PLEKHG7/MT1A/MYL2/NUBP1/NEDD9/NEU1/A/TP1A2/NEATC3/NFYB/NHLH2/NMBR/NOV/NPPC/NRAS/NTE3/OAS2/OPRL1/ORB2C1/ORB3A2/P2R/6/PAFAH2/ATP5B/IL21R/PALM/ARHGEF3/PARK2/SPOCK3/UTP1L1/LEF1/DDX47/C/END1/PRR16/ANGPT4/PDE4C/PDE7A/CL10/T73/SIRT6/PDE6B/ATP8A2/PGAM2/P13/PK3GG/PTX2/PKH01/PLA2G2A/PLAGL1/PKAG3/PML/RIIP1/Y3/FXYD6/GPR84/IL20RB/PNLP/RIK4/TLR9/TREM1/CYTL1/POMC/SSH1/PON1/RIN2/POU2AF1/ZDPHC13/APBB1P/ROBO4/FBLN1/BNC2/MED18/PALMD/BANP/PPP1CB/PPP1CC/PWIL2/ELP3/ARHGFE10/PRM16/DNAJC17/GOLPH3/ZNF532/PPP2R2B/FANCI/MOBLA/TRPV6/SMPP3/SLC30A10/CNOT11/CHRNA9/SYBU/LIMS2/VAC14/PARVA/PRKAR1B/IFT122/MCTP2/LMBRD1/PAG1/CSD1/PRKDI/WSB2/MYNN1/BIN3/MAPK3/MAP2K2/PRKRIR/PROC/MRAP/PRMT8/MASP1/HTRAI/SLAMF8/CD42E1/PSMB4/PAK6/ARNTL2/RGMA/PRDM11/LPAR5/PSMD7/SLURP1/A/CTR3B/PTGFR/PLEKHG5/TEEN2/GATAD2B/ERMN/METTL4/MARK4/CCAR2/PTPRE/PKN/CREZF/FAM60A/ACTA2/RASGRF2/TRIM27/RGR/RGS12/RTZ/PPA3/S100A4/S100A6/BGL/AP/5CT/CCL11/CCL17/NPAS3/NOD2/STRA6/SFRP2/CXCR5/ARHGAP9/TRAZB/GZF1/SGK1/MICAL1/TMEM237/VP33A/BMP4/ZNF649/SLC8A1/SLC9A3/BMIPR1B/SLIT1/BRD9/ZSCAN18/BOK/SOX9/BPI/STAT2/STK3/STK10/SUPT/BS12/VAAMP2/TAFA4/TBP/TCCEA1/TEAD3/TERF1/TGM2/TMP3/TLR5/TNFAIP3/TFEB/TNFRSF1A/TNMB/TRA1/T/RAF5/TRPC6/PHLDA2/TWIST1/CCR2/TNFRSF4/UCP1/VAARS/WNT10B/YWHAG/ZAP70/ZNF7/CA7/ZNF124/ZNF177/CACNA1E/PTP4A1/CACNB2/PAX8/CXCR4/FZD5/RAB7A/CARD14/BCL2L4/LST1/TMEM204/NLRX1/ZNF665/CSPP1/ZC3H14/GPRI57/ZNF606/ZC3H12A/RAB11FIP1/CPBE4/C6orf25/COL18A1/ZNF436/CALR/UNC93B1/SLIRP/CNPS/COLQ/CAS7/CAP2/B/SH3BGRL3/SCRT1/HIST1H3A/ANTXR1/SLAZ/CMAHP/ZNF397/NR0B2/CASQ1/HOPX/PARD6B/TTBK1/LIF1/LIF2/SPINK7/TRIM65/KDM2B/LOX3/MGARP/CBX2/RAE1/HITM1/GAS7/S/CIN/CDK10/RUNX1/TP63/RUNX3/SERPINA6/RS2/ACTN1/CRADD/FADD/TNFRSF11A/ALDH1A2/SPHK1/BDJ31/CCNA1/SKAP2/LIMD1/TSPAN18/CCR12/ERI1/PRC1/STAR13/PIAS2/ZFAND2A/MAP3K6/SYTY1/LDB2/CBFA2T2/RSAD2/AURKB/DAPL1/CD8A/REEP6/TRIP10/ADIPOQ/ARHGAP29/LV86/RAB3D/H2AF1/SMAD5-ZFAND2A/MAP3K6/SYTY1/LDB2/CBFA2T2/RSAD2/AURKB/DAPL1/CD8A/REEP6/TRIP10/ADIPOQ/ARHGAP29/LV86/RAB3D/H2AF1/SMAD5-AS1/RAB36/ARHGFE10/MICAL2/N4BP1/VGLL4/NUP93/RAPGEF2/ULK2/USP6NL1/CD79A/ZBTB39/TELO2/RABGAP1/JOSEC1/FGF19/NR1H4</p>
------------	----------------------------------	---------	------------	----------	----------	----------	--

GO:0044707	single- multicellular organism process	419/901	6214/17046	1.36E-10	5.78E-08	4.55E-08	<p>AB11/CDH3/CDH13/FAF1/RCAN2/CKNKB2/CDKN1C/SPEG/MRV11/TRDN/SPON2/ZBTB18/TACC2/PDPN/DMRT2/CELF1/CELF2/TBR1/GIB6/ADCY3/TMED10/LECT1/ESM1/CHGA/C/HL31/CHRNA3/CHRNA2/CHRNA5/GPRIN1/CIDEA/FAT3/CLN5/CCR1/ZG16B/SLC38A10/SEZ6/CNP/COL9A3/COL11A1/COM9/SC11/ZHP42/ADM/IL13/IRA/OR2A14/CP51/CRABP1/ZNF358/CRYBB3/FAM103A/AFPCDD1/CSTA/CTGF/SMDY1/CYLD/ADRB3/ESCCO2/CY11A1/TRPV3/RNF168/COCH/NRP6/DIO3/DLIG2/DMBT1/DNMT3A/ABAT/DRD4/DTNA/EEF1/EFNA2/EGFR/EGR3/EIF4G1/A2M/EMIL1/EPHA3/EPH4/ESR1/F11/FAT2/SP8/FGF10/RASA3/SBNO2/ACIN1/FOXO2/FOXO1/EXPH5/AKR1B1/SPG2/O/NFASC/EPB4113/FLNB/DIP2A/NEEDD4L/PSD3/RYPB/MORC3/NAK8/P2/SSK2/VGLL2/MTOR/DFNB31/PNKD/TENM4/LCE2B/GATM/GU93/FGF22/NPTN/GIB2/AMPD2/SDCBP2/DK3/VPS4A/AMPD3/BMP10/GNAS/GPDR1/FLVCR1/SCG3/GSTP1/TMOD4/GUCY1A3/NME7/HSPO90A1/HS90A81/HTR3A/HTR5A/ID3/RSP02/FMNI/BAHR12/I/ELX/NR4A1/JACACB/HPCA/APBA2/HOX4/HOX5/HOX6/HOX3/HRH1/HS1181/HS1782/ACAD1/HS90A1/HS90A81/HTR3A/HTR5A/ID3/RSP02/FMNI/BAHR12/I/GF1/GF2/CYR61/CE1C/CE1D/CE2D/IL1RN/IL6/AQP2/IL12RB2/AQP5/INHBA/IRF1/AQP9/ISL1/ITGA7/ITGB2/IVL/JUP/HLS1/KCNH2/KCN8/KCNMB1/KDR/ACAT1/AMIGO3/INSC/HES5/SLC6A7/RESPI8/AFF3/LAMA3/STMN1/ORZ5/LCK/LDLR/ARHGDI1A/GALS9/LHCGR/ILG1/IMNA/LMO2/LIT8/SBNO2/MC2R/MCC/MEF2D/MAP3K1/MEOX1/MEOX2/JM/FNG/MGAT1/MITF/HLX8/MYH4/MYL2/DRGL/NEU1/ATP1A2/NEFAT3/NHLH2/NOV/NPPC/NRAS/NTF3/OR3L1/OR3L2/SLC22A18/ATP5B/PALM/PARK2/UTP11L/LEF1/CEND1/ANGPT4/C11orf73/SIRT6/PDE6B/ATP8A2/PGAM2/PIK3CG/PTX2/PKHD1/PKM/PLA2G2A/PLAGL1/PML/RIPPL3/IL20RB/NPLUP/TLR9/TREM1/CYTL1/POMC/SSH1/MOV10L1/APBB1/IP/ROB4/MXRAB/BNC2/BANP/PPP1CB/HERC6/PPP1CC/HERP2/ELP3/SMPD3/CHRNA9/IRF52/PAFVA/PRKAR1B/IFT122/ERNAD4/MCTP2/CSGALNACT1/PRKD1/BIN3/MAPK3/MA/P2K2/PROC/HTRA1/PSMB4/RGMA/TRPC7/PSMD7/SLURP1/PIEKHG5/TEMN2/ERMN/RDH14/METT14/MARK4/PXN/ACTA2/RASGRF2/TRIM27/RGR/RPL29/S100A4/S100A6/BGLAP/SC7/CCL11/NPAS3/NOD2/STRA6/SRRP2/CXCR5/TRAB2/GZF1/DNAI2/SGK1/BNMP1B/SLIT1/BOK/SOX9/PIPI/STK3/SUPT6H/BSZT2/TCGA1/ZEB1/ACT1/TEAD3/TGM2/TCHH/TMP3/TLE3/TLR5/TNFAIP3/TNFRSF1A/TNXB/TRPC4/TRPC6/PLD2A2/TNFRSF4/TNFRSF4/WNT10B/YWHAG/ZAP70/ZNF7/CACNA1E/PTP4A1/CACNB2/PA/X8/CXCR4/FZD5/RAB7A/PPDPF/LST1/TMEM204/NLRX1/CALD1/ZC3H12A/RAB11B/P1/G6orf25/COL18A1/CALR/COLQ/CAST/CAP2B/SH3BGR1/SCRT1/HIST1H3A/SPATA16/BFSP2/N/R0B2/CASQ1/HOPX/PARD8B/TTBK1/TRIM63/KDM2B/LCX3/CBX2/IFTM1/GAS7/SCIN/RUNX1/TP63/RUNX3/IRS2/ACTN1/FADD/TNFRSF11A/ALDH1A2/SPHK1/STBD1/LIMD1/PIAS2/LDB2/ESAM/SLC16A3/CBFA2T2/RSAD2/AURKB/RCS1/CD8A/ADIPOQ/H2AFY/MTLS/ARHGFE10/MICAL2/RAPGEF2/ULK2/CD79A/FGF19</p>
GO:0048518	positive regulation of biological process	347/901	4960/17046	2.79E-10	1.11E-07	8.73E-08	<p>AB11/CDH3/TANK/TSPAN5/CDH13/FAF1/CDKN1C/CTRG1/TRDN/SPON2/PITRM1/PDPN/DMRT2/CELF1/TBR1/HCST/ADPCV3/REER1/ESM1/CHGA/CHI3L1/ERLIN2/PSI1/EGLN2/CIDEA/CCR1/SLC5B1/SEZ6/MAP3K8/ADM/IL13/RA/EGFLAM/CP51/MIB2/MPP7/CTGF/SMYD1/SH3D19/CYLD/ADR83/FTM1/TRPV3/CITEDA4/DBB1/RNF168/BHLHA15/COCH/NLRP6/DIO3/DMBT1/DNMT3A/ABAT/DRD4/EEF1/EEF2/EGFR/EGR3/EIF4G1/A2M/UNC13D/EPHA1/EPHA3/ESR1/F11/SPATA13/FCGR2A/FGA/FGF10/RASA3/PPM1E/SBNO2/ACIN1/FOXO2/TBC1D9/FOXO1/EXPH5/AKR1B1/SPG2/O/NFASC/EPB4113/FLNB/DIP2A/NEEDD4L/PSD3/RYPB/MORC3/NAK8/P2/SSK2/VGLL2/MTOR/DFNB31/PNKD/TENM4/LCE2B/GATM/GU93/FGF22/NPTN/GIB2/AMPD2/SDCBP2/DK3/VPS4A/AMPD3/BMP10/GNAS/GPDR1/FLVCR1/SCG3/GSTP1/TMOD4/GUCY1A3/NME7/HSPO90A1/HS90A81/HTR3A/HTR5A/ID3/RSP02/FMNI/BAHR12/I/ELX/NR4A1/JACACB/HPCA/APBA2/HOX4/HOX5/HOX6/HOX3/HRH1/HS1181/HS1782/ACAD1/HS90A1/HS90A81/HTR3A/HTR5A/ID3/RSP02/FMNI/BAHR12/I/GF1/GF2/CYR61/CE1C/CE1D/CE2D/IL1RN/IL6/AQP2/IL12RB2/AQP5/INHBA/IRF1/AQP9/ISL1/ITGA7/ITGB2/IVL/JUP/HLS1/KCNH2/KCN8/KCNMB1/KDR/ACAT1/AMIGO3/INSC/HES5/SLC6A7/RESPI8/AFF3/LAMA3/STMN1/ORZ5/LCK/LDLR/ARHGDI1A/GALS9/LHCGR/ILG1/IMNA/LMO2/LIT8/SBNO2/MC2R/MCC/MEF2D/MAP3K1/MEOX1/MEOX2/JM/FNG/MGAT1/MITF/HLX8/MYH4/MYL2/DRGL/NEU1/ATP1A2/NEFAT3/NHLH2/NOV/NPPC/NRAS/NTF3/OR3L1/OR3L2/SLC22A18/ATP5B/PALM/PARK2/UTP11L/LEF1/CEND1/ANGPT4/C11orf73/SIRT6/PDE6B/ATP8A2/PGAM2/PIK3CG/PTX2/PKHD1/PKM/PLA2G2A/PLAGL1/PML/RIPPL3/IL20RB/NPLUP/TLR9/TREM1/CYTL1/POMC/SSH1/MOV10L1/APBB1/IP/ROB4/MXRAB/BNC2/BANP/PPP1CB/HERC6/PPP1CC/HERP2/ELP3/SMPD3/CHRNA9/IRF52/PAFVA/PRKAR1B/IFT122/ERNAD4/MCTP2/CSGALNACT1/PRKD1/BIN3/MAPK3/MA/P2K2/PROC/HTRA1/PSMB4/RGMA/TRPC7/PSMD7/SLURP1/PIEKHG5/TEMN2/ERMN/RDH14/METT14/MARK4/PXN/ACTA2/RASGRF2/TRIM27/RGR/RPL29/S100A4/S100A6/BGLAP/SC7/CCL11/NPAS3/NOD2/STRA6/SRRP2/CXCR5/TRAB2/GZF1/DNAI2/SGK1/BNMP1B/SLIT1/BOK/SOX9/PIPI/STK3/SUPT6H/BSZT2/TCGA1/ZEB1/ACT1/TEAD3/TGM2/TCHH/TMP3/TLE3/TLR5/TNFAIP3/TNFRSF1A/TNXB/TRPC4/TRPC6/PLD2A2/TNFRSF4/TNFRSF4/WNT10B/YWHAG/ZAP70/ZNF7/CACNA1E/PTP4A1/CACNB2/PA/X8/CXCR4/FZD5/RAB7A/PPDPF/LST1/TMEM204/NLRX1/CALD1/ZC3H12A/RAB11B/P1/G6orf25/COL18A1/CALR/COLQ/CAST/CAP2B/SH3BGR1/SCRT1/HIST1H3A/SPATA16/BFSP2/N/R0B2/CASQ1/HOPX/PARD8B/TTBK1/TRIM63/KDM2B/LCX3/CBX2/IFTM1/GAS7/SCIN/RUNX1/TP63/RUNX3/IRS2/ACTN1/FADD/TNFRSF11A/ALDH1A2/SPHK1/STBD1/LIMD1/PIAS2/LDB2/ESAM/SLC16A3/CBFA2T2/RSAD2/AURKB/RCS1/CD8A/ADIPOQ/H2AFY/MTLS/ARHGFE10/MICAL2/RAPGEF2/ULK2/CD79A/FGF19</p>
GO:0048731	system development	292/901	4014/17046	3.05E-10	1.14E-07	8.94E-08	<p>AB11/CDH3/CDH13/FAF1/RCAN2/CKNKB2/CDKN1C/SPEG/MRV11/TRDN/SPON2/ZBTB18/TACC2/PDPN/DMRT2/CELF1/CELF2/TBR1/GIB6/ADCY3/TMED10/LECT1/ESM1/CHGA/CHI3L1/ERLIN2/PSI1/EGLN2/CIDEA/CCR1/SLC5B1/SEZ6/MAP3K8/ADM/IL13/RA/EGFLAM/CP51/MIB2/MPP7/CTGF/SMYD1/SH3D19/CYLD/ADR83/FTM1/TRPV3/CITEDA4/DBB1/RNF168/BHLHA15/COCH/NLRP6/DIO3/DMBT1/DNMT3A/ABAT/DRD4/EEF1/EEF2/EGFR/EGR3/EIF4G1/A2M/UNC13D/EPHA1/EPHA3/ESR1/F11/SPATA13/FCGR2A/FGA/FGF10/RASA3/PPM1E/SBNO2/ACIN1/FOXO2/TBC1D9/FOXO1/EXPH5/AKR1B1/SPG2/O/NFASC/EPB4113/FLNB/DIP2A/NEEDD4L/PSD3/RYPB/MORC3/NAK8/P2/SSK2/VGLL2/MTOR/DFNB31/PNKD/TENM4/LCE2B/GATM/GU93/FGF22/NPTN/GIB2/AMPD2/SDCBP2/DK3/VPS4A/AMPD3/BMP10/GNAS/GPDR1/FLVCR1/SCG3/GSTP1/TMOD4/GUCY1A3/NME7/HSPO90A1/HS90A81/HTR3A/HTR5A/ID3/RSP02/FMNI/BAHR12/I/ELX/NR4A1/JACACB/HPCA/APBA2/HOX4/HOX5/HOX6/HOX3/HRH1/HS1181/HS1782/ACAD1/HS90A1/HS90A81/HTR3A/HTR5A/ID3/RSP02/FMNI/BAHR12/I/GF1/GF2/CYR61/CE1C/CE1D/CE2D/IL1RN/IL6/AQP2/IL12RB2/AQP5/INHBA/IRF1/AQP9/ISL1/ITGA7/ITGB2/IVL/JUP/HLS1/KCNH2/KCN8/KCNMB1/KDR/ACAT1/AMIGO3/INSC/HES5/SLC6A7/RESPI8/AFF3/LAMA3/STMN1/ORZ5/LCK/LDLR/ARHGDI1A/GALS9/LHCGR/ILG1/IMNA/LMO2/LIT8/SBNO2/MC2R/MCC/MEF2D/MAP3K1/MEOX1/MEOX2/JM/FNG/MGAT1/MITF/HLX8/MYH4/MYL2/DRGL/NEU1/ATP1A2/NEFAT3/NHLH2/NOV/NPPC/NRAS/NTF3/OR3L1/OR3L2/SLC22A18/ATP5B/PALM/PARK2/UTP11L/LEF1/CEND1/ANGPT4/C11orf73/SIRT6/PDE6B/ATP8A2/PGAM2/PIK3CG/PTX2/PKHD1/PKM/PLA2G2A/PLAGL1/PML/RIPPL3/IL20RB/NPLUP/TLR9/TREM1/CYTL1/POMC/SSH1/MOV10L1/APBB1/IP/ROB4/MXRAB/BNC2/BANP/PPP1CB/HERC6/PPP1CC/HERP2/ELP3/SMPD3/CHRNA9/IRF52/PAFVA/PRKAR1B/IFT122/ERNAD4/MCTP2/CSGALNACT1/PRKD1/BIN3/MAPK3/MA/P2K2/PROC/HTRA1/PSMB4/RGMA/TRPC7/PSMD7/SLURP1/PIEKHG5/TEMN2/ERMN/RDH14/METT14/MARK4/PXN/ACTA2/RASGRF2/TRIM27/RGR/RPL29/S100A4/S100A6/BGLAP/SC7/CCL11/NPAS3/NOD2/STRA6/SRRP2/CXCR5/TRAB2/GZF1/DNAI2/SGK1/BNMP1B/SLIT1/BOK/SOX9/PIPI/STK3/SUPT6H/BSZT2/TCGA1/ZEB1/ACT1/TEAD3/TGM2/TCHH/TMP3/TLE3/TLR5/TNFAIP3/TNFRSF1A/TNXB/TRPC4/TRPC6/PLD2A2/TNFRSF4/TNFRSF4/WNT10B/YWHAG/ZAP70/ZNF7/CACNA1E/PTP4A1/CACNB2/PA/X8/CXCR4/FZD5/RAB7A/PPDPF/LST1/TMEM204/NLRX1/CALD1/ZC3H12A/RAB11B/P1/G6orf25/COL18A1/CALR/COLQ/CAST/CAP2B/SH3BGR1/SCRT1/HIST1H3A/SPATA16/BFSP2/N/R0B2/CASQ1/HOPX/PARD8B/TTBK1/TRIM63/KDM2B/LCX3/CBX2/IFTM1/GAS7/SCIN/RUNX1/TP63/RUNX3/IRS2/ACTN1/FADD/TNFRSF11A/ALDH1A2/SPHK1/STBD1/LIMD1/PIAS2/LDB2/ESAM/SLC16A3/CBFA2T2/RSAD2/AURKB/RCS1/CD8A/ADIPOQ/H2AFY/MTLS/ARHGFE10/MICAL2/RAPGEF2/ULK2/CD79A/FGF19</p>

GO:0009653	anatomical structure morphogenesis	205/901	2579/17046	3.27E-10	1.15E-07	9.01E-08	AB11/CDH13/FARP1/CDKN1C/SPON2/PDPN/DWIRT2/TBR1/GIB6/LEP1/ESM1/CHB11/FRMD6/CNP/COL9A3/C111A1/COMP/S3121/ADM/CPM/ZNF358/FAM101A/CTGF/SH3D19/1/3/CYL0/COCH/ECC41/FENNA2/EGFR/EGR3/TMEM17/UINC13D/EPHA1/EPH3/EPH4/ESR1/SP8/FGA/FGF10/RASA3/VASH1/BTBD3/SBNO2/FOXO1/FOXK2/SBNO2/NFASC/EPB41/L3/FLNB/NEEDD4/ARHGAP18/ARHGAP23/TMEM14/GAS2/FGF22/DKK3/BMP10/GNAS/FLVCR1/TMOD4/ANXA2/SOX8/NRG1/HLX/NR4A1/HOBX3/HOXC4/HOXD3/HSP90AA1/HSP90A/B1/D3/RSP02/FMN1/BAH12/IGF1/IGF2/CYR61/IL1RN/IL6/FOXK2/AQP5/INHBA/ISL1/ITG7/ITGB2/ITGB7/KOR/HES5/AFF3/LAMA3/STMN1/ARHGDA/LGL1/SMAD3/MEF2D/MA/P3K1/MEOX1/MEOX2/MIF2/LHX8/MYL2/NFATC3/NOV/NPPC/NRAS/NTF3/ATP5B/PALM/PARK2/LEF1/CEND1/ANGPT4/SIRT6/ATP8A2/PK3CG/PTX2/PKH01/PML/RIK4/SSH1/RO/BO4/FBLIM1/BNC2/PALMD/CHRNA9/LIMS2/PAIVA/IJT122/CSGALNACT1/PKRD1/BN3/MAK3/MAP2K2/TRPC7/PSMD7/TENM2/ERMN/PXN/AC/TA2/RASGRF2/S100A4/S100A6/BLGAP/CCL11/STRA6/SFRP2/GZ1/DNAI2/SKG1/PS3A/BMP4/BMPR1B/SULT1/SOX9/STK3/ZEB1/ACT1/TGM2/TL3/TNFAIP3/TRPC4/TRPC6/PHLDA2/TWIST1/CCR2/WNT10B/CACNB2/PAX8/FZD5/ST1/ZC3H12A/C6orf25/COL18A1/CALR/SURP/CAS2/CAP2B/ANTXR1/CASQ1/HOPX/PARD6B/TBK1/KOM2B/L/OX3/GAS7/RUNX1/TP63/RUNX3/IRS2/ACTN1/ALDH1A2/SPHK3/LJM1D1/ADIPQO/MICAL2/RAPGEF2/ULK2/FGF19
GO:0006928	movement of cell or subcellular component	152/901	1789/17046	1.37E-09	4.55E-07	3.58E-07	AB11/CDH13/SPON2/PDPN/TBR1/ADCY3/CHGA/KIF12/AP3S1/FRMD6/CR1/COL9A3/APCDD1/KLK3/CTGF/DNAH6/DNAH8/FENNA2/EGFR/EGR3/DNAH12/EPHA1/EPH3/EPH4/PAT2/SPATA13/PHACTR1/FGF10/RASA3/VASH1/FOXK2/NFASC/GAPDH5/FGF22/BMP10/GPER1/JFAR2/NME17/HAS1/SOX8/NRG1/4MCL1/HRH1/HSP90AA1/HSP90A/1/YR61/IL1RN/IL6/IL15/ISL1/ITG7/ITGB2/ITGB7/JUP/KDR/KIF25/LAMA3/STMN1/LCK/LCP1/ARHGDA/LGALS9/LMYNA/SMAD3/ACR3/ARHGAP1/ARHGAP23/NOV/NRAS/NTF3/P2RY6/ATP5B/PALM/LEF1/CEND1/ANGPT4/PK3CG/PTX2/PKH01/SPA17/PML/TREM1/ROB04/ELP3/PARVA/IFT122/PRKD1/BN3/MAK3/MAP2K2/PROC/PSMB4/PAK6/RGMA/TRPC7/PSMD7/PLERKHS/TENM2/PAM60A/RASGRF2/CCL11/CCL17/NOD2/SFRP2/CXCR5/DNAI2/SKG1/BMP4/SLC8A1/BMPR1B/SULT1/SOX9/STK3/ZEB1/ACT1/TRPC4/TRPC6/PHLDA2/TWIST1/CCR2/WNT10B/CACNB2/PAX8/FZD5/ST1/ZC3H12A/C6orf25/COL18A1/CALR/SURP/CAS2/CAP2B/ANTXR1/CASQ1/HOPX/PARD6B/TBK1/KOM2B/L/OX3/GAS7/RUNX1/TP63/RUNX3/IRS2/ACTN1/ALDH1A2/SPHK3/LJM1D1/ADIPQO/MICAL2/RAPGEF2/ULK2/FGF19
GO:0048869	cellular developmental process	271/901	3716/17046	1.54E-09	4.84E-07	3.81E-07	AB11/CDH13/SPON2/ZBTB18/TACC2/PDPN/CELF1/TBR1/LECT1/GPRIN1/CLN5/FRM D6/CCR1/SEZ6/CNP/COL9A3/C111A1/SCLT1/ZFP42/ADM/IL13IRA/CP51/FAM101A/APCDD1/CSTA/CTGF/SMYD1/SH3D19/CYLD/ADR83/ESCO2/CYP11A1/BEH1/HA15/COCH/DNMT1/DNMT3A/EEF2/EFNA2/EGFR/EGR3/EIF4G1/A2M/ELK4/TMEM17/EMIL1/U/NC13D/EPHA1/EPH3/EPH4/ESR1/FGA/FGF10/RASA3/BTBD3/SBNO2/ACIN1/FOXO1/FOXK2/FOXO1/EXPH5/SPG20/NFASC/EPB41.13/FLNB/LOT2/NEEDD4/SYNE1/PSD3/ARHGAP18/MAK3/PI3K/PTX2/TSSK2/MTOR/DFNB31/TENM4/GAS2/LCE2B/GAPDH5/FGF22/NPTN/BNP10/GNAS/GPER1/FFAR2/FLVCR1/TMOD4/ANXA2/SOX8/KCNIP2/NRG1/HLA-B/HLA-D/A/ANXA13/HLX/NR4A1/HOBX3/HOXD3/HSP90AA1/HSP90A/1/D3/RSP02/FMN1/BAH12/IGF1/IGF2/CYR61/LCE1C/LCE1D/LCE2D/IL6/FOXK2/INHBA/IRF1/ISL1/ITG7/ITGB2/ITGB7/IVJ/JUP/PHL51/KDR/NSC/HES5/LAMA3/STMN1/LCK/ARHGDA/LGALS9/LGL1/LMNA/SMAD3/MEF2D/MAK3/MEOX1/MIF2/MITF/LHX8/MYL2/NEU1/NFATC3/NHLH2/NOV/NPPC/NRAS/NTF3/ATP5B/PALM/PARK2/LEF1/CEND1/SIRT6/PTX2/PKH01/PLA2G2A/PLA2G1/SSH1/SSH1/MOVI01/ROB04/MKRN8/FBLIM1/PALMD/HERC6/PPP1C/PIWIL2/ELP3/SMPD3/PAIVA/IJT122/PRKD1/BN3/MAK3/MAP2K2/IRAP/HTRAI/CDCA25E1/PSMB4/RGMA/TRPC7/TENM2/ERMN/RDH14/PXN/AZ/RASGRF2/S100A4/S100A6/BLGAP/CCL11/CCL17/SFRP2/DNAI2/SKG1/TMEM237/NP53A/BMP4/SLC8A1/BMPR1B/SULT1/BOV/SOX9/STK3/SUPT6H/TA4B4/CEA1/ZEB1/ACT1/TEAD3/TCHH/TNFRSF1A/TRPC4/TRPC6/TWIST1/UCP1/WNT10B/YWHAG/ZAP70/CACNB2/PAX8/CXCR4/FZD5/PDPDF/LST1/TMEM204/ZC3H12A/C6orf25/COL18A1/CALR/SURP/CAS2/CAP2B/SCR1/SPATA16/ANTXR1/BFSP2/CASQ1/HOPX/PARD6B/TBK1/LOXL3/CBX2/IFTM1/GAS7/SCIN/RUNX1/TP63/RUNX3/IRS2/ACTN1/FADD/TNFRSF11A/ALDH1A2/LJM1D1/ADIPQO/H2AFY/MTLS5/ARRHGEF10/RAPGEF2/ULK2/CD79A/FGF19
GO:0048513	organ development	218/901	2848/17046	2.23E-09	6.63E-07	5.21E-07	AB11/CDH13/CDKN1C/SPEG/ZBTB18/TACC2/PDPN/TBR1/GIB6/TMED10/LECT1/CHB11/CHRNA1/CLN5/CCR1/SLC38A10/SEZ6/CNP/COL9A3/C111A1/COMP/ZFP42/ADM/IL13IRA/CPS1/PS1/FAM101A/APCDD1/CSTA/CTGF/SMYD1/CYLD/ESCO2/CYP11A1/DRD4/ECE1/EEF2/EFNA2/EGFR/EGR3/EMIL1/EPH3/EPH4/ESR1/FGA/FGF10/8BTBD3/SBNO2/ACIN1/FOXO1/FOXK2/FOXO1/EXPH5/ARRB1/SPG20/FLNB/MLC1/NUP210/N/DOA/HLX/ACAC8/HPCA/HOXB3/HOXCA/HOXD3/HSD11B1/HSD17B2/HSP90AA1/HTR5A/D3/RSP02/FMN1/BAH12/IGF1/IGF2/CYR61/LCE1C/LCE1D/LCE2D/IL6/AQP2/AQP5/INHBA/IRF1/ISL1/ITG7/ITGB7/IVJ/JUP/KCNJ8/KDR/ACAT1/AMIGO3/NSC/HES5/LCGA1/STMN1/LCK/LGALS9/UHCGR/UMNA/LMO2/LOX1/TB/SMAD3/MC2R/MEF2D/MAK3/MEOX1/MEOX2/MITF/LHX8/MYL2/NFATC3/NOV/NPPC/NRAS/NTF3/LEF1/CEND1/C11orf73/SIRT6/PDE6B/ATP8A2/PTX2/PKH01/PKM/PLAGL1/PML/RIPLV3/CYTL1/BNC2/HERC6/SMPD3/CHRNA9/LIMS2/PAIVA/IJT122/CSGALNACT1/BN3/MAK3/MAP2K2/HTRAI/ACTA2/S100A4/BGLAP/SCC1/CC11/STRA6/SFRP2/TRA2B/GZF1/VPS33A/BMP4/SLC8A1/BMPR1B/SULT1/BOV/SOX9/STK3/ZEB1/ACT1/TGM2/TCHH/TLR5/TLR6/TLR9/TLR10B/SFRP2/C6orf25/COL18A1/CALR/CAS2/BFSP2/NR0B2/CA/SQ1/HOPX/TTBK1/KOM2B/LOXL3/SCIN/RUNX1/TP63/RUNX3/IRS2/ACTN1/FADD/TNFRSF11A/ALDH1A2/SPHK3/LJM1D1/ADIPQO/H2AFY/MTLS5/ARRHGEF10/RAPGEF2/ULK2/CD79A/FGF19
GO:0010033	response to organic substance	207/901	2687/17046	3.90E-09	1.04E-06	8.19E-07	CDH13/CDKN1C/TOR1A1/SPON2/GIB6/NPFRF2/ADCY3/TMED10/LECT1/CHB11/CHRNA1/CHRNA2/CHRNA5/CIDEA/AFPS1/CCR1/CNP/ADM/IL13IRA/CP51/CTGF/CYP11A1/CI/TED4/DOO57/ZNF366/HLH1A15/DNMT3A/ABAT1/DRO4/AGXT/EGFR/EGR3/EIF4G1/EPH3/ESR1/FGA/FGF10/RASA3/SBNO2/FOXO1/ARRB1/SPG20/FLNB/MLC1/NUP210/N/EDD4/ARHGAP18/MTOR/STAP2/FBXO2/GATM/FGF22/NPTN/GIB2/BMP10/GNAS/GPER1/FFAR2/BMP10/GSTP1/GUCY1A3/HAS1/NRGI1/HLA-B/HLA-DPA1/HLA-E/HLA-F/NR4A1/HPCA/HRH1/HSD17B2/HSPAL1/HSP90AA1/HSP90A/1/HTR3A/HTR5A/IGF2/CYR61/IL1R1/IL1RL1/IL6/LOR4/IL11R/IL12RB2/IL15RA/INHBA/IRF1/AQP9/ISL1/ITIH4/JUP/KCNJ8/KDR/ACAT1/IPO5/HES5/AFF3/LCK/ARHGDA/LGALS9/LHCGR/UMNA/LMO2/LOX1/TB/PTN/SMAD3/MEI/MAK3/MEI/MOVI10/ATP1A2/NPPC/NRAS/OAS2/OPRL1/P2RY6/IL12R/ARHGAP3/PARK2/LEF1/PIK3CG/PTX2/PKM/PRKAG3/PML/IL20RB/TLR9/SSH1/POU1/PPP1CB/PPP1CC/CHRNA9/SYBU/PRKAR1B/IL1MBRD1/PRKD1/MAK3/MAP2K2/HTRAI/PSMBA/RGMA/PSMD7/P/IGFR/PLERKHS/PTPRE/PXN/RASGRF2/IRIT2/BGLAP/CCL11/CCL17/NOD2/SFRP2/CXCR5/BMP4/SLC8A1/SLC9A3/8MPR1B/SOX9/STAT2/BST2/VAMP2/ZEB1/ACT1/TIMP3/TLR5/TNFAIP3/TNFRSF11A/TWIST1/CCR2/TNFRSF4/WNT10B/CACNA1E/PAK8/FZD5/RAB7A/CACNA1E/TMEM204/ZC3H12A/CEB4/CALR/NR0B2/CASQ1/IL1F10/TRIM63/IMGAR2/BAE1/JIFTM1/RUNX1/RUNX3/IRS2/FADD/TNFRSF11A/ALDH1A2/SPHK3/HSPB1/ARRHGEF2/FGF19/NR1H4

GO:0044700	single organism signaling	378/901	5624/17046	4.74E-09	1.13E-06	8.88E-07	<p>AKT3/CHRNA1/CDH3/TANK/TSPAN5/CDH13/FARP1/KLRG1/R/CAN2/KCNMB2/CDKN1C/TCIRG1/MRV1/TRDN/PDPN/HCS7/NPFER2/ADCY3/LECT1/ESM1/CH131/ERLIN2/EGLN2/PTH2/P/DAP1/CHRNA1/CHRNA2/CHRNA3/SORCS1/CIDEA/PANX3/AP3S1/CCR1/SEZ6/TNFAIP8L1/CNP/MAP3K8/ADM/IL13RA/ORA2A4/CRABP1/IMB2/NPP7/APCDD1/CTGF/SGOL1/PRM1L/CYLD/ADRB3/DOB1/ZNF366/BHLHA15/NLRP6/DL2/DMBT1/ABAT/DRD4/DTNACE1/EPNAX2/EGRF/EGR3/EIF4G1/AZM/TMEM117/EPHA1/EPHA3/EPHB4/ESR1/SPATA13/FCGR2A/FGA/FGF10/FHIT/RASA3/FOXJ1/FOXK2/FOXO1/AKR1B1/SPG20/NFASC/FLNB/RHOBTB2/NUP210/NEDDL4/PSD3/LARP1/PPP1R13B/PUM2/ARHGAP18/MAPK8IP2/TSSK2/MTOR/GABBR1/ASGEF1C/ALS2CJ/PNKD/TENM4/ACOT11/RGS22/PLEK2/ADGRF1/RPS6K1/GIAs/FGF22/NFTN/GB2/SDCBP2/PDE7B/DK3C/CYTH4/GLS3/GPR162/BMP10/GNAS/GP/R26/GPER1/FFAR2/GRB10/GRIK4/GSTP1/GUCY1A3/NMIE7/GPR132/ANXAZ/SOX8/KCNIP2/NRGI1/ANXAG/HLA-B/HLA-DOA/HLA-DPA1/HLA-E/HLA-F/HR4A1/HPCA/APBA2/HOXD3/HRH1/HSP90AA1/HSP90AB1/HTR3A/HTRS4/R/SPO2/IGF1/IGF2/CYR61/GPR142/IL1R1/IL1RN/IL6/IL10RA/IL11RA/IL12RB2/IL15RA/INHBA/IRF1/ISL1/ITGA7/ITGB2/ITGB7/IUP/CD82/KCNH2/KCNJ8/KCNJ9/KCNMB1/KDR/HES5/STMN1/ORA2S/LCK/LCP1/LDLUR/ARHGAP1A/GALNS/LHCGR/LGL1/LMNA/RAB19/LTB1/TBP1/SMAD3/MC/2R/MCC/MAP3K1/MFN6/SCGB2A1/NITF/MOVI0/MPZ/PLEKHG7/NEDD9/ATP1A2/INFAT3/KNMBR/NOV/NPPC/NRAS/NTF3/OAS2/OPRL1/ORA2C1/ORA3Z/P2RY6/IL21R/PALM/ARH/GEF3/PARK2/SPOCK3/LEF1/DDX47/ANGPT4/PDE4C/PDE7A/PDE6B/PGAM2/PIK3CG/PTX2/PKHDI/PLA2G2A/PRKAG3/PML/GPR84/IL20RB/PNUP/TLR9/TREM1/CYTL1/POMC/RIN2/ZDHHCL3/APBB1P/PPP1C/ARHGAP10/MOBIJA/SMPD3/CHRNA9/SYBU/LMMS2/VAC14/PRKAR1B/IFT122/MCTP2/LMBRD1/PRKDI1/WSB2/MAP3K/MAP2K2/PRKR1/R/HTRA1/CDCA25E1/LPAR5/PSMD7/PTGFR/PLEKHG5/TENM2/CARZ/PTPRE/ARG52/RIT2/S100A4/S100A6/SCT/CC11/CCL17/NOD2/STR/A6/SFRP2/CXCR5/ARHGAP9/SGK1/MICAL1/TMEM237/BMP4/SLC6A12/SLC8A1/BMPR1B/BOK/SOX9/STAT2/STK3/STK10/BST2/NAVMP2/ZEB1/TEAD3/TGM2/TLE3/TLUBS/TNFAIP3/TNFRSF1A/TNXB/TRAF1/TRAF5/TWIST1/CCR2/TNFRSF4/WNT10B/YWHAG/ZAP70/CA7/CACNA1E/CACNB2/PAX8/CXCR4/FZD5/RAB7A/CARD14/BCL2L14/TMEM204/NLRX1/GPR157/RAB11FP1/CPEB4/C6orf25/CALR/UNC93B1/CAPS/COLQ/HIST1H3A/ANTXR1/SLA2/CVMAH/NR0B2/CASQ1/IL1F10/TRIM63/RAE1/HFTM1/CDK10/RUNX1/TP63/RUNX3/RS2/CRADD/FADD/TNFRSF11A/ALDH1A2/SPHK1/SKAP2/LIMD1/TSPAN18/CCR2/PRC1/STARD13/PIAS2/MAP3K6/SYTT/RSAD2/AURK8/DAP1/CD8A/TIRP10/ADIPOO/ARHGAP29/L186/RAB3D/SMAD5/AS1/RAB36/ARHGAP10/NUP93/RAPGEF2/ULK2/CD79A/TELO2/IGSE1/FGF19/NR1H4</p>
GO:0023052	signaling	378/901	5629/17046	5.32E-09	1.22E-06	9.59E-07	<p>AKT3/AB1/CDH3/TANK/TSPAN5/CDH13/FARP1/KLRG1/R/CAN2/KCNMB2/CDKN1C/TCIRG1/MRV1/TRDN/PDPN/HCS7/NPFER2/ADCY3/LECT1/ESM1/CH131/ERLIN2/EGLN2/PTH2/P/DAP1/CHRNA1/CHRNA2/CHRNA3/SORCS1/CIDEA/PANX3/AP3S1/CCR1/SEZ6/TNFAIP8L1/CNP/MAP3K8/ADM/IL13RA/ORA2A4/CRABP1/IMB2/NPP7/APCDD1/CTGF/SGOL1/PRM1L/CYLD/ADRB3/DOB1/ZNF366/BHLHA15/NLRP6/DL2/DMBT1/ABAT/DRD4/DTNACE1/EPNAX2/EGRF/EGR3/EIF4G1/AZM/TMEM117/EPHA1/EPHA3/EPHB4/ESR1/SPATA13/FCGR2A/FGA/FGF10/FHIT/RASA3/FOXJ1/FOXK2/FOXO1/AKR1B1/SPG20/NFASC/FLNB/RHOBTB2/NUP210/NEDDL4/PSD3/LARP1/PPP1R13B/PUM2/ARHGAP18/MAPK8IP2/TSSK2/MTOR/GABBR1/ASGEF1C/ALS2CJ/PNKD/TENM4/ACOT11/RGS22/PLEK2/ADGRF1/RPS6K1/GIAs/FGF22/NFTN/GB2/SDCBP2/PDE7B/DK3C/CYTH4/GLS3/GPR162/BMP10/GNAS/GP/R26/GPER1/FFAR2/GRB10/GRIK4/GSTP1/GUCY1A3/NMIE7/GPR132/ANXAZ/SOX8/KCNIP2/NRGI1/ANXAG/HLA-B/HLA-DOA/HLA-DPA1/HLA-E/HLA-F/HR4A1/HPCA/APBA2/HOXD3/HRH1/HSP90AA1/HSP90AB1/HTR3A/HTRS4/R/SPO2/IGF1/IGF2/CYR61/GPR142/IL1R1/IL1RN/IL6/IL10RA/IL11RA/IL12RB2/IL15RA/INHBA/IRF1/ISL1/ITGA7/ITGB2/ITGB7/IUP/CD82/KCNH2/KCNJ8/KCNJ9/KCNMB1/KDR/HES5/STMN1/ORA2S/LCK/LCP1/LDLUR/ARHGAP1A/GALNS/LHCGR/LGL1/LMNA/RAB19/LTB1/TBP1/SMAD3/MC/2R/MCC/MAP3K1/MFN6/SCGB2A1/NITF/MOVI0/MPZ/PLEKHG7/NEDD9/ATP1A2/INFAT3/KNMBR/NOV/NPPC/NRAS/NTF3/OAS2/OPRL1/ORA2C1/ORA3Z/P2RY6/IL21R/PALM/ARH/GEF3/PARK2/SPOCK3/LEF1/DDX47/ANGPT4/PDE4C/PDE7A/PDE6B/PGAM2/PIK3CG/PTX2/PKHDI/PLA2G2A/PRKAG3/PML/GPR84/IL20RB/PNUP/TLR9/TREM1/CYTL1/POMC/RIN2/ZDHHCL3/APBB1P/PPP1C/ARHGAP10/MOBIJA/SMPD3/CHRNA9/SYBU/LMMS2/VAC14/PRKAR1B/IFT122/MCTP2/LMBRD1/PRKDI1/WSB2/MAP3K/MAP2K2/PRKR1/R/HTRA1/CDCA25E1/LPAR5/PSMD7/PTGFR/PLEKHG5/TENM2/CARZ/PTPRE/ARG52/RIT2/S100A4/S100A6/SCT/CC11/CCL17/NOD2/STR/A6/SFRP2/CXCR5/ARHGAP9/SGK1/MICAL1/TMEM237/BMP4/SLC6A12/SLC8A1/BMPR1B/BOK/SOX9/STAT2/STK3/STK10/BST2/NAVMP2/ZEB1/TEAD3/TGM2/TLE3/TLUBS/TNFAIP3/TNFRSF1A/TNXB/TRAF1/TRAF5/TWIST1/CCR2/TNFRSF4/WNT10B/YWHAG/ZAP70/CA7/CACNA1E/CACNB2/PAX8/CXCR4/FZD5/RAB7A/CARD14/BCL2L14/TMEM204/NLRX1/GPR157/RAB11FP1/CPEB4/C6orf25/CALR/UNC93B1/CAPS/COLQ/HIST1H3A/ANTXR1/SLA2/CVMAH/NR0B2/CASQ1/IL1F10/TRIM63/RAE1/HFTM1/CDK10/RUNX1/TP63/RUNX3/RS2/CRADD/FADD/TNFRSF11A/ALDH1A2/SPHK1/SKAP2/LIMD1/TSPAN18/CCR2/PRC1/STARD13/PIAS2/MAP3K6/SYTT/RSAD2/AURK8/DAP1/CD8A/TIRP10/ADIPOO/ARHGAP29/L186/RAB3D/SMAD5/AS1/RAB36/ARHGAP10/NUP93/RAPGEF2/ULK2/CD79A/TELO2/IGSE1/FGF19/NR1H4</p>
GO:0061448	connective tissue development	35/901	224/17046	7.76E-09	1.71E-06	1.35E-06	<p>LECT1/CH131/COL11A1/COMP/FAM101A/CTGF/FOXK2/S/GP20/BMP10/IGF1/IGF2/CYR61/GPR142/IL1R1/IL1RN/IL6/IL10RA/IL11RA/IL12RB2/IL15RA/INHBA/IRF1/ISL1/ITGA7/ITGB2/ITGB7/IUP/CD82/KCNH2/KCNJ8/KCNJ9/KCNMB1/KDR/HES5/STMN1/ORA2S/LCK/LCP1/LDLUR/ARHGAP1A/GALNS/LHCGR/LGL1/LMNA/RAB19/LTB1/TBP1/SMAD3/MC/2R/MCC/MAP3K1/MFN6/SCGB2A1/NITF/MOVI0/MPZ/PLEKHG7/NEDD9/ATP1A2/INFAT3/KNMBR/NOV/NPPC/NRAS/NTF3/OAS2/OPRL1/ORA2C1/ORA3Z/P2RY6/IL21R/PALM/ARH/GEF3/PARK2/SPOCK3/LEF1/DDX47/ANGPT4/PDE4C/PDE7A/PDE6B/PGAM2/PIK3CG/PTX2/PKHDI/PLA2G2A/PRKAG3/PML/GPR84/IL20RB/PNUP/TLR9/TREM1/CYTL1/POMC/RIN2/ZDHHCL3/APBB1P/PPP1C/ARHGAP10/MOBIJA/SMPD3/CHRNA9/SYBU/LMMS2/VAC14/PRKAR1B/IFT122/MCTP2/LMBRD1/PRKDI1/WSB2/MAP3K/MAP2K2/PRKR1/R/HTRA1/CDCA25E1/LPAR5/PSMD7/PTGFR/PLEKHG5/TENM2/CARZ/PTPRE/ARG52/RIT2/S100A4/S100A6/SCT/CC11/CCL17/NOD2/STR/A6/SFRP2/CXCR5/ARHGAP9/SGK1/MICAL1/TMEM237/BMP4/SLC6A12/SLC8A1/BMPR1B/BOK/SOX9/STAT2/STK3/STK10/BST2/NAVMP2/ZEB1/TEAD3/TGM2/TLE3/TLUBS/TNFAIP3/TNFRSF1A/TNXB/TRAF1/TRAF5/TWIST1/CCR2/TNFRSF4/WNT10B/YWHAG/ZAP70/CA7/CACNA1E/CACNB2/PAX8/CXCR4/FZD5/RAB7A/CARD14/BCL2L14/TMEM204/NLRX1/GPR157/RAB11FP1/CPEB4/C6orf25/CALR/UNC93B1/CAPS/COLQ/HIST1H3A/ANTXR1/SLA2/CVMAH/NR0B2/CASQ1/IL1F10/TRIM63/RAE1/HFTM1/CDK10/RUNX1/TP63/RUNX3/RS2/CRADD/FADD/TNFRSF11A/ALDH1A2/SPHK1/SKAP2/LIMD1/TSPAN18/CCR2/PRC1/STARD13/PIAS2/MAP3K6/SYTT/RSAD2/AURK8/DAP1/CD8A/TIRP10/ADIPOO/ARHGAP29/L186/RAB3D/SMAD5/AS1/RAB36/ARHGAP10/NUP93/RAPGEF2/ULK2/CD79A/TELO2/IGSE1/FGF19/NR1H4</p>
GO:0065008	regulation of biological quality	236/901	3225/17046	2.26E-08	4.80E-06	3.77E-06	<p>CSGALNACT1/MAPK3/ACTA2/SFRP2/BMP4/BMPR1B/SOX9/ZEB1/WNT10B/SCIN/RUNX3</p> <p>CDH3/KCNMB2/TCIRG1/MRV1/TRDN/ZBTB18/PDPN/GIB6/ADCY3/CHGA/EGLN2/CHRNA1/CHRNA2/CHRNA3/CHRN4/CHRN5/CIDEA/CLN5/CCR1/SLC51B/C15orf27/Z7G16B/SEZ6/CNP/ADM/IL13RA/CP51/CRABP1/CTGF/ADRB3/CYPL1A1/FTTM1/DDB1/BHLHA15/COCH/NLRP6/DIO3/ABAT/DRD4/EECE1/AZM/ESR1/F11/FGA/FGF10/ACIN1/FOXK2/FOXO1/AKR1B1/SPG20/EPB413/FLNB/FLT2/ATP11A/NEDDL4/SYNE1/ARHGAP18/MORC3/MAPK8IP2/MTOR/SLC37A4/DNFBP1/STEAP2/GAS2/PABPC1/NPTN/AMPOD/DK3/GLS2/AMPOD3/GNAS/GPR26/GPER1/FAR2/FLVCR1/SCG3/GSTP1/BRF1/TM004/GUCY1A3/ANXAZ/SERPIND1/SOX8/KCNIP2/ANXAG/HKI/ACACB/HRH1/ACADU/HSP90AB1/HTR3A/FMNI1/BARHL2/NMIE9/GEF1/IGF2/IL1R1/ILRN/IL6/AQP5/INHBA/IRF1/AQP9/ISL1/ITGA7/ITGB2/IUP/ATP9B/KCNH2/KCN8/KCNMB1/KDR/AMIGOS3/LCK/DL/LGALS9/LTB1/SMAD3/MAP3K1/MIF2/MY12/NUBP1/ATP1A2/NOV/NPPC/NRAS/OPRL1/ATP5B/ANO7/PALM/PAR2/LEF1/PALM/ANGPT4/PTP68/ATP8A2/PIK3CG/PKHDI/PML/IL20RB/TLR9/TREM1/CYTL1/POMC/SSH1/APBB1P/FBULM1/PALMD/SMIPD3/SLC30A10/CHRNA9/SYBU/PARVA/PRKARI/PRKDI1/MAPK3/PROCS/SLAMF8/COCA2SE1/TRPC7/ACTR3B/ERMIN/RDH14/METTL4/CCAR2/PXN/AC/TA2/RASGEF2/REC2/TRIM27/RP3/BGLAP/SCT/CC11/ABHD4/NOD2/STR/A6/SGK1/BMP4/SLC441/SLC6A12/SLC8A1/SLC9A3/SLIT1/SOX9/STK3/NAVMP2/CEA1/TERF1/TGM2/TNFAI/P3/TRPC4/TRPC6/CCR2/NARS/WNT10B/YWHAG/CYTL1/CACNA1E/PAX8/CXCR4/RAB7A/TM1/ZC3H12A/RAB11FP1/C6orf25/CALR/COLO/CAPZB/SH3BGLR3/HIST1H3A/ATP13A4/NR0B2/CASQ1/TBKI/GAS7/SCIN/TP63/RS2/ACTN1/FADD/TNFRSF11A/ALDH1A2/LIMD1/SYTT/ILDB2/ESAM/SLC16A3/SMDT1/ADIPOO/RAB3D/MY15/RAPGEF2/ULK2</p>

GO:0098602	single organism cell adhesion	68/901	704/17046	1.03E-06	0.00011	8.44E-05	CDH3/CDH9/PDPN/PK3/MAP3K8/CSTA/CYLD/DDOST/EGFR/EGR3/UNC13D/EPHA1/FGA/NFASC/FLOT2/MTOR/GNAS/HLA-DOA/HLA-DPA1/HLA-E/HLX/ZC3H12D/IGF1/IGF2/CYR61/IL1RN/IL6/IRF1/ITGA7/ITGB2/ITGB7/JUP/LCK/LCP1/LGALS9/SMAD3/MF12/NFATC3/NOV/LEF1/PK3CG/PKH01/IL20R8/APBB1IP/FBLIM1/LIMS2/PARVA/PAG1/TENM2/PXN/NO2D/BMP4/SOX9/STK10/ZEB1/TNKB/CRR2/TNFRSF4/ZAP70/FZD5/CALR/ANTRX1/ESAM/RASD2/CD8A/ADIPOQ	68
GO:0042127	regulation of cell proliferation	114/901	1385/17046	1.08E-06	0.00011	8.74E-05	ABU1/CDH3/CDH13/CDKN1C/SPG6/TGCRG1/GIB6/LECT1/ESM1/B4GALT7/ADM/IL13RA/CTGF/EGFR/EGR3/EPHA1/ESR1/FGF10/VASH1/FOXO1/AKR1B1/MORC3/MTOR/FBXO2/BMP10/GPER1/GSTP1/ANXA2/SOX8/NRNG1/HLA-DPA1/HLA	114
GO:006915	apoptotic process	134/901	1700/17046	1.20E-06	0.00012	9.52E-05	C1D/GIB6/CH13/EGLN2/CARD16/CIDEA/ANKRD9/COMP/MAP3K8/ADM/IL13RA/CTGF/CYLD/DDB1/DNM13A/DSG3/EGFR/EGR3/ESR1/FGA/FGF10/FHIT/ACIN1/FOXO2/FOXO1/EP134	134
GO:0010646	regulation of cell communication	197/901	2731/17046	1.42E-06	0.00014	0.00011	B4L13/DIP2A/PPP1R13B/ARHGEB18/RYBP/RNF1448/GAS3/SL2/BMP10/GPER1/GSTP1/GZMA/SOX8/NRNG1/ANXA6/HS90AB1/ID3/IGF1/CYR61/IL1RN/IL6/NHBA/IRF1/ISL1/JTGB2/2/KOR/LCK/ARHGDI1/LGALS9/LMNA/SMAD3/MEF2D/MAP3K1/MPZ/NTF3/PFAFH2/ARHGEF3/PARK2/UTP111/LEF1/DDX41/ANGPT4/PK3CG/PLAGL1/PLEC/PML/PPP2R2B/LIMS2/PRKDI/MAPK3/PROC/PSMB4/PAK6/PSMD7/PTGFR/PIEKG65/CCAR2/RASGEF2/SCT/NO2D/SFRP2/SGK1/BMP4/BMPR1B/BOK/SOX9/STK3/STK10/ACTC1/TERF1/TGM2/TNF/AIP3/TNFRSF1A/TRAF1/TRAF5/PTN/STK10/ACTC1/TERF1/TGM2/TNF/M2B/SCIN/TP63/RUNX3/IRS2/ACTN1/CRADD/FADD/ALDH1A2/SPHK1/MAP3K6/AURKB/DAPL1/ADIPOQ/LY86/RAPGEF2	197
GO:0050793	regulation of developmental process	149/901	1953/17046	1.82E-06	0.00018	0.00014	CDH3/SPAN5/CDH13/FARP1/RCAN2/CDKN1C/TRDN/HICST/NPFR2/LECT1/ESM1/CH13/LJ/CIDEA/CCR1/SEZ6/TNF/AIP8L1/MAP3K8/ADM/IL13RA/MIB2/MPP7/APCDD1/CTGF/CYLD/ADRB3/ZNF366/NLRP6/ABAT/YDR4/EGFR/A2M/ESR1/SPATA13/FGA/FGF10/RASA3/FOXO1/AKR1B1/SPG20/ROHBT2/NEEDD4/PSD3/LARP1/PUM2/ARHGEF18/MAPK8IP2/MTOR/ALS2CL/PNKD/RGS22/FGF22/NPTN/DKK3/CYTH4/BMP10/GNAS/GPER1/FAR2/GRB10/GSTP1/ANXA2/NRNG1/HKI1/HS90AB1/RSPD2/IGF1/IGF2/CYR61/IL1RN/IL6/NHBA/IRF1/ISL1/JUP/KDR/HES5/LCK/ARHGDI1/LGALS9/LHCG8/LGL1/LMNA/LTPB1/SMAD3/MCC/MAP3K1/MFNG/PLEKHG7/ATP1A2/NOV/NRAS/NTF3/PALM/ARHGEF3/PARK2/LEF1/PDE4C/PDE6B/PK3CG/PKH3/PLA2G2A/PML/TLR9/POW2/DHHC13/PPP1CC/ARHGEF10/SYB/ILIMS2/PRKAR1B/IFT122/LMBRD1/PAG1/PRKDI/MAPK3/MAP2K2/HTR/A1/PSMB4/PAK6/PSMD7/PIEKG65/CCAR2/PTPR/PXN/RASGEF2/RGS12/S100A4/SCT/CCL11/NO2D/SFRP2/ARHGAP9/TMEM237/BMP4/SLC8A1/BMPR1B/SOX9/STK2/STK3/STK10/ACTC1/TERF1/TGM2/TNF/3/ST2/VAMP2/ZEB1/TLIS/TNFAIP3/TNFRSF1A/TNAX/TRAFA1/TRAFA5/TWIST1/WNT10B/YWHAG/ZAP70/CA7/CACNA1E/PAX8/CXCR4/FZD5/RAB7A/CARD14/BCL2L14/TMEM204/NL/RX1/RAB11FP1/CALR/SLA2/OMAH/ANR082/CDK10/RUNX1/TP63/RUNX3/IRS2/CRADD/FADD/TNFRSF11A/SPHK1/MAP3K6/SYTY7/RSAD2/CD8A/TRIP10/ADIPOQ/ARHGAP29/LY86/ARHGEF10/RAPGEF2/TELO2/IOSEC1/FGF19	149
GO:0098609	cell-cell adhesion	75/901	816/17046	1.87E-06	0.00018	0.00014	PHA3/ESR1/FGA/FGF10/VASH1/ACIN1/FOXO2/FOXO1/SPG20/EPH4L13/FLOT2/NEEDD4/ARHGEF18/MTOR/TENM4/GAS2/NPTN/BMP10/GNAS/GPER1/FLVCR1/SOX8/NRNG1/HLA-DPA1/HLA-E/HLX/ZC3H12D/IGF1/IGF2/CYR61/IL1RN/IL6/IRF1/ITGA7/ITGB2/ITGB7/JUP/AMIGO3/CDHR4/LCK/LCPI/LGALS9/SMAD3/NFATC3/NOV/LEF1/PK3CG/PKH01/IL20R8/APBB1IP/FBLIM1/LIMS2/PARVA/PAG1/PCDHGCA/PCDHGB7/PCDHGB8/PCDHGA11/TENM2/NO2D/PCDH20/BMP4/SOX9/STK10/ZEB1/TNKB/CRR2/TNFRSF4/ZAP70/FZD5/SLA2/FADD/ESAM/RSA/D2/CD8A/ADIPOQ	75
GO:0008219	cell death	140/901	1816/17046	2.27E-06	0.00021	0.00017	C1D/GIB6/CH13/EGLN2/CARD16/CIDEA/ANKRD9/COMP/MAP3K8/ADM/IL13RA/PARP4/CTGF/CYLD/DDB1/DNM13A/DSG3/EGFR/EGR3/ESR1/FGA/FGF10/FHIT/ACIN1/FOXO2/FOXO1/EPH4L13/DIP2A/PPP1R13B/ARHGEB18/RYBP/RNF1448/GAS2/CUL1/GLS2/BMP10/GPER1/GSTP1/DOBA/NOX3/NRNG1/ANXA6/HS90AB1/ID3/IGF1/CYR61/IL1RN/IL6/NHBA/IRF1/ISL1/JTGB2/KDR/LCK/ARHGDI1/LGALS9/LMNA/SMAD3/MEF2D/MAP3K1/MEOX2/MPZ/NOV/NTF3/PFAFH2/ARHGEF3/PARK2/UTP111/LEF1/DDX41/ANGPT4/PK3CG/PKH01/KM/PLAGL1/PLEC/PML/PPP2R2B/LIMS2/PRKDI/MAPK3/PROC/PSMB4/PAK6/PSMD7/PTGFR/PIEKG65/MARK4/CCAR2/RASGEF2/SCT/NO2D/SFRP2/SGK1/BMP4/BMPR1B/BOK/SOX9/STK3/STK10/ACTC1/TERF1/TGM2/TNFAIP3/TNFRSF1A/TRAF1/TRAFA5/PHLDA2/TWIST1/TNFRSF4/WNT10B/YWHAG/PAX8/CXCR4/FZD5/CARD14/BCL2L14/FAM188A/ZC3H12A/C/PEBA/COL18A1/CLPTM1L/CALR/CAST/KDM2B/SCIN/TP63/RUNX3/IRS2/ACTN1/CRADD/FADD/ALDH1A2/SPHK1/MAP3K6/AURKB/DAPL1/ADIPOQ/LY86/RAPGEF2	140
GO:0016265	death	140/901	1816/17046	2.27E-06	0.00021	0.00017	C1D/GIB6/CH13/EGLN2/CARD16/CIDEA/ANKRD9/COMP/MAP3K8/ADM/IL13RA/PARP4/CTGF/CYLD/DDB1/DNM13A/DSG3/EGFR/EGR3/ESR1/FGA/FGF10/FHIT/ACIN1/FOXO2/FOXO1/EPH4L13/DIP2A/PPP1R13B/ARHGEB18/RYBP/RNF1448/GAS2/CUL1/GLS2/BMP10/GPER1/GSTP1/DOBA/NOX3/NRNG1/ANXA6/HS90AB1/ID3/IGF1/CYR61/IL1RN/IL6/NHBA/IRF1/ISL1/JTGB2/KDR/LCK/ARHGDI1/LGALS9/LMNA/SMAD3/MEF2D/MAP3K1/MEOX2/MPZ/NOV/NTF3/PFAFH2/ARHGEF3/PARK2/UTP111/LEF1/DDX41/ANGPT4/PK3CG/PKH01/KM/PLAGL1/PLEC/PML/PPP2R2B/LIMS2/PRKDI/MAPK3/PROC/PSMB4/PAK6/PSMD7/PTGFR/PIEKG65/MARK4/CCAR2/RASGEF2/SCT/NO2D/SFRP2/SGK1/BMP4/BMPR1B/BOK/SOX9/STK3/STK10/ACTC1/TERF1/TGM2/TNFAIP3/TNFRSF1A/TRAFA1/TRAFA5/PHLDA2/TWIST1/TNFRSF4/WNT10B/YWHAG/PAX8/CXCR4/FZD5/CARD14/BCL2L14/FAM188A/ZC3H12A/C/PEBA/COL18A1/CLPTM1L/CALR/CAST/KDM2B/SCIN/TP63/RUNX3/IRS2/ACTN1/CRADD/FADD/ALDH1A2/SPHK1/MAP3K6/AURKB/DAPL1/ADIPOQ/LY86/RAPGEF2	140

GO:0019722	calcium-mediated signaling	21/901	1125/17046	2.32E-06	0.00017	0.00021	0.00017	CDH13/RCAN2/BHLHA15/DRO4/EGFR/NRG1/HPCA/IGF1/KDR/ATP2A2/INFATC3/MCTP2/PTGFR/TENM2/SCLC8A1/ZAP70/CXCR4/SLA2/CASQ1/SPHK1/CD8A	21
GO:0032720	negative regulation of tumor necrosis factor production	11/901	38/17046	2.73E-06	0.00019	0.00025	0.00019	CIDEA/GSTP1/LGALS9/POMC/TRIM27/NOD2/BP1/TNFAIP3/TWIST1/ZC3H12A/ADIPOQ	11
GO:0002376	immune system process	175/901	2392/17046	2.76E-06	0.00019	0.00025	0.00019	AB11/TANK/CD300LD/KLRG1/CDKN1C/SPON2/HCS1/ADCY3/CHGA/CGR1/MAP3K8/ADM/IL31RA/CYLD/ESCO2/DDOST1/RNF68/COCH/NLRP6/DMBT1/EEF2/EFNA2/EGFR/EGR3/A2M/EMIL1/JUNC13D/FCGR2A/FGA/FGF10/RASA3/SBNO2/ACIN1/FOXJ1/FOXO1/FLOT2/PUM2/MITOR/SCL37A4/FGF2/AMPPD3/GNAS/GPER1/FFAR2/FLVCR1/GZMA/ANXA2/NRSG1/HLA-B/HLA-DOA/HLA-DPA1/HLA-E/HLA-F/HLX/NR4A1/HOXB3/HRH1/HSP90AA1/HSP90AB1/ZC3H12B/CD300E/IGF1/IGF2/L1RL1/L1RLN/IL6/IL16/IL16/INHBA/IRF1/AQP9/ITGB2/ITGB7/KCNJ8/KDR/HES5/LCK/LCP1/LGALS9/LMO2/LTB/SMAD3/MAP3K1/MEOX1/MITE/MOV10/NEATC3/NOV/NRAS/OAS2/IL21R/LEF1/ANGPT4/PIK3CG/PTX2/PML/L20R8/TLR9/TREM1/POU2AF1/APBB1IP/HERC6/SMPP3/PRKAR1B/PAG1/PRKDJ/MAPK3/MAP2K2/PROC/MASP1/HTRA1/PSMB4/PSMD7/DEFB134/BGLAP/CCL11/CCL17/NOD2/TINAGL1/SFRP2/CKCR5/VPS33A/BMP4/SOX9/BP1/STAT3/STK3/STK10/SUPT6H/BST2/VAMP2/TCEA1/ZEB1/TLR5/TNFAIP3/CCR2/TNFRSF4/WNT10B/ZAP70/CAT7/CXCR4/FZD5/RAB7A/LST1/NLRX1/ZC3H12A/C6orf25/CALR/JUNC93B1/HST1H3A/SLA2/ILL1F10/IFTM1/SCIN/RUNX1/RUNX3/IRS2/ACTN1/FAOD/TNFRSF11A/ENDOU/SKAP2/ESAM/SCL16A3/RSAD2/IL32/CD8A/ADIPOQ/ly86/NUP93/RAPGEF2/CD79A/FGF19	175
GO:0019222	regulation of metabolic process	386/901	6084/17046	3.16E-06	0.00022	0.00028	0.00022	AB11/CDH3/ZNF783/DH13/MBNL2/FARP1/RCAN2/CDKN1C/D1/ZBTB18/PITRMI/DMRT2/CELF1/TBRI/NPFRF2/ADCY3/PNRC1/TMED10/HNRPUL1/CHB1L1/ERLIN2/PSIP1/EGLN1/386 2/CARD16/ZBED9/CIDEA/CGR1/SCL51B/MAP3K8/ZFP42/ADM/IL31RA/ZNF358/LDLRAD3/CSTA/ZNF738/CTGF/SMYD1/SH3D19/CYLD/ADRB3/ESCO2/ZNF782/ZNF709/ZNF781/CTE/D4/RNF168/ZNF366/BHLHA15/NLRP6/DLG2/DNMT3A/DRD4/VECE1/EEF2/EGFR/EGR3/PATL2/EIF4G1/AZM/ELK4/EPHA1/EPHA3/ESR1/SPATL3/PHACTR1/SP8/FGA/FGF10/FHIT/XR/N2/RASA3/PPP1M1E/SBNO2/TRAK1/MSRB2/ACIN1/FOXJ1/FOXQ2/TBC1D9B/FOXO3/GG3/DIP2A/FLOT2/TBC1D1/NEBD4/PSD3/LARP1/PUM2/ARHGFB18/RYPB/MAPK8IP2/VGLL2/MTOR/GABBR1/RASGEF1C/RNF448/ZNF549/ALS3C1/PKNO2/RGS22/FBXO2/GAPDH5/PABPC1/DNAJC2/FGF22/NPTN/DK3/CYTH4/BMP10/ZNF638/GNAS/ZNF311/ZNF844/GPER1/DOX7/GRB10/ZBTB44/DNAIC15/GSTP1/GTF2B/BRE1/JUC12A3/GZMA/ANXA2/SEPRIN1/SOX8/NRGI1/HK1/HK2/HMGGA1/NR4A1/ACACB/HPCA/APBAZ/HOXB3/HOXC4/HOXC5/HOX6/HOX7/AGFG2/HRH1/ACADL/HSP90AA1/HSP90AB1/TFAP2E/ID3/CO128A1/BARRH12/IGF1/IGF2/CYR61/IL1RN/IL16/FOXK2/INHBA/IRF1/SL1/TGB2/ITIH3/ITIH4/JU/PUSP50/HLS1/KDR/RIF25/PO5/HES5/AFF3/LCK/DLX1/ARHGDI1A/LGALS9/LHCG/LGL1/LMNA/LMO2/LTB/SMAD3/MC2R/MEI1/ME2/MEF2D/MAP3K1/MEOX1/MEOX2/MF12/MIT1/FLHX8/MOV10/PLEKHG7/INFAT3/NFYB/NHLH2/NOV/NPC/NRAS/NTF3/OPR1/JPALM/ARHGFE3/PARK2/SPOCK3/LEF1/PRR16/ANGU12/SIRT6/PGAM2/P3/PK3CG/PTX2/PKHDJ/PLA2G2A/PIAGL1/PML/RIPPL3/PNUP/RPK4/TLR9/CYTL1/PONC/SSH1/RIN2/POU2AF1/RNCC2/MED18/BANP/PPP1C/PWIL2/ELP3/ARHGEF10L/PRMT6/DNAIC17/ZNF532/PPP2R2B/FANCI/CNOT11/VACL4/PRKAR1B/CSDJ/PRKDJ/MTYNN/MAPK3/MAP2K2/MRAP/PRMT8/MASP1/HTRA1/SLAMF8/CD425E1/PSMB4/PAK6/ARNTL2/RGMA/RDM11/P/SMID7/PTGFR/PLEKHG5/TENM2/GATAD2B/METTL4/CCAR2/PXN/CREBZF/ACTA2/RASGRF2/TRIM27/RGS12/SCT/CCL11/CCL17/NP33/NO22/SFRP2/ARHGAP9/TRA2B/GZF1/SGK1/BMP4/ZNF649/BMP18/BRD9/ZSCAN18/BOK/SOX9/STAT2/STK3/STK10/SUPT6H/BST2/TA4B/TBP/TCEA1/TCRB2/ZEB1/ACTC1/TEAD3/TERF1/TIMP3/TLB3/TLB5/TNFAIP3/TNFRSF1A/TNXXB/TRAFF1/TRAFF5/PHLDA2/TWIST1/CCR2/TNFRSF4/UCP1/ARX/WM108/YWHAG/ZNF17/ZNF124/ZNF177/PAX8/CXCR4/FZD5/RAB7A/CARD14/ZNF665/ZC3H14/ZNF606/ZC3H12A/CPEB4/ZNF436/CALR/SLRP/CAS1/S3H3BGR13/SCRT1/HIST1H3A/SLA2/ZNF397/NROB2/HOPX/SPINK7/TRIM63/KOM2B/LOX13/CBX2/GAS7/CDK10/RUNX1/TP63/RUNX3/SERP1/MA6/IRS2/ACTN1/CRADD/TNFRSF11A/ALDH1A2/SPHK1/BUDB1/CCNA1/LUMID1/ERH1/STAR13/PIAS2/ZFAND2A/MAP3K6/LDB2/CBFA2T2/AURKB/DAP1/ADIPOQ/ARHGAP2/9/H2AFY/ARHGFE10/MICAL2/ZNABP1/VGLL4/RAPGEF2/ULK2/USP6L/ZBTB39/RABGAP1/IOSEC1/FGF19/NR1H4	386
GO:0032989	cellular component morphogenesis	115/901	1432/17046	3.19E-06	0.00022	0.00028	0.00022	AB11/FARP1/SPON2/PDPN/TBR1/LEP1/FRMD6/CNP/COL9A3/SC11/SH3D19/CYLD/COCH/EFNA2/EGFR/TWEM17/JUNC13D/EPHA1/EPHA3/EPH4/FGA/FGF10/RASA3/8TB3/SPG115 20/NFASC/EPB41.3/F1NB/NEBD4/ARHGFE18/MAPK8IP2/TENM4/GAS2/FGF22/BMP10/TMOD4/NRG1/HSP90AA1/HSP90AB1/JPMN1/BARHL2/IL6/SL1/ITGA7/ITGB2/ITGB7/KDR/S/TM1/ARHGDI1A/LG1/SMAD3/MAP3K1/MR12/MY12/NRAS/NTF3/PALM1/PARK2/LEF1/ATP8A2/PKHD1/SSH1/FBLN1/PALM1/PARVA/FE1122/BINI/MAPK3/MAP2K2/CD425E1/PSMB4/RGMA/TRPC7/PSMD7/TENM2/ERIN/PXN/RASGRF2/S100A4/CCL11/SFRP2/DNAI2/SGK1/TMEM23/VPS33A/BMP4/BMP18/SULT1/SOX9/ACT1/TRPC4/TRPC6/TWIST1/CACNB2/PAX8/LST1/C6orf25/COL18A1/CALR/SLRP/CAPZB/ANTXR1/CASQ1/PARD6B/ITBK1/OXL3/GAS7/RUNX3/IRS2/ACTN1/LUMID1/RAPGEF2/ULK2/FGF19	115
GO:0030036	actin cytoskeleton organization	52/901	511/17046	4.53E-06	0.0003	0.00038	0.0003	AB11/FAM101A/CTGF/EPHA1/EPHA3/PHACTR1/FGF10/PPM1E/MSRB2/LIMCH1/EPH413/FLNB/ARHGFB18/MTOR/PLEK2/BMP10/TMOD4/FMNI/LCP1/LG1/SMAD3/MAP3K1/M/52 Y12/NEED9/NTF3/PARK2/SSH1/PARVA/TTC17/BIN3/PAK6/ACTR3B/ERIN/TWIM27/CCL11/PARVG/MICAL1/BST2/ACTC1/TNXXB/CALR/CAPZB/SH3BGR13/ANTXR1/CASQ1/GAS7/SCI/N/ACT1/TRIP10/ARHGFE10/MICAL2/IOSEC1	52
GO:0035556	intracellular signal transduction	179/901	2478/17046	4.58E-06	0.0003	0.00038	0.0003	AB11/TANK/CDH13/FARP1/RCAN2/MRVI1/HCS1/NPFRF2/ADCY3/CH13L1/CCR1/SEZB/TNFAIP8L1/MAP3K8/ADM/IL31RA/MBI2/CTGF/SGOL1/PPM1L/CYLD/ADRB3/BHLHA15/NLRP6/DRO4/EGFR/A2M/ESR1/SPATL3/FGA/FGF10/FHIT/RASA3/FOXO1/AKR1B1/HOBTB2/PSD3/AARP1/PPP1R13B/PUM2/ARHGFE18/MAPK8IP2/TSSK2/MTOR/RASGEF1C/ALS2C1/AC/OTL1/PLEK2/FGF22/SDCBP2/CYTH4/BMP10/GNAS/GPER1/GSTP1/GUCY1A3/NRG1/ANK4A1/HPCA/HRH1/HTRA1/IGF1/ATP8A2/PKHD1/SSH1/FBLN1/PALM1/PARVA/FE1122/BINI/MAPK3/MAP2K2/CD425E1/PSMB4/RGMA/TRPC7/PSMD7/TENM2/ERIN/PXN/RASGRF2/S100A4/CCL11/SFRP2/DNAI2/SGK1/TMEM23/VPS33A/BMP4/BMP18/SULT1/SOX9/ACT1/TRPC4/TRPC6/TWIST1/CACNB2/PAX8/LST1/C6orf25/COL18A1/CALR/SLRP/CAPZB/ANTXR1/CASQ1/PARD6B/ITBK1/OXL3/GAS7/RUNX3/IRS2/ACTN1/LUMID1/RAPGEF2/ULK2/FGF19	179

GO:1903556	negative regulation of tumor necrosis factor superfamily cytokine production	11/901	40/17046	4.76E-06	0.00039	0.0003	CIDEA/GSTP1/LGALS9/POMC/TRIM27/NOD2/BPI/TNFAIP3/TWIST1/ZC3H12A/ADIPOQ	11
GO:0048646	anatomical structure formation involved in morphogenesis	92/901	1090/17046	4.76E-06	0.00039	0.0003	AB11/CDH13/PDPN/DMMT2/BR1/LECT1/ESM1/CH131/COL11A1/SC11/ADM/CTGF/CYLD/EGFR/TMEM17/UINC13D/EPHA1/EPHB4/FGF10/VASH1/SBNO2/FOXK2/NFASC/EPB4113/TFENM4/BMP10/GNAS/TMOD4/ANXA2/SOX8/NRA4/HOXB3/FMN1/CRY61/L6/INHBA/ISL1/TGAT/ITGB2/KDR/HES5/LAMA3/MEOX2/MYL2/NFATC3/NOV/ATP5B/LEF1/CEND1/ANGPT4/ATP8A2/PK3CG/PTX2/PKHDI/PML/ROBO4/PARVA/IFT122/PRKD1/MAKP3/IMP2K2/HTRA1/CC111/S18A6/SFRP2/DNAI2/TMEM237/VPS33A/BMP4/SOX9/STK3/ACTC1/TGM2/TNFAIP3/TWIST1/CCR2/60625/ZC3H12A/C60625/COL18A1/CAST/CASQ1/HOPX/KDM2B/RUNX1/TP63/ACTN1/SPHK1	92
GO:0032680	regulation of tumor necrosis factor production	17/901	91/17046	4.82E-06	0.00039	0.0003	SPON2/CIDEA/GSTP1/HLA-E/ISL1/LGALS9/TLR9/POMC/TRIM27/NOD2/BPI/TNFAIP3/TWIST1/CCR2/ZC3H12A/FADD/ADIPOQ	17
GO:0032879	regulation of localization	159/901	2151/17046	4.94E-06	0.00039	0.00031	CDH3/CDH13/TRDN/PDRN/TBR1/RRR1/CHGA/CIDEA/CCR1/SLC51B/CYLD/ITIM1/TRPV3/NLRP6/ABAT7/DRD4/EGFR/UINC13D/EPHA1/SPATA13/FGA/FGF10/VASH1/FOXK2/EXPH5/MILC1/TBC1D1/NUP210/NEDD4/MAKP3/MTOR/GLSZ/APS4A/BMP10/GNAS/CACR2B/GR26/GPER1/FEAR2/GRB10/ANXA2/HAS1/KCNP2/NRG1/ANKA13/HLA-E/ACACB/HPCA/HSPA1L/HSP90A81/IGF1/CRY61/IL1RN/IL6/INHBA/ISL1/UP/KCNH2/KCNJ9/KDR/PO5/LAMA3/STMN1/LCK/LCP1/LGALS9/ILGL1/LMNA/SMAD3/MCC/MAP3/K1/ATP1A2/NFATC3/NOV/NTF3/OPRL1/PZRY6/PARK2/LEF1/ANGPT4/PDE4C/SIRT6/ATP8A2/PK3CG/PTX2/PKHDI/PML/FXYD6/TLR9/POMC/PON1/ROBO4/ELP3/GOLPH3/TRPV6/SMPD3/SLC30A10/SYBU/PRKAR1B/LMBRD1/PRKD1/MAKP3/IMP2K2/FAM60A/SRFGF2/TRIM27/CC111/NOD2/SFRP2/SK1/BMP4/SLC8A1/SLC9A3/SOX9/STK10/SUPTEH/BS/TZ/NAVMP2/TRPC6/PHLDA2/TWIST1/CCR2/TNFRSF4/YNHAG/CA7/CACNA1E/PTPAA1/CACNB2/PAX8/FZD5/RAB7A/ZC3H12A/RAB11FP1/COL18A1/CALY/SH3BGR1/3/SCRT1/NR0B2/CASQ1/PARD6B/RAE1/ITIM1/SCIN/IRS2/ACTN1/FADD/TNFRSF11A/SPHK1/SY77/RSAD2/REEP6/ADIPOQ/RAB3D/NUP93/RAPGEF2/RABGAP1L/FGF19	159
GO:0061061	muscle structure development	55/901	554/17046	5.05E-06	0.0004	0.00031	SPFG/PTB138/CHRNA1/COL11A1/ADM/SMYD1/BHLHA5/EGFR3/FGF10/FOXK2/FLNB/FLT2/SYNE1/VGLL2/MTOR/BMP10/TMOD4/SOX8/NRG1/HIX/ID3/IGF1/IGF2/IL6/ISL1/TGFA7/7/LMNA/SMAD3/MEF2D/MEOX2/NTF2/NFATC3/NOV/NRAS/NTF3/LEF1/SIRT6/PTX2/PLAGL1/BN3/CC111/STRAG8/BMP4/SLC8A1/SOX9/SUPT6H/ZEB1/ACTC1/TWIST1/WNT10B/TMEM204/CALB/CAST/CASQ1/HOPX	55
GO:0009887	organ morphogenesis	78/901	884/17046	5.38E-06	0.00042	0.00033	TBR1/GI86/COL11A1/COMP/ADM/FAM101A/CTGF/EGFR/EPHB4/ESR1/FGF10/FOXK2/BMP10/GNAS/FLVCR1/SOX8/NRG1/HIX/HOXB3/HOXC4/HOXB3/ID3/RSPO2/FMN1/IGF1/IGF2/CYR61/IL6/AQP5/INHBA/ISL1/HES5/SMAD3/MEF2D/LHX8/MYL2/NPCO/LEF1/SIRT6/ATP8A2/PTX2/PML/BNC2/CHRNA9/LIMS2/PARVA/IFT122/CSGALNACT1/MAKP3/MA/P2K2/HTRA1/ACTA2/BGLAP/CC111/STRAG6/SFRP2/GZF1/BMP4/SLC8A1/BMPR1B/SLIT1/SOX9/ZEB1/ACTC1/TGM2/TLE3/TNFAIP3/PHLDA2/TWIST1/WNT10B/PAX8/FZD5/COL18A1/KDM2B/TP63/ALDH1A2/IMCAL2	78
GO:0008360	regulation of cell shape	21/901	132/17046	5.66E-06	0.00043	0.00034	PDPN/COCH/EPB4113/ARRHGF18/GAS2/IL6/TGFA7/ITGB2/KDR/PALM/FBLN1/PALMD/PARVA/CD42SE1/ERMIN/PXN/CC111/SLIT1/TTBK1/GAS7/LIMD1	21
GO:0032640	tumor necrosis factor production	17/901	93/17046	6.54E-06	0.00049	0.00038	SPON2/CIDEA/GSTP1/HLA-E/ISL1/LGALS9/TLR9/POMC/TRIM27/NOD2/BPI/TNFAIP3/TWIST1/CCR2/ZC3H12A/FADD/ADIPOQ	17
GO:0016337	single organismal cell-cell adhesion	62/901	657/17046	6.57E-06	0.00049	0.00038	CDH3/CDH9/PDPN/PK3/MAKP38/CSTA/CYLD/DDOST/EGFR/EGR3/FGA/NFASC/FLT2/MTOR/GNAS/HLA-DOA/HLA-DPA1/HLA-DOA/ZC3H12D/IGF1/IGF2/CYR61/IL1RN/IL6/IRF1/TGAT/ITGB2/ITGB7/JUP/LCK/LCP1/LGALS9/SMAD3/NFATC3/NOV/LEF1/PK3CG/PKHDI/IL20RB/APBB1P/FBLN1/LIMS2/PARVA/PAG1/TENM2/NOD2/BMP4/SOX9/STK10/ZEB1/TNXX/CCR2/TNFRSF4/ZAP70/FZD5/SLAZ/FADD/ESAM/RSAD2/CD8A/ADIPOQ	62
GO:0043067	regulation of programmed cell death	106/901	1314/17046	6.64E-06	0.00049	0.00038	EGLN2/CARD16/CIDEA/ANKRD9/COMP/MAKP38/ADM/IL13RA/CTGF/CYLD/DOB1/EGFR/EGR3/ESR1/FGA/FGF10/ACIN1/FOXK2/FOXO1/DP2A/ARHGEF18/GLS2/BMP10/GPER1/GS1/TPI/GZMA/SOX8/NRG1/HSP90A81/ID3/IGF1/CYR61/IL1RN/IL6/INHBA/ISL1/KDR/LCK/ARHGAP10/LGALS9/LMNA/SMAD3/MAKP31/MTF/IMP2/NTF3/PAFAH2/ARHGEF3/PARK2/UTP11A/LEF1/ANGPT4/PK3CG/PKHDI/PML/LIMS2/PROC/PSMB4/PAK6/PSMD7/PTGFR/PLEKHG5/MARK4/CCAR2/RASGEF2/SCT/NOD2/SFRP2/SK1/BMP4/BMPR1B/BOK/SOX9/STK3/STK10/ACTC1/TERF1/TGM2/TNFAIP3/TRAF1/TRAF5/TWIST1/TNFRSF4/WNT10B/YNHAG/PAX8/CARD14/BC12L14/CPEB4/COL18A1/CALR/CAST/KDM2B/SCIN/TP63/RUNX3/RS2/A/CTN1/CRADD/FADD/ALDH1A2/SPHK1/MAKP36/AURKB/ADIPOQ/RAPGEF2	106
GO:0008283	cell proliferation	135/901	1775/17046	7.16E-06	0.00052	0.00041	AB11/CDH3/CDH13/CDKN1C/SPG1/CTGIRG1/TACC2/PDPN/GI86/LECT1/ESM1/BAGAL7/PDAP1/ADM/IL13RA/CTGF/DMMT1/DPH1/EGFR/EGR3/BML1/EPHA1/ESR1/ESR2/VASH1/F10XC2/FOXO1/AKR1B1/LARP1/NORX3/MTOR/TENM4/FBXO2/BMP10/GPER1/GS1P1/ANXA2/SOX8/NRG1/HLA-DPA1/HLA-DOA/HMGGA1/NRA4/TFAP2E/ZC3H12D/IGF1/IGF2/CYR61/IL6/IL12RB2/IL15RA/INHBA/IRF1/ITGB2/ITGB7/JUP/KDR/HES5/LCK/LGALS9/SMAD3/MCC/MTF/NEU1/NOV/NPCC/NRAS/NTF3/LEF1/CEND1/SIRT6/ATP8A2/PK3CG/PTX2/PKHDI/PLA2G2A/PML/RIPPL1/3/IL20RB/CNOT11/LIMS2/IFT122/CSGALNACT1/PRKD1/IMP2K2/PKRIR/HTRA1/SLURP1/PTGFR/TM27/RPAS3/S100A6/CC111/NOD2/SFRP2/SK1/BMP4/BMPR1B/BOK/SOX9/STK3/BS2/ZEB1/TNFAIP3/TRAF5/TWIST1/TNFRSF4/WNT10B/ZAP70/FZD5/SLIT1/COL18A1/CALR/RETNLB/KDM2B/JITM1/SCIN/CDK10/RUNX1/TP63/RUNX3/IRS2/FADD/TNFRSF11A/ALDH1A2/SPHK1/SKAP2/PRC1/ADIPOQ/AY86/RAPGEF2/CD79A/FGF19	135

GO:0002682	regulation of immune system process	110/901	1391/17046	1.07E-05	0.00071	0.00056	AB11/TNK/KLRG1/SPON2/HCS7/CCR1/MAP3K8/IL31RA/CYL2/COCH/NLRP6/DMBT1/EGFR/EGR3/A2M/UNC13D/FCGR2A/FGF10/RASA3/ACIN1/FOXO1/FLOT2/PUM2/MTOR/SLC37A4/FGF22/GNAS/GPER1/FFAR2/NRG1/HLA-B/HLA-DQA/HLA-DPA1/HLA-E/HLA-F/HLX/NR4A1/HSP90AA1/HSP90AB1/ZC3H12D/IGF1/IGF2/IL6/INHBA/IRF1/ITGB2/ITGB7/KDR/HES5/LCK/LGALS9/SMAD3/MAP3K1/MIFF/MOV10/NFATC3/NOV/NRAS/LEF1/PML/IL20R8/TLR9/TREM1/PAG1/MAPK3/MAP2K2/MASP1/HTRA1/PSMB4/PSMD7/PTPRE/RASGRF2/TRIM27/BGLAP/SOX9/BPI/NO22/BMP4/SOX9/BPI/NO22/STK10/SUPT6B/BST2/ZEB1/TLR5/TNF/ALIP3/CCR2/TNFRSF4/ZAP70/CA7/FZD5/LST1/NLRX1/ZC3H12A/CALR/UNC93B1/HIST1H3M/SLAZ/HITM1/SCIN/RUNX1/IRS2/FADD/SKAP2/RSAD2/CD8A/ADIPOQ/NUPI93/RAIPGEF2/C/D79A/FGF19
GO:0050678	regulation of epithelial cell proliferation	32/901	265/17046	1.12E-05	0.00073	0.00058	CDH3/CDH13/CDKN1C/LECT1/EGFR/EGR3/FGF10/VASH1/MTOR/NR4A1/IGF1/IL6/KDR/SMAD3/MCC/PLA2G2A/LIMS2/JF122/PRKD1/HTRA1/SLURP1/CCL11/NO22/SFRP2/BMP4/SOX9/TNFAIP3/TWIST1/WNT10B/TP63/RUNX3/ALDH1A2
GO:2000145	regulation of cell motility	57/901	599/17046	1.22E-05	0.00079	0.00062	CDH13/CCR1/EGFR/EPHA1/SPATA13/FGF10/VASH1/FOXO2/BMP10/GPER1/HAS1/IGF1/CYR61/IL1RN/IL6/KDR/LAMA3/LGALS9/LMNA/SMAD3/MCC/MAP3K1/NOV/INTF3/P2RY6/LEF1/ANGPT4/PTX2/ROBO4/ELP3/PRKQ1/MAP2K2/FAM60A/CCL11/NO22/SFRP2/SGK1/BMP4/SCLC8A1/SOX9/STK10/BST2/PHLDA2/TWIST1/CCR2/PTP4A1/COL18A1/CALR/SH3BGR1/3/SCRT1/PAR6B/IFITM1/IRS2/FZD/SPHK1/ADIPOQ/RAIPGEF2
GO:0006796	phosphate-containing compound metabolic process	196/901	2808/17046	1.33E-05	0.00085	0.00067	AKT3/ABI1/GNE/FARP1/CDKN1C/SPG6/RCKD7/TCIRG1/HCS7/NPFR2/ADCV3/CH13L1/ACOT7/ALPK2/CCR1/CNP/APOA1B/MAP3K8/ADM/IL31RA/UBI/CP1/CP51/TRPM6/CTGF/PP/MI1/MBOAT1/ADRB3/FTM1/JADAL/NLRP6/DLG2/DRD4/EGFR/ENO3/ADCK3/EPHA1/EPHA3/EPH4/FGF10/FHIT/RAS3/PPM1E/FOXO/MORC3/MAPK8IP2/TSSK2/MTOR/GA/BBR1/GAK/GAPDH5/RPS6K1/FGF22/NPTN/AMPO2/PDE7B/AMPO3/BMP10/GNAS/PIG1/HEM5/GPER1/DOK7/GRB10/DNAJC15/GSTP1/GUCY1A3/NAME7/ANXA2/NRGI/HK1/AC/ACB/HPCA/HRH1/HSP90AB1/DUDD1/ANME9/IGF1/IGF2/CYR61/IL1RN/IL6/IL12RB2/INHBA/INPP5A/ISL1/ITGB2/KCNH2/KDR/HES5/LCK/LDLR/LGALS9/LHCSR/SMAD3/MC2R/MEI1/M/EG/MAP3K1/MGAT1/MOC51/NUDT1/AMVH4/NDUFBA1/ATP1A2/NPCC/NRAS/INTF3/OAS2/OPR1/ATP5B/PALM/VPARK2/ANGPT4/PDE4C/PDE7A/SIRT6/PDE6B/PGAM2/PIGC/PIK3CG/PKH1/PKM/PLA2G2A/PRKAG3/PML/RIPK4/TLR9/SSH1/PON1/LP/CA2/PPP1CB/PPP2R2B/SMO3/AC14/PRKAR1B/CSGALNACT1/PRKD1/MAPK3/MAP2K2/MKAP/S/LAMF8/PSMB4/PAK6/PSMD7/MARK4/PTPRE/PXN/RASGRF2/TRIM27/SCT/CCL11/CCL17/NO22/SFRP2/SGK1/CEBK/BMP4/BMPRI1B/SOX9/STK3/STK10/TNFAIP3/TNFRSF1A/TNXB/TWIST1/CCR2/TNFRSF4/UPP1/WWHAG/ZAP70/PTP4A1/CXCR4/FZD5/CARD14/TBK1/CDK10/KMO/RUNX3/IRS2/TNFRSF1A/STK19/SYNI2/SPHK1/LIMD1/MAP3K6/AURKB/ADIPOQ/H2AFY/ENTPD3/RAPGEF2/ULK2/LPGAT1/FGF19
GO:0071706	tumor necrosis factor superfamily cytokine production	17/901	98/17046	1.35E-05	0.00086	0.00067	SPON2/CIDEA/GSTP1/HLA-E/ISL1/LGALS9/TM6/PTM2/NO22/BPI/TNFAIP3/TWIST1/CCR2/ZC3H12A/FADD/ADIPOQ
GO:1902531	regulation of intracellular signal transduction	115/901	1479/17046	1.42E-05	0.00088	0.00069	CDH13/FARP1/RCAN2/HCS7/NPFR2/CH13L1/CCR1/SEZ6/TNFAIP3/IL31RA/MIB2/CTGF/CYD/ADRB3/NLRP6/DRD4/EGFR/A2M/ESR1/SPATA13/FGA/FGF10/RASA3/FOX/O1/AKR1B1/RHOBTB2/PSD3/PUM2/ARHGAP18/MAPK8IP2/MTOR/ALS2/FGF22/CYTH4/BMP10/GNAS/GPER1/GSTP1/NRGI/IGF1/IGF2/CYR61/IL1RN/IL6/INHBA/ISL1/KDR/HES5/LCK/ARHGAP18/LGALS9/LHCSR/MAP3K1/PILEKHG7/NOV/NRAS/INTF3/ARHGAP18/PIK3CG/PKH1/PLA2G2A/TLR9/ZDHHC13/ARHGAP10/LMBRD1/PRKD1/MAPK3/MAP2K2/PSMB4/PAK6/PSMD7/PILEKHG5/CCR2/ARX/RASGRF2/S100A4/CCL11/CCL17/NO22/SFRP2/ARHGAP9/BMP4/SOX9/STK3/BST2/TNFAIP3/TNFRSF1A/TNXB/TNFAIP5/TWIST1/ZAP70/CXCR4/FZD5/CARD14/NLRX1/SLAZ/FADD/TNFRSF1A/SPHK1/LIMD1/STARD13/MAP3K6/CD8A/TRIP10/ADIPOQ/ARHGAP29/ARHGAP10/RAPGEF2/TELO2/IGSE21/IGF19
GO:0048584	positive regulation of response to stimulus	138/901	1848/17046	1.42E-05	0.00088	0.00069	AB11/CDH3/TANK/TSPAN5/CDH13/CDKN1C/SPON2/HCS7/ESM1/CH13L1/CCR1/MAP3K8/IL31RA/MIB2/MPP7/CTGF/CYD/ADRB3/RNF168/COCH/NLRP6/DMBT1/DRD4/EGFR/A2M/FCGR2A/FGA/FGF10/RASA3/FOXO2/AKR1B1/LARP1/PUM2/MAPK8IP2/MTOR/FGF22/NPTN/MIP10/GNAS/GPER1/FFAR2/GRB10/NRGI/HK1/HLA-B/HLA-DPA1/HLA-E/HLX/HMG1/HSP90AA1/HSP90AB1/RSPO2/IGF1/IGF2/CYR61/IL1RN/IL6/IL12RB2/INHBA/IRF1/ISL1/ITGB2/JUP/KDR/HES5/LCK/LGALS9/LHCSR/SMAD3/MAP3K1/MFNG/NFATC3/NOV/NRAS/INTF3/PARK2/PIK3CG/PLA2G2A/PML/TLR9/ZDHHC13/LIMS2/PAG1/PRKD1/MAPK3/MAP2K2/MASP1/PSMB4/PSMD7/PILEKHG5/CCR2/PXN/RASGRF2/S100A4/CCL11/CCL17/NO22/STRA6/SFRP2/BMP4/BMPRI1B/SOX9/STK3/BST2/TLR5/TNFAIP3/TNFRSF1A/TNFAIP5/TWIST1/WHAG/ZAP70/CXCR4/FZD5/CARD14/BCL2L14/NLRX1/CALR/UNC93B1/SLAZ/HOPX/CDK10/TP63/RUNX3/IRS2/CRADD/FADD/TNFRSF1A/SPHK1/SKAP2/MAP3K6/RSAD2/CD8A/ADIPOQ/LY86/RAPGEF2/CD79A/FGF19
GO:0001501	skeletal system development	48/901	478/17046	1.49E-05	0.00092	0.00072	AB11/CDKN1C/DMRT2/LECT1/CH13L1/SLC38A10/COL11A1/COMP/FAM101A/CTGF/FOXO2/BMP10/GNAS/FLVCR1/ANXA2/HOXB3/HOXC4/HOXC5/HOXC6/HOXD3/RSPO2/FMNI1/IGF1/IGF2/CYR61/HES5/SMAD3/MIEF2/CYTL11/BNC2/CSGALNACT1/MAPK3/BGLAP/SFRP2/BMP4/BMPRI1B/SOX9/ZEB1/TWIST1/WNT10B/Gsof25/SCIN/RUNX1/T/PE3/RUNX3
GO:0042592	homeostatic process	112/901	1434/17046	1.53E-05	0.00093	0.00073	CDH3/TCIRG1/TRDN/ZBTB18/GBB6/ADCV3/EGLN2/CHRNA1/CIDEA/CIN5/CCR1/ZIG16B/ADM/IL31RA/CP51/CTGF/ADRB3/DBB1/BHLHA15/ABAT/DRD4/ESR1/ACIN1/FOXO1/AKR1B1/NEDD4/SLC37A4/DFNB31/STEAP2/NPTN/AMPO2/AMPD3/GNAS/GPER1/FFAR2/FLVCR1/GSTP1/ANXA6/HK1/ACAD/ANME9/IGF1/IL1RN/IL6/AQP2/AQP5/INHBA/AQP9/KC/NH2/KDR/LCK/LDLR/LGALS9/MF1Z/NUBPL/ATP1A2/NOV/OPRL4/ATP5B/PARK2/SIRT6/PDE6B/PIK3CG/PKH1/PML/IL20R8/TLR9/CYTL11/POMC/SLC30A10/CHRNA9/SYBU/PRKAR1B/PRKD1/SJAMF8/TRPC2/RPA3/BGLAP/CCL11/ABHD4/NO22/SGK1/BMP15/SCN4A/SLC8A1/SLC9A3/SOX9/TCEA1/TERF1/TGM2/TNFAIP3/TRPC4/TRPC6/CCR2/CA7/CACNA1E/CXCR4/RANK1/CALR/SH3BGR1/ATP13A4/CASQ1/TP63/IRS2/FADD/TNFRSF1A/LDB2/SMDT1/ADIPOQ/MTLS
GO:0001525	angiogenesis	42/901	398/17046	1.57E-05	0.00094	0.00074	CDH13/LECT1/ESM1/CH13L1/ADM/CTGF/EGR3/EPHA1/EPHA4/FGF10/VASH1/FOXO2/ANXA2/NR4A1/HOXB3/CYR61/IL6/ISL1/KDR/MEOX2/NFATC3/NOV/ATP5B/LEF1/ANGPT4/PIK3CG/PTX2/PML/ROBO4/PARVA/PRKD1/CCL11/SFRP2/BMP4/TNFAIP3/TWIST1/CCR2/FZD5/ZC3H12A/COL18A1/RUNX1/SPHK1
GO:0001503	ossification	38/901	348/17046	1.84E-05	0.0011	0.00086	CCR1/COL11A1/FAM101A/CTGF/EGFR/SNO2/FOXO2/SOX8/D3/RSPO2/IGF1/IGF2/CYR61/IL6/SMAD3/MIEF2/NPPC/ATP5B/LEF1/CSGALNACT1/PRKD1/RDH14/BGLAP/SFRP2/BMP4/SLC8A1/BMPRI1B/SOX9/TWIST1/WNT10B/IFTM1/TP63/RUNX3/TNFRSF1A/LIMD1/RSAD2

GO:0008285	negative regulation of cell proliferation	57/901	608/17046	1.88E-05	0.00111	0.00111	0.00087	AB11/CDH13/CDKN1C/SPEC/GI86/LECT1/B4GAL1/ADM/FGF10/VASH1/MORC3/FBXO2/GPER1/GSTP1/HMGAL1/ZC3H12D/IGF1/IL6/INHBA/IRF1/LGALS9/SMAD3/MCC/NOV/NPPC/ABEN1/SIRT6/ATP8A2/PLA2G2A/PML/RIPPL3/IL20RB/LIMS2/IFT122/PRKRIR/SLURP1/SFRP2/BMP4/BMPR1B/SOX9/STK3/ZE1/TFNAP3/WNT10B/FZD5/LST1/COL18A1/KDM2B/FTIM1/SCN10/RUNX1/RUNX3/ALDH1A2/SKAP2/ADIPOQ/RAPGEF2	57
GO:0031323	regulation of cellular metabolic process	340/901	5352/17046	1.92E-05	0.00112	0.00112	0.00088	9/CIDEA/CCR1/SLC1B1/MMP3/8ZF2P4/ADM/IL13RA/ZNF358/STA/ZNF738/CTGF/SNVD19/CYLD/ADRB3/ESCO2/ZNF782/ZNF709/ZNF781/CITED4/RNF168/ZNF366/BHLH/AL5/NLRP6/DIG2/DNMT3A/DRD4/CEC1/EEF2/EGFR/EGR3/PATL2/EIF4G1/AZM1/ELK1/EPHA1/ESR1/SP8/FGF10/FHIT/XRNI2/RASA3/PPM1E/SBNO2/TRAK1/MRBR2/ACIN1/FOX/L1/FOX2/FOXO1/SPG20/NEDD4/LARP1/PUM2/RFBP/MAPK8IP2/VGLL2/MTOR/GABRR1/RNF144B/ZNF549/PNK0/FBXO2/GAPDH5/PABPC/DNAJC2/FGF22/NPTN/DKK3/BMP10/ZNF638/GNAS/ZNF311/ZNF844/GPER1/DOCK7/GRB10/ZBTB44/DNAJC15/GSTP1/GT2B8/BRE1/GUCY1A3/GZMA/ANXA2/SERPIND1/SOX8/NRG1/HK1/HLX/HMGAL1/NR4A1/ACACB/H/PCA/HOXB3/HOXC4/HOXC6/HOXC8/HRH1/ACAD11/HS90AA1/HS90AA2/TFAP2E/ID3/COL28A1/BARHL2/IGF1/IGF2/CYR61/IL1RN/IL6/IL16/FOKK2/INHBA/IRF1/ISL1/TGFB2/ITIH3/ITIH4/LIP/USP50/HILS1/KDR/KIF25/HESS/AFF3/LCK/LDLR/LGALS9/LHCGR/LMNA/LMO2/1TB/SMAD3/MC2R/ME1/ME2/MEF2D/MAP3K1/MEOX1/MEOX2/MP2/MITF/ALH8/MOVL0/NFATC3/NFYB/NHLH2/NPPC/NRAS/NTF3/ORL1/PALM/PARK2/SPOCK3/LEF1/PRR16/ANGPT4/SIRT6/PGAM2/PI3/PK3CG/PTX2/PKH01/PLA2G2A/PLA2G1/PML/RIPPL3/RIPK4/TLR9/CYTL1/POMC/SSH1/POU2AF1/BNCF/MED18/BANP/PPP1CB/PWILL2/EU3/PRMT6/DNAJC17/ZNF532/PPP2R2B/CNCT11/VAC14/PRKAR1B/GSD1/PRKDI1/MYNN/MAK3/MAP2K2/MRAP/PRMT8/MASPL1/HTRA1/SLAMF8/PSMB4/PAK6/ARNTL2/RGMA/PRDM11/PSMD7/TENM2/GATAD2B/METTL14/CCAR2/PXN/CREBZ/RASGRF2/TRIM27/SC/T/CCL11/CCL17/NPASP3/NOD2/SFRP2/TTRA2B/GZF1/SGK1/BMP4/ZNF649/BMPR1B/BRO9/ZSCAN18/BOK/SOX9/STAT2/STK3/STK10/SUP16H/BST2/TAI4B/TBP/TCEA1/TCEB2/ZE1/T/EAD3/TERF1/TIMP3/TFLE3/TLR5/TNFAIP3/TNFRSF1A/TNKB/TRAF1/TRAFS/PHLDA2/TWIST1/CCR2/TNFRSF4/UCP1/NARS/WNT10B/WYHAG/ZNF7/ZNF124/ZNF177/PAX8/CXCR4/FZD5/RAB7A/CARD14/ZNF665/ZC3H14/ZNF606/ZC3H12A/CPEB4/ZNF436/CALR/SURP/CAST/SCRT1/HIST1H3A/SLA2/ZNF397/NR0B2/HOPX/SPINK7/KDM2B/LOX13/CBX2/GAS7/CDK10/RUNX1/TP63/RUNX3/SERPINA6/IRS2/ACTN1/CRADD/FADD/TNFRSF11A/SPHK1/BLD31/CCNA1/LUMDI1/PIAS3/ZFAND2A/MAP3K6/LDB2/CBFA2T2/AURKB/DAPL1/ADIPOQ/H2AFY/MICAL2/NBP1/VGLL4/RAPGEF2/ILK2/ZBTB39/FGF19/NR1H4	340
GO:0010941	regulation of cell death	109/901	1395/17046	1.98E-05	0.00114	0.00114	0.0009	EGLN2/CARD16/CIDEA/ANKRD9/COMP/MAP3K8/ADM/IL13RA/CTGF/CYLD/DB1/DNMT3A/EGFR/EGR3/ESR1/FGA/FGF10/ACIN1/FOX2/FOXO1/DIP2A/ARHGFB18/GLS2/BMP10/GPER1/GSTP1/GZMA/SOX8/NRG1/HS90AA1/ID3/IGF1/CYR61/IL1RN/IL6/INHBA/ISL1/KDR/LCK/ARHGDI1/KDR/LCK/ARHGDI1/MITF/MIP2/NOV/NITF3/PAFAH2/ARHG/EF3/PARK2/UTP11/LEF1/ANGPT4/PK3/CG/PKH1/PML/LIMS2/PRKDI1/PROC/PSMB4/PAK6/PSMD7/PTGFR/PLEKHG5/MARK4/CCAR2/SFRP2/SCT/NOD2/SFRP2/SGK1/BMP4/BMPR1B/BOK/SOX9/STK3/STK10/ACT1/TERF1/TGM2/TFNAP3/TRAF1/TRAFS/TWIST1/TNFRSF4/WNT10B/WYHAG/PAX8/CARD14/BCL2L14/CPEB4/COL18A1/CALR/CAST/KDM2B/SCN17/TP63/RUNX3/IRS2/ACTN1/CRADD/ALDH1A2/SPHK1/MAP3K6/AURKB/ADIPQ/RAPGEF2	109
GO:0009967	positive regulation of signal transduction	105/901	1334/17046	2.10E-05	0.0012	0.0012	0.00095	CDH3/TPAN5/CDH13/CDKN1C/HCT/ESM1/CH13/1/SMI1/MAP3K8/IL13RA/MIB1/MPP7/CTGF/ADRB3/DRD4/EGFR/FGA/FGF10/RASA3/AKR1B1/PUM2/MAPK8IP2/MTOR/F/GF22/NPTN/BMP10/GNAS/GPER1/GRB10/NRG1/RSP2/IGF1/IGF2/CYR61/IL1RN/IL6/INHBA/ISL1/JUP/KDR/HES5/LCK1/LGALS9/LHCGR/SMAD3/MAP3K1/MFNG/NOV/NRAS/NTF3/PARK2/PK3CG/PLA2G2A/PML/TLR9/ZDHHC13/LIMS2/PAG1/PRKDI1/MAPK3/MAP2K2/PSMB4/PSMD7/PLEKHG5/CCAR2/PXN/RASGRF2/STB00A4/CCL11/CCL17/NOD2/SFRP2/BMP4/BMPR1B/SOX9/STK3/BST2/TLR5/TNFRSF1A/TRAFS/WNT10B/WYHAG/ZAP70/CXCR4/FZD5/CARD14/BCL2L14/SLA2/CDK10/TP63/RUNX3/IRS2/CRADD/FADD/TNFRSF11A/SPHK1/S/KAP2/MAP3K6/RSAD2/CD8A/ADIPOQ/LY86/RAPGEF2/FGF19	105
GO:0060537	muscle tissue development	37/901	338/17046	2.24E-05	0.00127	0.00127	0.001	SPEG/ZBTB18/CHRNA1/COL11A1/SMYD1/FOX2/FLNB/VGLL2/TENM4/BMP10/SOX8/NRG1/HX1/ISL1/LMNA/SMAD3/MEF2D/MEOX2/MYL2/NFATC3/NRAS/LEF1/SIRT6/PTX2/PLA2G11/BN3/STR6A/BMP4/SLC8A1/SOX9/ACT1/TWIST1/WNT10B/CALR/CASO1/TP63/ALDH1A2	37
GO:0045669	positive regulation of osteoblast differentiation	12/901	55/17046	2.36E-05	0.00133	0.00133	0.00104	GNAS/IGF1/CYR61/IL6/NPPC/PRKDI1/SFRP2/BMP4/BMPR1B/WNT10B/ITIM1/TP63	12
GO:0001944	vasculature development	53/901	557/17046	2.46E-05	0.00137	0.00137	0.00108	CDH13/PDPN/LECT1/ESM1/CH13/ADM/CTGF/EGR3/EPHA1/ROBO4/PARVA/PRKD1/ACTA2/CCL11/STR6A/SFRP2/BMP4/TFNAP3/TWIST1/CCR2/FZD5/TMEM204/ZC3H12A/COL18A1/NFATC3/NOV/ATP8B/LEF1/ANGPT4/PK3CG/PTX2/PML/ROBO4/PARVA/PRKD1/ACTA2/CCL11/STR6A/SFRP2/BMP4/TFNAP3/TWIST1/CCR2/FZD5/TMEM204/ZC3H12A/COL18A1/RUNX1/ALDH1A2/SPHK1/RAPGEF2	53
GO:0010243	response to organonitrogen compound	76/901	893/17046	2.51E-05	0.00139	0.00139	0.00109	TCIRG1/NPFFR2/ADCV3/TMEOX1/CHRNA1/CHRNA2/CHRNA3/AP3S1/ADM/CP51/CTGF/CYP11A1/DNMT3A/ABAT/DRD4/AGX1/EGFR/EGR3/EIF4G1/FGA/FGF10/RASA3/FOX2/FOXO1/AKR1B1/MTOR/GATM/FGF22/GNAS/GPER1/GRB10/NRG1/NR4A1/HPCAR/HRH1/HTR3A/IGF2/IL1RN/IL6/AQP9/JUP/PO5/LCK/ATP1A2/NRAS/PARK2/PK3CG/PKM/PRKAG3/TLR9/SSH1/CHRNA9/PRKAR1B/LMBRD1/MAPK3/MAP2K2/PSMB4/PSMD7/PTPRE/PXN/RASGRF2/NOD2/SLC8A1/SOX9/VAMP2/ZEB1/TIMP3/TFNAP3/WNT10B/CPEB4/MGARP/IRS2/A/ADIPQ/RAPGEF2/FGF19/NR1H4	76
GO:0040012	regulation of locomotion	60/901	659/17046	2.71E-05	0.00148	0.00148	0.00117	CDH13/TBRI/CCR1/JEGFR/EPHA1/SPATL3/FGF10/VASH1/SPATL3/FGF10/VASH1/IGF1/CYR61/IL1RN/IL6/IL6/KDR/LAMA3/LGALS9/LMNA/SMAD3/MCC/MAP3K1/NOV/NITF3/P2RY6/LEF1/ANGPT4/PTX2/ROBO4/ELP3/PRKDI1/MAP2K2/FAM60A/CCL11/NOD2/SFRP2/SGK1/BMP4/SLC8A1/SOX9/STK10/BST2/PHLDA2/TWIST1/CCR2/PTP441/CXCR4/COL18A1/CALB/SH3BGRL3/SCRT1/PAR6B/ITIM1/IRS2/FADD/SPHK1/ADIPOQ/RAPGEF2	60
GO:0045321	leukocyte activation	59/901	647/17046	3.03E-05	0.00164	0.00164	0.00129	CHGA/MAP3K8/IL13RA/CYLD/DDOST/RNF168/EGR3/JUNC13D/FGF10/SBNO2/FLOT2/MTOR/HLA-DQA1/HLA-DPA1/HLA-E/HLX/ZC3H12D/IGF1/INHBA/IRF1/ITGB2/LCK/LCP1/LGALS9/SMAD3/NFATC3/IL21R/LEF1/PK3CG/IL2ORB/APBB1IP/PAG1/PTPRE/NOD2/CXCR5/BMP4/BPI/SUPT6H/BST2/VAMP2/ZEB1/TNFAIP3/CCR2/TNFRSF4/ZNF70/CXCR4/FZD5/LST1/ZC3H12A/SLA2/IRS2/FADD/SKAP2/RSAD2/CD8A/CD79A	59

GO:0045667	17/901	105/17046	3.43E-05	0.00173	0.00136	GNAS/ID3/IGF1/CYR61/L6/SWAD3/NPPC/PRKD1/SFRP2/BMP4/BMPRI1/TWIST1/WNT10B/IFITM1/TP63/LIMD1/PIAS2	17
GO:1901700	112/901	1462/17046	3.53E-05	0.00177	0.00139	TCIRG1/SPON2/GIB6/NPFR2/ADC3/AP33/CNP/ADM/CP51/CTGF/CYP11A1/DNMT3A/ABAT/DRD4/AGXT/EGFR/EGR3/EIF4G1/EPAH3/ESR1/FGA/FGF10/RASA3/SBNO2/FOXCF2/FOXCI/AXR1/AKR1B1/MILCI/MTOR/GATM/GA3/FGF22/GIB2/GNAS/GPER1/FPAR2/GRB10/GSTP1/NRG1/NR4A1/HPCA/HSD17B2/HTR3A/HTR5A/IGF2/IL1R1/IL1RN/L6/LOR4/AQP2/IL12RB2/INHBA/AQP9/JUP/KCNJ8/PO5/LCK/LGALS9/MEJ1/ATP1A2/NPPC/NRAS/OPRL1/P2RY6/PARK2/LEF1/PIK3CG/SSH1/CHRNA9/M/P2K2/PSMB4/PSMD7/PTGFR/PTPR/PTRE/PXN/RASGRF2/BGLAP/NOD2/BMP4/SLC8A1/SOX9/VAMP2/ZEB1/ACTC1/TIMP3/TLR5/TNFAIP3/TPRC6/ITRMP6/WTNT10B/CACNA1E/ZC3H12A/CFEB4/COL18A1/CALB/NR0B2/TRIM63/MGARPR/RS2/TNFRSF11A/ALDH1A2/ADIPQO/LY86/RAPGEF2/FGF19/NR1H4	112
GO:0014070	67/901	768/17046	3.60E-05	0.00179	0.0014	ADC3/CHRNA1/CHRNA2/CHRNA5/CIDEA/ADM/CP51/CTGF/CYP11A1/CITED4/ZNF366/DNMT3A/ABAT/DRD4/AGXT/EGFR/EGR3/ESR1/FGA/FGF10/MILCI/GIB2/GNAS/GPER1/GUC	67
GO:0042692	37/901	346/17046	3.73E-05	0.00184	0.00144	Y1A3/NRAA1/HPCA/HRH1/HSP90A1/HTR3A/HTR5A/IL1RN/IL6/INHBA/AQP9/ISL1/JUP/KCNJ8/ACAT1/LOX/SWAD3/ATP1A2/OPRL1/P2RY6/PARK2/LEF1/PIK3CG/SSH1/CHRNA9/M/SPG/ADM/SWYD1/BH1H415/FGF10/FLT2/SYNE1/MTOR/BMP10/TMOD4/SOX8/NRG1/ID3/IGF1/IGF2/ISL1/LMNA/MYL2/NEFATC3/NOV/NTEF3/LEF1/PTX2/BIN3/CCL17/BMP4/SLC37/8A1/SOX9/SUPTB1/ZEB1/ACTC1/WNT10B/TMEM204/CALB/CAST/CASQ1/HOPX	37
GO:0023056	112/901	1467/17046	4.07E-05	0.00199	0.00156	CDH3/TSPAN5/CDH13/CDKN1C/TRDN/HCT1/ESM1/CH1B1/CCR1/MAP3K8/IL13RA/MIB2/MPP7/CTGF/CYLD/ADR83/ABAT/DRD4/EGFR/FGA/FGF10/RASA3/AKR1B1/LARP1/PUM2/MAPK8IP2/MTOR/FGF22/NPTN/BMP10/GNAS/GPER1/GRB10/NRG1/RSP02/IGF1/IGF2/CYR61/IL1RN/IL6/INHBA/ISL1/JUP/KDR/HES5/LCK/LGALS9/LHCGR/SMAD3/MAP3K1/MFNG/NOV/NRAS/NTEF3/PARK2/PIK3CG/PLA2G2A/PML/TLR9/ZDHHC13/UMSZ/PAG1/PRKD1/NAKPK3/MAP2K2/PSMB4/PSMD7/PLEKHG5/CCAR2/PXN/RASGRF2/S100A4/SC1/CCL11/CCL17/NOD2/SFRP2/BMP4/BMPRI1/SOX9/STK3/BST2/VAMP2/TLR5/TNFRSF1A/TRAFA5/WNT10B/CALB/NR0B2/TRIM63/MGARPR/AE1/ALDH1A2/ADIPQO/RAPGEF2/CDK10/TP63/RUNX3/IRS2/CRADD/FADD/TNFRSF11A/SPHK1/SKAP2/MAP3K6/RSAD2/CD8A/ADIPQO/LY86/RAPGEF2/FGF19	112
GO:0010647	113/901	1485/17046	4.32E-05	0.00209	0.00164	CDH3/TSPAN5/CDH13/CDKN1C/TRDN/HCT1/ESM1/CH1B1/CCR1/MAP3K8/IL13RA/MIB2/MPP7/CTGF/CYLD/ADR83/ABAT/DRD4/EGFR/FGA/FGF10/RASA3/AKR1B1/LARP1/PUM2/MAPK8IP2/MTOR/FGF22/NPTN/BMP10/GNAS/GPER1/GRB10/NRG1/RSP02/IGF1/IGF2/CYR61/IL1RN/IL6/INHBA/ISL1/JUP/KDR/HES5/LCK/LGALS9/LHCGR/SMAD3/MAP3K1/MFNG/NOV/NRAS/NTEF3/PARK2/PIK3CG/PLA2G2A/PML/TLR9/ZDHHC13/UMSZ/PAG1/PRKD1/NAKPK3/MAP2K2/PSMB4/PSMD7/PLEKHG5/CCAR2/PXN/RASGRF2/S100A4/SC1/CCL11/CCL17/NOD2/SFRP2/BMP4/BMPRI1/SOX9/STK3/BST2/VAMP2/TLR5/TNFRSF1A/TRAFA5/WNT10B/WHAG/ZAP70/CA7/CXR4/FZD5/CARD14/BC1L14/SLA2/NR0B2/CDK10/TP63/RUNX3/IRS2/CRADD/FADD/TNFRSF11A/SPHK1/SKAP2/MAP3K6/RSAD2/CD8A/ADIPQO/LY86/RAPGEF2/FGF19	113
GO:0051241	76/901	908/17046	4.40E-05	0.00211	0.00166	CDH3/MRV1/LECT1/CIDEA/CCR1/SEZ6/ADM/FAM101A/CYLD/ADR83/TRPV3/F11/FGA/VASH1/FOXCF2/SFG2/BMP10/GNAS/GSTP1/GUCY1A3/ANXA2/SOX8/HIX/ID3/RSP02/IGF1/IL6/INHBA/IRF1/ISL1/HES5/ARHGAP10/GALNS9/SMAD3/MCC/ATP1A2/NOV/NPPC/NRAS/LEF1/CEND1/ANGPT4/PIK3CG/PML/IL20RB/TLR9/POMC/LIMS2/IFT122/PROC/TRIM27/SCT/NOV2/SFRP2/BMP4/SULT1/SOX9/BPT/STK3/BST2/TNFAIP3/TWIST1/CCR2/TNFRSF4/PXN/NLRX1/ZC3H12A/RAB11/FP1/CALR/RUNX1/TP63/LIMD1/CBFAZT2/ADIPQO/RAPGEF2/ULK2	76
GO:0009889	252/901	3834/17046	4.52E-05	0.00211	0.00166	CTGF/ZNF783/CDH13/CDKN1C/C1D/ZBTB18/DVMT2/CELF1/TBR1/NPFR2/PNRC1/HNRNPUL1/ERLIN2/PSIP1/EGLN2/ZBED9/CIDEA/SLC15B/ZFP42/ADM/IL13RA/ZNF358/ZNF738/N2/SBNO2/TRAK1/MSR82/FOXO1/FOXO2/ZNF782/ZNF709/ZNF781/CITED4/RNF168/ZNF366/BHLHA15/DNMT3A/DRD4/EEF2/EGFR/EGR3/PATL2/EIF4G1/ELK4/ESR1/SP8/FGF10/HHIT/XR844/GPER1/GRB10/ZBTB44/GSTP1/GTF2B/BRF1/GUCY1A3/SOX8/NRG1/HLX/HMGA1/NRAA1/HPCA/HOXB3/HOX4/HOX5/HOX6/HOX3/HRH1/ACAC1/ACAC2/ACAC3/ACAC4/ACAC5/ACAC6/ACAC7/ACAC8/ACAC9/ACAC10/ACAC11/ACAC12/ACAC13/ACAC14/ACAC15/ACAC16/ACAC17/ACAC18/ACAC19/ACAC20/ACAC21/ACAC22/ACAC23/ACAC24/ACAC25/ACAC26/ACAC27/ACAC28/ACAC29/ACAC30/ACAC31/ACAC32/ACAC33/ACAC34/ACAC35/ACAC36/ACAC37/ACAC38/ACAC39/ACAC40/ACAC41/ACAC42/ACAC43/ACAC44/ACAC45/ACAC46/ACAC47/ACAC48/ACAC49/ACAC50/ACAC51/ACAC52/ACAC53/ACAC54/ACAC55/ACAC56/ACAC57/ACAC58/ACAC59/ACAC60/ACAC61/ACAC62/ACAC63/ACAC64/ACAC65/ACAC66/ACAC67/ACAC68/ACAC69/ACAC70/ACAC71/ACAC72/ACAC73/ACAC74/ACAC75/ACAC76/ACAC77/ACAC78/ACAC79/ACAC80/ACAC81/ACAC82/ACAC83/ACAC84/ACAC85/ACAC86/ACAC87/ACAC88/ACAC89/ACAC90/ACAC91/ACAC92/ACAC93/ACAC94/ACAC95/ACAC96/ACAC97/ACAC98/ACAC99/ACAC100/ACAC101/ACAC102/ACAC103/ACAC104/ACAC105/ACAC106/ACAC107/ACAC108/ACAC109/ACAC110/ACAC111/ACAC112/ACAC113/ACAC114/ACAC115/ACAC116/ACAC117/ACAC118/ACAC119/ACAC120/ACAC121/ACAC122/ACAC123/ACAC124/ACAC125/ACAC126/ACAC127/ACAC128/ACAC129/ACAC130/ACAC131/ACAC132/ACAC133/ACAC134/ACAC135/ACAC136/ACAC137/ACAC138/ACAC139/ACAC140/ACAC141/ACAC142/ACAC143/ACAC144/ACAC145/ACAC146/ACAC147/ACAC148/ACAC149/ACAC150/ACAC151/ACAC152/ACAC153/ACAC154/ACAC155/ACAC156/ACAC157/ACAC158/ACAC159/ACAC160/ACAC161/ACAC162/ACAC163/ACAC164/ACAC165/ACAC166/ACAC167/ACAC168/ACAC169/ACAC170/ACAC171/ACAC172/ACAC173/ACAC174/ACAC175/ACAC176/ACAC177/ACAC178/ACAC179/ACAC180/ACAC181/ACAC182/ACAC183/ACAC184/ACAC185/ACAC186/ACAC187/ACAC188/ACAC189/ACAC190/ACAC191/ACAC192/ACAC193/ACAC194/ACAC195/ACAC196/ACAC197/ACAC198/ACAC199/ACAC200/ACAC201/ACAC202/ACAC203/ACAC204/ACAC205/ACAC206/ACAC207/ACAC208/ACAC209/ACAC210/ACAC211/ACAC212/ACAC213/ACAC214/ACAC215/ACAC216/ACAC217/ACAC218/ACAC219/ACAC220/ACAC221/ACAC222/ACAC223/ACAC224/ACAC225/ACAC226/ACAC227/ACAC228/ACAC229/ACAC230/ACAC231/ACAC232/ACAC233/ACAC234/ACAC235/ACAC236/ACAC237/ACAC238/ACAC239/ACAC240/ACAC241/ACAC242/ACAC243/ACAC244/ACAC245/ACAC246/ACAC247/ACAC248/ACAC249/ACAC250/ACAC251/ACAC252/ACAC253/ACAC254/ACAC255/ACAC256/ACAC257/ACAC258/ACAC259/ACAC260/ACAC261/ACAC262/ACAC263/ACAC264/ACAC265/ACAC266/ACAC267/ACAC268/ACAC269/ACAC270/ACAC271/ACAC272/ACAC273/ACAC274/ACAC275/ACAC276/ACAC277/ACAC278/ACAC279/ACAC280/ACAC281/ACAC282/ACAC283/ACAC284/ACAC285/ACAC286/ACAC287/ACAC288/ACAC289/ACAC290/ACAC291/ACAC292/ACAC293/ACAC294/ACAC295/ACAC296/ACAC297/ACAC298/ACAC299/ACAC300/ACAC301/ACAC302/ACAC303/ACAC304/ACAC305/ACAC306/ACAC307/ACAC308/ACAC309/ACAC310/ACAC311/ACAC312/ACAC313/ACAC314/ACAC315/ACAC316/ACAC317/ACAC318/ACAC319/ACAC320/ACAC321/ACAC322/ACAC323/ACAC324/ACAC325/ACAC326/ACAC327/ACAC328/ACAC329/ACAC330/ACAC331/ACAC332/ACAC333/ACAC334/ACAC335/ACAC336/ACAC337/ACAC338/ACAC339/ACAC340/ACAC341/ACAC342/ACAC343/ACAC344/ACAC345/ACAC346/ACAC347/ACAC348/ACAC349/ACAC350/ACAC351/ACAC352/ACAC353/ACAC354/ACAC355/ACAC356/ACAC357/ACAC358/ACAC359/ACAC360/ACAC361/ACAC362/ACAC363/ACAC364/ACAC365/ACAC366/ACAC367/ACAC368/ACAC369/ACAC370/ACAC371/ACAC372/ACAC373/ACAC374/ACAC375/ACAC376/ACAC377/ACAC378/ACAC379/ACAC380/ACAC381/ACAC382/ACAC383/ACAC384/ACAC385/ACAC386/ACAC387/ACAC388/ACAC389/ACAC390/ACAC391/ACAC392/ACAC393/ACAC394/ACAC395/ACAC396/ACAC397/ACAC398/ACAC399/ACAC400/ACAC401/ACAC402/ACAC403/ACAC404/ACAC405/ACAC406/ACAC407/ACAC408/ACAC409/ACAC410/ACAC411/ACAC412/ACAC413/ACAC414/ACAC415/ACAC416/ACAC417/ACAC418/ACAC419/ACAC420/ACAC421/ACAC422/ACAC423/ACAC424/ACAC425/ACAC426/ACAC427/ACAC428/ACAC429/ACAC430/ACAC431/ACAC432/ACAC433/ACAC434/ACAC435/ACAC436/ACAC437/ACAC438/ACAC439/ACAC440/ACAC441/ACAC442/ACAC443/ACAC444/ACAC445/ACAC446/ACAC447/ACAC448/ACAC449/ACAC450/ACAC451/ACAC452/ACAC453/ACAC454/ACAC455/ACAC456/ACAC457/ACAC458/ACAC459/ACAC460/ACAC461/ACAC462/ACAC463/ACAC464/ACAC465/ACAC466/ACAC467/ACAC468/ACAC469/ACAC470/ACAC471/ACAC472/ACAC473/ACAC474/ACAC475/ACAC476/ACAC477/ACAC478/ACAC479/ACAC480/ACAC481/ACAC482/ACAC483/ACAC484/ACAC485/ACAC486/ACAC487/ACAC488/ACAC489/ACAC490/ACAC491/ACAC492/ACAC493/ACAC494/ACAC495/ACAC496/ACAC497/ACAC498/ACAC499/ACAC500/ACAC501/ACAC502/ACAC503/ACAC504/ACAC505/ACAC506/ACAC507/ACAC508/ACAC509/ACAC510/ACAC511/ACAC512/ACAC513/ACAC514/ACAC515/ACAC516/ACAC517/ACAC518/ACAC519/ACAC520/ACAC521/ACAC522/ACAC523/ACAC524/ACAC525/ACAC526/ACAC527/ACAC528/ACAC529/ACAC530/ACAC531/ACAC532/ACAC533/ACAC534/ACAC535/ACAC536/ACAC537/ACAC538/ACAC539/ACAC540/ACAC541/ACAC542/ACAC543/ACAC544/ACAC545/ACAC546/ACAC547/ACAC548/ACAC549/ACAC550/ACAC551/ACAC552/ACAC553/ACAC554/ACAC555/ACAC556/ACAC557/ACAC558/ACAC559/ACAC560/ACAC561/ACAC562/ACAC563/ACAC564/ACAC565/ACAC566/ACAC567/ACAC568/ACAC569/ACAC570/ACAC571/ACAC572/ACAC573/ACAC574/ACAC575/ACAC576/ACAC577/ACAC578/ACAC579/ACAC580/ACAC581/ACAC582/ACAC583/ACAC584/ACAC585/ACAC586/ACAC587/ACAC588/ACAC589/ACAC590/ACAC591/ACAC592/ACAC593/ACAC594/ACAC595/ACAC596/ACAC597/ACAC598/ACAC599/ACAC600/ACAC601/ACAC602/ACAC603/ACAC604/ACAC605/ACAC606/ACAC607/ACAC608/ACAC609/ACAC610/ACAC611/ACAC612/ACAC613/ACAC614/ACAC615/ACAC616/ACAC617/ACAC618/ACAC619/ACAC620/ACAC621/ACAC622/ACAC623/ACAC624/ACAC625/ACAC626/ACAC627/ACAC628/ACAC629/ACAC630/ACAC631/ACAC632/ACAC633/ACAC634/ACAC635/ACAC636/ACAC637/ACAC638/ACAC639/ACAC640/ACAC641/ACAC642/ACAC643/ACAC644/ACAC645/ACAC646/ACAC647/ACAC648/ACAC649/ACAC650/ACAC651/ACAC652/ACAC653/ACAC654/ACAC655/ACAC656/ACAC657/ACAC658/ACAC659/ACAC660/ACAC661/ACAC662/ACAC663/ACAC664/ACAC665/ACAC666/ACAC667/ACAC668/ACAC669/ACAC670/ACAC671/ACAC672/ACAC673/ACAC674/ACAC675/ACAC676/ACAC677/ACAC678/ACAC679/ACAC680/ACAC681/ACAC682/ACAC683/ACAC684/ACAC685/ACAC686/ACAC687/ACAC688/ACAC689/ACAC690/ACAC691/ACAC692/ACAC693/ACAC694/ACAC695/ACAC696/ACAC697/ACAC698/ACAC699/ACAC700/ACAC701/ACAC702/ACAC703/ACAC704/ACAC705/ACAC706/ACAC707/ACAC708/ACAC709/ACAC710/ACAC711/ACAC712/ACAC713/ACAC714/ACAC715/ACAC716/ACAC717/ACAC718/ACAC719/ACAC720/ACAC721/ACAC722/ACAC723/ACAC724/ACAC725/ACAC726/ACAC727/ACAC728/ACAC729/ACAC730/ACAC731/ACAC732/ACAC733/ACAC734/ACAC735/ACAC736/ACAC737/ACAC738/ACAC739/ACAC740/ACAC741/ACAC742/ACAC743/ACAC744/ACAC745/ACAC746/ACAC747/ACAC748/ACAC749/ACAC750/ACAC751/ACAC752/ACAC753/ACAC754/ACAC755/ACAC756/ACAC757/ACAC758/ACAC759/ACAC760/ACAC761/ACAC762/ACAC763/ACAC764/ACAC765/ACAC766/ACAC767/ACAC768/ACAC769/ACAC770/ACAC771/ACAC772/ACAC773/ACAC774/ACAC775/ACAC776/ACAC777/ACAC778/ACAC779/ACAC780/ACAC781/ACAC782/ACAC783/ACAC784/ACAC785/ACAC786/ACAC787/ACAC788/ACAC789/ACAC790/ACAC791/ACAC792/ACAC793/ACAC794/ACAC795/ACAC796/ACAC797/ACAC798/ACAC799/ACAC800/ACAC801/ACAC802/ACAC803/ACAC804/ACAC805/ACAC806/ACAC807/ACAC808/ACAC809/ACAC810/ACAC811/ACAC812/ACAC813/ACAC814/ACAC815/ACAC816/ACAC817/ACAC818/ACAC819/ACAC820/ACAC821/ACAC822/ACAC823/ACAC824/ACAC825/ACAC826/ACAC827/ACAC828/ACAC829/ACAC830/ACAC831/ACAC832/ACAC833/ACAC834/ACAC835/ACAC836/ACAC837/ACAC838/ACAC839/ACAC840/ACAC841/ACAC842/ACAC843/ACAC844/ACAC845/ACAC846/ACAC847/ACAC848/ACAC849/ACAC850/ACAC851/ACAC852/ACAC853/ACAC854/ACAC855/ACAC856/ACAC857/ACAC858/ACAC859/ACAC860/ACAC861/ACAC862/ACAC863/ACAC864/ACAC865/ACAC866/ACAC867/ACAC868/ACAC869/ACAC870/ACAC871/ACAC872/ACAC873/ACAC874/ACAC875/ACAC876/ACAC877/ACAC878/ACAC879/ACAC880/ACAC881/ACAC882/ACAC883/ACAC884/ACAC885/ACAC886/ACAC887/ACAC888/ACAC889/ACAC890/ACAC891/ACAC892/ACAC893/ACAC894/ACAC895/ACAC896/ACAC897/ACAC898/ACAC899/ACAC900/ACAC901/ACAC902/ACAC903/ACAC904/ACAC905/ACAC906/ACAC907/ACAC908/ACAC909/ACAC910/ACAC911/ACAC912/ACAC913/ACAC914/ACAC915/ACAC916/ACAC917/ACAC918/ACAC919/ACAC920/ACAC921/ACAC922/ACAC923/ACAC924/ACAC925/ACAC926/ACAC927/ACAC928/ACAC929/ACAC930/ACAC931/ACAC932/ACAC933/ACAC934/ACAC935/ACAC936/ACAC937/ACAC938/ACAC939/ACAC940/ACAC941/ACAC942/ACAC943/ACAC944/ACAC945/ACAC946/ACAC947/ACAC948/ACAC949/ACAC950/ACAC951/ACAC952/ACAC953/ACAC954/ACAC955/ACAC956/ACAC957/ACAC958/ACAC959/ACAC960/ACAC961/ACAC962/ACAC963/ACAC964/ACAC965/ACAC966/ACAC967/ACAC968/ACAC969/ACAC970/ACAC971/ACAC972/ACAC973/ACAC974/ACAC975/ACAC976/ACAC977/ACAC978/ACAC979/ACAC980/ACAC981/ACAC982/ACAC983/ACAC984/ACAC985/ACAC986/ACAC987/ACAC988/ACAC989/ACAC990/ACAC991/ACAC992/ACAC993/ACAC994/ACAC995/ACAC996/ACAC997/ACAC998/ACAC999/ACAC1000/ACAC1001/ACAC1002/ACAC1003/ACAC1004/ACAC1005/ACAC1006/ACAC1007/ACAC1008/ACAC1009/ACAC1010/ACAC1011/ACAC1012/ACAC1013/ACAC1014/ACAC1015/ACAC1016/ACAC1017/ACAC1018/ACAC1019/ACAC1020/ACAC1021/ACAC1022/ACAC1023/ACAC1024/ACAC1025/ACAC1026/ACAC1027/ACAC1028/ACAC1029/ACAC1030/ACAC1031/ACAC1032/ACAC1033/ACAC1034/ACAC1035/ACAC1036/ACAC1037/ACAC1038/ACAC1039/ACAC1040/ACAC1041/ACAC1042/ACAC1043/ACAC1044/ACAC1045/ACAC1046/ACAC1047/ACAC1048/ACAC1049/ACAC1050/ACAC1051/ACAC1052/ACAC1053/ACAC1054/ACAC1055/ACAC1056/ACAC1057/ACAC1058/ACAC1059/ACAC1060/ACAC1061/ACAC1062/ACAC1063/ACAC1064/ACAC1065/ACAC1066/ACAC1067/ACAC1068/ACAC1069/ACAC1070/ACAC1071/ACAC1072/ACAC1073/ACAC1074/ACAC1075/ACAC1076/ACAC1077/ACAC1078/ACAC1079/ACAC1080/ACAC1081/ACAC1082/ACAC1083/ACAC1084/ACAC1085/ACAC1086/ACAC1087/ACAC1088/ACAC1089/ACAC1090/ACAC1091/ACAC1092/ACAC1093/ACAC1094/ACAC1095/ACAC1096/ACAC1097/ACAC1098/ACAC1099/ACAC1100/ACAC1101/ACAC1102/ACAC1103/ACAC1104/ACAC1105/ACAC1106/ACAC1107/ACAC1108/ACAC1109/ACAC1110/ACAC1111/ACAC1112/ACAC1113/ACAC1114/ACAC1115/ACAC1116/ACAC1117/ACAC1118/ACAC1119/ACAC1120/ACAC1121/ACAC1122/ACAC1123/ACAC1124/ACAC1125/ACAC1126/ACAC1127/ACAC1128/ACAC1129/ACAC1130/ACAC1131/ACAC1132/ACAC1133/ACAC1134/ACAC1135/ACAC1136/ACAC1137/ACAC1138/ACAC1139/ACAC1140/ACAC1141/ACAC1142/ACAC1143/ACAC1144/ACAC1145/ACAC1146/ACAC1147/ACAC1148/ACAC1149/ACAC1150/ACAC1151/ACAC1152/ACAC1153/ACAC1154/ACAC1155/ACAC1156/ACAC1157/ACAC1158/ACAC1159/ACAC1160/ACAC1161/ACAC1162/ACAC1163/ACAC1164/ACAC1165/ACAC1166/ACAC1167/ACAC1168/ACAC1169/ACAC1170/ACAC1171/ACAC1172/ACAC1173/ACAC1174/ACAC1175/ACAC1176/ACAC1177/ACAC1178/ACAC1179/ACAC1180/ACAC1181/ACAC1182/ACAC1183/ACAC1184/ACAC1185/ACAC1186/ACAC1187/ACAC1188/ACAC1189/ACAC1190/ACAC1191/ACAC1192/ACAC1193/ACAC1194/ACAC1195/ACAC1196/ACAC1197/ACAC1198/ACAC1199/ACAC1200/ACAC1201/ACAC1202/ACAC1203/ACAC1204/ACAC1205/ACAC1206/ACAC1207/ACAC1208/ACAC1209/ACAC1210/ACAC1211/ACAC1212/ACAC1213/ACAC1214/ACAC1215/ACAC1216/ACAC1217/ACAC1218/ACAC1219/ACAC1220/ACAC1221/ACAC1222/ACAC1223/ACAC1224/ACAC1225/ACAC1226/ACAC1227/ACAC1228/ACAC1229/ACAC1230/ACAC1231/ACAC1232/ACAC1233/ACAC1234/ACAC1235/ACAC1236/ACAC1237/ACAC1238/ACAC1239/ACAC1240/ACAC1241/ACAC1242/ACAC1243/ACAC1244/ACAC1245/ACAC1246/ACAC1247/ACAC1248/ACAC1249/ACAC1250/ACAC1251/ACAC1252/ACAC1253/ACAC1254/ACAC1255/ACAC1256/ACAC1257/ACAC1258/ACAC1259/ACAC1260/ACAC1261/ACAC1262/ACAC1263/ACAC1264/ACAC1265/ACAC1266/ACAC1267/ACAC1268/ACAC1269/ACAC1270/ACAC1271/ACAC1272/ACAC1273/ACAC1274/ACAC1275/ACAC1276/ACAC1277/ACAC1278/ACAC1279/ACAC1280/ACAC1281/ACAC1282/ACAC1283/ACAC1284/ACAC1285/ACAC1286/ACAC1287/ACAC1288/ACAC1289/ACAC1290/ACAC1291/ACAC1292/ACAC1293/ACAC1294/ACAC1295/ACAC1296/ACAC1297/ACAC1298/ACAC1299/ACAC1300/ACAC1301/ACAC1302/ACAC1303/ACAC1304/ACAC1305/ACAC1306/ACAC1307/ACAC1308/ACAC1309/ACAC1310/ACAC1311/ACAC1312/ACAC1313/ACAC1314/ACAC1315/ACAC1316/ACAC1317/ACAC1318/ACAC1319/ACAC1320/ACAC1321/ACAC1322/ACAC1323/ACAC1324/ACAC1325/ACAC1326/ACAC1327/ACAC1328/ACAC1329/ACAC1330/ACAC1331/ACAC1332/ACAC1333/ACAC1334/ACAC1335/ACAC1336/ACAC1337/ACAC1338/ACAC1339/ACAC1340/ACAC1341/ACAC1342/ACAC1343/ACAC1344/ACAC1345/ACAC1346/ACAC1347/ACAC1348/ACAC1349/ACAC1350/ACAC1351/ACAC1352/ACAC1353/ACAC1354/ACAC1355/ACAC1356/ACAC1357/ACAC1358/ACAC1359/ACAC1360/ACAC1361/ACAC1362/ACAC1363/ACAC1364/ACAC1365/ACAC1366/ACAC1367/ACAC1368/ACAC1369/ACAC1370/ACAC1371/ACAC1372/ACAC1373/ACAC1374/ACAC1375/ACAC1376/ACAC1377/ACAC1378/ACAC1379/ACAC1380/ACAC1381/ACAC1382/ACAC1383/ACAC1384/ACAC1385/ACAC1386/ACAC1387/ACAC1388/ACAC1389/ACAC1390/ACAC1391/ACAC1392/ACAC1393/ACAC1394/ACAC1395/ACAC1396/ACAC1397/ACAC1398/ACAC1399/ACAC1400/ACAC1401/ACAC1402/ACAC1403/ACAC1404/ACAC1405/ACAC1406/ACAC1407/ACAC1408/ACAC1409/ACAC1410/ACAC1411/ACAC1412/ACAC1413/ACAC1414/ACAC1415/ACAC1416/ACAC1417/ACAC1418/ACAC1419/ACAC1420/ACAC1421/ACAC1422/ACAC1423/ACAC1424/ACAC1425/ACAC1426/ACAC1427/ACAC1428/ACAC1429/ACAC1430/ACAC1431/ACAC1432/ACAC1433/ACAC1434/ACAC1435/ACAC1436/ACAC1437/ACAC1438/ACAC1439/ACAC1440/ACAC1441/ACAC1442/ACAC1443/ACAC1444/ACAC1445/ACAC1446/ACAC1447/ACAC1448/ACAC1449/ACAC1450/ACAC1451/ACAC1452/ACAC1453/ACAC1454/ACAC1455/ACAC1456/ACAC1457/ACAC1458/ACAC1459/ACAC1460/ACAC1461/ACAC1462/ACAC1463/ACAC1464/ACAC1465/ACAC1466/ACAC1467/ACAC1468/ACAC1469/ACAC1470/ACAC1471/ACAC1472/ACAC1473/ACAC1474/ACAC1475/ACAC1476/ACAC1477/ACAC1478/ACAC1479/ACAC1480/ACAC1481/ACAC1482/ACAC1483/ACAC1484/ACAC1485/ACAC1486/ACAC1487	

GO:0045778	positive regulation of ossification	14/901	79/17046	6.02E-05	0.00264	0.00207	GNAS/IGF1/CYR61/IL6/SMAD3/NPPC/PRKD1/SFRP2/BMP4/SLC8A1/BMP1B/WNT10B/IFTM1/TP63	14
GO:0045597	positive regulation of cell differentiation	66/901	768/17046	6.48E-05	0.00282	0.00222	CCR1/SEZ6/ADM/CTGF/SMYD1/DMBT1/EGFR3/EIF4G1/JUNC13D/EPHA3/FGA/ACIN1/NEED4L/MTOR/TENM4/MPTN/BMP10/GNAS/GPER1/SOX8/NRG1/HLX/HOXD3/IGF1/CYR61/IL6/INHBA/KDR/LCK/ARHGDI1/LGALS9/SMAD3/NEU1/NPPC/PALM/PARK2/LEF1/ATP8A2/PLA2G2A/PML/PRKD1/MAIP2K2/SFRP2/BMP4/BMPR1B/SOX9/STKS2/EEB1/TEAD3/TWIST1/WNT10B/ZAP70/PAX8/CXCR4/ZC3H12A/CALR/HOPX/IFTM1/SCN/RUNX1/TP63/FADD/CBFA2T2/ADIPOQ/H2AFY/RAPGEF2	66
GO:0044281	small molecule metabolic process	166/901	2375/17046	6.81E-05	0.00294	0.00231	LC/CTGF/PNMT1/MBOAT1/ADRB3/CPY11A1/ADA1/DIO3/DLG3/DNMT3A/ABAT/DRD4/AGXT/ENOS1/ALAS1/FAH/FHIT/FOXO1/AKR1B1/NUP210/MTOR/FOXA1/SLC37A4/GABRR1/P/KO/ACOT11/GATM/GAPDH5/AMPD2/PDE7B/DKK3/SLZ5/AMPD3/DHHD/GNAS/THES1/GURJ/GRB10/DNAJC15/GSTP1/GUCY1A3/NNME7/PADI1/HAS1/HKI1/ACACB/HPCA/HRH1/HSD11B1/ACADL/HSP90AA1/NNME5/IGF1/IGF2/IL1RN/IL6/INP5A/ACAT1/DLIR/ILHGR/MC2R/ME1/ME2/MGAT1/NDUFT1/MYH4/NUBP1/NDUFB4/NEU1/ATP1A2/NFYB/NPPO/AS2/OPRL1/ATP5B/PALM/PARK2/SPOCK3/CHST15/PDE4C/PCYOX1/PDE7A/SIRT6/PDE6B/PGAM2/PIK3CG/PKMX/PLA2G2A/PKAG3/SLCO1C1/PNLP/CYTL1/POMC/PON1/CYP2W1/LPCAT2/PPP1CB/PPP1CC/SPMPD3/VAC14/PRKAR1B/LMBRD1/CSGALNACT1/PRKD1/APOBR/MAPK3/MRAP/PSMB4/PSMD7/RDH14/SCT/STRA6/CERK/SLC4A1/VAMP2/TNFRSF1A/TNXX8/PHLDA2/TWIST1/CCR2/UCP1/UPT1/VARS/CA7/CACNA1E/PAX8/CEERS4/QTIRT1/NROB2/RAE1/KMO/HS2/ALDH1A2/SYND1/SPHK1/CH25H/SLC16A3/ADIPOQ/ENTPD3/NUP93/IGATT1/FGF19/NR1H4	166
GO:0001568	blood vessel development	50/901	536/17046	6.89E-05	0.00295	0.00232	CDH13/LECT1/ESM1/CH1B1/ADM/CTGF/EGFR3/EPHA1/EPH4/FGF10/VASH1/FOXO2/FOXO1/FLVCR1/ANXA2/NR4A1/HOXB3/CYR61/IL6/ISL1/ITGA7/KDR/LOX/MEOX2/NFATC3/NO5/V/ATP5B/LEF1/ANGPT4/PIK3CG/PTX2/PML/ROBO4/PARVA/PRKD1/ACTA2/CCL11/STRA6/SFRP2/BMP4/TNFAIP3/TWIST1/CCR2/FZD5/ZC3H12A/COL18A1/RUNX1/ALDH1A2/SPHK1/RAPGEF2	50
GO:0022603	regulation of anatomical structure morphogenesis	70/901	830/17046	7.01E-05	0.00298	0.00234	PDPN/DNMT2/TBR1/LECT1/CH1B1/ADM/SH3D3/CYLD/COCH/JUNC13D/EPHA1/EPHA3/ESR1/FGA/FGF10/VASH1/FOXO2/SPG20/EPH413/NEED4L/ARHGFE18/TENM4/GAS2/BMP10/SOX8/SPPO2/IBARHL2/IL1RN/IL6/ISL1/ITGA7/ITGB2/KDR/ARHGDI1/SMAD3/MIF2/PALM/PARK2/LEF1/ANGPT4/PML/SSH1/FBLIM1/PALMD/UMS2/PARVA/PRKD1/MAIP2K2/CDC42SE1/ERMN/PXN/CCL11/SFRP2/BMP4/SOX9/TNFAIP3/TWIST1/CCR2/PAX8/LST1/CALR/CAPZB/TTBK1/GAS7/RUNX1/SPHK1/LUMDI/ADIPOQ/RAPGEF2/ULK2	70
GO:0019220	regulation of phosphate metabolic process	117/901	1568/17046	7.23E-05	0.00305	0.0024	ABLI/FARP1/CDKN1C/NFPR2/ADCY3/CH1B1/CCR1/MAP3K8/ADM/IL13RA/CTGF/ADRB3/NLRP6/DLG2/DRD4/EGFR/EPHA1/FGA/FGF10/RAS/AS3/PRM1E/FOXO1/MAPK8IP2/MTOR/GABRR1/GAPDH5/FGF22/NPTN/BMP10/GNAS/GPER1/DOK7/GRB10/DNAJC15/GSTP1/GUCY1A3/ANXA2/NRG1/HPCA/HRH1/HSP90AB1/IGF1/IGF2/CYR61/IL1RN/IL6/INHBA/ISL1/TGB2/KDR/HES5/LCK/LDLR/LGALS9/LHGR/SMAD3/MC2R/ME1/ME2/MAP3K1/NPPC/NRAS/NTF3/OPRL1/PALM/PARK2/ANGPT4/SIRT6/PGAM2/PIK3CG/PKHD1/PLA2G2A/PML/TLR9/ELP3/PPP2R2B/VAC14/PRKAR1B/PRKD1/MAPK3/MAP2K2/MRAP/SLAMF8/PSMB4/PAK6/PSMD7/PXN/PASGRF2/TRIM27/SCT/CCL11/CCL17/NOD2/SFRP2/BMP4/SOX9/STK3/STK10/TNFAIP3/TNFRSF1A/TNXX8/TWIST1/CCR2/TNFRSF4/YWHAG5/CXCR4/FZD5/CDK10/IRS2/TNFRSF11A/SPHK1/MAP3K6/ADIPOQ/H2AFY/RAPGEF2/FGF19	117
GO:0006753	nucleoside phosphate metabolic process	56/901	624/17046	7.43E-05	0.00311	0.00245	GNE/TCIRG1/NPFR2/ADCY3/ACOT7/CNP/APOA1BP/ADM/ADRB3/ADAL/DLG2/DRD4/ENO2/FHIT/GABRR1/GAPDH5/AMPD2/PDE7B/AMPD3/GNAS/GPER1/DNAJC15/GUCY1A3/NME7/HKI1/ACACB/HPCA/NNME9/IGF1/LHGR/MC2R/ME1/ME2/MGAT1/NDUFT1/MYH4/NDUFB4/ATP1A2/NPPC/OAS2/OPRL1/ATP5B/PALM/PDE6B/PDE6B/PGAM2/PKM/CSGALNACT1/MRAP/SCT/UCP1/KMO/ENTPD3	56
GO:0070371	ERK1 and ERK2 cascade	27/901	228/17046	7.47E-05	0.00311	0.00245	CH1B1/CCR1/CTGF/NLRP6/EGFR/FGA/FGF10/GPER1/GSTP1/IGF1/CYR61/IL6/KDR/LGALS9/PKHD1/PLA2G2A/MAPK3/MAIP2K2/CCL11/CCL17/NOD2/BMP4/SOX9/TNFRSF11A/ADIP2/OQ/RAPGEF2/FGF19	27
GO:0071407	cellular response to organic cyclic compound	37/901	359/17046	8.15E-05	0.00337	0.00265	ADCY3/CP51/CYP11A1/EGFR/EGFR3/ESR1/FGA/MLC1/GNAS/GPER1/NR4A1/HRH1/HSP90AB1/IL1RN/IL6/INHBA/AQP9/ISL1/JUP/SMAD3/ATP1A2/P2RY6/PARK2/LEF1/PIK3CG/SSH1/BGLAP/BMP4/SLC8A1/WNT10B/NROB2/TRIM63/MGARP/RAE1/ADIPOQ/RAPGEF2/NR1H4	37
GO:0019221	cytokine-mediated signaling pathway	48/901	512/17046	8.49E-05	0.00349	0.00274	CCR1/IL13RA/EIF4G1/FLNB/NUP210/GSTP1/HLA-B/HLA-DPA1/HLA-E/HLA-F/HSP90AB1/IL1RN/IL6/IL10RA/IL11RA/IL12RB2/IL15RA/IRF1/LTB/OAS2/IL21R/PARK2/PML/IL20RB/MAPK3/PSMB4/PSMD7/CCL11/CCL17/CXCR5/STAT2/BS2/TNFRSF1A/CIR2/TNFRSF4/CXCR4/CARD14/IL1F10/RAE1/IFTM1/FADD/TNFRSF11A/SPHK1/CCR2/RSAD2/ADIPOQ/NUP93	48
GO:0033993	response to lipid	65/901	761/17046	8.81E-05	0.00359	0.00283	SPON2/GIB6/ADCY3/CNP/ADM/CP51/CTGF/CYP11A1/GTID4/ZNF366/DNMT3A/DRD4/AGXT/EGFR/EPHA3/ESR1/FGA/FGF10/SBNO2/MLC1/GIB2/GNAS/GPER1/FFAR2/GSTP1/NR4A1/HSD17B2/HTRA5/IL1RN/IL6/IL10RA/IL12RB2/INHBA/ISL1/KCNJ8/LGALS9/LOX/ATP1A2/OPRL1/P2RY6/LEF1/PTX2/PON1/MAPK3/PTGFR/BGLAP/NOD2/BMP4/SLC9A3/SOX9/TNFAIP3/TNFAIP3/WNT10B/RAB7A/ZC3H12A/CALR/NROB2/TRIM63/MGARP/TNFRSF11A/ALDH1A2/ADIPOQ/LY86/NR1H4	65

GO:0008152	metabolic process	624/901	10817/17046	9.98E-05	0.00386	0.00304	AKT3/ABI1/CDH3/GNE/ZNF783/TSPAN5/CDH13/SUGP2/MBNL2/FARP1/RCAN2/CDKN1C/SPEG/BCKDK/TCIRG1/ABCAN9/C1D7/ZBTB18/PTTRM1/MTTH5/PDPN/DWRT2/CELF1/CELF2/7 BR1/HCS7/NPFRR2/ADCY3/PNRC1/TMED10/SLC27A2/LECT1/ADAM25/9HNRNP/UL1/RPP1/CH13/1/ERLUN2/PSIP1/CH13/2/EGLN2/84GALT7/RF12/ACOTT7/EXOC3/ADPRH11 /CARD16/ZBED9/CIDEA/GBP4/ALPK2/GALNT15/C1CA1/CLNS/MRPL52/CRR1/SLC15/1/CNP/ADAC3/APOA1B/NEU4/ADOC3/CO111A1/GALM/MAP3K8/ZFP42/ADM/IL13RA/EGFL AM/UBLCP1/HUS1B/CPD/CPM/CP51/NDUFAT6/PXDNL/CRABP1/ZNF358/TRPM6/MB12/PARP4/LDLRAD3/BSG1CT/MGAT5B/CSTA/KLC3/ZNF738/CTGF/SMYD1/PPM1L/SH3D19/CYB 561/CYLD/MBON1/ADRB3/ESCO2/CYP11A1/ZNF782/FTM1/ADAL/ZNF709/ZNF781/CTEDA/DDB1/ONRF2/DDOST/RFNF168/ZNF366/BLH1A15/NLRP6/DIO3/DL2/DNAH6/DNAH 8/DNMT3A/ABAT/DPH1/DRD4/EEF1/AGT7/EGFR/EGR3/PATL2/EF4G1/A2M/ELK4/LPH/DNAH12/FENQ2/ADK3/EPHA3/EPH4/ESR1/ALAS1/F11/FAH/SPATA13/PRSS 54/RFNF182/PHACTR1/SP8/FGA/FGF10/FHIT/XRN2/RASA3/PPM1E/SBNQ2/TRAK1/MRNB2/ACIN1/FOXJ1/FOXJ2/TBC1D9B/FOXO1/AKR1B1/GGAG3/DIP2A/FLT2/TBC1D1/NUP210/ ATP11A/NEED4L/PSD3/LARP1/PUN2/ARHGFE18/RYPB/MORC3/MAPK8IP2/TSSK2/NGLL2/MTOR/FUCA1/SLC37A4/GABB81/PASGEF1C/RNF144B/ZNF549/5T6GALNAC3/GAK/SAM M50/ALS2/CPND/TENM4/ACOT11/LTN1/RGS22/STEA2/FBXL21/FBXO2/LCE2B/SAC2/MGAT1/GGAT5/GBG17/GAD7/H5/SLC17A5/RFS6K1/PABPC1/DNAJC2/FGF22/NPTN/AMPD2/PDE7B /DK3/CYTH4/GLS2/VPS4A/AMPD3/DHDB/BMP10/ZNF638/GNAS/ZNF311/TMPRSS12/PIGW/ZNF844/THYM5/GPER/YEOT/DOCK7/GRB10/MRPS188/ZBTB44/DNAJC15/GSTP1/GT F2B/BRF1/GUCY1A3/NME7/PADI1/GZMA/ANXAZ/HAS4/SERPIND1/SOX8/NRG1/HK1/HLX/HMGA1/NR4A1/ACACB/HPCA/MPBA2/HOXB3/HOXC5/HOXD3/AGFG2/H RH1/HSD11B1/HSD17B2/ACAD11/HSP90A1/HSP90A1/DUPD1/ADAMT15/TFAP2E/ID3/ZC3H12D/COZ28A1/FMNI1/BAHR12/NME9/IGF1/IGF2/CYR61/LCE1C/LCE1D/LCE2 D/ILRN/IL6/IL12RB2/PRSS41/IL16/FOXK2/INHA/INPP5A/RE1/AOP9/ISL1/TIGB2/ITIH3/ITIH4/IVL/IUP/USP50/HILS1/ATP9B/KCNH2/KDR/ACAT1/KIF25/PO5/MRT15/HES5/AFF3/L CK/MUC21/ILDR/ARHGDI1/GALS9/LHCGR/ILGL1/LMNA/LMO2/LOX1/TB/SMAD3/MC2R/MEI1/ME2/MEF2D/MAP3K1/MEK1/MEDK2/MF12/MFNQ/MGAT1/MITF/LHX8/MOCS1/ MOV10/PLEKHG7/NUDT1/MYH4/NUBP1/NDUFB4/DRG1/NEU1/ATP1A2/INFAT3/CFYB/NHLH2/NOV/NPPC/NRAS/NTF3/OAS2/OPRL1/PAFAH2/ATP5B/PALM/ARHGFE3/PARK2/SP OCK3/UTP11L/LEF1/DDX47/PRR16/CHST15/ANGPT4/PDE4C/PCYOX1/PDE7A/SIRT6/PDE6B/ATP8A2/GALNT7/PGAM2/P13/PI3C/PIK3CG/PI3TX2/PKH01/PKM/PLA2G2A/PLAGL1/PRK AG3/PML/RIPPL3/SLC1C1/PNLI/PIPK4/TLR9/TREM1/CTY11/POMC/SSH1/PONI/RINZ/MOVI01/NOF2/UF1Z/DHHC13/BNC2/JMED18R/CYP2Z1/RRP25/LPCAT2/IBANP/PPP1CB/HE M/NN/APOBB/MAPK3/MAP2K2/PROC/MRAP/PRMT8/MASP1/HTRA1/SLAMF8/CD425E1/PSMB4/PAK6/ARNTL2/RGMA/PRDM11/PSMD7/PTGER/PLEKHG5/TENM2/GATA2B/KL HL/RDHL4/METTL4/MARK4/CCAR2/PTPR/PXN/CREBZF/ABHD17C/ACTA2/RASGRF2/RFC2/TRIM27/RGR/RGS12/EXOC4/RP3/RPL8/RPL29/SCY/CCL11/CCL17/ABHD4/MRPS14/P RS22/NPAS3/NOD2/STRA6/SFRP2/MAP1L3B2/ARHGAP9/TRA2B/GZE1/DNAI2/SGK1/MICAL1/CERK/VPS33A/BMP4/SLCAA1/ZNF649/BMPR1B/BRD9/ZSCAN18/BOK/SOX9/SRFB8/ STAT2/STK3/STK10/SUPT6H/BST2/NAVMP2/TAH48/TBP/CEA1/TCB2/ZEB1/ACTL1/TEAD3/TEF1/TGM2/TIMP3/TLB5/TNFAIP3/TNFRSF1A/TNXB/TRAF1/TRA5/TPRM2/PHL A2/TWIST1/CCR2/TNFRSF4/UCP1/UPP1/VARS/MG2/ZNF67/ZNF7/CA7/ZNF124/ZNF177/CACNA1E/PTPA41/MOOS/PXAR3/CXCR4/FZD5/RAB7A/ER13/CARD14/GOPD3/C ERS4/ZNF665/EPHX3/ZC3H14/ERMP1/TMEM62/ZNF606/ZC3H12A/FAAP100/CEB4/COL18A1/ZNF436/FEEDF1/CALR/OTRT1/SLRP/CAPS/COLO/CAST/SH3BGR3/SCRT1/HIST1H3A/ DYNLBB2/SLA2/ATP13A4/ZNF397/NR0B2/HOPX/TBK1/SPINK7/TRIM63/KDM2B/LOXL3/GTBPB3/CBX2/RAE1/GAS7/CDK10/KMO/RUNX1/TP63/RUNX3/SERPINA6/IRS3/ACTN1/CR ADD/FADD/TNFRSF11A/ALDH1A2/STK19/SYND1/SPHK1/BJUD31/CCNA1/ENDOU1/STBD1/LMD1/CH25H/ERH1/STARD13/PIAS2/ZFAND2A/MAP3K6/LDB2/SLC16A3/CBEA2T/RSAD2/ AURKB/DAP1/CCDC102A/NEURL3/SDR42E1/ADIPOQ/ARHGAP29/RAB3D/H2AFY/ENTPD3/PREPL/ARHGFE10/MICAL2/N4BP1/VGLL4/NUP93/RAPGEF2/ULK2/USP6NL/ZBTB39/RAB GAP1/QSOX1/UPGAT1/FGF19/NR1H4
GO:0002062	chondrocyte differentiation	15/901	93/17046	0.0001	0.00392	0.00308	COL11A1/FAM101A/CTGF/SMAD3/MEF2D/NOV/NPPC/CYLL1/SFRP2/BMP4/BMPR1B/SOX9/WNT10B/SCIN/RUNX3
GO:0009117	nucleotide metabolic process	55/901	617/17046	0.0001	0.00392	0.00308	GNE7/CIRG1/NPFRR2/ADCY3/ACOTT/CNP/APOA1B/ADM/ADR83/ADAL/DL2G2/DRD4/ENO2/FHIT/GABBR1/GAPDH5/AMPD2/PDE7B/AMPD3/GNAS/GPER1/DNAJC15/GUCY1A3/N ME7/HK1/ACACB/HPCA/NME9/IGF1/LHCGR/MC2R/ME1/ME2/MGAT1/NUDT1/MYH4/NDUF84/ATP1A2/NPPC/OAS2/OPRL1/ATP5B/PALM/PDE4C/PDE7A/SIRT6/PDE6B/PGAM2/P KM/CSSGALNACT1/MRAP/SCT/CCR2/UPP1/KMO
GO:0006935	chemotaxis	67/901	796/17046	0.00011	0.004	0.00315	CDH13/SPON2/TBRI1/CHGA/CCR1/CO19A3/EFNA2/EGFR/EGR3/EPHA1/EPHA3/EPH4/FGF10/RASAS/NFASC/FGF22/FFAR2/SERPIND1/NRGI/NR4A1/HRH1/HSP90A1/HSP90AB1/ CYR61/IL6/IL16/IL17/ITGB2/KDR/LGALS9/SMAD3/NOV/NRAS/NTF3/LEF1/PIK3CG/TREM1/PARVA/PRKDJ1/MAPK3/MAP2K2/PSMB4/RGMA/TRPC7/PSMD7/PLEKHG5/TENM2/RASG REF2/CCL11/CCL17/NOD2/CXCR5/BMP4/BMPR1B/SLIT1/TPRC4/TPRC6/CCR2/CACNB2/CXCR4/CALR/RUNX3/IRS2/TNFRSF11A/CCR2/RAPGEF2/FGF19
GO:0042330	taxis	67/901	796/17046	0.00011	0.004	0.00315	CDH13/SPON2/TBRI1/CHGA/CCR1/CO19A3/EFNA2/EGFR/EGR3/EPHA1/EPHA3/EPH4/FGF10/RASAS/NFASC/FGF22/FFAR2/SERPIND1/NRGI/NR4A1/HRH1/HSP90A1/HSP90AB1/ CYR61/IL6/IL16/IL17/ITGB2/KDR/LGALS9/SMAD3/NOV/NRAS/NTF3/LEF1/PIK3CG/TREM1/PARVA/PRKDJ1/MAPK3/MAP2K2/PSMB4/RGMA/TRPC7/PSMD7/PLEKHG5/TENM2/RASG REF2/CCL11/CCL17/NOD2/CXCR5/BMP4/BMPR1B/SLIT1/TPRC4/TPRC6/CCR2/CACNB2/CXCR4/CALR/RUNX3/IRS2/TNFRSF11A/CCR2/RAPGEF2/FGF19
GO:0048878	chemical homeostasis	77/901	949/17046	0.00011	0.00407	0.0032	TCIRG1/TRDN/GIB6/ADCY3/CLN5/CCR1/ADM/CP51/DOB1/BLH1A15/DRD4/ESR1/ADAM1/NEED4L/SLC37A4/STEA2/NPTN/GNAS/GPER1/FFAR2/FLVCR1/GSTP1/ANXAG/HK1/ACAD L/IGF1/IL1R1/IL6/AOP2/AOP5/AOP9/KCNH2/KDR/LCK/LDLR/MR/NUBP1/ATP1A2/OPRL1/ATP5B/PARK2/SIRT6/PDE6B/PK3CG/PKH01/PML/POMC/SLC30A10/CHRNA9/SYBU/PRK AR/IB/PRKDJ1/SLAMF8/TRPC7/CCL11/ABHD4/SK1/BMP4/SLCAA1/SLC8A1/SLC9A3/TGM2/TRPC4/TRPC6/CCR2/CA7/CACNA1E/CXCR4/RAB7A/CALR/ATP13A4/CASQ1/TP63/IRS2/S MDT1/ADIPOQ/MTL5
GO:0048514	blood vessel morphogenesis	45/901	475/17046	0.00011	0.00408	0.00321	CDH13/LECT1/ESM1/CHBL1/ADM/CTGF/EGR3/EPHA1/EPH4/FGF10/WASH1/FOXK2/ANXA2/NR4A1/HOXB3/CYR61/IL6/ISL1/ITGA7/KDR/MEK2/NFATC3/NOV/ATP5B/LEF1/ANGRP 4/PK3CG/PTX2/PML/ROBO4/PARVA/PRKDJ/CCL11/STR46/SFRP2/BMP4/TNFAIP3/TWIST1/CCR2/FZD5/ZC3H12A/COL18A1/RUNX1/SPHK1/RAPGEF2
GO:0014706	striated muscle tissue development	34/901	324/17046	0.00011	0.00408	0.00321	SPEG/ZBTB18/CHRNA1/CO11A1/SMYD1/FOXK2/FLNB/VGLL1/TENM4/BMP4/NOV/SOX8/NRGI/HLX/IL1/IL1A/SMAD3/MEF2D/MEK2/MLY2/NFATC3/NRAS/LEF1/SIRT6/PTX2/PLA GL1/BN3/BMP4/SLC8A1/ACTC1/TWIST1/WNT10B/CALR/CASQ1/ALDH1A2

GO:0018130	heterocycle biosynthetic process	253/901	3911/17046	0.00013	0.00447	0.00352	ZNF783/CDH13/CDKN1C/TCIRG1/C1D/ZBTB18/MTFHS/DMRT2/TBR1/NPFRZ/ADCY3/PNRC1/HNRNPUL1/ERLIN2/PSIP1/EGLN2/ACOT7/ZBED9/CIDEA/ZFP42/ADM/IL3/RA/CP51/0/NF358/ZNF738/CTGF/SMYD1/CYLD/ADRB3/ZNF781/CTE4/DDB1/NNF1/68/ZNF366/BLHA15/DNMT3A/DRD4/EGFR/EGR3/ELK4/ESR1/ALAS1/SP8/FGF10/FHIT/XRN2/SBNO2/TRAK1/MSR82/FOXO1/NUP210/NEED4/RVBP/GABBR1/ZNF549/DNAJC2/AMPD2/DK3/GLS2/AMPD3/BMP10/ZNF638/GNAS/ZN F311/ZNF844/GPER1/ZBTB44/GTF2B/BRE1/GUCY1A3/NME7/SOX8/NRG1/HLX/HMGCA1/ACACB/HPC4/HOXC6/HOXD3/TFAP2E/ID3/BARHL2/NMIE9/IGF1/IGF2/CYR61/IL6/IL16/FOXK2/INHBA/IRF1/ISL1/JUP/USP50/HLS1/HESS/AFF3/LGAL59/LHCGR/LMO2/SMAD3/MC2N3/ME1/MEF2D/MEOX1/MEOX2/MITE/LHX8/MOCS1/MOV1/0/DRG1/NFATC3/NFYB/NHLH2/NPC/NTF3/OAS2/OPRL1/ATP5B/PALM/PARK2/LEF1/SIRT6/PKHD1/PKAG3/PRK4/RIPL3/PRKAG3/PRK4/RIPL3/CYTL1/POMC/POU2AF1/BNC2/MED18/RP43/RP18/PLP29/SC/TPAS3/NOD2/SFRP2/GZF1/SGK1/BMP4/ZNF649/BMPRL1/BRD9/ZSCAN18/SOX9/STAT1/2/STK3/SUPT6H/TAFA48/TBP/TCEA1/TCEB2/ZEB1/TEAD3/TERF1/TFE1/TFE3/TFNFAIP3/TFNFRS4/TRAFF1/TRAFF5/TFWIST1/UCP1/UPP1/WNT10B/YWHAG/ZNF124/ZNF177/PAH8/FZD5/CARD14/ZNF665/ZNF606/ZC3H12A/ZNF436/CALB/QTRT1/SLURP/SCRT1/HIST1H3A/SLA2/ZNF397/NR0B2/HOPX/KDM2B/LOX3/CBX2/RAE1/GAST/KMO/RUNX1/TP63/RUNX3/ACTN1/FADD/TNFRSF11A/SPHK1/BDU31/CCNA1/LIMD1/PIAS2/LDB2/CBFA27/AURKB/ADIPQ/H2AFY/MICAL2/VGLL4/NUP93/ZBTB39/NR1H4
GO:0043207	response to external biotic stimulus	67/901	802/17046	0.00013	0.00448	0.00352	SPON2/GJBE/HNRNPUL1/CHGA/CNP/ADM/CP51/CY11A1/COCH/NLRP6/DMBT1/UNC13D/FGA/FGF10/SBNO2/ACINI/PUW2/SIC37/AA/GSTP1/GUCY1A3/HLA-B/HLA-E/HMGCA1/IL1RN/IL6/IL1LORA/IL2RB2/IRF1/KCNJ8/STMN1/LCK/LGAL59/SMAD3/OAS2/PLA2G2A/PML/TLRS/TREM1/MAPK3/HTRA1/SLAMF8/PTGER/CREBZ/ACTA2/DEFB134/CCL11/NOD2/BPI/STAT2/BST2/TLRS/TFNFAIP3/TNFRSF1A/CA7/CCR4/FZD5/NLRX1/ZC3H12A/UNC93B1/HIST1H3A/HITM1/FADD/TNFRSF11A/RSAD2/CD8A/XY86/NUP93
GO:0051707	response to other organism	67/901	802/17046	0.00013	0.00448	0.00352	SPON2/GJBE/HNRNPUL1/CHGA/CNP/ADM/CP51/CY11A1/COCH/NLRP6/DMBT1/UNC13D/FGA/FGF10/SBNO2/ACINI/PUW2/SIC37/AA/GSTP1/GUCY1A3/HLA-B/HLA-E/HMGCA1/IL1RN/IL6/IL1LORA/IL2RB2/IRF1/KCNJ8/STMN1/LCK/LGAL59/SMAD3/OAS2/PLA2G2A/PML/TLRS/TREM1/MAPK3/HTRA1/SLAMF8/PTGER/CREBZ/ACTA2/DEFB134/CCL11/NOD2/BPI/STAT2/BST2/TLRS/TFNFAIP3/TNFRSF1A/CA7/CCR4/FZD5/NLRX1/ZC3H12A/UNC93B1/HIST1H3A/HITM1/FADD/TNFRSF11A/RSAD2/CD8A/XY86/NUP93
GO:0019438	aromatic compound biosynthetic process	253/901	3915/17046	0.00014	0.00469	0.00369	NF358/ZNF738/CTGF/SMYD1/CYLD/ADRB3/ZNF781/CTE4/DDB1/NNF1/68/ZNF366/BLHA15/DNMT3A/DRD4/EGFR/EGR3/ELK4/ESR1/ALAS1/SP8/FGF10/FHIT/XRN2/SBNO2/TRAK1/MSR82/FOXO1/NUP210/NEED4/RVBP/GABBR1/ZNF549/DNAJC2/AMPD2/DK3/GLS2/AMPD3/BMP10/ZNF638/GNAS/ZN F311/ZNF844/GPER1/ZBTB44/GTF2B/BRE1/GUCY1A3/NME7/SOX8/NRG1/HLX/HMGCA1/ACACB/HPC4/HOXC6/HOXD3/TFAP2E/ID3/BARHL2/NMIE9/IGF1/IGF2/CYR61/IL6/IL16/FOXK2/INHBA/IRF1/ISL1/JUP/USP50/HLS1/HESS/AFF3/LGAL59/LHCGR/LMO2/SMAD3/MC2N3/ME1/MEF2D/MEOX1/MEOX2/MITE/LHX8/MO10/DRG1/NFATC3/NFYB/NHLH2/NPC/NTF3/OAS2/OPRL1/ATP5B/PALM/PARK2/LEF1/SIRT6/PKHD1/PKAG3/PRK4/RIPL3/PRKAG3/PRK4/RIPL3/CYTL1/POMC/POU2AF1/BNC2/MED18/RP43/RP18/PLP29/SC/TPAS3/NOD2/SFRP2/GZF1/SGK1/BMP4/ZNF649/BMPRL1/BRD9/ZSCAN18/SOX9/STAT1/2/STK3/SUPT6H/TAFA48/TBP/TCEA1/TCEB2/ZEB1/TEAD3/TERF1/TFE1/TFE3/TFNFAIP3/TFNFRS4/TRAFF1/TRAFF5/TFWIST1/UCP1/UPP1/WNT10B/YWHAG/ZNF124/ZNF177/PAH8/FZD5/CARD14/ZNF665/ZNF606/ZC3H12A/ZNF436/CALB/QTRT1/SLURP/SCRT1/HIST1H3A/SLA2/ZNF397/NR0B2/HOPX/KDM2B/LOX3/CBX2/RAE1/GAST/KMO/RUNX1/TP63/RUNX3/ACTN1/FADD/TNFRSF11A/SPHK1/BDU31/CCNA1/LIMD1/PIAS2/LDB2/CBFA27/AURKB/ADIPQ/H2AFY/MICAL2/VGLL4/NUP93/RAPGEF2/ZBTB39/NR1H4
GO:0006163	purine nucleotide metabolic process	45/901	480/17046	0.00014	0.00469	0.00369	TCIRG1/NPFRZ/ADCY3/ACOT7/ADM/ADRB3/DLG2/DRD4/ENO2/FHIT/GABBR1/GAPDH5/AMPD2/PDE7B/AMPD3/GNAS/GPER1/DNAJC15/GUCY1A3/NMIE7/HK1/ACACB/HPCA/NMIE9/IGF1/LHCGR/MC2R/NUDT1/MYH4/NDUFB4/ATP1A2/NPPC/OAS2/OPRL1/ATP5B/PALM/PDE4C/PDE7A/SIRT6/PDE68/PGAM2/PKM/MRAP/SCT/CCR2
GO:0030155	regulation of cell adhesion	52/901	581/17046	0.00014	0.00475	0.00373	CDH13/MAP3K8/EGFLAM/CYLD/EGR3/UNC13D/EPHA1/EPHA3/FGA/FOXK2/FLTOTZ/MTOR/CYTH4/NR6G1/HLA-DOA/HLA-DPA1/HLA-E/HLX/ZC3H12D/FMN1/IGF1/IGF2/CYR61/IL1RN/IL6/IRF1/KDR/LAMA3/LCK/ARHGAP14/GALS9/SMAD3/MF12/ATP5B/LEF1/PIK3CG/PML/IL20RB/APBB1/PPP/PCB/PAG1/NOD2/SR P2/BMP4/SOX9/ZEB1/TGM2/CCR2/ZAP70/CALR/FADD/ADIPQ
GO:0034654	nucleobase-containing compound biosynthetic process	249/901	3846/17046	0.00014	0.00476	0.00374	ZNF783/CDH13/CDKN1C/TCIRG1/C1D/ZBTB18/DMRT2/TBR1/NPFRZ/ADCY3/PNRC1/HNRNPUL1/ERLIN2/PSIP1/EGLN2/ACOT7/ZBED9/CIDEA/ZFP42/ADM/IL3/RA/ZNF358/ZNF738/CTGF/SMYD1/CYLD/ADRB3/ZNF781/CTE4/DDB1/NNF1/68/ZNF366/BLHA15/DNMT3A/DRD4/EGFR/EGR3/ELK4/ESR1/SP8/FGF10/FHIT/XRN2/SBNO2/TR AK1/MSR82/FOXO1/NUP210/NEED4/RVBP/GABBR1/ZNF549/DNAJC2/AMPD2/DK3/GLS2/AMPD3/BMP10/ZNF638/GNAS/ZNF311/ZNF844/GPER1/ZBTB44/GTF2B/BRE1/GUCY1A3/NME7/SOX8/NRG1/HLX/HMGCA1/NR4A1/ACACB/HPC4/HOXB3/HOXC6/HOXD3/TFAP2E/ID3/BARHL2/NMIE9/IGF1/IGF2/CYR61/IL6/IL16/FOXK2/INHBA/IRF1/ISL1/JUP/USP50/HLS1/HESS/AFF3/LGAL59/LHCGR/LMO2/SMAD3/MC2N3/ME1/MEF2D/MEOX1/MEOX2/MITE/LHX8/MO10/DRG1/NFYB/NHLH2/NPC/NTF3/OAS2/OPRL1/ATP5B/PALM/PARK2/LEF1/SIRT6/PKHD1/PKAG3/PRK4/RIPL3/PRKAG3/PRK4/RIPL3/CYTL1/POMC/POU2AF1/BNC2/MED18/BANP/ELP3/P RMT6/DNAJC17/ZNF532/CNOT11/PRKDI/MYNN/MAPK3/MRAP/PRMT8/PAK6/ARNTL2/RGMA/PRDM11/TEMM2/GATAD2B/CCAR2/CREBZ/RFC2/TRIM27/R 29/SC/TPAS3/NOD2/SFRP2/GZF1/SGK1/BMP4/ZNF649/BMPRL1/BRD9/ZSCAN18/SOX9/STAT1/2/STK3/SUPT6H/TAFA48/TBP/TCEA1/TCEB2/ZEB1/TFE1/TFE3/TFNFAIP3/TFN FRS4/TRAFF1/TRAFF5/TFWIST1/UCP1/UPP1/WNT10B/YWHAG/ZNF124/ZNF177/PAH8/FZD5/CARD14/ZNF665/ZNF606/ZC3H12A/ZNF436/CALB/QTRT1/SLURP/SC RT1/HIST1H3A/SLA2/ZNF397/NR0B2/HOPX/KDM2B/LOX3/CBX2/RAE1/GAST/KMO/RUNX1/TP63/RUNX3/ACTN1/FADD/TNFRSF11A/SPHK1/BDU31/PIAS2/LDB2/CB FA27/AURKB/ADIPQ/H2AFY/MICAL2/VGLL4/NUP93/ZBTB39/NR1H4
GO:0009260	ribonucleotide biosynthetic process	28/901	251/17046	0.00016	0.00515	0.00405	TCIRG1/NPFRZ/ADCY3/ACOT7/ADM/ADRB3/DRD4/GABBR1/AMPD2/AMPD3/GNAS/GPER1/GUCY1A3/NMIE7/ACACB/HPCA/NMIE9/LHCGR/MC2R/NPPC/OPRL1/ATP5B/PALM/PK W/MRAP/SCT/CCR2/UPP1

GO:0071345	cellular response to cytokine stimulus	56/901	642/17046	0.00016	0.00515	0.00405	CHI3L1/CCL11/IL13RA/CYP11A1/EIF4G1/FGA/SBN2/FLNB/NUP210/GPER1/GSTP1/HLA-B/HLA-DPA1/HLA-E/HLA-F/HSP90AB1/IL1R1/IL1RN/IL16/IL10RA/IL12RB2/IL15RA/IRF1/LGALS9/IT1B/OAS2/IT1B/PARK2/LEF1/PML/IL20RB/MAPK3/PSMB4/PSMD7/CCL11/CCL17/CXCR5/SOX9/STAT2	56
GO:0001775	cell activation	71/901	868/17046	0.00016	0.00516	0.00406	/BST2/TNFRSF1A/CXCR2/TNFRSF4/CXCR4/CARD14/IL1F10/RAE1/JFITM1/FADD/TNFRSF1A/SPHK1/CCL2/RSAD2/ADIPQO/NUIP3 CHGA/MAP3K8/IL13RA/CTGF/CYLD/WBP2NL/DSD01/RNF168/EGR3/AQM1/CD3D/FGA/FGF10/SBN2/FLT2/MTOR/GNAS/SCG3/HLA-DOA/HLA-DPA1/HLA-E/HLX/ZCH312D/IGF1/IGF2/IL6/INHBA/IRF1/ITGB2/LCK/LCP1/LGALS9/SMAD3/NFATC3/IL21R/LEF1/PIK3CG/IL20RB/APBB1IP/PAG1/MAPK3/TRPC7/SURP1/PTPRE/NOD2/CXCR5/B	71
GO:0034097	response to cytokine	62/901	732/17046	0.00016	0.00522	0.00411	MPA/BPI/SUPT6H/BST2/NVAMP2/ZEB1/TNFAIP3/TRPC6/CCR2/TNFRSF4/ZAP70/CXCR4/FZD5/LST1/ZC3H12A/CAS1/SLAZ/ACTN1/FADD/SKAP2/RSAD2/CD8A/CD79A	62
GO:0060255	regulation of macromolecule metabolic process	327/901	5249/17046	0.00016	0.00563	0.00417	CHI3L1/CCL11/IL13RA/CYP11A1/DOO1/EIF4G1/FGA/SBN2/FLNB/NUP210/GPER1/GSTP1/HLA-B/HLA-DPA1/HLA-E/HLA-F SOX9/STAT2/BST2/TIMP3/TNFRSF1A/CCR2/TNFRSF4/CXCR4/CARD14/IL1F10/RAE1/JFITM1/FADD/TNFRSF1A/ALDH1A2/SPHK1/CCR2/RSAD2/ADIPQO/NUIP3	327
GO:0061138	morphogenesis of a branching epithelium	23/901	189/17046	0.00017	0.00563	0.00417	AB11/CDC43/ZNF783/CDH13/MBNL2/FARP1/CDKN1C/CID/ZBTB18/DMM2/CELF1/TBR1/NPFR2/ADCV3/PNRC1/TMED10/HNRNPUL1/CHI3L1/ERLIN2/PSIP1/EGLN2/CARD16/ZBED 9/CIDEA/CCR1/SCS1B/MAP3K8/ZFP42/IL13RA/ZNF358/IL2RAD3/CSTA/ZNF738/CTGF/SMD3/SHD9/CYLD/AORR8/ESCO2/ZNF782/ZNF709/ZNF781/CITED4/RNF168/ZNF366/B HLA15/NLRP6/DLGG/DMNT3A/DRD4/EEF1/EEF2/EGFR/EGR3/PATL2/EIF4G1/A2M/ELK4/ESR1/S98/FGA/FGF10/FHIT/XRN2/RASA3/PPP1E/SBN2/TRAK1/MRSR2/ACIN1/ FOXL1/FOXO1/FOXO1/SPG20/GGA3/DIP2A/FLT2/NEDD4/LARP1/PUOM2/RYBP/MAPK8IP2/VGLL2/MTOR/RNF144B/ZNF549/FBXO2/GAPDH5/PABPC1/DNAIC2/FGF22/NPTN/DK3 /BMP10/ZNF638/GNAS/ZNF311/ZNF844/GPER1/DOK7/GRB10/ZBTB44/GSTP1/GT2B/RNF17/GZMA/ANXA2/SERPIND1/SOX8/NRG1/HLX/HMGAL1/NR4A1/APBA2/HOXB3/HOXC4/H OXC5/HOXC6/HOXD3/HSP90AB1/TFA2E/ID3/COL28A1/BARHL2/IGF1/IGF2/CYR61/IL1RN/IL6/IL1F/FOXK2/INHBA/IRF1/ISL1/ITGB2/ITIH4/IJUP/USP50/HLS1/KDR/HES5/AF3 /LCK/LGALS9/LMNA/LMO2/ITB/SMAD3/MEF2D/MAP3K1/MEOX1/MEOX2/MEF2/MEF1/UXH8/MOV10/NFATC3/NFYB/NHLH2/NOV/NPPC/NRAS/NTF3/OPRL1/PARK2/SPOCK3/LEF1/ PRR16/ANGPT4/SIRT6/PGAM2/PI3/PIK3CG/PTX2/PKH01/PLA2G2A/PLAGL1/PML/RIPPL3/RIK4/TLR9/CYTL1/POW/SSH1/POU2AF1/BNC2/MEI18/BANIP/PPP1CB/PPP1CC/PWIL 2/ELP3/PRMT6/DNAIC17/ZNF532/PPP2R2B/FANCI/CNOT11/PRKAR1B/PRKDI1/MYNN/MAK3/MAP2K2/PRMT8/MAS91/HTRA1/PSMB4/PAK6/ARNTL2/RGMA/PRDM11/PSMD7/PT GFR/TEHM2/GATA2B/METTL14/CCAR2/PXN/CREBZF/ACTA2/RASGRF2/TRIM27/CCL11/CCL17/NPAS3/NOD2/SRR2/TBA2B/GZF1/SGK1/BMP4/ZNF649/BMIPR1B/BRD9/ZSCAN18/ BOK/SOX9/STAT2/STK10/SUPTHG/BST2/TAFA4/TBP/TECA1/TCBE2/ZEB1/ACTC1/TEAD3/TERF1/LEL3/TNFAIP3/TNFRSF1A/TNXP/TRAF1/TRAF5/PHLDA2/TWIST1/CCRL/ TNFRSF4/UCP1/WARS/WNT10B/WWAG/ZNF17/ZNF124/ZNF177/PAX8/CXCR4/CEB1/CARD14/ZNF665/ZC3H14/ZNF646/ZNF436/CALR/SURP/CAST/SCRT1/ HIST1H3A/SLAZ/ZNF97/NR0B2/HOPX/SPINK7/TRIM63/KDM2B/LOXL3/CBX2/GAS7/CDK10/RUNX1/TP63/RIUX3/SERPINA6/IRS2/ACTN1/CRADD/FADD/TNFRSF11A/ALDH1A2/SPH KJ/BU31/CCNA1/LIMD1/ER11/PIAS2/ZFAND2A/MAP3K6/LDB2/CBFA2T2/AURKB/ADIPQO/H2AF1/VJGL4/IRAPGEF2/ZBTB39/FGF19/NR1H4	23
GO:0031348	negative regulation of defense response	18/901	130/17046	0.00017	0.00563	0.00417	ADM/ESR1/FGF10/FOXO2/SOX8/RSPO2/IGF1/IL6/KDR/NFATC3/LEF1/PTX2/PML/PXN/CCL11/SFRP2/GZF1/BMP4/SOX9/TGM2/PAK8/FEZ5/TP63	18
GO:0035295	tube development	52/901	585/17046	0.00017	0.00536	0.00422	NLRP6/A2M/GPER1/GSTP1/HLA-B/HLA-E/ISL1/LGALS9/SMAD3/NOV/IL20RB/HTRA1/PSMB4/NOD2/TNFAIP3/TNFRSF1A/NLRX1/ADIPQO	52
GO:0009152	purine ribonucleotide biosynthetic process	27/901	240/17046	0.00018	0.00559	0.0044	TCIRG1/NPFR2/ADCV3/ACOTT/ADM/ADRB3/DRD4/GABRR1/AMPD2/AMPD3/GNAS/GPER1/GUCY1A3/NMIE7/ACACB/HPCA/NME9/IHCGR/MC2R/NPPC/OPRL1/ATP5B/PALM/PK M/MRAP/SCT/CCR2	27
GO:0046390	ribose phosphate biosynthetic process	28/901	253/17046	0.00018	0.0056	0.0044	TCIRG1/NPFR2/ADCV3/ACOTT/ADM/ADRB3/DRD4/GABRR1/AMPD2/AMPD3/GNAS/GPER1/GUCY1A3/NMIE7/ACACB/HPCA/NME9/IHCGR/MC2R/NPPC/OPRL1/ATP5B/PALM/PK M/MRAP/SCT/CCR2	28
GO:0040007	growth	72/901	887/17046	0.00018	0.0056	0.0044	CDH13/CDKN1C/CELF1/ESM1/EGLN2/CHRNA1/COMP/ADM/CTGF/ADRB3/DIO3/DMBT1/ESR1/FGF10/XRN2/FOXO2/SPG20/EPB4113/NEDD4/MTOR/TENM4/GATM/BMP10/GNAS7 /FLVCR1/NRG1/HLX/ACACB/APBA2/ZC3H12D/RSP02/FMN1/BARHL2/IGF1/CYR61/IL6/INHBA/SMAD3/MT1A/MTL2/MYD88/NOV/NPPC/PARK2/LEF1/SIRT6/ATP8A2/PKM/P ML/BNC2/PRMT6/BIN3/HTRA1/CCAR2/CCL11/NOD2/STRA6/SRR2/SGK1/BMP4/BMPR1B/SULT1/SOX9/STK3/BST2/TIMP3/WNT10B/COLO/Q/HOPX/SPHK1/ULK2	72
GO:0048534	hematopoietic or lymphoid organ development	61/901	720/17046	0.00018	0.00561	0.00441	AB11/CDKN1C/CCRL1/IL13RA/CYLD/ESCO2/EEF2/F2FN/AZ/EGR3/EML1/FGF10/SBN2/ACIN1/FOXK1/MTOR/GNAS/FLVCR1/ANXA2/HLA-B/HLA- DOA/HLX/HOXB3/IL6/INHBA/IRF1/KDR/HES5/LCK/LGALS9/LMO2/LTB/MEOX1/MTIT/NEAT3/LEF1/PTX2/PML/HERC6/SMPD3/BGLAP/SRR2/CXCR5/VPS33A/BMP4/STK3/TCEA1/Z EB1/WNT10B/ZNF70/FZD5/C6orf25/SCIN/RUNX1/RUNX3/ACTN1/FADD/TNFRSF11A/RSAD2/CD8A/ADIPQO/CD79A	61

GO:0070372	regulation of ERK1 and ERK2 cascade	25/901	215/17046	0.00018	0.00561	0.00441	CHI3L1/CCL1/CTGFG/NLRP6/EGFR/FGA/FGF10/GPER1/GSTP1/GF1/CYR61/IL6/KDR/LGALS9/PKH1/PLA2G2A/MAPK3/CCL11/CCL17/NOD2/BMP4/TNFRSF11A/ADIPOQ/RAPGEF2/GF19	25
GO:0051094	positive regulation of developmental process	83/901	1059/17046	0.00019	0.00567	0.00446	DMRT2/CELF1/CHI3L1/CCL1/CTGFG/SWYD1/DIO3/DMBT1/EGR3/EIF4G1/UNC130/EPHA1/EPHA3/FGA/FGF10/ACIN1/FOXO2/NEDD4/MTOR/TENM4/NPTN/BMP10/GN/AS/GPER1/SOX8/NRG1/HUX/HMG1/ACACB/HOX3/GF1/CYR61/IL6/INHBA/ISL1/KDR/AMIGO3/LCK/ARHGDA1/GAL/S9/SMAD3/NEU1/NPPC/PALM/PARK2/LEF1/ANGPT4/ATP8A2/PLA2G2A/PML/PRKD1/MAP2K2/CCL11/SFRP2/BMP4/SCL3A1/BMP19/SOX9/STK3/ZEB1/TEAD3/TNFAIP3/TWIST1/WNT10B/ZAP70/PAX8/CXCR4/ZC3H12A/CALR/HOPX/IFITM1/SCIN/RUNX1/TP63/FADD/SPHK1/CBEA2T2/ADIPOQ/H2AFV/RAPGEF2	83
GO:0007015	actin filament organization	31/901	293/17046	0.00019	0.00567	0.00446	ABIL1/FAM101A/CTGF/EPHA1/PHACTR1/PMI1E/MTOR/TM004/FMN1/LCP1/SMAD3/MAP3K1/NEDD9/PARK2/SSH1/TTCL1/BIN3/ACTR3B/ERMIN/TRIM27/CCL11/MICAL1/ACTC1/CAPZB/SH3BGR1/3/GAS7/SCIN/ACTN1/ARHGEF10/MICAL2	31
GO:0001763	morphogenesis of a branching structure	24/901	203/17046	0.00019	0.00567	0.00446	ADM/ESR1/FGF10/FOXO2/SOX8/RSP02/GF1/IL6/KDR/NFATC3/LEF1/PTX2/PML/ERMN/PXN/CCL11/SFRP2/GZF1/BMP4/SOX9/TGM2/PAX8/EZD5/TP63	24
GO:0006140	regulation of nucleotide metabolic process	24/901	203/17046	0.00019	0.00567	0.00446	NPF2/ADM/ADRB3/DRD4/GABBR1/GAPDH/GNAS/GPER1/DNAJC15/GUCY1A3/HPCA/IGF1/LHCGR/MC2R/ME1/ME2/NPPC/OPRL1/PALM/SIRT6/PGAM2/MRAP/SCT/CCR2	24
GO:0007267	cell-cell signaling	89/901	1154/17046	0.00019	0.00567	0.00446	KCNMB2/NPF2/ADCY3/CHRNA1/CHRNA2/CHRNA3/PANX3/CCR1/SEZ6/CNP/ADM/CTGF/ADRB3/BHLHA15/DLG2/ABAT/DRD4/DNA/EPNA2/EGR3/JG/FGF10/FOXO1/IMAP8B2/GABBR1/PNKD/GIA3/NPTN/GI2/PDE7B/GS2/GNAS/GPER1/FFAR2/GRIK4/SOX8/KCNP2/APBA2/HRH1/HTR3A/CYR61/IL1RN/IL6/INHBA/ISL1/ITGB2/KCNH2/KCNJ8/KCNJ9/KCNMB1/LTB/NPZ/NTPIA2/NOV/NTF3/OPRL1/PARK2/PDE4C/POMC/SMPO3/CHRNA9/SYBU/PRKAR1B/RASGEF2/RT2/SCT/CCL17/SFRP2/BMP4/SCL3A1/SOX9/BST2/VAMP2/YWHAG/CA7/CACNA1E/CACNB2/PAX8/EZD5/ARAB1/PPP1/COI1/NR0B2/TP63/IRS2/TNFRSF11A/SYT7/ADIPOQ/RAB3D/RAPGEF2	89
GO:0009187	cyclic nucleotide metabolic process	23/901	191/17046	0.00019	0.00576	0.00453	NPF2/ADCY3/CNP/ADM/ADRB3/DRD4/GABBR1/AMPD2/PDE7B/GNAS/GPER1/GUCY1A3/HPCA/LHCGR/MC2R/NPPC/OPRL1/PALM/PDE4C/PDE7A/MRAP/SCT/CCR2	23
GO:0019219	regulation of nucleobase-containing compound metabolic process	235/901	3617/17046	0.00019	0.00576	0.00453	ZNF783/CDH13/MBNL2/CDKN1C/C1D/ZBTB18/DMRT2/CELF1/TBR1/NPF2/PNRC1/HNRNPUL1/ERLIN2/PSIP1/EGLN2/ZBED9/GIDEA/EZFP42/ADM/IL131RA/ZNF358/ZNF738/SWYD1/CYLD/ADRB3/ESCO2/ZNF782/ZNF709/ZNF781/CTE2D/RNF168/BHLHA15/DNMT3A/DRD4/EGFR/EGR3/ELK4/ESR1/SP8/FGF10/FHIT/XRN2/SBN02/TRAK1/MSRB2/ACIN1/FOXO1/FOXO2/FOXO3/GUCY1A3/G2MA/SOX8/NRG1/HUX/HMG1A1/NR4A1/HPCA/HOX83/HOX4/HOX5/HOX6/HOX3/JFAP2E/ID3/BARHL2/GF1/IGF2/CYR61/IL6/IL16/FOXO2/INHBA/RF1/TF2B/BRE1/GUCY1A3/G2MA/SOX8/NRG1/HUX/HMG1A1/NR4A1/HPCA/HOX83/HOX4/HOX5/HOX6/HOX3/JFAP2E/ID3/BARHL2/GF1/IGF2/CYR61/IL6/IL16/FOXO2/INHBA/RF1/ISL1/JUP/USP50/HLS1/HES5/AFF3/IGALS9/LHCGR/LMNA/LMO2/SMAD3/MC2R/ME1/ME2/MEF2D/MEOX1/MEOX2/MITT/LHX8/MOV10/NFATC3/NFYB/NHLH2/NPPC/NTF3/OPRL1/PALM/PARK2/LEF1/SIRT6/PGAM2/PTX2/PKH1/PLAG1/PM1/PPP1/PPP2/RIPK4/TLR9/CY11/POMC/POU2AF1/BNC2/MED18/BANP/ELP3/PRMT6/DNAJC17/ZNF532/CNOT11/PRK1/MIYNN/MAPK3/MRAP/PRMT8/HTRA1/PAK6/ARNTL2/RGMA/PRDM11/TENM2/GATAD2B/CCAR2/CREBZF/TRIM27/SCT/NPAS3/NOD2/SFRP2/TRA2B/GZF1/SGK1/BMP4/ZNF64/9/BMPR1B/BRD9/ZSCAN18/SOX9/STAT2/STK3/SUPT6H/TAFA7/TBP/CEA1/TCEB2/ZEB1/TEAD3/TFR1/TLF3/TNFAIP3/TNFRSF1A/TRAJ1/TRAJ5/TWIST1/CCR2/TNFRSF4/UCP1/WW110B/ZNF7124/ZNF177/PAX8/EZD5/CARD14/ZNF665/ZC3H12A/ZNF606/ZC3H12A/ZNF436/CALR/SLRP/SCRT1/HIST1H3A/SLA2/HOPX/KDM2B/LOXL3/CBX2/GA57/RUNX1/TP63/RUNX3/ACTN1/FADD/TNFRSF11A/SPHK1/BUD31/CCNA3/LIMD1/PIAS2/IDB2/CBEA2T2/AURKB/ADIPOQ/H2AFV/MICAL2/VGLL4/ZBTB39/NR1H4	235
GO:0006952	defense response	119/901	1639/17046	0.00019	0.00576	0.00453	ABIL1/TANK/KLRG1/TGIRG1/SPON2/ADCY3/CHGA/CHI3L1/CCR1/MAP3K8/ADM/IL131RA/PARP4/CYLD/DDOST/COCH/NLRP6/DMBT1/DRD4/EGFR/EIF4G1/A2M/UNC13D/FCGR2A/FGA/FGF10/RAS3/SBN02/ACIN1/FOXO1/PU1M2/MAPK8/P2/MTOR/SLC37A4/FGF22/GPER1/FFAR2/GSTP1/NRG1/HLA-B/HLA-E/HLA-F/NR4A1/HRH1/HSP90A1/HSP90A8/CD300E/IL1R1/IL1RN/IL6/INHBA/IRF1/ISL1/ITGB2/ITIH4/KCNJ8/LCK/LGALS9/SMAD3/MAP3K1/MOV10/NFATC3/NOV/NRAS/OAS2/PIK3CG/PLA2G2A/PML/IL20RB/TLR9/TREM1/PRKAR1B/PRKDI/MAPK3/IMP2K2/MASP1/HTRA1/SLAMF8/PSMD7/PTPRCAP/RASGRF2/TRIM27/DEFB134/CCL11/CCL17/NOD2/BMPR1B/BPI/STAT2/BST2/TUBS/TNFAIP3/TNFRSF1A/CCR2/TNFRSF4/ZAP70/CA7/CACNA1E/CXCR4/NLRX1/UNC93B1/HIST1H3A/IL1F10/IFITM1/IRS2/FADD/TNFRSF11A/SPHK1/CCR12/R/SAD2/IL32/CDBA/ADIPOQ/L186/NUP93/RAPGEF2/FGF19	119
GO:0070873	regulation of glycogen metabolic process	8/901	32/17046	0.0002	0.00589	0.00463	MTOR/GRB10/GF1/IGF2/PPP1C9/PHILDA2/IRS2	8
GO:0014032	neural crest cell development	10/901	49/17046	0.0002	0.00594	0.00467	FOXO2/SOX8/NRG1/ISL1/LEF1/PTX2/SOX9/TWIST1/ALDH1A2/FGF19	10

GO:0051704	multi-organism process	151/901	2174/17046	0.00021	0.00609	0.00479	AB11/TCIRG1/SPON2/CELF1/GJB6/ADCY3/ADAM29/HNRNPULL1/CHGA/PSIP1/CNP/ZFP42/ADM/CP51/CYP11A1/DDB1/WBP2/NL/COCH/NLRP6/DMBT1/DNMT3A/ABAT/DRD4/EIF4G1/UNC13D/ESR1/FGM/FGF10/XRN2/SBNO2/ACIN1/ANKR1B1/NUP210/NEEDD4/PUM2/MAPK8/P2/TSSK2/MTOR/SLC37A4/GAPDH5/GJB2/VPS4A/GNAS/IZUMO1/GSTP1/GTF2B/GUCYA3/SOX8/HLA-B/HLA-E/HMGAI/HSPA1L/HSP90A1/IGF1/IL1R1/IL1RN/IL6/IL10RA/IL12RB2/IL16/INHBA/IRF1/ITGB7/HILS1/KCNJB/KDR/PO5/KRT7/STMN1/LCK/LDLR/LGALS9/LHCGR/LMNA/SMAD3/NP/PC/OS2/PARK2/LEF1/PGAM2/P/3/PLA2G2A/SPA17/PML/TLR9/TREM1/MOY10L1/PWIL2/PROTEG/WDR33/VACL4/LMBRD1/MAPK3/HTTRA1/SLAMF8/PSMB4/PSMD7/PTGFR/CREB/ZF/ACTA2/TRIM27/RPL8/DEFB134/RP29/CCL11/NPAS3/NOD2/BMP4/SLC20A2/BMPRI1B/SOX9/BP/STAT2/TAFA4B/TBP/TCEA1/TCEB2/TEAD3/TLR5/TNFAIP3/TNFRSF1A/CCR2/CA7/CXCR4/FZD5/RAB7A/CDC86/NLRX1/ZC3H12A/CALR/UNC93B1/SLURP/CAST/HIST1H3A/SPATA16/KDM2B/RAEL1/IFITM1/TP63/FADD/TNFRSF11A/CCNA1/ENDOU/R/SAD2/CDBA/LY86/MTLS/NUP93/USF6NL
GO:0034329	cell junction assembly	25/901	217/17046	0.00021	0.00611	0.0048	CDH3/CDH9/CDH12/CDH13/PRK3/MPP7/EPHA3/NFASC/EPB413/GIB2/FMNI1/JUP/KDR/LAMA3/SMAD3/P/LEC/FBUIM1/LIMS2/PARVA/PXN/FZD5/PARD6G/PARD6B/ACTN1/RAPGEF2
GO:0051272	positive regulation of cellular component movement	35/901	349/17046	0.00021	0.00619	0.00486	CDH13/PDPN/CCR1/EGFR/EPHA1/FGF10/FOXO2/GPER1/IGF1/CYR61/IL6/KDR/STMN1/LGALS9/SMAD3/NITF3/P2RY6/LEF1/ANGPT4/ELP3/PRKDJ/MAP2K2/CCL11/BMP4/SLC8A1/S/OX9/TWIST1/CCR2/PTP4A1/COL18A1/CALR/IRS2/FAOD/SPHK1/RAPGEF2
GO:0044264	cellular polysaccharide metabolic process	14/901	89/17046	0.00023	0.00649	0.00511	CP51/MTOR/GRB10/HAS1/IGF1/IGF2/PRKAG3/POMC/PPP1CB/PPP1CC/CSGALNACT1/PHLDA2/IRS2/STBD1
GO:0050776	regulation of immune response	72/901	894/17046	0.00023	0.00649	0.00511	AB11/TANK/KLRG1/SPON2/HCS7/MAP3K8/CYLD/COCH/NLRP6/DMBT1/EGFR/A2M/UNC13D/FCGR2A/FGF10/RASA3/FOXO1/PUM2/MTOR/FGF22/FFAR2/NRG1/HLA-B/HLA-DPA1/HLA-E/HLA-F/HXL/NR4A1/HSP90A1/HSP90A1/IL6/IRF1/ITGB2/ITGB7/LCK/LGALS9/SMAD3/MAP3K1/MOY10/NFATC3/NRAS/L2OR8/TLR9/PAG1/MAPK3/MAP2K2/MAS1/PSMB4/PSMD7/R/ASGR2/TRIM27/NOD2/STAT2/SUPT6H/BST2/ILR5/TNFAIP3/CCR2/ZAP70/FZD5/NLRX1/UNC93B1/SLAZ/IFITM1/IRS2/FAD/SCAD2/CD8A/RAPGEF2/CD79A/FGF19
GO:0055082	cellular chemical homeostasis	53/901	607/17046	0.00023	0.00652	0.00513	TCIRG1/TRON/GIB6/CILNS/CCR1/ADM/PRO4/ESR1/FOXO/NEEDD4/NPTM/GPER1/FLVCR1/ANXA6/HK1/IL1R1/AQP2/AQP5/AQP9/LCK/NUBP1/ATP1A2/OPRL1/ATP5B/PDPE6B/PIK3CG/PKH41/PML/SLC30A10/CHRNA9/SYBU/PRKDI/SLAMF8/TRPC7/CCL11/SGK1/BMP4/SLC4A1/SLC8A1/TGMD2/TRPC4/TRPC6/CR2/CA7/CACNAIE/CXCR4/RAB7A/CALR/ATP13A4/CASQ1/IRS2/SMDT1/MTLS
GO:0007167	enzyme linked receptor protein signaling pathway	89/901	1161/17046	0.00023	0.00656	0.00516	AB11/CDH3/CDH13/CDKN1C/CHRG1/ADCY3/LECT1/ESM1/GIDEA/AP351/IL13IRA/CTGF/PPM1L/FNNA2/EGFR/F1F4G1/EPHA1/EPHA3/EPH4/FGF10/RASA3/FOXO2/FOXO1/SPG20/N/EDD4/ARHGEF18/MTOR/FGF22/NPTN/BMP10/GPER1/GRB10/NRG1/NR4A1/HSP90A1/IGF1/IGF2/CYR61/NHBA/JUP/KDR/HES5/LCK/ARHGDI4/LTBR1/SMAD3/MAP3K1/MOY10/NOV/NPPC/NRAS/NITF3/ARHGEF3/LEF1/ANGPT4/PRKAG3/PML/TLR9/PPP1CB/LMBRD1/PAG1/PRKDI/MAPK3/MAP2K2/HTRA1/PSMB4/RGMA/PSMD7/PLEKHG5/PTPRE/PXN/RASGRF2/IRITZ/SFRP2/BMP4/BMP4/BMP4/SOX9/ZEB1/ZAP70/RAB7A/TMEM204/IRS2/SPHK1/CD8A/ADIPOQ/RAPGEF2/FGF19
GO:0048736	appendage development	21/901	169/17046	0.00023	0.00656	0.00516	COMP/ZNF358/ECEL1/SP8/FGF10/GNAS/FLVCR1/RSPO2/FMNI1/AFF3/MEOX2/LEF1/PTX2/IFT122/SFRP2/BMP4/BMPRI1B/SOX9/TWIST1/TP63/ALDH1A2
GO:0060173	limb development	21/901	169/17046	0.00023	0.00656	0.00516	COMP/ZNF358/ECEL1/SP8/FGF10/GNAS/FLVCR1/RSPO2/FMNI1/AFF3/MEOX2/LEF1/PTX2/IFT122/SFRP2/BMP4/BMPRI1B/SOX9/TWIST1/TP63/ALDH1A2
GO:1901699	cellular response to nitrogen compound	57/901	667/17046	0.00023	0.00656	0.00516	TCIRG1/ADCY3/AP351/CP51/CYP11A1/DNMT3A/EGFR/EGR3/EIF4G1/FGF10/RASA3/FOXO2/FOXO1/AKR1B1/MTOR/FGF22/GNAS/GPER1/GRB10/NRG1/NR4A1/HRH1/IGF2/LIRN/AQP9/JUP/PO5/LCK/SMAD3/NRAS/PARK2/PK3CG/PRKAG3/TLR9/SSH1/PRKAR1B/LMBRD1/MAPK3/MAP2K2/PSMD7/PTPRE/PXN/RASGRF2/NOD2/SLC8A1/SOX9/VAMP2/ZEB1/WNT10B/CPEB4/MGARF/IRS2/ADIPOQ/RAPGEF2/F/GF19/NR1H4
GO:0006828	manganese ion transport	5/901	12/17046	0.00024	0.00658	0.00517	SLC30A10/TRPC4/TRPC4/TRPC4
GO:0048145	regulation of fibroblast proliferation	13/901	79/17046	0.00024	0.00658	0.00517	BAG1/EGFR/ESR1/FGF10/MORC3/GSTP1/ANXA2/IGF1/NRAS/SIRT6/PML/S100A6/SPHK1
GO:0065009	regulation of molecular function	175/901	2588/17046	0.00024	0.00661	0.00519	AB11/CDH3/FARP1/RCAN2/CDKN1C/TRDN/PITRM1/NPFRF2/ADCY3/CHI3L1/CARD16/MAP3K8/CSTA/CTGF/CYLD/ADRB3/DLG2/DRD4/EGFR/A2M/EPHA1/EPHA3/ESR1/SPATA13/P/HACTR1/FGF10/RASA3/PPM1L/TBC1D9B/TBC1D1/NEEDD4/PSD3/ARHGEF18/MAPK8/P2/MTOR/GABRR1/RASGEF1C/ALSZC1/RSZ22/FGF22/CYTH4/GNAS/GPER1/DOCK7/DNAIC15/GSTP1/GZMA/ANXA2/SERPIND1/KCNIP2/NRG1/HPCA/AGFG2/HSP90A1/HSP90A1/03/COL28A1/IGF1/IGF2/CYR61/IL1RN/IL6/SL1/TH3/ITH4/JUP/PO5/LCK/ARHGDI4/LGALS9/LHCGR/IL6L1/SMAD3/MAP3K1/MFNG/PLEKHG7/ATP1A2/NHLH2/NRAS/NITF3/OPRL1/PALM/ARHGEF3/PARK2/SPOC3/LEF1/ANGPT4/PI3/PK3CG/PTX2/PKH41/PML/FXYD6/PNLIP/RIPK4/TLR9/CYTL1/PONI1/RIN2/ELP3/ARHGEF10L/PP2R2B/VACL14/PRKAR1B/PRKDI/MAPK3/MAP2K2/PRMT8/SLAMF8/CD42SE1/PSMB4/PAN6/PSMD7/PLEKHG5/CCR2/PXN/CREBZ/RASGRF2/TRIM27/GS12/CCL11/CCL17/NOD2/SFRP2/ARHGAP9/SGK1/BMP4/BOK/STK3/STK10/BST2/VAMP2/TCEA1/TERF1/TERF2/TNFAIP3/TNFB/TNFR1/TRAF1/TRAF5/TRPC6/TWIST1/CCR2/TNFRSF4/WNT10B/VWHAG/CACNB2/CXCR4/FZD5/CARD14/ZC3H12A/CASF18/NROB2/HOPX/SPINK7/TP63/SERPINA6/IRS2/CRADD/FADD/TNFRSF11A/SPHK1/STARD13/PIAS2/MAP3K6/AURKB/ADIPOQ/ARHGAP29/H2AF1/ARHGEF10/RAPGEF2/USP6/NRABGAP1/JOSEC1/FGF19

GO:0000904	cell morphogenesis involved in differentiation	76/901	958/17046	0.00024	0.00661	0.00519	FARP1/SPON2/TBRI1/LECT1/FRMD6/CNP/COI9A3/EFNA2/EGFR/UNC13D/EPHA1/EPHA3/EPH4/FGA/FGF10/RASA3/BTBD3/SPG20/NFASC/FLNBB/NEBD4L/MAPK8IP2/FGF22/NRG1/HSP90A1/HSP90AB1/HSP90AB2/PRK11/ITGB7/STMN1/ARHGDI1/LG11/SNAD3/MAP3K1/MFIZ/INRA5/NTF5/LEF1/ATP8A2/JSSH1/PAVVA/MAPK3/MAP2K2/PSM8A/RGM4/TRP/C7/PSMD7/TENN2/PXN/RASGEF2/S100A4/S100A6/SFRP2/VNFRP2/CACNB2/PAX8/C6orf25/COL18A1/CALR/ANTXR1/PARD6B/LOXL3/RUNX3/RIS2/ACTN1/RAPGEF2/ULK2/FGF19	76
GO:0009790	embryo development	76/901	958/17046	0.00024	0.00661	0.00519	XI/ATP8A2/HOXB3/HOXC4/HOXC5/HOXC6/HOXD3/HSD17B2/ID3/RSPD2/IGF1/CYR61/LIRN/INHBA/ISL1/ITGAT/ITGB2/KOR/HESS/RESP1B/AF3/LAMA3/LMO2/SMAD3/MEOX1/MEOX2/MGAT3/LEF1/ATP8A2/PITX2/RIPPLY3/CHRNA9/JFT122/SCI/STRA6/SFRP2/BMP4/SLC8A1/SOX9/STK3/ZE11/PAX8/FZD5/HOPX/KDM2B/RUNX4/TP63/ALDH1A2/ADIPOQ/MICAL2	76
GO:0071840	cellular component organization or biogenesis	351/901	5713/17046	0.00025	0.00674	0.00553	AKT3/ABI1/CDH9/TFSPAN5/CDH12/CDH13/FARP1/TCIRG1/TRDN/SPON2/CID1/TACC2/PDPN/CELF1/TBRI1/SEPT19/ADC3/TMED10/LECT1/RRF1/ESM1/CHGA/PSIP1/PKP3/EGFLN2/ATXN2L/BAGAL1/EXOC3/CHRNA1/CHRNA2/GPRIN1/CIDEA/CLOTNF/PANX3/CLN5/MRP152/FRMD6/SLC51B/SEZ6/CNP/POA1BP/COL19A3/COI11A1/COMP/SLTI1/ZFP42/AD/ME/EGFLAM/NDUFA6/MPP7/FAM101A/CTGF/SMYD3/SGOL1/SH3D19/CYLD/ITIM1/DOB1/WBP2NL/DDOST/RNF168/BHLHA15/COCH/DLGG2/DMNT3A/DSG3/EFNA2/EGFR/PATL2/A2M/ELK4/TMEM17/EM11/UNC13D/EPHA1/EPHA3/EPH4/ESR1/ALAS1/SPAT13/PHACTR1/FGA/FGF10/RASA3/PPM1E/BTBD3/MSTRB2/ACIN1/LIMCH1/FOXK2/SPG20/NFASC/EPB413/FINB/FLT2/MCL1/TBC1D1/NUP210/ATP11A/NEBD4L/SYNE1/PUJ2/ARHGFE18/RYPB/MAPK8IP2/MTOR/SLC37A4/SAMM50/DEFB31/ALSZC1/TEENM4/GAS2/SACS/PLEK2/DNAIC2/FGF22/NPTN/GIB2/GSL2/VPS4A/BMP10/PIGW/IZUMO1/GRR26/GPER1/MRP5188/DNAIC15/TMMD4/HAS1/KCNP2/NRGI/ANXA6/HK1/ANXA13/HMGA1/A/CACB/HPCA/VACADL/HSPAL1/HSP90A1/HSP90A2/HC11D2/COL28A1/FMN1/BARHL2/UG1/IGF2/CYR61/LIG1/ADP2/AQP2/AQP9/INHBAA/AQP9/ISL1/ITGAT/ITGB2/ITGB7/ITP/USP50/HILS1/ATP9B/KDR/ACAT1/KIF25/KRT15/AMIGO3/INSC/HESS/LAMA3/STMN1/LCP1/ARHGDI1/LG11/LUNNA/LOX/ITBP1/SMAD3/MEI1/MAP3K1/MFIZ/ITTE/MPZ/MYH4/NTL2/NUBP1/NEOD9/NEU/NOV/NRAS/NTF3/ATP9B/ANO7/PALM/PARK2/UTP11/LEF1/DDX47/PBR16/ANGPT4/C11orf73/ATP8A2/XRNP2/PLA2G2A/PLEC/PRKAG3/PML/TREM1/SSH1/BLUML1/PALMD/LPCAT2/BANP/PWIL2/EUP3/PRMT6/GOLPH3/LMS188P1/PEX6/UMS2/UMS2/PARVA/TTCT1/ITF122/CSGALNACT1/PRKD1/BIN3/MAPK3/MAP2K2/TRPV5/PRMT8/HTRA1/SLAMF8/CD42SE1/PSMB4/PAK6/RGM4/TRPC7/PSMD7/ACTR3B/TEENM2/GATAD2B/ERMIN/MARK4/CCR2/RPN/RASGEF2/RC2/TRIM27/EXOC4/PA3/R/PL8/RPL29/S100A4/S100A6/CCL11/MRP514/PARV6/NOD2/SRRP2/DNAI2/SGK3/MICAL1/TMEM237/VPS3A/BMP4/BMPRI1B/SLIT1/BRD9/SOX9/SRPF8/STAT2/SUPT6H/BST2/VAMP2/TCEB2/ACTC1/TERF1/CHHT/TFN1AP3/TNFRSF1A/TNXB/TNFA1/TRPC4/TRPC6/TWIST1/WNT10B/YWHAG/CA7/CACNB2/PAX8/CXCR4/FZD5/COI18A1/CALR/COI21A1/SURP/CAPS/COI4/CANPZB/HIST1H2BM/SH3BGRL3/HIST1H3A/DYNLBR2/ANTXR1/BFSP2/CASQ1/HOPX/PARD6G/PARD6B/TTBK1/KDM2B/LOXL3/MGARP9/CBX2/RAE1/GAS75/CIN/TP63/RUNX3/RIS2/ACTN1/FADD/SPHK1/CCNA1/SKAP2/LIMB2/LIMD1/ER11/MAP7/PRC1/SY17/LD82/CBAF22/TAURK8/TRIP10/ADIPOQ/H2AF2/ARRHGE10/MICAL2/NUP93/RAPGEF2/ULK2/USP6NL/IOSEC1/FGF19	351
GO:0070588	calcium ion transmembrane transport	22/901	182/17046	0.00025	0.00674	0.00553	TRDN/C15orf27/TRPM6/TRPV3/DRD4/RASA3/ATP1A2/OPRL1/PK3GG/TLR9/TRPV6/CHRNA9/TRPV5/TRPC7/BMP4/SLC6A1/TRPCA/TRPC6/TRPM22/CACNAIE/CACNB2/SMIDT1	22
GO:0071132	mesenchyme morphogenesis	8/901	33/17046	0.00025	0.00674	0.00553	FOXK2/ISL1/SMAD3/LEF1/ACTA2/SOX9/ACTC1/TWIST1	8
GO:006816	calcium ion transport	35/901	352/17046	0.00025	0.00674	0.00553	TRDN/CLCA1/CCR1/C15orf27/TRPM6/CTGF/TRPV3/BHLHA15/DRD4/RASA3/CBA2R2B/GPER1/ANXA6/CLK/ATP1A2/NEATC3/OPRL1/PK3GG/PML/TLR9/TRPV6/CHRNA9/PRKD1/TRPV5/TRPC7/TRIM27/BMP4/SLC8A1/TRPCA/TRPC6/TRPM22/CACNAIE/CACNB2/CASQ1/SMIDT1	35
GO:1901137	carbohydrate derivative biosynthetic process	61/901	729/17046	0.00025	0.00674	0.00553	SLC17A5/AMPD3/AMPD3/GNAS/PIGW/GPER1/EOGT/GUCY1A3/NME7/HAS1/ACACB/HPCA/NME9/IGF1/AMUC21/LHCGR/MC2R/MGAT1/NEU1/NPPC/OAS2/OPRL1/ATP5B/PALM/C	61
GO:009607	response to biotic stimulus	68/901	837/17046	0.00026	0.00703	0.00553	HST15/SIRT6/GALNT1/PIGC/PKM/CYTL1/CSGALNACT1/MRAP/SCT/BMPRI1B/CCR2/UPP1/MOGS/CALB/QTR1	68
GO:1901135	carbohydrate derivative metabolic process	89/901	1167/17046	0.00027	0.00727	0.00572	SPON2/GIB6/HNRNPUL1/CHGA/CNP/ADM/CPS1/CYP11A1/COCH/NLRP6/DMBT1/UNC13D/FGA/FGF10/SSNO2/ACIN1/PUJ2/SLC37A4/GSTP1/GUCY1A3/HLA-B/HLA-E/HMGA1/LIRN/LIG1/LLORA/IL12RB2/IRF1/KCNJ8/STMN1/LCK/LGALS9/SMAD3/OAS2/PLA2G2A/PML/TLR9/TREM1/MAPK3/HTRA1/SLAMF8/PTGER/CREB/ACTA2/DEFB134/CCL11/NOD2/SYNDIG1L/BPI/STAT2/BST2/TLR5/TNFAIP3/TNFRSF1A/CX7/CXCR4/FZD5/NLRX1/ZC3H12A/UNC93B1/HIST1H3A/JFTM1/FADD/TNFRSF1A/RSD2/CD8A1/Y86/NUP93	89
GO:1900034	regulation of cellular response to heat	12/901	70/17046	0.00028	0.00727	0.00572	GNMT/CIK3/NPFPR2/ADCY3/LECT1/B4GALT1/ACOTT1/GALNT15/SC51B/NEU/COL11A1/ADM/EGFLAM/PARP4/BSG1CT/MGAT5B/MB0AT1/ADR3/ADAL/DDOST/DLGG2/DMNT3A/DRD4/ENOD2/TRAK1/FOXJ1/AKR1B1/FUC1A1/GABRR1/ST16GALNAC3/FBXO2/GBGTT1/GAPDH5/SLC17A5/AMPD2/PDE7B/AMPD3/GNAS/PIGW/GPER1/EOGT/DNAIC15/GUCY1A3/AM/E7/HAS1/HK1/JACACB/HPCA/NME9/IGF1/TH3/ITH4/MUC21/LHCGR/MC2R/MGAT1/NUDT1/AMYH4/NDUFB4/NEU1/ATP1A2/NPPC/OAS2/OPRL1/ATP5B/PALM/SPOCK3/CHST15/P/DE4C/PDE7A/SIRT6/PDE6B/GALNT1/PGAM2/PIGG/PKM/PLA2G2A/CYTL1/SMPP3/CSGALNACT1/MRAP/SCT/CEK1/BMPRI1B/CCR2/UPP1/MOGS/CALB/QTR1	12
GO:0072521	purine-containing compound metabolic process	47/901	524/17046	0.00028	0.00735	0.00578	NUP210/MTOR/DNAIC2/HSPA11/HSP90A1/C11orf73/MAPK3/CCAR2/RPA3/RAE1/NUP93	47
							TCIRG1/NPFPR2/ADCY3/ACOTT1/ADM/ADR3/ADAL/DLGG2/DMNT3A/DRD4/ENOD2/FHIT/GABRR1/GAPDH5/AMPD2/PDE7B/AMPD3/GNAS/GPER1/DNAIC15/GUCY1A3/NNM7/HK1/A/CACB/HPCA/NME9/IGF1/LHCGR/MC2R/NUDT1/AMYH4/NDUFB4/ATP1A2/NPPC/OAS2/OPRL1/ATP5B/PALM/PDE6B/PDE6B/PGAM2/PKM/MRAP/SCT/CCR2	

GO:1902578	single-organism localization	242/901	3769/17046	0.00031	0.00798	0.00627	AB11/CDH3/TPANS/KCNMB2/TCIRG1/TRDN/ABCA9/ADCY3/TMED10/SLC27A2/RER1/CHGA/CHI3L1/PPK3/EXOC3/CHRNA1/CHRNA2/CHRNA5/GIDEA/PANX3/AP3S1/CLCA1/CCR1/SLC51B/C15orf27/SLC38A10/CNP/ADM/TRPM6/KLC3/CTGF/ABCC13/SH3BP1/CYB5B61/CYLD/TRPV3/DDOST/BHLH1A15/NLRP6/DLGG2/ABAT/DRD4/AGXT/EGFR/A2M/U	242
GO:0005977	glycogen metabolic process	12/901	71/17046	0.00032	0.00798	0.00628	NC130/SLC10A4/FCGR2A/FGA/FGF10/RASA3/TRAK1/EXPH5/NFASC/EPBA113/FLNB/LOT2/MILC1/NUPT210/ATP11A/NEDD4L/SYNE1/MORC3/MAK8IP2/MTOR/SLC37A4/SAMM50/STEAP2/SLC17A5/GIA3/GIB2/GLS2/VPS4A/GNAS/CRACR2/PIGW/GPR26/GRB10/FLVCR1/GRIK4/DNAIC15/SCG3/NNM17/ANXA2/KCNIP2/NGR1/ANXA6/HKI1/ANXA13/HLA-E/ACACB/HPCA/HSPA1/HSP90A11/HSP90A1/HTR3A/IGF1/IGF2/IL1RN/IL6/AQP2/AOP5/INHBA/AQP9/ISL1/ITGB2/ITGB7/JUP/ATP9B/KCNH2/KCNJ8/KCNJ9/KCNMB1/PO5/INSC/TOMM20/SLC6A17/LCK/LDLR/LGALS9/LLGL1/LMNA/SMA03/MFI2/ATP1A2/NEAT3/NOV/INT3/OPRL1/SLC22A18/P2RY6/ATP5B/ANO7/PALM/PARK2/PDE4C/PCYOX1/CL1orf73/SIRT6/ATP8A2/PIK3CG/PRKAG3/PNL/XYND6/SLCO1C1/PNLIP/TLR9/TREM1/POMC/PON1/ZDHHC13/GOLPH3/SLC47A1/SLC29A3/TRPV6/SMPD3/SLC30A10/CHRNA9/SYBU/PEX26/PRKAR1B/IFT122/LMBRD1/PRK11/APOBR/MAK3/IMP2/K2/TRPV5/CDCA25E1/TRPC7/RASGEF2/TRIM27/EXOC4/RPL8/RP29/S100A6/SC7/NOD2/TINAGL1/STRA6/SFRP2/SGK1/VP	12
GO:0060438	trachea development	6/901	19/17046	0.00032	0.00807	0.00635	CACNA1E/CACNB2/PAX8/FZD5/RAB7A/RAB11/FP1/CAIR/COLO/SLC25A18/MFSD1/ATP13A4/NR0B2/MONJA/CASQ1/MGAR/PRAE1/SLC43A1/SCIN/IRS2/ACTN1/TNFRSF11A/SPHK1/INAP7/SYTY/SLC16A3/RSAD2/SMO1/ADIPOQ/RAB3D/NUP93/RAP6EEZ/USP6NL/FGF19/NR1H4	6
GO:0002694	regulation of leukocyte activation	38/901	399/17046	0.00033	0.00831	0.00654	CPS1/MTOR/GRB10/IGF1/IGF2/PRKAG3/POMC/PPP1CB/PPP1CC/PHLDA2/IRS2/STBD1	38
GO:0035265	organ growth	17/901	126/17046	0.00034	0.00851	0.0067	RSPO2/IEF1/MAPK3/MAK2/K2/BMP4/SOX9	17
GO:0009259	ribonucleotide metabolic process	43/901	471/17046	0.00035	0.0086	0.00676	MAP3K8/IL13RA/CYLD/EGR3/UNC13D/FGF10/FGF11/FLOT2/MTOR/GPER1/HLA-DOA/HLA-DPA1/HLA-E/HLX/ZC3H12D/IGF1/IGF2/IL6/INHBA/IRE1/LCK/LGALS9/IL20RB/PAG1/PTPRE/NOD2/BMP4/BPI/SUPT6H/ZEB1/TNFAP3/CCR2/TNFRSF4/ZAP70/IST1/ZC3H12A/SLA2/IRS2/FADD	43
GO:0051046	regulation of secretion	54/901	633/17046	0.00036	0.00878	0.0069	COMP/ESR1/FGF10/FOXO2/TENM4/BMP10/FLVCR1/NGR1/HLX/ACACB/RPO2/IGF1/NPPC/SIRT6/BNC2/SOX9/STK3	54
GO:0050679	positive regulation of epithelial cell proliferation	19/901	150/17046	0.00036	0.00881	0.00693	TCIRG1/NPFR2/ADCY3/ACOT7/ADM/ADRB3/DLGG2/DRD4/ENO2/GABBR1/GARDHS/AMPD2/PDE7B/AMPD3/GNAS/GPER1/DNAIC15/GUCY1A3/NME7/HKI1/ACACB/HPCA/NME9/IG	19
GO:0006073	cellular glucan metabolic process	12/901	72/17046	0.00036	0.00883	0.00694	F1/LHCGR/MC2R/MYH4/NDUFB4/ATP1A2/NPPC/OPRL1/ATP5B/PALM/PDE4C/PDE7A/SIRT6/PDE6B/PGAM2/PKM/MRAP/SC7/CCR2/UPP1	12
GO:0044042	glucan metabolic process	12/901	72/17046	0.00036	0.00883	0.00694	CHGA/CIDEA/NLRP6/ABAT/DRD4/UNC13D/FGA/FGF10/EXPH5/VPS4A/GNAS/GPER1/FFAR2/NGR1/HLA-E/IGF1/IL1RN/IL6/INHBA/ISL1/LGALS9/IL11/NOV/OPRL1/PARK2/PDE4C/PML/TLR9/POMC/GOLPH3/ITRPV6/SMPD3/SYBU/PRKAR1B/TRIM27/SC7/NOD2/SGK1/VAMP2/TWIST1/	12
GO:0071593	lymphocyte aggregation	38/901	401/17046	0.00037	0.00889	0.00699	CDH3/CDH13/EGFR/EGR3/FGF10/MTOR/NR4A1/IGF1/IL6/KDR/PRKDI1/HTRAI/CCL11/NOD2/BMP4/SOX9/TNFAP3/TWIST1/TP63	38
GO:0043588	skin development	26/901	238/17046	0.00037	0.00889	0.00699	CPS1/MTOR/GRB10/IGF1/IGF2/PRKAG3/POMC/PPP1CB/PPP1CC/PHLDA2/IRS2/STBD1	26
GO:0009150	purine ribonucleotide metabolic process	42/901	458/17046	0.00037	0.00889	0.00699	CPS1/MTOR/GRB10/IGF1/IGF2/PRKAG3/POMC/PPP1CB/PPP1CC/PHLDA2/IRS2/STBD1	42
GO:0055085	transmembrane transport	94/901	1258/17046	0.00037	0.00892	0.00701	E/HLX/ZC3H12D/IGF1/IGF2/IL6/IRE1/ITGB2/LCK/LCP1/LGALS9/SMA03/NEATC3/LEF1/PIK3CG/IL20RB/AFBB1IP/PAG1/NOD2/BMP4/STK10/ZEB1/CCR2/TNFRSF4/ZAP70/FZD5/SLA2/FADD/RSAD2/CD8A	94

GO:0034113	heterotypic cell-cell adhesion	9/901	44/17046	0.00041	0.00985	0.00775	FGA/NFASC/ILIRN/ITGA7/ITGB2/ITGB7/JUP/PARVA/ADIPOQ	9
GO:0052652	cyclic purine nucleotide metabolic process	19/901	152/17046	0.00042	0.01009	0.00794	NPFER2/ADCY3/ADM/ADRB3/DRD4/GABBR1/AMPD2/GNAS/GPER1/GUCYJA3/HPCA/LHCGR/MC2R/NPPC/OPRL1/PALM/MRAP/SCT/CCR2	19
GO:0009612	response to mechanical stimulus	22/901	189/17046	0.00043	0.01009	0.00794	CH13L1/COL11A1/ANKRD23/IL6/IRF1/JUP/LCK/MAP3K1/ATP1A2/ATP8A2/CHRNA9/MAPK3/BGLAP/STRA6/BMP4/SLC8A1/SOX9/TIMP3/TLRS/TNFRSF1A/CRADD/FADD	22
GO:0006936	muscle contraction	29/901	280/17046	0.00043	0.01009	0.00794	MIRVIL/TRDN/CHRNA1/CTGF/DNA/BMP10/GPER1/TMOD4/GUCYJA3/KCNIP2/ANXA6/KCNH2/LCK/MYH4/MYL2/ATP1A2/ATP8A2/PGAM2/PIK3CG/PXN/ACTA2/SLC8A1/ACTC1/CA	29
GO:0031325	positive regulation of cellular metabolic process	179/901	2688/17046	0.00044	0.01025	0.00806	LDI/CASQ1/TRIM63/SPHK1/STBD1/RCSDB1 ABRI/CDH3/CDH13/CDKN1C/DMRT2/TBR1/ADCY3/CH13L1/ERLIN2/PSIP1/CCR1/CCR2/FOXO1/LARP1/MAK8IP2/VGLL2/MTOR/RNF144B/GAPDH/S/PABPC1/DNAIC2/FGF22/NPTN/BMP10/GNAS/GPER1/DOK7/GRB10/G /EGFR/ESR1/FGA/FGF10/RASA3/SBNO2/FOXO2/FOXO1/LARP1/MAK8IP2/VGLL2/MTOR/RNF144B/GAPDH/S/PABPC1/DNAIC2/FGF22/NPTN/BMP10/GNAS/GPER1/DOK7/GRB10/G STP1/BRE1/GUCYJA3/ANXA2/SOX8/NRG1/HKI/HMGAI/NRA1/ACACB/HPCA/HRH1/HSP90AA1/HSP90AB1/TFAP2E/BARHL2/IGF1/IGF2/CYR61/IL1RN/IL6/FOXK2/INHBA/IRF1/SL1 /JUP/KDR/HES5/LCK/LDLR/LGALS9/LHCGR/LMNA/LMO2/ITB1/SMAD3/MC2R/MEF2D/MAC3K1/MEOX1/MEOX2/MH2/MITF/NFATC3/NFYB/NHLH2/NPPC/NRAS/NTF3/OPRL1/PARK 2/LEF1/PRR16/ANGPT4/PIK3CG/PTX2/PLA2G2A/PLAGL1/PMU/RIK4/TLR9/CYTL1/POMC/BANP/PWIL2/FANCI/PRKAR1B/PRKD1/MAPK3/MAP2K2/MRAP/PSMB4/PAK6/ARNTL2/R GMA/PSMD7/PXN/RASGRF2/TRIM27/SCT/CCL11/CCL17/NPASA3/NOO2/SFRP2/TRAZB/BMP4/ZNF649/BMPRI1/BO/K/SOX9/STK10/SUPT6H/TBPT/CEA1/TCBEZ/ZEB1/TEAD3/T LB5/TNFAIP3/TNFRSF1A/TRA1/TRA5/TWIST1/CCR2/WNT10B/PAX8/CXCR4/FZD5/CARD14/ZC3H12A/CALR/CDK10/RUNX1/TP63/RUNX3/IRS2/CRADD/FADD/TNFRSF11A/SPHK1/ PIAS2/ZFAND2A/MAP3K6/LDB2/CBFA2T2/ADIPOQ/MICAL2/RAPGEF2/FGF19/NR1H4	179
GO:0051240	positive regulation of multicellular organismal process	96/901	1297/17046	0.00044	0.0104	0.00818	TRDN/SPON2/DMRT2/CELF1/CH13L1/CCR1/CCR2/SEZ6/ADM/CP51/CTGF/DIO3/ABAT7/DRD4/EGR3/EIF4G1/EPHA7/EPHA3/FGA/FGF10/ACINI/FOXO2/NEDD4L/PUM2/TENM4/NPTN/BMP 10/GNAS/GPER1/FFAR2/SOX8/NRG1/HLA-DPA1/HLA- E/HLX/ACACB/HOXD3/HRH1/IGF1/CYR61/IL6/IL12RB2/INHBA/IRF1/ISL1/KDR/AMIGO3/LCK/ARHGDI1/LGALS9/ITB1/SMAD3/NEUJ/NPPC/OPRL1/PALM/PARK2/LEF1/ANGPT4/ATP8 A2/ILX/PAL/IL20RB/TLR9/PRKD1/MAP2K2/SCT/CCL11/NOO2/SFRP2/BMP4/SLC8A1/BMPRI1B/SOX9/ZEB1/TEAD3/TLRS/TNFAIP3/TWIST1/CCR2/WNT10B/PAX8/CXCR4/FZD5/NL RX1/IFITM1/SCIN/RUNX1/TP63/FADD/TNFRSF11A/SPHK1/CBFA2T2/RSAD2/ADIPOQ/H2AFY/RAPGEF2	96
GO:0071605	monocyte chemotactic protein-1 production	4/901	8/17046	0.00046	0.0106	0.00834	GSTP1/LGALS9/TWIST1/ADIPOQ	4
GO:0071637	regulation of protein-1 production	4/901	8/17046	0.00046	0.0106	0.00834	GSTP1/LGALS9/TWIST1/ADIPOQ	4
GO:0072282	metanephric nephron tubule morphogenesis	4/901	8/17046	0.00046	0.0106	0.00834	SOX8/HES5/SOX9/PAX8	4
GO:0009190	cyclic nucleotide biosynthetic process	19/901	153/17046	0.00046	0.01063	0.00836	NPFER2/ADCY3/ADM/ADRB3/DRD4/GABBR1/AMPD2/GNAS/GPER1/GUCYJA3/HPCA/LHCGR/MC2R/NPPC/OPRL1/PALM/MRAP/SCT/CCR2	19
GO:0048146	positive regulation of fibroblast proliferation	10/901	54/17046	0.00046	0.01065	0.00837	EGFR/ESR1/FGF10/ANXA2/IGF1/NRAS/SIRT6/PML/S100A6/SPHK1	10

GO:0044271	cellular nitrogen compound biosynthetic process	274/901	4363/17046	0.00047	0.01065	0.00837	ZNF783/CDH13/CDKN1C/TCIRG1/C1D/ZBTB18/MTFHS/DMRT7/CELF1/TBR1/NPFER/ADCY3/PNR1/HNRNPUL1/ERLIN2/PSIP1/EGLN1/ACOT7/ZBED9/CIIDEA/NRPLS2/ZFP42/ADM1/IL31RA/CP51/ZNF358/ZNF738/CTGF/SMYD1/CYLID/ADR83/ZNF782/ADAL/ZNF709/ZNF781/CTED4/DDB1/DDOST/RNF168/ZNF709/VGLL2/MTOR/GABRR1/ZNF549/STGG/ATL2/EIF4G1/ELK4/ESR1/ALIAS1/SP8/EYF10/FHIT/XRN2/SBN02/TRAK1/MRSB2/FOXJ1/FOXO2/FOXO1/NUP210/NEEDD4L/LARP1/PUIM2/RYBP/VGLL2/MTOR/GABRR1/ZNF549/STGG/ALNAC3/PABPC1/DNAJC2/AMPD3/DMK3/GLS2/AMPD3/BMP10/ZNF638/GNAS/BNF111/ZNF844/GPER1/MPS188/ZBTB44/GTF2B/BRF1/GUCY1A3/NUME7/SOX8/NRGI/HLX/HMGA1/NRAA1/ACACB/HPCA/HOXB3/HOXC4/HOXD5/HOXC6/HOXD9/HSP90AA1/HSP90AB1/TTABP2E/ID3/BARHL2/NUME9/IGF1/IGF2/CYR61/IL6/IL16/FOXK2/INHBA/IRF1/ISL1/JUP/USP5/0/HLSL/HSS5/AF3/LGALS9/LHCGR/LMO2/SMAD3/MC2R/ME1/NEF2D/MEOX1/MEOX2/JMITF/LHX8/MOVD0/DRG1/NFATC3/NFYB/NHLH2/NPPCNTF3/OAS2/ORPL1/ATP5B/PALM/PARK2/LEF1/PRR18/SIRT6/PTX2/PKHD1/PKM/PLAGL1/PRKAG3/PML/RPPL3/RPK4/TLR9/CYTL1/POMC/POU2AF1/BNCF2/MED18/BANP/PWIL2/ELP3/PRMT6/DNAIC17/ZNF53/2/CNOT11/PRKD1/MYNN1/MAPK3/MRAP/PRMT8/PAK6/ARNTL2/RGMA/PRDM11/TENM2/GATA2B/METTL14/CCAR2/CREBZF/RFC2/TRIM27/NGS12/RPA3/RPL8/RPL29/SC/T/MPF5/14/IMPAS3/NOD2/SERP2/GZF1/SKK1/BMP4/ZNF649/BMPR19/BRO9/ZSCAN18/SOX9/SRP68/STAT2/STK3/SUPT6H/TA48/TBF/TCF1/TCCEB2/ZEB1/TEAD3/TERF1/TLE3/TLRS/TNFAI3/TNFRSF1A/TRAF1/TRAFA5/TWIST1/CCR2/TNFRSF4/UCP1/JUPP1/VAARS/WNT10B/MYHAG/ZNF7124/ZNF177/PAH8/FZD5/CARD14/CERS4/ZNF665/ZNF606/ZC3H12A/CPBE4/ZNF436/CALR/QTRT1/SLRP/SCRT1/HIST1H3A/SLA2/ZNF397/NR0B2/HOPX/KDM2B/LOX3/CBX2/RAE1/IGAS7/KMO/RUNX1/TP63/RUNX3/ACTN1/FADD/TNFRSF11A/SPHK3/BUO3/1/CNAT1/LIMD1/PIAS2/LDB2/CBFA272/AURKB/ADIPOQ/H2AF1/MICAL2/VGLL4/NUP93/ZBTB39/NR1H4	30/901	295/17046	0.00047	0.01065	0.00837	CDH3/APCDD1/CSTA/CTGF/EGFR/FGF10/EXPH5/FLNBL/FLOT2/CE2B/GNAS/CE1C/LCE1D/LCE2D/INHBA/IVL/KRT15/HES5/LAMA3/NF3/PITX2/BMP4/SOX9/TCHH/WNT10B/RUNX3/1/TP63/RUNX3/LDB2/H2AF1
GO:0008544	epidermis development	30/901	295/17046	0.00047	0.01065	0.00837	CDH3/APCDD1/CSTA/CTGF/EGFR/FGF10/EXPH5/FLNBL/FLOT2/CE2B/GNAS/CE1C/LCE1D/LCE2D/INHBA/IVL/KRT15/HES5/LAMA3/NF3/PITX2/BMP4/SOX9/TCHH/WNT10B/RUNX3/1/TP63/RUNX3/LDB2/H2AF1						
GO:0055080	cation homeostasis	49/901	566/17046	0.00047	0.01076	0.00846	TCIRG1/TRDN/CLINS/CCR1/ADM/DRD4/ESR1/NEEDD4/STEP2/NPTN/GPER1/FLVCR1/ANXA6/KCNH2/KDR/LCK/MF12/NUBP1/ATPIA2/OPRL1/ATP5B/PARK2/PDE6B/PIK3CG/PKH1D1/PML/SLC30A10/CHRNA9/PRKD1/SLAMF8/TRPC7/CC111/S6K1/BMP4/SLC4A1/SLC8A1/SLC9A3/TGMD2/TRP4/TRPC6/CCR2/CA7/CXCR4/BA87A/CALR/ATP13A4/CASQ1/SMO1/MT/15						
GO:0034330	cell junction organization	26/901	242/17046	0.00048	0.01079	0.00849	CDH3/CDH9/CDH12/CDH13/PKP3/MPP7/EPHA3/NFASC/EPB41L3/GIB2/FMN1/JUP/KDR/LAMA3/SMAD3/MIPZ/PLEC/FBLIM1/LIMS2/PARVA/PXN/FZD5/PARD6G/PARD6B/ACTN1/R/26						
GO:0051145	smooth muscle cell differentiation	9/901	45/17046	0.00049	0.01108	0.00871	ADM/FGF10/NFATC3/NTF3/PITX2/BMP4/SOX9/ZEB1/TMEM204						
GO:0006468	protein phosphorylation	118/901	1662/17046	0.0005	0.01115	0.00877	AKT3/ABI1/CDKN1C/SPEG/BCDKK/HCST/NPFER/ADCY3/CH1L1/ALPK2/CRR1/MAP3K8/IL131A/TRPM6/CTGF/PPM1L/ADR83/NLRP6/DRD4/EGFR/ADCK5/EPHA1/EPHA3/EPH8A/FGA/FGF10/RASA3/PPM1E/FOXO1/MORC3/MAPK8P2/TSSK2/MTOR/GAK/PSK1/FGF2/NPTN/BMP10/GPER1/DOCK7/GSTP1/ANX2/NRGI/HS90A81/IGF1/IGF2/CYR61/IL1RN/IL6/IL12RB2/INHBA/ISL1/TGDB2/KCNH2/KOR/HES5/LCK/LGALS9/SMAD3/MAP3K1/NRAS/NTF3/OPRL1/PARK2/ANGPT4/PIK3CG/PKH1D1/PLA2G2A/PRKAG3/PML/RIPK4/TLRS/ELP3/PR/1B/PKHD1/MAPK3/MAP2K2/PSMB4/PAK6/PSMD7/MARK4/PXN/RASGEF2/TRIM27/CC111/CCL17/NOD2/ZFRP2/SKK1/BMP4/BMPR18/SOX9/STK3/STK10/TNFAIP3/TNFRSF1A/TNFB/TWIST1/TNFRSF4/YWHAG/ZAP70/CXCR4/FZD5/CARD14/TTBK1/CDK10/RUNX3/IRS2/TNFRSF11A/STK19/SPHK1/MAP3K6/AURKB/ADIPOQ/H2AF1/RAPEGF2/ULK2/FGF19/19						
GO:0070374	positive regulation of ERK1 and ERK2 cascade	19/901	154/17046	0.0005	0.01119	0.0088	CH1L1/CCR1/CTGF/EGFR/FGA/FGF10/GPER/IL6/KDR/LGALS9/PLA2G2A/MAPK3/CCL17/CCL17/NOD2/BMP4/TNFRSF11A/RAPEGF2/FGF19						
GO:0060326	cell chemotaxis	24/901	217/17046	0.00051	0.01135	0.00892	CHGA/CCR1/EGR3/FFAR2/NRA41/HRH1/IL6/IL16/ITGB2/LGALS9/NOV/LEF1/PIK3GG/TREM1/PARVA/PRKD1/PIK3GG/CC111/CCL17/NOD2/CCR2/CXCR4/CALR/TNFRSF11A						
GO:0048732	gland development	38/901	408/17046	0.00051	0.01135	0.00892	CDKN1C/CP51/EGFR/ESR1/FGA/FGF10/DNK3/NRG1/HLX/HOXB3/HOXD3/IGF1/IGF2/IL6/ISL1/ACAT1/SMAD3/NFATC3/LEF1/PTX2/PKM/PML/ILMS2/CC111/STRA6/BMP4/SOX9/TG/38						
GO:0070486	leukocyte aggregation	38/901	408/17046	0.00051	0.01135	0.00892	MZ/TNFAIP3/PAK8/PPP2R2/CAST/IRX1/TP63/IRS2/FADD/TNFRSF11A/ALDH1A2 E/HLX/ZC3H12D/IGF1/IGF2/IL6/IRF1/ITGB2/LCK/ICP1/LGALS9/SMAD3/NFATC3/LEF1/PIK3GG/IL20RB/APBB1P/PAG1/NOD2/BMP4/STK10/ZEB1/CCR2/TNFRSF4/ZAP70/FZD5/SLA2/FADD/RSD2/CD8A						
GO:1902533	positive regulation of intracellular signal transduction	72/901	921/17046	0.00053	0.01178	0.00927	CDH13/HCS2/CH1L1/CCR1/MAP3K8/IL131A/MIB2/CTGF/ADR83/DRD4/EGFR/FGA/FGF10/RASA3/AKR1B1/PUIM2/MAPK8P2/MTOR/FGF2/GNAS/GPER1/NRGI/IGF1/IGF2/IL1RN/IL6/ISL1/KDR/HES5/LCK/LGALS9/LHCGR/MAP3K1/NRAS/NTF3/PARK2/PIK3CG/PLA2G2A/TLR9/ZDHHC13/PRKD1/MARK3/MAP2K2/PSMB4/PSMD7/PLEKHG5/PXN/RASGEF2/S100A4/CCL11/CCL17/NOD2/BMP4/SOX9/STK3/BST2/TNFRSF1A/TRAFA5/ZAP70/CXCR4/FZD5/CARD14/CDK10/IRS2/FADD/TNFRSF11A/SPHK1/MAP3K6/CD8A/ADIPOQ/RAPGEF2/FGF19						
GO:0002040	sprouting angiogenesis	10/901	55/17046	0.00054	0.0119	0.00935	CDH13/ESM1/EGR3/EPH8A/FOXO2/NRA41/KDR/LEF1/PARVA/BMP4						
GO:0021781	glial cell fate commitment	5/901	14/17046	0.00055	0.01199	0.00943	SOX8/NRGI/HES5/NTF3/SOX9						
GO:0044262	cellular carbohydrate metabolic process	28/901	271/17046	0.00055	0.01207	0.00949	GNF5/SLC51B/CP51/FOXO1/AKR1B1/MTOR/GAPDH5/GPER1/GRB10/HAS1/HK1/HRH1/IGF1/IGF2/IL6/LHCGR/PARK2/SIRT6/PGAM2/PRKAG3/POMC/PPP1CB/PPP1CC/CSGALNACT1/PHLA2/IRS2/STBD1/ADIPOQ						

GO:0019693	ribose phosphate metabolic process	43/901	482/17046	0.00056	0.0122	0.00959	TCIRG1/NPFR2/ADCY3/ACOTT/ADM/ADR83/DLIG2/DRD4/ENO2/GABBR1/GAPDH5/AMPD2/PDE7B/AMPD3/GNAS/GPER1/DNAJC15/GUCY1A3/NME7/HK1/ACACB/HPCA/NME9/IGFI/LHCGR/MC2R/NMY4/NDUFB4/ATP1A2/NPPC/OPRL1/ATP5B/PALM/PDEAC/PDE7A/SIRT6/PDE6B/PGANM2/PKM/MRAP/SCT/CCR2/UPT1	43
GO:0045595	regulation of cell differentiation	99/901	1356/17046	0.00058	0.01248	0.00982	TBR1/CCR1/SEZ6/ADM/FAM101A/CTGF/SMTD1/CYLD/BHLHA15/DMBT1/EGR3/EIF4G1/UNC13D/EPHA3/FGA/FGF10/ACINI1/FOXQ2/FOXO1/SFG20/FLOT2/NEDD4L/MTOR/TENM4/NPTN/BMP10/GNAS/GPER1/SOX8/NRG1/HLA-B/HLA-DOA/HLX/HOX83/HOXD3/OD3/BARHL2/IGF1/CYR61/IL6/INHBA/IRF1/ISL1/JUP/KDR/HESS/LCK/ARHGDI1/LGALS9/SMAD3/MF12/MITF/NEU1/NOV/NPCC/NTF3/PALM/PARK2/LEF1/ATP8A2/PLA2G2A/PML/SSH1/PRK01/MPAP2K2/BGLAP/CCL17/SFRP2/BMP4/BMP18/SOX9/STK3/SUPT6H/ZEB1/TEAD3/TNFRSF14/TWIST1/WNT10B/NWHAG/ZAP70/PAX8/CXCR4/ZC3H12A/CALR/SCRT1/HOPX/IFITM1/SCIN/RUNX3/TP63/RUNX3/FADD/LIMD1/PIAS2/CBFA2T2/ADIPQO/HZAFY/RAPGEF2/ULK2	99
GO:0031076	embryonic camera-type eye development	8/901	37/17046	0.00058	0.01251	0.00984	FGF10/PITX2/STRA6/ZEB1/TWIST1/FZD5/KDM2B/ALDH1A2	8
GO:0002407	dendritic cell chemotaxis	6/901	24/17046	0.00059	0.01259	0.0099	CCR1/LGALS9/PIK3CG/CCR2/CXCR4/CALR	6
GO:0006109	regulation of carbohydrate metabolic process	19/901	156/17046	0.00059	0.01259	0.0099	SILCS1B/FOXO1/MTOR/GAPDH5/GPER1/GRB10/HRH1/IGF1/IGF2/IL6/LHCGR/PARK2/SIRT6/PGANM2/POVIC/PPP1CB/PHLDA2/IRS2/ADIPQO	19
GO:2000147	positive regulation of cell motility	33/901	341/17046	0.0006	0.0129	0.01015	CDH13/CCR1/EGFR/EPHA1/FGF10/FOXQ2/GPER1/IGF1/CYR61/IL6/KDR/GALS9/SMAD3/NTF3/P2RY6/LEF1/ANGPT4/ELP3/PRKD1/MPAP2K2/CCL11/BMP4/SLC8A1/SOX9/TWIST1/CCR2/PTP4A4/COL18A1/CALR/IRS2/FADD/SPHK1/RAPGEF2	33
GO:0007274	neuromuscular synaptic transmission	7/901	29/17046	0.00063	0.01343	0.01056	CHRNA1/CHRNA2/CHRNA5/DTNA/EGR3/NTF3/CHRNA9	7
GO:0030802	regulation of cyclic nucleotide biosynthetic process	17/901	133/17046	0.00065	0.01365	0.01074	NPFR2/ADM/ADR83/DRD4/GABBR1/GNAS/GPER1/GUCY1A3/HPCA/LHCGR/MC2R/NPPC/OPRL1/PALM/MRAP/SCT/CCR2	17
GO:0051093	negative regulation of developmental process	58/901	710/17046	0.00065	0.01365	0.01074	CDH3/LECT1/CCR1/SEZ6/FAM101A/CYLD/ADR83/BHLHA15/FGF10/VASH1/FOXQ2/FOXO1/SPG20/GNAS/GPER1/SOX8/HLX/ID3/RSPQ2/IGF1/IL6/INHBA/IRF1/ISL1/HESS/ARHGDI1/SMAD3/MF12/NOV/NPCC/NRAS/PARK2/LEF1/CEND1/ANGPT4/PML/LIMS2/HFT122/CCL17/SFRP2/BMP4/SLIT1/SOX9/STK3/ZEB1/TWIST1/CCR2/WNT10B/PAX8/CALR/HOPX/RUNX1/TP63/LIMD1/CBFA2T2/ADIPQO/RAPGEF2/ULK2	58
GO:0070838	divalent metal ion transport	37/901	399/17046	0.00065	0.01375	0.01081	TRDN/CLCA1/CCR1/C15orf27/TRPM6/CTGF/TRPV9/BHLHA15/DRD4/RASA3/CBACR2B/GPER1/ANXA6/LCK/ATP1A2/NFATC3/OPRL1/PIK3CG/PML/TLR9/ZDHHC13/TRPV6/SLC30A10/CHRNA9/PRKD1/TRPV5/TRPC7/TRIM27/BMP4/SLC8A1/TRPC4/TRPC6/TRPM2/CACNA1E/CACNB2/CASQ1/SMDT1	37
GO:0010628	positive regulation of gene expression	114/901	1608/17046	0.00066	0.01375	0.01081	CDH3/CDH13/CDKN1C/DMRT2/TBR1/ERLIN2/PSIP1/IL13/RA/CTGF/CTED4/BHLHA15/EEF2/EGFR/ESR1/FGF10/SBNQ2/FOXC2/FOXO1/LARP1/VGLL2/MTOR/PABPC1/DNAIC2/BMP10/GPER1/BRF1/SOX8/HMGAI1/NRAA1/HOXD3/TFAP2E/BARHL2/IGF1/IGF2/CYR61/IL6/FOXQ2/INHBA/IRF1/ISL1/JUP/HESS/LCK/LGALS9/LMNA/LMO2/SMAD3/MF2D/MEOX1/MEOX2/MF12/MITF/NFATC3/NFYB/NHLH2/NTF3/PARK2/LEF1/PR16/PTX2/PLAGL1/RIPK4/TUR9/CYLL1/POVIC/BANP/PWIL2/PRKD1/MAPK3/ARNTL2/RGMA/PTGFR/ACTA2/TRIM27/NPAS3/NOD2/SFRP2/TRA2B/BMP4/ZNF649/BMP18/SOX9/STK3/SUPT6H/TBP/TCEA1/TCEB2/ZEB1/ACT1/TEAD3/TNFRSF1A/TRAFF1/TRAFF5/TWIST1/WNT10B/PAX8/FZD5/CARD14/ZC3H12A/CALR/NR0B2/RUNX1/TP63/RUNX3/FADD/TNFRSF1A/ALDH1A2/SPHK1/PIAS2/LDB2/GBEA2T2/HZAFY/MICAL3/NR1H4	114
GO:0030097	hemopoiesis	56/901	680/17046	0.00066	0.01375	0.01081	AB11/GDNK1/CCR1/IL13/TRA/CYLD/ESCO2/EEF2/EFNA2/EGR3/EM11/SBNQ2/ACINI1/MTOR/GNAS/FLVCR1/ANXA2/HLA-B/HLA-DOA/HLX/HOX83/IL6/INHBA/IRF1/KDR/HESS/LCK/LGALS9/LMO2/MEOX1/MITF/NFATC3/LEF1/PML/HERC6/SMPD3/BGLAP/SFRP2/VPS33A/BMP4/STK3/TCEA1/ZEB1/WNT10B/ZAP70/FZD5/CBOR2/SCIN/RUNX1/RUNX3/ACTN1/FADD/TNFRSF1A/RSAD2/CD8A/ADIPQO/CD79A	56
GO:0009165	nucleotide biosynthetic process	31/901	315/17046	0.00066	0.01375	0.01081	TCIRG1/NPFR2/ADCY3/ACOTT/ADM/ADR83/DRD4/GABBR1/AMPD2/AMPD3/GNAS/GPER1/GUCY1A3/NME7/HK1/ACACB/HPCA/NME9/LHCGR/MC2R/ME1/NPPC/OAS2/OPRL1/ATP5B/PALM/PKM/MRAP/SCT/CCR2/UPT1/KMO	31
GO:0030003	cellular cation homeostasis	43/901	486/17046	0.00066	0.01375	0.01081	TCIRG1/TRON/CLNS/CCR1/ADM/DRD4/ESR1/NEDD4L/NPTN/GPER1/FLVCR1/ANXA6/LCK/NUBP1/ATP1A2/OPRL1/ATP1A2/OPRL1/ATP5B/PDE6B/PIK3CG/PKH1/PML/SLC30A10/CHRNA9/PRKD1/SLAMF8/TRPC7/CCL11/SGRK1/BMP4/SLC4A1/SLC8A1/GSM2/TRPC4/TRPC6/CCR2/CA7/CXCR4/RAB7A/CALR/ATP13A4/CASQ1/SMDT1/MTLS	43

GO:0070489	T cell aggregation	37/901	400/17046	0.00069	0.01382	0.01087	MAP3K8/CYL1D/DOST/EGFR3/FLTOT2/MTOR/HLA-DOA/HLA-DPA1/HLA-E/HLX/ZC3H12D/IGF1/IGF2/IL6/IRF1/JTGB2/LCK/LCP1/LGALS9/SMAD3/NFATC3/LEF1/PIK3CG/IL20RB/APBB1P/PAG1/NOD2/BMP4/ZEB1/CCR2/TNFRSF4/ZAP70/FZD5/SLA2/FADD/RSAD2/CD8A	37
GO:0071320	cellular response to cAMP	9/901	47/17046	0.00069	0.01382	0.01087	CP51/CYP11A1/EGR3/AQP9/PIK3CG/SLC8A1/WNT10B/ADIPOQ/RAPGEF2	9
GO:0018108	peptidyl-tyrosine phosphorylation	31/901	316/17046	0.0007	0.01397	0.01098	ABI1/IL13RA/EGFR/EPHA1/EPHA3/EPHB4/FGF10/MTOR/NPTN/DOK7/NRG1/IGF1/IGF2/IL6/IL12RB2/ISL1/JTGB2/KOR/HESS/LCK/NTF3/ANGPT4/MAPK3/MAP2K2/PXN/TRIM27/NO	31
GO:0071396	cellular response to lipid	35/901	372/17046	0.0007	0.01398	0.011	RSN2/ADCY3/CPS1/CYP11A1/EGFR/EPHA3/ESR1/SBN2/MIC1/GNAS/GPER1/FAR2/GSTP1/NR4A1/IL6/INHBA/ISL1/ATP1A2/P2RY6/LEF1/MAPK3/PTGFR/BGLAP/BMP4/SOX9/TL	35
GO:0002695	negative regulation of leukocyte activation	17/901	134/17046	0.0007	0.01399	0.01101	S5/TNFAIP3/WNT10B/ZC3H12A/NR0B2/TRIM63/MGAR2/ALDH1A2/LY86/NR1H4 IL31RA/CYL1D/GPER1/HLX/ZC3H12D/INHBA/IRF1/LGALS9/IL20RB/PAG1/BMP4/BPI/TNFAIP3/CCR2/IL11/ZC3H12A/SLA2	17
GO:0042327	positive regulation of phosphorylation	73/901	946/17046	0.0007	0.01399	0.01101	ABI1/ADCY3/CH13L1/CCR1/MAP3K8/IL31RA/CTGF/ADRB3/DRD4/EGFR/FGA/FGF10/RASA3/MAPK8IP2/MTOR/GAPDH5/FGF2/NPTN/BMP10/GPER1/DOK7/GRB10/ANKA2/NRGL1/HSP90AB1/IGF1/IGF2/CYR61/IL1IRN/IL6/INHBA/ISL1/KDR/HE5/LCK/LGALS9/MAP3K1/NRAS/NTF3/OPRL1/ANGPT4/PIK3CG/PLA2G2A/TLR9/PRKAR1B/PRKDI/MAPK3/MAP2K2/PSMB4/PAK6/PSMD7/PXN/RASGEF2/CCL11/CCL17/NOD2/SRR2/BMP4/SOX9/STK3/STK10/TNFRSF1A/CXR4/FZD5/CARD14/CDK10/RS2/TNFRSF1A/ADIPOQ/RAPGEF2/FGF19	73
GO:0014033	neural crest cell differentiation	10/901	57/17046	0.00073	0.01436	0.01129	FOX2/SOX8/NRGI1/SL1/LEF1/PITX2/SOX9/TWIST1/ALDH1A2/FGF19	10
GO:0050865	regulation of cell activation	39/901	430/17046	0.00073	0.01436	0.01129	MAP3K8/IL31RA/CTGF/CYL1D/EGFR3/UNC13D/FGF10/FLTOT2/MTOR/GPER1/HLA-DOA/HLA-DPA1/HLA-E/HLX/ZC3H12D/IGF1/IGF2/IL6/INHBA/IRF1/LCK/LGALS9/IL20RB/PAG1/PTPRE/NOD2/BMP4/BPI/SUPT6H/ZEB1/TNFAIP3/CCR2/TNFRSF4/ZAP70/IL11/ZC3H12A/SLA2/IRS2/FADD	39
GO:0050777	negative regulation of immune response	15/901	111/17046	0.00073	0.01445	0.01136	NLRP6/A2M/HLA-B/HLA-E/HLX/LGALS9/IL20RB/MASP1/PSMB4/TRIM27/NOD2/BST2/TNFAIP3/CCR2/NLRX1	15
GO:2000026	regulation of multicellular organismal development	105/901	1465/17046	0.00075	0.01464	0.01151	CDH3/DMRT2/TBR1/ECT1/CH13L1/CCR1/SEZ6/ADM/FAM101A/CTGF/CYL1D/DMBT1/EGFR3/EIF4G1/EPHA1/EPHA3/ESR1/FGF10/VASH1/ACIN1/FOX2/SPG20/NEED4/MTOR/TENM4/NPTN/BMP10/GNAS/GPER1/SOX8/NRGI1/HLA-B/HLA-DOA/HLX/ACACB/HOXB3/HOXD3/RPO2/BAHL2/IGF1/CYR61/IL1IRN/IL6/INHBA/IRF1/ISL1/KDR/AMIGO3/HESS/LAMA3/LCK/ARHGAP10/GALNS9/SMAD3/MITF/NEU1/NRAS/NTF3/PALM/PARK2/LEF1/CEND1/ANGPT4/ATP8A2/PML/SSH1/LIM52/PRKD1/MMP18/SULT1/SOX9/STK3/SUPT6H/ZEB1/TNFAIP3/TNFRSF1A/PHLDA2/TWIST1/CCR2/WNT10B/YWHAG/ZAP70/PAX8/CXCR4/CALR/COLO/SCRT1/HOPX/SCN/RUNX1/TP63/FADD/SPHK1/CBFA2T2/ADIPOQ/H2AFY/RARGEF2/ULK2	105
GO:0072511	divalent inorganic cation transport	37/901	402/17046	0.00075	0.0147	0.01156	TRDN/CLCA1/CCR1/C15orf27/TRPM6/CTGF/TRPV3/BHLHA15/DRD4/RASA3/CXCR2B/GPER1/ANKA6/LCK/ATP1A2/NFATC3/OPRL1/PIK3CG/PML1/TLR9/ZDHHC13/TRPV6/SLC30A10/CHRNA9/PRKD1/TRPV5/TRPC7/TRIM27/BMP4/SLC8A1/TRPC4/TRPC6/TRPM2/CACNA1E/CACNB2/CASQ1/SMDT1	37
GO:0032870	cellular response to hormone stimulus	56/901	684/17046	0.00076	0.01472	0.01158	TCIRG1/NPFFR2/ADCY3/AP3S1/CPS1/CYP11A1/EGFR/EGFR3/EIF4G1/ESR1/FGF10/RASA3/FOXO1/MTOR/FGF2/GNAS/GPER1/GRB10/NR4A1/IGF2/IL6/INHBA/ISL1/LCK/LHCGR/LMO2/ATP1A2/NRAS/P2RY6/LEF1/PRKAG3/TLR9/PRKAR1B/LMBRD1/MAPK3/MAP2K2/PSMB4/PSMD7/PTGFR/PTPRE/PXN/RASGEF2/BMP4/NAVMP2/WNT10B/PAX8/NROB2/TRIM63/MGAR2/IRS2/ADIPOQ/RAPGEF2/FGF19/NR1H4	56
GO:0006171	cAMP biosynthetic process	16/901	123/17046	0.00076	0.01473	0.01158	NPFFR2/ADCY3/ADM/ADRB3/DRD4/GABRR17/GNAS/GPER1/HPCA/LHCGR/MC2R/OPRL1/PALM/MRAP/SCT/CCR2	16
GO:0044723	single-organism carbohydrate metabolic process	55/901	669/17046	0.00076	0.01475	0.0116	GNB/BAGAL17/GALNT15/CIN5/SLC5B/NEUA/GALM/CPS1/PARP4/B3GLCT/MGAT5B/DDOST/ENO2/TRAK1/FOXO1/AKR1B1/MTOR/FUCA1/SLC37A4/ST6GALNAC3/GBGT1/GAPDH5/SLC17A5/DHHDH/GPER1/EOGT/GRB10/HAS1/HK1/HRH1/IGF1/IGF2/IL6/MUC21/LHCGR/MGAT1/NEU1/OAS2/PARK2/CHST15/SIRT6/GALNT7/PGAM2/PKM/PRKAG3/POMC/PPP1C/B/PPP1CC/CSGALNACT1/PHLDA2/MOGS/CALR/IRS2/STBD1/ADIPOQ	55
GO:0018212	peptidyl-tyrosine modification	31/901	318/17046	0.00077	0.01491	0.01172	ABI1/IL13RA/EGFR/EPHA1/EPHA3/EPHB4/FGF10/MTOR/NPTN/DOK7/NRG1/IGF1/IGF2/IL6/IL12RB2/ISL1/JTGB2/KOR/HESS/LCK/NTF3/ANGPT4/MAPK3/MAP2K2/PXN/TRIM27/NO	31
GO:0061323	cell proliferation	5/901	15/17046	0.00079	0.01506	0.01184	D2/SFRP2/TNFRSF1A/ZAP70/ADIPOQ BMP10/ISL1/PITX2/BMP4/SOX9	5
GO:0003338	involved in heart morphogenesis	7/901	30/17046	0.00079	0.01506	0.01184	FGF10/SOX8/FMN1/HESS/BMP4/SOX9/PAX8	7

GO:0002862	negative regulation of inflammatory response to antigenic stimulus	4/901	9/17046	0.00079	0.01506	0.01185	NLRP6/IL20RB/PSMB4/NOD2	4
GO:1901293	nucleoside phosphate biosynthetic process	31/901	319/17046	0.00081	0.0155	0.01219	TCIRG1/NPFR2/ADCY3/ACOT7/ADM/ADR83/DRD4/GABBR1/AMPD2/AMPD3/GNAS/GPER1/GUCY1A3/NMIE1/ACACB/HPCA/NME9/LHCGR/MC2R/ME1/NIPPC/OAS2/OPRL1/ATP5B31/PALM/PKM/NRAP/SCT/CCR2/UPP1/KMO	31
GO:0071704	organic substance metabolic process	555/901	9633/17046	0.00083	0.01579	0.01242	AKT3/ABI1/CDH3/GNF/ZNF783/TSPAN5/DH13/USP2/MBNL2/PARP/CDKN1C/SPERG/BCKKB/CIRG1/CID1/ZBTB18/PITRM1/MTFHS/PPDN/DMRT2/CELF1/CELF2/TBR1/HCS2/NPFFFR2/ADCY3/PNRC1/TMED10/SLC7A2/LECT1/A/DAM29/HNRNPUL1/RPPI1/HIBADH/CH13/1/ERLIN2/ACOT7/EXOC3/ADPRHL1/CARD16/ZBED9/CIDEA/A1LPK2/GALNT15/CLCA1/CLNS/MRP152/CCR1/SLC51B/CNP/APOA1BP/NEU4/COUS93/COL11A1/GALM/MAP3K8/ZFP42/ADM/IL13RA/EGFLAM/UBICP1/HUS1B/CPD/CPM/CP51/PXDN/CRABP1/ZNF358/TRPM6/MIB2/PARP4/IDLIRAD3/B3GLCT/MGAT5B/CSTA/ZNF738/CTGF/SMYD1/PPM1/SH3D19/CYLD/MBOAT1/ADRB3/ESCO2/CYP11A1/ZNF782/HTM1/ADAL/ZNF709/ZNF781/CITED4/DBB1/LONRF2/DDOST/RNF168/ZNF366/BHLHA15/NLRP6/DIO3/DLG2/DNMT3A/ABAT/DPH1/DRD4/ECE1/AGXT/EEF2/EGFR/EGR3/PATL2/EIF4G1/A2M/ELK4/UPH/ENO2/ADCK5/EPHA1/EPHA3/EPHA4/ESR1/ALAS1/F11/FAH/PRSS54/RNF182/SP8/FGA/FGF10/FHIT/XRN2/RASA3/PPM1E/SBNO2/TRAK1/MSR82/ACIN1/FOXL1/FOX2/FOXO1/AKR1B1/GGA3/DIP2A/FLOT2/NUP210/NEEDD4/LARP1/PUM2/RYBP/MORC3/MAPK8IP2/TSSK2/VGLL2/MTOR/FUCA1/SLC37A4/GABBR1/RNF144B/ZNF549/STGALINAC3/GAK/SAMM50/PNK0/TEMM4/ACOT11/LTN1/FBXO2/LCE2B/SACS/GATM/GBGT1/GAPDH/SLC12A5/RP56K1/DNAUC2/FGF22/NPTN/AMPD2/PDE7B/DKK3/GS2/NP54A/AMPD3/DHHD4/BMP10/ZNF638/GNAS/ZNF311/TPRSS12/PIGW/ZNF844/THEM5/GPER1/EOGT/DOK7/GRB10/MRPS18B/ZBTB44/DNAUC15/GSTP1/GTF2B/BRF1/GUCY1A3/NMIE7/PAD1/GZMA/ANXA2/HAS3/SERPIND1/SOX8/NRG1/HK1/HLX/HMGAI1/NR4A1/ACACB/HPCA/APBA2/HOXB3/HOXC5/HOXD3/HRH1/ATP1A2/NFATC3/NFYB/NHLH2/NOV/NPPADU/HSPAL1/HSP90AA1/HSP90A81/DUPD1/ADAMTSL5/TFAP2E/ID3/ZC3H12D/COL28A1/FMN1/BARH2/NM9/GF1/GF2/CYR61/LCE1C/LCE2D/IL1RN/IL6/IL12RB2/PRSS41/IL16/FOXK2/INHBA/NP5A/IRF1/SL1/TGFB2/ITH3/ITH4/IVU/JUP/USP50/HLS1/KCNH2/KDR/ACAT1/HES5/AFF3/CLK/MUC21/IDL1B/LGALS9/LH-CGR/LMNA/LMO2/LOX1/TB/SMA/D3/MC2R/ME1/ME2/MEF2D/MAPK3/MAP2K2/PROC/MRAP/PRMT8/MASP1/HTRA1/PSMB4/PAK6/ARNTL2/RGMA/PRDM11/PSMD7/PTGFR/PTENM2/GATAD2B/KLHL8/RDH14/METTL1/WRP25/LPCAT2/BANP/PPP1CB/HERG6/PPP1CC/PIWIL2/ELP3/PRMT6/DNAIC17/ZNF532/PPP2R2B/FANCF/WDR33/5/MPD3/CNOT11/VAC14/PRKARI/B/LMBRD1/CSGALNACT1/PRK11/MSR2/MYNN/APOBR/MAPK3/MAP2K2/PROC/MRAP/PRMT8/MASP1/HTRA1/PSMB4/PAK6/ARNTL2/RGMA/PRDM11/PSMD7/PTGFR/PTENM2/GATAD2B/KLHL8/RDH14/METTL14/MARK4/CCAR2/PTPRE/PXN/CREBZF/ACTA2/RASGEF2/RFC2/TRIM27/RGR/RGS12/EXOC4/RP43/RPL8/RPL29/SCT/CCL11/CCL17/ABHD4/MRPS14/PRSS22/NPAS3/NOD2/STRA6/SFRP2/TRA2B/GZF1/SGK1/CERK/BWIP4/ZNF649/BWIP18/BRD9/ZSCAN18/BOK/SOX9/SRP68/STAZ2/STK3/STK10/SUPT6H/BST2/NAVAMP2/TAFA4B/TBP/TCFA1/TCFB2/ZEB1/ACTC1/TEAD3/TERF1/TGM2/TIMP3/TLE3/TNFAIP3/TNFRSF1A/TNXB/TRAFA1/TRAFA5/PHLDA2/TWIST1/CCR2/TNFRSF4/UCP1/UPP1/AVARS/WNT10B/VWHAG/ZAP70/ZNF7/ZNF124/ZNF177/P1P4A1/MOGS/PAX8/CXCR4/FZD5/RAB7A/ER3/CARD14/GDPD3/CERS4/ZNF665/EPH3/3/CH14/ERMP1/ZNF608/ZC3H12/FAAP100/CEB4/COL18A1/ZNF436/EEPDI/CALR/QTRT1/SLIRP/COX/CAST/SCRT1/HIST1H3A/SLA2/ZNF397/NR0B2/HOPX/TTBK1/SPINK7/TRIM63/KDM2B/LOX1/GTBP3/CBX2/RAE1/GAS7/CDK10/KMO/RUNX1/TP63/RUNX3/SERPINA5/RS2/ACTN1/CRADD/FADD/TNFRSF11A/ALDH1A2/STK19/SYNU2/SPHK1/BUID31/CCNA1/ENDOU/STBD1/LIMD1/CH25H/ERL1/PIAS2/ZFAND2A/MAP3K6/LDB2/SLC16A3/CBFA2T2/AU14/RK/NEUR13/SDR42E1/ADIPQ/RAB3D/H2AF1/ENTPD3/PREPL/MICAL2/IN4BP1/VGLL4/NUP93/RAPGEF2/ULK2/ZBTB39/LPGAT1/FGF19/NR1H4/ADM/CP51/CTGF/CYP11A1/CITED4/STAP2/NPTN/PER1/FLVCR1/ANXA6/KCNH2/KDR/LCK/WF12/NUBP1/ATP1A2/OPRL1/ATP5B/PARK2/PDE6B/PIK3CG/PKH11/PML/SLC30A10/CHRNA9/PRKD1/SLAMF8/TRPC7/CCL11/SGK1/BMP4/SLC4A1/SLC8A1/SLC9A3/TGM2/TRPC4/TRPC6/CCR2/CA7/CXCR4/RAB7A/CALR/ATP13A4/CASQ1/SMDT1/MTL5	36
GO:0048545	response to steroid hormone	36/901	390/17046	0.00084	0.01582	0.01244	BMP4/SLC9A3/TIMP3/CALB/NR0B2/TRIM63/MGARP/ALDH1A2/ADIPQ/NR1H4	36
GO:0032881	regulation of polysaccharide metabolic process	8/901	39/17046	0.00084	0.01584	0.01246	MITOR/GRB10/GF1/IGF2/POMC/PPP1CB/PHLDA2/IRS2	8
GO:0098771	inorganic ion homeostasis	49/901	581/17046	0.00084	0.01584	0.01246	TCIRG1/TRON/CLNS/CCR1/ADM/DRD4/ESR1/NEEDD4/STAP2/NPTN/PER1/FLVCR1/ANXA6/KCNH2/KDR/LCK/WF12/NUBP1/ATP1A2/OPRL1/ATP5B/PARK2/PDE6B/PIK3CG/PKH11/PML/SLC30A10/CHRNA9/PRKD1/SLAMF8/TRPC7/CCL11/SGK1/BMP4/SLC4A1/SLC8A1/SLC9A3/TGM2/TRPC4/TRPC6/CCR2/CA7/CXCR4/RAB7A/CALR/ATP13A4/CASQ1/SMDT1/MTL5	49
GO:0005976	polysaccharide metabolic process	14/901	101/17046	0.00085	0.01584	0.01246	CP51/MTOR/GRB10/HAS1/IGF1/IGF2/PRKAG3/POMC/PPP1CB/CSGALNACT1/PHLDA2/IRS2/STBD1	14
GO:0010876	lipid localization	31/901	320/17046	0.00086	0.01599	0.01258	ABC9A/SLC27A2/CIDEA/SLC51B/FTM14/DRD4/SLC10A4/ATP11A/WP54A/FAR2/ACACB/IL6/INHBA/AQP9/ATP9B/LDLR/ANO7/PARK2/ATP8A2/SLC01C1/PNLI/POMC/PONI/APOBR1/ABHD4/STRA6/ZC3H12A/IRS2/TNFRSF11A/ADIPQ/NR1H4	31

GO:0043255	regulation of carbohydrate biosynthetic process	12/901	79/17046	0.00086	0.01599	0.01258	FOXO1/MTOR/GPER1/GRB10/HRH1/IGF1/IGF2/IL6/LHCGR/PPP1CB/IRS2/ADIPOQ	12
GO:0048568	embryonic organ development	38/901	420/17046	0.00089	0.01639	0.01289	CDKN1C/IGB6/COL11A1/ADM/EGFR/FGF10/FOXO2/GATM/GNAS/FLVCR1/HLX/HOXB3/HOXC/HOXD3/ID3/CTRB1/KDR/LMO2/SMAD3/LEF1/ATP8A2/PTX2/CHRNA9/IFT122/SCT/538	38
GO:0030817	regulation of cAMP biosynthetic process	15/901	113/17046	0.00089	0.01639	0.01289	TRAG/BMP4/SLC8A1/SOX9/STK3/ZEB1/TWIST1/PA88/FZD5/KDM2B/RUNX1/ALDH1A2/MICAL2 NPFER2/ADM/ADRB3/DRD4/SABBR1/GNAS/GPER1/HPCA/LHCGR/MC2R/OPRL1/PALM/MRAP/SCT/CCR2	15
GO:0042325	regulation of phosphorylation	97/901	134/17046	0.00089	0.01639	0.01289	AB11/CDKN1C/NPFR2/ADC3/CH13L1/CCR1/MAP3K8/IL31RA/CTGF/ADRB3/NLRP6/DRD4/EGFR/EPHA1/FGA/FGF10/RASA3/PPM1E/FOXO1/MAPK8IP2/MTOR/GAPDH5/FGF22/NP	97
GO:0051173	positive regulation of nitrogen compound metabolic process	117/901	1672/17046	0.0009	0.0165	0.01297	TN/BMP10/GPER1/DOK7/GRB10/DNAJL5/GSTP1/ANXA2/NRG1/HS90AB1/IGF1/IGF2/CYR61/IL1RN/IL6/NHBA/ISL1/TG2/KDR/HESS/LCK/LGALS9/SMAD3/MAP3K1/NRAS/NTF3/OPRL1/PARK2/ANGPT4/SIRT6/PIK3CG/PKH01/PLA2G2A/PAL/TLR9/ELP3/VACL4/PRKAR1B/PRK01/MAPK3/MAP2K2/SLAMF8/PSMB4/PAK6/PSMD7/PXN/RASGRF2/TRIM27/CCL11/CCL17/NOD2/SFRP2/BMP4/SOX9/STK3/STK10/TNFAIP3/TNFRSF1A/TNXP8/TWIST1/TNFRSF4/YWHAG/CXCR4/FZD5/CAK1D4/CDK10/IRS2/TNFRSF1A/SPHK1/MAP3K6/ADIPOQ/H2AF1/RAPGEF2/FGF19	117
GO:0007159	leukocyte cell-cell adhesion	39/901	435/17046	0.00091	0.01661	0.01306	CDH13/CDKN1C/DNMT2/TBR1/ERLIN2/PSI1/ADM/IL131RA/ADRB3/CITED4/RNF168/BUHA15/EEF2/EGFR/ESR1/FGF10/SBNO2/FOXO2/FOXO1/LARP1/VGILL2/MTOR/GAPDH5/PA8	39
GO:0001667	ameboid-like cell migration	28/901	280/17046	0.00092	0.01683	0.01323	PCI/DNACC2/BMP10/GNAS/GPER1/BRF1/GUCY1A3/SOX8/HMGA1/NRA41/HPCA/HS90AA1/HS90AB1/TFAP2E/BAH1L2/IGF1/IGF2/CYR61/IL6/FOXK2/INHBA/IRF1/ISL1/JUP/HESS/LGALS9/LHCGR/LMNA/LMO2/SMAD3/MC2R/MEF2D/MEOX1/MEOX2/MTF/NFATC3/NFYB/NHLH2/NPPC/NTF3/PARK2/LEF1/PRR16/PTX2/PLAGL1/RIPK4/TLR9/CYTL4/POMC/BA	28
GO:0007507	heart development	40/901	450/17046	0.00092	0.01683	0.01323	NP/PW1L2/PRK01/MAPK3/MRAP/ARNTL2/RGNA/TRIM27/SCT/NPAS3/NOD2/SFRP2/TRA2B/BMP4/ZNF649/BMPR1B/SOX9/STK3/SUPT6H/TBP/TCEA1/TCEB2/ZEB1/TEAD3/TLR5/TNFRSF1A/TRAF1/TRAF5/TWIST1/WNT10B/PA88/FZD5/CAK1D4/CALR/RUNX1/TP63/RUNX3/FADD/TNFRSF1A/SPHK1/PIAS2/LDB2/CBFAZ2/MICAL2/NR1H4	40
GO:0034109	homotypic cell-cell adhesion	41/901	465/17046	0.00094	0.01705	0.01341	MAP3K8/CYLD/DDOST/EGR3/FGA/FLOT2/MTOR/GNAS/HLA-DOA/HLA-DPA1/HLA-E/HLX/ZC3H12D/IGF1/IGF2/IL6/IRF1/ITGB2/IUP/LC/LCP1/LGALS9/SMAD3/NFATC3/LEF1/PIK3CG/IL20RB/APBB1IP/PAG1/NOD2/BMP4/STK10/ZEB1/CCR2/TNFRSF4/ZAP70/FZD5/SLA2/FADD/RSAD2/CD8A	41
GO:0050728	negative regulation of inflammatory response	13/901	91/17046	0.00096	0.01742	0.0137	NLRP6/GPER1/GSTP1/ISL1/SMAD3/NOV/IL20RB/PSMB4/NOD2/TNFAIP3/TNFRSF1A/NLRX1/ADIPOQ	13
GO:0001818	negative regulation of cytokine production	22/901	201/17046	0.00098	0.01776	0.01397	E/HLX/ZC3H12D/IGF1/IGF2/IL6/IRF1/ITGB2/ITGB7/LCK/LCP1/LGALS9/SMAD3/NFATC3/LEF1/PIK3CG/IL20RB/APBB1IP/PAG1/NOD2/BMP4/STK10/ZEB1/CCR2/TNFRSF4/ZAP70/FZD5/SLA2/FADD/RSAD2/CD8A	22
GO:0050927	positive regulation of positive chemotaxis	6/901	23/17046	0.001	0.01788	0.01406	CDH3/CIDEA/CYLD/GSTP1/IL6/NHBA/LGALS9/LEF1/PM1/IL20RB/TLR9/POMC/TRIM27/NOD2/BB1/BS12/TNFAIP3/TWIST1/TNFRSF4/NLRX1/ZC3H12A/ADIPOQ	6
GO:0072243	metanephric nephron epithelium development	6/901	23/17046	0.001	0.01788	0.01406	SOX8/ACAT1/HESS/SOX9/PA88/ADIPOQ	6

GO:0006112	energy reserve metabolic process	19/901	164/17046	0.00108	0.0186	0.01463	ADCY3/CPS1/ADRB3/MTOR/GNAS/GRB10/ACACCB/GF1/GF2/PRKAG3/POMC/PPP1CC/PRKAR1B/VAMP2/PHIDA2/CACNA1E/IRS2/STBD1	19
GO:0022008	neurogenesis	109/901	1548/17046	0.0011	0.01878	0.01477	FARP1/CDKN1C/SPON2/ZBTB18/TACC2/TBR1/GPRIN1/CLN5/SEZ6/CNP/COL9A3/SC11/ADM/APCDD1/CYP11A1/DNMT3A/EFNA2/EGFR/EIF4G1/EM11/EPHA1/EPHA3/EPHB4/FGF10/RASA3/ITBD3/SFG20/NFASC/EPB4112/NEDD4/PSD3/NAKKB1B2/DNFB31/TENM4/FGF22/NPTN/GPER1/SOX8/KCNP2/NR61/HOXB3/HOXD3/HSP90AA1/HSP90AB1/ID3/RSP02/FMN1/ARHL2/GF1/IL6/INHBA/ISL1/HES5/STMN1/ARHGDI1/LG1/LHX8/NEU1/NRAS/NTF3/PCALM/PARK2/LEF1/CEND1/ATP8A2/PTX2/SSH1/MXR8/PPP1CC/ELP3/PRKDI1/MAPK3/MAKP2/PSMB4/RGMA/TRPC7/PSMD7/TENM2/RASGRF2/S100A6/SK1/BMP4/BMP1B/SLIT1/BOK/SOX9/ZEB1/TRPC4/TRPC6/TWIST1/WNT10B/WHAG/CACNB2/CXCR4/FZD5/LST1/CALB1/SCRT1/PAR6B/GAS7/RUNX1/RUNX3/IRS3/ALDH1A2/CBFA2T2/ARHGFE10/RARGFE2/ULK2/FGF19	109
GO:0001101	response to acid chemical	28/901	284/17046	0.00115	0.01955	0.01538	CPS1/CTGF/CYP11A1/DNMT3A/EGFR/EPHA3/AKR1B1/MTOR/GNAS/FFAR2/HPCAH/SD1B2/IL6/AQP2/IFOS/P2RN6/PONI1/PTGFR/BMP4/SOX9/ZEB1/TIMP3/WNT10B/CPEB4/COL1281/ALDH1A2/ADIPOQ/NR1H4	28
GO:0010906	regulation of glucose metabolic process	13/901	93/17046	0.00118	0.02009	0.0158	FOXO3/MTOR/GRB10/GF1/GF2/IL6/PARK2/PGAM2/POMC/PPP1CB/PHLDA2/IRS2/ADIPOQ	13
GO:0045747	positive regulation of Notch signaling pathway	7/901	32/17046	0.00119	0.02009	0.0158	TSPAN5/FGF10/HES5/MFNG/NOV/NOD2/TP63	7
GO:0030198	extracellular matrix organization	34/901	369/17046	0.00119	0.02009	0.0158	B4GALT7/COL9A3/COL11A1/COMP/EGFLAM/CTGF/A2M/FGA/FOXC2/BMP10/ANXA2/HAS1/HSP90AB1/COL28A1/CYR61/ITGA7/ITGB2/ITGB7/NDR/LANAA3/LCP1/LOX/LTBP1/SMA D3/MR12/PLEC/CSGALNACT1/SFRP2/BMP4/SOX9/TNX8/COL18A1/COL21A1/ACTN1	34
GO:0035239	tube morphogenesis	33/901	355/17046	0.0012	0.02012	0.01582	ADM/EGFR/ESR1/FGF10/FOXC2/SOX8/HLX/RSP02/FMN1/GF1/KDR/HES5/SMAD3/NFATC3/LEF1/PTX2/PML/FTL22/PXN/CCL11/STRA6/SFRP2/GZF1/BMP4/SOX9/STK3/ZEB1/TG M2/TWIST1/PAX8/KDM2B/TP63/MICAL2	33
GO:0001942	hair follicle development	12/901	82/17046	0.0012	0.02012	0.01582	CDH3/APCDD1/EGFR/FGF10/GNAS/INHBA/SOX9/WNT10B/RUNX1/TP63/RUNX3/LDB2	12
GO:0022404	molt cycle process	12/901	82/17046	0.0012	0.02012	0.01582	CDH3/APCDD1/EGFR/FGF10/GNAS/INHBA/SOX9/WNT10B/RUNX1/TP63/RUNX3/LDB2	12
GO:0022405	hair cycle process	12/901	82/17046	0.0012	0.02012	0.01582	CDH3/APCDD1/EGFR/FGF10/GNAS/INHBA/SOX9/WNT10B/RUNX1/TP63/RUNX3/LDB2	12
GO:0032940	secretion by cell	68/901	886/17046	0.00123	0.02046	0.01609	ADCY3/TMED10/CHGA/CHI3L1/EXOC3/CIDEA/CCR1/ADM/CTGF/ABAT/DRD4/A2M/UNC13D/FGA/FGF10/EXPH5/STEAP2/GLS2/NPS4A/GNAS/GPER1/FFAR2/SCG3/HLA-E/FGF1/GF2/IL1RN/IL6/INHBA/ISL1/GALS9/ILG1/NOV/PARK2/PD44/PIK3CG/PML/TLR9/TREM1/POMC/GOLPH3/TRPV6/SMPD3/SYBU/PRKAR1B/TRIM27/EXOC4/SCY/NOD2/V PS33A/SLCGA12/VAMP2/TWIST1/CCR2/TNFRSF4/CACNA1E/PAX8/RAB7A/RAB11FIP1/NR0B2/MON1A/SGN/IRS2/ACTN1/SYTT/RSAD2/ADIPOQ/RAB3D	68
GO:0043062	extracellular structure organization	34/901	370/17046	0.00124	0.02069	0.01627	B4GALT7/COL9A3/COL11A1/COMP/EGFLAM/CTGF/A2M/FGA/FOXC2/BMP10/ANXA2/HAS1/HSP90AB1/COL28A1/CYR61/ITGA7/ITGB2/ITGB7/NDR/LANAA3/LCP1/LOX/LTBP1/SMA D3/MR12/PLEC/CSGALNACT1/SFRP2/BMP4/SOX9/TNX8/COL18A1/COL21A1/ACTN1	34
GO:0035518	histone H2A monoubiquitination	4/901	10/17046	0.00126	0.02085	0.0164	DDB1/RNF168/RYBP/KDM2B	4
GO:0072173	metanephric tubule morphogenesis	4/901	10/17046	0.00126	0.02085	0.0164	SOX8/HES5/SOX9/PAX8	4
GO:0018149	peptide cross-linking	9/901	51/17046	0.00127	0.0209	0.01644	EGFLAM/CSTA/LCE2B/LCE1C/LCE1D/LCE2D/NL/SPOCK3/TGM2	9
GO:0050926	regulation of positive chemotaxis	6/901	24/17046	0.00127	0.0209	0.01644	CDH13/FGF10/IL16/KDR/SMAD3/NTF3	6

GO:0009266	response to temperature stimulus	22/901	206/17046	0.00136	0.02186	0.01719	PSIP1/ADM/ADR83/TRPV3/FOXO1/NUP210/MTOR/ACOT11/DNAIC2/HSPA1L/HSP90AA1/HSP90AB1/IGF1/IL1R1/IL6/C11orf73/MAKP3/CCAR2/RPA3/CASQ1/RAE1/NUP93	22
GO:1901564	organonitrogen compound metabolic process	135/901	1996/17046	0.00137	0.02203	0.01732	BCKDK/TCIRG1/MTHF5/CELF1/NPFR2/ADCV3/TMED10/HIBADH/EGLN2/BAGALT7/ACOT7/CLN5/MRPL52/APOA1BP/NEU4/ADM/EGFLAM/CPS1/PPM1L/MBOAT1/ADRB5/ADAL/D DOST/DIO3/DLGG/DNMT3A/NBAT/DRD4/ECCE1/AGXT/EEF2/PATL2/EIF4G1/ENO2/ALAS1/FAH/FHIT/AKR1B1/LARP1/PUW2/MTOR/FUCA1/GABBR1/ST6GALNAC3/PNKD/GATM/GAP DH5/PABPC1/AMPD2/PDE7B/GLS1/GNAS/GPER1/MRPS18B/DNAIC15/GSTP1/GUCY1A3/NME7/PADI1/HAS1/HKI1/ACACB/HPCA/ACAD1/BAH12/NNM59/IGF1/CYR61/IL6/IT IH3/ITH4/ACAT1/LDLR/LHCGR/MC2R/ME1/ME2/MOCS1/NUDT1/MYH4/NDUFB4/NEU1/ATP1A2/NPPC/OAS2/OPRL1/ATP5B/PALM/PARK2/SPOCK3/PRR36/CHST15/PDE4C/PCYOX 1/PDE7A/SIRT6/PDE6B/PGAM2/PKM/PLA3G2A/PML/CYTL1/POMC/PON1/LPCAT2/PWIL2/SMPP3/CNOT11/MBR01/CSGALNACT1/PRKD3/MAPK3/MRAP/PSMB4/PSMD7/METTL1 4/RPL8/RPL29/SCT/MRPS14/NO22/CEK1/SRFB6/CCR2/UPP1/VARS/PAX8/CPEB4/CALR/QTRT1/KMO/SPHK1/NR1H4	23
GO:0097191	extrinsic apoptotic signaling pathway	23/901	220/17046	0.00142	0.02276	0.0179	CYLD/FGA/FGF10/GPER1/GSTP1/NRG1/IGF1/NHBA/LMNA/SMAD3/DDX47/PML/SFRP2/BMP1R1B/BOX/STK3/TNFAIP3/TNFRSF1A/TRAF1/BC1L14/RUNX3/CRADD/FADD	23
GO:0009615	response to virus	34/901	373/17046	0.00142	0.02276	0.0179	SPON2/HNRNPUL1/DNMT1/UNC13D/ACIN1/PUW2/SLC37A4/HMGAL/IL6/IRF1/KCNJ8/STMN1/LCK/GALS9/OAS2/PML/TREM1/HTRA1/CREBZF/ACTA2/CCL11/STAT2/BST2/TNFAIP 3/CA7/CXCR4/NLRX1/UNC93B1/HISTH3A/FITM1/FADD/RSAD2/CDBA/NUP93	34
GO:0048729	tissue morphogenesis	48/901	581/17046	0.00146	0.02318	0.01822	COL11A1/ADM/EGFR/ESR1/FGF10/FOXL1/FOXK2/BMP10/SOX8/NRG1/RSPO2/FMN1/IGF1/CYR61/IL6/NHBA/SL1/KDR/HES5/SMAD3/MYL2/NFATC3/LEF1/SIRT6/ATP8A2/PTRX2/P ML/RIPK4/IFT122/PXN/ACTA2/CCL11/SFRP2/GZF1/BMP4/SOX9/STK3/ACTC1/TGM2/TWIST1/PAX8/FZD5/KDM2B/RUNX1/TP63/RUNX3/ALDH1A2/MICAL2	48
GO:0032760	regulation of tumor necrosis factor production	9/901	52/17046	0.00146	0.02318	0.01822	SPON2/HLA-E/ISL1/GALS9/TLR9/NOD2/TWIST1/CCR2/FADD	9
GO:2001238	positive regulation of extrinsic apoptotic signaling pathway	9/901	52/17046	0.00146	0.02318	0.01822	CYLD/GPER1/NHBA/PML/BMP1R1B/STK3/BC1L14/RUNX3/FADD	9
GO:0019637	organophosphate metabolic process	75/901	1004/17046	0.00147	0.02318	0.01822	GNF/TCIRG1/NPFR2/ADCV3/ACOT7/CNP/APOA1BP/ADM/CPS1/MBOAT1/ADRB3/FITM1/ADAL/DLG2/DRD4/ENO2/FHIT/GABBR1/GAPDH5/AMPD2/PDE7B/AMPD3/GNAS/PIGW1/T HEM5/GPER1/DNAIC15/GUCY1A3/NME7/HKI1/ACACB/HPCA/HRH1/NNM59/IGF1/INPP5A/LDLR/LHCGR/MC2R/ME1/ME2/MOCS1/NUDT1/MYH4/NDUFB4/ATP1A2/NPPC/O AS2/OPRL1/ATP5B/PALM/PDE4C/PDE1A/SIRT6/PDE6B/PGAM2/PIGC/PIK3CG/PKM/PLA2G2A/PON1/LPCAT2/SMPD3/VAC14/CSGALNACT1/MRAP/SCT/CCR2/UPP1/KMO/SY NJ2/ENTPD3/LPGAT1	75
GO:0098773	skin epidermis development	12/901	84/17046	0.00149	0.02337	0.01837	CDH3/APCDD1/EGFR/FGF10/GNAS/NHBA/SOX9/WNT10B/RUNX1/TP63/RUNX3/LDB2	12
GO:0060337	type I interferon signaling pathway	11/901	73/17046	0.00149	0.02337	0.01837	HLA-B/HLA-E/HLA-F/HSP90AB1/IRF1/OAS2/STAT2/BST2/IHITM1/FADD/RSAD2	11
GO:0071357	cellular response to type I interferon	11/901	73/17046	0.00149	0.02337	0.01837	HLA-B/HLA-E/HLA-F/HSP90AB1/IRF1/OAS2/STAT2/BST2/IHITM1/FADD/RSAD2	11
GO:0010556	regulation of macromolecule biosynthetic process	228/901	362/17046	0.0015	0.0234	0.0184	ZNF783/CDH13/CDKN1C/C1D/ZBTB18/DNMT2/CELF1/TBR1/PNRC1/HNRNPUL1/FRUN2/PSIP1/EGIN2/ZBED9/CIDEA/SLC51B/ZFP42/IL13/RA/ZNF558/ZNF738/CTGF/SMYD1/CYLD/E SCO2/ZNF782/ZNF709/ZNF781/CITE04/RNF168/ZNF366/BHLHA15/DNMT3A/EEF2/EGFR/EGR3/PATL2/EIF4G1/ELK4/ESR1/SP8/FGF10/FHIT/XRN2/SBNO2/TRAKI1/MR8B2/FOXJ1/F OX2/FOXO1/SPG20/NEEDD4/LARP1/PUW2/RYP7/VGLL2/MTOR/ZNF549/PABPC1/DNAIC2/DK3/BMP10/ZNF638/ZNF311/ZNF844/GPER1/GRB10/ZBTB44/GSTP1/GTF2B/BRF1/S OX8/NRG1/HLX/HMGA1/NRA41/HOXB3/HOXC4/HOXC5/HOXC6/HOXD3/TFAP2E/ID3/BAH12/IGF1/IGF2/CYR61/IL6/IL16/FOXK2/NHBA/IRF1/ISL1/LIP/USP50/HLS1/KDR/HES5/A FF3/LGALS9/LMNA/LMO2/LTB/SMAD3/MEF2D/MEOX1/MEOX2/MITF/LHX8/MOV10/NFAT3/NRFB/NHLH2/NTF3/PARK2/LEF1/PRR16/SIRT6/PITX2/PKH01/PLAGL1/PML/RIPPL3/ RIPK4/TLR9/CYTL1/POMC/POU2AF1/BNCC2/MED18/BANP/PPP1CB/PWIL2/ELP3/PRMT6/DNAIC17/ZNF532/CNOT11/PRKD1/MYNN/MAPK3/PRMT8/HTRA1/PAKG/ARNTL2/RGMA/ PRDM11/TENM2/GATAD2B/METTL14/CCAR2/CREBZF/TRIM27/NPAS3/NOD2/SFRP2/GZF1/SGK1/BMP4/ZNF649/BMP1R1B/BRD9/ZSCAN18/SOX9/STAT2/STK3/SUPT6H/TA48/TBP/ TCEA1/TCB2/ZEB1/TEAD3/TERF1/TELE3/TNFAIP3/TNFRSF14/TRAF1/TRAF5/TWIST1/CCR2/TNFRSF4/UCP1/VARS/WNT10B/ZNF77/ZNF124/ZNF177/PAX8/FZD5/CARD14/ZNF665/ZN F606/ZC3H12A/CPEB4/ZNF436/CALR/SURP5/CR1/HIST1H3A/SLA2/ZNF397/NRO82/HOPX/KDM2B/LOC13/CBX2/GAS7/RUNX4/TP63/RUNX3/RS2/ACTN1/FADD/TNFRSF11A/SPHK 1/BDU331/CCNA1/LIMD1/PIAS2/LDB2/CBFA2T2/AURKB/ADIPQO/H2AF1/MICAL2/VGLL4/ZBTB39/NR1H4	228

GO:0009892	negative regulation of metabolic process	159/901	2412/17046	0.0015	0.02341	0.01841	<p>FARP1/CDKN1C/C1D/ZBTB18/CELF1/ERLIN2/CIDEA/CCR1/CDSTA/CTGF/SMYD1/CYLD/RNF168/ZNF366/NLRP6/DLG2/DNMT3A/DRD4/EGFR/PATL2/A2M/ELK4/EPHA1/ESR1/PHACTR1/FGA/FHIT/PPM1E/SBNO2/ACIN1/FOXO2/FOXO1/DIP2A/FLT2/NEEDD4/PUM2/RYBP/MTOR/GABRR1/PABPC1/DNAJC2/DKX3/GPER1/GRBB10/DNAJC15/GSTP1/GZNA/A/INXA2/SERPIND1/SOX8/NR61/HMGACB/ACACB/HPC4/HOXB3/HOXC6/ACADL/HSP90A1/ID3/COL28A1/IGF1/IL16/INHBA/IRF1/ISL1/ITIH3/ITIH4/IL13/KIF25/PO5/HESS1/GALS9/SMAAD3/MITF/MOV10/NPPC/NTF3/OPRL1/PALM/PARK2/SPOCK3/ALF1/SIRT6/P13/P1K3CG/PTX2/PKHD1/LR9/BANP/PWIL2/PRMT6/DNAJC17/CNOT11/PRKAR1B/MAP2K4/MASP1/CDC42SE1/PSMB4/PSMD7/TENN2/GATAD2B/METT14/CCAR2/CREBZF/TRIM27/NOD2/SFRP2/GZF1/BMP4/ZNF649/SOX9/SUPT6H/BST2/TBP/ZEB1/TERF1/TNMP3/TNFAIP3/TWIST1/CCR2/TNFRSF4/WNT10B/YWHAG/ZNF177/ZC3H14/ZC3H12A/CEP84/CALR/SURP/CAST/SCRIPT1/HIST1H3A/SLA2/NROB2/HOPX/SPINK7/KDM2B/LOX13/CBX2/TP63/RUNX3/SERPINA6/IRS2/FADD/LIMD1/ERL1/PIAS2/CBEA2/ZTAURK8/DAPL1/ADIPOQ/H2AF1/N4BP1/RAPGEF2/FGF19/NR1H4</p>	159
GO:0044249	cellular biosynthetic process	328/901	5425/17046	0.00151	0.02347	0.01846	<p>CDH3/GNE/ZNF783/CDH13/CDKN1C/TCIRG1/C1D/ZBTB18/MTHFS/DMRT2/CELF1/TBR1/NPFR2/ADCT3/PNRC1/SLC27A2/HNRNPUL1/ERLIN2/PSIP1/EGLN2/BAGAL1/ACO17/ZBE/D9/CIDEA/GALNT15/NMRP15/SLC51B/NEU4/ZFP42/ADAM13/IRF4/PS1/ZNF358/PARP4/B3GLCT/MGAT5B/ZNF738/CTGF/SMYD1/PPM1L/CYLD/MBOAT1/ADRB3/ESCO2/CYP11A1/ZNF782/IFTM1/ADAL/ZNF709/ZNF781/CTEDA4/DOB1/DDOST/RNF168/ZNF366/BHLHA15/DNMT3A/ABAT/DPH1/DRD4/AGX2/EEF2/EGFR/EGR3/PATL2/EH4G1/ELK4/ESR1/ALAS1/S/P8/FGF10/HIT1/ARN2/SBNO2/TRAK1/MSRB2/FOXO1/AKR1B1/NUP210/NEEDD4/LARP1/PUM2/RVBP/VGLT1/MTOR/GABRR1/ZNF549/ST6GALNAC3/GATM/G8GT1/S/LC17A5/PABPC1/DNAJC2/AMPD2/DKX3/GLS2/AMPD3/BMP10/ZNF638/GNAS/ZNF844/GPER1/EGOT/GRB10/MRPS18B/ZBTB44/GSTP1/GTF2B/BRF1/GUCY1A3/NM/E7/PAD1/HAS1/SOX8/NR61/HLX/HMGAL1/NR4A1/ACACB/HPC4/HOXB3/HOXC4/HOXC5/HOXC6/HOXD3/HRH1/ACADL/HSP90A1/HSP90A11/TFAP2E/ID3/BARHL2/NME9/IGF1/GF2/CYR61/IL6/IL16/FOXK2/INHBA/IRF1/ISL1/JUP/USP50/ACATI/HESS1/AFK3/MUC21/LDLR/LGALS9/LHGR/LMO2/LTB/SMAD3/MC2R/MEI/MEF2D/MEOX1/MEOX2/MGAT1/MITF/LHX8/MOCS1/MOV10/DRG1/NEU1/NFAT3/NFYB/NHLH2/NPPC/NTF3/QASZ/OPRL1/ATP5B/PALM/PARK2/LEF1/PRR16/GHST15/SIRT6/GALNT7/PIGC/PIK3CG/PTX2/PKHD1/MITF/LHX8/MOCS1/MOV10/DRG1/NEU1/NFAT3/NFYB/NHLH2/NPPC/NTF3/QASZ/OPRL1/ATP5B/PALM/PARK2/LEF1/PRR16/GHST15/SIRT6/GALNT7/PIGC/PIK3CG/PTX2/PKHD1/A/ALD1A2/SYNU2/SPHK1/BUD31/CNNA1/LIMD1/CH25H/PIAS2/LDB2/CBEA2/ZTAURK8/ADIPOQ/H2AFY/MICAL2/NG2/IL14/NUP93/RAPGEF2/ZBTB39/LPGAT1/FGF19/NR1H4</p>	328
GO:0048754	branching morphogenesis of an epithelial tube	18/901	156/17046	0.00152	0.02352	0.0185	<p>ESR1/FGF10/FOXO2/SOX8/RSPO2/IGF1/KDR/NFAT3/LEF1/PTX2/PMI/PXN/CCL11/SFRP2/GZF1/BMP4/SOX9/PAX8</p>	18
GO:0002221	pattern recognition receptor signaling pathway	19/901	169/17046	0.00155	0.02395	0.01883	<p>TANK/MAP3K8/CYLD/NLRP6/DMBT1/PUM2/FFAR2/IRF1/TIGB2/MAP3K1/IL19/MAPK3/NOD2/TLR5/TNFAIP3/NLRX1/JUNC93B1/FADD/RSAD2</p>	19
GO:0072273	metanephric nephron morphogenesis	6/901	25/17046	0.0016	0.02465	0.01938	<p>SOX8/FMN1/HESS1/BMP4/SOX9/PAX8</p>	6
GO:0051249	regulation of lymphocyte activation	32/901	347/17046	0.00161	0.02478	0.01949	<p>MAP3K8/CYLD/EGR3/FGF10/FLT2/MTOR/HLA-DOA/HLA-DPA1/HLA-E/HLX/ZC3H12D/IGF1/GF2/IL6/INHBA/IRF1/LCK/LGALS9/IL20RB/PAG1/NOD2/BMP4/SUPT6H/ZEB1/TNFAIP3/CCR2/TNFRSF4/ZAP70/SLT1/SLA2/IRS2/FADD</p>	32
GO:0030500	regulation of bone mineralization	10/901	63/17046	0.00162	0.0248	0.0195	<p>CCR1/FAM101A/SMAD3/BGLAP/BMP4/SLC8A1/BMPR1B/SOX9/TWIST1/WNT10B</p>	10
GO:0050880	regulation of blood vessel size	16/901	132/17046	0.00162	0.02487	0.01956	<p>KCNMB2/MRV11/ADM/CP51/ADRB3/ECE1/FGA/FOXC2/GPER1/GUCY1A3/HRH1/KCNJ8/ATP1A2/NPCC/ACTA2/SLC8A1</p>	16
GO:0030335	positive regulation of cell migration	31/901	333/17046	0.00163	0.02488	0.01957	<p>CDH13/CCR1/EGFR/EPHA1/FGF10/FOXO2/GPER1/IGF1/CYR61/IL6/KOR/LGALS9/SMAD3/NTF3/P2RY6/LEF1/ANGPT4/ELP3/PRKD1/CCL11/BMP4/SLC8A1/SOX9/CCR2/PTP44A1/COL11/8A1/CALR/IRS2/FADD/SPHK1/RAPGEF2</p>	31
GO:0060348	bone development	19/901	170/17046	0.00166	0.02527	0.01987	<p>ABI1/SLC38A10/COMP/FAM101A/GNAS/ANXA2/IGF1/MEF2D/NPCC/CSGALNACT1/BGLAP/SFRP2/BMP4/BMPR1B/SOX9/TWIST1/C6orf25</p>	19
GO:0060341	regulation of cellular localization	82/901	1122/17046	0.00167	0.0253	0.01989	<p>CDH3/TRDN/RER1/CHGA/CIDEA/SLC51B/CYLD/ABAT/DRD4/EGFR/JUNC13D/FGA/EXPH5/MUC1/NEEDD4/MTOR/GLS2/VPS4A/GNAS/GPR26/GPER1/FFAR2/NR61/ANXA13/HLA-E/HPC4/HSPAL1/HSP90A1/IGF1/IL1RR/IL6/INHBA/ISL1/JUP/PO5/CP1/ILGALS9/LIGL1/LMNA/SMAD3/ATP1A2/NOV/PARK2/PDE4C/PML1/LR9/POMC/GOIPH3L/TRP6/SWMPD3/S/YBU/PRKAR1B/PRK01/MAKP3/MAP2K2/TRIM27/SCY/NOD2/SFRP2/BMP4/SLC8A1/SUPT6H/BST2/VAMP4/TWIST1/CCR2/TNFRSF4/VWHAG/CACNA1E/PAX8/FZD5/RAB7A/RAB11F1/P1/NROB2/CASQ1/IRS2/SPHK1/SYTY/RSAD2/REEP6/ADIPOQ/RAB3D</p>	82

GO:0034340	interferon induction	11/901	74/17046	0.00167	0.0253	0.01989	HLA-B/HLA-E/HLA-F/HSP90AB1/IRF1/OAS2/STAT2/BST2/IHTM1/FADD/RSAD2	11
GO:0048546	digestive tract morphogenesis	9/901	53/17046	0.00168	0.02544	0.02	EGFR/FGF10/HLX/SMAD3/PTX2/STRA6/SFRP2/BMP4/TP63	9
GO:1902105	regulation of leukocyte differentiation	23/901	223/17046	0.0017	0.02564	0.02036	CCR1/CYLD/EGR3/ACIN1/MTOR/GNAS/HLA-B/HLA-DOM/HLX/IL6/INHBA/IRF1/LCX/LGALS9/MITF/LEF1/BGLAP/BMP4/ZEB1/ZAP70/RUNX1/FADD/ADIPOQ	23
GO:2000112	regulation of cellular macromolecule biosynthetic process	222/901	3525/17046	0.00175	0.02628	0.02067	ZNF783/CDH13/CDKN1C/CIDZ/BTB18/DWMT2/CELF1/TBR1/PNRC1/HNRNPULL1/ERLIN2/PSIP1/EGIN2/ZBED9/CIDEA/SLS1B/ZFP42/IL31RA/ZNF358/ZNF738/SMYD1/CYLD/FSCC2/ZNF782/ZNF709/ZNF781/CITE4/RNF168/ZNF366/BHLHA15/DNMT3A/EEF2/EGFR/EGR3/PATL2/EIF4G1/ELK4/ESR1/SRP81/ZNF844/GPER1/GRB10/ZBTB44/GTF2B/BRF1/SOX8/NRG1/HLX/HMGGA1/NRA41/HOXB3/HOXC4/HOXCS/HOXC5/HOXC6/HOXD3/TFAP2E/ID3/BAR/HL2/GF1/GF2/CYR61/IL6/IL6/FOXK2/INHBA/IRF1/ISL1/JUP/USP50/HLS1/HES5/AFF3/LGALS9/LMNA/LMO2/SMAD3/MEF2D/MEOX1/MEOX2/MITF/LHX8/MOV10/NFATC3/NFYB/NHLH2/NTF3/PARK2/LEF1/SIRT6/PTX2/PKH2/PLA/LAGL1/PML/RIPPL3/RIPK4/TLR9/CYTL1/POM/C/POU2AF1/BNC2/MEI18/BANP/PPP1CB/PWIL2/ELP3/PRMT6/DNAIC17/ZNF532/CNOT11/PRK01/MIYNN/MAK3/PRMT8/HTRA1/PAK6/ARNTL2/RGMA/PRDM11/TENM2/GATAD2B/METTL4/CCAR2/CREB2/TRIM27/NP35/NOB2/SFRP2/GZF1/SGK1/BMP4/ZNF649/BMPR1B/BRD9/TA48/TBP/TCEA1/TCEB2/ZEB1/TEA D3/TEF1/TL3/TFE1P3/TFNRF1A/TFRAF1/TFRAF5/TWIST1/TFNRF5/UCP1/VARS/WNT108/ZNF124/ZNF177/PAX8/FZD5/CARD14/ZNF665/ZNF606/ZC3H12A/CEPBA/ZNF436/CALR/SURP/SCRIPT1/HIST1H3A/SLA2/ZNF397/NR082/HOPX/KDM2B/LOXL3/CBX2/GAS7/RUNX1/TP63/RUNX3/IRS2/FADD/TNFRSF11A/SPHK1/BUD31/CCNA1/UMD1/PIAS2/LDB2/C	222
GO:0035150	regulation of tube size	16/901	133/17046	0.00176	0.02638	0.02074	BEA2T2/AURKB/ADIPOQ/H2AFY/MICAL2/VGLL4/ZBTB39/NR1H4 KCNMB2/MRV11/ADM/CP51/ADR83/ECE1/FCA/FOX2/GPER1/GUCY1A3/HRH1/KCNJ8/ATP1A2/NPPC/ACTA2/SLC8A1	16
GO:0035051	cardiocyte differentiation	14/901	109/17046	0.00179	0.0268	0.02108	SPEG/MTOR/TENM4/BMP10/NRG1/ISL1/LMNA/MYL2/PTX2/BMP4/SLC8A1/ACTC1/TWIST1/CALR	14
GO:0044093	positive regulation of molecular function	115/901	1672/17046	0.00181	0.02709	0.0213	ABI1/CDH3/FARP1/TRDN/PTRM1/ADCY3/CH3L1/MAP3K8/CTGF/ADRB3/DRD4/EGFR/EPHA1/ESR1/SPATA13/FGF10/RASA3/TBC1D9B/TBC1D1/PSD3/ARHGGEF18/MAPK8IP2/RAS G1/ALS2/CL/RS22/FGF22/CYTH4/GNAS/GPER1/DOCK7/DNAIC15/ANXA2/NRG1/HPC/A/GEG2/HSP90AB1/GF1/GF2/CYR61/IL1R1/IL6/ISL1/JUP/LC/ARHGDA/LGALS9/LHCR/L/LG1/SMAD3/MAB3K1/MFNG/PLEKHG7/NHLH2/NRAS/NTF3/ARHGGEF3/PARK2/ANGPT4/PIK3CG/PTX2/PML/PLIP/RIPK4/TLR9/CYTL1/POML/IRN2/ARHGGEF10/PRKAR1B/PRK01/M APK3/MAP2K2/PSMB4/PAK6/PSMD7/PLEKHG5/PXN/RASGRF2/TRIM27/RGS12/CCL11/CCL17/NOB2/SFRP2/ARHGAP9/SGK1/BMP4/BOX/STK3/STK10/TCEA1/TFRAF1/TFRAF5/PRC6/TWIST1/WNT108/CXGR4/FZD5/CARD14/SH3BGR13/IRS2/CRADD/FADD/TNFRSF11A/SPHK1/STARD13/MAP3K6/ADIPOQ/ARHGAP29/ARHGGEF10/RAPGEF2/USP6NL/RABGAP11/QSOE C1/EGF19	115
GO:1903506	regulation of nucleic acid-templated transcription	205/901	3227/17046	0.00182	0.02713	0.02134	ZNF783/CDH13/CDKN1C/CIDZ/BTB18/DWMT2/TBR1/PNRC1/HNRNPULL1/ERLIN2/PSIP1/EGIN2/ZBED9/CIDEA/ZFP42/IL31RA/ZNF358/ZNF738/SMYD1/CYLD/ZNF782/ZNF709/ZNF781/81/CITE4/RNF168/ZNF366/BHLHA15/DNMT3A/EGFR/EGR3/ELK4/ESR1/SP8/FGF10/FHT/HRN2/SBNO2/TRAK1/MSRB2/FOX11/FOX2/FOX3/SPG30/NEED4L/RYPB/NGL2/MTOR /ZNF549/DNAIC2/DKK3/BMP10/ZNF638/ZNF311/ZNF844/GPER1/ZBTB44/GTF2B/BRF1/SOX8/NRG1/HLX/HMGGA1/NRA41/HOXB3/HOXC4/HOXCS/HOXC5/HOXC6/HOXD3/TFAP2E/ID3/BAR HL2/GF1/GF2/CYR61/IL6/IL6/FOXK2/INHBA/IRF1/ISL1/JUP/USP50/HLS1/HES5/AFF3/LGALS9/LMNA/LMO2/SMAD3/MEF2D/MEOX1/MEOX2/MITF/LHX8/MOV10/NFATC3/NFYB /NHLH2/NTF3/PARK2/LEF1/SIRT6/PTX2/PKH2/PLA/LAGL1/PML/RIPPL3/RIPK4/TLR9/CYTL1/POMC/POU2AF1/BNC2/MEI18/BANP/ELP3/PRMT6/DNAIC17/ZNF532/CNOT11/PRK01 /MIYNN/MAK3/PRMT8/HTRA1/PAK6/ARNTL2/RGMA/PRDM11/TENM2/GATAD2B/CCAR2/CREB2/TRIM27/NP35/NOB2/SFRP2/GZF1/SGK1/BMP4/ZNF649/BMPR1B/BRD9/ZSCA N18/SOX9/STAT2/STK3/SUPT6H/TFAP4B/TBP/TCEA1/TCEB2/ZEB1/TEAD3/TFE3/TFNFAIP3/TFNRF5/TFRAF1/TFRAF5/TWIST1/TFNRF4/UCP1/WNT108/ZNF124/ZNF177/TPA38/F ZD5/CARD14/ZNF665/ZNF606/ZC3H12A/ZNF436/CALR/SURP/SCRIPT1/HIST1H3A/SLA2/ZNF397/NR082/HOPX/KDM2B/LOXL3/CBX2/GAS7/RUNX1/TP63/RUNX3/ACTN1/FADD/TNFR SF11A/SPHK1/BUD31/CCNA1/UMD1/PIAS2/LDB2/CBEA2T2/AURKB/ADIPOQ/H2AFY/MICAL2/VGLL4/ZBTB39/NR1H4	205
GO:0001656	metaphosis development	12/901	86/17046	0.00183	0.02719	0.02138	FGF10/FOX2/SOX8/ID3/FMNI/AQP2/ACAT1/HES5/BMP4/SOX9/PAK8/ADIPOQ	12
GO:0006355	regulation of transcription, DNA-templated	204/901	3210/17046	0.00184	0.02725	0.02143	ZNF783/CDH13/CDKN1C/CIDZ/BTB18/DWMT2/TBR1/PNRC1/HNRNPULL1/ERLIN2/PSIP1/EGIN2/ZBED9/CIDEA/ZFP42/IL31RA/ZNF358/ZNF738/SMYD1/CYLD/ZNF782/ZNF709/ZNF781/81/CITE4/RNF168/ZNF366/BHLHA15/DNMT3A/EGFR/EGR3/ELK4/ESR1/SP8/FGF10/FHT/HRN2/SBNO2/TRAK1/MSRB2/FOX11/FOX2/FOX3/SPG30/NEED4L/RYPB/NGL2/MTOR /ZNF549/DNAIC2/DKK3/BMP10/ZNF638/ZNF311/ZNF844/GPER1/ZBTB44/GTF2B/BRF1/SOX8/NRG1/HLX/HMGGA1/NRA41/HOXB3/HOXC4/HOXCS/HOXC5/HOXC6/HOXD3/TFAP2E/ID3/BAR HL2/GF1/GF2/CYR61/IL6/IL6/FOXK2/INHBA/IRF1/ISL1/JUP/USP50/HLS1/HES5/AFF3/LGALS9/LMNA/LMO2/SMAD3/MEF2D/MEOX1/MEOX2/MITF/LHX8/MOV10/NFATC3/NFYB /NHLH2/NTF3/PARK2/LEF1/SIRT6/PTX2/PKH2/PLA/LAGL1/PML/RIPPL3/RIPK4/TLR9/CYTL1/POMC/POU2AF1/BNC2/MEI18/BANP/ELP3/PRMT6/DNAIC17/ZNF532/CNOT11/PRK01 /MIYNN/MAK3/PRMT8/HTRA1/PAK6/ARNTL2/RGMA/PRDM11/TENM2/GATAD2B/CCAR2/CREB2/TRIM27/NP35/NOB2/SFRP2/GZF1/SGK1/BMP4/ZNF649/BMPR1B/BRD9/ZSCA N18/SOX9/STAT2/STK3/SUPT6H/TFAP4B/TBP/TCEA1/TCEB2/ZEB1/TEAD3/TFE3/TFNFAIP3/TFNRF5/TFRAF1/TFRAF5/TWIST1/TFNRF4/UCP1/WNT108/ZNF124/ZNF177/TPA38/F ZD5/CARD14/ZNF665/ZNF606/ZC3H12A/ZNF436/CALR/SURP/SCRIPT1/HIST1H3A/SLA2/ZNF397/NR082/HOPX/KDM2B/LOXL3/CBX2/GAS7/RUNX1/TP63/RUNX3/ACTN1/FADD/TNFRSF11A/S PHK1/BUD31/CCNA1/UMD1/PIAS2/LDB2/CBEA2T2/AURKB/ADIPOQ/H2AFY/MICAL2/VGLL4/ZBTB39/NR1H4	204

GO:0010604	positive regulation of macromolecule metabolic process	171/901	2632/17046	0.00184	0.02725	0.02143	AB11/CDH3/CDH13/CDKN1C/DWMT2/TBR1/ADCY3/CH13L1/ERLIN2/PSIP1/EGLN2/CCR1/SILCS1B/MAP3K8/IL131RA/CTGF/SH3D19/ADRB3/CTTED4/RNF168/BHLHA15/DRD4/ECE1/EEF12/EGFR/ESR1/FGA/FGF10/RASA3/SBNO2/FOXO2/FOXO1/GGA3/LARP1/MAPK8IP2/NGLL2/MTOR/RNF148B/PABPC1/DNAJC2/FGF22/NPTN/BMP10/GPER1/DOCK7/BRF1/ANXA2/SOX8/NRG1/HMGAI1/NRAA1/HOXD3/HSP90AB1/TFAP2E/BARHL2/IGF1/IGF2/CYR61/IL1RN/IL6/FOXK2/INHBA/IRF1/ISL1/JUP/KDR/HES5/LCK/LGALS9/LMNA/LMO2/LTB/SMAD3/MEF2D/MAP3K1/MEOX1/MEOX2/MEF2/MITF/NEFAT3/NFYB/NHLH2/NRAS/NTF3/OPRL1/PARK2/LEF1/PRR16/ANGPT4/PK3CG/PTX2/PLA2G2A/PLA2G1/PLM/RIPK4/TLR9/CYTL1/POMC/BANP/PWIL2/FANCJ/PRKAR1B/PRKDI1/MAPK3/MAP2K2/PSMB4/PAK6/ARNTL2/RGMA/PSMD7/PTGFR/PXN/ACTA2/RASGEF2/TRIM27/CCL11/CCL17/NPAS3/NOD2/SFRP2/TRA2B/BMP4/ZNF649/BMPR1B/BOK/SOX9/STK3/STK10/SUP1G/H/TBP/TCEA1/TCEB2/ZEB1/ACTC1/TEAD3/TNFAP3/TNFRSF1A/TRAF1/TRAF5/TWIST1/CCR2/WNT10B/PAX8/CXCR4/FZD5/RAB7A/CARD14/ZC3H12A/CALR/NROB2/CDX10/RUNX4/TP63/RUNX3/RSZ/CRADD/FADD/TNFRSF11A/ALDH1A2/SPHK1/PIAS2/ZFAND2A/MAP3K6/LDB2/CBFA2T2/ADIPOQ/H2AF1/MICAL2/RAPGEF2/FGF19/NR1H4	24/901	238/17046	0.00185	0.02773	0.02147	SPEG/SWYD1/BHLHA15/MTOR/BMP10/TMOD4/NRG1/IGF1/IGF2/LMNA/MYL2/NFATC3/NOV/LEF1/PTX2/BIN3/BMP4/SIC8A1/ACTC1/WNT10B/CALR/CAST/CASQ1/HOPX	24
GO:0000165	differentiation MAPK cascade	61/901	790/17046	0.00187	0.02754	0.02166	NPFER2/CH13L1/CCR1/MAP3K8/IL131RA/CTGF/PPM1L/ADRB3/NLRP6/DRD4/EGFR/FGA/FGF10/RASA3/FOXO1/MAPK8IP2/FGF22/BMP10/GPER1/GSTP1/NRG1/IGF1/IGF2/CYR61/IL1RN/IL6/INHBA/KDR/LGALS9/MAP3K1/NRAS/NTF3/PARK2/PIK3CG/PKHD1/PLA2G2A/TLR9/MAPK3/MAP2K2/PSMB4/PAK6/PSMD7/PXN/RASGEF2/CCL11/CCL17/NOD2/SFRP2/BM14/SOX9/STK3/TNNB/CXCR4/FZD5/CDK10/IRS2/TNFRSF11A/MAP3K6/ADIPOQ/RAPGEF2/FGF19	61/901	790/17046	0.00187	0.02754	0.02166	NPFER2/CH13L1/CCR1/MAP3K8/IL131RA/CTGF/PPM1L/ADRB3/NLRP6/DRD4/EGFR/FGA/FGF10/RASA3/FOXO1/MAPK8IP2/FGF22/BMP10/GPER1/GSTP1/NRG1/IGF1/IGF2/CYR61/IL1RN/IL6/INHBA/KDR/LGALS9/MAP3K1/NRAS/NTF3/PARK2/PIK3CG/PKHD1/PLA2G2A/TLR9/MAPK3/MAP2K2/PSMB4/PAK6/PSMD7/PXN/RASGEF2/CCL11/CCL17/NOD2/SFRP2/BM14/SOX9/STK3/TNNB/CXCR4/FZD5/CDK10/IRS2/TNFRSF11A/MAP3K6/ADIPOQ/RAPGEF2/FGF19	61
GO:1900542	regulation of purine nucleotide metabolic process	21/901	198/17046	0.00188	0.02759	0.02169	NPFER2/ADM/ADRB3/DRD4/GABBR1/GAPDH5/GNAS/GPER1/DNAJC15/GUCY1A3/HPCA/IGF1/LHCGR/MC2R/NPPC/OPRL1/PALM/SIRT6/MRAP/SCT/CCR2	21		0.00188	0.02759	0.02169	NPFER2/ADM/ADRB3/DRD4/GABBR1/GAPDH5/GNAS/GPER1/DNAJC15/GUCY1A3/HPCA/IGF1/LHCGR/MC2R/NPPC/OPRL1/PALM/SIRT6/MRAP/SCT/CCR2	21
GO:0061029	eyelid development in camera-type eye	4/901	11/17046	0.0019	0.02765	0.02175	INHBA/MAP3K1/STRA6/TWIST1	4		0.0019	0.02765	0.02175	INHBA/MAP3K1/STRA6/TWIST1	4
GO:0080184	response to phenylpropanoid	4/901	11/17046	0.0019	0.02765	0.02175	CIDEA/CYP11A1/FGA/BGLAP	4		0.0019	0.02765	0.02175	CIDEA/CYP11A1/FGA/BGLAP	4
GO:0022414	reproductive process	81/901	1111/17046	0.0019	0.02765	0.02175	CDKN1C/CELF1/ADCY3/ADAM29/COL9A3/ZFP42/ADM/CYP11A1/WBP2NL/DNMT3A/ABAT/DRD4/EGFR/ESR1/FGF10/XRN2/AKR1B1/MAPK8IP2/SSK2/MTOR/GAPDH5/GIIB2/GNAS81/ZUMO1/HAS1/SOX8/HSD17B2/HSPA1L/HSP90AB1/IGF1/CYR61/IL1R1/IL1RN/INHBA/HILS1/KDR/LGALS9/LHCGR/LMNA/MC2R/LHX8/NPPC/OPRL1/LEF1/PGAM2/P13/PTX2/SPA17/MOVL0L1/PWIL2/WDR33/HTRA1/PTGFR/TRIM27/RPL29/NPAS3/STRA6/SFRP2/BMP4/SIC8A1/BMIPR1B/BOK/SOX9/STK3/TAFA4/TBP/TEAD3/TLR5/PHLDA2/FZD5/CALR/SLRP/CA5T/SPATA16/ANTXR1/KDM2B/CBX2/TP63/CCNA1/ENDOU/MTLS	81/901	1111/17046	0.0019	0.02765	0.02175	CDKN1C/CELF1/ADCY3/ADAM29/COL9A3/ZFP42/ADM/CYP11A1/WBP2NL/DNMT3A/ABAT/DRD4/EGFR/ESR1/FGF10/XRN2/AKR1B1/MAPK8IP2/SSK2/MTOR/GAPDH5/GIIB2/GNAS81/ZUMO1/HAS1/SOX8/HSD17B2/HSPA1L/HSP90AB1/IGF1/CYR61/IL1R1/IL1RN/INHBA/HILS1/KDR/LGALS9/LHCGR/LMNA/MC2R/LHX8/NPPC/OPRL1/LEF1/PGAM2/P13/PTX2/SPA17/MOVL0L1/PWIL2/WDR33/HTRA1/PTGFR/TRIM27/RPL29/NPAS3/STRA6/SFRP2/BMP4/SIC8A1/BMIPR1B/BOK/SOX9/STK3/TAFA4/TBP/TEAD3/TLR5/PHLDA2/FZD5/CALR/SLRP/CA5T/SPATA16/ANTXR1/KDM2B/CBX2/TP63/CCNA1/ENDOU/MTLS	81
GO:0032651	regulation of interleukin-1 beta production	8/901	44/17046	0.00192	0.02778	0.02185	GSTP1/ISL1/LGALS9/SMAD3/PML/NOD2/TNFAIP3/SPHK1	8		0.00192	0.02778	0.02185	GSTP1/ISL1/LGALS9/SMAD3/PML/NOD2/TNFAIP3/SPHK1	8
GO:0055008	cardiac muscle tissue morphogenesis	9/901	54/17046	0.00193	0.02778	0.02185	COL11A1/FOXO2/BMP10/NRG1/ISL1/MYL2/SIRT6/PTX2/ACTC1	9		0.00193	0.02778	0.02185	COL11A1/FOXO2/BMP10/NRG1/ISL1/MYL2/SIRT6/PTX2/ACTC1	9
GO:0060350	endochondral bone morphogenesis	9/901	54/17046	0.00193	0.02778	0.02185	COMP/GNAS/MEF2D/NPPC/BNC2/CSGALNACT1/BMP4/BMPR1B/SOX9	9		0.00193	0.02778	0.02185	COMP/GNAS/MEF2D/NPPC/BNC2/CSGALNACT1/BMP4/BMPR1B/SOX9	9
GO:1903557	positive regulation of tumor necrosis factor superfamily cytokine production	9/901	54/17046	0.00193	0.02778	0.02185	SPOPN2/HLA-E/ISL1/LGALS9/TLR9/NOD2/TWIST1/CCR2/FADD	9		0.00193	0.02778	0.02185	SPOPN2/HLA-E/ISL1/LGALS9/TLR9/NOD2/TWIST1/CCR2/FADD	9

GO:0051252	regulation of RNA metabolic process	211/901	3337/17046	0.00193	0.02784	0.02189	ZNF783/CDH13/MBNL2/CDKN1C/C1D/ZBTB18/DMRT2/CELF1/TBR1/PNRC1/HNRNPUL1/ERLIN2/PSIP1/ERLIN2/ZBED9/CIDEA/ZFP42/L3IRA/ZNF358/ZNF738/SMYD1/CYLD/ZNF782/ZNF709/ZNF781/CITEDA/RNF168/ZNF366/BHLHA15/DNMT3A/EGFR/EGR3/ELK4/ESR1/SP8/FGF10/FHIT/XRN2/SBNO2/TRAK1/MSRB2/ACIN1/FOXL1/FOXO2/FOXO1/SPG20/NEED4/RYBP/VGLL2/MTOR/ZNFE549/PABPC1/DNAC2/DKK3/BMP10/ZNF638/ZNF331/ZNF844/GPER1/ZBTB44/GTF2B/BRE1/SOX8/NRG1/HLX/HMGAI/NRAA1/HOXB3/HOXC4/HOXC5/HOXC6/HOXC7/TFAP2E/ID3/BARHL2/GF1/GF2/CYR61/IL6/FOXK2/NHBA/RF1/SL1/JUP/USP50/HLS1/HES5/AFK3/LGALS9/LMNA/LMO2/SMAD3/MIEF2D/MEOX1/MEOX2/MITF/LHX8/MOV10/NFATC3/NFYB/NHLH2/NTF3/PARK2/LEF1/SIRT6/PHYX2/PKH01/PLA2L1/POMC/POU2AF1/BNC2/MED18/BANP/ELP3/PRMT6/DNAI1/ZNF532/CNOT11/PRK01/MYNN/MAFK3/PRMT8/HTRA1/PAK6/ARNTL2/RGMA/PRDM11/TENM2/GATAD2B/CCAR2/CREBZF/TRIM27/NP43/NOD2/SFRP2/TRA2B/GZF1/SGK1/BMP4/ZNF649/BMPRI1B/BRD9/2SCAN18/SOX9/STAT2/STK3/SUPT6H/TAFA4B/TBP/TCEA1/TCEB2/ZEB1/TEAD3/TLE3/TNFAP3/TNFRSF1A/TRAF1/TRAF5/TWIST1/TNFRSF4/UCP1/WNT10B/ZNF7/ZNF124/ZNF177/PAX8/FZD5/CARD14/ZNF665/ZCH14/ZNF606/ZCH12/ZNF436/CALR/SURP/SCRT1/HIST1H3A/SLA2/ZNF397/NR0B2/HOPX/KDM2B/LOXL3/CBX2/GAS7/RUNX1/TP63/RUNX3/ACTN1/FA0D/TNFRSF11A/SPHK1/BLD3/PIAS2/LDB2/CBFA2T2/AURKB/ADIP00/H2AFY/MICAL2/NGL4/ZBTB39/NR1H4	5
GO:0030878	thyroid gland development	5/901	18/17046	0.00196	0.02795	0.02198	FGF10/HOXB3/HOXD3/SMAD3/PAX8	5
GO:0071371	cellular response to gonadotropin stimulus	5/901	18/17046	0.00196	0.02795	0.02198	CYP11A1/EGR3/NHBA/LHCGR/PAX8	5
GO:0072077	renal vesicle morphogenesis	5/901	18/17046	0.00196	0.02795	0.02198	SOX8/FMN1/BMP4/SOX9/PAX8	5
GO:0070848	response to growth factor	65/901	855/17046	0.00197	0.02795	0.02198	CDKN1C/ADCY3/LECT1/CIDEA/CPS1/CTGF/CYPL1A1/EGFR/EGR3/FGF10/RASA3/FOXO1/SPG20/NEED4/AHGF1B/MTOR/FGF22/NPTN/BMP10/GRB10/HAS1/NRG1/NR4A1/HTR3/65A/CYR61/LLR1/KDR/HES5/CKARHGDI/ALTB1/SMAD3/MAFK3/MOVI10/NRAS/ARHGFB3/LEF1/PML/PPP1CB/PPP1CC/PRKAR1B/PRK01/MAFK3/MAP2K2/HTRA1/PSMBA4/RGMA/PSMD7/PLEKHG5/PXN/RASGRF2/RIT2/BGLAP/SFRP2/BMP4/BMPRI1B/SOX9/ZEB1/TWIST1/TMEM204/RUNX1/RUNX3/IRS2/RAPGEF2/FGF19	65
GO:1903035	negative regulation of response to wounding	17/901	147/17046	0.00197	0.02795	0.02198	NLRP6/F11/FGA/GPER1/GSTP1/ANXA2/ISL1/SMAD3/NOV1/LZOR8B/PROC/PSMBA4/NOD2/TNF- α /P3/TNFRSF1A/NLRX1/ADIP00	17
GO:0036336	dendritic cell migration	6/901	26/17046	0.00198	0.02795	0.02198	CCR1/LGALS9/PIK3CG/CCR2/CXCR4/CALR	6
GO:0060561	apoptotic process involved in morphogenesis	6/901	26/17046	0.00198	0.02795	0.02198	FOXO2/CYR61/LEF1/PML/PAX8/FZD5	6
GO:0072207	metanephric epithelium development	6/901	26/17046	0.00198	0.02795	0.02198	SOX8/ACAT1/HES5/SOX9/PAX8/ADIP00	6
GO:2000826	regulation of heart	6/901	26/17046	0.00198	0.02795	0.02198	FOXO2/BMP10/ISL1/BMP4/SOX9/TWIST1	6
GO:0019538	protein metabolic process	304/901	5009/17046	0.00199	0.02798	0.022	AKT3/ABI1/GNE/TSPAN5/FARP1/CDKN1C/SREG/CKCKK/PTRM1/CELF1/HCS1/NPFR2/ADCY3/TMED10/LECT1/ADAM29/CH3L1/ERLIN2/EGLN2/B4GALT7/EXO3/ADPRHL1/CARD11/6/ALPK2/GALNT15/CLCA1/CLIN5/MRPL52/CCR1/SLC51B/NEU4/CO1L1A1/MAFK3/IL3IRA/EGFLAM/UBLCP1/CPD/CPM/CP51/TRPM6/MIB2/PARR4/LDIRAD3/B3GLCT/MGAT5B/CS/TA/ZNF738/CTGF/SMYD1/PPM1L/SH3D19/CYLD/ADR83/ESCO2/DDDB1/LONRF2/DOST/RNF168/NLRP6/DLG2/DPH1/DRD4/ECE1/EEF2/EGFR/PAT12/EIF4G1/A2M/ELK4/ADCK5/EP/HA1/EPHA3/EPHA4/F11/PRSS4/RNF182/FGA/FGF10/FHIT/RASA3/PPM1E/TRAJ1/MSRB2/FOXO1/FOXO3/FGA3/FLOT2/NUP210/NEED4/LARP1/PUM2/RYPB/MORC3/MAFK8IP2/TSSK2/MTOR/RNF144B/STGALNAC3/GAK/SAMM50/TENM4/LTN1/FBXO2/LCCE2/SACS/GBG1/SLC17A5/RPS6K1/PABPC1/DNAC2/FGF22/NPTN/VPS4A/BMP10/TMPS/S12/PIGW/GPER1/EOGT/DOCK7/MRPS18B/GSTP1/PAD1/GZMA/ANXA2/SERPIND1/NRG1/HSPA1/HSP90A8/DUDD1/ADAMTS15/COL28A1/BARHL2/IGF1/IGF2/CYR61/LCE1/CCE1D/IL1R/IL6/IL2LRB2/PRSS4/INHBA/RF1/SL1/TG22/THB3/INH4/IVL/USP50/KCNH2/KDR/HES5/CK/NUC21/LDLR/LGALS9/LMNA/LOXL3/SMAD3/MAFK3/1/MF12/MGAT1/MOCS1/NEU1/NRAS/NTF3/OAS2/OPRL1/PARK2/SPOCK3/LEF1/PRR16/CHST15/ANGPT4/PCYOX1/SIRT6/GALNT7/P3/PIGC/PIK3CG/PKH01/PLA2G2A/PRKAG3/PML/R/1P/KA/TLR9/TREM1/CYTL1/POWC/SSH1/BANP/PPP1CB/HERC6/PPP1CC/PWIL2/ELP3/PRMT6/PPP2R2B/FANCI/CNOT11/PRKAR1B/CSGALNACT1/PRK01/MSB2/MAFK3/MAFK2/K/OC/PRMT8/MASP1/HTRA1/PSMBA4/PAK6/PSMD7/TENM2/KLHL8/METTL14/MARK4/CCAR2/PIPRE/PXN/RASGRF2/TRIM27/RGR/EXOC4/RP1B/RL29/CCL11/CCL17/MRPS14/PRSS2/NOD2/SFRP2/SK1/BMP4/BMPRI1B/BOK/SOX9/SRFB8/STK3/STK10/SUPT6H/BST2/NWMP2/TCEB2/TERF1/TGM2/TIMP3/TNFAIP3/TNFRSF1A/TNMB/TRAF5/TWIST1/CCR2/TNFRSF4/IVARS/WNT10B/YWHAG/ZAP70/PTP4A1/MOGS/CXCR4/FZD5/RAB7A/CARD14/ERMP1/CPBE4/CALR/CAST/HOPX/TTBK1/SPINK7/TRIM63/KDM2B/CBX2/RAE1/CDK10/TP63/RUNX3/SERPINA6/IRS2/GRADD/FADD/TNFRSF11A/STK19/SPHK1/ENDOU/PIAS2/ZFAND2A/MAFK6/AURKB/NEURL3/ADIP00/RAB3D/H2AFY/PREPL/N4BP1/NUP93/RAPGEF2/ULK2/FGF19	304

GO:0010557	positive regulation of macromolecule biosynthetic process	107/901	1544/17046	0.00206	0.0289	0.02275	CDH13/CDKN1C/DMRT2/TBR1/ERLIN2/PSIP1/SLIC3/7A2/HIBADH/CH3L1/ERLIN2/EGIN2/B4GALT1/ACOTT7/GDEA/GALNT15/CLIN5/MRPL52/CRR1/SLC51B/CNF/APOA1B/P/NEU4/CO19A3/COL11A1/GALM/MAP3K8/ADAM/IL3/RA/EGFLAM/HUS1B/CP51/NDUFA6/PXDNL/CFRBP1/PARP4/B3GCT/MGAT5B/CTGF/SMYD1/PPM1L/CYB5G1/MBOAT1/ADRB3/ESCO2/CYP11A1/FITM1/ADA/DDB1/DOOST/RNF168/NLRP6/DIOS/DL2/DNMT3A/ABAT/DPH1/DRD4/AGT/FEF2/EGFR/A2M/ELK4/UPH1/ENOD2/ESR1/JALAS1/F1L/PAH/FGA/F/G10/FHIT/RASA3/TRAK1/MSRB2/ACIN1/FOOY1/AKR1B1/NUPT210/LARP1/SIC37A4/GABBR1/ST6GALNAC3/PNKD/ACOTT11/STEAP2/FBXO2/GATM/GBC11/GAPDH5/SLIC17A5/FGF2/AMPD2/PDE7B/DK3/GLS2/AMPD3/DHHDH/BMP10/GNAS/PIGW/THEM5/GPER1/EOGT/GRB10/MRPS18B/DNAJC15/GSTP1/GUCY1A3/NME7/PAD1L/ANXA2/HAS1/NRG1/HK1/HMGAL/ACACB/HPCA/HRH1/HSD11B1/HSD17B2/ACADL/HSP90AA1/NME5/GFY/GFZ/CR6/IL1R1/IL1R1/JL6/INHA/INPP5A/ISL1/USP50/KCNH2/KDR/ACAT1/KRT15/MUC21/LDLR/LGALS9/LHCR/LOX/SMAD3/MC2R/MEI1/MEZ/MAP3K1/MGAT1/MOC51/NUDT1/NM14/NUBP1/NUF1A2/NFATC3/NFYB/NPCC/NRAS/NTF3/OAS2/OPRL1/PAFAH2/ATP5B/PALM/PARK2/SPOCK3/LEF1/CHST15/PDE4C/PCYOX1/PDE7A/SIRT6/PDE6B/GALNT7/PGAM2/PIGC/PIK3CG/PKH01/PKM/PLA2G2A/PRKAG3/PML/SLC01C1/PNLP/TREM1/CYTL1/POMC/PON1/CYP2W1/LPCAT2/PPP1CB/PPP1CC/PIWIL2/ELP3/PRMT6/FANCI/WDR33/SMPD3/VACL1/PRKARI/IMBRD1/CSGALNACT1/CSD1/PRKDI1/APOBR/MAPK3/MAP2K2/MRAP/PRMT8/MAS1/PSMB4/PAK6/PSMD7/RDHL4/PXN/RASGRF2/RFC2/RPA3/SC1/CCL11/CCL17/ABHD4/MRPS14/NUD2/STRAG/SFRP2/MIC AL1/CEK1/VPS33A/BMP4/SCL4A1/BMPR1B/SOX9/STAT2/STK3/STK10/SUPT6H/VAMP2/TCEA11/TERF1/TNFRSF1A/TNXB/PHLDA2/TWIST1/CCR2/UCP1/UPP1/VARS/WNT10B/CA7/CACNA1E/MOGS/PAX8/CXCR4/FZD5/RAB7A/GDPD3/CERS4/EPH3/FAAIP100/COL18A1/EEPDI/CALR/QTRT1/CAPS/CO1Q5/H3BGR/3/NR0B2/HOPX/KDM2B/LOXL3/RAE1/CDK10/KMO/S/ERIP1/IRS2/TNFRSF11A/ALDH1A2/SYNY2/SPHK1/STBD1/CH25H/MAP3K6/SIC16A3/ADIPOQ/H2AFY/ENTP3/IRS2/NUD2/NUD9/RAPEF2/ULK2/LPGAT1/FGF19/NR1H4
GO:0050708	regulation of protein secretion	33/901	367/17046	0.00207	0.02893	0.02275	CIDEA/ABAT/DRD4/FGA/EXPH5/GNAS/GPER1/FEAR2/HLA-E/IGF1/IL6/ISL1/LGALS9/ILGL1/NOV/PARK2/PDE4C/PML/TLR9/GOLPH3/3/SYBU/PRKARI/8/RAB11/FIP1/NR0B2/IRS2/SYT7/IRSAD2
GO:0044710	single-organism metabolic process	303/901	4994/17046	0.00207	0.02893	0.02275	CDB3/GNE/BCDK2/TOIRG1/MTFHS/PDPN/NPFFR2/ADCY3/SIC27A2/HIBADH/CH3L1/ERLIN2/EGIN2/B4GALT1/ACOTT7/GDEA/GALNT15/CLIN5/MRPL52/CRR1/SLC51B/CNF/APOA1B/P/NEU4/CO19A3/COL11A1/GALM/MAP3K8/ADAM/IL3/RA/EGFLAM/HUS1B/CP51/NDUFA6/PXDNL/CFRBP1/PARP4/B3GCT/MGAT5B/CTGF/SMYD1/PPM1L/CYB5G1/MBOAT1/ADRB3/ESCO2/CYP11A1/FITM1/ADA/DDB1/DOOST/RNF168/NLRP6/DIOS/DL2/DNMT3A/ABAT/DPH1/DRD4/AGT/FEF2/EGFR/A2M/ELK4/UPH1/ENOD2/ESR1/JALAS1/F1L/PAH/FGA/F/G10/FHIT/RASA3/TRAK1/MSRB2/ACIN1/FOOY1/AKR1B1/NUPT210/LARP1/SIC37A4/GABBR1/ST6GALNAC3/PNKD/ACOTT11/STEAP2/FBXO2/GATM/GBC11/GAPDH5/SLIC17A5/FGF2/AMPD2/PDE7B/DK3/GLS2/AMPD3/DHHDH/BMP10/GNAS/PIGW/THEM5/GPER1/EOGT/GRB10/MRPS18B/DNAJC15/GSTP1/GUCY1A3/NME7/PAD1L/ANXA2/HAS1/NRG1/HK1/HMGAL/ACACB/HPCA/HRH1/HSD11B1/HSD17B2/ACADL/HSP90AA1/NME5/GFY/GFZ/CR6/IL1R1/IL1R1/JL6/INHA/INPP5A/ISL1/USP50/KCNH2/KDR/ACAT1/KRT15/MUC21/LDLR/LGALS9/LHCR/LOX/SMAD3/MC2R/MEI1/MEZ/MAP3K1/MGAT1/MOC51/NUDT1/NM14/NUBP1/NUF1A2/NFATC3/NFYB/NPCC/NRAS/NTF3/OAS2/OPRL1/PAFAH2/ATP5B/PALM/PARK2/SPOCK3/LEF1/CHST15/PDE4C/PCYOX1/PDE7A/SIRT6/PDE6B/GALNT7/PGAM2/PIGC/PIK3CG/PKH01/PKM/PLA2G2A/PRKAG3/PML/SLC01C1/PNLP/TREM1/CYTL1/POMC/PON1/CYP2W1/LPCAT2/PPP1CB/PPP1CC/PIWIL2/ELP3/PRMT6/FANCI/WDR33/SMPD3/VACL1/PRKARI/IMBRD1/CSGALNACT1/CSD1/PRKDI1/APOBR/MAPK3/MAP2K2/MRAP/PRMT8/MAS1/PSMB4/PAK6/PSMD7/RDHL4/PXN/RASGRF2/RFC2/RPA3/SC1/CCL11/CCL17/ABHD4/MRPS14/NUD2/STRAG/SFRP2/MIC AL1/CEK1/VPS33A/BMP4/SCL4A1/BMPR1B/SOX9/STAT2/STK3/STK10/SUPT6H/VAMP2/TCEA11/TERF1/TNFRSF1A/TNXB/PHLDA2/TWIST1/CCR2/UCP1/UPP1/VARS/WNT10B/CA7/CACNA1E/MOGS/PAX8/CXCR4/FZD5/RAB7A/GDPD3/CERS4/EPH3/FAAIP100/COL18A1/EEPDI/CALR/QTRT1/CAPS/CO1Q5/H3BGR/3/NR0B2/HOPX/KDM2B/LOXL3/RAE1/CDK10/KMO/S/ERIP1/IRS2/TNFRSF11A/ALDH1A2/SYNY2/SPHK1/STBD1/CH25H/MAP3K6/SIC16A3/ADIPOQ/H2AFY/ENTP3/IRS2/NUD2/NUD9/RAPEF2/ULK2/LPGAT1/FGF19/NR1H4
GO:0003012	muscle system process	31/901	339/17046	0.00215	0.02996	0.02356	MIRV1/TRDN/CHRNA1/CTGF/DTNA/BMP10/GPER1/TMOD4/GUCY1A3/KCNP2/ANXA6/IGF1/KCNH2/LCK/MYH4/MYL2/ATP1A2/NFATC3/ATP8A2/PGAM2/PIK3CG/PXN/ACTA2/SLC8A1/ACTC1/CALD1/CASO1/TRIM63/SPHK1/STBD1/RCSO1
GO:0044765	single-organism transport	226/901	3611/17046	0.00217	0.03011	0.02368	AB1L/CDH3/KCNMB2/TCR2/1/TRDN/ABCA9/SPON2/COG5/ADG3/3/TMED10/SLC27A2/RER1/CHGA/CH3L1/EXOC3/CHRNA1/CHRNA2/CHRNA5/CIDEA/PANX3/AP351/CLCA1/CCR1/S/LS3B/C15orf27/SLC38A10/CNP/ADM/TRPM6/MC3/CTGF/ABCC13/SH3D19/CYB5G1/CYD1/TPR13/DOOST/BHLHA15/NI/IRP6/ABAT/DRD4/AGT/EGFR/A2M/UNCL13/S/SLC10A4/FCG R2A/FGA/FGF10/RASA3/TRAK1/EXPH5/NFASC/MC1/NUPT210/ATP11A/NEDD4/MAPK8/2/MTOR/SLC37A4/SAMM50/STEAP2/SLC17A5/GAIA3/GIB2/GLS2/VPS4A/GNAS/CRACR2B/GRP26/GPER1/FFAR2/GRB10/FLVCR1/GRIK4/DNAJC15/SCG3/NME7/ANXA2/KCNP2/NRG1/ANXA6/HKI/ANXA13/HLA-E/ACACB/HPCA/HSPA1L/HSP90AA1/HSP90AB1/HTR3A/IGF1/IGF2/IL1R1/IL6/AQP2/AQP5/INHBA/AQP9/ISL1/1/JUP/ATP9B/KCNH2/KCN8/1/KCN9/1/KCNMB1/PO55/TOMM20L/SLC6A17/LCK/LDLR/LGALS9/ILGL1/LMNA/SMAD3/WIF2/ATP1A2/NFATC3/NOV/NTF3/OPRL1/SLC22A18/P2RY6/ATP5B/ANOT7/PALM/PARK2/PDE4C/PCYOX1/C11orf73/SIRT6/ATP8A2/PIK3CG/PRKAG3/PML/FXYD6/SLC01C1/PNLP/TLR9/TREM1/POMC/PON1/ZDHHC13/GOLPH3/SLC7A1/SLC29A3/RRP6/SMPD3/SLC30A10/CHRNA9/SYBU/CEX26/PRKARI/IFT122/LMBRD1/PRKDI1/APOBR/MAPK3/MAP2K2/TRPV5/CDC42SE1/TRPC7/RASGRF2/EXOC4/RPL29/S100A6/STRAG/SFRP2/SGKI1/VPS33A/BMP4/SCL4A1/SLC6A12/SLC8A1/SLC9A3/SLC20A2/SRP68/SUPT6H/VAMP2/TGM2/TRAPPC10/TRPC6/TRPM2/TWIST1/CCR2/TNFRSF4/UCP1/VWHAG/CA7/CACNA1E/CACNB2/PAX8/FZD5/RAB7A/RAB11/FIP1/CALR/SLC25A18/MEF5D7/ATP13A4/INR0B2/1/MON1A/CASQ1/MGARP/RAE1/SLC43A1/SCIN/IRS2/ACTN1/TNFRSF11A/SPHK1/SYT7/SLC16A3/IRSAD2/SMO1/ADIP OQ/RAB3D/NUP93/USP6L/FGF19/NR1H4
GO:0042246	tissue regeneration	9/901	55/17046	0.0022	0.03044	0.02394	FGF10/GATM/IGF1/NOV/PKM/BN3/TIMP3/WNT10B/HOPX
GO:0016051	carbohydrate biosynthetic process	20/901	188/17046	0.0023	0.03177	0.02499	EN02/FOXO1/AKR1B1/MTOR/GAPDH5/GPER1/GRB10/HAS1/HRH1/IGF1/IGF2/IL6/HICG/CHST15/PGAM2/PRKAG3/PPP1CB/CSGALNACT1/IRS2/ADIPOQ
GO:0045944	positive regulation of transcription from RNA polymerase II promoter	72/901	973/17046	0.00231	0.03186	0.02506	CDH13/DMRT2/TBR1/ERLIN2/PSIP1/HLHA15/FGFR/FGF10/SBNO2/FOXO2/FOXO1/VGLL2/GPER1/SOX8/HMGAL1/NRA41/TFAP2E/BARHL2/IGF1/IGF2/CYRG61/IL6/FOXK2/INHBA/IRF1/ISL1/HES5/1/LMNO2/SMAD3/MEF2D/MEOX2/MITF/NFATC3/HLH2/NTF3/PARK2/LEF1/PTX2/PLAGL1/TLR9/CYTL1/POMC/PRKD1/MAPK3/ARNTL2/RGMA/N ODZ/SFRP2/BMP4/ZNF649/BMPR1B/SOX9/STEAD3/ZEB1/TEAD3/TNFRSF1A/TWIST1/WNT10B/PAX8/FZD5/RUNX1/TP63/FADD/PIAS2/LDB2/CBFAZT2/MICAL2/NR1H4
GO:0042476	odontogenesis	14/901	112/17046	0.00232	0.03191	0.02509	ADM/FGF10/DB3/RSPO2/AQP5/INHBA/HLH8/LEF1/PTX2/HTRA1/BGLA9/BMP4/TWIST1/TP63
GO:0048705	skeletal system morphogenesis	22/901	215/17046	0.00234	0.03211	0.02525	COL11A1/COMP/FAM101A/CTGF/FOXC2/GNAS/FLVCR1/HOXB3/HOXD3/FMN1/SMAD3/MEF2D/NPPC/BNC2/CSGALNACT1/SFRP2/BMP4/BMPR1B/SOX9/ZEB1/TWIST1/WNT10B

GO:0045935	positive regulation of nucleobase-containing compound metabolic process	110/901	1604/17046	0.00251	0.03362	0.02644	CDH13/CDKN1C/DMRT2/TBR1/ERLIN2/PSIP1/ADM/L31RA/ADRB3/CTED4/RNF168/BHLHA15/EGFR/ESR1/FGF10/SBNO2/FOXO2/FOXO3/FOXO4/VGLL2/MTOR/GAPDH5/PABPC1/DNAJC2/BMP10/GNAS/GPER1/BRF1/GUCY1A3/SOX8/HMG1A1/NRAA1/HPCA/TFAP2E/BAHHL2/IGF1/IGF2/CYR61/L6/FOXK2/INHBA/IRF1/ISL1/JUP/HES5/LGALS9/LHCGR/LMNA/LMO2/SMA/D3/MCZR/MEF2D/MEOX1/MEOX2/MITF/NFATC3/NFYB/NHLH2/NPPC/NTF3/PARK2/LEF1/PITX2/PLAGL1/IRPK4/TLR9/CYTL1/POMC/BANP/PRKD1/MARK3/MRAP/ARNTL2/RGMA/T/RIM27/SCT/NP43/NOD2/SFRP2/TRA2B/BMP4/ZNF649/BMPR1B/SOX9/STK3/SUPT6H/TBP/TCEA1/TCEB2/ZEB1/TEAD3/TNFRSF1A/TRA1/TRA5/TWIST1/WNT10B/PAX8/FZD5/CA/RD14/CALB/RUNX1/TP63/RUNX3/FAOD/TNFRSF11A/SPHK1/PIAS2/LDB2/CBAZT2/MICAL2/NR1H4	110
GO:0042303	molting cycle	13/901	101/17046	0.00252	0.03362	0.02644	CDH3/APCDD1/TRPV3/EGFR/FGF10/GNAS/INHBA/SOX9/WNT10B/RUNX1/TP63/RUNX3/LDB2	13
GO:0042633	hair cycle	13/901	101/17046	0.00252	0.03362	0.02644	CDH3/APCDD1/TRPV3/EGFR/FGF10/GNAS/INHBA/SOX9/WNT10B/RUNX1/TP63/RUNX3/LDB2	13
GO:1901342	regulation of vasculature development	21/901	203/17046	0.00255	0.03362	0.02644	LECT1/CH13L1/ADM/EPHA3/VASH1/FOXO2/IL6/ISL1/KDR/ANGPT4/PML/PRKD1/CCL11/SFRP2/BMP4/TNFAIP3/TWIST1/CCR2/RUNX1/SPHK1/RAPGEF2	21
GO:0072087	renal vesicle development	5/901	19/17046	0.00255	0.03362	0.02644	SOX8/FMN1/BMP4/SOX9/PAX8	5
GO:0006366	transcription from RNA polymerase II promoter	124/901	1842/17046	0.00257	0.03362	0.02644	ZNF783/CDH13/CDKN1C/ZBTB18/DMRT2/TBR1/ERLIN2/PSIP1/EGLN2/CTGF/RNF168/ZNF366/BHLHA15/DNMT3A/EGFR/ELK4/ESR1/FGF10/SBNO2/TRA1/FOXO2/FOXO3/N/EDD4L/RYB9/VGLL2/MTOR/SL2/BMP10/GPER1/GTF2B/SOX8/HMG1A1/NRAA1/HOX83/HOXC5/HOXC6/TFAP2E/ID3/BAHHL2/IGF1/IGF2/CYR61/IL6/FOXK2/INHBA/IRF1/ISL1/HES5/LMO2/SMA/D3/MEF2D/MEOX1/MEOX2/MITF/NFATC3/NHLH2/NTF3/PARK2/LEF1/PITX2/PLAGL1/PRKAG3/RIPPLY3/TLR9/CYTL1/POMC/POUZAF1/MEF18/ELP3/PRMT6/DNAJC1/PRKD1/MAPK3/ARNTL2/RGMA/TENM2/GATAD2B/TRIM27/NP43/NOD2/SFRP2/GZF1/BMP4/ZNF649/BMPR1B/ZSCAN18/SOX9/STAT3/SUPT6H/TA4B/TBP/TCEA1/TCEB2/ZEB1/T/EAD3/TNFRSF1A/TWIST1/UCP1/WNT10B/YWHAG/ZNF177/PAX8/FZD5/CALR/SCRIPT1/SLA2/NR0B2/HOPX/KDM2B/CBX2/RUNX3/FADD/BDU31/CCNA1/PIAS2/LDB2/C/BFAZT2/AURKB/H2AFY/MICAL2/NR1H4	124
GO:0072507	divalent inorganic cation homeostasis	33/901	372/17046	0.00257	0.03362	0.02644	TRDN/CCR1/ADM/DRD4/ESR1/NPTN/GPER1/ANXAG/KDR/LCK/ATP1A2/OPRL1/PAR2/PDE6B/PIK3CG/PKH01/PML/SLC30A10/CHRNA9/PRKD1/TRPC7/CCL11/BMP4/SIC8A1/TGM2/TRPC4/TRPC6/CCR2/CXCR4/CALR/ATP13A4/CASQ1/SMO1	33
GO:0050848	regulation of calcium-mediated signaling	8/901	46/17046	0.00257	0.03362	0.02644	CDH13/RCAN2/DRD4/NRG1/IGF1/ZAP70/SLA2/CD8A	8
GO:0048699	generation of neurons	102/901	1471/17046	0.00257	0.03362	0.02644	FARP/CDKN1C/SPON2/ZBTB18/TBR1/GPRIN1/CLNS5E2B/CNP/COU9A3/SCLT1/ADM/DNMT3A/FENAZ/EGFR/EIF4G1/EMLL1/EPHA1/EPHA3/EPHBA/FGF10/RASA3/BTBBD3/SPG20/N/FASC/EPB41L3/NEDD4L/PB3D3/MAPK8IP2/DFNB31/TENM3/FGF22/NPTN/GPER1/SOX8/KCNIP2/NRGI/HOXB3/HOXD3/HSP90A1/ID3/RSP02/FMN1/BAHHL2/LG/INHBA/ISL1/HES5/STIM1/ARHGDA/LGL1/LHX8/NEU1/NRAS/NTF3/PALM/PARK2/LEF1/CEND1/ATP8A2/PITX2/SSH1/PPP1CC/ELP3/PRKD1/MAPK3/MAP2K2/PSMB4/RGMA/TRPC7/PSM/D7/TENM2/RASGRF2/S100A6/SGK1/BMP4/BMPR1B/SLIT1/SOX9/ZEB1/TRPC4/TRPC6/TWIST1/WNT10B/YWHAG/CACNB2/CXCR4/FZD5/LST1/CALR/SCRIPT1/PARD6B/GAS7/RUNX1/RUNX3/IRS2/ALDH1A2/CBAZT2/RAPGEF2/ULK2/FGF19	102
GO:0071363	cellular response to growth factor stimulus	63/901	833/17046	0.00259	0.03362	0.02644	CDKN1C/ADCY3/LECT1/CIDEA/GPS1/CTGF/CYP11A1/EGFR/EGR3/FGF10/RASA3/FOXO1/SPG20/NEDD4L/ARHGFE18/MTOR/FGF22/NPTN/BMP10/GRB10/HAS1/NR4A1/HTR36/A/CYR61/KOR/HES5/LCK/ARHGDI/LTBP1/SMA/D3/MAP3K1/MOV10/NRAS/ARHGFE3/LEF1/PML/PPP1CC/PRKRI1B/PRKD1/MAPK3/MAP2K2/HTRA1/PSMB4/RGMA/PSMD7/PLEKHG5/PXN/RASGRF2/RIT2/BGLAP/SFRP2/BMP4/BMPR1B/SOX9/ZEB1/TWIST1/TMEM204/RUNX1/IRS2/RAPGEF2/FGF19	63
GO:0000738	DNA catabolic process, exonucleolytic	3/901	6/17046	0.00261	0.03362	0.02644	XRN2/ER3/EN1	3
GO:0009838	abscission	3/901	6/17046	0.00261	0.03362	0.02644	SPG20/PSFA4/AURKB	3
GO:0032960	regulation of inositol triphosphate biosynthetic process	3/901	6/17046	0.00261	0.03362	0.02644	GPER1/HRH1/LHCGR	3
GO:0043031	negative regulation of macrophage activation	3/901	6/17046	0.00261	0.03362	0.02644	IL131RA/BPI/ZC3H12A	3
GO:0060019	radial glial cell differentiation	3/901	6/17046	0.00261	0.03362	0.02644	FGF10/HES5/LEF1	3

GO:0072049	comma-shaped body morphogenesis	3/901	6/17046	0.00261	0.03362	0.02644	HES5/BMP4/PAX8	3
GO:0072174	metanephric tubule formation	3/901	6/17046	0.00261	0.03362	0.02644	SOX8/SOX9/PAX8	3
GO:1902031	regulation of NADP metabolic process	3/901	6/17046	0.00261	0.03362	0.02644	ME1/ME2/PGAM2	3
GO:0045087	innate immune response	73/901	994/17046	0.00262	0.03362	0.02644	ABII1/TANK/KLRG1/SPON2/ADCV3/CHGA/MAP3K8/CYLD/DDOST2/COCH/DMBT1/EGFR/A2M/UNC13D/FCGR2A/FGA/FGF10/RASA3/FOXO1/MTOR/FGF22/GPER1/FFAR2/NRG1/HLA-B/HLA-DPA1/HLA-E/HLA-F/NR4A1/HSP90AA1/HSP90AB1/CD300E/IRF1/ITGB2/LCK/LGALS9/MAP3K1/NOV10/NFATC3/NRAS/OAS2/PIK3CG/PML/TLR9/TREM1/PRKAR1B/PRKDI1/MAPK3/MAP2K2/MASP1/PSMB4/PSMD7/RASGRF2/TRIM27/DEFB134/CCL11/CCL17/NOD2/STAT2/BST2/TLR5/TNFAIP3/CCR2/ZAP70/NLRX1/UNC93B1/ITIM1/IRS2/FADD/RSAD2/LY86/RAPGEF2/FGF19	73
GO:0050790	regulation of catalytic activity	142/901	2151/17046	0.00262	0.03362	0.02644	ABII1/CDH3/FARP1/RCAN2/CDKN1C/PITRM1/NPFR2/ADCY3/CH13L1/CARD16/MAP3K8/CSTA/CTGF/ADRB3/DLGG2/DRD4/EGFR/A2M/EPHA1/EPHA3/ESR1/SPATA13/PHACTR1/FGF10/RASA3/PPM1E/TBC1D9B/TBC1D10/PSD3/ARHGFE18/MAPK8IP2/MTOR/GABBR1/RASGEF1/ALS2C/RS22/FGF22/CYTH4/GNAS/GPER1/DOCK/DNAJC15/GSTP1/GZMA/ANXA2/SERPIND1/NRG1/HPC/AAGFG2/HSP90AA1/HSP90AB1/COI28A1/GF2/CYR61/L1LRN/L16/ITH4/ITIH4/ITPO5/LCK/ARRHGDI/ALGAL59/LHCGR/LLGL1/SMAD3/MAP3K1/PLEKHG7/NRAS/NTF3/PALLM/ARHGFE3/PARK2/SPOCK3/LEF1/ANGPT4/PI3/PK3CG/PML/PNLIP/TLR9/RIN2/ELP3/ARHGFE10/PPP2R2B/VAC14/PRKAR1B/PRKDI1/MAPK3/MAP2K2/SLAMF8/CDC425/E1/PSMB4/PAX6/PSMD7/PLEKHG5/CAR2/PXN/RASGRF2/TRIM27/RGS12/CCL17/NOD2/SFRP2/ARHGAP9/SGK1/BMP4/ROK/STK3/STK10/BST2/TCEA1/TERF1/TIMP3/TNFAIP3/TNX8/CCR2/TNFRSF4/WWHAG/CXCR4/FZD5/CARD14/CAST/SH3BGR13/SPINK7/TP63/SERPINA6/IRS2/CRAOD/FADD/TNFRSF11A/STAR13/MAP3K6/ADIPOQ/ARHGAP29/H2AFY/ARHGFE10/RAPGEF2/USP6N1/BABGAP1/OSECL1/FGF19	142
GO:0050866	negative regulation of cell activation	17/901	151/17046	0.00263	0.03362	0.02644	IL13RA/CYLD/GPER1/HLX/ZC3H12D/INHBA/IRF1/LGALS9/IL20RB/PAG1/BMP4/BPI/TNFAIP3/CCR2/LST1/ZC3H12A/SLA2	17
GO:0055123	digestive system development	17/901	151/17046	0.00263	0.03362	0.02644	CDKN1C/CP51/EGFR/FGF10/FOXL1/HLX1/IGF1/IGF2/SMAD3/PTX2/SCT/STRA6/SFRP2/BMP4/PPDPF/TP63/ALDH1A2	17
GO:0032675	regulation of interleukin-6 production	12/901	90/17046	0.0027	0.0345	0.02713	SPON2/HLA-B/IL6/ISL1/LGALS9/TLR9/NOD2/BPI/TNFAIP3/TWIST1/NLRX1/ZC3H12A	12
GO:0046689	response to mercury ion	4/901	12/17046	0.00273	0.03465	0.02725	GATM/AQP2/AQP9/PGAM2	4
GO:0080439	trachea morphogenesis	4/901	12/17046	0.00273	0.03465	0.02725	RSPO2/MAPK3/MAP2K2/BMP4	4
GO:0051051	negative regulation of transport	36/901	418/17046	0.00277	0.03518	0.02766	TRDN/CHGA/CIDEA/CYLD/DRD4/NEEDD4/MTOR/GRB10/ANXA2/NRG1/ANXA13/IL1RN/IL6/INHBA/KCNH2/LGALS9/ATP1A2/NOV/OPRL1/PARK2/PDE4C/SIRT6/PML/TLR9/LMBRD1/PRKDI1/TRIM27/SCT/BST2/TWIST1/CCR2/TNFRSF4/RAB11/HP1/IRS2/RSAD2/ADIPOQ	36
GO:1901653	cellular response to peptide	40/901	478/17046	0.0028	0.03536	0.02781	TCIRG1/ADCY3/AP3S1/CP51/CY11A1/EGFR/EF4G1/FGF10/RASA3/FOXO1/AKR1B1/MTOR/FGF22/GNAS/GPER1/GRB10/NRG1/NR4A1/IGF2/LCK/NRAS/PRKAG3/TLR9/PRK40/AR1B/LMBRD1/MAPK3/MAP2K2/PSMB4/PSMD7/PTPRE/PXN/RASGRF2/NOD2/VAMP2/NGARP/IRS2/ADIPOQ/RAPGEF2/FGF19	40
GO:0051048	negative regulation of secretion	19/901	178/17046	0.00281	0.03536	0.02781	CHGA/CIDEA/DRD4/NRG1/IL1RN/IL6/INHBA/LGALS9/NOV/PARK2/PDE4C/PML/TRIM27/SCT/CCR2/TNFRSF4/RAB11/HP1/RSAD2/ADIPOQ	19
GO:0042060	wound healing	53/901	678/17046	0.00281	0.03536	0.02781	CDH3/KCNMB2/MRVI1/NLRP6/A2M/F11/FGA/FGF10/FOXO2/GATM/GNAS/SCG3/GUCY1A3/ANXA2/SERPIND1/NRG1/IGF1/IGF2/CYR61/IL6/IRF1/ITGB2/KCNMB1/LCK/LOX/SMAD3/MAP3K1/NOV/NRAS/ANGPT4/PIK3CG/PKM/TREM1/APBB1IP/PRKAR1B/BIN3/MAPK3/PROC/TRPC7/BMP4/SIC1/CA1/TIMP3/TNFAIP3/TRPC6/WNT10B/C6orf25/CAPZB/HIST1H3A/HOPX/ACTN1/SYT7/ESAM/SLC16A3	53
GO:0055074	calcium ion homeostasis	31/901	345/17046	0.00281	0.03536	0.02781	TRDN/CCR1/ADM/DRD4/ESR1/NPTN/GPER1/ANXA6/KDR/LCK/ATP1A2/OPRL1/PDE6B/PIK3CG/PKHD1/PML/CHRNA9/PRKDI1/TRPC7/CCL11/BMP4/SIC1/CA1/TIMP3/TNFAIP3/TRPC6/WNT10B/C6orf25/CAPZB/HIST1H3A/HOPX/ACTN1/SYT7/ESAM/SLC16A3	31
GO:008154	actin polymerization or depolymerization	17/901	152/17046	0.00282	0.03536	0.02781	R2/CXCR4/CALB/ATP13A4/CASO1/SMO1/ABII1/MSRB2/MTOR/IMOD4/FWIN1/MAP3K1/SSH1/TTC11/ACTR3B/TRIM27/CCL11/MICAL1/CAPZB/SH3BGR13/GAS7/SCIN/MICAL2	17

GO:1901652	response to peptide	47/901	585/17046	0.00283	0.03538	0.02782	TCIRG1/NPFR2/ADCY3/AP351/ADM/CP51/CTGF/CYP11A1/EGFR/EIF4G1/FGF10/RASAS3/FOXO1/FOXO2/FOXO3/GPER1/GRB10/NRG1/NRA41/IGF2/IL6/LCK/NRAS/PKM/PRKAG3/TLR9/PRKAR1B/LMBRD1/MAPK3/MAP2K2/PSMB4/PSMD7/PTPR/PTN/PTNIP3/MGARP/IRS2/ADIPQO/RAPGEF2/FGF19/EEF2/LARP1/MTOR/PABPC1/BARRHL2/CYR61/IL6/PRR16/PWILZ/MAPK3/NODD	47
GO:0034250	positive regulation of cellular amide metabolic process	11/901	79/17046	0.00284	0.03548	0.0279		11
GO:0030182	neuron differentiation	95/901	1359/17046	0.00285	0.0355	0.02791	FARP1/CDKN1C/SPON2/ZBTB18/TBR1/GPRIN1/CLN5/SEZ6/CNP/COL9A3/SCLT1/ADM/DNMT3A/EFNA2/EGFR/EIF4G1/EPHA1/EPHA3/EPHB4/FGF10/RASAS3/BTBD3/SPG20/NFASC/E/95/PB413/NEDD4/PSD3/MAPK8IP2/DFNB31/TEMNA4/FGF22/NPTN/SOX8/KCNP2/NRGI1/HOX8/HS90AA1/HS90AB1/HS90AB2/HS90AB3/HS90AB4/HS90AB5/HS90AB6/HS90AB7/HS90AB8/HS90AB9/HS90AB10/HS90AB11/HS90AB12/HS90AB13/HS90AB14/HS90AB15/HS90AB16/HS90AB17/HS90AB18/HS90AB19/HS90AB20/HS90AB21/HS90AB22/HS90AB23/HS90AB24/HS90AB25/HS90AB26/HS90AB27/HS90AB28/HS90AB29/HS90AB30/HS90AB31/HS90AB32/HS90AB33/HS90AB34/HS90AB35/HS90AB36/HS90AB37/HS90AB38/HS90AB39/HS90AB40/HS90AB41/HS90AB42/HS90AB43/HS90AB44/HS90AB45/HS90AB46/HS90AB47/HS90AB48/HS90AB49/HS90AB50/HS90AB51/HS90AB52/HS90AB53/HS90AB54/HS90AB55/HS90AB56/HS90AB57/HS90AB58/HS90AB59/HS90AB60/HS90AB61/HS90AB62/HS90AB63/HS90AB64/HS90AB65/HS90AB66/HS90AB67/HS90AB68/HS90AB69/HS90AB70/HS90AB71/HS90AB72/HS90AB73/HS90AB74/HS90AB75/HS90AB76/HS90AB77/HS90AB78/HS90AB79/HS90AB80/HS90AB81/HS90AB82/HS90AB83/HS90AB84/HS90AB85/HS90AB86/HS90AB87/HS90AB88/HS90AB89/HS90AB90/HS90AB91/HS90AB92/HS90AB93/HS90AB94/HS90AB95/HS90AB96/HS90AB97/HS90AB98/HS90AB99/HS90AB100	95
GO:0010629	negative regulation of gene expression	96/901	1376/17046	0.00287	0.03569	0.02807	CDKN1C/CLD/ZBTB18/CELF1/CCR1/CTGF/SWDD1/CYLD/RNF168/ZNF366/DNMT3A/PATL2/A2M/EIF4/ESR1/SBN02/ACIN1/FOXO2/FOXO1/DIP2A/FLT2/NEDD4/PUM2/RVBP/PAB96/PC1/DKK3/GPER1/SOX8/NRGI1/HMGAI/HOXB3/ID3/IRF1/ISL1/HLS1/HESS1/LGALS9/SMAD3/MITF/MOV10/PARK2/LEF1/SIRT6/PTX2/PKH01/PML/RIPPLY3/TLR9/PWILZ/PRMT6/DNAJC17/CNOT11/MAP2K2/MASP1/TEM2/GATAD2B/METTL14/CCAR2/CREBZF/TRIM27/NOD2/SFRP2/GZFF1/BMP4/ZNF649/SOX9/TBP/ZEB1/TNFAIP3/TWIST1/TNFRSF4/WNT10B/ZNF177/ZC3H14/ZC3H12A/CPEB4/CAUR/SCRT1/HIST1H3A/SUA2/NROB2/HOPX/KDM2B/LOXL3/CBX2/TP63/RUNX3/LUMD1/ER11/PIAS2/CBFA2T2/AURKB/ADIPQO/H2AFY/FGF19/NR1H4	96
GO:0007399	nervous system development	143/901	2174/17046	0.0029	0.03582	0.02817	FARP1/CDKN1C/SPON2/ZBTB18/TACC2/TBR1/GPRIN1/CLN5/SEZ6/CNP/COL9A3/SCLT1/ADM/ZNF358/APCDD1/CYP11A1/DLG2/DNMT3A/EFNA2/EGFR/EGFR3/EIF4G1/EMIL1/EPHA1/EPHA3/EPHB4/FGF10/RASAS3/BTBD3/SPG20/NFASC/EPB41L3/NEDD4/PSD3/MAPK8IP2/MTOR/DFNB31/TEMNA4/FGF22/NPTN/SOX8/KCNP2/NRGI1/HLX/HPCA/APBA2/HOXB3/HOXD3/HS90AA1/HS90AB1/HS90AB2/HS90AB3/HS90AB4/HS90AB5/HS90AB6/HS90AB7/HS90AB8/HS90AB9/HS90AB10/HS90AB11/HS90AB12/HS90AB13/HS90AB14/HS90AB15/HS90AB16/HS90AB17/HS90AB18/HS90AB19/HS90AB20/HS90AB21/HS90AB22/HS90AB23/HS90AB24/HS90AB25/HS90AB26/HS90AB27/HS90AB28/HS90AB29/HS90AB30/HS90AB31/HS90AB32/HS90AB33/HS90AB34/HS90AB35/HS90AB36/HS90AB37/HS90AB38/HS90AB39/HS90AB40/HS90AB41/HS90AB42/HS90AB43/HS90AB44/HS90AB45/HS90AB46/HS90AB47/HS90AB48/HS90AB49/HS90AB50/HS90AB51/HS90AB52/HS90AB53/HS90AB54/HS90AB55/HS90AB56/HS90AB57/HS90AB58/HS90AB59/HS90AB60/HS90AB61/HS90AB62/HS90AB63/HS90AB64/HS90AB65/HS90AB66/HS90AB67/HS90AB68/HS90AB69/HS90AB70/HS90AB71/HS90AB72/HS90AB73/HS90AB74/HS90AB75/HS90AB76/HS90AB77/HS90AB78/HS90AB79/HS90AB80/HS90AB81/HS90AB82/HS90AB83/HS90AB84/HS90AB85/HS90AB86/HS90AB87/HS90AB88/HS90AB89/HS90AB90/HS90AB91/HS90AB92/HS90AB93/HS90AB94/HS90AB95/HS90AB96/HS90AB97/HS90AB98/HS90AB99/HS90AB100	143
GO:0070167	regulation of biomineral tissue development	10/901	68/17046	0.0029	0.03582	0.02817	CCR1/FAM101A/SMAD3/BGLAP/BMP4/SCL8A1/BMP1B/SOX9/TWIST1/WNT10B	10
GO:0071260	cellular response to mechanical stimulus	10/901	68/17046	0.0029	0.03582	0.02817	IRF1/MAPK3/ATP1A2/MAPK3/BMP4/SOX9/TLR5/TNFRSF1A/CRADD/FADD	10
GO:0032101	regulation of response to external stimulus	60/901	790/17046	0.00295	0.03612	0.0284	CDH13/TBR1/CCR1/NLRP6/A2M/F11/FGA/FGF10/SBN02/ACIN1/LARP1/PUM2/MTOR/SIC37A4/GPER1/FFAR2/GSTP1/ANXA2/HKI1/LILR1/IL16/IL6/SLI/LDR/LCK/LGALS9/SMAD3/NOV/NTF3/PARK2/PDE6B/PIK3CG/PLA2G2A/PML/IL20RB/TLR9/TREM1/PRK01/MAP2K2/PROC/MASP1/HTRA1/PSMB4/NOD2/STAT2/TNFAIP3/TNFRSF1A/CCR2/CA7/CXCR4/FZD5/RA87A/NLRX1/CALB/HIST1H3A/HOXY/TNFRSF1A/ADIPQO/L1/Y86/NUP93	60
GO:0048598	embryonic morphogenesis	46/901	571/17046	0.00296	0.03612	0.0284	CDKN1C/GBB6/COL11A1/ADM/ZNF358/ECE1/SFRP10/FOXO2/TEMNA4/GNAS/FLVCR1/SOX8/HLX/HOXB3/HOXC4/HOXD3/RSPO2/CYR61/LILRN/INHBA/ITGA7/ITGB2/HESS1/AFK3/LAMA3/SMAD3/LEF1/ATP8A2/CHRNA9/IFT122/STRAG/SFRP2/BMP4/SOX9/STK3/ZEB1/TWIST1/PAX8/FZD5/KDM2B/TP63/ALDH1A2/ADIPQO/MICAL2	46
GO:0005979	regulation of glycolysis biosynthetic process	6/901	28/17046	0.00297	0.03612	0.0284	MTOR/GRB10/IGF1/IGF2/PPP1CB/IRS2	6
GO:0010962	regulation of glucan biosynthetic process	6/901	28/17046	0.00297	0.03612	0.0284	MTOR/GRB10/IGF1/IGF2/PPP1CB/IRS2	6
GO:0034698	response to gonadotropin	6/901	28/17046	0.00297	0.03612	0.0284	CYP11A1/EGR3/GBB6/INHBA/LHCGR/PAX8	6
GO:0002698	negative regulation of immune effector process	12/901	91/17046	0.00297	0.03612	0.0284	A2M/HLA-B/HLA-E/HLX/LGALS9/IL20RB/MASP1/HTRA1/NOD2/BS2/CCR2/NLRX1	12

GO:0042307	positive regulation of protein import into nucleus	12/901	91/17046	0.00297	0.03612	0.0284	EGFR/HSP90A/B1/GFI1/IL6/JUP/PO5/LGALS9/SMAD3/TLR9/SFRP2/BMP4/SPHK1	12
GO:1904018	positive regulation of vasculature development	14/901	115/17046	0.00297	0.03612	0.0284	CH3L1/ADM/EPHA1/FOXO2/ISL1/KDR/ANGPT4/PRKD1/CCL11/SFRP2/TWIST1/RUNX1/SPHK1/RAPGEF2	14
GO:0006874	cellular calcium ion homeostasis	30/901	332/17046	0.003	0.03643	0.02865	TRDN/CCR1/ADM/DRD4/ESR1/NPTN/GPER1/ANXA6/LCK/ATP1A2/OPRL1/PDE6B/PIK3CG/PKHD1/PMIL/CHRNA9/PRKD1/TRPC7/CCL11/BMP4/SLC8A1/TGM2/TRPC4/TRPC6/CCR2/CXCR4/CAUR/ATP13A4/CASQ1/SMAD1	30
GO:0007519	skeletal muscle tissue development	17/901	153/17046	0.00302	0.0365	0.0287	ZBTB18/CHRNA1/SMYD1/FLNB/VGLL2/SOX8/HLX/MEF2D/MEOX2/NFATC3/NRAS/PTX2/PLAGL1/BN3/TWIST1/WNT10B/CASQ1	17
GO:0030799	regulation of cyclic nucleotide metabolic process	17/901	153/17046	0.00302	0.0365	0.0287	NPFRR2/ADM/ADRB3/DRD4/GABBR1/GNAS/GPER1/GUCY1A3/HPCA/LHCGR/MC2R/NPPC/OPRL1/PALM/MRAP5/CT/CCR2	17
GO:0060485	menschyma development	21/901	206/17046	0.00304	0.03663	0.02881	EPHA3/FGF10/FOXO2/SOX8/NRG1/ISL1/SMAD3/MEOX1/LEF1/PTX2/BNC2/ACTA2/S100A4/SFRP2/BMP4/SOX9/ACTC1/TWIST1/LOXL3/ALDH1A2/FGF19	21
GO:0048608	reproductive structure development	34/901	391/17046	0.00308	0.03704	0.02913	CDKN1C/COL9A3/ZFP42/ADM/CYP11A1/EGFR/ESR1/FGF10/GI82/SOX8/HSD17B2/HSP90A/B1/GFI1/CYR61/INHBA/KDR/LHCGR/MC2R/LHX8/LEF1/PTX2/HTRA1/STRA6/SFRP2/BMP4/SLC8A1/BMPR1B/BO/K/SOX9/STK3/TLR5/PHLDA2/FGF5/TP63	34
GO:0043122	regulation of I-kappa kinase/NF-kappaB signaling	22/901	220/17046	0.00311	0.03717	0.02923	MIB2/CYLD/NLRP6/ESR1/GSTP1/LGALS9/NOV/PARK2/TLR9/ZDHHC13/PRKD1/PLEKHG5/S100A4/NOD2/BST2/TNFAIP3/TNFRSF1A/TRAF5/NLRX1/FAOD/SPHK1/ADIPOQ	22
GO:0045934	negative regulation of nucleobase-containing compound metabolic process	90/901	1280/17046	0.00311	0.03717	0.02923	CDKN1C/C1D/ZBTB18/SMYD1/CYLD/RNF168/ZNF366/DNM13A/DRD4/ELK4/ESR1/SBNO2/ACIN1/FOXO2/FOXO1/NEDD4L/RYBP/GABBR1/PABPC1/DNAIC2/DKK3/GPER1/DNAIC15/GZMA/SOX8/NRG1/HMGCL/HPCA/HOXB3/HOXC6/ID3/IRF1/ISL1/HILS1/HESS/SMAD3/MITF/NPPC/OPRL1/PALM/LEF1/SIRT6/PTX2/PKHD1/PMIL/RIPPY3/TLR9/PRMT6/DNAIC17/TENM2/GATAD2B/CCAR2/CREBZF/TRIM27/NOD2/SFRP2/GZF1/BMP4/ZNF649/SOX9/TFEB1/TERF1/TNFAIP3/TWIST1/CCR2/TNFRSF4/WNT10B/ZNF177/ZC3H14/ZC3H12A/CALR/SUURP/SCRT1/HIST1H3A/SLAZ/NROB2/HOPX/KDM2B/LOXL3/CBX2/TP63/RUNX3/LIMD1/PIAS2/CBFA2T2/AURKB/ADIPOQ/H2AFY/NR1H4	90
GO:0030326	embryonic limb morphogenesis	15/901	128/17046	0.00311	0.03717	0.02923	ZNF358/ECE1/SP8/GNAS/FLVCR1/RSP02/AFF3/LEF1/PTX2/IFT122/SFRP2/BMP4/TWIST1/TP63/ALDH1A2	15
GO:0035113	embryonic appendage morphogenesis	15/901	128/17046	0.00311	0.03717	0.02923	ZNF358/ECE1/SP8/GNAS/FLVCR1/RSP02/AFF3/LEF1/PTX2/IFT122/SFRP2/BMP4/TWIST1/TP63/ALDH1A2	15
GO:0006954	inflammatory response	47/901	588/17046	0.00312	0.03717	0.02923	KLRG1/CH3L1/CCR1/PARP4/NLRP6/A2M/UNC13D/FGM/SBNO2/GPER1/IFAR2/GSTP1/HRH1/IL1RL1/IL1RLN/IL6/ISL1/ITGB2/ITIH4/LGALS9/SMAD3/NFATC3/NOV/PK3CG/PLA2G2A/IL20RB/TLR9/PRKD1/MAS1/PSMB4/CCL11/CCL17/NOD2/BMPR1B/TLR5/TNFAIP3/TNFRSF1A/CCR2/TNFRSF4/CXCR4/NLRX1/IL1F10/TNFRSF11A/SPHK1/CCR2/ADIPOQ/LY86	47
GO:0030004	cellular monovalent inorganic cation homeostasis	11/901	80/17046	0.00314	0.03734	0.02997	TCIRG1/CLNS1/NEEDD4L/ATP1A2/ATP5B/SLAMF8/SGK1/SLC4A1/SLC8A1/SLC8A1/CA7/RAB7A	11
GO:0051235	maintenance of location	21/901	207/17046	0.00322	0.03818	0.03003	TRDN/CIDEA/HTT1/EPB41L3/FLNB/SYNE1/MORC3/IFAR2/HK1/ACACB/IL6/JUP/LCK/ITBP1/PMIL/SLC30A10/ABHD4/ZC3H12A/CAIR/CASQ1/SCIN	21
GO:008015	blood circulation	35/901	407/17046	0.00323	0.03825	0.03008	KCNMB2/MRVI1/TRDN/CELF2/CHGA/ADM/CPS1/CTGF/ADRB3/ABAT/ECCE1/FGA/FOXO2/BMP10/GPER1/GUCY1A3/KCNIP2/HRH1/JUP/KCNH2/KCNJ8/MEOX2/MTYL2/ATP1A2/NPPC/OPRL1/PK3CG/POMC/ACTA2/SGK1/SLC8A1/ACT1/CACNA1E/HOPX/ADIPOQ	35

GO:0072234	metanephric nephron tubule development	5/901	20/17046	0.00325	0.03845	0.03024	SOX8/ACAT1/HES5/SOX9/PAX8	5
GO:0050801	ion homeostasis	50/901	636/17046	0.00327	0.03854	0.03031	TCIRG1/TRDN/CLNS/CCR1/ADM/CP51/DRD4/ESR1/NEDD4/STEA2/NPTN/GPER1/FLVCR1/ANXA6/KCNH2/KDR/LCK/MFI2/NUBP1/ATP1A2/OPRL1/ATP5B/PARK2/PDE6B/PIK3CG/PRKHD1/PML/SLC30A10/CHRNA9/PRKD1/SLAMF8/TRPC7/CCL11/SGK1/BMP4/SLC4A1/SLC8A1/SLC9A3/TGM2/TRPC6/CCR2/CA7/CXCR4/RAB7A/CALR/ATP13A4/CASQ1/SMDT1/MTLS	50
GO:0044711	single-organism biosynthetic process	107/901	1567/17046	0.00329	0.03875	0.03047	CDH3/TCIRG1/MTHS/NPFR2/ADCY3/SLC27A2/ERLIN2/BAG1/ACOT7/MRPL52/ADM/CP51/CTGF/PPM1L/BOAT1/ADAL/DOB1/ABAT/DPH1/DRD4/A3/GXT/EEF2/ENO2/ALAS1/FOXO1/AKR1B1/MTOR/GABBR1/STGGALNAC3/GATM/GBG1/GAPDH5/AMPD2/DKX3/GLS2/ANP3/GNAS/PIGW/GPER1/GRB10/NRPS188/GSTP1/GUCY1A3/NME1/PADI1/HAS1/ACACB/HPCA/HRH1/HSO1B1/HSO1B2/ACADL/NMME5/IGF1/IGF2/CRY61/L6/ACAT1/LDLR/LHCR/M/C2R/ME1/NPPC/QAS2/OPRL1/ATP5B/PALM/GHST15/PGAM2/PIGC/PIK3CG/PKM/PLA2G2A/PRKAG3/PML/CYTL1/LPCAT2/PPP1CB/VAC14/CSGALNACT1/PRKD1/MRAP/RFC2/RPA3/SCT/MRPS14/BMP4/TERF1/CCR2/UPP1/CERS4/QTRT1/KMO/IRS2/ALDH1A2/SYNU2/SPHK1/CH25H/SDR42E1/ADIPOQ/RAPGEF2/IGGAT1/FGF19/NR1H4	107
GO:0055002	striated muscle cell development	15/901	129/17046	0.00336	0.03941	0.03099	SPEG/BMP10/TMOD4/IGF1/LMNA/MYL2/NFATC3/LEF1/PTX2/BN3/BMP4/SLC8A1/ACTC1/MNT10B/CASQ1	15
GO:0035137	hind limb morphogenesis	7/901	38/17046	0.00337	0.03941	0.03099	GNAS/RSPO2/FWNI1/AFF3/PTX2/BMP4/TWIST1	7
GO:0072210	metanephric nephron development	7/901	38/17046	0.00337	0.03941	0.03099	SOX8/FWNI1/HES5/BMP4/SOX9/PAX8/ADIPOQ	7
GO:0051223	regulation of protein transport	53/901	684/17046	0.00337	0.03941	0.03099	CIDEA/SLCS1B/CYLD/ABAT/DRD4/EGFR/FGA/EXPH5/MTOR/GLS2/GNAS/GPR26/GPER1/FFAR2/GSTP1/HLA-B/HLA-E/HPCA/HSPA1/HSP90A81/IGF1/L6/SL1/JUP/PO5/LCP1/LGALS9/LGL1/SWAD3/NOV/PARK2/PDE4C/PML/TLR9/GOLPH3L/SYBU/PRKAR1B/TRIM27/NOD2/SFRP2/BMP4/VAMP2/TWIST1/TNFRSF4/CACNA1E/FZD5/RAB11F1P1/NR0B2/IRS2/SPHK1/SYTT/RSAD2/ADIPOQ	53
GO:1904035	regulation of epithelial cell apoptotic process	8/901	48/17046	0.00339	0.03954	0.03109	FGA/GPER1/IL6/KDR/BMP4/TNF/AINP3/COL18A1/CAST	8
GO:0043410	positive regulation of MAPK cascade	45/901	560/17046	0.00342	0.03978	0.03128	CH13L/CCR1/MAP3K8/CTGF/ADRB3/DRD4/EGFR/FGA/FGF10/RASA3/MAPK8IP2/FGF22/GPER1/IRG1/IGF1/IGF2/IL1RN/IL6/KDR/LGALS9/MAP3K1/IRAS/NTF3/PIK3CG/PLA2G2A/TLR9/MAPK3/MAP2K2/PSMB4/PSMD7/PXN/RASGRF2/CCL11/CCL17/NOD2/BMP4/STK3/CXCR4/FZD5/CDK10/IRS2/TNFRSF11A/MAP3K6/RAPGEF2/FGF19	45
GO:0031347	regulation of defense response	55/901	716/17046	0.00342	0.03978	0.03128	TANK/MAP3K8/CYLD/COCH/MIIPPE/DMBT1/A2M/SBNO2/ACIN1/PUM3/SLC37A4/GPER1/FFAR2/GSTP1/HLA-B/HLA-E/HSP90A81/IL1RL1/IL6/IRF1/ISL1/TGB2/LCK/LGALS9/SMAD3/MAP3K1/NFATC3/NOV/IRAS/PIK3CG/PLA2G2A/PQO/ADIPQ/NUP93	55
GO:0055001	muscle cell development	16/901	142/17046	0.00343	0.03979	0.03129	SPEG/ADM/BMP10/TMOD4/IGF1/LMNA/MYL2/NFATC3/LEF1/PTX2/BN3/BMP4/SLC8A1/ACTC1/MNT10B/CASQ1	16
GO:0006811	ion transport	99/901	1435/17046	0.00346	0.03999	0.03145	KCNMB2/TCIRG1/TRDN/SLC27A2/CHRNA1/CHRNA2/CHRNA3/CLCA1/CCR1/SLCS1B/CL50F27/SLC38A10/TRPM6/CTGF/TRPV3/BHLHA15/DRD4/AGXT/SLC10A4/RASA3/MLC1/ATP11A/NEDD4L/MAPK8IP2/STEA2/SLC17A5/GLS2/CRACR2B/GPER1/GRK4/KCNIP2/ANXA6/ACACB/HTR3A/IL1RN/AQP2/AQP5/AQP9/ATP9B/KCNH2/KCNJ8/KCNJ9/KCNMB1/SLCGA17/LCK/LDLR/HMFI2/ATP1A2/NFATC3/OPRL1/SLC22A18/P2RY6/ATP5B/ANO7/PARK2/PCYOX1/ATP8A2/PIK3CG/PML/FXYD6/SLCO1C1/TLR9/ZDHHHC13/SLC47A1/TRPV6/SLC30A10/CHRNA9/PRKD1/TRPV5/TRPC7/RASGRF2/TRIM27/S100A6/SGK1/BMP4/SLC4A1/SLC6A12/SLC8A1/SLC9A3/SLC20A2/VAMP2/TRAPP10/TRPC4/TRPC6/TRPM2/TWIST1/UCP1/CA7/CACNA1E/CACNB2/ATP13A4/CASQ1/SLC43A1/IRS2/TNFRSF11A/SLC16A3/SMDT1/NR1H4	99
GO:0003013	circulatory system process	35/901	409/17046	0.00349	0.04033	0.03172	KCNMB2/MRV11/TRDN/CELF2/CHGA/ADM/CP51/CTGF/ADRB3/ABAT/EEC1/FGA/FOXO2/BMP10/GPER1/GUCY1A3/KCNIP2/HRH1/JUP/KCNH2/KCNJ8/MEOX2/MYL2/ATP1A2/NPPC/OPRL1/PIK3CG/POMC/ACTA2/SGK1/SLC8A1/ACTC1/CACNA1E/HOPX/ADIPOQ	35
GO:0055065	metal ion homeostasis	42/901	515/17046	0.00354	0.04084	0.03212	TCIRG1/TRDN/CCR1/ADM/DRD4/ESR1/NEDD4/STEA2/NPTN/GPER1/FLVCR1/ANXA6/KCNH2/KDR/LCK/MFI2/NUBP1/ATP1A2/OPRL1/PARK2/PDE6B/PIK3CG/PRKHD1/PML/SLC30A10/CHRNA9/PRKD1/TRPC7/CCL11/SGK1/BMP4/TGM2/TRPC4/TRPC6/CCR4/CXCR4/CALR/ATP13A4/CASQ1/SMDT1/MTLS	42
GO:1904591	positive regulation of protein import	12/901	93/17046	0.00356	0.0409	0.03216	EGFR/HSP90A81/IGF1/IL6/JUP/PO5/LGALS9/SMAD3/TLR9/SFRP2/BMP4/SPHK1	12
GO:0035116	embryonic hind limb morphogenesis	6/901	29/17046	0.00358	0.0409	0.03216	GNAS/RSPO2/AFF3/PTX2/BMP4/TWIST1	6

GO:0060740	prostate gland epithelium morphogenesis	6/901	29/17046	0.00358	0.0409	0.03216	ESR1/FGF10/IGF1/BMP4/SOX9/TP63	6
GO:0061036	positive regulation of cartilage development	6/901	29/17046	0.00358	0.0409	0.03216	BMP10/CYR61/SMAD3/BMP4/BMP4/BMP4/SOX9	6
GO:0009890	negative regulation of biosynthetic process	95/901	1370/17046	0.0036	0.04105	0.03228	CDKN1C/CD/2B/TB18/CELF1/ERLIN2/SMYD1/CYLD/RNF168/ZNF366/DNMT3A/DRD4/PATL2/ELK4/ESR1/SBNO2/FOXO2/FOXO3/NEEDD4/RYBP/GABBR1/DNAJC2/DNK3/GPER1/GRB19510/GSTP1/SOX8/NRG1/HMGAI/HPCA/HOXB3/HOXC6/ACAD1/ID3/IL6/INHBA/IRF1/ISL1/HILS1/HES5/SMAD3/MITF/OPRL1/PALM/LEF1/SIRT6/PITX2/PKH01/PML/RIPPLY3/TLR9/PRMT6/DNAIC17/TENM2/GATAD2B/METTL14/CCAR2/CREBZF/TRIM27/NOD2/SFRP2/GZF1/BMP4/ZNF649/SOX9/TBP/ZEB1/TERF1/TNFAP3/TWIST1/CCR2/TNFRSF4/WNT10B/ZNF177/ZC3H12A/CEP84/CALR/SCRI1/HIST1H3A/SLA2/NR0B2/HOXB/KDM2B/LOX3/CBX2/TP63/RUNX3/LIMD1/PIAS2/CBF42T2/AURKB/ADIPQ/H2A/RAPGEF2/FGF19/NR1H4	95
GO:0061458	leukocyte reproductive system development	34/901	395/17046	0.00361	0.04116	0.03237	CDKN1C/COX9A3/ZFP42/ADM/CYP11A1/EGFR/ESR1/FGF10/G1B2/SOX8/HSD17B2/HSP90AB1/IGF1/CYR61/INHBA/KDR/LHCGR/MC2R/LHX8/LEF1/PITX2/HTRA1/STRA6/SFRP2/BMP4/SLC8A1/BMP4/BOK/SOX9/STK3/TLR5/PHLDA2/FZD5/TP63	34
GO:0030595	chemotaxis	18/901	169/17046	0.00366	0.04167	0.03277	CHGA/CCR1/FFAR2/HRH1/HRH1/IL6/ITGB2/LGALS9/NOV/PIK3CG/TREM1/CCL11/CCL17/NOD2/CCR2/CXCR4/CALR/TNFRSF11A	18
GO:0048762	mesenchymal cell differentiation	17/901	156/17046	0.00369	0.04182	0.03289	EPHA3/FGF10/FOXO2/SOX8/NRG1/ISL1/SMAD3/LEF1/PITX2/S100A4/SFRP2/BMP4/SOX9/TWIST1/LOX3/ALDH1A2/FGF19	17
GO:0019318	hexose metabolic process	23/901	237/17046	0.00369	0.04182	0.03289	GALM/B3GLCT/ENO2/FOXO1/AKR1B1/MTOR/FUCA1/SLC37A4/GAPDH5/GRB10/HK1/IGF1/IGF2/IL6/PARK2/CHST15/PGAM2/PKM/POMC/PPP1CB/PHLDA2/IRS2/ADIPOQ	23
GO:0050727	regulation of inflammatory response	24/901	251/17046	0.0037	0.04182	0.03289	NLRP6/A2M/SBNO2/GPER1/FFAR2/GSTP1/LIR1/IL6/ISL1/SMAD3/NOV/PIK3CG/PLA2G2A/IL20RB/TLR9/MASP1/PSMB4/NOD2/TNFAP3/TNFRSF1A/CCR2/NLRX1/TNFRSF11A/ADIPOQ	24
GO:0031324	negative regulation of cellular metabolic process	141/901	2154/17046	0.00371	0.04182	0.03289	FARP1/CDKN1C/C1D/ZBTB18/CELF1/ERLIN2/CARD16/CST4/SMYD1/CYLD/RNF168/ZNF366/NLRP6/DLG2/DNMT3A/DRD4/PATL2/A2M/ELK4/EPHA1/ESR1/FHIT/PPM1E/SBNO2/ACI1/FOXO2/FOXO1/NEEDD4/RYBP/MTOR/GABBR1/PABPC1/DNAJC2/DNK3/GPER1/GRB10/DNAIC15/GSTP1/G2MA/ANXA2/SERPIND1/SOX8/NRG1/HMGAI/ACACB/HPCA/HOXB3/HOXC6/ACAD1/HSP90AB1/ID3/COX28A1/IGF1/IL6/INHBA/IRF1/ISL1/ITIH3/ITIH4/HILS1/KIF25/HES5/SMAD3/MITF/NPPC/NTF3/OPRL1/PALM/PARK2/SPOCK3/LEF1/SIRT6/PI3/PK3C/G/PITX2/PKH01/PML/RIPPLY3/TLR9/PRMT6/DNAIC17/PRKAR1B/MASP1/PSMB4/PSMD7/TENM2/GATAD2B/METTL14/CCAR2/CREBZF/TRIM27/NOD2/SFRP2/GZF1/BMP4/ZNF649/SOX9/SUPT6H/BST2/TBP/ZEB1/TERF1/TIMP3/TNFAP3/TWIST1/CCR2/TNFRSF4/WNT10B/WWHAG/ZNF177/ZC3H12A/C3H12A/CEP84/CALR/SLRP/CAST/SCRT1/HIST1H3A/SLA2/NR0B2/HOPX/SPINK7/KDM2B/LOX3/CBX2/TP63/RUNX3/SERPINA6/IRS2/IFADD/LIMD1/PIAS2/CBF42T2/AURKB/DAPL1/ADIPOQ/H2A/RAPGEF2/FGF19/NR1H4	141
GO:0006941	striated muscle contraction	14/901	118/17046	0.00376	0.04213	0.03313	CHRNA1/CTGF/DINA/BMP10/KCNH2/MYL2/ATP1A2/ATP8A2/PGAM2/PIK3CG/SLC8A1/ACTC1/CASQ1/RCSQ1	14
GO:0007169	transmembrane receptor protein tyrosine kinase signaling pathway	65/901	879/17046	0.00377	0.04213	0.03313	AB11/CDH3/CDH13/TCIRG1/ADCY3/LETT1/ESM1/AP3S1/IL13RA/CTGF/EFNA2/EGFR/EIF4G1/EPHA1/EPHA3/EPH4/FGF10/RASA3/FOXO2/FOXO1/ARHGFE1B/MTOR/FGF22/NPTN/GPER1/GRB10/NRG1/NRAA1/HSP90A1/IGF1/IGF2/IJUP/KDR/LCK/ARHGAP1/MOV10/NRAS/NTF3/ARHGFE3/ANGPT4/PRKAG3/TLR9/PRKAR1B/LMBRD1/PAG1/PRKQ1/MAK3/MA/PK2/PSMB4/PSMD7/PLEKHG5/PTPRE/PXN/PASGFR2/RIT2/SOX9/ZAP70/RAB7A/TMEM204/IRS2/SPHK1/CD8A/ADIPOQ/RAPGEF2/FGF19	65
GO:0009617	response to bacterium	38/901	456/17046	0.00377	0.04213	0.03313	SPON2/GIB6/CHGA/CNP/ADM/CP51/CYPL1A1/COCH/NLRP6/DMBT1/FGA/FGF10/SBNO2/GSTP1/HLA-B/HLA-E/IL1RN/IL6/IL10RA/IL12RB2/KCNJ8/LGALS9/PLA2G2A/TLR9/TREM1/MARK3/SLAMF8/PTGFR/DEFB134/NOD2/BPI/TLR5/TNFAP3/TNFRSF1A/FZD5/ZC3H12A/TNFRSF11A/Y86	38
GO:0072044	collecting duct development	4/901	13/17046	0.00378	0.04213	0.03313	AKR1B1/AQP7/BMP4/PAX8	4
GO:0072189	ureter development	4/901	13/17046	0.00378	0.04213	0.03313	SOX8/BMP4/SOX9/ALDH1A2	4
GO:2000479	regulation of cAMP-dependent protein kinase activity	4/901	13/17046	0.00378	0.04213	0.03313	NPFRR2/PRKAR1B/ADIPOQ/RAPGEF2	4

GO:0072503	cellular divalent inorganic cation homeostasis	31/901	352/17046	0.0038	0.04231	0.03327	TRDN/CCR1/ADM/DRD4/ESR1/NPTN/GPER1/ANXA6/LCK/ATP1A2/OPRL1/PDE6B/PIK3CG/PKH1/PRPC7/CCL11/BMP4/SLC8A1/TGM2/TRPCA/TRP31/C6/CCR2/CXCR4/CALR/ATP13A4/CASQ1/SMDT1	31
GO:0032649	interferon-gamma production	11/901	82/17046	0.00381	0.0424	0.03334	HLA-DPA1/IL12RB2/INHBA/ISL1/LGALS9/IL20RB/TLR9/NOD2/CCR2/FZD5/FADD	11
GO:0045766	positive regulation of angiogenesis	13/901	106/17046	0.00386	0.0428	0.03366	CH3L1/ADM/EPHA1/FOXC2/ISL1/KDR/ANGPT4/PRKD1/CCL11/SFRP2/TWIST1/RUNX1/SPHK1	13
GO:1903522	regulation of blood circulation	22/901	224/17046	0.00387	0.0428	0.03366	KCNMB2/TRDN/CELF2/ADM/CP51/CTGF/ECE1/FGA/NEDD4/BMP10/GPER1/KCNIP2/HRH1/JUP/KCNH2/MYL2/ATP1A2/NPPC/PIK3CG/SLC8A1/CACNA1E/HOPX	22
GO:0032635	interleukin-6 production	12/901	94/17046	0.00389	0.04294	0.03377	SFON2/HLA-B/IL6/ISL1/LGALS9/TLR9/NOD2/IRP1/TNFAIP3/TWIST1/NLRX1/ZC3H12A	12
GO:0048863	stem cell differentiation	23/901	238/17046	0.00389	0.04294	0.03377	A2M/EPHA3/FGF10/FOXC2/SOX8/NRG1/SL1/HES5/SMAD3/MEOX1/LEF1/PITX2/S100A4/SFRP2/BMP4/SOX9/TEAD3/TWIST1/PAX8/LOXL3/TP63/ALDH1A2/FGF19	23
GO:0051090	regulation of sequence-specific DNA binding transcription factor activity	30/901	338/17046	0.0039	0.04295	0.03377	CYLD/ESR1/ID3/IL6/JUP/LGALS9/NHLH2/PKH1/IRIPK4/TLR9/CYTL1/PRKD1/MAPK3/CHEBZ/TRIM27/NOD2/SGKJ/STK3/TNFAIP3/TRAF1/TRAF5/TWIST1/TNFRSF4/WNT10B/CARD11/4/ZC3H12A/NR0B2/TNFRSF11A/SPHK1/PIAS2	30
GO:0006875	cellular metal ion homeostasis	37/901	442/17046	0.00392	0.04301	0.03382	TCIRG1/TRDN/CCR1/ADM/DRD4/ESR1/NEDD4/NPTN/GPER1/FLVCR1/ANXA6/LCK/NUBP1/ATP1A2/OPRL1/PDE6B/PIK3CG/PKH1/PM1/SLC30A10/CHRNA9/PRKD1/TRPC7/CCL11/SGKJ/BMP4/SLC8A1/TGM2/TRPCA/TRPC6/CCR2/CXCR4/CALR/ATP13A4/CASQ1/SMDT1/MTLS	37
GO:0002704	negative regulation of leukocyte mediated immunity	7/901	39/17046	0.00393	0.04301	0.03382	HLA-B/HLA-E/LGALS9/IL20RB/NOD2/BST2/CCR2	7
GO:0034121	regulation of toll like receptor signaling pathway	7/901	39/17046	0.00393	0.04301	0.03382	NLRP6/IRF1/TLR9/NOD2/TLR5/TNFAIP3/RSAD2	7
GO:0045216	cell-cell junction organization	21/901	211/17046	0.00403	0.04403	0.03463	CDH3/CDH9/CDH12/CDH13/PRK3/MPP7/EPHA3/NFAS/EPB41L3/GIB2/FMNI1/JUP/KDR/SMAD3/MP2/LIMS2/PXN/FZDS/PARD6G/PARD6B/ACTN1	21
GO:0030324	lung development	19/901	184/17046	0.00406	0.04432	0.03486	PDPN/CHI3L1/CTGF/FGF10/HSD11B1/RSPO2/GFI1/KDR/NSC/LOX/C11orf73/PITX2/MAPK3/MAP2K2/STRA6/BMP4/SOX9/HOPX/ALDH1A2	19
GO:0035767	endothelial cell chemotaxis	5/901	21/17046	0.00409	0.04434	0.03487	EGR3/NR4A1/NOV/PRKD1/PLEKHG5	5
GO:1901020	negative regulation of calcium ion transmembrane transporter activity	5/901	21/17046	0.00409	0.04434	0.03487	TRDN/DRD4/ATP1A2/OPRL1/TLR9	5
GO:1903170	negative regulation of calcium ion transmembrane transport	5/901	21/17046	0.00409	0.04434	0.03487	TRDN/DRD4/ATP1A2/OPRL1/TLR9	5

GO:0035270	endocrine system development	15/901	132/17046	0.00418	0.04527	0.0356	CDKN1C/FGF10/FOXO1/DKK3/HOXB3/HOXD3/IL6/ISL1/SMAD3/PITX2/STRA6/BMP4/SOX9/PAX8/ALDH1A2	15
GO:0050680	negative regulation of epithelial cell proliferation	13/901	107/17046	0.00419	0.04529	0.03562	CDKN1C/LECT1/WASH1/MCC/PLA2G2A/JMS2/IFT122/SLURP1/SFRP2/BMP4/SOX9/WNT10B/RUNX3	13
GO:0009306	protein secretion	38/901	459/17046	0.0042	0.04529	0.03562	CH3L1/CIDEA/ABAT/DRD4/FGA/EXPH5/GNAS/GPER1/FFAR2/HLA-E/IGF1/IL1RN/IL6/ISL1/LGALS9/ILG1L/NOV/PARK2/PDE4C/PML/TLR9/TREM1/GOLPH3L/SYBU/PRKAR1B/TRIM27/NOD2/VAMP2/TWIST1/TNFRSF4/CACNA1E/RAB11F1P1/NR0B2/MON1A/IRS2/SYT1/RSAD2/RA83D	38
GO:1903531	negative regulation of secretion by cell	17/901	158/17046	0.00421	0.04529	0.03562	CHGA/CIDEA/DRD4/IL1RN/IL6/INHBA/LGALS9/NOV/PARK2/PDE4C/PML/TLR9/TREM1/TNFRSF4/RAB11F1P1/RSAD2/ADIPOQ	17
GO:0005975	carbohydrate metabolic process	62/901	835/17046	0.00421	0.04529	0.03562	GNE/CH3L1/CH3L2/B4GALT7/GALNT15/CLN5/SLC51B/NEU4/GALM/CP51/PARP4/B3GLCT/MGAT5B/ADR83/DDOST/ENO2/TRAK1/FOXO1/AKR1B1/NUIP210/MTOR/FUCA1/SLC37A4/ST6GALNA3/G8T11/GAPDH5/SLC17A5/DHHDH/GPER1/EOGT/GRB10/HAS1/HK1/HRH1/IGF1/IGF2/IL6/MUC21/LHCGR/MEI/MGAT1/NEU1/OAS2/PARK2/CHST15/SIRT6/GALNT7/PGAM2/PKM/PRKAG3/POMC/PPP1CB/PPP1CC/CSGALNACT1/PHLDA2/MOGS/CALR/RAE1/IRS2/STBD1/ADIPOQ/NUIP93	62
GO:0045893	positive regulation of transcription, DNA-templated	94/901	1362/17046	0.00431	0.04618	0.03631	CDH13/CDKN1C/DWMT2/TBR1/ERLIN1/IL13/RA/CTED4/BHLHA15/EGFR/ESR1/FGF10/SBNQ2/FOXO1/VGLL2/MTOR/DNAIC2/BMP10/GPER1/BRF1/SOX8/HMGA1/NR4A1/TFAP2E/BARHL2/IGF1/IGF2/CYR61/IL6/FOXO2/INHBA/IRF1/ISL1/JUP/HES5/LGALS9/LMNA/LMO2/SMAD3/MEF2D/MEOX1/MEOX2/MITF/NFATC3/NFYB/NHLH2/NTF3/PARK2/L/TEAD3/TNFRSF1A/TRAF1/TRAFS/TWIST1/WNT10B/PAX8/FZD5/CARD14/RUNX1/TP63/RUNX3/FADD/TNFRSF11A/SPHK1/PIAS2/LDB2/CBFA2T2/MICAL2/NR1H4	94
GO:1903508	positive regulation of nucleic acid-templated transcription	94/901	1362/17046	0.00431	0.04618	0.03631	CDH13/CDKN1C/DWMT2/TBR1/ERLIN1/IL13/RA/CTED4/BHLHA15/EGFR/ESR1/FGF10/SBNQ2/FOXO1/VGLL2/MTOR/DNAIC2/BMP10/GPER1/BRF1/SOX8/HMGA1/NR4A1/TFAP2E/BARHL2/IGF1/IGF2/CYR61/IL6/FOXO2/INHBA/IRF1/ISL1/JUP/HES5/LGALS9/LMNA/LMO2/SMAD3/MEF2D/MEOX1/MEOX2/MITF/NFATC3/NFYB/NHLH2/NTF3/PARK2/L/TEAD3/TNFRSF1A/TRAF1/TRAFS/TWIST1/WNT10B/PAX8/FZD5/CARD14/RUNX1/TP63/RUNX3/FADD/TNFRSF11A/SPHK1/PIAS2/LDB2/CBFA2T2/MICAL2/NR1H4	94
GO:0044282	small molecule catabolic process	29/901	326/17046	0.00436	0.04659	0.03664	BCKDK/MTHFS/SLC27A2/HIBADH/ACOT7/CRABP1/ABAT/AGXT/ENO2/FAH/MTOR/PNKD/GAPDH5/GLSZ/DHHDH/HK1/ACADL/ACAT1/LDLR/NUDT1/PCYOX1/PGAM2/PKM/PONI/SM PD3/TWIST1/SMO/IRS2/ADIPOQ	29
GO:0060440	trachea formation	3/901	7/17046	0.00439	0.04683	0.03682	MAPK3/MAP2K2/BMP4	3
GO:0002252	immune effector process	53/901	693/17046	0.00439	0.04683	0.03682	AB11/SPON2/CHGA/RNF168/DMBT1/A2M/JUNC13D/FCGR2A/SBNQ2/ACIN1/PUM2/SLC37A4/FFAR2/HLA-B/HLA-E/HLX/HS90AA1/HSP90AB1/IL6/IRF1/KCNJ8/LCK/LCP1/LGALS9/OAS2/LEF1/PIK3CG/PM1/IL20RB/TREMI1/APBB1P/MAPK3/MASP1/HTRA1/NOD2/STAT2/SUPT6H/BST2/VAMP2/TNFAP3/CCR2/TNFRSF4/CA7/FZD5/NRX1/JUNC3B1/HISTH3A/SLAZ/JHTM1/FADD/RSAD2/CD8A/NUIP93	53
GO:0007422	peripheral nervous system development	10/901	72/17046	0.00442	0.04697	0.03694	CYP11A1/EGR3/NFASC/SOX8/NR61/ISL1/NTF3/RUNX1/RUNX3/ARRHGEF10	10
GO:0043010	camera-type eye development	26/901	283/17046	0.00442	0.04697	0.03694	CDKN1C/DRD4/FGF10/FOXO2/SOX8/HPCA/AQP5/INHBA/HES5/SMAD3/MAP3K1/MITF/PDE6B/ATP8A2/PITX2/IFT122/STRA6/BMP4/BMP10/SOX9/ZEB1/TWIST1/FZD5/BFSP2/KD M2B/ALDH1A2	26
GO:0060541	respiratory system development	21/901	213/17046	0.00449	0.04763	0.03746	SPEG/PDPN/CH3L1/CTGF/FGF10/HSD11B1/RSPO2/IGF1/KDR/INSC/LOX/LEF1/C11orf73/PITX2/MAPK3/MAP2K2/STRA6/BMP4/SOX9/HOPX/ALDH1A2	21
GO:0032637	interleukin-8 production	9/901	61/17046	0.00452	0.04784	0.03762	CH3L1/FFAR2/LGALS9/TLR9/NOD2/BPI/TLR5/FADD/ADIPOQ	9
GO:0070663	regulation of leukocyte proliferation	19/901	186/17046	0.00457	0.04827	0.03796	FGF10/GSTP1/HLA-DPA1/HLA-E/ZC3H12D/IGF1/IGF2/IL6/IRF1/LGALS9/IL20RB/BMP4/TNFAP3/CCR2/TNFRSF4/ZAP70/LST1/RS2/FADD	19

GO:0005575	cellular_componen	942/942	16277/17046	3.63E-20	2.48E-17	2.20E-17	<p>AKT3/ABI1/CDH3/ITANK/SMIM6/CD300L/D/GNE/ZNF783/CCDC180/CDH9/TSFANS/CDH12/CDH13/SUGP2/MBNL1/FARP1/KLRKAN2/KCNMB2/CDKN1C/SPFEG/BCKDK/TCIRG1/MRV1L/TRO1/ABCA9/SPON2/C1D/COG5/ZBTB18/PIRTRM1/TACCC2/MTHE5/PDPNP/DMRT2/CELFI1/CELF2/TBR11/SEF19/GJB6/HCS1/NPFR2/ADC3/PIRNC1/MTMED10/SLC27A2/LECT1/RER1/ESM1/ADAM29/HNRNPUL1/RP114/HBADH/CHGA/CHL1/ERLIN1/ERLIN2/PSIP1/CHIL3/EGN2/PXMP4/ATXN21/B4GAL1/PTH2/KIF12/ACOT17/EXOC3/CHRNA1/CHRNA2/CHRNA5/GPRIN1/SORCS1/CIDEA/CTDNF7/GBP4/ALPK2/PANX3/ARBP7/GALNT3/AP351/CLCA1/C10orf90/FAT3/CLNS1/MRPL52/FRMO6/CCR1/SLC18/CL10orf2/SPATA33/ZG168/SLC38A10/SEZ6/KRT40/TNFAIP8L1/MOBSA/CNTP/APOA1BP/NEU4/CO19A3/COL11A11/VP068/GALM/COMP/SLT1/MAP3K8/ZFP442/ADM/IL13/IRA/EGFLAM/UBLCP1/HUS1B/C7orf34/OA2A4/CPD/CPM/CP51/NDUFAP6/PXDN/CRAP1/ZNF358/TRPM6/MI2B/PAR6/MPPT7/LDLRAD3/FAM101A/B3GLCT/CEP128/LYSMD4/MGAT5B/APCDD1/CSTA/KLC3/ZNF38/CTG F/ABCC13/MR3/S/MPD1/SGOL1/PPM1/LRRC34/S/HD19/CYBS61/CYLD/MB0A1/ADR83/ANKRD46/ESCO2/CYP11A1/ZNF782/FTTM1/ADAL/TPRV3/ZNF709/ZNF781/CALM16/CTE DA/DBB1/WBP2NL/DDOST/RNF168/ZNF366/BHLHA15/COCH/PPP1R18/NLRP6/DIO3/DL62/DKMT1/DNAH6/DNAH8/ENMT3A/ABAT/DPH1/DRO4/D5G5/DTNA/ECE1/AGXT/FEZF/E FNA2/EGFR/EGR3/FATL2/EIF4G1/AZM1/ELK4/ANKRD23/TMEM17/LPH/EMIL1/ANM14/SMIMA12/SLD10A4/SMIMA14/ENMT3A/EPH84/ESR1/ALAS1/FL11/FAH/F/ SPATA13/PRSS54/FCGR2A/RNF182/PHACTR1/SP8/FGF10/FHIT/XRN2/RASA3/PPM1/VA5H1/RTB3/SBNO2/TRAK1/MSR2/ACIN1/FOXJ1/FOXQ2/TBC1D9B/FOXO1/EXPH5 /AKR1B1/SPG20/NFAS/EPH4L13/GG43/FLNB/DIP2A/FLDT2/MIC1/TBC1D1/IRHOB1B2/NU210/SELL13/ATP11A/NEED4/SYNE1/PSD3/LARP1/PPP1R13B/PUM2/ARHGFE18/RBP/ MORC3/MAPK8IP2/TSK2/AGL2/VGLL2/WDR27/SLC37A4/GABRR1/RASGEF1C/RNF144B/ZNF549/CCDC110/STGALNAC3/TWEM15/ANUT1/MSR1/DSC9R/GAK/SAMM50/DFN B31/ALS2CL/PNKD/SEC31B/TENM4/ACOT11/FAM169A/RA114/RGS22/STEAP2/GAS2/FBXK121/FBXO2/LCE2B/SACS/GATM/GBGT1/GAPDH5/PLEK2/SLC17A5/ADGRF1/RPS6KCI/PA8P C1/AKAP8L/GJA3/DNAIC2/FGF27/NPTN/GJB2/CLU1/AMPD2/SDCBP2/PDE7B/DK3/CYTH4/GLS2/VP54A/AMPD3/GPR162/DHD/IMP10/ZNF638/GNAS/ZNF311/CRACR2B/TMPR SS12/PIGW/IZUMOI1/ZNF844/THEM5/GPR26/GPER1/EOGT/DOK7/DCBLD1/FFAR2/TRIM42/GRB10/MRPS18B/FLVCR1/GRK4/ZBTB44/DNAIC15/SCG3/GSTP1/GTF2B/BRF1/TW0D4 /GUCY1A3/CCDC106/NMIE7/GPR132/PAD11/GZMA/ANXA2/HAS1/SEIRIND1/SOX8/KCNIP2/NRGG1/ANXA6/HK1/HLA-B/HLA-DOA/HLA-DPA1/ANXA13/HLA-E/HLA-FH1X/HMG41/ACACB/HPC/CPBAZ/HOXB3/HOXC4/HOXD3/HOXE3/HOXC6/HOXD3/AGFG2/HRH1/HSD11B1/SD17B2/ACAD1/HSFPA11/HSF90AA1/HSF90AB1/HTR3A/HTR5A/DUP D1/ADAMTSL5/ANKRD45/TFAP2E/ID3/ZC3H12/D/28A1/RSP02/MS4A10/FMNI1/CD300E/BARHL1/NMIE5/JG1/IGF2/CYR61/GPR142/LCE1C/LCE1D/LCE2D/LRL1/LILRN/LIL6/LI0 CN8/KCN9/KCNMB1/KDR/ACAT1/KIF25/KR71/KR135/AMIGO3/INSC/TOMM20/CELC17A/HES3/SLC6A17/RESIP18/CDHR4/AFF3/LAIR2/LANMA3/STMNI1/ORZAS/LCK/LCP1/JM UC21/LD1R/ARHGDI1/GALS9/LHGR/LGL1/C11orf87/LMNA/LMO2/RAB19/LOX/PPP1R1B/STAM3/MC2R/MCC1/ME2/MEF2D/MAP3K1/MEOX1/MEOX2/MFI2/MFNG/MGAT1/SCGB2A1/MITF/LHX8/ASGR1/MOCS1/MOV10/MPZ1/IGF4/MTT1/MYH4/MYL2/NUBP1/NDUF84/DRG1/NEED9/NEU1/ATP1A2/NFATC3/NFYB/NHLH2/NMBR/NOV/ NPPC/NRAS/NTF3/OAS2/WRAP73/OPRL1/ORZC1/ORZC2/SLC22A18/P2R6/PAFAH2/ATP5B/IL21R/DEF6/ANO7/PALM/ARHGFS3/PARK2/SPOCK3/BOLA1/UTP11/LEF1/DDX47/CEN D1/CHST15/ANGPT4/PDE4C/PCYOX1/JPDE7A/C11orf73/SIRT6/PDF66/HIGD1B/ATP8A2/GALNT7/PGAM2/PB1/PIC/PIK3C/G/PTX2/PKHDI1/PKM/PLA2G2A/PLAGL1/SPA17/LRP1B/PL EC/PRKAG3/PML/RIP13/FXYD6/GPR84/IL20R8/SLC10C1/PNLIP/RIPK4/TLR9/TREM1/CYTL1/POMC/SSH1/PON1/INIG2/MOV10/POU2AF1/ZDHHC13/APPB1P/ROBO4/MXR8A/F BLIM1/BNC2/MED18/PALMD/CYP2W1/RPP25/LPCAT2/BANP/PPP1CB/FAM118A/HERC6/PPP1CC/PIWI1/ELP3/ARMT9/10L/PRMT6/DNAJC17/GOLPH3/LZF533/PPP2R2B/FANC/ MOBI.A/SLC47A1/SLC29A3/MIS18BP1/WDR33/TRPV6/SMPD3/SLC30A10/CNOT11/CHRNA9/SYBLU/PEX26/LIMS2/FRMD4A/VAI14/CARX/PAIVA/PRKAR1B/TTC17/IFT122/CFAP44 /ERMARD/MCTP2/LMBRD1/CSGALNACT1/PAG1/CISD1/PRKDI1/WSB2/MYNN1/BN3/APOBR/MAPK3/MAP2K2/PCDHGC4/PCDHGB7/PCDHGB3/PCDHGALL/PRKRIR/PROX/MRAP/TRP V5/PRMT8/MASP1/HTRAI/SLAMF8/CD42SE1/PSMB4/PAG6/ARNTL2/RGMA/CEACAM19/PRDM11/TRPCL7/PAR5/PSM107/SURP1/ACTR3B/PTGFR/PLEKHG5/TENN2/GAT2B/ER 1/KCNIP2/NRGG1/HLA-B/HLA-DOA/HLA-DPA1/ANXA13/HLA-E/HLA-</p>
GO:0005886	plasma membrane	336/942	4464/17046	2.51E-11	5.73E-09	5.07E-09	<p>AKT3/ABI1/CDH3/CD300L/CDH9/TSFANS/CDH12/CDH13/FARP1/KLRG1/KCNMB2/TCIRG1/TRDN/PDPN/GJB6/HCS1/NPFR2/ADC3/TMED10/ADAM29/ERLIN2/PKP3/CHRNA1/CHRNA2/CHRNA5/GPRIN1/PANX3/CLCA1/FAT3/FRMD6/CCR1/SLC51B/C15orf27/SEZ6/CNP1/SPY6B/IL13RA/ORA2A14/CPM/TRPM6/MPP7/LDLRAD3/APCDD1/CSTA/CTGF/KKR3/SH3 D19/CYLD/ADR83/TRPV3/MURP6/DIO3/DLG2/DRD4/DSG3/DTNA/ECE1/EEF2/EFNA2/EGFR/TMEM17/LPH/SLC10A4/ENO2/EPHA1/EPHA3/EPHA4/ESR1/FL1/FAT2/SPATA13/FCGR2 A/FGA/FGF30/RASA3/ACIN1/SPG20/NFASC/EPH4L13/FLNB/FLT2/MILC1/RHOBTB2/ATP11A/NEED4/SYNE1/PSD3/PPP1R13B/GABRR1/TENM4/RGS22/STEAP2/LCE2B/PLEK2/SLC1 7A5/ADGRF1/GJA3/NPTN/GJB2/SDCBP2/CYTH4/VP54A/GPR162/GNAS/IZUMOI1/GPR26/GPER1/GPR26/GPER1/GPR26/DOK7/FFAR2/GRB10/FLVCR1/GRK4/GSTP1/GUCY1A3/GPR132/GZMA/ANXA2/HAS 1/KCNIP2/NRGG1/HLA-B/HLA-DOA/HLA-DPA1/ANXA13/HLA-E/HLA-</p> <p>F/HPCA/APBA2/HRH1/HSF90AA1/HSF90AB1/HTR3A/HTR5A/FMNI1/CD300E/IGF1/IGF2/GPR142/LCE1C/LCE1D/LCE2D/IL1R1/LILRN/IL6/IL10RA/AQP2/IL11/IRA/IL12RB2/PRSS41/IL16 /AQP5/INPP5A/AQP9/ITGA7/ITGB2/ITGB7/ITIH4/VL/JUP/CD82/ATP98/KCNH2/KCNJ8/KCNJ9/KCNMB1/KDR/SLC6A17/CDHR4/ORA2A5/LCK/LCP1/MUC21/LDLR/LHCGR/LGL1/RAB1 9/LPP1/TB/SMAD3/MC2R/MCC/MR2/ASGR1/MP2/NUBP1/NEUJ/ATP1A2/NMBR/NRAS/OPRL1/ORA2C1/ORA2C2/SLC22A18/P2RY6/DEF6/ANO7/PALM/PCYOX1/PDE6B/ATP8 A2/PIK3CG/PKHDI1/PKM1/SPA17/PLECFXYD6/GPR84/IL20R8/SLC10C1/TLR9/TREM1/SSH1/APBB1P/BNC2/CYP2W1/FANCI/SLC47A1/TRPV6/SMPD3/SLC30A10/CHRNA9/LIMS2/PA IVA/PRKAR1B/TTC17/LMNB1/PAG1/PRKDI1/APOBR/MAPK3/MAP2K2/PCDHGC4/PCDHGB7/PCDHGB3/PCDHGALL/PRKRIR/PROX/MRAP/TRP V5/PRMT8/MASP1/HTRAI/SLAMF8/CD42SE1/PSMB4/PAG6/ARNTL2/RGMA/CEACAM19/PRDM11/TRPCL7/PAR5/PSM107/SURP1/ACTR3B/PTGFR/PLEKHG5/TENN2/GAT2B/ER 1/KCNIP2/NRGG1/HLA-B/HLA-DOA/HLA-DPA1/ANXA13/HLA-E/HLA-</p> <p>F/HPCA/APBA2/HRH1/HSF90AA1/HSF90AB1/HTR3A/HTR5A/FMNI1/CD300E/IGF1/IGF2/GPR142/LCE1C/LCE1D/LCE2D/IL1R1/LILRN/IL6/IL10RA/AQP2/IL11/IRA/IL12RB2/PRSS41/IL16 /AQP5/INPP5A/AQP9/ITGA7/ITGB2/ITGB7/ITIH4/VL/JUP/CD82/ATP98/KCNH2/KCNJ8/KCNJ9/KCNMB1/KDR/SLC6A17/CDHR4/ORA2A5/LCK/LCP1/MUC21/LDLR/LHCGR/LGL1/RAB1 9/LPP1/TB/SMAD3/MC2R/MCC/MR2/ASGR1/MP2/NUBP1/NEUJ/ATP1A2/NMBR/NRAS/OPRL1/ORA2C1/ORA2C2/SLC22A18/P2RY6/DEF6/ANO7/PALM/PCYOX1/PDE6B/ATP8 A2/PIK3CG/PKHDI1/PKM1/SPA17/PLECFXYD6/GPR84/IL20R8/SLC10C1/TLR9/TREM1/SSH1/APBB1P/BNC2/CYP2W1/FANCI/SLC47A1/TRPV6/SMPD3/SLC30A10/CHRNA9/LIMS2/PA IVA/PRKAR1B/TTC17/LMNB1/PAG1/PRKDI1/APOBR/MAPK3/MAP2K2/PCDHGC4/PCDHGB7/PCDHGB3/PCDHGALL/PRKRIR/PROX/MRAP/TRP V5/PRMT8/MASP1/HTRAI/SLAMF8/CD42SE1/PSMB4/PAG6/ARNTL2/RGMA/CEACAM19/PRDM11/TRPCL7/PAR5/PSM107/SURP1/ACTR3B/PTGFR/PLEKHG5/TENN2/GAT2B/ER 1/KCNIP2/NRGG1/HLA-B/HLA-DOA/HLA-DPA1/ANXA13/HLA-E/HLA-</p> <p>F/HPCA/APBA2/HRH1/HSF90AA1/HSF90AB1/HTR3A/HTR5A/FMNI1/CD300E/IGF1/IGF2/GPR142/LCE1C/LCE1D/LCE2D/IL1R1/LILRN/IL6/IL10RA/AQP2/IL11/IRA/IL12RB2/PRSS41/IL16 /AQP5/INPP5A/AQP9/ITGA7/ITGB2/ITGB7/ITIH4/VL/JUP/CD82/ATP98/KCNH2/KCNJ8/KCNJ9/KCNMB1/KDR/SLC6A17/CDHR4/ORA2A5/LCK/LCP1/MUC21/LDLR/LHCGR/LGL1/RAB1 9/LPP1/TB/SMAD3/MC2R/MCC/MR2/ASGR1/MP2/NUBP1/NEUJ/ATP1A2/NMBR/NRAS/OPRL1/ORA2C1/ORA2C2/SLC22A18/P2RY6/DEF6/ANO7/PALM/PCYOX1/PDE6B/ATP8 A2/PIK3CG/PKHDI1/PKM1/SPA17/PLECFXYD6/GPR84/IL20R8/SLC10C1/TLR9/TREM1/SSH1/APBB1P/BNC2/CYP2W1/FANCI/SLC47A1/TRPV6/SMPD3/SLC30A10/CHRNA9/LIMS2/PA IVA/PRKAR1B/TTC17/LMNB1/PAG1/PRKDI1/APOBR/MAPK3/MAP2K2/PCDHGC4/PCDHGB7/PCDHGB3/PCDHGALL/PRKRIR/PROX/MRAP/TRP V5/PRMT8/MASP1/HTRAI/SLAMF8/CD42SE1/PSMB4/PAG6/ARNTL2/RGMA/CEACAM19/PRDM11/TRPCL7/PAR5/PSM107/SURP1/ACTR3B/PTGFR/PLEKHG5/TENN2/GAT2B/ER 1/KCNIP2/NRGG1/HLA-B/HLA-DOA/HLA-DPA1/ANXA13/HLA-E/HLA-</p> <p>2/CXCR4/FZD5/CARD14/TMEM204/IGF1R1/BBP1/STAT2/STK10/BST2/VAMP2/TGMD2/TLR5/TNFRSF41/TRAF5/TRPC4/TRPC6/CCR2/TNFRSF4/ZAP70/CACNA1E/ITP4A1/CACNB /ITPRIP/INSD1/ACTN1/FAOD/TNFRSF11A/SPHK1/ENDOU/SKAP2/STBD1/TSFAN18/CCR2/MAP7/PRC1/SYTT/ESAM/SLC16A3/CD8A/TRIP10/LY86/RAB3D/ENTPD3/RAPGEF2/USP6NL/ CD79A</p>

GO:0044464	cell part	856/942	14556/17046	1.50E-07	2.05E-05	1.81E-05	<p>AKT3/ABI1/CDH3/JANK/CD300L/D/GNE/ZNF783/CDH9/TSPAN5/CDH12/CDH13/SUGP2/MBNL2/FARP1/CLR/G1/RCANZ/KCNMB2/CDK1/C/SPEG/BCDK/TCIRG1/MRVL1/TRDN/ABCA9/CLD/COG5/ZBTB18/PITRM1/TACC2/MTH5/PDPN/DWMT2/CELF1/CELF2/TBR1/SEPT9/IGB6/HGST/NPFRZ/ADCY3/PNRC1/TMED10/S/SLC27A2/LECT1/REB1/ADAM29/HNRXPULL1/RPP4/HIBADH/CHGA/CHL3/ERLIN2/PSIP1/PKP3/EGLN2/PXMP4/ATXN2/LBKAL2/ACOT7/EXO3/CHRNA1/CHRNA2/CHRNAS/GRIN1/CIDEA/GBPA/ALPK2/PANX3/RBP7/GALNT15/AP351/CLCA1/C10orf90/FAT3/CLNS/MRPL52/FRMD6/COR1/SLC38A10/SE26/TMFAP81/MOBS3A/CNP/APOA11BP/NEU4/CO19A3/COL11A1/LYPD6B/GALM/SLC11/MAR38/ZFP42/ADM/IL13RA/UBLCP1/HUS1B/ORZ14/CPM/GPS1/NDUFA56/PXDN1/CRABP1/ZNF538/TRPM6/MBZ2/PAR4/MPP7/LDLRAD3/FAM101/709/ZNF781/CALLM6/GTDED4/DOB1/WBP2NI/DDOST/RNF168/ZNF366/HUHA15/PPP1R18/NLRP6/DIO3/DLG2/DMB1/DNAH6/DNAH8/DNMT3A/ABAT/DPH1/DRD4/DSG3/DTMA/ECE1/AGXT/EEF2/EFNA2/EGFR/EGFR3/PATL2/EIF4G1/A2M/ELK4/ANKRD23/TMEM17/LIPH/EML1/JUNCL3D/DNAH12/SLC10A4/SMM14/ENO2/ADC5/EPHA1/EPHA3/EPH4/ESR1/ALAS1/F11/FAH/FAT2/SPATA13/PRSS54/FCGR2A/RNF1B2/PHACTR1/SP8/FGA/FGF10/FHIT/XRN2/RASA3/PPM1E/WASH1/BTBD3/TRAK1/MSTR2/ACIN1/FOXO1/FOXO2/FOXO3/EXP/H5/AKR1B1/SPG20/NFASC/EPB41L3/GGA3/FLNB/DIP2A/LOT2/MILC1/TBC1D1/RHOBTB2/NUB2/SEL1L3/ATP11A/NEEDD4/SYNE1/PSD3/LARP1/PPP1R13B/PUN2/ARHGFE18/RYBP/MORC3/MAPK8IP2/TSSK2/VGLL2/JMTR/FUCAL1/WDR27/SLC37A4/GABBR1/RASGEF1C/RNF144B/ZNF549/CCDC110/STG6A1NAC3/NUTM1/GAK/SAMM50/DFNB31/ALS2CL/PN/KD/SEC3B/TENM4/ACOT11/FAM169A/RAI14/RGS22/STEAP2/GAS2/FBLX2/FBXO2/LCCE2B/SACS/GATTM/GBG1/GAPDHS/PLEK2/SLC17A5/ADGRE1/RFS6K1/PABPC1/AKAP8L/G1A3/DNAIC2/FGF22/NPTN/GIB2/AMPD2/SDCBP2/PDE7B/CYTH4/GLS2/NPS4A/AMPD3/GPR162/DHHD/BNP10/ZNF638/GNAS/ZNF311/CBACR2B/P1GWI/ILJLMO1/ZNF844/THEM5/GPR26/GPER1/EOGT/DOK7/FFAR2/TRIM42/GRB10/MRPS18B/FLVCR1/GRK4/ZBTB44/DNAUC15/SCG3/GSTP1/GT2B/BRF1/TMDD4/GUCY1A3/CCDC106/NME1/GPR132/PADI1/GZM1/A/ANXA2/HAS1/50X8/KCNIP2/NRGI/ANXA6/HK1/HLA-B/HLA-DOA/HLA-DPA1/ANXA13/HLA-E/HLA-F/HLX/HMGA1/NRA41/ACACB/HPC/APPB4/HOXB3/HOXC5/HOXC6/HOXD3/HRH1/HSD11B1/HSD17B2/ACADL/HSPAL1/HSP90A11/HSP90A1/HTR3A/HTR5A/DUPD1/TTA/P2E/D3/ZC3H12D/COL28A1/RSPD2/FMIN1/CD300E/BAHHL2/NMIE9/IGF1/GF2/GPR142/LCE1/LCE1D/LCE1E/LIR1/LIR2/LIR3/LIR4/AQP2/IL11RA/IL11RB2/IL15RA/PRSS41/IL16/FOXK2/AQP5/INPP5A/IRF1/AQP9/ISL1/ITGA7/ITGB2/ITGB7/ITHA4/ITIH4/VLJUP/CD82/USP50/HLS1/ATP9B/KCNH2/KCN9/KCNMB1/KOR/ACAT1/KIF25/IFOS/KRT5/KRT15/IN5C/TOMM20/CLC17A/HES5/SLC6A17/RESP18/CDHR4/AFF3/STMN1/ORB25/LC/PCP1/JMUC21/LDIR/ARHGDA/LGALS9/LHCCR/LG/LJ/LMNA/LMO2/RAB19/LOX/PPP1R13B/SMAD3/MC2R/MCC/MEL/MEF2D/MAP3K1/MEOX1/MEOX2/MEF2/MFN2/MFN3/MGAT1/MITF/LHX8/ASGR1/MOCS1/MOV10/MPZ/MTL1/NUDT1/MYH4/MYL2/NUBP1/NDUFB4/DRG1/NED09/NEU1/ATP1A2/INFAT3/NFYB/NHLH2/NNBR/NOV/NPPC/NRAS/NTR3/OAS2/WRAP73/OPRL1/OR2C1/OR3A2/SLC22A18/P2RY6/PAFAH2/ATP5B/DEF6/ANO7/PALM/ARHGFE3/P/ARL2/BOLA1/UTP11L/LEF1/DDX47/CHST15/PDE4C/PCYOX1/PDE7A/CL1orf73/SIR16/PDE6B/ATP8A2/GALNT7/PGAM2/P/IGC/PK3CG/PTX2/PKH1/PKM/PLA2G2A/PLAGL1/SPA17/PLECC/PRKAG3/PMI/RIPPLY3/FXYD6/GPR84/IL20R9/SC1C1/RIPK4/TLR9/TREM1/PONC/SSH1/POM1/RIN2/MOV10L1/POU2AF1/ZDHHCL3/APBB1P/MXRAB/FBLIM1/BNC2/MED18/PALMD/CYP2W1/RPP25/ALPCAT2/BANP/PPP1CB/HERC6/PPP1CC/PIWI/L2/ELP3/ARHGEF10L/PRMT6/DNAIC17/GOIPH31/ZNF532/PPP2R2B/FANCI/MOBS1A/SLC47A1/SLC29A3/MIS18BP1/WDR33/TRPV6/SMPD3/SLC30A10/CNOT11/CHRNA9/SYBU/PEX26/LIMS2/FMRD4/VAC14/CARXO/PARVA/PRKAR1B/TTTC17/IFT122/CFAP44/ERMAR0/MCTP2/LMIBRDJ/CSGALNACT1/PAG1/CISD1/PRKDI1/W5B2/MYNN/BIN3/APP/BR/MAPK3/MAP2K2/PCDHG4/PCDHG8/PCDHG11/PRKRIR/PROC/MRAP/TRPV5/PRMT8/HTRA1/SLC29A3/MISDC42SE1/PSMB4/PAK6/ARNTL2/RGMA/PRDM11/TRPC7/LPARE/PSMD7/ACTR3B/PTGFR/PLEKHG5/TENM2/GATAD28/ERMN/KLHL8/RDHL4/METTL14/MARK4/CCR2/PTPRCA/P/PTPRE/PXN/CREBZ/FAM60A/ACTA2/RASGR2/RFC2/TRIM27/RGR/RGS12/RII2/EXO4/RP3/RPL8/DEFB134/RPL29/S100A4/S100A5/S100A6/BGLAP/CCL11/ABHD4/MRPS14/NP43/C19orf33/PARV6/NOD2/STRAG/CXCR5/MAP1L3C3B2/ARHGAP9/TRA2B/GZF1/DNAI2/SGK1/CLDN25/SYND1G1/MIKAL1/CEPK/PCDH20/VPS33A/BMP4/SLC4A1/SPATS2/</p>
------------	-----------	---------	-------------	----------	----------	----------	--

GO:0016020	membrane	522/942	8177/17046	1.50E-06	0.00016	0.00016	0.00014	AKT3/ABI1/CDH3/SMIM6/CD300LD/CCDC180/CDH9/TSPAN5/CDH12/CDH13/FARP1/KLRG1/KCNMB2/TCIRG1/MIRV1/TRDN/ABCAN9/COG5/PDPN/CELF1/GBI6/HGST/NPFR2/ADCY3/TMED10/SLC27A2/LECT1/REK1/ADAM29/CHGA/ERL2/PRK3/PXMP4/ATXN2L/8AGALT7/EXO3/CHRNA1/CHRNA2/CHRNA5/GPRIN1/SORCS1/PANX3/GAUNT15/AP351/CLCA1/FAT3/CIN5/MRPL52/FRMDE/CRC1/SLC51B/CL5orf27/SLC38A0/SEZB/CNP/NEU4/YPDF6/SLCT1/IL13RA/ORZ1A1/CPD/CPM/CP51/NDUFAF6/TRPM6/PAR64/MPP7/LDLRAD3/B3GL/CT/NSMD4/MGAT5/APCDD1/CTA/CTGF/ABCC13/XKR3/PPM11/SH3D19/CYB5G1/CYD/MBOA1/ADRB3/ANKRD46/CYP11A1/FTM1/TRP3/DDOST/NLRP6/DIO3/DLGG/DMBT1/DRD4/DSG3/DTNM/EEEL1/EEF2/EEN2/EGFR/EH4G1/TMEM17/UPH/UNC13D/SLC10A4/SMIM14/ENO2/ADCK5/EPHA1/EPHA3/EPHA4/ESR1/F11/FAT2/SPATA13/FCGR2A/RNF182/FGA/FGF10/XRN2/RASA3/ACIN1/TBC1D9B/SPG20/NFASC/EPB413/GGA3/FLNB/FLOT2/JM1LC/RHOB/TB2/NUIP210/SELE1/ATP11A/NEBD4L/SYNE1/PDS3/LARP1/PPP1R13B/PUM2/MTOR/SLC37A4/GABBR1/RNF144B/ST6GALNAC3/TMEM151A/GAK/SAMM50/PNKD/SEC31B/TENM4/FAM169A/RGS22/STEA2/LCE2B/GATTM/GBGT1/PLEK2/SLC17A5/ADGRF1/RP56K1/PABPC1/GIA3/DNAUC2/NPTN/GIB2/SDCBP2/CTH4/VP54A/GPR163/GNAS/TNIPR312/PIGW/JUNMO1/GPR26/GPER1/DOK7/DCBLD1/FFAR2/GRB10/MRPS18B/FLVCR1/GRIK4/DNAI1/C15/SCG3/GSTP1/GUCY1A3/GPR132/GZMA/ANXA2/HAS1/KCNIP2/NRG1/ANXA6/HKI1/HLA-B/HLA-DOA/HLA-DPA1/ANXA13/HLA-E/HLA-F/NR4A1/ACACB/HPCA/APBA2/AGFG2/HRH1/HSD11B1/HSI17B2/ACADL/HSP90AA1/HSP90AB1/HTR3A/HTR5A/MS4A10/FMNI1/CD300E/IGF1/IGF2/GPR142/LCE1C/LCE1D/LCE2D/IL1R1/IL1RN/IL6/IL13RA/IL2RB2/IL15RA/PRSS41/IL16/AQP5/INPP5A/AQP9/ITGA7/ITGB2/ITGB7/ITIH4/INL/JUP/CD82/ATP9B/KCNH2/KCNJ8/KCNJ9/KCNMB1/KDR/A/CAT1/PO5/ANMIGO3/TOMM20L/CLEC17A/SLC6A17/CDHR4/STMN1/ORZ2A5/LCK/LCP1/MUC21/LDLR/LHCGR/LGL1/C11orf87/LMNA/RAB19/LPP/LTB/SMD3/MC2R/MCC/MF12/MFNG/MGAT1/ASGR1/MPZ/NUBP1/NDUFB4/DRG1/NEU1/ATP1A2/NMBR/NRAS/OAS2/OPRL1/OR2C1/ORS3A2/SLC22A18/P2RY6/ATP5B/IL21R/DEF6/ANO7/PALM/DDX47/CEPND1/C/HST15/PCYOX1/PD56B/HIGD1B/ATP8A2/GALNT7/PIGC/PIK3CG/PKHD1/PKM/PLA2G2A/SPAI7/LRP1B/PLECP/ML1/FXYD6/GPR84/IL20RB/SLCO1C1/RIPK4/TLR9/TREM1/SSH1/ZDHH/C13/APBB1IP/ROBO4/MXRA8/BNC2/PALMD/CYP2W1/LPCAT2/FAM118A/GOLPH3L/PPP2R2B/FANCI/SLC47A1/SLC29A3/TRPV6/SMPD3/SLC30A10/CHRNA9/SYBU/PEX26/LIMS2/VAC14/PARVA/PRKAR1B/TTCL1/IFT122/ERNARD/MCTP2/LMBRD1/CSGALNACT1/PAG1/CISD1/PRKD1/APOBR/MAPK3/MAP2K2/PCDHGC4/PCDHGB7/PCDHGB3/PCDHGA11/MRAP/TRPV5/PRMT8/SLAMF8/CDCK2SE1/RGMA/CEACAM19/TRPC7/LIPAR5/PSMD7/PTGFR/PLK4HGS/TENM2/RNF150/RDH14/PTPCAP/PTPRE/PXN/RASGRF2/TRIM27/RGR/RGS12/RIT2/EXO4/RPL8/CTXN3/RPL29/S100A6/MRPS14/PARVG/NOD2/STRAG/CXCR5/MAP1C3B2/DNAI2/SGK1/CLDN25/SYNDIG1/CERK/PCDH20/TMEM237/NPS33A/SLC4A1/ZLG16/SLC6A12/SLC8A1/SLC9A3/SLC20A2/BNIP1B/TMEM108/LYNX1/BOK/BPI/STAT2/STK10/BST2/VAMP2/ACTC1/TGM2/TLR5/TRAPP10/TNFRSF1A/TNFRSF1A/IFILR1/ERFMP1/CALCR2/TNFRSF4/UCP1/WWHAG/ZAP70/CACNA1E/PTP4A1/CACNB2/MOGS/CXCR4/FZD5/RAB7A/REEP5/CARD14/GDDP3/BCL2L14/LST1/CERS4/TMEM204/NLRX1/GFLR1/WRM1/CALD1/PSCA/FAM188A/TME M62/GPR157/ZC3H12A/RAB11/FIP1/C6orf25/CUPTM1/CALR/UNC93B1/CAPS/CAST/GSG1/HIST1H3A/SLC25A18/ANTXR1/SLA2/MFSD7/CMAHP/BFSP2/ATP13A4/YIP4/CASQ1/PARD6G/FAXC/PARD6B/LOXL3/MGARP/RAE1/SLC43A1/IFTM1/ITPRIP/KMO/IR52/ACTN1/FADD/TNFRSF11A/SYNU2/SPHK1/ENDOU/SKAP2/STBD1/SLAMF9/TSPAN18/CH25H/CCR2/MAP7/PRC1/STAR013/SYTT/ESAM/SLC16A3/RSAD2/SMDT1/IL37/CD8A/REEP6/TRIP10/SDR42E1/NY86/RAB3D/ENTPD3/RAB36/NUP93/RAPGEF2/ULK2/USP6NL/CD79A/TELO2/TMCC2/NOSEC1/LPGAT1.
GO:0030054	cell junction	96/942	1073/17046	1.62E-06	0.00016	0.00016	0.00014	ABI1/CDH3/CDH13/FARP1/GBG/PRK3/CHRNA1/CHRNA2/CHRNA5/FRMD6/EGFLAM/MPP7/LDLRAD3/DLGG2/DSG3/DTNM/EGFR/ANKRD23/FAT2/PHACTR1/AKR1B1/NFASC/EPB413/FLNB/FLOT2/PSD5/ARHGFB18/GABBR1/GAK/SLC17A5/PABPC1/GJA3/GB2/GPER1/DOK7/MRPS18B/GRIK4/ANXA6/HMG1/HOX5/HTR3A/FMNI1/GPR142/ITGA7/JUP/KDR/SLC6A17/LCK/LCP1/LPP/NEED9/NEU1/ATP1A2/NOV/ANO7/C11orf73/PLECG/APBB1P/FBLIM1/PPP1CB/CHRNA9/LIMS2/FRMD4A/PARVA/MAPK3/MAP2K2/PLEKHG5/TENM2/PXN/RPL8/PARVG/CLDN25/SLC8A1/SRP68/VAMP2/ACTC1/TGM2/TRPC4/ITGM2/ITPRIP/KMO/IR52/ACTN1/FADD/TNFRSF11A/SYNU2/SPHK1/ENDOU/SKAP2/STBD1/SLAMF9/TSPAN18/CH25H/CCR2/MAP7/PRC1/STAR013/SYTT/ESAM/SLC16A3/RSAD2/SMDT1/IL37/CD8A/REEP6/TRIP10/SDR42E1/NY86/RAB3D/ENTPD3/RAB36/NUP93/RAPGEF2/ULK2/USP6NL/CD79A/TELO2/TMCC2/NOSEC1/LPGAT1.

GO:0005737	cytoplasm	604/942	9735/17046	3.88E-06	0.00033	0.00029		<p>AKT3/ABI1/CDH3/ITANK/GNE/CDH13/MBNL2/FARP1/RCAJ2/CDKN1/C/BCKDK/TCIRG1/MRV11/TRDN/ABCA9/CIID/COG5/PITRM1/ITAC2/MTTHFS/CELF1/CELF2/SEPT9/GIB6/ADCY3/TMED10/SLC27A2/REB1/HIBADH/CHGA/CH13L1/ERLIN2/PSIP1/EGLN2/PXAMP4/ATXN2L1/B4GAL17/KIF112/ACOT7/EXOC3/CDDEA/GB94/RBP7/GAINT15/APS31/CLCA1/CL10orf90/CLN5/MRPL52/FRMD6/CCRI1/SPATA3/SLC38A10/SEZ6/TFNFA/SPB1/CNP/AF0A1/BPNEU1/CO19/1/3/CLLI1/GALM1/SCLT1/MAP3K8/2/P42/ADM/CP51/NDUFAP6/PCXDNI/CRABP1/MIB2/PAP94/MPPT7/FAM101A/B3GLCT/CEP128/MGAT58/GSTA/KLG3/CTGF/MYD1/SKGL1/PDML1/SB91/CYD/MBOX1/ESCT/COXP1A1/FTM1/ADAL/CALML6/CTED4/DOB1/WB PZNU/DDOST/RNF168/PPP1R18/NLRP6/DIO3/DMB1/1/DNAH6/DNAH8/DMNMT3/ABAT/DPH1/DRD4/D5G3/DTNA/ECE1/EEF2/EGFR/EGR3/PATL2/EIF4G1/A2M/ELK4/ANKRD23/EMVL/JUNCL3D/DNAH12/SVM114/ENOZ/ADCS/EPHA3/EPH84/ESR1/ALAS1/FAH/SPATA13/PRESS4/NF182/PHACTR1/FGA/FHIT/RASA3/PPM1E/VASH1/BTBD3/TRAJK/MSR8Z/ACIN1/FOXO1/EXPH5/AKR1B1/SPG20/EPB413/GGA3/FLNB/FLT2/MCL1/TBC1D1/ARHOB2/NUP210/ATP11A/NEDD4/SYNE1/LARP1/PPP1R138/PUM2/ARHGFE18/RYPB/MAFK8/PP2/TSSK2/VGLL2/MTOR/FUCA1/SLC37M4/GABRR1/RNF148B/CDDC110/ST6GALNAC3/NTM1/1/GAK/SAMM50/FNB31/A152/CI/PNKD/SEC13B/TEJNM4/ACOT11/RAI14/RGS22/STEA P2/GAS2/FBXL21/FBXO2/LCE2B/SACS/GATM1/G8T1/GAPDH3/PLEK2/S17A5/RPS6K1/PA8C1/AKAP8L/DNAJ2/CFGF22/PTN1/GBZ2/AMPD2/SDCBP2/PDE7B/GLS2/VPS4A/ANP D3/DHHDH/BMP10/ZNF638/GNAS/CRACR2B/P/GW/IZUMO1/THYM5/GPER1/EOGT/GRB10/MRPS188/FLVCR1/DNAJC15/SCG3/GSTP1/TWOD4/GUCY1A3/CCDC106/PADI1/ANXA2/H AS1/SOX8/KCNP2/NRG1/ANXA6/HKI/HLA-B/HLA-DOA/HLA-DPA1/ANXA13/HLA-E/HLA-F/HMEG1/NR4A1/ACAB6/HPCA/A/PBA2/HDXX6/HRH1/HS1782/ABAD/HSR1/HSP90AA1/HSP90AB1/HTR3A/HTR5A/DUPD1/D3/ZC3H12D/COL28A1/FMN1/BAHRL2/NME9/IGF1/IGF2/GPR142/ICE1/CCE1D/ILRN/ALG/AOP2/IL5RA/IL16/AQP2/IL5RA/IL16/AQP2/IFSL/ITGA7/ITIH4/VL/UP/ATP9B/KCNH2/KCNJ8/KDR/ACAT1/MF25/PO5/KRT7/INSC/TO MM20L/SLC6A17/RESP18/AFF3/STMN1/LCK/CP1/MUC2/1/IDL/ARHGEDIA/IGALS9/HCCR/LIG1/LJMN/ARAB19/1/PP1/SMA83/MC2R/MCC/MEI/ME2/MEF2D/MAP3K1/MEOX1/M EOX2/MFNG/MGAT1/MIF/MOCS1/MOV10/MPZ/MTJA/NUDT1/MYH4/MYL2/NUJBP1/NDUFB4/DWNT9/NEU1/ATP1A2/NFATC3/NM8R/NOV/NPPC/NRAS/NTF3/OAS2/WRA P73/OPRL1/ORB2/SLC22A18/PAFAH2/ATP5B/DEF6/ANO7/PALM/ARHGFE3/PARK2/BOLA1/UTP11/LEF1/CHST15/PDE4C/PCYOX1/PDE7A/C11orf73/SIRT6/PDE6B/ATP8A2/GAINT 7/P6AM2/PIGC/PIK3CG/PTX2/PIKHD1/PKM/PLA2G2A/PLA3/1/SPA17/PLEC/PRKAG3/PPP1R2B/FA/ANC/MOBI1/SLC29A3/SMPD3/CNOT11/CHRNA9/SYBU/PEX26/LIM52/FRMD4A/V AT2/PPP1CB/HERC6/PPP1CC/PWILZ/ELP3/ARHGFE10/PRMT6/DNAJC17/GOLPH3/PMP2R2B/F/ANCI/MOBI1/SLC29A3/SMPD3/CNOT11/CHRNA9/SYBU/PEX26/LIM52/FRMD4A/V AC14/CARKO/PARVA/PRKAR1B/ITC17/IFT112/ERNARDJ/UMBRD1/CSGALNACT1/CUSD1/PRKJ1/BN3/NAK3/MAKP3/MAKP2K2/PROC/MRAB/PRMT8/HTRAI/CDC24SE1/PSMBA/PAKE6/ARNT L2/RGMA/PRDM11/TRPC1/PSMD7/ACTR3B/PTGFR/PLK4HG5/TENM2/ERVMN/HRH14/METT1L4/MAR4/KCCAR2/PTPRE/PKN1/ACTA2/RASGRF2/RFC2/TRIM27/RGS3Z/EXOCA/RPL8/R PL29/S100A4/S100A6/BGLAP/MRPS14/NPASA3/PARV/GNOD2/MAP1LC3B2/ARHGAP9/GZF1/DNAJ2/SBGL1/MICAL1/CERK/VPS33A/BMP4/SPAT5/ZSG16/SLC8A1/ BOV/BI/SRP68/STAT2/STK3/STK10/BST2/VAMP2/TAF4B/TBP/JCEB2/ZEB1/ACT1/TERF1/TGM2/TIMP3/TFRAPC10/TNFAP3/TFNRSF1A/TRAF1/TRAF5/TRPC4/TRPC6/PHLDA2/CCR 2/UCP1/UPP1/VARS/YWHAG/ZAP70/CA7/PTP4A1/MOGS/CXCR4/FZD5/RAB7A/ER13/CARD14/BCL2L14/LS1/CERS4/NLRX1/CSP1/ZC3H14/ERMP1/CAID1/2NF606/ZC3H12A/RAB1 1/FP1/FAAP100/CPEB4/RNF39/C6orf25/COL18A1/ZNF436/CALR/CO12A1/UNC93B1/OTR1/SLRP/CAPS/CAST/CA/P2B/SH3BGL3/SSGI/CCDC3/DYMR22/SLC25A18/SPATA16/AN TXR1/SLA2/CNMAHP/BSP2/ATP13A4/YIP4/ZNF397/NR0B2/CASQ1/PARD6G/PARD6B/TBKI/TRIM63/LOXL3/PTPBP3/MGAR/PAE1/CIorf198/GAS7/SCN1/KMO/RUNX1/TP63/RU NX3/RSZ2/ACTN1/CRAD/FADD/ALDH1A2/SYNI2/SPHK1/CNNA1/ENDOU/SKAP2/STBD1/HSP81/LIMD1/CH25H/ER11/MAP7/PRC1/STARD13/ZFAND2A/MAP3K6/SYTT7/RSAD2/SMDT 1/AURKB/REEP6/TRIP10/ADIP02/ARHGAP29/RAB3D/PREP1/RAB36/MTSL/ARHGFE10/RAPGEF2/ULK2/USP6N1/CD79A/KIAA0513/DZAP2/TELO2/RABGAP1L/LPGAT1</p>
GO:0005615	extracellular space	102/942	1213/17046	1.15E-05	0.00088	0.00078	<p>CDH13/SPON2/CH13L1/CH13Z/CLQTNF7/CDH12/KIF12/ACOT7/CLQTNF7/CLCA1/CLN5/ZG168/SEZ6/CNP/AF0A1/BPNEU1/CO19/1/3/CLLI1/GALM1/SCLT1/MAP3K8/2/P42/ADM/CP51/NDUFAP6/PCXDNI/CRABP1/MIB2/PAP94/MPPT7/FAM101A/B3GLCT/CEP128/MGAT58/GSTA/KLG3/CTGF/MYD1/SKGL1/PDML1/SB91/CYD/MBOX1/ESCT/COXP1A1/FTM1/ADAL/CALML6/CTED4/DOB1/WB PZNU/DDOST/RNF168/PPP1R18/NLRP6/DIO3/DMB1/1/DNAH6/DNAH8/DMNMT3/ABAT/DPH1/DRD4/D5G3/DTNA/ECE1/EEF2/EGFR/EGR3/PATL2/EIF4G1/A2M/ELK4/ANKRD23/EMVL/JUNCL3D/DNAH12/SVM114/ENOZ/ADCS/EPHA3/EPH84/ESR1/ALAS1/FAH/SPATA13/PRESS4/NF182/PHACTR1/FGA/FHIT/RASA3/PPM1E/VASH1/BTBD3/TRAJK/MSR8Z/ACIN1/FOXO1/EXPH5/AKR1B1/SPG20/EPB413/GGA3/FLNB/FLT2/MCL1/TBC1D1/ARHOB2/NUP210/ATP11A/NEDD4/SYNE1/LARP1/PPP1R138/PUM2/ARHGFE18/RYPB/MAFK8/PP2/TSSK2/VGLL2/MTOR/FUCA1/SLC37M4/GABRR1/RNF148B/CDDC110/ST6GALNAC3/NTM1/1/GAK/SAMM50/FNB31/A152/CI/PNKD/SEC13B/TEJNM4/ACOT11/RAI14/RGS22/STEA P2/GAS2/FBXL21/FBXO2/LCE2B/SACS/GATM1/G8T1/GAPDH3/PLEK2/S17A5/RPS6K1/PA8C1/AKAP8L/DNAJ2/CFGF22/PTN1/GBZ2/AMPD2/SDCBP2/PDE7B/GLS2/VPS4A/ANP D3/DHHDH/BMP10/ZNF638/GNAS/CRACR2B/P/GW/IZUMO1/THYM5/GPER1/EOGT/GRB10/MRPS188/FLVCR1/DNAJC15/SCG3/GSTP1/TWOD4/GUCY1A3/CCDC106/PADI1/ANXA2/H AS1/SOX8/KCNP2/NRG1/ANXA6/HKI/HLA-B/HLA-DOA/HLA-DPA1/ANXA13/HLA-E/HLA-F/HMEG1/NR4A1/ACAB6/HPCA/A/PBA2/HDXX6/HRH1/HS1782/ABAD/HSR1/HSP90AA1/HSP90AB1/HTR3A/HTR5A/DUPD1/D3/ZC3H12D/COL28A1/FMN1/BAHRL2/NME9/IGF1/IGF2/GPR142/ICE1/CCE1D/ILRN/ALG/AOP2/IL5RA/IL16/AQP2/IL5RA/IL16/AQP2/IFSL/ITGA7/ITIH4/VL/UP/ATP9B/KCNH2/KCNJ8/KDR/ACAT1/MF25/PO5/KRT7/INSC/TO MM20L/SLC6A17/RESP18/AFF3/STMN1/LCK/CP1/MUC2/1/IDL/ARHGEDIA/IGALS9/HCCR/LIG1/LJMN/ARAB19/1/PP1/SMA83/MC2R/MCC/MEI/ME2/MEF2D/MAP3K1/MEOX1/M EOX2/MFNG/MGAT1/MIF/MOCS1/MOV10/MPZ/MTJA/NUDT1/MYH4/MYL2/NUJBP1/NDUFB4/DWNT9/NEU1/ATP1A2/NFATC3/NM8R/NOV/NPPC/NRAS/NTF3/OAS2/WRA P73/OPRL1/ORB2/SLC22A18/PAFAH2/ATP5B/DEF6/ANO7/PALM/ARHGFE3/PARK2/BOLA1/UTP11/LEF1/CHST15/PDE4C/PCYOX1/PDE7A/C11orf73/SIRT6/PDE6B/ATP8A2/GAINT 7/P6AM2/PIGC/PIK3CG/PTX2/PIKHD1/PKM/PLA2G2A/PLA3/1/SPA17/PLEC/PRKAG3/PPP1R2B/FA/ANC/MOBI1/SLC29A3/SMPD3/CNOT11/CHRNA9/SYBU/PEX26/LIM52/FRMD4A/V AT2/PPP1CB/HERC6/PPP1CC/PWILZ/ELP3/ARHGFE10/PRMT6/DNAJC17/GOLPH3/PMP2R2B/F/ANCI/MOBI1/SLC29A3/SMPD3/CNOT11/CHRNA9/SYBU/PEX26/LIM52/FRMD4A/V AC14/CARKO/PARVA/PRKAR1B/ITC17/IFT112/ERNARDJ/UMBRD1/CSGALNACT1/CUSD1/PRKJ1/BN3/NAK3/MAKP3/MAKP2K2/PROC/MRAB/PRMT8/HTRAI/CDC24SE1/PSMBA/PAKE6/ARNT L2/RGMA/PRDM11/TRPC1/PSMD7/ACTR3B/PTGFR/PLK4HG5/TENM2/ERVMN/HRH14/METT1L4/MAR4/KCCAR2/PTPRE/PKN1/ACTA2/RASGRF2/RFC2/TRIM27/RGS3Z/EXOCA/RPL8/R PL29/S100A4/S100A6/BGLAP/MRPS14/NPASA3/PARV/GNOD2/MAP1LC3B2/ARHGAP9/GZF1/DNAJ2/SBGL1/MICAL1/CERK/VPS33A/BMP4/SPAT5/ZSG16/SLC8A1/ BOV/BI/SRP68/STAT2/STK3/STK10/BST2/VAMP2/TAF4B/TBP/JCEB2/ZEB1/ACT1/TERF1/TGM2/TIMP3/TFRAPC10/TNFAP3/TFNRSF1A/TRAF1/TRAF5/TRPC4/TRPC6/PHLDA2/CCR 2/UCP1/UPP1/VARS/YWHAG/ZAP70/CA7/PTP4A1/MOGS/CXCR4/FZD5/RAB7A/ER13/CARD14/BCL2L14/LS1/CERS4/NLRX1/CSP1/ZC3H14/ERMP1/CAID1/2NF606/ZC3H12A/RAB1 1/FP1/FAAP100/CPEB4/RNF39/C6orf25/COL18A1/ZNF436/CALR/CO12A1/UNC93B1/OTR1/SLRP/CAPS/CAST/CA/P2B/SH3BGL3/SSGI/CCDC3/DYMR22/SLC25A18/SPATA16/AN TXR1/SLA2/CNMAHP/BSP2/ATP13A4/YIP4/ZNF397/NR0B2/CASQ1/PARD6G/PARD6B/TBKI/TRIM63/LOXL3/PTPBP3/MGAR/PAE1/CIorf198/GAS7/SCN1/KMO/RUNX1/TP63/RU NX3/RSZ2/ACTN1/CRAD/FADD/ALDH1A2/SYNI2/SPHK1/CNNA1/ENDOU/SKAP2/STBD1/HSP81/LIMD1/CH25H/ER11/MAP7/PRC1/STARD13/ZFAND2A/MAP3K6/SYTT7/RSAD2/SMDT 1/AURKB/REEP6/TRIP10/ADIP02/ARHGAP29/RAB3D/PREP1/RAB36/MTSL/ARHGFE10/RAPGEF2/ULK2/USP6N1/CD79A/KIAA0513/DZAP2/TELO2/RABGAP1L/LPGAT1</p>	
GO:004421	extracellular region part	238/942	3516/17046	0.00023	0.01579	0.01397	<p>ABH1/CCDC180/CDH113/SPON2/ZBTB18/TMED10/SLC27A2/LECT1/CH13L1/ERLIN2/CH13L2/KIF12/ACOT7/CLQTNF7/CLCA1/CLN5/ZG168/SEZ6/CNP/AF0A1/BPNEU1/CO19/1/3/CLLI1/GALM1/SCLT1/MAP3K8/2/P42/ADM/CP51/NDUFAP6/PCXDNI/CRABP1/MIB2/PAP94/MPPT7/FAM101A/B3GLCT/CEP128/MGAT58/GSTA/KLG3/CTGF/MYD1/SKGL1/PDML1/SB91/CYD/MBOX1/ESCT/COXP1A1/FTM1/ADAL/CALML6/CTED4/DOB1/WB PZNU/DDOST/RNF168/PPP1R18/NLRP6/DIO3/DMB1/1/DNAH6/DNAH8/DMNMT3/ABAT/DPH1/DRD4/D5G3/DTNA/ECE1/EEF2/EGFR/EGR3/PATL2/EIF4G1/A2M/ELK4/ANKRD23/EMVL/JUNCL3D/DNAH12/SVM114/ENOZ/ADCS/EPHA3/EPH84/ESR1/ALAS1/FAH/SPATA13/PRESS4/NF182/PHACTR1/FGA/FHIT/RASA3/PPM1E/VASH1/BTBD3/TRAJK/MSR8Z/ACIN1/FOXO1/EXPH5/AKR1B1/SPG20/EPB413/GGA3/FLNB/FLT2/MCL1/TBC1D1/ARHOB2/NUP210/ATP11A/NEDD4/SYNE1/LARP1/PPP1R138/PUM2/ARHGFE18/RYPB/MAFK8/PP2/TSSK2/VGLL2/MTOR/FUCA1/SLC37M4/GABRR1/RNF148B/CDDC110/ST6GALNAC3/NTM1/1/GAK/SAMM50/FNB31/A152/CI/PNKD/SEC13B/TEJNM4/ACOT11/RAI14/RGS22/STEA P2/GAS2/FBXL21/FBXO2/LCE2B/SACS/GATM1/G8T1/GAPDH3/PLEK2/S17A5/RPS6K1/PA8C1/AKAP8L/DNAJ2/CFGF22/PTN1/GBZ2/AMPD2/SDCBP2/PDE7B/GLS2/VPS4A/ANP D3/DHHDH/BMP10/ZNF638/GNAS/CRACR2B/P/GW/IZUMO1/THYM5/GPER1/EOGT/GRB10/MRPS188/FLVCR1/DNAJC15/SCG3/GSTP1/TWOD4/GUCY1A3/CCDC106/PADI1/ANXA2/H AS1/SOX8/KCNP2/NRG1/ANXA6/HKI/HLA-B/HLA-DOA/HLA-DPA1/ANXA13/HLA-E/HLA-F/HMEG1/NR4A1/ACAB6/HPCA/A/PBA2/HDXX6/HRH1/HS1782/ABAD/HSR1/HSP90AA1/HSP90AB1/HTR3A/HTR5A/DUPD1/D3/ZC3H12D/COL28A1/FMN1/BAHRL2/NME9/IGF1/IGF2/GPR142/ICE1/CCE1D/ILRN/ALG/AOP2/IL5RA/IL16/AQP2/IL5RA/IL16/AQP2/IFSL/ITGA7/ITIH4/VL/UP/ATP9B/KCNH2/KCNJ8/KDR/ACAT1/MF25/PO5/KRT7/INSC/TO MM20L/SLC6A17/RESP18/AFF3/STMN1/LCK/CP1/MUC2/1/IDL/ARHGEDIA/IGALS9/HCCR/LIG1/LJMN/ARAB19/1/PP1/SMA83/MC2R/MCC/MEI/ME2/MEF2D/MAP3K1/MEOX1/M EOX2/MFNG/MGAT1/MIF/MOCS1/MOV10/MPZ/MTJA/NUDT1/MYH4/MYL2/NUJBP1/NDUFB4/DWNT9/NEU1/ATP1A2/NFATC3/NM8R/NOV/NPPC/NRAS/NTF3/OAS2/WRA P73/OPRL1/ORB2/SLC22A18/PAFAH2/ATP5B/DEF6/ANO7/PALM/ARHGFE3/PARK2/BOLA1/UTP11/LEF1/CHST15/PDE4C/PCYOX1/PDE7A/C11orf73/SIRT6/PDE6B/ATP8A2/GAINT 7/P6AM2/PIGC/PIK3CG/PTX2/PIKHD1/PKM/PLA2G2A/PLA3/1/SPA17/PLEC/PRKAG3/PPP1R2B/FA/ANC/MOBI1/SLC29A3/SMPD3/CNOT11/CHRNA9/SYBU/PEX26/LIM52/FRMD4A/V AT2/PPP1CB/HERC6/PPP1CC/PWILZ/ELP3/ARHGFE10/PRMT6/DNAJC17/GOLPH3/PMP2R2B/F/ANCI/MOBI1/SLC29A3/SMPD3/CNOT11/CHRNA9/SYBU/PEX26/LIM52/FRMD4A/V AC14/CARKO/PARVA/PRKAR1B/ITC17/IFT112/ERNARDJ/UMBRD1/CSGALNACT1/CUSD1/PRKJ1/BN3/NAK3/MAKP3/MAKP2K2/PROC/MRAB/PRMT8/HTRAI/CDC24SE1/PSMBA/PAKE6/ARNT L2/RGMA/PRDM11/TRPC1/PSMD7/ACTR3B/PTGFR/PLK4HG5/TENM2/ERVMN/HRH14/METT1L4/MAR4/KCCAR2/PTPRE/PKN1/ACTA2/RASGRF2/RFC2/TRIM27/RGS3Z/EXOCA/RPL8/R PL29/S100A4/S100A6/BGLAP/MRPS14/NPASA3/PARV/GNOD2/MAP1LC3B2/ARHGAP9/GZF1/DNAJ2/SBGL1/MICAL1/CERK/VPS33A/BMP4/SPAT5/ZSG16/SLC8A1/ BOV/BI/SRP68/STAT2/STK3/STK10/BST2/VAMP2/TAF4B/TBP/JCEB2/ZEB1/ACT1/TERF1/TGM2/TIMP3/TFRAPC10/TNFAP3/TFNRSF1A/TRAF1/TRAF5/TRPC4/TRPC6/PHLDA2/CCR 2/UCP1/UPP1/VARS/YWHAG/ZAP70/CA7/PTP4A1/MOGS/CXCR4/FZD5/RAB7A/ER13/CARD14/BCL2L14/LS1/CERS4/NLRX1/CSP1/ZC3H14/ERMP1/CAID1/2NF606/ZC3H12A/RAB1 1/FP1/FAAP100/CPEB4/RNF39/C6orf25/COL18A1/ZNF436/CALR/CO12A1/UNC93B1/OTR1/SLRP/CAPS/CAST/CA/P2B/SH3BGL3/SSGI/CCDC3/DYMR22/SLC25A18/SPATA16/AN TXR1/SLA2/CNMAHP/BSP2/ATP13A4/YIP4/ZNF397/NR0B2/CASQ1/PARD6G/PARD6B/TBKI/TRIM63/LOXL3/PTPBP3/MGAR/PAE1/CIorf198/GAS7/SCN1/KMO/RUNX1/TP63/RU NX3/RSZ2/ACTN1/CRAD/FADD/ALDH1A2/SYNI2/SPHK1/CNNA1/ENDOU/SKAP2/STBD1/HSP81/LIMD1/CH25H/ER11/MAP7/PRC1/STARD13/ZFAND2A/MAP3K6/SYTT7/RSAD2/SMDT 1/AURKB/REEP6/TRIP10/ADIP02/ARHGAP29/RAB3D/PREP1/RAB36/MTSL/ARHGFE10/RAPGEF2/ULK2/USP6N1/CD79A/KIAA0513/DZAP2/TELO2/RABGAP1L/LPGAT1</p>	
GO:0042588	xymogen granule	5/942	12/17046	0.00029	0.01812	0.01603	<p>TMED10/DWBT1/ZG16/VAMP2/RAB3D</p>	

All DMC Molecular Function	Description	GeneRatio	BgRatio	pvalue	p.adjust	qvalue	geneID	Count
GO:0003674	molecular_function	893/893	15274/17046	1.62E-44	1.63E-41	1.44E-41	<p>AKT3/ABI1/CDH3/TANK/CD300LD/GNE/ZNF783/CDH9/TSPAN5/CDH12/CDH13/SUGP2/MBNL2/FARP1/KLRG1/RCAN2/KCNMB2/CDK11C/SFPG6/BCKDK/TGRCG1/MRV17/TRDN/ABCA9/SPON2/CD/COG5/ZBTB38/PTIRM1/TACC2/MHFS/DMRT2/CELF1/CELF2/TBR1/REPL1/SEPT9/HCTST/PPFR2/ADCY3/PNRC1/TMED10/SLC27AZ/RER1/ESM1/ADAM29/HNRNPUL1/RPP14/HIBADH/CH13L/ERLIN2/PSIP1/CHH3L2/PKP3/EGLN2/TP53TG1/PKXMP4/ATXNL2/UBAGALT7/KIF12/ACOT7/PDAP1/EXO3/CHRNA1/CHRNA2/ADPRHL1/CHRNA5/CARD16/GP/RLN1/SORCS1/ZBED9/PWMP2A/CIDEA/GB94/ALPK2/PANX3/RBP7/GALNT15/AP531/CICL1/FAT3/CLN5/MPRI5/FRMD6/CCR1/SLC51B/C15orf27/ZG16B/SLC38A10/KRT40/TNFAIP1/AMOB3A/CNP/ADAACL3/LRRIQ3/APOA1BP/NEU4/COL9A3/COL11A1/GALM/COMP/SLIT1/MAIP3K8/ZF42/ADAM/IL13RA/EGFAM/UBLCP1/ORZAL4/CPD/CPM/CP51/INDUF6/PHYDL/CRABP1/ZNF358/TRPM6/CRYBB3/MB2/PARP4/MPPT7/LDIRAD3/FAM101A/B3GLCT/MGAT5B/APCDD1/CSTA/KL3/ZNF738/CTGF/ABCC13/SMYD1/SGOL1/PPM11/LRRC34/SH3D19/CY8561/CYLD/MBON1/ADRB3/ESCG2/CYP11A1/ZNF782/FITM1/ADA4/TRPV3/ZNF709/ZNF781/CALML6/CITED4/DBI1/WBP2NL/LONRF2/DDOST/RNF168/RBM46/ZNF366/BHLHA15/COCH/PPP1R18/NLRP6/DIO3/DLG2/DMBT1/DNAH6/DNAH8/DNM1T3A/ABAT/DPH1/DRD4/DSG3/DTNA/ECE1/AGXT/EEF2/EFNA2/EGFR/EGR3/PATL2/EIF4G1/A2M/ELK4/ANKRD23/LPH/EM11/JUNCL30/ZBTB7C/DNAH12/SLC10A4/ENO2/ADCK5/EPHA1/EPHA3/EPH4/ESR1/ALAS1/F11/FAH/FAT2/SPATA13/PRESS4/FCGR2A/RNF182/PHACTR1/SP8/FGA/FGF10/FHIT/XRN2/RASAS3/RNF44/PPM1E/VASH1/TRAK4/M5RB2/ACIN1/LIMCH1/FOXO1/EXPH5/AKR1B1/SPG20/NFAS/EPBA113/GG43/FLNB/DIP2A/FLOT2/MLC1/TBC1D1/RHOBTB2/NUP210/ATP11A/KLHL18/NEDD41/SYNE1/PSD3/LARP1/PPP1R13B/PUM2/ARHGFB/RYPB/MORC3/MAKBP2/TSK2/VGLL2/MTOR/FUCA1/WDR27/TTL10/SLC37A4/GABBR1/PAASGEF1C/RNF448/ZNF549/CCDC110/ST6GALNAC3/NUTM1/DSCB9/GAK/SAMM50/DFNB31/ALS2CL/PNKD/TENM4/ACOT11/LTN1/RGS22/STEAP2/FBXL2/FBXO2/LCE2B/SACS/GATM/GBG11/GAPDHS/SLC17AS/ADGRF1/RP56BK1/PABP1/AKAP8L/GA3/DNAIC2/FGF22/NPTN/GIB2/AMPD2/SDCBP2/PDE7B/CYTH4/GLS2/VPS4A/AMPD3/GPR162/DHDB/BMP10/ZNF638/GNAS/C11orf31/ZNF311/CRACR2B/TMPRSS12/PIGW1/ZUO1/ZNF844/THEM5/GPER1/EOGT/DOK7/DCBLD1/FFAR2/TRIM42/GRB10/MRPS18B/FLVCR1/GRIK1/ZBTB44/DNAIC15/SCG3/GSTP1/GTF2B/BRE1/TM0D4/GUCY1A3/CCDC106/NMIE7/GPR132/PAD11/GZMN/ANXA2/HAS1/SERPIND1/SOX8/KCNP2/NRG1/ANXA6/HKI1/HLA-B/HLA-DOA/HLA-DPA1/ANXA13/HLA-E/HLA-F/HIX/HMGA1/NR4A1/ACACB/HPCA/APBA2/HOXB3/HOXC4/HOXC5/HOXC6/HOXD3/AGFG2/HRH1/HSD11B1/HSD11B2/ACADL/HSPA1L/HSP90AA1/HSP90AB1/HTR3A/HTRA5/DUPD1/ADAMTSL5/ANKRD45/TTPA2E/ID3/C3H12D/COL28A1/RSP02/FMN1/BARHL2/NNIE9/GF1/IGF2/CYR61/GPR142/CELC/CELD1/CE2D/LCE2D/LIL1/LILRN/L6/IL10RA/AQP2/IL11RA/IL12RB2/IL15RA/PRSS41/IL16/FOXK2/AQP5/INHBA/INPP5A/IRF-3/AQP9/ISL1/TGAT7/TGEB2/TGEB7/ITH3/ITH4/IVL/JUP/CD82/USP50/HLS1/ATP9B/KCNH2/KCNH3/KCNJ8/KCNJ9/KCNMB1/KDR/ACAT1/KIF25/IPO5/KRT7/KRT15/C17orf82/GLEC17A/HES5/SLC6A17/CDHR4/RBM12B/AFF3/LAIR2/LAM3/STMN1/ORZAS1/LCK/CP1/LDLR/ARHGDA/LGALS9/LHCGR/LGL1/C11orf87/UMNA/LMO2/RAB19/LOX/ZNF833P/LPP/LTB1/TBP1/SMAD3/MC2R/MCC/ME1/ME2/MEF2D/MAP3K1/MEOX1/MEOX2/WF2/MFNG/MGAT1/SCGB2A1/MITF/LHX8/ASGR1/MOCS1/MOV10/MPZ/PLEKHG7/MT1A/NUDT1/MYH4/MY12/NUB1/NDFU84/DRG1/NEO9/NEUJ/ATP1A2/NFATC3/NFYB/NHLH2/NMBR/NOV/NPPC/NFRAS/MTF3/OAS2/RNF165/OPRL1/ORC1/ORB3A2/SLC22A18/P2RY6/PAFAH2/ATP5B/IL21R/DEF6/ANOT7/PALM/ARHGFE3/PARK2/SPOCK3/BOLA1/UTP11L/LEF1/DDX47/PRR16/CHST15/ANGPT4/PDE4C/PCYOX1/PDE7A/C11orf73/SIRT6/PDE6B/ATP8A2/GALNT7/PGAM2/P3/PICG/PIK3C/GPITX2/PKH81/PKM/P1A2G2/P1A2GL/SPAL1/LRP1B/PLEC/PRKAG3/PML/FXYD6/GPR84/IL20RB/SLC01C1/PNLIP/RIPK4/TLR9/TREM1/CYLL1/POVIC/SSH1/PONI/RINZ/MOV10/L1/POUZAF1/ZDHHC13/APBB1P/ROBO4/MXR56/BNC2/MED18/CYP2W1/RPP25/LPCAT2/TTC12/BANP/PPP1CB/FAM118A/HERC6/PPP1CC/PWIL2/ELP3/ARHGEF10L/PRMT6/DNAAC17/GOIPH3L/ZNF532/PPP2R2B/FANCI/MOBI4/SLC47A1/SLC29A3/MIS18BP1/WDR33/1/TRPV6/SMPD3/SLC30A10/CNOT11/CHRNA9/TTHUMPDI1/SYRBY/PEX26/FRMD4A/VACL4/CARDK/PARVA/PRKAR1B/TTC17/FTL22/MCTP2/LMBRD1/CSGALNACT1/PAG1/C1SD1/PRKDI1/MYNN/BIN3/APOBR1/MAK3/MAK2/PCDHGC4/PCDHGB7/PCDHGB8/PCDHGA11/PRKRR/PROCMR/AR/TPV5/PRMT7/HTRA1/SLAMF8/CD42SE1/PSMB4/PAK6/ARNTL2/RGMA/PRDM11/TRPC7/PAB5/PSMD7/SUURP1/ACTR3B/PTGFR/PLEKHG5/TENN2/GATA2B/ERMN/RNF150/RDHL4/METTL14/MARK4/CCAR2/PTPRE/PXN/CREBZF/AB</p>	893

GO:0005488	binding	774/893	12915/17046	7.46E-17	3.75E-14	3.33E-14	<p>AKT3/ABI1/CDH3/ITANK/CD300L/D/GNE/ZNF783/CDH9/ITSPAN5/CDH12/CDH13/SUGP2/MBNL2/FARP1/KLRG1/RCANZ/CDKNI1C/SPREG/BCKDK/TCIRG1/MRVL1/TRDN/ABCA9/SPON2/774</p> <p>C1D/COG5/ZBTB18/PITRMI1/TACC2/MTHFS/DWIRT2/CELF1/CELE2/TBR14/RPR12/SEPT9/HCS17/PDPR2/ADCY3/PNRC1/TMED10/S1C27A2/REB1/ESM1/ADAM29/HNRNPULL/RPP14/HIBADH/CHIHL1/ERLIN2/PSIP1/CH1L2/PKP3/EGLN2/PXMP4/ATXN2/ATXN2/ATXN2/ADPRL1/CHRNA1/SORCS1/ZBED9/PWWP2A/CIDEA/GBP4/ALPK2/RBP7/GALNT15/AP3S1/CLCA1/FAT3/CLN5/FIRM/D6/CCR1/SLC18B/ZG168/KRT40/TNF4/P811/MB03A/CNP/LRRIQ3/POX1/IBP/NEU4/COL11A1/GALM/COMPI/SCLT1/MAP3K8/ZFP42/ADM/IL13/IRA/EGFLAM/UBLCP1/CPD/CPM/CP51/PXDNJ/CRABP1/ZNF358/TRN06/CRY8B3/MB2/PAR04/MPP7/LDIRAD3/FAM101A/MGAT5B/APCDD1/CS1A/KLC3/ZNF738/CTGF/ABCC13/SMYD1/SGOL1/PPM11/SH3D19/CV5B51/CELD1/ADRB3/ZNF1181/ADAL/ZNF709/ZNF783/CA1MLM6/DBB1/WBP2N1/LONRF2/DDOSTA/RN168/RBM46/ZNF366/BHLHA15/COCH/PPP1R18/NLRP6/DLGG2/DMBT1/DNAH6/DNAH8/DNM1T3A/ABAT/DPH1/DRD4/DG3/DTNA/ECE1/AGXT/EEF2/EJNA2/EGFR/EGR3/PAT12/EIF4G1/A2M/YELK4/ANKRD23/LIPH/EM11/JUNC13D/ZBTB7C/DNAH12/ENO2/ADCK5/EPHA1/EPHA3/EPH4/ESR1/ALAS1/F11/FAH/FAT2/SPATA13/FCGR2A/RNF182/PHACTR1/SP8/FGA/FGF10/FHIT/XRN2/RASA3/RNF44/PPM1E/VASH1/TRAK1/MSRB2/ACINI1/FOXO1/FOXO2/FOXO3/FOXO4/EXPH5/SPG20/NFASC/EPH4L3/EGX3/FLNB/DIP2A/FLT2/MILCI/TBCLD1/RHOBT2/NUP210/ATP11A/KLHL18/NEED4L/SYNE1/LARP1/PPP1R13B/FOXO1/FTL1/STEA2/FBXO2/SAK5/GBG11/GAPDH5/RPS6K1/PABPC1/AKAP8L/GIA3/DNAJC2/FGF22/NF549/CCDC110/NUTM1/NAK/SAMM50/DFNB31/ALS2/C/PLNKO/TENN4/ACO111/TIN1/STEA2/FBXO2/SAK5/GBG11/GAPDH5/RPS6K1/PABPC1/AKAP8L/GIA3/DNAJC2/FGF22/NPTN/AMPD2/SDCBP2/PDE7B/CYTH4/GLS2/VPS4A/AMPD3/BMP10/ZNF638/GNAS1/C11orf31/ZNF311/CRACR2B/ZUMO1/ZNF844/THFEM5/GPER1/DOCK7/DCBLD1/FFAR4/TFAM42/ZRB10/FLVCR1/ZBTB44/DNAJC15/SCG3/GSTP1/GTF2B/BRF1/TM0D4/GUCY1A3/CCDC106/NME7/PADI4/GZMA/ANXA2/SERPIND1/SOXB8/KCNIP2/NRG1/ANXA6/HK1/HLA-B/HLA-DOA/HLA-DPA1/ANXA13/HLA-E/HLA-F/HLX/HMGAI1/NRA41/ACACB/HPCA/APBAZ/HOXB3/HOXC4/HOXC5/HOXC6/HOXC8/HRH1/ACAD1/HSPA1L/HSP90AA1/HSP90A81/HTR3A/ADAMTSL5/ANKRD45/TFAP2E1/D3/ZC3H12D/RSP02/FMNI1/BARHL2/IGF1/IGF2/CYR61/LCE2D/IL1R1/IL1RN/IL6/IL10RA/IL12/2/BB2/IL10R4/IL12/BB2/IL12/BB2/IL15R/IL16/FOXK2/ACQP5/INHBA/INP5A/IRE1/USL1/ITGA7/ITGB2/ITGB7/ITIH4/IVL/JUP/CD82/HILS1/ATP9B/KCNH2/KCNJ8/KCNJ9/KDR/ACAT1/KIF25/JP05/KRT7/KRT15/C17orf82/CLEC17A/HESS/CDH8/RBM12B/AFB3/LAIR2/LAMA3/STMN1/LCK/LCP1/LDLR/ARHG9A/IGALS9/LHCGR/LGL1/C11orf87/LMNA/LMOM2/RAB19/LOX/ZNF833P/LPP/LTB/LTBP1/SMAD3/MC2R/MCC/ME1/ME2/MEF2D/MAP3K1/AMEOX1/MEOX2/MF2/MFNG/MGA11/SCGB2A1/MITF/LHX8/ASGR1/MOCS1/MOV10/MTIA/NUDT1/MYH4/MYL2/NUB1/DRG1/NEED9/ATP1A2/NEAFC3/NFYB/NHLH2/NOV/NPPC/NRAS/NTF3/OAS2/RNF165/OPRL1/SLC22A18/PZRY6/PAFAH2/ATP5B/DEF6/PALM/ARHGFE3/PARK2/SPOCK3/BOLAJ1/UTP1L1/LEF1/DDX47/PRR16/C-HST15/ANGK4/PDE4/C11orf73/SIRT6/PDE68/ATP8A2/GALNT7/PGAM2/PIK3C3/PITX2/PKH01/PKM1/PLA2G2A/PLA2G3/PLA17/IRP1B/PLEC/PRKAG3/PMAL/FXYD6/RLR2/TLR4/TLR5/ANGK4/TLR9/TREM1/CYLL1/POMC/SSH1/PON1/MOV10L1/POU2AF1/ZDHHC13/ARBB1P/FBLN11/BORCS6/BNC2/MED18/CY2P2W1/RP25/LPCA12/TTC12/BANP/PPP1CB/FAM118A/PPP1CC/PIWIL2/ELP3/PRMT6/DNAJC17/GOLPH3/ZNF532/PPP2R2B/FANCI/MOBI1/MIS18BP1/WDR33/TRPV6/SMPD3/CNOT11/CHRNA9/THUMPDI1/SYBU/PEX26/LIMS2/FRMD4A/VAC14/CAKOD/PARVA/PRKAR1B/TTC17/IIFT122/ACTP2/LMBRD1/CSGALNACT1/PAG1/CISD1/PRK01/MYNN/BN3/MAPK3/MAP2K2/PCDHGC4/PCDHGB7/PCDHG83/PCDHGA11/PRKRIP/PROC/MRBP/TRPV5/PRMT8/MASP1/HTRA1/PSM84/PAG6/ARNTL2/RGMA/TRPC7/PSMD7/SLURP1/ACTR3B/TENM2/GATAD2B/ERMIN/RNF150/METTL14/MARK4/CCAR2/PTPRE/PXN/CREBZF/FAM60A/ACTA2/RASGRF2/RFC2/TRIM27/RGR/RIT2/EXOCD4/PA3/RPL18/RPL29/S100A4/S100A5/S100A6/BGLAP/JCT/CCL11/CCL17/MRPS3/PARYG/NO22/TINAGL1/SFRP2/CXCR5/ARHGAP9/TRA2B/GZF1/DNAI2/SSG11/MICAL1/CERK/PCDH20/VPS33A/BMP4/SLC4A1/SPATS2/ZNF649/ZG16/SLC6A12/SLC8A1/SLC9A3/BMPRI1B/SUT1/BRD9/ZSCAN18/BOG/SOX9/BBP/SRP68/STAT2/STK3/STK10/SUPT6H/BST2/VAMP2/TA4B/TBP1/CEA1/TCBE2/ZEB1/ACTC1/TEAD3/TERF1/TGM2/TCHHT/TIMP3/ULE3/TLR5/TFAP2C10/TNFAP3/TFNRF5/TFNRF5A/TNXB1/TRAFF1/TRAFF5/TRPC4/TRPC6/TWIST1/CCR2/VARS/ZNFHIT2/WNT10B/YWHAG/ZAP70/ZNF124/ZNF127/C7orf72/ZNF124/ZNF124/ZNF124/ZNF127/CCDNB2/PAX8/CXCR4/IFZD5/RAB7A/ERI3/REEP5/CCDC86/CARD14/GDPPD3/BCCL11/4/</p>
------------	---------	---------	-------------	----------	----------	----------	---

GO:0005515	protein binding	594/893	9755/17046	3.42E-09	1.15E-06	1.02E-06 AKT3/ABI1/TANK/CD300L/DGNE/ZNF783/TSPAN5/CDH13/FARP1/KIRG1/CDKN1C/SPEG/BCKDK/TCIRG1/MRV11/TRDN/SAPON2/CI-D/COG5/ZBTB18/TACC2/DMRT2/CELF1/SEPT9/H- CST/NPFR2/ADCY3/PNRC1/TMED10/SLIC27A2/REB1/ESM1/HNRP1L1/ERLIN2/PSP1/PR3/EGGNE/PXNP4/ATXN2L/BAGAL7/KIF12/ACOT7/EXO3/CHRNA5/GPRIN1/SORCS1/P- WWW2A/CIDEA/RBP7/AP3S1/CLNS3/FRMD6/CCR1/SLCS3/IRF4/IBP1/IRIQ3/APOA1BP/NEUA/CO11A1/CONOMP/SLC11/MAIP3/KS/ADM/IL13RA/UBLPC1/CP51/CRABP1/TRP M6/CRYBB3/MIB2/PARP4/MPP7/FAM101A/MGAT5B/APCDD1/CSTA/KLC3/CTGF/SMYD1/SH3D19/CYB5L1/CYD/ADRB3/DBB1/WBP2NL/DOST/RNF168/ZNF366/BHLHA1 5/COCH/PPP1R1B/DLG2/DMBT1/DNM3A/ABA7/DPH1/DRD4/DTNA/ECE1/AGX7/EEF2/EFNA2/EGFR/PATL2/EIF4G1/A2M/ELK4/ANKRD33/EML1/UNC13D/ADCK5/EPHA1/EPHA3/E- PHB4/ESR1/ALAS1/E11/FAH/SPATA13/FCGR2A/RNF182/PHACTR1/FGAF/FGF10/PHIT/PMV1E/HTH1/TRAK1/MSRB2/ACIN1/UMCH3/FOXK2/TBC1D9B/FOXO1/EXPH5/SPG20/NFASC /EPB413/GGA3/FLNB/DIP2A/FLTOT2/MCL1/TBC1D11/NUP210/ATP11A/KLHL18/NEDD4/SLYX1/LARP1/PPR1R13/PUM2/RYN2/VTG2/VGLL2/MTOR/WDR27/TTTT10/G ABBR1/RNF1448/CCDC110/NTM1/GAK/SAMM50/DFNB2/ALG3/CLPK/PNKO/TEMM4/LTN1/FOXO2/SACS/GAPDH5/HPSC6K1/PAAP/C1/GIA3/DNAJC2/GF22/NPTN/AMPPD/S DCBP2/GLS2/VPS4A/BMP110/GNAS/CRACR2B/ZUMO1/ZNF844/THEM5/GPER1/DOK7/FFAR2/TRIM42/GRB10/VLCV/FLVCR1/ZBTB44/DNAIC15/GSTP1/GTF2B/BRF1/TMOD4/GUCY1A3/ CDC106/ANME7/GZMA/ANXA2/SOX8/KCNIP2/NRG1/ANXA6/HK1/HLA-B/HLA-DOA/HLA-E/HLA- F/HLX/HMGA1/NR4A1/ACAC8/HPCA/APBA2/HOXC4/HOXB3/HPA11/HS90A0A1/HS90A8/ADAMTSL5/ANKRD5/TFAP2E/ID3/RSP02/FMN1/BAHRH2/GF1/GF2/CYR61/LCE2D/L 1H1/L1RNL/L6/L10RA/L12R82/L15RA/L16/FOXK2/AQP5/INHBA/INPP5A/IRF1/SL1/ITGAT7/ITGB7/ITIH4/IVL/ITJUB/CDB2/HIL51/KCNH2/KCNJ8/KCNJ9/KDR/ACAT1/KIF25/PO 5/KRT7/KRT15/C17orf82/HESS/PRBM12B/LAIR2/LAMA3/STMN1/LCK/LCP1/LDLR/ARHGDA/LGALS9/LGL1/C11orf87/LMNA/LMO2/LOX/LOPP/LTB1/TBP1/SMAD3/MC2R/MCC/MEF2 D/MAIP3K1/MEOX1/MEOX2/MF02/SCGB2A1/MITF/LHX8/ASGR1/MOV10/MT1A/NUDT1/MYH4/MY12/NUBP1/JRGG/NEO29/ATP1A2/NFATC3/NFYB/NHLH2/NOV/NPPC/NRAS/NTF 3/OAS2/OPRL1/SLC22A18/P2RY6/ATP5B/DEF6/PALM/ARHGFE3/PARK2/BOLA1/UTP11L/LEF1/DDX47/PRR17/ANNGT4/PDE4C/C11orf73/SIRT6/PK3/CG/PTX2/PKHDI/PKM/SPA17/ PLEC/PRKAG3/PML/FXYD6/IL20RB/RIPK4/TLB9/TREM1/CYTL1/POMC/SSH1/PONI/POU2AF1/APBB1P/FBLIM1/BORCS6/MED18/RPP25/TTCL2/BNAP/PPP1CB/FAM118A/PPP1CC/E LP3/PRMT6/GOLPH3/PPP2R2B/FANCI/MOBI4/MIS18BP1/TRPV6/CNOT11/SYBU/PEX26/FRMD4/VAC14/CARKO1/PARVA/PRKAR1B/TTCC11/IFIT122/LMBRD1/PAG1/PRKD1/ BIN3/MAIP3/MAP2K2/PRKRR/PROCMRAP/TRPV5/PRMT8/MA5P1/HTRA1/PSMB4/PAK6/ARNTL2/RGMA/TPC7/PSMD7/SLURP1/ACTR3B/TEMN2/GATAD2B/ERMN/MARK4/CCA R2/PTRP/RYX/CREBZF/FAM60A/ACTA2/RASGEF2/REC2/TRIM27/RGR/RIT2/EXO4/PPA3/SL00A4/SL00A5/SL00A6/SCT/CLL1/CCL17/NPAs3/PARV6/NOD2/TINAGL1/SFRP2/CX R5/ARHGAP9/TRA2B/DNAI2/DNAI2/SGKI/MICAL1/CERK/VPS33A/BMP4/SLC4A1/ZNF649/ZG16/SLC6A12/SLC8A1/SLC9A3/BMPRI1B/SLIT1/BRD9/BOK/FOXO9/STAT2/STK3/STK10/SUPT6H/B ST2/NAIP2/TF48/TBP/TCEA1/TCEB2/ZEB1/ACTC1/TEAD3/TEFR1/TGMD2/TCHH/TIMP3/TLF3/TLS/TRAPPC10/TNFAP3/TPNFRS/FLA/TNXL/TRA51/TRAF5/TRPC4/TRPC6/TWIST1/CC R2/NAV5/WNT10B/YWHAG/ZAP70/ZNF124/ZNF177/CACNB2/PAX8/CXCR4/FZD5/RAB7A/REEF5/CCDC86/CARD14/BCL2L14/NLX3/IGF1R1/ZMYM1/CSPP1/ZC3H14/CALD1/FAM18 8A/ZC3H12A/RAB11FP1/FAAP100/CPEBA/COL18A1/ZNF436/CALR/SJLRP/COLO/CYST/CAST/CAI/IR/SH3/SH3BP1/HIST1H3A/SLC25A18/ANTXR1/SLAZ/BFSP2/NPFI4/ZNF 397/NR0B2/HOPX/PARD6G/PARD6B/ILF10/SPINK7/RETNLB/TRIM63/KDM2B/LOXL3/GTPBP3/MGARF/CBX2/RAE1/HTM1/GAS7/SCIN/CDK10/RUNX1/TP63/RUNX3/IRS2/ACTN1/ CRADD/FADD/TNFRSF11A/SYNJ2/SPKH1/BUD31/CNNA1/ENDOU/SKAP2/STBD1/LIMD3/THAP3/CCR12/MAP7/PRC1/STAND13/PIAS2/STY71/LDB2/SLC16A3/CBFAZ2/RSAD2/AURKB/ DAP1/RCSD1/L132/CD8A/REEP6/TPRP10/ADIPOQ/ARHGAP29/RAB3D/H2AF1/ENTPD3/ARHGFE10/MICAL2/N4BP1/VGLL4/RAPGEF7/ULK2/USP6NL/CD79A/DAZAP2/TELO2/RABGA P1L/TMCC2/FGF19/NR1H4	594
GO:0043169	cation binding	264/893	3856/17046	4.55E-07	0.00011	0.0001 CDH3/TANK/GNE/CDH9/CDH12/CDH13/MBNL2/SPON2/ZBTB18/PITRM1/MTHF5/DMRT2/RFP12/ADCY3/ADAM29/EGLN2/BGAL7/CHRNA1/CHRNA2/ADPHL/CHRNA5/GALNT1 5/CLCA1/FA13/MOBSA/APOA1BP/COLL1A1/COMP/MAP3K8/ZEP42/CPD/CPM7/PS1/PXDNI/ZNF358/TRPV6/MIB2/MGAT5B/SMYD1/PPM11/CYB5L1/CYLD/ESCO2/CYP11A1/ZNF7 82/ADAL/ZNF709/ZNF781/CALM16/LONRF2/RNF168/ZNF366/DNMT3A/ABA7/DRD4/DGSG/DTNA/ECE1/EGR3/EML1/ZBTB7C/ENO2/ESR1/FAH/FAH2/RNF182/SP8/XRN2/RAS43/R NF44/PPM1E/MSRB2/LIMCH1/TBC1D9B/ATP11A/RVBP/MOIR3/TSK2/RNF148B/ZNF549/PNKD/LTN1/STEAP2/GBGT1/AKAP4B/AMPPD2/PDE7B/AMPPD3/ZNF638/NGAS/ZNF311/CR ACR2B/ZNF844/TRIM42/ZBTB44/GTF2B/BRF1/NME7/PAD11/ANXA2/KCNIP2/ANR4A1/ACACB/HPCA/AGFG/HRH1/HTR3A/ADAMTSL5/ZC3H12D/FOKK2/ISL1/ITGAT7 /ITGB2/ITGB7/ATP9B/ACAT1/CLEC17A/CDHR4/LCP1/LDLR/LMO2/LOX/ZNF833P/PPP1/ITBP1/SMAD3/MEI4/ME2/MAP3K1/MF12/MFNG/MGAT1/HH8/ASGR1/MOCS1/MT1A/NUDT 1/MY12/NUBP1/ATP1A2/OAS2/RNF165/PARK2/SPOCK3/PDE4C/PDE1A/SIRT6/PDE6B/ATP8A2/GALNT1/PKM/P1A2G2A/PJAL1/LRP1B/PML/PNLI/PLIP/PLIN1/MOVI10/LZDHH13/FBL IM1/BNC2/CYP2W1/LPCAT2/PPP1CB/PPP1CC/ELP3/3NF592/MOBI4/SMPD3/CHRNA9/UMS2/MCTP2/CSGALNACT1/GISD1/PRKD1/MIYNN/PCDHGC4/PCDHGB7/PCDHGB3/PCDHGA 11/PRKR/PROC/MASP1/GATAD2B/RNF150/PXN/TRIM27/S100A4/S100A5/S100A6/BGLAP/GZF1/MICAL1/CERK/NCDH20/ZNF649/SLC8A1/BMPRI1B/SUT1/ZSCAN18/STK3/TCEA1/ ZEB1/TGMD2/TCHH/TIMP3/TNFAP3/TRA1/TRA5/ZNHIT2/ZNF7/CA7/ZNF124/ZNF177/CACNAIE/ERB/GDPD3/ZNF665/ZMYM1/ZC3H14/ERMPI1/ZNF606/ZC3H12A/RNF39/COL18 A1/ZNF436/CALR/OVRT11/CAPS/SCRT1/ANTXR1/ATP13A4/ZNF397/CASQ1/TRIM63/KDM2B/LOXL3/SCIN/RUNX1/TP63/ACTN1/TNFRS11A/SPHK1/ENDOU/LIMD1/CH25H/THAP3/E R11/PIAS3/ZFAND2A/MAP3K6/STY71/CBPA2T2/RSAD2/AURKB/NEURL3/ARHGAP29/MTLS/MICAL2/RAPGEF2/ZBTB39/NR1H4	264

GO:0043167	ion binding	362/893	5637/17046	9.40E-07	0.00019	0.00017	<p>AKT3/CDH3/TANK/GNE/CDH9/CDH12/CDH13/MBNL2/SPG6/BCKD/ABCA9/SPON2/ZBTB18/PITRM1/MT/HFS/DVRT2/RFLP2/SEPT9/ADCY9/SLC27A2/ADAM29/EGLN2/BGAL17/KI362</p> <p>F12/ACOT7/CHRNA1/CHRNA2/ADPRHL3/CHRNA5/GBPA4/ALPK4/GALNT15/CLCA1/FAT3/MOBSA/ROA1/ALPK4/COMP/MAP3K8/ZFP42/CPD/CPM/CP5/1/PXDNL/CRABP1/ZNF338/TRPM6/MB2/MGAT5B/CTGF/ABCC13/SMYD1/PPM11/CYB5G1/CYLD/ESCO2/CCP11A1/ZNF783/CALML16/LONRF2/RNF168/ZNF366/LNR6/DNAH6/DNAH8/DNMT3A/ABAT/DRD4/DSG3/DTNACE1/AGXT/EEF2/EGFR/EGR3/UPH1/EMIL1/ZBTB7/DNAH12/ENO2/EHAI1/EPH4/ESR1/ALAS1/FAH/FAT2/RNF182/SP8/FGF10/XRN2/RASA3/RNF44/PPM1E/MSR2/LIMCH1/TBC1D98/RHOBTB2/ATP11A/RYP/MORC3/TSSK2/MTOR/TTL10/RNF144B/ZNF549/GAK/PNKO/LTN1/STEAP2/GBG1/RP56K1/AKAP1/AMPD2/PDE7B/VPS4A/AMPD3/ZNF638/GNAS/ZNF311/CRACR2B/ZNF844/TRIM42/ZBTB44/GT22/BRE1/GUCY1A3/NME4/ANXA2/SERPND1/KCNIP2/ANXA6/HKI1A/NXAL3/NRA41/ACACB/HPCA/AGFG2/HRH4/ACADL/HSP1A1/HSP90A1/HSP90AB1/HTB3A/ADAMTSL5/ZC3H12D/RSP02/CYR61/FOXK2/SIL1/JTGAT7/JTG82/JTG87/ATP9B/KCNJ8/KO/R/ACAT1/KIF25/CLC37A/CDHR4/LCK/LCP1/LDLR/LMO2/RAB19/LOW/ZNF833P/LPP/LTPB1/SMAD3/MEI1/ME2/MAP3K1/MF2/MFNG/MGAT1/HX8/ASGR1/MOCS1/MOV10/MT1A/NUDT1/MYH4/MYL2/NUBP1/DRG1/ATP1A2/NOV/NRAS/OAS2/RNF165/PFAFHA1/ZNF649/ARHGAP9/GZF1/5GK1/MICAL1/CEK1/PCDH20/BMP4/ZNF649/SLTRB3/GATAD2B/RNF150/MARK4/PKN/ACTA2/RFC2/TRIM27/IRIT2/RPL29/S100A4/S100A6/BGLAP/NO22/ARHGAP9/GZF1/5GK1/MICAL1/CEK1/PCDH20/BMP4/ZNF649/SLC8A1/BMPR1B/SUT1/ZSCAN1B/STK3/STK10/VAMP2/TCEA1/ZEB1/ACTC1/TGM2/TC4H/TIMP3/TNFAIP3/TNXB/TNRA1/TRA55/TRPC4/TNXC6/VARS/ZNHIT2/ZAP70/ZNF7/CA7/ZNF124/ZNF177/CACNA1E/RAB7A/ER13/GDPD3/NLRX1/ZNF665/ZMYM1/ZC3H14/ERMP1/ZNF606/ZC3H12A/RNF39/C6orf25/CO118A1/ZNF436/CALR/QTRT1/CAPS/SKRT1/ANTXR1/ATP13A4/ZNF397/CASQ1/TBK1/TRIM63/KDM2B/LOXL3/GTPBP3/SCIN/CDK10/KMO/RUNX1/TP63/RUNX3/ACTN1/TNFRSF11A/STK19/SPHK4/ENDOU/LIMD1/CH25H/THAP3/ER1/PIAS2/ZFAND2A/MAP3K6/SYTT7/CBFA2T2/RSAD2/AURK8/NEURL3/ADIPPOO/ARHGAP29/RAB3D/ENTPD3/RAB36/MTLS/MICAL2/RAPGEF2/ULK2/ZBTB39/NR1H4</p>
GO:0046872	metal ion binding	257/893	3777/17046	1.19E-06	0.0002	0.00018	<p>CDH3/TANK/GNE/CDH9/CDH12/CDH13/MBNL2/SPON2/ZBTB18/PITRM1/MT/HFS/DVRT2/RFLP2/ADCY9/ADAM29/EGLN2/BGAL17/ADPRHL1/GALNT15/CLCA1/FAT3/MOBSA/APO257</p> <p>A1BP/CO11A1/COMP/MAP3K8/ZFP42/CPD/CPM/CP5/1/PXDNL/CRABP1/ZNF338/TRPM6/MB2/MGAT5B/CTGF/ABCC13/SMYD1/PPM11/CYB5G1/CYLD/ESCO2/CCP11A1/ZNF783/CALML16/LONRF2/RNF168/ZNF366/LNR6/DNAH6/DNAH8/DNMT3A/ABAT/DRD4/DSG3/DTNACE1/AGXT/EEF2/EGFR/EGR3/UPH1/EMIL1/ZBTB7/DNAH12/ENO2/EHAI1/EPH4/ESR1/ALAS1/FAH/FAT2/RNF182/SP8/FGF10/XRN2/RASA3/RNF44/PPM1E/MSR2/LIMCH1/TBC1D98/RHOBTB2/ATP11A/RYP/MORC3/TSSK2/MTOR/TTL10/RNF144B/ZNF549/GAK/PNKO/LTN1/STEAP2/GBG1/RP56K1/AKAP1/AMPD2/PDE7B/VPS4A/AMPD3/ZNF638/GNAS/ZNF311/CRACR2B/ZNF844/TRIM42/ZBTB44/GT22/BRE1/GUCY1A3/NME4/ANXA2/SERPND1/KCNIP2/ANXA6/HKI1A/NXAL3/NRA41/ACACB/HPCA/AGFG2/HRH4/ACADL/HSP1A1/HSP90A1/HSP90AB1/HTB3A/ADAMTSL5/ZC3H12D/RSP02/CYR61/FOXK2/SIL1/JTGAT7/JTG82/JTG87/ATP9B/KCNJ8/KO/R/ACAT1/KIF25/CLC37A/CDHR4/LCK/LCP1/LDLR/LMO2/RAB19/LOW/ZNF833P/LPP/LTPB1/SMAD3/MEI1/ME2/MAP3K1/MF2/MFNG/MGAT1/HX8/ASGR1/MOCS1/MOV10/MT1A/NUDT1/MYH4/MYL2/NUBP1/DRG1/ATP1A2/NOV/NRAS/OAS2/RNF165/PFAFHA1/ZNF649/ARHGAP9/GZF1/5GK1/MICAL1/CEK1/PCDH20/BMP4/ZNF649/SLTRB3/GATAD2B/RNF150/MARK4/PKN/ACTA2/RFC2/TRIM27/IRIT2/RPL29/S100A4/S100A6/BGLAP/NO22/ARHGAP9/GZF1/5GK1/MICAL1/CEK1/PCDH20/BMP4/ZNF649/SLC8A1/BMPR1B/SUT1/ZSCAN1B/STK3/STK10/VAMP2/TCEA1/ZEB1/ACTC1/TGM2/TC4H/TIMP3/TNFAIP3/TNXB/TNRA1/TRA55/TRPC4/TNXC6/VARS/ZNHIT2/ZAP70/ZNF7/CA7/ZNF124/ZNF177/CACNA1E/RAB7A/ER13/GDPD3/NLRX1/ZNF665/ZMYM1/ZC3H14/ERMP1/ZNF606/ZC3H12A/RNF39/C6orf25/CO118A1/ZNF436/CALR/QTRT1/CAPS/SKRT1/ANTXR1/ATP13A4/ZNF397/CASQ1/TBK1/TRIM63/KDM2B/LOXL3/GTPBP3/SCIN/CDK10/KMO/RUNX1/TP63/RUNX3/ACTN1/TNFRSF11A/STK19/SPHK4/ENDOU/LIMD1/CH25H/THAP3/ER1/PIAS2/ZFAND2A/MAP3K6/SYTT7/CBFA2T2/RSAD2/AURK8/NEURL3/ADIPPOO/ARHGAP29/RAB3D/ENTPD3/RAB36/MTLS/MICAL2/RAPGEF2/ULK2/ZBTB39/NR1H4</p>
GO:0005102	receptor binding	100/893	1310/17046	7.80E-05	0.01121	0.00994	<p>TRDN/C1D/TACC2/HCT119/NPFR2/SLC27A2/REF2/FESM1/ADM/CTGF/ADRB3/ZNF366/DLG2/AGXT/EFNA2/A2M/FGA/FGF10/TRAK1/FLOT2/FGF22/NPTN/BMP10/GNAS/IZUMO1/DO100</p> <p>K7/GRB10/GTF2B/NRG1/HLA-B/HLA-E/HLA-F/HMGA1/HSP90A1/RSP02/IGF1/IGF2/CYR61/LIR1/LIRN/LI6/L16/INHBA/ISL1/KCNJ8/KOR/LAMA3/LCK/LT/SMAD3/NOV/NPC/NTF3/ATP5B/PALM/PARK2/LEF1/ANGPT4/PIK3CG/LR9/CYLL/POW1C/LMBRD1/MRAP/RGM5/SLURP1/TEMM2/PXN/S100A4/SCT/CLL1/CLL17/SFRP2/BMP4/SUIT1/TLRS/TNXB/TRA1/CCR2/WNT10B/YWHAG/ZAP70/CALR/SH3BGL3/NR0B2/LI1F10/RET/NLB/IRS2/ACTN1/FADD/ENDOU/CCR2/MAP7/PIAS2/IL32/CD8A/ADIPPOO/RAPGEF2/FGF19/NR1H4</p>
GO:0060089	molecular transducer activity	119/893	1631/17046	0.00011	0.01382	0.01225	<p>KLRG1/NPFR2/CHRNA1/CHRNA2/CHRNA5/SORCS1/CCR1/MAP3K8/IL13RA/ORA2A14/MB2/AORB3/NLRP6/DMBT1/DRD4/EGFR/EPHA1/EPHA3/EPHA4/ESR1/GABBR1/ADGRF1/NP1TN/GPR162/GNAS/GPR26/GPER1/FFAR2/GRIK4/GUCY1A3/GPR132/HLA-DOA/HLA-DPA1/NR4A1/HRH1/HTR3A/HTR5A/GPR142/LIR1/LI10RA/LI11RA/LI12RB2/LI15RA/ITGB2/ITGB7/ITGPA/KCNH2/KOR/STMN1/ORA25/LDLR/LGAL5/LHCGR/LTBR1/SMAD3/MC2R/MCC/MAP3K1/ASGR1/ASGR2/OPRL1/OR2C1/OOR2A2/P2RY6/LI2IR/LEF1/PKH1/LRP1B/GPR84/LI20RB/TLR9/TREM1/ZDHHC13/ROBO4/CHRNA9/VAC14/APOBR/MAPK3/SLAMF8/RGMA/LPAR5/PTGFR/PLEKHG5/PTPRE/TIM27/RGR/RGS12/TMAGL1/CXCR5/SLC20A2/BMPR1B/STAT2/STK3/STK10/BST2/TNFRSF1A/TRA55/CCR2/TNFRS4/PAX8/CXCR4/FZD5/GPR157/ANTXR1/NR0B2/TRIM63/LOXL3/HFTM1/IRS2/TNFRSF11A/SPHK4/ENDOU/SLAMF9/CCR2/MAP3K6/CD8A/RAPGEF2/CD79A/NR1H4</p>
GO:0004896	cytokine receptor activity	13/893	80/17046	0.00025	0.02766	0.02452	<p>CCR1/IL13RA/LI1R1/LI10RA/LI12RB2/IL15RA/ITGB2/ITGB7/ITGPA/KCNH2/KOR/STMN1/ORA25/LDLR/LGAL5/LHCGR/LTBR1/SMAD3/MC2R/MCC/MAP3K1/ASGR1/ASGR2/OPRL1/OR2C1/OOR2A2/P2RY6/LI2IR/LEF1/PKH1/LRP1B/GPR84/LI20RB/TLR9/TREM1/ZDHHC13/ROBO4/CHRNA9/VAC14/APOBR/MAPK3/SLAMF8/RGMA/LPAR5/PTGFR/PLEKHG5/PTPRE/TIM27/RGR/RGS12/TMAGL1/CXCR5/SLC20A2/BMPR1B/STAT2/STK3/STK10/BST2/TNFRSF1A/TRA55/CCR2/TNFRS4/PAX8/CXCR4/FZD5/GPR157/ANTXR1/NR0B2/TRIM63/LOXL3/HFTM1/IRS2/TNFRSF11A/SPHK4/ENDOU/SLAMF9/CCR2/MAP3K6/CD8A/RAPGEF2/CD79A/NR1H4</p>
GO:0008092	cytoskeletal protein binding	62/893	761/17046	0.00036	0.03482	0.03086	<p>ABLI/FARP1/KIF12/MB2/FAM101A/KLC3/PPP1R1B/EGFR/ANKRD23/VEML1/PHACTR1/MSR2/LIMCH1/EPB41L3/FLNB/SYNE1/MAP8BIP2/BMP10/TM0D4/ANXA2/HPCA/FMN1/KIF25/STMN1/LCP1/MYH4/MYL2/PARK2/PLEC/SSH1/FBLN1/SYBU/PARVA/BN3/ACTR3B/ERMIN/MARK4/PKN/S100A4/S100A6/PARVG/NO22/MICAL1/SLC4A1/SLC8A1/VAMP2/ACTC1/TERR1/CXCR4/CAD1/CAZB/ANTXR1/TRIM63/RAE1/GAS7/SCIN/ACTN1/PRC1/IRCS1/RAB3D/ARHGEE10/MICAL2</p>
GO:0003779	actin binding	35/893	363/17046	0.00038	0.03482	0.03086	<p>MB2/PPP1R1B/EGFR/PHACTR1/MSR2/LIMCH1/EPB41L3/FLNB/SYNE1/TM0D4/HPCA/FMN1/LCP1/MYH4/MYL2/PARK2/PLEC/SSH1/PARVA/ACTR3B/ERMIN/S100A4/PARVG/NO22/MICAL1/SLC4A1/CXCR4/CAID1/CAZB/ANTXR1/GAS7/SCIN/ACTN1/IRCS1/MICAL2</p>

Hypomethylated DMC, Biological Process	Description	GeneRatio	BgRatio	pvalue	p.adjust	qvalue	geneid	Count
GO:0008150	biological_process	590/590	15230/17046	3.93E-30	2.05E-26	1.78E-26	AKT3/ABI1/TANK/CD300LD/GNE/ZNF783/CDH9/CDH12/SUGP2/FARP1/KLRIG1/RCAN2/CDKN1C/SPCG/MRV1/ITRDN5/PON2/COG5/PITRM1/TACC2/MTHFS/PDPN/CELF1/GBI6/PNR C17/TMED10/LECT1/REJ1/ESM1/ADAM29/HNRNPULL/RPP14/CHGA/CH31/ERL1/CH32/TPS37G1/ATXN2/KIF12/ACOT7/PDAP1/EXOCS/CHRNA1/CHRNA2/CARD 16/GPRIN1/SORCS1/CIOTNF7/GBR4/PANX3/RBP7/GALNT15/AP351/FAT3/CLN5/MRPL53/CCR1/SLCS1B/SEZ26/TNFAIP83/NEU4/CO19A3/COMP/MAP3K8/ADM1/L3 1RA/EGF/LAM/UBLCP1/HUS1B/ORZ14/CPM/CP51/NDUF4F6/PXDNL/GRABP1/ZNF358/RYRBB3/MI02/PARF4/MPPP7/LDLRAD3/FAM101A/B3GLCT/MAG38/CSTA/KLC3/ZNF738/AB CC13/SMYD1/SGOL1/PPM1L/SH3D19/CYLD/MBOAT1/ESCO2/CYP11A1/ZNF782/DDB1/LONRF2/DDOST/ZNF366/BH1H415/DIO3/D1G2/DMBT1/DNAH6/ABAT/DPH1/DNA/AGXT/E EF2/EPNA2/EIF4G1/A2M/ELK4/ANKRD23/LIPH/SLC10A4/ENO2/ADCK5/EPHA1/ESR1/IFI1/FAH/FAF2/SPATA13/PRSS54/FCGR2A/PHACTR1/FGA/FGF10/PHIT/BTBD3/SBNO2/TRAK1/ M5RB2/FOXLI1/FOXK2/EXPH5/ARR1B1/NFASC/EPB41L3/GGA3/DIP2A/FLOT2/MLC1/TBC1D1/RHOB/TBZ2/NUJ2/10/NEED4L/SYNE1/PSD3/PPP1R13B/PUM2/ARHGFE18/RNBP/MORC3 /MAPK8IP2/TSSK2/VGLL2/SLC37A4/RASGEF1C/RNF144B/ZNF549/ST6GALNAC3/SANM50/DFNB31/ALS2CL/PNKD/SEC31B/ACOTT1/STEAP2/GAS2/FBXL21/LCE2B/SACS/GATM/GB GTL/PLEK2/SLC17A5/ADGRE1/RPS6K1/PABPC1/AKAP8L/DNAJC2/FGF22/NPTN/CLUL1/PDE7B/CYTH4/AMIPD3/DH/DH1/BMP10/ZNF638/ZNF311/TMPRSS12/ZNF844/THEM5/GPR26 /EOGT/FFAR2/GRB10/MRPS18B/GRIK4/DNAJC15/SCG3/TMOD4/GUCY1A3/GPR132/PADI1/HAS1/SOX8/HK1/HLA-DOA/HLA- DPA1/ANXA13/NRA4A1/ACACB/HOXC4/AGFG2/HRH1/HSD11B1/HSPA1L/HSP90A11/HTR3A/DUPD1/ADAMTS15/ANKRD45/TFAP2E/D3/ZC3H12D/RSPD2/CD300E/NME9/IGF1/IGF2 /GPR142/LCE1C/LCE1D/LCE1E/LIR1/LIRN/LI10RA/AOP2/LI11RA/LI12RB2/LI15RA/PRSS41/LI16/FOXK2/AQP5/INHBA/INP5A/IRF1/AQP9/ITGA7/ITGB2/ITGB7/ITIH4/ITIL/ITUP/CD8 2/USP50/KCNH2/KCNJ8/KCNJ9/KCNMB1/KDR/KIF25/PO5/AMIGO3/HES5/AFF3/LAMA3/STMN1/ORZ15/LCP1/MUC21/LDLR/ARHGDA/LGAL59/LCGR/LMNA/LMO2/RAB19/SRRD/ LPP/MC2B/MCC/ME2/MFNG/MGAT1/SCGB2A1/MIIT/LHX8/ASGR1/MOCS1/MOV10/NP2/PLEKHG7/NYH4/MYL2/NUBP1/NDUFB4/DRG1/NEU1/ATP1A2/NFATC3/NHLH2/NPCC/N RAS/OAS2/OPRL1/ORZ32/SLC22A18/P2RY6/PFAH2/ATP5B/LI21R/ANOT7/PARK2/SPOCK3/UTP11L/PRR16/CHST15/PCYOX1/C11orf73/SIRT6/PDE6B/ATP8A2/PB/PITX2/PK HD1/PKM/PLA2G2A/PLAGL1/LRP1B/PRKAG3/PVL/RIPPLY3/FXYD6/GPR84/SLCO1C1/NLUP/TLR9/TREM1/SSH1/RIN2/POUZAF1/APBB1IP/ANKRA8/FBLN1/MED18/PALMD/CYP2W1 /RPP25/BANP/PPP1CB/HERC6/ELP3/DNAJC17/SOLPH3L/PPP2R2B/FANCI/MOBI1A/SLC47A1/SLC29A3/MS18BP1/TRPV6/SLC30A10/CHRNA9/PEX26/FRMD4A/CARXO/PARVA/PKRA R1B/TTC17/IFT122/ERMA2/MCTP2/LMBRD1/CSGALNACT1/PAG1/CISD1/W5B2/MYNN/APOBR/MAK3/PRKRIR/PROC/MRAP/TRPV5/PRMT8/HTRA1/SLAMF8 /CD42SE1/PAK6/ARNTL2/RGMA/PRDM11/PSMD7/SLURP1/PTGFR/PLEKHG5/TEANM2/GATAD2B/ERMIN/KLHL8/RDHL4/MARK4/PTPRE/CREBZF/ABHD17C/FAM60A/ACTA2/RFC2/T RIM27/RGR/RGS12/RIT2/RP3B/GLAP/SCT/CCL11/ABHD4/MRPS14/PRSS22/NP35/PARG/NOD2/TNAGL1/STRA6/MAP1LC3B2/ARHGAP9/GZFF/JDNJA2/PCDH20/TMEM237/VP53 3A/BMP4/SLC44A1/ZNF649/ZG16/SLC6A12/SLC8A1/SLC9A3/SLC20A2/BMPRI1B/SUIT1/BRD9/ZSCAN18/TMEM108/BOX/BI/SRPG8/STAT2/STK3/SUPT6H/BST2/TCEB2/ZEB1/TEAD3/T ERF1/TGM2/TCHH/TNFAIP3/TNFRSF1A/TRA5/TRPC6/TRPM2/CCR2/TNFRSF4/UCP1/WNT108/ZAP70/ZNF7/CA7/CACNA1E/MOGS/RAB7A/ER3/CCDC86/CARD14/BCL2L14/LST1/C ERS4/ZNF665/CSPP1/ERMP1/CALD1/FAM188A/TMEM62/GPR157/ZC3H12A/FAAP100/CPBEA4/Coot25/ZNF436/EEPD1/CLPTML1/CALR/COL21A1/QTRT1/SIRP/CAST/CAPZB/DYNL RB2/SLC25A18/SPATA16/ANTXR1/MFSD7/CMAMP/BSP2/ATP13A4/ZNF397/NROB2/MONI1/CASQ1/HOPX/PARD6G/KRBA1/TTBK1/RETNLB/TRIM63/GTPBP3/RAE1/SLC43A1/IFT M1/SCIN/CDK10/KMO/RUNX1/TP63/RUNX3/SERPINA6/IRS2/ACTN1/CRAOD/TNFRSF1A/ALDH1A2/STK19/SYNU2/SPHK1/BUDB3/CCNA4/ENDOD/SKAP2/STBD1/HSPB3/TSPAN18/C H25H/CCR12/ERL1/PRCI/STARD13/PIAS2/MAP3K6/SYTY/ESAM/SLC16A3/CBFAZ12/AURKB/DAPL1/CD8A/CCDC102A/NEURL3/TRIP10/ADIPOQ/ENTPD3/PREP1/RAB36/MIC AL2/N48P1/VGLL4/NUP93/RAPGEF2/CD79A/ZBTB39/OSEC1/LPGAT1/FGF19/NR1H4	590

GO:0050794	regulation of cellular process	394/590	9347/17046	1.23E-09	9.87E-07	8.56E-07	<p>AKT3/ABI1/TANKZF783/FARP1/KLRG1/RCAN2/CDKN1C/SPEG/MRV11/TRDN/SPON2/PTRM1/TACC2/PDPN/CELF1/GIB6/PNRC1/TMED10/LECT1/RRER1/ESM1/HNRPUL1/CHGA/CHIB1/ERLIN2/EGLN2/ATXN2L/PDAP1/CHRNA1/CHRNA2/CARD16/SORCS1/AP351/CCR1/SLCS1B/SEZ6/ZNFAIP8L1/COMP/MA3K8/ADM/IL131RA/EGFLAM/HUS1B/OR2A14/CRABP1/ZNF358/MBZ1/MPP7/FAM101A/CSTA/ZNF738/SMYD1/SGOL1/PPM1L/SHB19/CYD/ESCO2/ZNF782/DOB1/ABAT/DTNA/AGXT/EEF2/EFNA2/EIF4G1/AZM/ELK4/EPHA1/ESR1/SPATA13/FCGR2A/FGA/FGF10/FHIT/SBNO2/TRAK1/MSR82/FOXL1/EPB4113/DIP2A/LOT2/MLC1/RHOBTB2/NUP210/NEED4L/PSD3/PPP1R13/B/PUM2/ARHGAP18/RVBP/MORC3/MAIR8IP2/TSSK2/VGLL2/RASGEF1C/RNF144B/ZNF549/ALS2C1/PNK0/ACOT11/GAS2/SAKS/PLEK2/ADGRF1/RP56KCI/PABPC1/DNAJC2/FGF2Z/NPTN/PDE7B/CYTH4/BMP10/ZNF638/ZNF311/ZNF844/GPR26/FFAR2/GRB10/GRK4/DNAI5/TM0D4/GUCY4A3/GPR132/HAS1/50X8/HKI/HLA-DOA/HLA-DPA1/ANXA13/NR4A1/ACACB/HOXC4/HRH1/HSPA11/HSP90AB1/HTR3A/TFAP2E/ID3/ZC3H12D/RSP02/NNM5/FGF1/GF2/GPR142/LIL1R1/LIL1R2/IL10RA/IL11RA/IL12RB2/IL15RA/IL16/FOXK2/INHBA/IRF1/ITGA7/ITGB2/ITGB7/ITIH4/ITIH4/UP/CD82/USP50/KCNH2/KCNH8/KCNJ9/KDR/KIF25/PO5/AMIG03/HES5/AF3/LAMA3/STMN1/OR2A5/LCP1/LDLR/ARHGDA/LGALS9/LHCGR/LMNA/LMO2/RAB19/MC2R/MCC/MEZ/MFNG/SCGB2A1/MITF/LHX8/MOV10/LMP2/PLEKHG7/MYL2/NHLH2/NPPC/NRAS/OAS2/OPRL1/OR2C1/OR3A2/P2RY6/PFAFH2/ATP5B1/IL12R/PARK2/SPOCK3/UTP111/PRR16/C11orf73/SIRT6/PD66B/ATP8A2/P13/PTX2/PHK1/PLA2G2A/PLAGL1/PRKAG3/PML/RIPPL3/FYD6/GPR84/PNLIP/TLR8/TREM1/SSH1/RIN2/POU2AF1/APBB1P/FBLIM1/MED18/PALMD/IBANP/PPP1CE/ELP3/DNAJC17/GOLPH3/PPP2R2B/FANCI/MOB1A/TPRV6/SLC30A10/CHRN9/PARVA/PRKAR1B/FTL122/MCTP2/LMBRD1/PAG1/CISD1/MSB2/MYNN/MAF3/KN2/PRKRR/PROX/MRAP/PRMT8/HTRA1/SLMFB8/CD42SEL/TPRP6/ARNTL2/RGMA/PRDM11/PSMD7/SLURP1/PTGER/PLEKHG5/TEEN2/GATAD2B/ERMN/MAK4/PTPRE/CREBZF/FAM60A/TRIM27/RGR/RGS12/RIT2/RPA3/BGLAP/SCT/CC111/NPAS3/NO22/STRA6/ARHGAP9/GZF1/TMEM237/BMP4/ZNF649/SLC8A1/BMPR1B/SLIT1/BRD9/ZSCAN18/BOK/BPI/STAT2/STK3/SUPT6H/BST2/TCEB2/ZEB1/TEAD3/TERF1/TGM2/ZNFAP3/TNFRSF1A/TRAFF5/TPRC6/CCR2/TNFRSF4/UCP1/WNT10B/ZAP70/ZNF7/CA7/CACNA1E/RAB7A/CARD14/BCL2L14/LST1/ZNF665/CSPP1/GPR157/ZC3H12A/CPEB4/C6orf25/ZNF436/CALR/SLURP/CAST/CA/PZB/ANTXR1/CMVHP/ZNF397/NR0B2/CASQ1/HOPX/TTBK1/TRIM63/RAE1/IFITM1/SCIN/CDK10/RUNX1/TP63/RUNX3/SERPINA6/IBS2/ACTN1/CRADD/TNFRSF11A/ALDH1A2/SPHK1/BUD31/CCNA1/SKAP2/TSPAN18/CCR2/PRCI/STAR013/PIAS2/MA3K6/SYTT7/CBFA2T2/RSAD2/AURKB/DAP1/CD8A/TRIP10/ADIPQ/RAB36/MICAL2/N4BP1/VGLL4/NUP93/RAPGEF2/CD79A/ZBTB39/IQSECI1/FGF19/NR1H4</p>
GO:0050789	regulation of biological process	410/590	9837/17046	1.32E-09	9.87E-07	8.56E-07	<p>AKT3/ABI1/TANKZF783/FARP1/KLRG1/RCAN2/CDKN1C/SPEG/MRV11/TRDN/SPON2/PTRM1/TACC2/PDPN/CELF1/GIB6/PNRC1/TMED10/LECT1/RRER1/ESM1/HNRPUL1/CHGA/CHIB1/ERLIN2/EGLN2/ATXN2L/PDAP1/CHRNA1/CHRNA2/CARD16/SORCS1/AP351/CCR1/SLCS1B/SEZ6/TNFAIP8L1/COMP/MA3K8/ADM/IL131RA/EGFLAM/HUS1B/OR2A14/CRABP1/ZNF358/MBZ1/MPP7/LDLRAD3/FAM101A/CSTA/ZNF738/SMYD1/SGOL1/PPM1L/SH3D19/CYD/ESCO2/ZNF782/DOB1/ABAT/DTNA/AGXT/EEF2/EFNA2/EIF4G1/AZM/ELK4/EPHA1/ESR1/SPATA13/FCGR2A/FGA/FGF10/FHIT/SBNO2/TRAK1/MSR82/FOXL1/EPB4113/DIP2A/LOT2/MLC1/RHOBTB2/NUP210/NEED4L/PSD3/PPP1R13/B/PUM2/ARHGAP18/RVBP/MORC3/MAIR8IP2/TSSK2/VGLL2/RASGEF1C/RNF144B/ZNF549/ALS2C1/PNK0/ACOT11/GAS2/SAKS/PLEK2/ADGRF1/RP56KCI/PABPC1/DNAJC2/FGF2Z/NPTN/PDE7B/CYTH4/BMP10/ZNF638/ZNF311/ZNF844/GPR26/FFAR2/GRB10/GRK4/DNAI5/TM0D4/GUCY4A3/GPR132/HAS1/50X8/HKI/HLA-DOA/HLA-DPA1/ANXA13/NR4A1/ACACB/HOXC4/HRH1/HSPA11/HSP90AB1/HTR3A/TFAP2E/ID3/ZC3H12D/RSP02/NNM5/FGF1/GF2/GPR142/LIL1R1/LIL1R2/IL10RA/IL11RA/IL12RB2/IL15RA/IL16/FOXK2/INHBA/IRF1/ITGA7/ITGB2/ITGB7/ITIH4/ITIH4/UP/CD82/USP50/KCNH2/KCNH8/KCNJ9/KDR/KIF25/PO5/AMIG03/HES5/AF3/LAMA3/STMN1/OR2A5/LCP1/LDLR/ARHGDA/LGALS9/LHCGR/LMNA/LMO2/RAB19/MC2R/MCC/MEZ/MFNG/SCGB2A1/MITF/LHX8/MOV10/LMP2/PLEKHG7/MYL2/NHLH2/NPPC/NRAS/OAS2/OPRL1/OR2C1/OR3A2/P2RY6/PFAFH2/ATP5B1/IL12R/PARK2/SPOCK3/UTP111/PRR16/C11orf73/SIRT6/PD66B/ATP8A2/P13/PTX2/PHK1/PLA2G2A/PLAGL1/PRKAG3/PML/RIPPL3/FYD6/GPR84/PNLIP/TLR8/TREM1/SSH1/RIN2/POU2AF1/APBB1P/FBLIM1/MED18/PALMD/IBANP/PPP1CE/ELP3/DNAJC17/GOLPH3/PPP2R2B/FANCI/MOB1A/TPRV6/SLC30A10/CHRN9/PARVA/PRKAR1B/FTL122/MCTP2/LMBRD1/PAG1/CISD1/MSB2/MYNN/MAF3/KN2/PRKRR/PROX/MRAP/PRMT8/HTRA1/SLMFB8/CD42SEL/TPRP6/ARNTL2/RGMA/PRDM11/PSMD7/SLURP1/PTGER/PLEKHG5/TEEN2/GATAD2B/ERMN/MAK4/PTPRE/CREBZF/FAM60A/TRIM27/RGR/RGS12/RIT2/RPA3/BGLAP/SCT/CC111/NPAS3/NO22/STRA6/ARHGAP9/GZF1/TMEM237/BMP4/ZNF649/SLC8A1/BMPR1B/SLIT1/BRD9/ZSCAN18/BOK/BPI/STAT2/STK3/SUPT6H/BST2/TCEB2/ZEB1/TEAD3/TERF1/TGM2/ZNFAP3/TNFRSF1A/TRAFF5/TPRC6/CCR2/TNFRSF4/UCP1/WNT10B/ZAP70/ZNF7/CA7/CACNA1E/RAB7A/CARD14/BCL2L14/LST1/ZNF665/CSPP1/GPR157/ZC3H12A/CPEB4/C6orf25/ZNF436/CALR/SLURP/CAST/CA/PZB/ANTXR1/CMVHP/ZNF397/NR0B2/CASQ1/HOPX/TTBK1/TRIM63/RAE1/IFITM1/SCIN/CDK10/RUNX1/TP63/RUNX3/SERPINA6/IBS2/ACTN1/CRADD/TNFRSF11A/ALDH1A2/SPHK1/BUD31/CCNA1/SKAP2/TSPAN18/CCR2/PRCI/STAR013/PIAS2/MA3K6/SYTT7/CBFA2T2/RSAD2/AURKB/DAP1/CD8A/TRIP10/ADIPQ/RAB36/MICAL2/N4BP1/VGLL4/NUP93/RAPGEF2/CD79A/ZBTB39/IQSECI1/FGF19/NR1H4</p>

GO:0044700	single organism signaling	249/590	5624/17046	1.22E-06	0.00052	0.00052	0.00045	<p>AKT3/ABI1/TANK/FARP1/KLRG1/RKAN2/CDKN1C/MRVI1/TRDN/PPDN/LECT1/ESM1/CH13L1/ERLN2/EGLN2/PDAP1/CHRNA1/CHRNA2/SORCS1/AP3S1/CCR1/SEZ6/TNFAP8</p> <p>LJ/CNP/MAP3K8/ADM/IL13RA/ORZ4L4/CRABP1/MI82/PPP7/SGLI/PPM1L/CYLD/DOB1/ZNFX366/BHLHA15/DL32/DMBT1/ABAT/DNA/AGXT/ENNA2/EIF4G1/A2M/EPHA1/ESR1/</p> <p>SPATA13/FCGR2A/FGA/FGF10/FHIT/FOXL1/FOXCL2/ARRB1B/NFASC/RHOB/TB2/NUP210/NEDD4L/P5D3/PPP1R13B/PU12/ARHGEF18/MAPK8IP2/TSSK2/RASGEF1C/ALS2CL/PNKD/A</p> <p>COT11/PLEK2/ADGRF1/PP56KCI/FGF22/NPTN/PDE7B/CYTH4/BMP10/GPR26/FFAR2/GRB10/GRIK4/GUCY1A3/GPRI132/SOX8/HLA-DOA/HLA-</p> <p>DPAA1/NR4A1/HRH1/HSP90AB1/HTR3A/RSPQ2/IGF1/IGF2/GPRI42/IL1R1/IL1RN/IL10RA/IL11RA/IL12RB2/IL15RA/INHBA/IRF1/ITGA7/ITGB2/ITGB7/IJUP/CDB2/KCNH2/KCNJ8/KCNJ9</p> <p>/KCNMB1/KDR/HES5/STMN1/ORZ4L4/LCP1/LDLR/ARHGDI3/LGALS9/LHCSR/LMNA/RAB19/MC2R/MCC/MFG/SGB2A1/MITF/MOV10/MP2/PLEKHG7/ATP1A2/NFATC3/NPPC/NR</p> <p>AS/OAS2/OPRL1/OPR2C1/OR3A2/P2RY6/IL21R/PARK2/SPOCK3/PDE6B/PTX2/PKHD1/PLA2G2A/PRKAG3/PML/GPR84/PNLI9/TL89/TREM1/RN2/APBB1IP/PPP1CB/MOB1A/CHRNA9</p> <p>/PRKAR1B/FT1122/MCTP2/LMBRD1/PAG1/W5B2/MAPK3/MAP2K2/PRKRIR/HTRA1/CDCA25E1/PAK6/NGM/MAP3/PPP7/P1GFR/LEKHG5/TENM2/PTPRE/RGR/NGS12/RT2/SCY/CLL1/</p> <p>NOD2/STRA6/ARHGAP9/TMEM237/BMP4/SLC6A12/SLC8A1/BMPR1B/BOK/STAT2/STK3/BST1/ZEB1/TEAD3/TGMD2/TNFAP3/TNFRSF4/TRA5/CCR2/TNFRSF4/WNT10B/ZAP70/CA</p> <p>7/CACNA1E/RAB7A/CARD14/BC1L2L14/GPRI157/CPEB4/C6orf25/CALR/ANTXR1/CMAHP/NROB2/CASQ1/TTRIM63/RAE1/JFITM1/JFITM1/TP63/RUNX3/IRS2/CRADD/TNFRSF11</p> <p>A/ALDH1A2/SPHK1/SPKAP2/TSPAN18/CCR2/PRC1/STAR13/PIAS2/MAP3K6/SIT1/RAS2/AURK8/DAP1L/CDBA/TRIP10/ADOIPOQ/RAB36/NUP93/RAPGEF2/CD79A/IOSEC1/FGF19/</p> <p>NR1H4</p>
GO:0023052	signaling	249/590	5629/17046	1.32E-06	0.00052	0.00052	0.00045	<p>AKT3/ABI1/TANK/FARP1/KLRG1/RKAN2/CDKN1C/MRVI1/TRDN/PPDN/LECT1/ESM1/CH13L1/ERLN2/EGLN2/PDAP1/CHRNA1/CHRNA2/SORCS1/AP3S1/CCR1/SEZ6/TNFAP8</p> <p>LJ/CNP/MAP3K8/ADM/IL13RA/ORZ4L4/CRABP1/MI82/PPP7/SGLI/PPM1L/CYLD/DOB1/ZNFX366/BHLHA15/DL32/DMBT1/ABAT/DNA/AGXT/ENNA2/EIF4G1/A2M/EPHA1/ESR1/</p> <p>SPATA13/FCGR2A/FGA/FGF10/FHIT/FOXL1/FOXCL2/ARRB1B/NFASC/RHOB/TB2/NUP210/NEDD4L/P5D3/PPP1R13B/PU12/ARHGEF18/MAPK8IP2/TSSK2/RASGEF1C/ALS2CL/PNKD/A</p> <p>COT11/PLEK2/ADGRF1/PP56KCI/FGF22/NPTN/PDE7B/CYTH4/BMP10/GPR26/FFAR2/GRB10/GRIK4/GUCY1A3/GPRI132/SOX8/HLA-DOA/HLA-</p> <p>DPAA1/NR4A1/HRH1/HSP90AB1/HTR3A/RSPQ2/IGF1/IGF2/GPRI42/IL1R1/IL1RN/IL10RA/IL11RA/IL12RB2/IL15RA/INHBA/IRF1/ITGA7/ITGB2/KCNH2/KCNJ8/KCNJ9</p> <p>/KCNMB1/KDR/HES5/STMN1/ORZ4L4/LCP1/LDLR/ARHGDI3/LGALS9/LHCSR/LMNA/RAB19/MC2R/MCC/MFG/SGB2A1/MITF/MOV10/MP2/PLEKHG7/ATP1A2/NFATC3/NPPC/NR</p> <p>AS/OAS2/OPRL1/OPR2C1/OR3A2/P2RY6/IL21R/PARK2/SPOCK3/PDE6B/PTX2/PKHD1/PLA2G2A/PRKAG3/PML/GPR84/PNLI9/TL89/TREM1/RN2/APBB1IP/PPP1CB/MOB1A/CHRNA9</p> <p>/PRKAR1B/FT1122/MCTP2/LMBRD1/PAG1/W5B2/MAPK3/MAP2K2/PRKRIR/HTRA1/CDCA25E1/PAK6/NGM/MAP3/PPP7/P1GFR/LEKHG5/TENM2/PTPRE/RGR/NGS12/RT2/SCY/CLL1/</p> <p>NOD2/STRA6/ARHGAP9/TMEM237/BMP4/SLC6A12/SLC8A1/BMPR1B/BOK/STAT2/STK3/BST1/ZEB1/TEAD3/TGMD2/TNFAP3/TNFRSF4/TRA5/CCR2/TNFRSF4/WNT10B/ZAP70/CA</p> <p>7/CACNA1E/RAB7A/CARD14/BC1L2L14/GPRI157/CPEB4/C6orf25/CALR/ANTXR1/CMAHP/NROB2/CASQ1/TTRIM63/RAE1/JFITM1/JFITM1/TP63/RUNX3/IRS2/CRADD/TNFRSF11</p> <p>A/ALDH1A2/SPHK1/SPKAP2/TSPAN18/CCR2/PRC1/STAR13/PIAS2/MAP3K6/SIT1/RAS2/AURK8/DAP1L/CDBA/TRIP10/ADOIPOQ/RAB36/NUP93/RAPGEF2/CD79A/IOSEC1/FGF19/</p> <p>NR1H4</p>
GO:0051716	cellular response to stimulus	277/590	6405/17046	1.40E-06	0.00052	0.00052	0.00045	<p>AKT3/ABI1/TANK/FARP1/KLRG1/RKAN2/CDKN1C/MRVI1/SPON2/PPN2/GI86/LECT1/ESM1/CHGA/CH13L1/ERLN2/EGLN2/TP52TG1/PDAP1/CHRNA1/CHRNA2/SORCS1/AP3S1/CCR</p> <p>1/SEZ6/TNFAP8/LJ/CNP/MAP3K8/ADM/IL13RA/HUS1B/ORZ4L4/CPS1/CRABP1/MI82/PPP7/SGLI/PPM1L/CYLD/ESCO2/CPV11A1/DDB1/ZNFX366/BHLHA15/DMBT1/DTNA/AGX</p> <p>T/EFNA2/EIF4G1/A2M/EPHA1/ESR1/FOXCL1/FOXCL2/ARRB1B/NFASC/RHOB/TB2/NUP210/NEDD4L/P5D3/PPP1R13B/PU12/ARHGEF18/M</p> <p>APK8IP2/TSSK2/SLC37A4/RASGEF1C/ALS2CL/ACOT11/PLEK2/ADGRF1/PP56KCI/DNAJC2/FGF22/NPTN/PDE7B/CYTH4/BMP10/GPR26/FFAR2/GRB10/GRIK4/DNAJC15/GUCY1A3/GP</p> <p>R132/HAS1/SOX8/HKI1/HLA-DOA/HLA-</p> <p>DPAA1/NR4A1/HRH1/HSP90AB1/HTR3A/RSPQ2/IGF1/IGF2/GPRI42/LCE1D/IL1R1/IL1RN/IL10RA/AQP2/IL11RA/IL12RB2/IL15RA/INHBA/IRF1/ACQP9/ITGA7/ITGB2/ITGB</p> <p>7/IJUP/CDB2/KCNH2/KDR/IPD5/HES5/STMN1/ORZ4L4/LCP1/LDLR/ARHGDI3/LGALS9/LHCSR/LMNA/LMO2/RAB19/MC2R/MCC/MFG/SGB2A1/MITF/ASGR1/MOV10/PLEKHG7/AT</p> <p>PLA2/NFATC3/NPPC/NRAS/OAS2/OPRL1/OR2C1/OR3A2/P2RY6/IL21R/PARK2/SPOCK3/CL10F73/SIRT6/PDE6B/PTX2/PKHD1/PLA2G2A/PRKAG3/PML/GPR84/PNLI9/TREM1/P</p> <p>SSH1/RIN2/APBB1IP/CYP2W1/PPP1CB/FANCI/MOB1A/CHRNA9/PARVA/PRKAR1B/FT1122/MCTP2/LMBRD1/PAG1/W5B2/MAP3/MAP2K2/PRKRIR/HTRA1/SLAMF8/CDCA25E1/PA</p> <p>6/RGMA/PSMD7/PTGFR/PLEKHG5/TENM2/PTPRE/RFC2/RGR/NGS12/RT2/RP43/BGLAP/CLL1/NOD2/STRA6/ARHGAP9/VPS33A/BMP4/SLC8A1/BMPR1B/BOK/STAT2/S</p> <p>TK3/BST1/ZEB1/TEAD3/TGMD2/TNFAP3/TNFRSF4/TRA5/CCR2/CPV11A1/WNT10B/ZAP70/CA7/CACNA1E/RAB7A/CARD14/BC1L2L14/GPRI157/ZC3H12A/FAA1/DOO/C</p> <p>PEB4/C6orf25/EEF1D/CALR/ANTXR1/CMAHP/NROB2/CASQ1/TTRIM63/RAE1/JFITM1/CDK10/RUNX1/TP63/RUNX3/IRS2/CRADD/TNFRSF11A/ALDH1A2/SPHK1/SPKAP2/STBD1/TSPAN</p> <p>18/CCR2/PRC1/STAR13/PIAS2/MAP3K6/RSAD2/AURK8/DAP1L/CD8A/TRIP10/ADOIPOQ/RAB36/NABP1/NUP93/RAPGEF2/CD79A/IOSEC1/FGF19/NR1H4</p> <p>CDKN1C/SPON2/GBB6/LECT1/CH13L1/EPHA1/CPV11A1/BHLHA15/EIF4G1/ESR1/FGA/FGF10/SBNO2/FOXO2/AKR1B1/MILC1/NUP210/NEDD4L/ARHGEF18/FGF22</p> <p>/NPTN/BMP10/FFAR2/GRB10/HAS1/HLA-</p>
GO:0071310	cellular response to organic substance	110/590	2092/17046	3.83E-06	0.00133	0.00133	0.00116	<p>DPAA1/NR4A1/HRH1/HSP90AB1/HTR3A/RSPQ2/IGF1/IGF2/GPRI42/IL1R1/IL1RN/IL10RA/IL11RA/IL12RB2/IL15RA/INHBA/IRF1/ACQP9/ITGA7/ITGB2/ITGB</p> <p>7/IJUP/CDB2/KCNH2/KDR/IPD5/HES5/STMN1/ORZ4L4/LCP1/LDLR/ARHGDI3/LGALS9/LHCSR/LMNA/LMO2/RAB19/MC2R/MCC/MFG/SGB2A1/MITF/ASGR1/MOV10/PLEKHG7/AT</p> <p>PLA2/NFATC3/NPPC/NRAS/OAS2/OPRL1/OR2C1/OR3A2/P2RY6/IL21R/PARK2/SPOCK3/CL10F73/SIRT6/PDE6B/PTX2/PKHD1/PLA2G2A/PRKAG3/PML/GPR84/PNLI9/TREM1/P</p> <p>SSH1/RIN2/APBB1IP/CYP2W1/PPP1CB/FANCI/MOB1A/CHRNA9/PARVA/PRKAR1B/FT1122/MCTP2/LMBRD1/PAG1/W5B2/MAP3/MAP2K2/PRKRIR/HTRA1/SLAMF8/CDCA25E1/PA</p> <p>6/RGMA/PSMD7/PTGFR/PLEKHG5/TENM2/PTPRE/RFC2/RGR/NGS12/RT2/RP43/BGLAP/CLL1/NOD2/STRA6/ARHGAP9/VPS33A/BMP4/SLC8A1/BMPR1B/BOK/STAT2/S</p> <p>TK3/BST1/ZEB1/TEAD3/TGMD2/TNFAP3/TNFRSF4/TRA5/CCR2/CPV11A1/WNT10B/ZAP70/CA7/CACNA1E/RAB7A/CARD14/BC1L2L14/GPRI157/ZC3H12A/FAA1/DOO/C</p> <p>PEB4/C6orf25/EEF1D/CALR/ANTXR1/CMAHP/NROB2/CASQ1/TTRIM63/RAE1/JFITM1/CDK10/RUNX1/TP63/RUNX3/IRS2/CRADD/TNFRSF11A/ALDH1A2/SPHK1/SPKAP2/STBD1/TSPAN</p> <p>18/CCR2/PRC1/STAR13/PIAS2/MAP3K6/RSAD2/AURK8/DAP1L/CD8A/TRIP10/ADOIPOQ/RAB36/NABP1/NUP93/RAPGEF2/CD79A/IOSEC1/FGF19/NR1H4</p> <p>CDKN1C/SPON2/GBB6/LECT1/CH13L1/EPHA1/CPV11A1/BHLHA15/EIF4G1/ESR1/FGA/FGF10/SBNO2/FOXO2/AKR1B1/MILC1/NUP210/NEDD4L/ARHGEF18/FGF22</p> <p>/NPTN/BMP10/FFAR2/GRB10/HAS1/HLA-</p>
GO:0007166	cell surface receptor signaling pathway	126/590	2511/17046	6.86E-06	0.00224	0.00224	0.00194	<p>DPAA1/NR4A1/HRH1/HSP90AB1/HTR3A/RSPQ2/IGF1/IGF2/GPRI42/IL1R1/IL1RN/IL10RA/IL11RA/IL12RB2/IL15RA/INHBA/IRF1/ACQP9/ITGA7/ITGB2/ITGB</p> <p>7/IJUP/CDB2/KCNH2/KDR/IPD5/HES5/STMN1/ORZ4L4/LCP1/LDLR/ARHGDI3/LGALS9/LHCSR/LMNA/LMO2/RAB19/MC2R/MCC/MFG/SGB2A1/MITF/ASGR1/MOV10/PLEKHG7/AT</p> <p>PLA2/NFATC3/NPPC/NRAS/OAS2/OPRL1/OR2C1/OR3A2/P2RY6/IL21R/PARK2/SPOCK3/CL10F73/SIRT6/PDE6B/PTX2/PKHD1/PLA2G2A/PRKAG3/PML/GPR84/PNLI9/TREM1/P</p> <p>SSH1/RIN2/APBB1IP/CYP2W1/PPP1CB/FANCI/MOB1A/CHRNA9/PARVA/PRKAR1B/FT1122/MCTP2/LMBRD1/PAG1/W5B2/MAP3/MAP2K2/PRKRIR/HTRA1/SLAMF8/CDCA25E1/PA</p> <p>6/RGMA/PSMD7/PTGFR/PLEKHG5/TENM2/PTPRE/RFC2/RGR/NGS12/RT2/RP43/BGLAP/CLL1/NOD2/STRA6/ARHGAP9/VPS33A/BMP4/SLC8A1/BMPR1B/BOK/STAT2/S</p> <p>TK3/BST1/ZEB1/TEAD3/TGMD2/TNFAP3/TNFRSF4/TRA5/CCR2/CPV11A1/WNT10B/ZAP70/CA7/CACNA1E/RAB7A/CARD14/BC1L2L14/GPRI157/ZC3H12A/FAA1/DOO/C</p> <p>PEB4/C6orf25/EEF1D/CALR/ANTXR1/CMAHP/NROB2/CASQ1/TTRIM63/RAE1/JFITM1/CDK10/RUNX1/TP63/RUNX3/IRS2/CRADD/TNFRSF11A/ALDH1A2/SPHK1/SPKAP2/STBD1/TSPAN</p> <p>18/CCR2/PRC1/STAR13/PIAS2/MAP3K6/RSAD2/AURK8/DAP1L/CD8A/TRIP10/ADOIPOQ/RAB36/NABP1/NUP93/RAPGEF2/CD79A/IOSEC1/FGF19/NR1H4</p> <p>CDKN1C/SPON2/GBB6/LECT1/CH13L1/EPHA1/CPV11A1/BHLHA15/EIF4G1/ESR1/FGA/FGF10/SBNO2/FOXO2/AKR1B1/MILC1/NUP210/NEDD4L/ARHGEF18/FGF22</p> <p>/NPTN/BMP10/FFAR2/GRB10/HAS1/HLA-</p>

GO:0070887	cellular response to chemical stimulus	124/590	2524/17046	2.28E-05	0.00518	0.00449	<p>CDKN1C/SPON2/GIB6/LECT1/CHGA/CHL3/EGLN2/AP351/CCR1/IL13/IRA/CP51/CYP11A1/BHLHA15/EIF4G1/ESR1/FGA/FGF10/SBN02/FOXO2/AKR1B1/MCL1/NUP210/NEEDD4L/ARH1/GEF18/FGF22/NPTN/BMP10/FFAR2/GRB10/HAS1/HLA-</p> <p>DPAA1/NR4A1/HRH1/HSP90AB1/HTR3A/IGF2/ACE1D/IL1R1/IL1RN/IL12RB2/IL13/IRAL/INHA/IRF1/AQP9/ITGB2/JUP/KCNH2/KDR/PO5/HESS/ARHGDI4/LGALS9/LHCGR/LMNA/UM02/MOV10/ATPLA2/NFATC3/NRAS/OAS2/P2RY6/IL21B/PARK2/PRKAG3/PML/ITR9/TREM1/SSH1/CY2P2W1/PPP1CB/PARVA/PRKAR1B/ALMBRD1/MAPK3/MAP2K2/HTRA1/SLAMF8/RGMA/PSMD7/PTGFR/PLEKHG5/PTPRE/RIT2/BGLAP/CLL11/NOD2/BNIP4/SLC8A1/BNIPR1B/STAT2/BST2/TCB2/ZEB1/TNFAIP3/TNFRSF1A/TRPC6/CCR2/JNFRSF4/WNT10B/CACNA1E/CARD14/ZC3H12A/CPEB4/CALR/NR0B2/TRIM63/RNF144B/ALSZCL/PABPC1/DNAJC2/FGF22/NPTN/CYTH4/BMP10/GPR26/FFAR2/GRB10/DNAJC15/GUCY1A3/SOX8/HKI1/HLA- G19/NR1H4</p>
GO:0009628	response to abiotic stimulus	63/590	1071/17046	2.48E-05	0.0053	0.0046	<p>GIB6/CHL3/EGLN2/ADM/CYP11A1/DOB1/ABAT/ANKRD23/AKR1B1/MIC1/NUP210/ACOT11/FBXL21/DNAJC2/HRH1/HSPA11/HSP90AB1/IGF1/IL1R1/AQP2/IRF1/AQP9/IVUJUP/KCNB1/LDBR/LMNA/ATP1A2/NFATC3/NPPC/C11orf73/PD68B/ATP8A2/PKM/PML/PNIP/PPP1CB/CHRNA9/MAPK3/RGR/RP43/BGLAP/SC7/CC111/STRA6/BMP4/SLC8A1/TCB2/TNFRSF1A/ITR9/CACNA1E/CPEB4/CASQ1/TRIM63/RAE1/KV02/TP63/CRADD/TNFRSF11A/AURKB/ADIPOQ/NABP1/NUP93</p>
GO:0048518	positive regulation of biological process	217/590	4960/17046	2.54E-05	0.0053	0.0046	<p>ABI1/TANK/FARP3/CDKN1C/TRDN/SPON2/PTRM1/JRER/ESM1/CHGA/CHL3/ERLIN2/EGLN2/CCR1/SLC51B/SEZ6/MAP3K8/ADM/IL13/IRAL/EGFLAM/CP51/MIB2/MPP7/SMYD1/SH3D19/CYLD/DOB1/BHLHA15/DOS3/DMBT1/ABAT/EEF2/EIF4G1/AZM/EPHA1/ESR1/F11/SPATA13/FCG2A/FGA/FGF10/SBN02/FOXO2/EXPH5/AKR1B1/GGA3/FLT02/MLC1/TBC1D1/NEEDD4L/PSD3/PUM2/ARHGEF18/MAPK8IP2/VGLL2/RAASGEF1C/RNF144B/ALSZCL/PABPC1/DNAJC2/FGF22/NPTN/CYTH4/BMP10/GPR26/FFAR2/GRB10/DNAJC15/GUCY1A3/SOX8/HKI1/HLA-</p> <p>DPAA1/ANXA13/NR4A1/ACACB/AGFG2/HRH1/HSPA11/HSP90AB1/TFAP2E/ID3/RSPO2/IGF1/IGF2/IL1RN/IL12RB2/JUP/KCNH2/KDR/PO5/AMIGO3/HESS/STMN1/LCP1/LDBR/ARHGDI4/LGALS9/LHCGR/LMNA/UM02/MC2R/MFNG/MITF/PLEKHG7/NEU1/NFATC3/NHLH2/NPPC/NRAS/OPR11/P2RY6/PARK2/JUTP11/PRR16/SIRT6/A TP8A2/PTX2/PKHD1/PLA2G2A/PLAGL1/PML/PNIP/TLR9/RIN2/APBB1IP/BNAP/ELP3/GOLPH3/F-ANCP/PRKAR1B/PAG1/MAPK3/MAP2K2/MRAP/HTRAI/PAK6/ARNT/SLT2/RGMA/PSM D7/PTGFR/PLEKHG5/TNMM2/MARK4/ACTA2/TRIM27/RGS12/SC7/CC111/NP4S3/NOD2/STRAG/ARHGAP9/BMP4/BNIPR1B/BOK/STK3/5UPT6H/BST2/TCB2/ZEB1/TEAD3/TERF1/TGM2/TNFAIP3/TNFRSF1A/TRA5/TPRC6/CCR2/TNFRSF4/WNT10B/ZAP70/CA7/RAB7A/CARD14/BC1L2L14/CSP1/ZC3H12A/CALR/NR0B2/HOPX/HITM1/SCIN/CDK10/RUNX1/TP63/RUNX3/IRS2/CRADD/TNFRSF11A/ALDH1A2/SPHK1/SKAP2/PRC1/STAR13/PIAS2/MAP3K6/SYT71/CBEA22/RSAD2/AURKB/CD8A/ADIPOQ/MICAL2/RAPGEF2/CD79A/IOSEC1/FGF19/NR1H4</p>
GO:0022610	biological adhesion	75/590	1348/17046	2.71E-05	0.00545	0.00473	<p>GNE/CDH9/CDH12/SPON2/PDPN/PK3/FAT3/CCR1/COM7/MAP3K8/EGFLAM/CSTA/CYLD/DDOST1/EPHA1/FAT7/FGA/FOXO2/NFASC/FLOT2/NPTN/CYTH4/BMP10/HAS1/HLA- DOA/HLA-</p> <p>DPAA1/HSP90AB1/ZC3H12D/IGF1/IGF2/IL1RN/IRF1/ITGA7/ITGB2/ITGB7/JUP/KDR/AMIGO3/HESS/LAMA3/LCP1/ARHGDI4/LGALS9/LPP/NFATC3/ATP5B/PKHD1/PML/APBB1IP/FBLI M1/PPP1CB/PARVA/PAG1/PCDHGB3/SLURP1/TENM2/BGLAP/CLL11/PARG/NO2/TINAGL1/PCDH20/BMP4/ZEB1/TGM2/CCR2/TNFRSF4/ZAP70/CALR/ANTXR1/ACTN1/ESAM/RS AD2/CD8A/ADIPOQ</p>
GO:0065008	regulation of biological quality	151/590	3225/17046	2.97E-05	0.00575	0.00499	<p>MIRV1/TRDN/PDPN/GIB6/CHGA/EGLN2/CHRNA1/CHRNA2/CLN5/CCR1/SLC51B/SEZ6/CNP/ADM/IL13/IRA/CP51/CRABP1/CYP11A1/DOB1/BHLHA15/DIO3/ARAT/A2M/ESR1/F11/FG A/FGF10/FOXO2/AKR1B1/EPB41L3/FLT02/NEEDD4L/SYNE1/ARHGEF18/MORC3/MAPK8IP2/SLC37A4/DFNB31/STEAP2/GAS2/PABPC1/NPTN/AMPD3/GPR26/FFAR2/SCG3/TMOD4/ GUCY1A3/SOX8/HKI1/ACACB/HRH1/HTR3A/ANME9/IGF1/IGF2/IL1R1/IL1RN/AQP2/AQP5/INHA/IRF1/AQP9/ITGB2/JUP/KCNH2/KCNMB1/KDR/AMIGO3/L DLR/LGALS9/MYL2/NUB1/ATP1A2/NPPC/NRAS/OPRL1/ATP5B/ANO7/PARK2/PRR16/SIRT6/PDE68/ATP8A2/PKHD1/PML/TLR9/TREM1/SSH1/APBB1IP/FBLIM1/PALMD/SLC30A10/ CHRNA9/PARVA/PRKAR1B/MAP3K3/PROC/SLAMF8/CD42SE1/ERMIN/RHD14/ACTA2/RFCC2/TRIM27/RP3/BGLAP/SC7/CC111/ABHD4/NOD2/STRA6/BMP4/SLC4A1/SLC6A12/SLC8A 1/SLC9A3/SLIT1/STK3/TERF1/TGM2/TNFAIP3/TRPC6/CCR2/WNT10B/CA7/CACNA1E/RAB7A/LST1/ZC3H12A/G6orf25/CALR/CAPZB/ATP13A4/NR0B2/CASQ1/TTBK1/SCIN/TP63/IRS2 /ACTN1/TNFRSF11A/ALDH1A2/SYT71/ESAM/SLC16A3/ADIPOQ/RAPGEF2</p>
GO:0061448	connective tissue development	21/590	224/17046	3.54E-05	0.0066	0.00573	<p>LECT1/CHL3/COMP/FAM103A/FOXO2/BMP10/SOX8/HOX4/RSPO2/IGF1/HESS/NPPC/CSGALNACT1/MAPK3/ACTA2/BMP4/BMP1R1B/ZEB1/WNT10B/SCIN/RUNX3</p>
GO:0009653	anatomical structure morphogenesis	125/590	2579/17046	3.93E-05	0.00707	0.00613	<p>ABI1/FAIRP1/CDKN1C/SPON2/PDPN/GIB6/LECT1/ESM1/CHL3/CNP/COL9A3/COMP/ADM/CPM/ZNF358/FAM101A/SHBD19/CYLD/EFNA2/EPHA1/ESR1/FGA/FGF10/BTB3/SBN02 /FOXO2/NFASC/EPB41L3/NEEDD4L/ARHGEF18/MAPK8IP2/GAS2/FGF22/BMP10/TMOD4/SOX8/NR4A1/HOX4/HSP90AB1/ID3/RSAD2/IGF1/IL1RN/FOXO2/AQP5/INHA /ITGA7/ITGB2/ITGB7/KDR/HESS/AFF3/LAMA3/STMN1/ARHGDI4/LHX8/MYL2/NFATC3/NPPC/NRAS/ATP5B/PARK2/SIRT6/ATP8A2/PTX2/PKHD1/PML/SSH1/FBLIM1/PALMD/CHRN A9/PARVA/HIT22/CSGALNACT1/MAPK3/MAP2K2/HTRA1/CD42SE1/RGMA/PSMD7/TENM2/ERMIN/ACTA2/CD42SE1/DNAI2/TMEM237/NP53A/BMP4/SLC8A1/ BMPR1B/SLIT1/STK3/ZEB1/TGM2/TNFAIP3/TRPC6/CCR2/WNT10B/LST1/ZC3H12A/G6orf25/CALR/SLURP/CAST/CAPZB/ANTXR1/CASQ1/TP63/RUNX3/IRS2/AC TN1/ALDH1A2/SPHK1/ADIPOQ/MICAL2/RAPGEF2/FGF19</p>
GO:0007155	cell adhesion	74/590	1343/17046	4.25E-05	0.00728	0.00632	<p>GNE/CDH9/CDH12/SPON2/PDPN/PK3/FAT3/CCR1/COMP/MAP3K8/EGFLAM/CSTA/CYLD/DDOST1/EPHA1/FAT7/FGA/FOXO2/NFASC/FLOT2/NPTN/CYTH4/BMP10/HAS1/HLA- DOA/HLA-</p> <p>DPAA1/ZC3H12D/IGF1/IGF2/IL1RN/IRF1/ITGA7/ITGB7/JUP/KDR/AMIGO3/HESS/LAMA3/LCP1/ARHGDI4/LGALS9/LPP/NFATC3/ATP5B/PKHD1/PML/APBB1IP/FBLIM1/PPP1CB/ PARVA/PAG1/PCDHGB3/SLURP1/TENM2/BGLAP/CLL11/PARG/NO2/TINAGL1/PCDH20/BMP4/ZEB1/TGM2/CCR2/TNFRSF4/ZAP70/CALR/ANTXR1/ACTN1/ESAM/RSAD2/CD8A/A DIPOQ</p>

GO:0019932	second-messenger-mediated signaling	20/590	2110/17046	4.33E-05	0.00728	0.00754	0.00632	RKAN2/MRV1/ADM/BHLHA15/GUCY1A3/HRH1/IGF1/KDR/LHCGR/ATP1A2/NFATC3/MCTP2/PTGFR/TENM2/SLC8A1/ZAP70/CASQ1/SPHK1/CD8A1/RAPGEF2	20
GO:0044707	single-multicellular organism process	261/590	6214/17046	4.62E-05	0.00754	0.00654	0.00654	AB11/FARP1/RCAN2/CDKN1C/SPEG/MRV1/TRDN/SPON2/TACC2/PDPN/CELF1/GIB6/TMED10/LECT1/ESM1/CHGA/CH13L1/CHRNA1/CHRNA2/GPRIN1/FAT3/CLIN5/CCR1/SEZ6/CNP1/CO9A3/COMP/ADM/IL13RA/ORA2A1/CP51/CRABP1/ZNF358/CRYBB3/FAM101A/CSTA/SMDY1/CYLD/ESCO2/CYP11A1/DIO3/DIG3/DMBT1/ABAT/DTNAA/EEF2/EFNA2/EIF4G1/A2M/EPHA1/ESR1/F11/FAT2/FGA/FGF10/BTD03/SBN02/FOXL1/FOXO2/EXPH5/AKR1B1/NFASC/EPB41L3/DIP2A/NEEDD4/PSD3/RYBP/MORC3/MAPK8IP2/TSSK2/VGLL2/DFNB31/PNKD/LCE2B/GATM/FGF2/NPTN/AMPD3/BMP10/FFAR2/SCG3/TMOD4/GUCT1A3/SOX8/HLA-DOA/HLA-DPA1/NR4A1/ACACB/HOX4/HRH1/HSD11B1/HSP90A1/HTR3A/ID3/RSPO2/AQP5/INHBA/IRF1/AQP9/ITGA7/ITGB2/ITLJ/UJ/DPA1/NR4A1/ACACB/HOX4/HRH1/HSD11B1/HSP90A1/HTR3A/ID3/RSPO2/AQP5/INHBA/IRF1/AQP9/ITGA7/ITGB2/ITLJ/UJ/DPA1/KCNH2/KCNJ8/KCNMB1/KDR/AMIGO3/HESS/AFF3/LAMA3/STMN1/ORA2A/ID1R/ARHGDA1/LGALS9/LHCGR/LMNA/LMO2/MC2R/MCC/MFNG/MGAT1/MITF/LHX8/MYH4/MYL2/DRG1/NEU1/ATP1A2/NFATC3/NHLH2/NPCC/NRAS/OPRL1/OR2A2/SLC22A18/ATP5B/PARK2/UTP11/CL10F73/SIRT6/POE6B/ATP8A2/PTX2/PKHDI/PKM/PLA2G2A/PLAGL1/RIPL1/RIPL3/PLIP/TLR9/TREM1/SSH1/FPBB1P/MXR48/BANP/PPP1CB/HERC6/ELP3/CHRNA9/PARVA/PKR1B/FTI122/ERMARD/MCTP2/CSGALNACT1/MAPK3/MAP2K2/PRO1/HTRA1/RGMA/PSMD7/SUURP1/PEKHG5/TENM2/ERMN/RDH14/MARK4/ACTA2/TRIM27/RGR/BGLAP/SCY/CC111/NP3AS3/NOD2/STRA6/GZF1/DNAI2/VPS33A/BMP4/SLC8A1/BM/PR1B/SLIT1/BOK/BPI/STK3/SUPT16H/BST2/ZEB1/ZEB2/TCOH/TNFAIP3/TNFRSF14/TRPC6/CCR2/TNFRSF4/WNT1/OBZAP70/ZNF7/CACNA1E/RAB7A/LST1/CAID1/ZC3H12A/C/GoF2/CALR/CAST/CAP2B/SPATA16/BFSP2/NR0B2/CASQ1/HOPX/ITBK1/TRIM63/ITIM1/CDK10/RUNX1/TP63/RUNX3/IRS2/CRADD/TNFRSF11A/SPHK1/SKAP2/STARD13/PIAS3/MAP3K6/M/SLC16A3/CBFA2T2/RSAD2/AURKB/CD8A/ADIPOQ/MICAL2/RAPGEF2/CD79A/FGF19	261
GO:0048583	regulation of response to stimulus	152/590	3283/17046	4.99E-05	0.00789	0.00685	0.00685	AB11/TANK/FARP1/KIRG1/RCAN2/CDKN1C/SPON2/LECT1/YESM1/CH13L1/CCR1/SEZ6/TNFAIP8L1/MAP3K8/ADM/IL13RA/MIB2/MPP7/CYLD/ZNF366/DMBT1/A2M/ESR1/F11/SPATA13/FCGR2A/FGA/FGF10/SBN02/FOXL1/FOXO2/AKR1B1/MICL1/RHOBT2/NUP210/NEEDD4/PSD3/PUM2/ARHGEF18/MAPK8IP2/SLC37A4/ALS2CL/DNAIC2/FGF22/NPTN/CYTH4/BMP10/FFAR2/GRB10/HK1/HLA-DPA1/NR4A1/HSPAL1/HSP90A1/RSPO2/IGF1/IGF2/IL1R1/IL1RN/IL16/INHBA/IRF1/ITGB2/ITGB7/IJUP/KDR/HES5/ARHGDA1/LGALS9/LHCGR/LMNA/MCC/MFNG/MOV10/PLEKHG7/NFATC3/NRAS/PARK2/CL10F73/SIRT6/POE6B/PKHDI/PLA2G2A/PML1/LR9/TREM1/PPP1CB/IFT122/LMBRO1/PAG1/MAPK3/MAP2K2/PRO1/PTRE/TRIM27/RGS12/RPA3/CLL11/NOD2/STRA6/ARHGAP9/TMEM237/BMP4/BMPR1B/STAT3/STK3/SUPT16H/BST2/ZEB1/ZEB2/TCOH/TNFAIP3/TNFRSF14/TRPC6/CCR2/TNFRSF4/WNT1/OBZAP70/ZNF7/CACNA1E/RAB7A/LST1/CAID1/ZC3H12A/C/GoF2/CALR/CAST/CAP2B/SPATA16/BFSP2/NR0B2/CASQ1/HOPX/ITBK1/TRIM63/ITIM1/CDK10/RUNX1/TP63/RUNX3/IRS2/CRADD/TNFRSF11A/SPHK1/SKAP2/STARD13/PIAS3/MAP3K6/RSAD2/CD8A/TRIP10/ADIPOQ/NUP93/RAPGEF2/CD79A/QSOX1/FGF19	152
GO:0008360	regulation of cell shape	15/590	132/17046	5.26E-05	0.00808	0.00701	0.00701	PDPN/EPB41L3/ARHG18/GAS2/ITGA7/ITGB2/KDR/FBLN1/PALMD1/PARVA/CDCA25E1/ERMN/CC111/ST1/TTBK1	15
GO:0018149	peptide cross-linking	9/590	51/17046	5.56E-05	0.00814	0.00706	0.00706	EGFLAM/CSTA/ICE2B/ICE1C/ICE1D/ICE2D/ML/SPOCK3/TGM2	9
GO:0032501	multicellular organismal process	268/590	6425/17046	5.62E-05	0.00814	0.00706	0.00706	AB11/FARP1/RCAN2/CDKN1C/SPEG/MRV1/TRDN/SPON2/TACC2/PDPN/CELF1/GIB6/TMED10/LECT1/ESM1/ADAM29/CHGA/CH13L1/CHRNA1/CHRNA2/GPRIN1/FAT3/CLIN5/CCR1/SEZ6/CNP1/COI9A3/COMP/ADM/IL13RA/ORA2A1/CP51/CRABP1/ZNF358/CRYBB3/FAM101A/CSTA/SMDY1/CYLD/ESCO2/CYP11A1/DIO3/DIG3/DMBT1/ABAT/DTNAA/EEF2/EFNA2/EI/FGF1/A2M/EPHA1/ESR1/F11/FAT2/FGA/FGF10/BTD03/SBN02/FOXL1/FOXO2/EXPH5/AKR1B1/NFASC/EPB41L3/DIP2A/NEEDD4/PSD3/RYBP/MORC3/MAPK8IP2/TSSK2/VGLL2/DFNB31/PNKD/LCE2B/GATM/FGF2/NPTN/AMPD3/BMP10/FFAR2/SCG3/TMOD4/GUCT1A3/HAS1/SOX8/HLA-DOA/HLA-DPA1/NR4A1/ACACB/HOX4/HRH1/HSD11B1/HSP90A1/HTR3A/ID3/RSPO2/IGF1/IGF2/IL1R1/IL1RN/AQP2/IL12RB2/AQP5/INHBA/IRF1/AQP9/ITGA7/ITGB2/ITLJ/UJ/DPA1/KCNH2/KCNJ8/KCNMB1/KDR/AMIGO3/HESS/AFF3/LAMA3/STMN1/ORA2A/ID1R/ARHGDA1/LGALS9/LHCGR/LMNA/MCC/MFNG/MGAT1/MITF/LHX8/MYH4/MYL2/DRG1/NEU1/ATP1A2/NFATC3/NHLH2/NPCC/NRAS/OPRL1/OR2A2/SLC22A18/ATP5B/PARK2/UTP11/CL10F73/SIRT6/POE6B/ATP8A2/PTX2/PKHDI/PKM/PLA2G2A/PLAGL1/PML/RIPL1/RIPL3/PLIP/TLR9/TREM1/SSH1/FPBB1P/MXR48/BANP/PPP1CB/HERC6/ELP3/CHRNA9/PARVA/PKR1B/FTI122/ERMARD/MCTP2/CSGALNACT1/MAPK3/MAP2K2/PRO1/HTRA1/RGMA/PSMD7/SUURP1/PTGFR/PLEKHG5/TENM2/ERMN/RDH14/MARK4/ACTA2/TRIM27/RGR/BGLAP/SCY/CC111/NP3AS3/NOD2/STRA6/GZF1/DNAI2/VPS33A/BMP4/SLC8A1/BMPR1B/SLIT1/BOK/BPI/STK3/SUPT16H/BST2/ZEB1/ZEB2/TCOH/TNFAIP3/TNFRSF14/TRPC6/CCR2/TNFRSF4/WNT1/OBZAP70/ZNF7/CACNA1E/RAB7A/LST1/CAID1/ZC3H12A/C/GoF2/CALR/CAST/CAP2B/SPATA16/BFSP2/NR0B2/CASQ1/HOPX/ITBK1/TRIM63/ITIM1/CDK10/RUNX1/TP63/RUNX3/IRS2/CRADD/TNFRSF11A/SPHK1/SKAP2/STARD13/PIAS3/MAP3K6/RSAD2/CD8A/ADIPOQ/MICAL2/RAPGEF2/CD79A/FGF19	268
GO:0006928	movement of cell or subcellular component	92/590	1789/17046	6.39E-05	0.00901	0.00782	0.00782	AB11/SPON2/PDPN/CHGA/KF12/AP31/CCR1/COI9A3/KLC3/DNAH6/EFNA2/EPHA1/FAT2/SPATA13/PHACTR1/FGF10/FOXO2/NEASC/FGF22/BMP10/FFAR2/HAS1/SOX8/NR4A1/HRH1/HSP90A1/IGF1/IL1RN/IL16/ITGA7/ITGB2/ITGB7/IJUP/KDR/KIF25/LAMA3/STMN1/LCP1/ARHGDA1/LGALS9/LMNA/MCC/MYH4/MYL2/ATP1A2/NRAS/P2R16/ATP5B/PTX2/PKHDI/PTRE/TRIM27/RGS12/RPA3/CLL11/NOD2/STRA6/ARHGAP9/TMEM237/BMP4/BMPR1B/STAT3/STK3/SUPT16H/BST2/ZEB1/ZEB2/TCOH/TNFAIP3/TNFRSF14/TRPC6/CCR2/TNFRSF4/WNT1/OBZAP70/ZNF7/CACNA1E/RAB7A/LST1/CAID1/ZC3H12A/C/GoF2/CALR/CAST/CAP2B/SPATA16/BFSP2/NR0B2/CASQ1/HOPX/ITBK1/TRIM63/ITIM1/CDK10/RUNX1/TP63/RUNX3/IRS2/CRADD/TNFRSF11A/SPHK1/SKAP2/STARD13/PIAS3/MAP3K6/RSAD2/CD8A/ADIPOQ/MICAL2/RAPGEF2/CD79A/FGF19	92
GO:0042127	regulation of cell proliferation	75/590	1385/17046	6.62E-05	0.00909	0.00789	0.00789	H1/HSP90A1/IGF1/IL1RN/IL16/ITGA7/ITGB2/ITGB7/IJUP/KDR/KIF25/LAMA3/STMN1/LCP1/ARHGDA1/LGALS9/LMNA/MCC/MYH4/MYL2/ATP1A2/NRAS/P2R16/ATP5B/PTX2/PKHDI/PTRE/TRIM27/RGS12/RPA3/CLL11/NOD2/STRA6/ARHGAP9/TMEM237/BMP4/BMPR1B/STAT3/STK3/SUPT16H/BST2/ZEB1/ZEB2/TCOH/TNFAIP3/TNFRSF14/TRPC6/CCR2/TNFRSF4/WNT1/OBZAP70/ZNF7/CACNA1E/RAB7A/LST1/CAID1/ZC3H12A/C/GoF2/CALR/CAST/CAP2B/SPATA16/BFSP2/NR0B2/CASQ1/HOPX/ITBK1/TRIM63/ITIM1/CDK10/RUNX1/TP63/RUNX3/IRS2/CRADD/TNFRSF11A/SPHK1/SKAP2/STARD13/PIAS3/MAP3K6/RSAD2/CD8A/ADIPOQ/MICAL2/RAPGEF2/CD79A/FGF19	75

GO:0009719	response to endogenous stimulus	83/590	1578/17046	7.17E-05	0.00959	0.00832	<p>CDKN1C/TMEM10/CHRNA1/CHRNA2/AP351/ADM/CP51/CYP11A1/ZNF366/ABAT/AGT/EIF4G1/ESR1/FGA/FGF10/FOXC2/AKR1B1/NEDD4L/ARHGFB18/STEAP2/GATM/FGF22/NPT/M/BL/RY/SSH1/PPP1CB/CHRNA4/AQ9P/JUP/JP05/HES5/LHCGR/LMO2/MOV10/ATP1A2/NRAS/OPRL1/SIC9A3/BMP4/PRKRA3/WNT1/OB/CPEB4/CALR/NR0B2/TRIM63/RUNX1/RUNX3/RSZ/ALDH1A2/ADIPQO/RAPGEF2/FGF19/NR1H4</p> <p>ABI1/TANK/FARP1/RCAN2/MRV1/CH1L1/CCR3/SEZ6/TNFAP81/MAP3K8/ADM/IL13RA1/MI1B2/SGOLL/PPM1A1/CYLD/BHLHA15/A2M/ESR1/SPATA13/FGA/FGF10/FHIT/AKR1B1/RH119</p> <p>OBTB2/PSD3/PPP1R1B/PUIM2/ARHGEF18/MARCKIP2/TSS2/RSAGEF1/ALS2/JACOT11/PLEK2/GF22/CYTH4/BMP10/GUCY1A3/NR4A1/HRH1/IGF2/IL1RN/NHBA/KCNH2/KDR/HES5/STMI1/LCP1/ARHGDI1/LGALS9/LHCR/RAB19/MOV10/PLEKHG7/ATP1A2/NFATC3/NRAS/PARK2/PKH01/PLA2G2A/PRKAG3/PML/TLR9/TREM1/RN2/PPP1CB/MOBLA/IFT122/MCTP2/LMBRD1/PAG1/WSB2/MAPK3/MAP2K2/PAGE/PSMD7/PTGFR/PLEKHG5/TENM2/RGS21/RIT2/CCL11/NOD2/ARHGAP9/BMP4/SIC8A1/BOX/STAT2/STK3/BST2/TEAD3/TNFAP3/TNFRSF1A/TNFRSF1A/TNFRSF1A/TNFRSF1A/TNFRSF1A/CDK14/CASQ1/IFTM1/CDK11/TP63/IRS2/GRS2/TNFRSF1A/SPHK1/PRK13/STARD13/MAP3K6/AURKB/CD8A/TFPI0/ADIPQO/RAB36/RAPGEF2/IOSECL1/EGF19</p>
GO:0051179	localization	221/590	5173/17046	0.0001	0.013	0.01128	<p>ABI1/TRON/SPON2/COG5/TACC2/PDPN/TMEM10/RER1/CHGA/CH1L1/PRK3/EXOC3/CHRNA1/CHRNA2/PANX3/RB7/AP351/CCR1/SICS1B/CNP/ADM/CRABP1/PARP4/MP7/LDLR183</p> <p>AD3/KL3/ABCC13/SH3D19/CYLD/ESCO2/DDO5/ST/BHLHA15/DL2G2/DMBT1/DNAH6/ABAT/AGT/A2M/SLC10A4/EPHA1/FAT2/SPATA13/FCGR2A/PHACTR1/FGA/FGF10/TRAKE1/FOX C2/EXPH5/NFASC/EPB413/GGA3/FLOT2/MCL1/TBC1D1/NUP210/NEDD4L/SYNE1/MORC3/MAPK8IP2/SLC37A4/SAMM50/SEC13B/STEAP2/SLC17A5/BMP10/GPR26/FEAR2/GRB10/GRK4/DNAIC1/SLC9A3/HAS1/SOX8/HKI1/ANKA13/NR4A1/ACACB/HRH1/HSPA14/HSP90AB1/HTR3A/IGF1/IGF2/IL1RN/AQP2/IL16/AQP5/NHBA/AQ9P/ITGA7/ITGB2/ITGB7/JUP/KC NH2/KCNJ8/KCNJ9/KCNMB1/KDR/PO5/LAMA3/STMI1/LCP1/LDLR/LGALS9/LMNA/RAB19/MCC/ASGR1/NUBP1/ATP1A2/NFATC3/NRAS/OPRL1/SLC22A1B/P2RY6/ATP5B/ANO7/P ARK2/PCYOX1/C11orf73/SIRT6/ATP8A2/PTX2/PKH01/LRP1B/PRKAG3/PML/FXYD6/SLOC1C1/PNUP1/TLR9/TREM1/RN2/BANP/ELP3/DNAIC17/GOLPH3/SLC47A1/SLC29A3/TRPV6/SLC30A10/CHRNA9/PEX2/PARVA/PRKAR1B/IFT122/LMBRD1/POBRR/MAPK3/MAP2K2/PROC/MRAP/TRPV5/CDC42SE1/PAK6/PLEKHG5/FAM60A/TRIM27/SCY/CCL11/ABHD4/NO D2/TINAGL1/STRAG/VPS33A/BMP4/SLC4A1/ZG16/SLC6A12/SLC6A1/SLC9A3/SLC20A2/SUIT1/SRP68/SUPT6H/BST2/TGME2/TNFAIP3/TNFRSF1A/STRPC6/TRPM2/CCR2/TNFRSF4/UCP1 /ZAP70/CA7/CACNA1E/RAB7A/ZC3H12A/CALR/SLRP/DYNLRB2/SLC35A18/MFSD7/ATP13A4/NR0B2/MON1A/CASQ1/RAE1/SLC43A1/IFTM1/SCIN/SERPINA6/IRS2/ACTN1/TNFRSF1 1A/SPHK3/ENDOUJ/STY7/ESAM/SLC16A3/RSAD2/AURKB/TRIP10/ADIPQO/RAB36/NUP93/RAPGEF2/FGF19/NR1H4</p> <p>RCAN2/BHLHA15/IGF1/KDR/ATP1A2/NFATC3/MCTP2/PTGFR/TENM2/SLC8A1/ZAP70/CASQ1/SPHK1/CD8A</p>
GO:0019722	calcium-mediated signaling	14/590	125/17046	0.00011	0.01323	0.01148	14
GO:0007275	multicellular organismal development	197/590	4527/17046	0.00011	0.01323	0.01148	197
GO:0030154	cell differentiation	157/590	3469/17046	0.00012	0.01383	0.012	157
GO:0002376	immune system process	115/590	2392/17046	0.00012	0.01414	0.01226	115
GO:0008283	cell proliferation	90/590	1775/17046	0.00013	0.01455	0.01262	90

GO:0034097	response to cytokine	44/590	732/17046	0.00027	0.02402	0.02084	CH3L1/CCR1/IL13/IRA/CYP11A1/DDOST/EIF4G1/FGA/SBN02/NUP210/HLA-DPA1/HSP90A8/IL11R1/IL1RN/IL10RA/IL11RA/IL12RB2/IL15RA/IRF1/ITH4/AFF3/LGALS9/OAS2/IL21R/PARK2/PML/MAPK3/PSMD7/CCL11/STAT2/BS2/TNFRSF1A/CCR2/TNFRSF4/CARD14/TRIM63/RAE1/IFITM1/TNFRSF1A/ALDH1A2/SPHK1/CCR2/RSAD2/ADIPOQ/NUP93	44
GO:0032720	negative regulation of tumor necrosis factor production	7/590	38/17046	0.00028	0.02476	0.02148	LGALS9/TRIM27/NOD2/BPI/TNFAIP3/ZC3H12A/ADIPOQ	7
GO:0045321	leukocyte activation	40/590	647/17046	0.00029	0.02482	0.02153	CHGA/MAP3K8/IL13/IRA/CYD/DDOST/FGF10/SBN02/FLOT2/HLA-DOA/HLA-DPA1/ZC3H12D/IGF1/IGF2/INHBA/IRF1/ITGA7/ITGB2/LCP1/LGALS9/NFATC3/IL21R/APBB1P/PAG1/PTPRE/NOD2/BMP4/BPI/SUPT6H/BS2/ZEB1/TNFAIP3/CCR2/TNFRSF4/ZAP70/IST1/Z	40
GO:0043207	response to external biotic stimulus	47/590	802/17046	0.0003	0.02482	0.02153	CH312A/IRS2/SKAP2/RSAD2/CD8A/CD79A	47
GO:0051707	response to other organism	47/590	802/17046	0.0003	0.02482	0.02153	SPON2/GJB6/HNRNPUL1/CHGA/CNP/ADM/CPS1/CYP11A1/DMBT1/FGA/FGF10/SBN02/PUM2/SIC37AA/GUCY1A3/IL1RN/IL10RA/IL12RB2/IRF1/KCNJ8/STMN1/LGALS9/OAS2/PLA2G2A/PML/TLR9/TREM1/MAPK3/HTRA3/SLAMF8/PTGFR/CREBZF/ACTA2/CCL11/NOD2/BPI/STAT2/BS2/TNFAIP3/TNFRSF1A/CA7/ZC3H12A/IFITM1/TNFRSF1A/RSAD2/CD8A/NU	47
GO:0035295	tube development	37/590	585/17046	0.00032	0.02592	0.02248	2G2A/PML/TLR9/TREM1/MAPK3/HTRA3/SLAMF8/PTGFR/CREBZF/ACTA2/CCL11/NOD2/BPI/STAT2/BS2/TNFAIP3/TNFRSF1A/CA7/ZC3H12A/IFITM1/TNFRSF1A/RSAD2/CD8A/NU	37
GO:0071407	cellular response to organic cyclic compound	26/590	359/17046	0.00033	0.0268	0.02325	PDPN/CHI3L1/ADM/CPS1/ZNF358/ESR1/FGF10/FOXO1/FOXO2/AKR1B1/SOX8/HSD11B1/RSP02/IGF1/AQP2/KDR/HESS/NFATC3/C11orf73/PTX2/PML/FT122/MAPK3/MAP2K2/SCT	26
GO:1903556	negative regulation of tumor necrosis factor superfamily cytokine production	7/590	40/17046	0.0004	0.03098	0.02687	/CCL11/STR46/GZF1/BMP4/SIC8A1/STK3/ZEB1/TGM2/HOPX/TP63/ALDH1A2/MICAL2	7
GO:0016337	single organismal cell-cell adhesion	40/590	657/17046	0.0004	0.03098	0.02687	RAPGEF2/NR1H4	40
GO:1901701	cellular response to oxygen-containing compound	54/590	975/17046	0.00043	0.03269	0.02886	CDH9/PDPN/PRK3/MAP3K8/CSTA/CYLD/DDOST/FGA/NFASC/FLOT2/HLA-DOA/HLA-DPA1/ZC3H12D/IGF1/IGF2/IL1RN/IRF1/ITGA7/ITGB2/ITGB7/JUP/ICP1/LGALS9/NFATC3/PKH2/APPB1P/FBLIM1/PARVA/PAG1/TENM2/NOD2/BMP4/ZEB1/CCR2/TNFRSF4/ZAP70	54
GO:0042221	response to chemical	169/590	3882/17046	0.00043	0.03269	0.02836	Y6/PARK2/PRKAG3/TLR9/SSH1/PRKARI1B/LMBRD1/MAPK3/MAP2K2/PSMD7/PTGFR/PTPRE/BGLAP/NOD2/SIC8A1/ZEB1/TNFAIP3/TRPG6/WNT10B/CACNA1E/ZC3H12A/CPEB4/TRIM63/IRS2/ALDH1A2/ADIPOQ/RAPGEF2/FGF19/NR1H4	169
GO:0098609	cell-cell adhesion	47/590	816/17046	0.00044	0.03275	0.02841	CDKN1C/SPON2/GJB6/TMED10/LECT1/CHGA/CH3L1/ERLIN2/EGLIN2/CHRNA1/CHRNA2/AP3S1/CCR1/CNP/CO19A3/ADM/IL13/IRA/ORA2A14/CPS1/PARP4/CYP11A1/DDOST/ZNF366/BHLHA15/ABAT/AGXT/EFNA2/EIF4G1/EPHA1/ESR1/FGA/FGF10/SBN02/FOXO2/AKR1B1/NFASC/MICL1/NUP210/NEEDD4/ARHGFB18/STEA2/PATM/FGF22/NPTN/BMP10/FFAR2/GRB10/GUCY1A3/HAS1/HLA-DPA1/NR4A1/HRH1/HSP1A1/HSP90A81/HTR3A/IGF2/LCE1D/IL1R1/IL1RN/IL10RA/AQP2/IL11RA/IL12RB2/IL15RA/IL15/INHBA/IRF1/AQP9/ITGB2/ITH4/JUP/KCNH2/KCNMB1/KDR/PO5/HESS/AFF3/ORA2A5/ARHGDI1/LGALS9/LHGR/LMNA/ILMO2/MOV10/ATP1A2/NFATC3/NPPC/NRAS/OAS2/OPRL1/ORA32/SLC22A18/P2RY6/IL12R/PARK2/PTX2/PKM/PRKAG3/PML/TLR9/TREM1/SSH1/CYP21A1/CYC30A10/CHRNA2/PARVA/PRKARI1B/LMBRD1/MAPK3/MAP2K2/HTRA3/SLAMF8/IGM1/PSMD7/PTGFR/PLEKHG5/TENM2/PTPRE/RTT2/BGLAP/CCL11/NOD2/BMP4/SLC8A1/SLC9A3/BMPRI1B/SIT1/SRP68/STAT2/BS2/ZEB1/TERF1/TNFAIP3/TNFRSF1A/TRPG6/TRPM2/CCR2/TNFRSF4/WNT10B/CACNA1E/RAB7A/CARD14/ZC3H12A/CPEB4/CALR/NR0B2/CASQ1/TRIM63/RAE1/IFITM1/RUNX1/RUNX3/IRS2/TNFRSF1A/ALDH1A2/SPHK1/HSPB3/CCR2/RSAD2/ADIPOQ/NUP93/RAPGEF2/FGF19/NR1H4	47

GO:0012501	programmed cell death	85/590	1718/17046	0.00045	0.03278	0.02844	8/GJB6/CH13L1/EGLN2/CARD16/COMP/MAP3K8/ADM/IL31RA/CYLD/DBB1/ESR1/FGA/FGF10/FHIT/FOXK2/EPBA41L3/DIP2A/PPP1R13B/ARHGFE18/RYBP/RNF144B/GAS2/BMP10/SOX10/HSP90A81/ID3/IGF1/IL1RN/NHBA/IRE1/JTGB2/KDR/ARHGDI2/LGALS9/LMNA/MPZ/PAFAH1B/PARK2/UTP11L/PKH11/PKML/PLAGL1/PKML/PPP2R2B/MAPK3/PROC/PAN6/PSMD7/PTGFR/PLEKHG5/MARK4/SCT/NOD2/BMP4/BMPR1B/BOK/STK3/TERF1/TGM2/TNFAP3/TNFRSF1A/TRAFS/TNFRSF1A/WNT10B/CARD14/BCL2L14/FAM188A/ZC3H12A/CPEB4/CLPTM11/CAUR/CAS1/SCIN/TP63/RUNX3/IRS2/ACTN1/CRADD/ALDH1A2/SPHK1/IMAP3K6/AURKB/DAPL1/ADIPQO/RAPGEF2	85
GO:0008643	carbohydrate transport	16/590	178/17046	0.00047	0.03419	0.02966	NUP210/SLC37A4/GRB10/HK1/IGF1/AQP2/AQP5/AQP9/SIRT6/PRKAG3/LMBRD1/RAE1/IRS2/ADIPQO/NUP93/FGF19	16
GO:0071345	cellular response to cytokine stimulus	39/590	642/17046	0.00049	0.03474	0.03014	CH13L1/CCR1/IL31RA/CYP11A1/EIF4G1/FGA/SBNO2/NUP210/HLA-DPA1/HSP90A81/IL1LR1/IL1RN/IL1ORA/IL1LR2/IL1LRA/IRF1/GALS9/OAS2/IL21R/PARK2/PML/MAPK3/PSMD7/CCL11/STAT2/BST2/TNFRSF1A/CCR2/TNFRSF4/CARD14/RAE1/IFITM1/TNFRSF11A/SPHK1/CR2/RSAD2/ADIPQO/NUP93	39
GO:0042476	odontogenesis	12/590	112/17046	0.0005	0.03474	0.03014	ADM/FGF10/ID3/RSPO2/AQP5/NHBA/HX8/PTX2/HITRA1/BGLAP/BMP4/TP63	12
GO:0046660	female sex differentiation	12/590	112/17046	0.0005	0.03474	0.03014	COL9A3/ESR1/FGF10/NHBA/KDR/LHCGR/LHX8/PTX2/STR46/BMP4/BMPR1B/TP63	12
GO:0042592	homeostatic process	73/590	1434/17046	0.00053	0.03633	0.03152	TRDN/GJB6/EGLN2/CHRNA1/CLN5/CCR1/ADM/IL31RA/CP51/DBB1/BHLHA15/ABAT/ESR1/AKR1B1/NEEDD4/SLC37A4/DFNB31/STEAP2/NPTN/AMPD3/FFAR2/HK1/NMIE9/IGF1/IL1R1/IL1RN/AQP2/AQP5/NHBA/AQP9/KCNH2/KDR/LDLR/LGALS9/NUP93/ATP1A2/OPRL1/ATP5B/PARK2/SIRT6/PDE6B/PKH1D1/PML/TLR9/SLC30A10/CHRNA9/PRKAR1B/SLAMF8/RFC2/RP3/BGLAP/CCL11/ABHD4/NOD2/BMP4/SLC4A1/SLC9A3/TERF1/TGM2/TNFAP3/TRPC6/CCR2/CA7/CACNA1E/RAB7A/CALR/ATP13A4/CA5Q1/TP63/IRS2/TNFRSF11A/ADIPQO	73
GO:1901698	response to nitrogen compound	53/590	961/17046	0.00054	0.03646	0.03163	TMED10/CHRNA1/CHRNA2/AP3S1/ADM/CP51/CYP11A1/ABAT/AGXT/EIF4G1/FGA/FGF10/FOXK2/AKR1B1/GATM/FGF22/GRB10/NRAA1/HRH1/HTR3A/IGF2/IL1LR1/IL1RN/AQP9/JU1/P/KCN18/IP05/ATP1A2/NRAS/PARK2/PKM/PRKAG3/TLR9/SSH1/CHRNA9/PRKAR1B/LMBRD1/MAPK3/MAP2K2/PSMD7/PTPRE/NOD2/BMP4/SLC8A1/ZEBI1/TNFAP3/WNT10B/CPEB4/IRS2/ADIPQO/RAPGEF2/FGF19/NR1H4	53
GO:0050793	regulation of developmental process	94/590	1953/17046	0.00055	0.03646	0.03163	PDPN/CELF1/ECT1/CH1L1/CCR1/SEZ6/ADM/FAM101A/SMYD1/SH3D19/CYLD/BHLHA15/DIO3/DMBT1/EIF4G1/EPHA1/ESR1/FGA/FGF10/FOXK2/EPBA41L3/FLOT2/NEEDD4/ARHGE F18/GAS2/NPTN/BMP10/SOX8/HLA-D0A/ACACB/ID3/RSPO2/IGF1/IL1RN/NHBA/IRE1/JTGA7/TGB2/JUP/KDR/AMIGO3/HESS/LAMA3/ARHGDI2/GALS9/LMNA/MITF/NEU1/NPPC/NRAS/PARK2/ATP8A2/PLA2G2A/PM L/SSH1/FB1L1M1/PALMD/PARVA/JFT122/MAP2K2/CDC42SE1/ERMN/BGLAP/CC111/WP33A/BMP4/SBC8A1/BMPR1B/SULT1/STK3/SUPT6H/ZEBI1/TEAD3/TNFAP3/TNFRSF1A/CCR2/WNT10B/ZAP70/LST1/ZC3H12A/CALR/CAPZB/HOPX/ITTBK1/IFITM1/SCIN/RUNX3/SPHK1/PIAS2/CBFA2T2/ADIPQO/RAPGEF2	94
GO:0010243	response to organonitrogen compound	50/590	893/17046	0.00055	0.03646	0.03163	TMED10/CHRNA1/CHRNA2/AP3S1/ADM/CP51/CYP11A1/ABAT/AGXT/EIF4G1/FGA/FGF10/FOXK2/AKR1B1/GATM/FGF22/GRB10/NRAA1/HRH1/HTR3A/IGF2/IL1LR1/IL1RN/AQP9/JUP/PO5/ATP1A2/NRAS/PARK2/PKM/PRKAG3/TLR9/SSH1/CHRNA9/PRKAR1B/LMBRD1/MAPK3/MAP2K2/PSMD7/PTPRE/NOD2/SLC8A1/ZEBI1/TNFAP3/WNT10B/CPEB4/IRS2/ADIPQO/RAP GEF2/FGF19/NR1H4	50
GO:0060439	trachea morphogenesis	4/590	12/17046	0.00056	0.0367	0.03184	RSPO2/MAPK3/MAP2K2/BMP4	4
GO:1901700	response to oxygen-containing compound	74/590	1462/17046	0.00057	0.0367	0.03184	SPO2/GJB6/AP3S1/CNF/ADM/CP51/CYP11A1/ABAT/AGXT/EIF4G1/ESR1/FGA/FGF10/SBNO2/FOXK2/AKR1B1/MLC1/GATM/FGF22/FFAR2/GRB10/NRAA1/HTR3A/IGF2/IL1LR1/IL1R 1/IL1LRA/AQP2/IL12RB2/NHBA/AQP9/JUP/KCN18/IP05/LGALS9/ATP1A2/NPPC/NRAS/OPRL1/P2R/6/PARK2/PKM/PRKAG3/TLR9/SSH1/PRKAR1B/LMBRD1/MAPK3/MAP2K2/PSM D7/PTGFR/PTPRE/BGLAP/NOD2/BMP4/SLC8A1/ZEBI1/TNFAP3/TRPC6/TRPM2/WNT10B/CACNA1E/ZC3H12A/CPEB4/CALR/NR0B2/TRIM63/IRS2/TNFRSF11A/ALDH1A2/ADIPQO/RA PGEF2/FGF19/NR1H4	74
GO:0009100	glycoprotein metabolic process	28/590	413/17046	0.00058	0.03674	0.03187	GNZ/LECT1/GALNT15/SLC51B/NEU4/EGF/LAM/PAAP4/B3GLCT/MGAT5B/DDOST/TRAK1/FOXJ1/ST6GALNAC3/GBGT1/SLC17A5/EOGT/IGF1/MUC21/MGAT1/NEU1/OAS2/SPOCK3/C 28 HST15/SIRT6/CSGALNACT1/BMPR1B/MOGS/CALR	28
GO:0048522	positive regulation of cellular process	183/590	4283/17046	0.00059	0.03674	0.03187	AB11/CDKN1C/TRDN/PDPN/RER1/ESM1/CH13L1/ERLUN2/CCR1/SLC51B/SEZ6/MAP3K8/ADM/IL31RA/EGFLAM/MI2B/MPP7/SMYD1/SH3D19/CYLD/DBB1/BHLHA15/DMBT1/ABAT/E EF2/EIF4G1/EPHA1/ESR1/FGA/FGF10/SBNO2/FOXK2/EXPH5/AKR1B1/FLOT2/NEEDD4/PUM2/ARHGEF18/MAPK8IP2/NGL2/RNF144B/PABPC1/DNAJC2/FGF22/NPTN/BMP10/GPR2 6/FFAR2/GRB10/GUCT1A3/SOX8/HK1/HLA-DPA1/ANXA13/NR4A1/ACACB/HRH1/HSPA11/HSP90A81/TFAP2E/ID3/RSPO2/IGF1/IGF2/IL1RN/IL12RB2/FOXK2/NHBA/IRE1/JUP/KCNH2/KDR/IP05/AMIGO3/HESS/STMN1/LCP1/L DLR/ARHGDI2/LGALS9/LHCGR/LMNA/LMO2/MC2R/MFNG/MITF/NEU1/NFATC3/NH1H2/NPPC/NRAS/OPRL1/P2RY6/PARK2/UTP11L/PRR16/PARK2/PTX2/PKH1D1/PLA2G2A /PLAGL1/PML/TLR9/APPB1P/BANP/ELP3/GOLPH3/FANG/PRKAR1B/PAG1/MAPK3/MAP2K2/MRAP/HITRA1/PARK6/ARNTL2/RGMM/PSMD7/PTGFR/PLEKHG5/TENM2/MARK4/TRIM 27/SC1/CCL11/NP3AS1/NOD2/BMP4/ZNF649/SLC8A1/BMPR1B/BOK/STK3/SUPT6H/ZEBI1/TEAD3/TERF1/TGM2/TNFAP3/TNFRSF1A/TRAFS/TRPC6/CCR2/TNFRSF4/WN T10B/ZAP70/CA7/RAB7A/CARD14/BCL2L14/CSPP1/ZC3H12A/CALR/NR0B2/HOPX/IFITM1/SCIN/CDK10/RUNX1/TP63/RUNX3/IRS2/CRADD/TNFRSF11A/ALDH1A2/SPHK1/SKAP2/P R C1/PIAS2/MAP3K6/SYTY/CBFA2T2/RSAD2/AURKB/CDBA/ADIPQO/MICAL2/RAPGEF2/FGF19/NR1H4	183

GO:0048731	system development	173/590	4014/17046	0.00059	0.03674	0.03187	0.03187	0.03187	0.03187	173	AB11/FARP1/CDKN1C/SPEG/SPON2/TAC2/PDPN/G1B6/TMED10/LECT1/ESM1/CH131/CHRNA1/GPRIN1/CLN5/CCR1/SEZ6/CNP/COL9A3/COMP/ADM/IL13RA/CP51/ZNF358/FAM101A/CSTA/SMYD1/CYLD/ESCO2/CYP11A1/DLG2/EEF2/EFNA2/EIF4A1/EPHA1/ESR1/FGA/FGF10/FOXC2/EXP5/AKR1B1/INFASC/EPB41.3/NEEDD4L/PSD3/MA PK8IP2/VGLL2/DFNB31/CEZB/GATM/FGF22/NPTN/BMP10/SOX8/HLA-DOA/NRA41/ACAC8/HOXC4/HSD11B1/HSP90A81/ID3/RSPD2/IGF1/IGF2/CE1C/LEC1D/LEE2D/AQP2/AQP5/INHBA/RUF1/ITGA7/IVL/JUP/KCNJ8/KOR/AMIGO3/HES5/STWN1/ARHG DIA/GALS9/LHCGR/LMNA/LMO2/MC2R/MITF/LHX8/MYL2/NEU1/NFATC3/INH1L2/NPPC/NRAS/ATP5B/PARK2/UTP11/CL1orf73/SIRT6/PDE6B/ATP8A2/PTX2/PKHD1/PKM/PLA6L 1/PML/RIPPLY/SSH1/AMK8A8/HERC6/ELP3/CHRNA9/PARVA/IFT1.22/CSGALNACT1/MAPK3/MAP2C/HTRA1/EGMA/PSMD7/TEMND1/MARK4/MAC2A2/BGLAP/SC7/CLL11/STRAG/GZF 1/VPS33A/BMP4/SILC8A1/BMPRI1B/SULT1/BOX/STK3/SUPT6H/ZEB1/TGMD2/TCHH/TNFAP3/TRPC6/CCR2/ZAP70/LTI/ZC3H12A/C6orf25/CALR/CAST/BFSP2/NROB2/CASQ 1/HOPX/TTRK1/SCIN/RUNX1/TP63/RUNX3/IRS3/ACTN1/TNFRSF11A/ADH1A2/SPHK1/CBFA2T2/RSAD2/CD8A/ADIPOQ/MICAL2/RAPGEF2/CD79A/FGF19
GO:0009966	regulation of signal transduction	110/590	2366/17046	0.00063	0.03856	0.03345	0.03345	0.03345	0.03345	110	FARP1/RCAN2/CDKN1C/LECT1/ESM1/CH131/CCR1/SEZ6/TNFAP8L1/MAP3K8/ADM/IL13RA/MIB2/MPP7/CYLD/ZNF366/ABAT/AZM/ESR1/SPATA13/FGA/FGF10/FOXLI1/AKR1B1/RHOBTB 2/NEED4L/PSD3/PUM2/ARHGFE18/MAPK8IP2/ALS2C/FGF22/NPTN/CYTH4/BMP10/GRB10/HSP90A81/RSPO2/IGF1/IGF2/IL1RN/INHBA/IRF1/JUP/KDR/HES5/ARHGDA/LGALS9/L HCGR/LMNA/MCC/MFNG/PLEKHG5/NRAS/PARK2/PDE6B/PKHD1/PLA2G2A/PML/TLR9/PPP1CB/IFT122/LMBRD1/PAG1/MAPK3/MAP2K2/HTRA1/PAG1/PAG6/PSMD7/PTPRE/RGS12/SC7/CLL11/NOD2/ARHGAP9/TMEM237/BMP4/BMPRI1B/STAT2/STK3/BST2/ZEB1/TNFAP3/TNFRSF1A/TRAFA5/WNT10B/ZAP70/RAB7A/CARD14/BCL2L14/CALR/CMAHP/CDK10/R UNX1/TP63/RUNX3/IRS2/CRADD/TNFRSF11A/SPHK1/SKAP2/STARD13/PIAS2/MAP3K6/RSAD2/CD8A/TRIP10/ADIPOQ/RAPGEF2/IOSECI/FGF19
GO:005082	cellular chemical homeostasis	37/590	607/17046	0.00064	0.03865	0.03353	0.03353	0.03353	0.03353	37	TRDN/G1B6/CLN5/CCR1/ADM/ESR1/NEED4L/NPTN/HK1/IL1R1/AQP2/AQP5/AQP9/NUBP1/ATP1A2/OPRL1/ATP5B/PDE6B/PKHD1/PML/SLC30A10/CHRNA9/SLAMF8/CLL11/BMP4/SLC4A1/SLC8A1/TGM2/TRPC6/CCR2/CA7/CACNA1E/RAB7A/CALR/ATP13A4/CASQ1/RS2
GO:1900034	regulation of cellular response to heat	9/590	70/17046	0.00066	0.03984	0.03456	0.03456	0.03456	0.03456	9	NUP210/DNAJC2/HSPA1L/HSP90A81/CL1orf73/MAPK3/RAB3/RAE1/NUP93
GO:0010646	regulation of cell communication	124/590	2731/17046	0.00068	0.04006	0.03475	0.03475	0.03475	0.03475	124	FARP1/RCAN2/CDKN1C/TRDN/LECT1/ESM1/CH131/CCR1/SEZ6/TNFAP8L1/MAP3K8/ADM/IL13RA/MIB2/MPP7/CYLD/ZNF366/ABAT/AZM/ESR1/SPATA13/FGA/FGF10/FOXLI1/AKR 1B1/RHOBTB2/NEEDD4L/PSD3/PUM2/ARHGFE18/MAPK8IP2/ALS2C/PKNO2/FGF22/NPTN/CYTH4/BMP10/GRB10/HSP90A81/RSPO2/IGF1/IGF2/IL1RN/INHBA/IRF 1/JUP/KDR/HES5/ARHGDA/LGALS9/LHCGR/LMNA/MCC/MFNG/PLEKHG7/ATP1A2/NRAS/PARK2/PDE6B/PKHD1/PLA2G2A/PML/TLR9/PPP1CB/PRKAR1B/IFT122/LMBRD1/PAG1/M APK3/MAP2K2/HTRA1/PAG6/PSMD7/PLEKHG5/PTPRE/RGS12/SC7/CLL11/NOD2/ARHGAP9/TMEM237/BMP4/SLC8A1/BMPRI1B/STAT2/STK3/BST2/ZEB1/TNFAP3/TNFRSF1A/TRAFA 5/WNT10B/ZAP70/CA7/CACNA1E/RAB7A/CARD14/BCL2L14/CALR/CMAHP/NR0B2/CDK10/RUNX1/TP63/RUNX3/IRS2/CRADD/TNFRSF11A/SPHK1/SKAP2/STARD13/PIAS2/MAP3K6 /SYT7/RSAD2/CD8A/TRIP10/ADIPOQ/RAPGEF2/IOSECI/FGF19
GO:0001763	morphogenesis of a branching structure	17/590	203/17046	0.00072	0.04146	0.03597	0.03597	0.03597	0.03597	17	ADM/ESR1/FGF10/FOXC2/SOX8/RSPO2/IGF1/KOR/NFATC3/PTX2/PML/ERMIN/CLL11/GZF1/BMP4/TGM2/TP63
GO:0005975	carbohydrate metabolic process	47/590	835/17046	0.00072	0.04146	0.03597	0.03597	0.03597	0.03597	47	GNE/CH131/CH132/GALNT15/CLN5/SLC51B/NEU4/CP51/PAR8A/B3GLCT/MGAT5B/DOOST/ENOD2/TRAK1/AKR1B1/NUP210/SLC37A4/ST6GALNA3/GBGT1/SLC17A5/DHHD/EOGT/GRB10/HAS1/HK1/HRH1/IGF1/IGF2/MUC21/LHCGR/MGAT1/NEU1/OAS2/PARK2/CHST15/SIRT6/PKM/PRKAG3/PPP1CB/CSGALNACT1/MOGS/CALR/RAE1/RS2/STBD1/ADIPOQ/NU P93
GO:0023051	regulation of signaling	122/590	2685/17046	0.00073	0.04146	0.03597	0.03597	0.03597	0.03597	122	FARP1/RCAN2/CDKN1C/TRDN/LECT1/ESM1/CH131/CCR1/SEZ6/TNFAP8L1/MAP3K8/ADM/IL13RA/MIB2/MPP7/CYLD/ZNF366/ABAT/AZM/ESR1/SPATA13/FGA/FGF10/FOXLI1/AKR 1B1/RHOBTB2/NEEDD4L/PSD3/PUM2/ARHGFE18/MAPK8IP2/ALS2C/PKNO2/FGF22/NPTN/CYTH4/BMP10/GRB10/HRH1/HSP90A81/RSPO2/IGF1/IGF2/IL1RN/INHBA/IRF1/JU P/KDR/HES5/ARHGDA/LGALS9/LHCGR/LMNA/MCC/MFNG/PLEKHG7/ATP1A2/NRAS/PARK2/PDE6B/PKHD1/PLA2G2A/PML/TLR9/PPP1CB/PRKAR1B/IFT122/LMBRD1/PAG1/MAPK3 /MAP2K2/HTRA1/PAG6/PSMD7/PLEKHG5/PTPRE/RGS12/SC7/CLL11/NOD2/ARHGAP9/TMEM237/BMP4/BMPRI1B/STAT2/STK3/BST2/ZEB1/TNFAP3/TNFRSF1A/TRAFA5/WNT10B/Z AP70/CA7/CACNA1E/RAB7A/CARD14/BCL2L14/CALR/CMAHP/NR0B2/CDK10/RUNX1/TP63/RUNX3/IRS2/CRADD/TNFRSF11A/SPHK1/SKAP2/STARD13/PIAS2/MAP3K6/SYT7/RSAD2 /CD8A/TRIP10/ADIPOQ/RAPGEF2/IOSECI/FGF19
GO:0002694	regulation of leukocyte activation	27/590	399/17046	0.00074	0.04146	0.03597	0.03597	0.03597	0.03597	27	MAP3K8/IL13RA/CYLD/FGF10/FT02/HLA-DOA/HLA-DPA1/ZC3H12D/IGF1/IGF2/INHBA/IRF1/LGALS9/PAG1/PTPRE/NOD2/BMP4/BPI/USPT6H/ZEB1/TNFAP3/CCR2/TNFRSF4/ZAP70/LTI/ZC3H12A/RS2
GO:0014070	response to organic cyclic compound	44/590	768/17046	0.00074	0.04146	0.03597	0.03597	0.03597	0.03597	44	CHRNA1/CHRNA2/ADM/CP51/CYP11A1/ZNF366/ABAT/AGCT/ESR1/FGA/FGF10/MLC1/GUCY1A3/NR4A1/HRH1/HSP90A81/HTR3A/IL1RN/INHBA/AQP9/JUP/KCNJ8/ATP1A2/OPRL1 /P2RY6/PARK2/SSH1/CHRNA9/MAPK3/PTGFR/BGLAP/NOD2/BMP4/SILC8A1/SLC9A3/WNT10B/CALR/NROB2/TRIM63/RAE1/ALDH1A2/ADIPOQ/RAPGEF2/NR1H4
GO:0009607	response to biotic stimulus	47/590	837/17046	0.00076	0.04146	0.03597	0.03597	0.03597	0.03597	47	SPON2/G1B6/HNRNPUL1/CHGA/CNP/ADM/CP51/CYP11A1/DMBT1/FGA/FGF10/SBNO2/PUM2/SLC37A4/GUCY1A3/IL1RN/IL10RA/IL12RB2/IRF1/KCNJ8/STWN1/LGALS9/OAS2/PLA 2G2A/PML/TLR9/TREM1/MAPK3/HTRA1/SLAMF8/PTGFR/CREBZF/ACT2/CLL11/NOD2/BPI/STAT2/BST2/TNFAP3/TNFRSF1A/CA7/ZC3H12A/IFTM1/TNFRSF11A/RSAD2/CD8A/NU P93
GO:0043031	negative regulation of macrophage activation	3/590	6/17046	0.00076	0.04146	0.03597	0.03597	0.03597	0.03597	3	IL131RA/BPI/ZC3H12A

GO:0002695	negative regulation of leukocyte activation	13/590	1134/17046	0.00077	0.04146	0.03597	IL131RA/CYLD/ZC3H12D/INHBA/IRF1/LGALS9/PAG1/BMP4/BR1/TNFNFAIP3/CCR2/LST1/ZC3H12A	13
GO:0046649	lymphocyte activation	34/590	548/17046	0.00077	0.04146	0.03597	MAP3K8/CYLD/DDOST/FGF10/FLOT2/HLA-DOA/HLA-DPA1/ZC3H12D/IGF1/IGF2/INHBA/IRF1/ITGB2/LCP1/LGALS9/NEFATC3/IL21R/APBB1/PAG1/NOD2/BMP4/SUPT6H/BST2/ZEB1/TNFNFAIP3/CCR2/TNFRSF4/ZAP70/LST1/IRS2/SKAP2/RSAD2/CD8A/CD79A	34
GO:0006915	apoptotic process	83/590	1700/17046	0.00078	0.04175	0.03622	8/HS90AB1/D3/IGF1/IL1RN/INHBA/IRF1/ITGB2/KDR/ARHGDI1/LGALS9/LMNA/MPZ/PAFAH2/PARK2/UTP11/PKH1/PLAGL1/PVLP/PPP2R2B/MAPK3/PROC/PAK6/PSMD7/PTGER/PLEKHG5/SCT/NOD2/BMP4/BMP4/BR1/BOK/STK3/TERF1/TGM2/TNFNFAIP3/TRA5/TNFRSF14/TRA5/TNFRSF4/IVNT10B/CARD14/BCL2L14/FAM188A/ZC3H12A/CPEB4/CLPTM11/CALR/CAS/T/SCIN/TP63/RUNX3/IRS2/ACTN1/CRADD/ALDH1A2/SPHK1/MAP3K6/AURKB/DAPL1/ADIPOQ/RAPGEF2	83
GO:0048286	lung alveolus development	7/590	45/17046	0.00083	0.04378	0.03798	PDN/FGF10/IGF1/KDR/STRA6/BMP4/HOPX	7
GO:0048367	regulation of programmed cell death	67/590	1314/17046	0.00087	0.04516	0.03918	EGLN2/CARD16/COMP/MAP3K8/ADM/IL31RA/CYLD/DBI/ESR1/FGA/FGF10/FOXO2/DIP2A/ARHGEF18/BMP10/SOX8/HS90AB1/ID3/IGF1/IL1RN/INHBA/KDR/ARHGDI1/LGALS9/ILMNA/MTF/MPZ/PAFAH2/PARK2/UTP11/PKH1/PVLP/PROX1/PAK6/PSMD7/PTGER/PLEKHG5/MARK4/BMP4/BR1/BOK/STK3/TERF1/TGM2/TNFNFAIP3/TRA5/TNFRSF4/WNT10B/CARD14/BCL2L14/CPEB4/CALR/CAS/T/SCIN/TP63/RUNX3/IRS2/ACTN1/CRADD/ALDH1A2/SPHK1/MAP3K6/AURKB/ADIPQ/RAPGEF2	67
GO:1901137	carbohydrate derivative biosynthetic process	42/590	729/17046	0.00087	0.04516	0.03918	IGNE/ACOT7/GALNT15/SIC51B/NEU4/ADM/PARP4/B3GCT/MGAT5B/DDOST/TRAK1/FOXO1/ST6GALNAC3/GBGT1/SLC17A5/AMIP3/EOGT/GUCY1A3/HAS1/ACACB/NME9/IGF1/MIUC21/LHCGR/MC2R/MGAT1/NEU1/NPPC/OAS2/OPRL1/ATP5B/CHST15/SIRT6/PKM/CSGALNACT1/MRAP/SCT/BMP4/BR1/BOK/STK3/TERF1/TGM2/TNFNFAIP3/TRA5/TNFRSF4/IVNT10B/CARD14/BCL2L14/FAM188A/ZC3H12A/CPEB4/CLPTM11/CALR/CAS/T/SCIN/TP63/RUNX3/IRS2/ACTN1/CRADD/ALDH1A2/SPHK1/MAP3K6/AURKB/DAPL1/ADIPOQ/RAPGEF2	42
GO:0061138	morphogenesis of a branching epithelium	16/590	189/17046	0.00091	0.04523	0.03924	ADM/ESR1/FGF10/FOXO2/SOX8/RSPO2/IGF1/KDR/NEFATC3/PTX2/PML/CCL11/GZF1/BMP4/TGM2/TP63	16
GO:0071417	cellular response to organonitrogen compound	37/590	619/17046	0.00091	0.04523	0.03924	AP3S1/CP51/CYP11A1/EI4/FGF10/FOXO2/AKR1B1/FGF2/GRB10/NRA41/HRH1/IGF2/IL1RN/AQP9/IJUP/PO5/NRAS/PARK2/PRKAG3/TLR9/SSH1/PRKAR1B/LMBRD1/MAPK3/MAP2K2/PSMD7/PTPRE/NOD2/SLC8A1/ZEB1/WNT10B/CPEB4/IRS2/ADIPQ/RAPGEF2/FGF19/NR1H4	37
GO:0001775	cell activation	48/590	868/17046	0.00093	0.04523	0.03924	CHGA/MAP3K8/IL31RA/CYLD/DDOST/A2M/FGA/FGF10/SBN2/FLOT2/SCG3/HLA-DOA/HLA-DPA1/ZC3H12D/IGF1/IGF2/INHBA/IRF1/ITGB2/LCP1/LGALS9/NEFATC3/IL21R/APBB1/PAG1/MAPK3/SLURP1/PTPRE/NOD2/BMP4/BR1/SUPT6H/BST2/ZEB1/TNFNFAIP3/TRPC6/CCR2/TNFRSF4/ZAP70/LST1/ZC3H12A/CAS/T/SCIN/TP63/RUNX3/IRS2/ACTN1/CRADD/ALDH1A2/SPHK1/MAP3K6/AURKB/ADIPQ/RAPGEF2	48
GO:0061061	muscle structure development	34/590	554/17046	0.00093	0.04523	0.03924	SPEG/CHRNA1/ADM/SWYD1/BHLHA15/FGF10/FOXO2/FLOT2/SCG3/HLA-DOA/HLA-DPA1/ZC3H12D/IGF1/IGF2/INHBA/IRF1/ITGB2/LCP1/LGALS9/NEFATC3/IL21R/APBB1/PAG1/MAPK3/SLURP1/PTPRE/NOD2/BMP4/BR1/SUPT6H/BST2/ZEB1/TNFNFAIP3/TRPC6/CCR2/TNFRSF4/ZAP70/LST1/ZC3H12A/CAS/T/SCIN/TP63/RUNX3/IRS2/ACTN1/CRADD/ALDH1A2/SPHK1/MAP3K6/AURKB/ADIPQ/RAPGEF2	34
GO:0009101	glycoprotein biosynthetic process	25/590	364/17046	0.00093	0.04523	0.03924	GNE/GALNT15/SLC51B/NEU4/PARP4/B3GCT/MGAT5B/DDOST/TRAK1/FOXO1/ST6GALNAC3/GBGT1/SLC17A5/AMIP3/EOGT/GUCY1A3/HAS1/ACACB/NME9/IGF1/MIUC21/BMP4/BR1/BOK/STK3/TERF1/TGM2/TNFNFAIP3/TRA5/TNFRSF4/IVNT10B/CARD14/BCL2L14/FAM188A/ZC3H12A/CPEB4/CLPTM11/CALR/CAS/T/SCIN/TP63/RUNX3/IRS2/ACTN1/CRADD/ALDH1A2/SPHK1/MAP3K6/AURKB/DAPL1/ADIPOQ/RAPGEF2	25
GO:0070374	positive regulation of ERK1 and ERK2 cascade	14/590	154/17046	0.00094	0.04523	0.03924	CH3L1/CCR1/FGA/FGF10/KDR/LGALS9/PLA2G2A/MAPK3/CCL11/NOD2/BMP4/TNFRSF14/RAPGEF2/FGF19	14
GO:0030036	actin cytoskeleton organization	32/590	511/17046	0.00094	0.04523	0.03924	AB11/FAM101A/EPHA1/PHACTR1/FGF10/MSRB2/EPB41L3/ARHGEF18/PLEK2/BMP10/TMO4/LCP1/MYL2/PARK2/SSH1/PARVA/TTC17/PAK6/ERMIN/TRIM27/CCL11/PARVG/BST2/CALR/CAZB/ANTXR1/CASQ1/SCIN/ACTN1/TRIP10/MICAL2/IQSEC1	32
GO:0044264	cellular polysaccharide metabolic process	10/590	89/17046	0.001	0.04737	0.04109	CP51/GRB10/HAS1/IGF1/IGF2/PRKAG3/PPP1CB/CSGALNACT1/IRS2/STBD1	10
GO:0034637	cellular carbohydrate biosynthetic process	9/590	74/17046	0.001	0.04737	0.04109	AKR1B1/GRB10/HAS1/IGF1/IGF2/PRKAG3/PPP1CB/CSGALNACT1/IRS2	9

GO:0070371	ERK1 and ERK2 cascade	18/590	228/17046	0.00101	0.04737	0.04109	CH13L1/CCR1/FGA/FGF10/GF1/KDR/LGALS9/PKH01/PLA2G2A/MAPK3/MAP2K2/CCL11/NOD2/BMP4/TNFRSF11A/ADIPOQ/RAPGEF2/FGF19	18
GO:0008219	cell death	87/590	1816/17046	0.00104	0.04796	0.04161	GJB6/CHI3L1/EGLN2/CARD16/COMP/MAP3K8/ADM/IL31RA/PARP4/CYLD/DBI/ESR1/FGA/FGF10/FHIT/FOXO2/EPBA4L13/DIP2A/PPP1R13B/ARHGGEF18/RYPB/RNF144B/GAS2/CLU11/BMP10/SOX8/HSP90A81/ID3/IGF1/LLRN/INHBA/IRF1/TGB2/KDR/ARHGDA/LGALS9/LMNA/MPZ/PFAH2/PARK2/UTP11L/PKH01/PKM/PLA3L1/PKM/PPP2R2B/MAPK3/PROC/PK6/PSMD7/PTGFR/PLEKHG5/MARK4/SCN/NOD2/BMP4/BMPR1B/BOX/STK3/TERF1/TGM2/TNFAIP3/TNFRSF1A/TRA5/TNFRSF4/WNT109/CARD14/BCL2L14/FAM188A/ZC3H12A/CPEB4/CLPTM1L/CALR/CAST/SCIN/TP63/RUNX3/IRS2/ACTN1/GRADD/ALDH1A2/SPHK1/MAP3K6/AURKB/DAPL1/ADIPOQ/RAPGEF2	87
GO:0016265	death	87/590	1816/17046	0.00104	0.04796	0.04161	GJB6/CHI3L1/EGLN2/CARD16/COMP/MAP3K8/ADM/IL31RA/PARP4/CYLD/DBI/ESR1/FGA/FGF10/FHIT/FOXO2/EPBA4L13/DIP2A/PPP1R13B/ARHGGEF18/RYPB/RNF144B/GAS2/CLU11/BMP10/SOX8/HSP90A81/ID3/IGF1/LLRN/INHBA/IRF1/TGB2/KDR/ARHGDA/LGALS9/LMNA/MPZ/PFAH2/PARK2/UTP11L/PKH01/PKM/PLA3L1/PKM/PPP2R2B/MAPK3/PROC/PK6/PSMD7/PTGFR/PLEKHG5/MARK4/SCN/NOD2/BMP4/BMPR1B/BOX/STK3/TERF1/TGM2/TNFAIP3/TNFRSF1A/TRA5/TNFRSF4/WNT109/CARD14/BCL2L14/FAM188A/ZC3H12A/CPEB4/CLPTM1L/CALR/CAST/SCIN/TP63/RUNX3/IRS2/ACTN1/GRADD/ALDH1A2/SPHK1/MAP3K6/AURKB/DAPL1/ADIPOQ/RAPGEF2	87
GO:0044281	small molecule metabolic process	109/590	2375/17046	0.00106	0.04833	0.04192	GNE/MTHS/PDPN/ERLIN2/EGLN2/ACOT7/CNP/NEU4/ADM/VEGFLAM/CPS1/NDUFAF6/CRABP1/B3GLCT/PPM1L/MBOATI1/CYP11A1/DIO3/DLG2/ABAT/AGXT7/ENO2/FAH/FHIT/ARR1B1/NUP1210/SLC37A4/PNKD/ACOT11/GATM/PDE7B/AMPD3/DHAP1/THM5/GRB10/DNAUC15/GUCY1A3/PADI1/HAS1/ACACB/HRH1/HSD11B1/NME9/IGF1/GF2/LLRN/INPP5A/LDLR/LHCSR/MC2R/ME2/MGAT1/MOC51/MYH4/NUBP1/NDUFB4/NEU1/ATP1A2/NPPC/OAS2/OPRL1/ATP5B/PARK2/SPOCK3/CHST15/PCYOX1/SRRT6/PDE6B/PKM/PLA3G2A/PKAG3/SLC10C1/PNLIP/CYP2W1/PPP1CB/PRKAR1B/LMBRD1/CSGALNACT1/APOBR/MAPK3/MRAP/PSMD7/RDH14/SCY/STRAG/SLC4A1/TNFRSF1A/CCR2/UCP1/CA7/CAGNAIE/CERS4/QTRT1/NR0B2/RAE1/KMO/IRS2/ALDH1A2/SYNI2/SPHK1/CH25H/SLC16A3/ADIPOQ/ENTPD3/NUP93/LPGAT1/FGF19/NR1H4	109
GO:0071320	cellular response to cAMP	7/590	47/17046	0.00108	0.04921	0.04269	CPS1/CYP11A1/AQP9/SLC8A1/WNT10B/ADIPOQ/RAPGEF2	7
GO:0001503	ossification	24/590	348/17046	0.0011	0.04965	0.04307	CCR1/FAM101A/SBNO2/FOXO2/SOX8/ID3/RSP02/IGF1/GF2/NPPC/ATP5B/CSGALNACT1/ROHL4/BGLAP/BMP4/SLC8A1/BMPR1B/WNT10B/HTM1/TP63/RUNX3/TNFRSF11A/PIAS2/RSAD2	24
Hypomethylated DMC, Cellular Component								
	Description	GeneRatio	logRatio	pvalue	p.adjust	qvalue	geneID	Count

GO:0005886	plasma membrane	229/617	4464/17046	8.17E-10		1.50E-07	1.60E-07	1.25E-05	1.33E-05	9.05E-08	14587/17046	570/617	cell	GO:0005623
<p>AKT3/ABI1/CD300L1/CDH9/CDH12/FARP1/IL1RA1/KLRG1/TRDN/PDPN/GIB6/TMED10/ADAM29/ERLIN2/PKP3/CHRNA1/CHRNA2/GPR11/PANX3/FAT3/CRR1/SLC51B/SEZ6/CNP/IL13RA/VR2A14/CPM/NPP7/LDLR/AD3/CD34/XKR3/SH3D19/CYLD/DIO3/DIG2/DTNW/EEF2/EPHA2/LIPH/SLC10A4/ENO2/EPAH1/ESR1/F11/FAT2/SPATA13/FCGR2A/FGA/FGF10/INPASC/EPB4-1L3/FLOT2/MILC1/RHOBTB2/NEDD4/SYNE1/PSD3/PPP1R3B/STEAP2/CE2B/PLEK2/SLC17A5/ADGRI1/NPTN/CYTH4/GPR26/FAR2/GRB10/GRIK4/GUCY1A3/GPR137/HAS1/HLA-DOA/HLA-DPA1/ANXA13/HRH1/HSP90AB1/HTR3A/CD300E/IGF1/IGF2/GPR142/LCE1L/CE2D/IL1R1/IL1RN/IL1ORA/AQP2/IL1RA/IL1R2B2/PRSS41/IL16/AQP5/INPP5A/AQP9/ITGA7/ITGB2/ITGB7/ITIH4/IVL/JUP/CD82/KCNH2/KCNJ9/KCNMB1/KOR/OR2A5/LCP1/MUC2/IL1R1/LHCGR/RA819/LPP/MC2R/MCC/ASGR1/MPZ/NUBP1/NEU1/ATP1A2/NRAS/OPR11/OPR2/OPR3/OPR4/OPR6/ATP5B/ANOT7/PCYOX1/P2RY6/ATP5B/ANOT7/PCYOX1/PD/E6B/ATP8A2/PK8/PK8/SLSHI/APBB1/PCYP2W1/FANG/SLC47A1/TRPV6/SLC30A10/CHRNA9/PARVA/PRKAR1B/ITC17/LMBRD1/PAG1/POB8/MAK3/MAP2K2/PCDHGB3/MAR8/TRPV5/BRMT8/CD425E1/RGMA/PTGFR/PLEKHG5/TEMN2/PTRPE/TRIM27/RGR/RGS12/RIT2/PARV6/NOD2/STRA6/DNAI2/CLDN2/PCDH2/SLC4A1/SLC6A2/SLC9A3/SLC20A2/SMR18/LVYX1/JBP1/STAT2/BST2/TGM2/TNFRSF1A/TRAFF5/TRFC6/TPM2/CCR2/TNFRSF4/ZAP70/CACNA1E/CARD14/IGF1R1/CALD1/PCSCA/GPR157/ZC3H12A/C6orf25/CALR/ANTXR1/BFS2/ATP13A4/PIPE4/CASQ1/PAIRD66/SLC43A1/IFITM1/ITPRIP/HS2/ACTN1/TNFRSF11A/SHPK1/ENDOU/SKAP3/STBD1/TSAN18/CGRL2/PRC1/SYTF/ESAM/SLC16A3/CD8A/TRIP10/ENTPD3/RAPGEF2/CD79A</p> <p>AKT3/ABI1/TANK/CD300L1/GNE/ZNF783/CDH9/COH12/SUGP2/FARP1/KLRG1/RCAN2/CDKN1C/SPERG/MRVI1/TRDN/CO55/PTTRM1/TACC2/MTH5/POPN/CELF1/GIB6/PNRC1/TME-D10/LECT1/RER1/ADAM29/HNRNPUL1/RP114/CHGA/CH13L1/ERLIN2/ERLIN3/EGLN2/ATXN2/KIF12/ACOT7/EXOC3/CHRNA1/CHRNA2/GPR11/GBP4/PANX3/RBP7/GALNT15/AP3S1/CL00190/FAT3/CLNS1/MRP152/CCR1/SLC51B/SPATA3/SEZ6/TNFAIP81/MOB3A/CNP/NEU4/COI9A3/MAP3X8/ADM1/IL13RA/UBI1CP1/HUS1B/OR2A14/CPM/CPS1/NDUF-AF6/PKD NL/CRABP1/ZNF358/MIB2/PARP4/MPP7/IL1RA/CD34/PCP2/CEP128/MGAT3B/CEST/KLC3/ZNF738/XKR3/SMYD1/SGOL1/PPM1L/SH3D19/CYLD/MB0AT1/ESCO2/CYP11A1/ZNF782/CALML6/DBB1/DODST/ZNF366/BHLHA15/PPP1R18/DIO3/DIG2/DMBT1/DNAH6/ABAT/DPH1/DTNW/AGXT/EEF2/EPHA2/EIF4G1/A2M/ELK4/ANKRD23/UPH1/SLC10A4/S MIM14/ENO2/ADCK5/EPHA1/ESR1/F11/FAH/FAT2/SPATA13/PRSS54/FCGR2A/PHACTR1/FGA/FGF10/PHIT/PTBD3/TRAQ1/MSRB2/FOXL1/FOXO2/EXPH5/AKR1B1/NFASC/EPB41/3/GGA3/DIP2A/FLOT2/MLC1/TBC1D1/RHOBTB2/NUP210/NEDD4L/SYNE1/PSD3/PPP1R3B/PUM2/ARHGFE18/RYBP/MORC3/MAKP8IP2/TSSK2/VGLL2/SLC37A4/RASGEF1C/RNF144B/ZNF549/CCDC110/ST66ALINAC3/SANM50/DFNB31/ALS3C1/PNKO/SEC31B/ACOT11/RAI14/STEAP2/GAS2/FBX121/CE2B/SACS/GATM/GBG1/PLEK2/SLC17A5/ADGRI1/RP56KCI1/PABPC1/AKAP8L/DNAIC2/FGF22/NPTN/PDE7B/CYTH4/AMPOD3/DHHDH/BMP10/ZNF638/ZNF311/ZNF844/THSM57/GPR26/EOGT/FFAR2/TRIM42/GRB10/MRPS18B/GRIK4/DNAI1/CS-C3/G3/TM004/GUCY1A3/GPR132/PAD11/HAS1/SOX8/HK1/HLA-DOA/HLA-DPA1/ANXA13/IR441/ACACB/HOX4/HRH1/HSD11B1/HSP90AB1/HTR3A/DUDD1/TFAP2E/D3/ZC3H12D/RSPO2/CD300E/NME9/IGF1/IGF2/GPR142/LCE1L/CE1D/LCE2D/IL1R1/IL1RN/IL1ORA/AQP2/IL13RA/IL1R2/IL13RA/PRSS54/IL16/FOXK2/AQP5/INP5A/IRF1/AQP9/ITGA7/ITGB2/ITGB7/ITIH4/IVL/JUP/CD82/USP50/KCNH2/KCNJ9/KCNMB1/KOR/KIF25/PO5/PO5/PO5/CLE17A/HESS/AFB3/STMN1/OPR2A5/LCP1/MUC3/IL1R1/ARHGDI4/LGAL59/LHCGR/LMNA/LMO2/RAB19/LPP/MC2R/MCC/ME2/MFNG/MGAT1/MITF/LHX8/ASGR1/MOCS1/MOV10/MPZ/MYH4/MYL2/NUBP1/NDUF84/DRE1/NEU1/ATP1A2/INPASC3/NHLH2/NPPC/NRAS/OAS2/OPR11/OPR2/OPR3/OPR4/OPR6/PAFAH2/ATP5B/ANOT7/PARK2/BOLA1/UTP11L/CHST15/PCYOX1/C11orf73/SIRT6/PDE6B/ATP8A2/PTX2/PKHD1/PML/PLA2G2A/PLAG1/PRKAG3/PML/RIPPLY3/XYB6/GPR84/SLC10C1/TLR9/2/REM1/SSH1/RIN2/POU2AF1/APBB1/MPX98/FBLN1/MEG18/PALMD/CYP2W1/RPP25/BANP/PPP1CB/HERC6/ELP3/DNAI1/GOI/PH3/PPP2R2B/FANCI/MOB1A/SLC47A1/SLC29A3/MIS18BP1/TRPV6/SLC30A10/CHRNA9/PEX26/FRMD4A/CAKRD/PARVA/PRKAR1B/TTC11/IT1L22/CFAP44/ERWARD/MCTP2/LMBRD1/CSGALNACT1/PAG1/CSUD1/W3B2/MYNN1/APOBR/MAPK3/MAP2K2/PCDHGB3/PRKRI/PROCK/MPAP/TRPV5/PRMT8/HTRA1/SLAMF8/CDCA25E1/PAK6/ARNT12/RGMA/PRDML1/PPP1R10/PLEKHG5/TEMN2/GATAD2B/E RMN/KLH18/RDH14/MARK4/PTPRE/GREBZF/FAM60A/ACTA2/REFC2/TRIM27/RGR/RGS12/RIT2/RPA3/BLGAP/CCL11/ABHD4/MRPS14/NPAS3/PARG/NOD2/STRA6/MAPI1/CD3B2/ARHGAP9/GZFI/DNAI2/CLDN25/PCDH20/TMEM23/VPS33A/BMP4/SPATS2/ZG16/SLC6A12/SLC9A3/SLC20A2/BMPR1B/SLIT1/Z5CAN18/LVYX1/BOK/BRP/SR P68/STAT2/STK3/SUPT6H/BST2/CEB2/ZEBI1/TEAD3/TERF1/TGM2/TCHE/TNFAIP3/TNFRSF4/TRAFF5/TRPM2/CCR2/TNFRSF4/UCP1/ZAP70/ZNF7/CA7/CACNA1E/MOGS/RA B7A/ERB3/CCDC86/CARD14/ESR6/BCI2L14/LST1/CEP54/IGF1R1/ZNF665/CSPP1/ERNMP1/CALD1/PCSCA/FAM188A/GPR157/ZC3H12A/FAAP100/CPEB4/C6orf25/ZNF496/CAIR/COL21A1/1/KRTAP2-1/QTRT1/SLIRP/CAST/CAZB/CDC3/DYNLRB2/SLC25A18/SPATA16/CRAT/1/ANTXR1/CVMAHP/BFS2/ATP13A4/PIPE4/ZNF397/NR0B2/MONJA/CASQ1/HOPX/PARD66/TBKI/TRIM63/GTRP83/RAE1/Clorf198/PPP1BP2/SLC43A1/IFITM1/ITPRIP/SCIN/KMO/ RUNX1/TP63/RUNX3/IRS2/ACTN1/CRADD/TNFRSF11A/ALDH1A2/STK19/SYNY2/SPHK1/BUDD31/CCNA1/ENDOU/SKAP3/STBD1/HSP90AB1/CH25H/CCR2/ERN1/PRC1/STAR13/PIAS2/MAP3K6/SYTF/ESAM/SLC16A3/CBFA2T2/RSAD2/AURKB/CD8A/CCDC102A/TRIP10/AD1POQ/ENTPD3/PREPL/RAB36/MICAL2/N4BP1/VGLL4/NUP93/RAPGEF2/CD79A/KAAO 513/DAZAP2/ZBTB39/IOSEC1/PLGAT1/FGF19/NR1H4</p>														

GO:0044464	cell part	567/617	14556/17046	4.17E-07	4.91E-05	4.60E-05	<p>AKT3/ABI1/TANK/CD300LD/GNE/ZNF783/CDH9/CDH12/SUGP2/FARP1/KLRG1/RCAN2/CDKN1C/SPERG/MRV11/TRDN/COG5/PIITRM1/TACC2/MTHF5/PDPN/CELF1/GIB6/PNRC1/TWME/D10/LECT1/REER1/ADAM29/HNRNPUL1/RPP14/CHGA/CH13L1/ERLIN2/PK93/EGLN2/ATXN2L/KIF12/ACOT7/EXOC3/CHRNA3/CHRNA2/GPRIN1/GBP4/PANX3/RBP7/GALNT15/AP351/CI0or90/FAT3/CLN5/MRP152/CCR1/SLCS18/SPATA33/SEZ6/TNFAP181/MOBSA/CNP/NEU4/COLO9A3/MAP3X8/ADMI/L31RA/UBI1CP1/HUS18/OZRA14/CPM/CPS1/NDU4F6/PXD/NL/CRABP1/ZNF358/MIB2/PARP4/MPP7/LDLRAD3/FAM101A/B3GL/CEP128/MGATS6/CS7A3/ZNF738/XKR3/SMD1/PPM1L/SKOR19/CYLD/MBOAT1/ESCO2/CYP11A1/ZNF782/CA1M16/DOB1/JDDOST/ZNF366/BHLHA15/PPP1R18/DIO3/DLGG2/DMB1/DNAH6/ABAT/DPH1/DTNA/AGXT/EEF2/EFNA2/EF4G1/A2M/ELK4/ANKRD23/LIPH/SLC10A4/S/MIM14/ENQ2/ADCK5/EPHA1/ESR1/F1/FAH/FAT2/SPATA13/PRSS54/FCGR2A/PNAC1/FCG/AGF10/FHIT/ITBD3/TRAJK/MSR82/FOXJ1/FOXC2/EXPH5/AKR1B1/NFASC/EPB4143/GGA3/DIP2A/FLOT2/MILC1/TBC1D1/RHOB1B2/NUP210/NEED4L/SYNE1/PSD3/PPP1R13B/PUM2/ARHGFE18/RYBP/MOKC3/MAPK8P2/TSSK2/VGL2/SLC37A4/RASGEF1C/RNF144B/ZNF549/CCDC110/ST66ALNAC3/SAMM50/DFNB31/ALS3C/PNKO/SEC31B/ACOT11/RAI14/STZF27/GAS2/FBX121/CE2B/SACS/GATM/GBGT1/PLEK2/SLC17A5/ADGRF1/RP56KCL1/PABPC1/AKAP8L/DNAIC2/FGF22/NPTN/PDE7B/CYTH4/AMPOD3/DHHD/BMP10/ZNF638/ZNF3117/ZNF844/GBR10/MRPS18B/GRIK4/DNAI4/DNAI4/SCG3/TMOD4/GUCY1A3/GPR132/PAD11/HAS1/SOX8/HK1/HLA-DOA/HLA-</p> <p>DPA1/ANXA13/NR4A1/ACACB/HOX4/HRH1/HSD11B1/HSPALL/HSP90A1/HTR3A/DUPD1/TFAP2E/D03/ZC3H12D/RSPD0/CD300E/NME9/IGF1/IGF2/GPRL42/LCEL1C/LCEL1D/CE2D/IL1R1/IL1RN/IL1ORA/AQP2/IL11RA/IL12RBZ/IL15RA/PRSS41/IL16/FOXO4/ABP5/INPP5A/IRF1/PAQP9/TGAT7/TGB2/ITGB7/ITIH4/IVL/JUP/CD82/USP50/KCNH2/KCNJ8/KCNJ9/KCNM/B1/KDR/MIF25/PO5/GLECT17A/HESS/AFF3/STMN1/OR2A5/LCP1/MUC21/LDLR/ARHGDI4/LGALS9/LHCGR/LVNA/LMO2/RAB19/LPP/MC2R/MCC/ME2/MFNG/MGAT1/MITF/LHX8/A/SGR1/MOCS1/JMOV10/MP2/MYH4/MYL2/NUBP1/NDUFB4/DRG1/NEU1/ATP1A2/NFATC3/NHLH2/NPPC/NRAS/OAS2/OPRL1/OR2K3/SLC22A18/P2RY6/PFAFAH2/ATP5B/AN/O7/PARK2/BOLA1/UTP11/CHST15/PCYOX1/C11oH73/SR16/PDE6B/ATP8A2/PTX2/PKX1/PLA2G2A/PLA6L1/PKRAK3/PML/RIPPL3/FXYD6/GPR84/SLC01C1/TLR9/TREM1/SSH1/RIN2/POUZAF1/APBB1IP/MXR48/FBLIM1/MED18/PALM0/CYP2W1/RPP25/BANP/PPP1CB/HERG6/EU3/DNAUC17/GOLPH3/PPP2R2B/FANCI/MOBI1/SLC47A1/SLC29A3/MI/S18BP1/TRPV6/SLC30A10/CHRNA9/PEX26/FRMD4A/CARND/PARVA/PRKAR1B/ITTC17/IFT122/CFAP44/FERMARD/IMCTP2/LMBRD1/CSGALNACT1/PAG1/CSDI1/W582/MYNN/POBR/MAPK3/MAP2K2/PCDHGB3/PRKRIR/PROC/MRAP/TRPV5/PRMT8/HTRA1/SLAMF8/CD425EJ/PAK6/ARNT12/RGMA/PRDM11/PSMD7/PTGFR/PLEKHG5/TEMN2/GATAD2B/ERMN/KLHL8/RDH14/MARK4/PTPRE/CREBZF/FAM60A/ACTA2/RKC2/TRIM27/RGR/RGS12/RIT2/RPA3/BGLAP/CCL11/ABHD4/MRPS14/NPAS3/PARV6/NOD2/STRAG/MAP1LC3B2/ARHGAP/9/GZF1/DNAI2/CLDN25/PCDH20/TMEM237/VPS33A/BMP4/SLC4A1/SPATS2/ZNF649/ZG16/SLC6A12/SLC8A1/SLC20A2/BNMR1B/ZSCAN18/LYXK1/BOK/BPI/SRP68/STAT2/STK3/SUPTGH/BST2/TCB2/ZEB1/TEAD3/TERF1/TGM2/TCHH1/TNFAIP3/TNFRSF1A/TRAF5/TRPC6/TRPV4/UCP1/ZAP70/ZNF7CA7/CACNA1E/MOGS/RAB7A/ERA3/C/CD86/CARD14/ESRG/BCL2L14/LST1/CEFS4/IGF1R1/ZNF665/CSPP1/EMRP1/CALD1/PSCA/FAM188A/GPR157/ZC3H12A/FAAP100/CPBE4/Ccor25/ZNF436/CALR/COI21A1/KRTAP2-1/QTRT1/SURP/CAST/CANP2B/CCDC3/DYNLRB2/SLC25A18/SPATA16/KRTAP17-1/ANTXR1/CMAHP/BFSP2/ATP13A4/MPF4/ZNF397/NROB2/CASO1/HOPX/PARP66/TBK1/TRIM63/GTPBP3/RAE1/C1orf198/PPE1P2/SLC43A1/IFTM1/ITPRIP/SCIN/KMO/RUNX1/T/P63/RUNX3/IRS2/ACTN1/CRADD/TNFRSF11A/ALDH1A2/STK19/SYNI2/SPHK1/BUO31/CCNA1/ENDOU/SKAP2/STBD1/HSPB3/TSPAN18/CH25H/CCR2/ERL1/PRCI/STARD13/PKASZ/MAP3K6/SYTT/ESAM/SLC16A3/CBFAZ2/RSAD2/AURKB/CD8A/CCDC102A/TRIP10/ADIPOQ/ENTPD3/PREP/RAB36/MICAL2/ABP1/NGL14/NUP93/RAPGEF2/CD79A/KIAA0513/DAZAP2/ZBTB39/IOSECL1/PGAT1/FGF19/NR1H4</p>
GO:0016020	membrane	351/617	8177/17046	3.80E-06	0.00037	0.00035	<p>AKT3/ABI1/SMMIM6/CD300LD/CDH9/CDH12/FARP1/KLRG1/MRV11/TRDN/COG5/PDPN/CELF1/GIB6/TWME10/LECT1/REER1/ADAM29/CHGA/ERLIN2/PK93/ATXN2L/EXOC3/CHRNA1/CHRNA2/GPRIN1/SORCS1/PANX3/GALNT15/AP351/FAT3/CLN5/MRP152/CCR1/SLCS18/SEZ6/CNP/NEU4/IL131RA/OR2A14/CPM/CPS1/NDU4F6/PARP4/MPP7/LDLRAD3/B3GLCT/MGAT5B/CSTA/ABCC13/XKR3/PPM1L/SH3D19/CYLD/MBOAT1/ANKRD46/CYP11A1/JDDOST/DIO3/DLGG2/DMB1/DTNA/EEF2/EFNA2/EF4G1/LIPH/SLC10A4/SWIM14/ENQ2/ADCK5/EPHA1/ESR1/F1/FAT2/SPATA13/SAMM50/PNKO/SEC31B/STEAP2/GAS2/LCE2B/GATM/GBGT1/PLEK2/SLC17A5/ADGRF1/RP56KCL1/PABPC1/DNAUC2/FGF22/NPTN/PDE7B/CYTH4/AMPOD3/DHHD/BMP10/ZNF638/ZNF3117/ZNF844/GBR10/MRPS18B/GRIK4/DNAI4/DNAI4/SCG3/TMOD4/GUCY1A3/GPR132/PAD11/HAS1/SOX8/HK1/HLA-DOA/HLA-</p> <p>DPA1/ANXA13/NR4A1/ACACB/HOX4/HRH1/HSD11B1/HSP90A1/HTR3A/DUPD1/TFAP2E/D03/ZC3H12D/RSPD0/CD300E/NME9/IGF1/IGF2/GPRL42/LCEL1C/LCEL1D/CE2D/IL1R1/IL1RN/IL1ORA/AQP2/IL11RA/IL12RBZ/IL15RA/PRSS41/IL16/FOXO4/ABP5/INPP5A/IRF1/PAQP9/TGAT7/TGB2/ITGB7/ITIH4/IVL/JUP/CD82/USP50/KCNH2/KCNJ8/KCNJ9/KCNM/B1/KDR/MIF25/PO5/GLECT17A/HESS/AFF3/STMN1/OR2A5/LCP1/MUC21/LDLR/ARHGDI4/LGALS9/LHCGR/LVNA/LMO2/RAB19/LPP/MC2R/MCC/ME2/MFNG/MGAT1/MITF/LHX8/A/SGR1/MOCS1/JMOV10/MP2/MYH4/MYL2/NUBP1/NDUFB4/DRG1/NEU1/ATP1A2/NFATC3/NHLH2/NPPC/NRAS/OAS2/OPRL1/OR2K3/SLC22A18/P2RY6/PFAFAH2/ATP5B/AN/O7/PARK2/BOLA1/UTP11/CHST15/PCYOX1/C11oH73/SR16/PDE6B/ATP8A2/PTX2/PKX1/PLA2G2A/PLA6L1/PKRAK3/PML/RIPPL3/FXYD6/GPR84/SLC01C1/TLR9/TREM1/SSH1/RIN2/POUZAF1/APBB1IP/MXR48/FBLIM1/MED18/PALM0/CYP2W1/RPP25/BANP/PPP1CB/HERG6/EU3/DNAUC17/GOLPH3/PPP2R2B/FANCI/MOBI1/SLC47A1/SLC29A3/MI/S18BP1/TRPV6/SLC30A10/CHRNA9/PEX26/FRMD4A/CARND/PARVA/PRKAR1B/ITTC17/IFT122/CFAP44/FERMARD/IMCTP2/LMBRD1/CSGALNACT1/PAG1/CSDI1/W582/MYNN/POBR/MAPK3/MAP2K2/PCDHGB3/PRKRIR/PROC/MRAP/TRPV5/PRMT8/HTRA1/SLAMF8/CD425EJ/PAK6/ARNT12/RGMA/PRDM11/PSMD7/PTGFR/PLEKHG5/TEMN2/GATAD2B/ERMN/KLHL8/RDH14/MARK4/PTPRE/CREBZF/FAM60A/ACTA2/RKC2/TRIM27/RGR/RGS12/RIT2/RPA3/BGLAP/CCL11/ABHD4/MRPS14/NPAS3/PARV6/NOD2/STRAG/MAP1LC3B2/ARHGAP/9/GZF1/DNAI2/CLDN25/PCDH20/TMEM237/VPS33A/BMP4/SLC4A1/SPATS2/ZNF649/ZG16/SLC6A12/SLC8A1/SLC20A2/BNMR1B/ZSCAN18/LYXK1/BOK/BPI/SRP68/STAT2/STK3/SUPTGH/BST2/TCB2/ZEB1/TEAD3/TERF1/TGM2/TCHH1/TNFAIP3/TNFRSF1A/TRAF5/TRPC6/TRPV4/UCP1/ZAP70/ZNF7CA7/CACNA1E/MOGS/RAB7A/ERA3/C/CD86/CARD14/ESRG/BCL2L14/LST1/CEFS4/IGF1R1/ZNF665/CSPP1/EMRP1/CALD1/PSCA/FAM188A/GPR157/ZC3H12A/FAAP100/CPBE4/Ccor25/ZNF436/CALR/COI21A1/KRTAP2-1/QTRT1/SURP/CAST/CANP2B/CCDC3/DYNLRB2/SLC25A18/SPATA16/KRTAP17-1/ANTXR1/CMAHP/BFSP2/ATP13A4/MPF4/ZNF397/NROB2/CASO1/HOPX/PARP66/TBK1/TRIM63/GTPBP3/RAE1/C1orf198/PPE1P2/SLC43A1/IFTM1/ITPRIP/SCIN/KMO/RUNX1/T/P63/RUNX3/IRS2/ACTN1/CRADD/TNFRSF11A/ALDH1A2/STK19/SYNI2/SPHK1/BUO31/CCNA1/ENDOU/SKAP2/STBD1/HSPB3/TSPAN18/CH25H/CCR2/ERL1/PRCI/STARD13/PKASZ/MAP3K6/SYTT/ESAM/SLC16A3/CBFAZ2/RSAD2/AURKB/CD8A/CCDC102A/TRIP10/ADIPOQ/ENTPD3/PREP/RAB36/MICAL2/ABP1/NGL14/NUP93/RAPGEF2/CD79A/KIAA0513/DAZAP2/ZBTB39/IOSECL1/PGAT1/FGF19/NR1H4</p>

GO:0003674	molecular_function	581/581	115274/17046	5.05E-26	5.40E-26	5.40E-29	6.22E-29	15274/17046	581/581	<p>AKT3/ABI1/TANK/CD300LD/GNE/ZNF783/CDH9/CDH12/SUGP2/FARP1/KLRG1/RCAN2/CDKN1C/SPEG/MRV11/TRDN5/SPON2/COG5/PITRM1/TACC2/MTHFS/CELF1/RFP/L2/PNRC1/JT/MED10/RERI/ESM1/ADAM29/HNRNPUL1/RPP14/CHI3L1/ERLIN2/CHI3L2/PKR3/EGFNL2/ATXN2L/KIF13L/ACOT7/PDAP1/EXOC3/CHRNA1/CHRNA2/CAIRD16/GPRIN1/SORCS1/GBP4/PANX3/RBP7/GALNT15/AP3S1/FAT3/CLN5/MRPL52/CCR1/SLC21A13/NEU4/COI9A3/COMP/MAAP3X8/ADM/IL31RA/EGFLAM/UBL/CP1/OR2A14/CPM/CP51/NDUFA6/PXDNL/CRAPB1/ZNF358/CRYBB3/MB2/PARP4/MPP7/LDIRARHGDI/LGALS9/CLN3/ZNF738/ABCC13/SMYD1/SGOL1/PPM11/SHD19/CYLD/MB0AT1/ESCO2/CYPL1A1/ZNF782/CALM16/DDB1/ONRF2/DDOST/ZNF366/BHLHA15/PPP1R18/DO3/DL2/DMBT1/DNAH6/ABA1/DPH1/DINA/AGXT/EEF2/E/FNA2/EFAG1/AZM/ELK4/ANKRD23/LIPH/SLC10A4/ENOD/ADCK5/EPHA1/ESR1/F11/FAH/FAT2/PAT8/SPRSS5/FCGR2A/PHACTR1/JFGA/FGF10/FHIT/TRAK1/MSRB2/FOXL1/FOX2/EXPH45/ACR1B1/NFASC/EPB413/GGA3/DP2A/FL0T2/MCL1/TBC1D1/RHOB1B2/NEDD4L/SYNE1/P5D1/PB13B/PUV2/ARHGFE18/RYPB/MORC3/MAPK8IP2/TSSK2/VGLL2/TTL10/SLC37A4/RASGEF1C/RNF144B/ZNF549/CCDC110/ST6GALNAC3/SAMM50/DNF831/ALS32C/PNKO/ACOT11/STEPAP2/FBXK12/LCE2B/SACS/GATM/EGGT1/SLC17A5/ADGRF1/RPS6K1/PABPC1/AKAP81/DNAJC2/JGF22/NPTN/PDE7B/CYTH4/AMPD3/DHBP/IMP10/NF638/C11orf31/ZNF313/TMPRSS12/ZNF844/THYM5/GPR26/BOGT7/FAR2/TRIM4/2/GRB10/MRPS188/GRIK4/DNAJC15/SCG3/TMOD4/GUCY1A3/GPR132/PADI1/HA51/SOX8/HK1/HLA-D0A-HLA-</p> <p>DPAL/ANXA13/NR4A1/ACACB/HOXC4/AGFG2/HRH1/HSD11B1/HSPT08A1/HTR3A/DUPD1/ADAMTSL5/ANKRD45/TFAP2E/ID3/ZC3H12D/RSPD2/NMIE9/IGF1/IGF2/GPR142/LCE1C/LCE2D/LRL1/LIRN/L10R/AQP2/L1L1RA/L12R/R2/L115RA/IL2R/IL15RA/AQP5/INHBA/INPSSA/IRF1/AQ09/ITGA7/ITGB7/ITIH4/NL/JUP/CDB2/USP50/KCNH2/KCNJ8/KCNJ9/KCNMB1/KOR/KIEF25/PO5/C17orf82/CLC17A/HES5/RBM12B/AFF3/LAIR2/LANMA3/STMN1/OR2A5/LCP1/LDIR/ARHGDI/LGALS9/LHCSR/C11orf87/LMINA/LMO2/RAB19/LPP/MCZ/MCC/MEZ/MFNG/MGAT1/SCGB2A1/MITF/LHX8/ASGR1/MOCS1/MOV10/MPZ/PLEKHG7/MYH4/MYL2/NUBP1/NDUFB4/DRG1/NEU1/ATP1A2/NFATC3/NH/LH2/NPPC/NRAS/OAS2/RNF165/OPRL1/OR2C1/OR3A2/SLC22A18/P2R16/PFAH4/ATP5B/IL21R/ANOT7/SPOCK3/BOAL1/UTP11/PRR16/CHST15/PCYOX1/C11orf73/SIRT6/DE6B/ATP8A2/P13/PTX2/PKHD1/PKM/PLA2G2A/PLAGL1/LRP1B/PRKAG3/PML/EXD6/GPR84/SLC1C1/PNLP/TLR9/TREM1/SSH1/RIN2/POUZAF1/APBB1P/MXR8A8/FBLM1/MED18/CY2W1/RPP25/TTC12/BANP/PPP1CB/HERC6/ELP3/DNAJC17/GOLPH3/PPP2R2B/FANG/MOBI1A/SLC47A1/SLC29A3/MIS18BP1/TRPV6/SLC30A10/CHRNA9/THUMPD1/PEX26/FRMD4A/CARD1/PARVA/PRKAR1B/TTC17/IFT122/MCTP2/LMBR10/CESGALNACT1/PAG1/CISD1/MYNN1/POBR/MAPK3/MAP2K2/PCDH8/PRKRR/PROC/MRAP/TRPV5/PRMT8/HTRA1/SLAMF8/CD42SE1/PAK6/ARNTL2/RGMA/PRDM11/P5MD7/SLURP1/PTGFR/PLEKH65/TEM2/GATA2B/ERMN/RNF150/RDH14/MARK4/PTPRE/CREBZF/ABHD17C/FAM60A/ACTA2/RFC2/TRIM27/RGR/RGS12/RIT2/RPA3/BGLAP/SC7/CLL1/ABHD4/MRPS14/RRS22/NPAS3/PARG/NO2/TINAG1/ARHGAP9/GZF1/DNAI2/CLDN25/PCDH20/VPS3A/BM/P4/SLC4A1/SPATS2/ZNF649/ZG16/SLC6A12/SLC8A1/SLC9A3/SLC20A2/BMPR1B/SLT1/BRD9/ZSCAN18/TMEM108/BOI/BP/SRP68/STAT2/STK3/SUPT6H/BST2/JCCEB2/ZEB1/JT/EA03/4/IGLRI1/ZNF665/CSPP1/ERMP1/CALD1/FAM188A/TFME62/GPR157/ZC3H12A/UCP1/WNT108/ZAP70/ZNF7/CA7/CACNA1E/MOCS/ARBT/ER3/CCDC86/CAIRD14/8/CLL14/CE5/ANTXR1/BFSP2/ATP13A4/YIP4/ZNF397/NROB2/CASQ1/HOPX/PARD6G/KRBA1/TBK1/RET/LN/TRIM63/GTTPB3/RAE1/PPFB7/SLC43A1/IFTM1/SGN/CDK10/KMO/RUNX1/TP63/RUNX3/SEPPINAG/IRS2/ACTN1/CRADD/TNFRSF11A/ALDH1A2/STK19/SYNI2/SPHK1/BUO31/CNAJ1/ENDOU/SKAP2/STBD1/SLAMF9/CH25H/CCR2/ERI1/PRCL1/STARD13/PIAS2/M/AP36/SYTY/SLC16A3/CBFAZ2/RSAD2/AURKB/DAP1/CD8A/CCDC102A/NEURL3/TRIP10/ADIPOQ/ENTPD3/PREP1/RAR36/MICAL2/N48P1/VGLL4/NUP93/RAPGEF2/CD79A/DAZAP2/ZBTB395/IOSEC1/LPGAT1/FGF19/NR1H4</p>
GO:0005488	binding	489/581	12915/17046	0.00014	0.00015	0.00015	3.40E-07	12915/17046	489/581	<p>AKT3/ABI1/TANK/CD300LD/GNE/ZNF783/CDH9/CDH12/SUGP2/FARP1/KLRG1/RCAN2/CDKN1C/SPEG/MRV11/TRDN5/SPON2/COG5/PITRM1/TACC2/MTHFS/CELF1/RFP/L2/PNRC1/JT/MED10/RERI/ESM1/ADAM29/HNRNPUL1/RPP14/CHI3L1/ERLIN2/CHI3L2/PKR3/EGFNL2/ATXN2L/KIF13L/ACOT7/PDAP1/EXOC3/CHRNA1/CHRNA2/CAIRD16/GPRIN1/SORCS1/GBP4/RBP7/GALNT15/AP3S1/FAT3/CLN5/CCR1/SLC21A13/NEU4/COI9A3/COMP/MAAP3X8/ADM/IL31RA/EGFLAM/UBLCP1/CPM/CP51/NDUFA6/PXDNL/CRAPB1/ZNF358/CRYBB3/MB2/PARP4/MPP7/LDIRARHGDI/LGALS9/CLN3/ZNF738/ABCC13/SMYD1/SGOL1/PPM11/SHD19/CYLD/MB0AT1/ESCO2/CYPL1A1/ZNF782/CALM16/DDB1/ONRF2/DDOST/ZNF366/BHLHA15/PPP1R18/DO3/DL2/DMBT1/DNAH6/ABA1/DPH1/DINA/AGXT/EEF2/EFNA2/EIF4G1/A2M/ELK4/ANKRD23/UHP/ANKD23/UPH/ESR1/F11/FAH/FAT2/SPATA13/FCG/R2A/PHACTR1/JFGA/FGF10/FHIT/TRAK1/MSRB2/FOXL1/FOX2/EXPH45/NFASC/EPB413/GGA3/DP2A/FL0T2/MCL1/TBC1D1/RHOB1B2/NUP210/NEDD4L/SYNE1/PPP1R13B/PUV2/RYPB/MORC3/MAPK8IP2/TSSK2/VGLL2/TTL10/RNF144B/ZNF549/CCDC110/SAMM50/DNF831/ALS32C/PNKO/ACOT11/STEP2/SACS/GBP2/RPS6K1/PABPC1/AKAP81/DNAJC2/JGF22/NPTN/PDE7B/CYTH4/AMPD3/BMP10/ZNF638/C11orf31/ZNF313/ZNF844/THYM5/FFAR2/TRIM42/GRB10/DNAIC15/SCG3/TMOD4/GUCY1A3/PADI1/SOX8/HK1/HLA-DOA/HLA-DPA1/ANXA13/NR4A1/ACACB/HOXC4/AGFG2/HRH1/HSPT08A1/HTR3A/DUPD1/ADAMTSL5/ANKRD45/TFAP2E/ID3/ZC3H12D/RSPD2/NMIE9/IGF1/IGF2/GPR142/RB2/IL15RA/IL16/FOXK2/AQP5/INHBA/INPSSA/IRF1/ITGA7/ITGB7/ITIH4/NL/JUP/CDB2/KCNH2/KCNJ8/KCNJ9/KCNMB1/KOR/KIEF25/PO5/C17orf82/CLC17A/HES5/RBM12B/AFF3/LAIR2/LANMA3/STMN1/OR2A5/LCP1/LDIR/ARHGDI/LGALS9/LHCSR/C11orf87/LMINA/LMO2/RAB19/LPP/MCZ/MCC/MEZ/MFNG/MGAT1/SCGB2A1/MITF/LHX8/ASGR1/MOCS1/MOV10/MPZ/PLEKHG7/MYH4/MYL2/NUBP1/NDUFB4/DRG1/NEU1/ATP1A2/NFATC3/NH/LH2/NPPC/NRAS/OAS2/RNF165/OPRL1/OR2C1/OR3A2/SLC22A18/P2R16/PFAH4/ATP5B/IL21R/ANOT7/SPOCK3/BOAL1/UTP11/PRR16/CHST15/PCYOX1/C11orf73/SIRT6/DE6B/ATP8A2/P13/PTX2/PKHD1/PKM/PLA2G2A/PLAGL1/LRP1B/PRKAG3/PML/EXD6/GPR84/SLC1C1/PNLP/TLR9/TREM1/SSH1/RIN2/POUZAF1/APBB1P/MXR8A8/FBLM1/MED18/CY2W1/RPP25/TTC12/BANP/PPP1CB/HERC6/ELP3/DNAJC17/GOLPH3/PPP2R2B/FANG/MOBI1A/SLC47A1/SLC29A3/MIS18BP1/TRPV6/SLC30A10/CHRNA9/THUMPD1/PEX26/FRMD4A/CARD1/PARVA/PRKAR1B/TTC17/IFT122/MCTP2/LMBR10/CESGALNACT1/PAG1/CISD1/MYNN1/POBR/MAPK3/MAP2K2/PCDH8/PRKRR/PROC/MRAP/TRPV5/PRMT8/HTRA1/SLAMF8/CD42SE1/PAK6/ARNTL2/RGMA/PRDM11/P5MD7/SLURP1/PTGFR/PLEKH65/TEM2/GATA2B/ERMN/RNF150/RDH14/MARK4/PTPRE/CREBZF/ABHD17C/FAM60A/ACTA2/RFC2/TRIM27/RGR/RGS12/RIT2/RPA3/BGLAP/SC7/CLL1/ABHD4/MRPS14/RRS22/NPAS3/PARG/NO2/TINAG1/ARHGAP9/GZF1/DNAI2/CLDN25/PCDH20/VPS3A/BM/P4/SLC4A1/SPATS2/ZNF649/ZG16/SLC6A12/SLC8A1/SLC9A3/SLC20A2/BMPR1B/SLT1/BRD9/ZSCAN18/TMEM108/BOI/BP/SRP68/STAT2/STK3/SUPT6H/BST2/JCCEB2/ZEB1/JT/EA03/4/IGLRI1/ZNF665/CSPP1/ERMP1/CALD1/FAM188A/TFME62/GPR157/ZC3H12A/UCP1/WNT108/ZAP70/ZNF7/CA7/CACNA1E/MOCS/ARBT/ER3/CCDC86/CAIRD14/8/CLL14/CE5/ANTXR1/BFSP2/ATP13A4/YIP4/ZNF397/NROB2/CASQ1/HOPX/PARD6G/KRBA1/TBK1/RET/LN/TRIM63/GTTPB3/RAE1/PPFB7/SLC43A1/IFTM1/SGN/CDK10/KMO/RUNX1/TP63/RUNX3/SEPPINAG/IRS2/ACTN1/CRADD/TNFRSF11A/ALDH1A2/STK19/SYNI2/SPHK1/BUO31/CNAJ1/ENDOU/SKAP2/STBD1/SLAMF9/CH25H/CCR2/ERI1/PRCL1/STARD13/PIAS2/M/AP36/SYTY/SLC16A3/CBFAZ2/RSAD2/AURKB/DAP1/CD8A/CCDC102A/NEURL3/TRIP10/ADIPOQ/ENTPD3/PREP1/RAR36/MICAL2/N48P1/VGLL4/NUP93/RAPGEF2/CD79A/DAZAP2/ZBTB395/IOSEC1/LPGAT1/FGF19/NR1H4</p> <p>AKT3/ABI1/TANK/CD300LD/GNE/ZNF783/CDH9/CDH12/SUGP2/FARP1/KLRG1/RCAN2/CDKN1C/SPEG/MRV11/TRDN5/SPON2/COG5/PITRM1/TACC2/MTHFS/CELF1/RFP/L2/PNRC1/JT/MED10/RERI/ESM1/ADAM29/HNRNPUL1/RPP14/CHI3L1/ERLIN2/CHI3L2/PKR3/EGFNL2/ATXN2L/KIF13L/ACOT7/PDAP1/EXOC3/CHRNA1/CHRNA2/CAIRD16/GPRIN1/SORCS1/GBP4/RBP7/GALNT15/AP3S1/FAT3/CLN5/CCR1/SLC21A13/NEU4/COI9A3/COMP/MAAP3X8/ADM/IL31RA/EGFLAM/UBLCP1/CPM/CP51/NDUFA6/PXDNL/CRAPB1/ZNF358/CRYBB3/MB2/PARP4/MPP7/LDIRARHGDI/LGALS9/CLN3/ZNF738/ABCC13/SMYD1/SGOL1/PPM11/SHD19/CYLD/MB0AT1/ESCO2/CYPL1A1/ZNF782/CALM16/DDB1/ONRF2/DDOST/ZNF366/BHLHA15/PPP1R18/DO3/DL2/DMBT1/DNAH6/ABA1/DPH1/DINA/AGXT/EEF2/EFNA2/EIF4G1/A2M/ELK4/ANKRD23/UHP/ANKD23/UPH/ESR1/F11/FAH/FAT2/SPATA13/FCG/R2A/PHACTR1/JFGA/FGF10/FHIT/TRAK1/MSRB2/FOXL1/FOX2/EXPH45/NFASC/EPB413/GGA3/DP2A/FL0T2/MCL1/TBC1D1/RHOB1B2/NUP210/NEDD4L/SYNE1/PPP1R13B/PUV2/RYPB/MORC3/MAPK8IP2/TSSK2/VGLL2/TTL10/RNF144B/ZNF549/CCDC110/SAMM50/DNF831/ALS32C/PNKO/ACOT11/STEP2/SACS/GBP2/RPS6K1/PABPC1/AKAP81/DNAJC2/JGF22/NPTN/PDE7B/CYTH4/AMPD3/BMP10/ZNF638/C11orf31/ZNF313/ZNF844/THYM5/FFAR2/TRIM42/GRB10/DNAIC15/SCG3/TMOD4/GUCY1A3/PADI1/SOX8/HK1/HLA-DOA/HLA-DPA1/ANXA13/NR4A1/ACACB/HOXC4/AGFG2/HRH1/HSPT08A1/HTR3A/DUPD1/ADAMTSL5/ANKRD45/TFAP2E/ID3/ZC3H12D/RSPD2/NMIE9/IGF1/IGF2/GPR142/RB2/IL15RA/IL16/FOXK2/AQP5/INHBA/INPSSA/IRF1/ITGA7/ITGB7/ITIH4/NL/JUP/CDB2/KCNH2/KCNJ8/KCNJ9/KCNMB1/KOR/KIEF25/PO5/C17orf82/CLC17A/HES5/RBM12B/AFF3/LAIR2/LANMA3/STMN1/OR2A5/LCP1/LDIR/ARHGDI/LGALS9/LHCSR/C11orf87/LMINA/LMO2/RAB19/LPP/MCZ/MCC/MEZ/MFNG/MGAT1/SCGB2A1/MITF/LHX8/ASGR1/MOCS1/MOV10/MPZ/PLEKHG7/MYH4/MYL2/NUBP1/NDUFB4/DRG1/NEU1/ATP1A2/NFATC3/NH/LH2/NPPC/NRAS/OAS2/RNF165/OPRL1/OR2C1/OR3A2/SLC22A18/P2R16/PFAH4/ATP5B/IL21R/ANOT7/SPOCK3/BOAL1/UTP11/PRR16/CHST15/PCYOX1/C11orf73/SIRT6/DE6B/ATP8A2/P13/PTX2/PKHD1/PKM/PLA2G2A/PLAGL1/LRP1B/PRKAG3/PML/EXD6/GPR84/SLC1C1/PNLP/TLR9/TREM1/SSH1/RIN2/POUZAF1/APBB1P/MXR8A8/FBLM1/MED18/CY2W1/RPP25/TTC12/BANP/PPP1CB/HERC6/ELP3/DNAJC17/GOLPH3/PPP2R2B/FANG/MOBI1A/SLC47A1/SLC29A3/MIS18BP1/TRPV6/SLC30A10/CHRNA9/THUMPD1/PEX26/FRMD4A/CARD1/PARVA/PRKAR1B/TTC17/IFT122/MCTP2/LMBR10/CESGALNACT1/PAG1/CISD1/MYNN1/POBR/MAPK3/MAP2K2/PCDH8/PRKRR/PROC/MRAP/PSMD7/SLURP1/TENM2/GATA2B/ERMN/RNF150/MARK4/PTPRE/CREBZF/FAM60A/ACTA2/RFC2/TRIM27/RGR/RITZ/RPA3/BGLAP/SC7/CLL1/MRPS14/NPAS3/PARG/NO2/TINAG1/ARHGAP9/GZF1/DNAI2/PCDH20/VPS3A/BMP4/SLC44A1/SPAT12/ZNF649/ZG16/SLC6A12/SLC8A1/SLC9A3/BMPRI1B/SLT1/BRD9/ZSCAN18/BOX/BP/SRP68/STAT2/STK3/SUPT6H/BST2/JCCEB2/ZEB1/TEAD3/TERF1/TGM2/JCHH/TNFAIP3/ZNF665/CSPP1/ERMP1/CALD1/FAM188A/TFME62/GPR157/ZC3H12A/UCP1/WNT108/ZAP70/ZNF7/CA7/CACNA1E/MOCS/ARBT/ER3/CCDC86/CAIRD14/8/CLL14/CE5/ANTXR1/BFSP2/ATP13A4/YIP4/ZNF397/NROB2/CASQ1/HOPX/PARD6G/KRBA1/TBK1/RET/LN/TRIM63/GTTPB3/RAE1/PPFB7/SLC43A1/IFTM1/SGN/CDK10/KMO/RUNX1/TP63/RUNX3/SEPPINAG/IRS2/ACTN1/CRADD/TNFRSF11A/ALDH1A2/STK19/SYNI2/SPHK1/BUO31/CNAJ1/ENDOU/SKAP2/STBD1/SLAMF9/CH25H/CCR2/ERI1/PRCL1/STARD13/PIAS2/M/AP36/SYTY/SLC16A3/CBFAZ2/RSAD2/AURKB/DAP1/CD8A/CCDC102A/NEURL3/TRIP10/ADIPOQ/ENTPD3/PREP1/RAR36/MICAL2/N48P1/VGLL4/NUP93/RAPGEF2/CD79A/DAZAP2/ZBTB395/IOSEC1/LPGAT1/FGF19/NR1H4</p>

GO:0060089	molecular transducer activity	90/581	1634/17046	2.80E-06	0.00081	0.01502	0.00076	90	KLRG1/CHRNA1/CHRNA2/SORCS1/CCR1/IL13RA/ORA2A14/MIB2/DMBT1/EPHA1/ESR1/ADGRF1/NPTN/GPR26/FFAR2/GRIK4/GUCY1A3/GPR132/HLA-DOA/HLA-DPA1/NR4A1/HRH1/HTR3A/GPR142/IL1R1/IL10RA/IL11RA/IL12RB2/IL15RA/ITGB2/ITGB7/KCNH2/KDR/STMN1/ORA2S/LDLR/LGALS9/LHCG/MC2R/MCC/ASGR1/OPRL1/ORB2C1/ORA32/P2RY6/IL21R/PRKHD1/LRP1B/GPR84/TLR9/TREM1/CHRNA9/APOB/RNAPK3/SLAMF8/RGMA/PTGFR/PTPRE/TRIM27/IRG8/TINAGL1/SLC20A2/BMPRL1B/TNFRSF4/GPR157/ANTXR1/NR1H4
GO:0004872	receptor activity	73/581	1364/17046	7.40E-05	0.01606	0.01502	0.01502	73	KLRG1/CHRNA1/CHRNA2/SORCS1/CCR1/IL13RA/ORA2A14/DMBT1/EPHA1/ESR1/ADGRF1/NPTN/GPR26/FFAR2/GRIK4/GUCY1A3/GPR132/HLA-DOA/HLA-DPA1/NR4A1/HRH1/HTR3A/GPR142/IL1R1/IL10RA/IL11RA/IL12RB2/IL15RA/ITGB2/ITGB7/KCNH2/KDR/STMN1/ORA2S/LDLR/LGALS9/LHCG/MC2R/MCC/ASGR1/OPRL1/ORB2C1/ORA32/P2RY6/IL21R/PRKHD1/LRP1B/GPR84/TLR9/TREM1/CHRNA9/APOB/RNAPK3/SLAMF8/RGMA/PTGFR/PTPRE/TRIM27/IRG8/TINAGL1/SLC20A2/BMPRL1B/TNFRSF4/GPR157/ANTXR1/NR1H4
GO:0004871	signal transducer activity	75/581	1444/17046	0.00015	0.02624	0.02453	0.02453	75	CHRNA1/CHRNA2/SORCS1/CCR1/MAP3K8/IL13RA/ORA2A14/MIB2/DMBT1/EPHA1/ESR1/ADGRF1/NPTN/GPR26/FFAR2/GRIK4/GPR132/HLA-DOA/HLA-DPA1/NR4A1/HRH1/HTR3A/GPR142/IL1R1/IL10RA/IL11RA/IL12RB2/IL15RA/ITGB2/JUP/KCNH2/KDR/STMN1/ORA2S/LGALS9/LHCG/MC2R/OPRL1/ORB2C1/ORA32/P2RY6/IL21R/G/PR84/TLR9/CHRNA9/MAPK3/RGMA/PTGFR/ALEKH5/PTPRE/TRIM27/IRG8/RGS12/BMPRL1B/STAT2/STK3/BST2/TNFRSF1A/TRAFF5/CCR2/TNFRSF4/GPR157/ANTXR1/NR0B2/TRIM63/IFITM1/IRS2/TNFRSF11A/SPHK1/CCR2/IL13RA/ORA2A14/MAP3K6/CD8A/RAPGEF2/CD79A/NR1H4
GO:0004896	cytokine receptor activity	10/581	80/17046	0.00038	0.04963	0.04641	0.04641	10	CCR1/IL13RA/IL1R1/IL10RA/IL11RA/IL12RB2/IL15RA/IL21R/CCR2/CCR2L2
GO:0005515	protein binding	372/581	9755/17046	0.0004	0.04963	0.04641	0.04641	372	AKT3/ABI1/TANK/CD300LD/GNE/ZNF783/FARP1/KLRG1/CDKN1C/SFEG/NRV11/TRDN/SPON2/COG5/TACC2/CELF1/PNRC1/TMED10/RER1/ESM1/HNRNPUL1/ERLIN2/PKBP3/EGLN2/ATXN2L/KIF32/ACOT7/EXO3/GPRIN3/SORCS1/RBP1/AP3S1/CLIN5/CCR1/SLCS1B/TNFAIP8L1/RRQ3/NEU4/COMP/MAP3K8/ADM/IL13RA/UBLCPT1/CPS1/CRABP1/CRYBB3/MIB2/PARP4/MP7/FAM101A/MGAT5B/CSTA/KLC3/SMYD1/SH3D19/CYLD/DOB1/DDB1/ZNF356/BHLHA15/PPP1R1B/DLGG/DMBT1/ABAT/DPH1/DTNA/AGXT/EEF2/EFNA2/EIF4G1/A2M/ELK4/ANKRD23/ADCK5/EPHA1/ESR1/F11/FAH/SPATA13/FCGR2A/PHACTR1/FGA/FGF10/FHIT/TRAK1/MR8B2/FOXO2/EXPH5/NFASC/EP84L13/GGAS3/DIP2A/FLOT2/MC1L/TBC1D1/NUP210/NEDD4L/SYNE1/PPP1R13B/PUM2/RYBP/MAPK8IP2/TSSK2/VGLL2/TLL10/RNF144B/CCDC110/SAMM50/DFNB31/ALS2CL/PNKO/SACS/RP56KCI/PAABPCL/AKAP8L/DNAIC2/FGF2/NPTN/BMP10/ZNF844/HEM5/FFAR2/TRIM42/GRB10/DNAIC15/TMOD4/GUCY1A3/SOX8/HK1/HLA-DOA/NR4A1/ACACB/HOXC4/HSPAL1/HSP90B81/ADAMTSL5/ANKRD45/TFAP2E/ID3/RSP02/IGF1/IGF2/LCE2D/IL1R1/IL1RN/IL10RA/IL12RB2/IL15RA/IL16/FOXK2/AQP5/INHBA/NP/PSA/RF1/ITGA7/ITGB2/ITGB7/ITIH4/IVU/JUP/CD82/KCNH2/KCNM8/KCNJ9/KDR/KIF25/PO5/C17orf82/HES5/RBM12B/LAIR2/LANAA3/STMN1/LCP1/LDLR/ARHGDA1/LGALS9/C11orf87/LVINA/LMO2/LPP/MC2R/MCC/SCGB2A1/MITE/HX8/ASGR1/MOV10/MYH4/MYL2/NUBP1/DRG1/ATP1A2/NFATC3/NHLH2/NPCC/NRAS/OAS2/OPRL1/SLC22A18/P2RY6/ATP5B/P/ARK2/BOLA1/UTP11/PRR16/C11orf73/SIRT6/PTX2/PKHD1/PKMX/PRKAG3/PML/FXYD6/TLR9/TREM1/SSH1/POU2AF1/PPB1P/FBLIM1/MED18/RP25/TTCL2/BANP/PPP1CB/ELP3/GOLPH3L/PPP2R2B/FANCI/MOB1A/MIS18BP1/TRPV6/PEX26/FRMD4A/CARD0/PKR/PRKAR1B/TTC17/FT122/LMBRD1/PKAG1/MAPK3/MAP2K2/PRKRIR/PROC/MRAP/TRPV5/PRMT8/HTRA1/PAK6/ARNTL2/RGMA/PSMD7/SUURP1/TENM2/GATAD2B/ERMN/MARK4/PTPRE/CREBZF/FAM60A/ACTA2/RFC2/TRIM27/RGR/IRIT2/RPA3/SCT/CCL11/NPAs3/PA/PGV/NOD2/TINAGL1/ARHGAP9/DNA2/NP533A/BMP4/SLC4A1/ZNF649/ZG16/SLC6A12/SLC8A1/SLC9A3/BMPR1B/SULT1/BRD9/BOX/STAT2/STK3/SUPT6H/BSZ2/TCB2/ZEB1/TEAD3/TERF1/TFW2/TCHH/TNFAIP3/TNFRSF1A/TRAFF5/TRPC6/CCR2/WNT10B/ZAP70/RAB7A/CCDC86/CARD14/CBL2L14/IGF1R/CSP1/CALD1/FAM188A/ZC3H12A/FARP100/CPEB4/ZNF436/ICALR/SUIRP/CAST/CAP2B/SLC25A18/ANTXR1/BFSP2/MPPE4/ZNF397/NR0B2/HOP/PARD6G/RETNLB/TRIM63/GTBPB3/RAE1/IFITM1/SCIN/CDK10/RUNX1/TP63/RUNX3/IRS2/ACTN1/CRADD/TNFRSF1A/SYNI2/SPHK1/BUD31/CCNA1/ENDOU/SKAP2/SITB01/CCR2/PRCI/STARD13/PIAS2/SYT7/SLC16A3/CBFA2T2/AURKB/DAPI1/CD8A/TRIP10/ADIPOOE1/NTPD3/MICAL2/N4BP1/VGLL4/RAPGEF2/CD79A/DZAP2/FGF19/NR1H4
Hypermethyated DMC, Biological Process	Description	GeneRatio	BgRatio	pvalue	p.adjust	qvalue	geneId	Count	

GO:0065007	biological regulation	235/311	10343/17046	9.80E-06	7.81E-06	7/ ZG168/ZFP42/APCDD1/CTGF/ADRB3/FITM1/TRPV3/ZNF709/ZNF781/CITED4/RNF168/COCH/NLRP6/DNMT3A/DRD4/ECE1/EGFR/EGR3/PAT12/TMEM17/UNC13D/EPHA3/EPH4/SP8/XRN2/RASA3/PPM1E/VASH1/ACIN1/TBC1D9B/FOXO1/SPG20/FLN8/LARP1/MOTOR/GABBR1/TENM4/RGS22/FBXO2/GAPDH5/AMPD2/SDCBP2/DKK3/GLS2/NPS4A/GP/R162/GNAS/CRACR2B/GPER1/DOK7/FLVCR1/ZBTB44/GSTP1/GTF2B/BRF1/ANME7/GZMA/ANXA2/SERPIND1/KCNIP2/ANXA6/HLA-B/HLA-E/HLA-F/HLX/HMGA1/HPCA/APBA2/HOXB3/HOXC5/HOXD6/HOXD3/ACADU/HSP90AA1/HTRSA/COI.28A1/FMN1/BAHR12/CYR61/IL6/SL1/THH3/ILG1/LTBP1/SMA/D3/MEI/MEF2D/MAP3K1/MEOX1/MEOX2/MF12/MIT1A/NEDD9/NFYB/NMBR/NOV/NTF3/PALM/ARHGFE10/PRMT6/ZNFS32/MPD3/CNOT11/SYBU/LIMS2/VACL14/PRK1/BIN3/MAS1/PSMB4/TRPC7/LPARE/PK4/CYTL1/POMC/PONI1/ZDHHC13/ROBO4/BNC2/PPP1CC/PIWIL2/ARHGFE10/PRMT6/ZNFS32/MPD3/CNOT11/SYBU/LIMS2/VACL14/PRK1/BIN3/MAS1/PSMB4/TRPC7/LPARE/ACTR3B/METTL14/CCAR2/PXN/RASGRF2/S100A4/S100A6/CCL17/SFRP2/CXCR5/TRA2B/SGK1/MICAL1/SOX9/STK10/VAMP2/TA4B/TBP/CEA1/ACTC1/TIMP3/TLE3/TLRS/TNXB/TRA/AF1/TRPC4/PHLDA2/TWIST1/VARS/WWHAG/ZNF124/ZNF177/PTP4A1/CACNB2/PAX8/CXCR4/FZD5/TMEM204/NLRX1/ZC3H14/ZNF606/RAB11FP1/COL18A1/UNC93B1/CAPS/COLO/SH3BGR13/SCRT1/HIST1H3A/SLA2/PARD6B/IL1F10/SPINK7/KDM2B/LOXL3/MGARP/CBX2/GAS7/FADD/LIMD1/ZFAND2A/LDB2/SMIDT1/REEP6/ARHGAP29/LY86/RAB3D/H2AFY/SMA05-AS1/MTLS/ARHGFE10/ULK2/USP6N1/TELO2/RABGAP1L
GO:0032501	multicellular organismal process	165/311	6425/17046	1.08E-05	8.61E-06	CDH3/CDH13/KCNMB2/ZBTB18/DNMT2/CELF2/TBR1/ADCG3/CHRNA5/CIDEA/ZG168/SLC38A10/COL11A1/SC1T1/ZFP42/APCDD1/CTGF/ADRB3/TRPV3/RNF168/COCH/NLRP6/DNMT3A/DRD4/ECE1/EGFR/EGR3/EMLI/EPHA3/EPH4/SP8/XRN2/RASA3/VASH1/ACIN1/FOXO1/FOXO3/SPG20/FLN8/MOTOR/TENM4/GAPDH5/GIA3/GIB2/AMPD2/SDCBP2/DKK3/NPS4A/GNA/S1ZUIMD1/GPER1/FLVCR1/GSTP1/ANME7/ANXA2/SERPIND1/KCNIP2/NRG1/ANXA6/HLA-B/HLA-E/HLA-F/HLX/HPCA/APBA2/HOXB3/HOXC5/HOXD6/HOXD3/ACADU/HSP90AA1/HTRSA/COI.28A1/FMN1/BAHR12/CYR61/IL6/SL1/THH3/ILG1/LTBP1/SMA/D3/MEI/MEF2D/MAP3K1/MEOX1/MEOX2/MF12/MIT1A/NEDD9/NFYB/NMBR/NOV/NTF3/PALM/ARHGFE10/PRMT6/ZNFS32/MPD3/CNOT11/SYBU/LIMS2/VACL14/PRK1/BIN3/MAS1/PSMB4/TRPC7/LPARE/ACTR3B/METTL14/CCAR2/PXN/RASGRF2/S100A4/S100A6/CCL17/SFRP2/CXCR5/TRA2B/SGK1/MICAL1/SOX9/STK10/VAMP2/TA4B/TBP/CEA1/ACTC1/TIMP3/TLE3/TLRS/TNXB/TRA/AF1/TRPC4/PHLDA2/TWIST1/VARS/WWHAG/ZNF124/ZNF177/PTP4A1/CACNB2/PAX8/CXCR4/FZD5/TMEM204/NLRX1/ZC3H14/ZNF606/RAB11FP1/COL18A1/UNC93B1/CAPS/COLO/SH3BGR13/SCRT1/HIST1H3A/SLA2/PARD6B/IL1F10/SPINK7/KDM2B/LOXL3/MGARP/CBX2/GAS7/FADD/LIMD1/ZFAND2A/LDB2/SMIDT1/REEP6/ARHGAP29/LY86/RAB3D/H2AFY/SMA05-AS1/MTLS/ARHGFE10/ULK2/USP6N1/TELO2/RABGAP1L
GO:0050789	regulation of biological process	226/311	9837/17046	1.15E-05	9.18E-06	CDH3/TSNAN5/CDH13/MBNL2/KCNMB2/ZBTB18/DNMT2/CELF2/TBR1/HCT5/NPFRR2/ADCV3/PSIP1/B4GALIT7/PTH2/CHRNA5/ZBED9/CIDEA/ANKRD9/FRMD6/ZFP42/APCDD1/CTGF/ADRB3/FITM1/TRPV3/ZNF781/CITED4/RNF168/COCH/NLRP6/DNMT3A/DRD4/ECE1/EGFR/EGR3/PAT12/TMEM17/UNC13D/EPHA3/EPH4/SP8/XRN2/RASA3/PPM1E/VASH1/ACIN1/TBC1D9B/FOXO1/SPG20/FLN8/LARP1/MOTOR/GABBR1/TENM4/RGS22/FBXO2/GAPDH5/AMPD2/DKK3/GLS2/NPS4A/GPR162/GNAS/CRACR2B/GPER1/DOK7/FLVCR1/ZBTB44/GSTP1/GTF2B/BRF1/ANME7/GZMA/ANXA2/SERPIND1/KCNIP2/NRG1/ANXA6/HLA-B/HLA-E/HLA-F/HLX/HMGA1/HPCA/APBA2/HOXB3/HOXC5/HOXD6/HOXD3/ACADU/HSP90AA1/HTRSA/COI.28A1/FMN1/BAHR12/CYR61/IL6/SL1/THH3/ILG1/LTBP1/SMA/D3/MEI/MEF2D/MAP3K1/MEOX1/MEOX2/MF12/MIT1A/NEDD9/NFYB/NMBR/NOV/NTF3/PALM/ARHGFE10/PRMT6/ZNFS32/MPD3/CNOT11/SYBU/LIMS2/VACL14/PRK1/BIN3/MAS1/PSMB4/TRPC7/LPARE/ACTR3B/METTL14/CCAR2/PXN/RASGRF2/S100A4/S100A6/CCL17/SFRP2/CXCR5/TRA2B/SGK1/MICAL1/SOX9/STK10/VAMP2/TA4B/TBP/CEA1/ACTC1/TIMP3/TLE3/TLRS/TNXB/TRA/AF1/TRPC4/PHLDA2/TWIST1/VARS/WWHAG/ZNF124/ZNF177/PTP4A1/CACNB2/PAX8/CXCR4/FZD5/TMEM204/NLRX1/ZC3H14/ZNF606/RAB11FP1/COL18A1/UNC93B1/CAPS/COLO/SH3BGR13/SCRT1/HIST1H3A/SLA2/PARD6B/IL1F10/SPINK7/KDM2B/LOXL3/MGARP/CBX2/GAS7/FADD/LIMD1/ZFAND2A/LDB2/REEP6/ARHGAP29/LY86/RAB3D/H2AFY/SMA05-AS1/ARHGFE10/ULK2/USP6N1/TELO2/RABGAP1L
GO:0044699	single-organism process	267/311	12449/17046	1.44E-05	1.15E-05	CDH3/TSNAN5/CDH13/KCNMB2/ZBTB18/DNMT2/CELF2/TBR1/SEP19/HCT5/NPFRR2/ADCV3/PSIP1/B4GALIT7/PTH2/CHRNA5/CIDEA/CLCA1/ANKRD9/FRMD6/C15orf27/ZG168/SLC38A10/ABO41BP/COL11A1/GALM/SC1T1/ZFP42/TRPM6/APCDD1/CTGF/CYB561/ADRB3/FITM1/ADAL/TRPV3/WBP2NL/RNF168/COCH/NLRP6/DNAH8/DNMT3A/DRD4/DSG3/ECE1/EGFR/EGR3/FITM1/TMEM17/EMLI/UNC13D/DNAH12/EPHA3/EPH4/ALAS1/SP8/XRN2/RASA3/PPM1E/VASH1/ACIN1/LIMCH1/FOXO1/SPG20/FLNB/ATP11A/LARP1/MOTOR/FUCA1/GABBR1/GAK/TENM4/RGS22/FBXO2/GAPDH5/GIA3/GIB2/AMPD2/SDCBP2/DKK3/GLS2/NPS4A/GPR162/GNAS/CRACR2B/PIGW1/TZUMO1/GPER1/FLVCR1/GSTP1/ANME7/GZMA/ANXA2/SERPIND1/KCNIP2/NRG1/ANXA6/HLA-B/HLA-E/HLA-F/HLX/HMGA1/HPCA/APBA2/HOXB3/HOXC5/HOXD6/HOXD3/HS17B2/ACADU/HSP90AA1/HTRSA/COI.28A1/FMN1/BAHR12/CYR61/IL6/SL1/THH3/ILG1/LTBP1/SMA/D3/MEI/MEF2D/MAP3K1/MEOX1/MEOX2/MF12/MIT1A/NEDD9/NFYB/NMBR/NOV/NTF3/PALM/ARHGFE10/PRMT6/ZNFS32/MPD3/CNOT11/SYBU/LIMS2/VACL14/PRK1/BIN3/MAS1/PSMB4/TRPC7/LPARE/ACTR3B/METTL14/CCAR2/PXN/RASGRF2/EXOC4/RPL29/S100A4/CCL17/SFRP2/CXCR5/TRA2B/SGK1/MICAL1/CERX/SOX9/STK10/VAMP2/TA4B/TBP/CEA1/ACTC1/TIMP3/TLE3/TLRS/TRAAPC10/TNXB/TRA/AF1/TRPC4/PHLDA2/TWIST1/JU/P1/VARS/WWHAG/PTP4A1/CACNB2/PAX8/CXCR4/FZD5/PPDPF/GDDP3/TMEM204/NLRX1/EPHX3/RAB11FP1/COL18A1/UNC93B1/CAPS/COLO/SH3BGR13/SCRT1/HIST1H3A/SLA2/PARD6B/IL1F10/SPINK7/KDM2B/LOXL3/MGARP/CBX2/GAS7/FADD/LIMD1/MAP7/LDB2/SMIDT1/RCSO1/SOR42E1/ARHGAP29/LY86/RAB3D/H2AFY/SMA05-AS1/ARHGFE10/ULK2/USP6N1/TELO2

GO:0009987	cellular process	285/311	13765/17046	6.00E-08	2.34E-05	1.86E-05	11/CHRNA5/ZBED9/CIDEA/ALPK2/CLCA1/ANKRD9/FRMD6/C15orf27/SC38A10/APOA1BP/COL11A1/SCNT1/ZFP42/TRPM6/ADCC1/CTGF/CYB561/ADRB3/ITIM1/ADAL/TRPV3/ZNF709/ZNF781/CITED4/WBP2NL/RNF168/COCH/NLRP6/DNAH8/DNMT3A/DRD4/DSG3/ECE1/EGFR/EGFR3/PATL2/TMEM17/EMIL1/UNC13D/DNAH12/EPHA3/EPHA4/ALAS1/RNF182/S/P8/ARN2/RASA3/PPM1E/VASH1/ACINI/LUMCH1/FOXO1/SPG20/FILN/ATP1/LARP1/MTOR/GABBR1/GAK/TENM1/ITN1/RS22/FBXO2/GAPDH5/GJA3/MS2/AMPD2/SDCBP2/DK3/GLS2/VPS4A/GPR162/GNAS/PIGV/ZUMOI/GPER1/DOCK7/FLVCL1/ZBTB44/GSTP1/GTF2B/BRF1/NME7/GZMA/ANXA2/SERPIND1/KCNIP2/NRG1/ANXA6/HLA-B/HLA-E/HLA-F/HILX/HMGAI/HPCA/APBA2/HOXB3/HOX5/HOX6/HOX7/HOX8/HOX9/HOX10/MEF2D/MEF2L/MAP3K1/MEOX1/MEOX2/MEF2/MTL1/NUD1/NEEDD9/NFYB/NMBR/NOV/NTF3/PALM/ARHGEF3/LEF1/DDX47/CEND1/A/LC6A17/LCK/LUGL1/LOX/MTB/LTB/LTP2/SMAD3/ME1/MEF2D/MP3K3/PIKC3G/SPA17/PLEC/IL20RB/RIPK4/CTTL1/POMC/PON1/MOVI0L1/ZDHHC13/ROBO4/BNC2/PCAT2/PPP1CC/PIWIL2/ARHGEF10L/PRTNFGF4/PDE4C/PDE7A/PTIP1/SGP3/SMPD3/CNOT11/SYB1/LIMS2/VAC14/PRKD1/BIN3/MAS1/PSMB4/PTPC7/LPAB5/ACTB38/MEIT1L1/CCAR2/PXN/RPL8/RPL29/S100A4/S100A6/CCL17/SFRP2/CXCR5/TRA2B/SGK1/MICAL1/CERK1/SOX9/STK10/VAMP2/TAFA48/TBP/TCEA1/ACTC1/TPM3/TLE3/TLR5/TRAPEL2/TNMB/TRAFA1/TRPC4/PHLDA2/TWIST1/UPP1/VARS/YWHAG/ZNF124/ZNF177/PTP441/CACNB2/PAX8/CXCR4/FZD5/PPDPF/TMEM204/NLRX1/EPHX3/ZH314/ZNF606/RAB11FP1/COL18A1/JUNC93B1/CAPS/COLO/HIST1H2BM/SH3BGR1/SCRIPT1/HIST1H3A/SLAZ/PAARD6B/ALI10/SPINK7/KDM2B/LOXL3/IMGARP/CBX2/GAS7/FADD/LIMD1/MA7/ZFAND2/ILDB2/ZREBP6/ARHGAP29/LY86/RA/B3D/H2AFY/SMAD5-AS1/MTLS/ARHGEF10/ULK2/USP6NL/TELO2
GO:0050794	regulation of cellular process	216/311	9347/17046	7.37E-08	2.63E-05	2.10E-05	11/CHRNA5/ZBED9/CIDEA/ALPK2/CLCA1/ANKRD9/FRMD6/C15orf27/SC38A10/APOA1BP/COL11A1/SCNT1/ZFP42/TRPM6/ADCC1/CTGF/CYB561/ADRB3/ITIM1/ADAL/TRPV3/ZNF709/ZNF781/CITED4/WBP2NL/RNF168/COCH/NLRP6/DNAH8/DNMT3A/DRD4/DSG3/ECE1/EGFR/EGFR3/PATL2/TMEM17/EMIL1/UNC13D/DNAH12/EPHA3/EPHA4/ALAS1/RNF182/S/P8/ARN2/RASA3/PPM1E/VASH1/ACINI/LUMCH1/FOXO1/SPG20/FILN/ATP1/LARP1/MTOR/GABBR1/GAK/TENM1/ITN1/RS22/FBXO2/GAPDH5/GJA3/MS2/AMPD2/SDCBP2/DK3/GLS2/VPS4A/GPR162/GNAS/PIGV/ZUMOI/GPER1/DOCK7/FLVCL1/ZBTB44/GSTP1/GTF2B/BRF1/NME7/GZMA/ANXA2/SERPIND1/KCNIP2/NRG1/ANXA6/HLA-B/HLA-E/HLA-F/HILX/HMGAI/HPCA/APBA2/HOXB3/HOX5/HOX6/HOX7/HOX8/HOX9/HOX10/MEF2D/MEF2L/MAP3K1/MEOX1/MEOX2/MEF2/MTL1/NUD1/NEEDD9/NFYB/NMBR/NOV/NTF3/PALM/ARHGEF3/LEF1/DDX47/CEND1/A/LC6A17/LCK/LUGL1/LOX/MTB/LTB/LTP2/SMAD3/ME1/MEF2D/MP3K3/PIKC3G/SPA17/PLEC/IL20RB/RIPK4/CTTL1/POMC/PON1/MOVI0L1/ZDHHC13/ROBO4/BNC2/PCAT2/PPP1CC/PIWIL2/ARHGEF10L/PRTNFGF4/PDE4C/PDE7A/PTIP1/SGP3/SMPD3/CNOT11/SYB1/LIMS2/VAC14/PRKD1/BIN3/MAS1/PSMB4/PTPC7/LPAB5/ACTB38/MEIT1L1/CCAR2/PXN/RPL8/RPL29/S100A4/S100A6/CCL17/SFRP2/CXCR5/TRA2B/SGK1/MICAL1/CERK1/SOX9/STK10/VAMP2/TAFA48/TBP/TCEA1/ACTC1/TPM3/TLE3/TLR5/TRAPEL2/TNMB/TRAFA1/TRPC4/PHLDA2/TWIST1/UPP1/VARS/YWHAG/ZNF124/ZNF177/PTP441/CACNB2/PAX8/CXCR4/FZD5/PPDPF/TMEM204/NLRX1/EPHX3/ZH314/ZNF606/RAB11FP1/COL18A1/JUNC93B1/CAPS/COLO/HIST1H2BM/SH3BGR1/SCRIPT1/HIST1H3A/SLAZ/PAARD6B/ALI10/SPINK7/KDM2B/LOXL3/IMGARP/CBX2/GAS7/FADD/LIMD1/MA7/ZFAND2/ILDB2/ZREBP6/ARHGAP29/LY86/RA/B3D/H2AFY/SMAD5-AS1/MTLS/ARHGEF10/ULK2/USP6NL/TELO2
GO:0044707	single-multicellular organism process	158/311	6214/17046	1.30E-07	4.29E-05	3.42E-05	11/CHRNA5/ZBED9/CIDEA/ALPK2/CLCA1/ANKRD9/FRMD6/C15orf27/SC38A10/APOA1BP/COL11A1/SCNT1/ZFP42/TRPM6/ADCC1/CTGF/CYB561/ADRB3/ITIM1/ADAL/TRPV3/ZNF709/ZNF781/CITED4/WBP2NL/RNF168/COCH/NLRP6/DNAH8/DNMT3A/DRD4/DSG3/ECE1/EGFR/EGFR3/PATL2/TMEM17/EMIL1/UNC13D/DNAH12/EPHA3/EPHA4/ALAS1/RNF182/S/P8/ARN2/RASA3/PPM1E/VASH1/ACINI/LUMCH1/FOXO1/SPG20/FILN/ATP1/LARP1/MTOR/GABBR1/GAK/TENM1/ITN1/RS22/FBXO2/GAPDH5/SDCBP2/DK3/GLS2/VPS4A/GPR162/GNAS/GPER1/DOCK7/ZBTB44/GSTP1/GTF2B/BRF1/NME7/GZMA/ANXA2/SERPIND1/KCNIP2/NRG1/ANXA6/HLA-B/HLA-E/HLA-F/HILX/HMGAI/HPCA/APBA2/HOXB3/HOX5/HOX6/HOX7/HOX8/HOX9/HOX10/MEF2D/MEF2L/MAP3K1/MEOX1/MEOX2/MEF2/MTL1/NUD1/NEEDD9/NFYB/NMBR/NOV/NTF3/PALM/ARHGEF3/LEF1/DDX47/CEND1/ANGPT4/PDE4C/PDE7A/PGRAM2/PKC3G/IL20RB/RIPK4/CTTL1/POMC/ZD/HHC13/ROBO4/BNC2/PTIP1/SGP3/SMPD3/CNOT11/SYB1/LIMS2/VAC14/PRKD1/BIN3/MAS1/PSMB4/PTPC7/LPAB5/ACTB38/MEIT1L1/CCAR2/PXN/RASGR2/S100A4/S100A6/CCL17/SFRP2/CXCR5/TRA2B/SGK1/MICAL1/SOX9/STK10/VAMP2/TAFA48/TBP/TCEA1/ACTC1/TPM3/TLE3/TLR5/TRAPEL2/TNMB/TRAFA1/PHLDA2/TWIST1/VARS/YWHAG/ZNF124/ZNF177/PTP441/CACNB2/PAX8/CXCR4/FZD5/TMEM204/NLRX1/ZH314/ZNF606/RAB11FP1/COL18A1/JUNC93B1/CAPS/COLO/SH3BGR1/SCRIPT1/HIST1H3A/SLAZ/PAARD6B/ALI10/SPINK7/KDM2B/LOXL3/IMGARP/CBX2/GAS7/FADD/LIMD1/MA7/ZFAND2/ILDB2/ZREBP6/ARHGAP29/LY86/RA/B3D/H2AFY/SMAD5-AS1/MTLS/ARHGEF10/ULK2/USP6NL/TELO2
GO:0048468	cell development	67/311	1998/17046	4.85E-07	0.00015	0.00012	11/CHRNA5/ZBED9/CIDEA/ALPK2/CLCA1/ANKRD9/FRMD6/C15orf27/SC38A10/APOA1BP/COL11A1/SCNT1/ZFP42/TRPM6/ADCC1/CTGF/CYB561/ADRB3/ITIM1/ADAL/TRPV3/ZNF709/ZNF781/CITED4/WBP2NL/RNF168/COCH/NLRP6/DNAH8/DNMT3A/DRD4/DSG3/ECE1/EGFR/EGFR3/PATL2/TMEM17/EMIL1/UNC13D/DNAH12/EPHA3/EPHA4/ALAS1/RNF182/S/P8/ARN2/RASA3/PPM1E/VASH1/ACINI/LUMCH1/FOXO1/SPG20/FILN/ATP1/LARP1/MTOR/GABBR1/GAK/TENM1/ITN1/RS22/FBXO2/GAPDH5/SDCBP2/DK3/GLS2/VPS4A/GPR162/GNAS/GPER1/DOCK7/ZBTB44/GSTP1/GTF2B/BRF1/NME7/GZMA/ANXA2/SERPIND1/KCNIP2/NRG1/ANXA6/HLA-B/HLA-E/HLA-F/HILX/HMGAI/HPCA/APBA2/HOXB3/HOX5/HOX6/HOX7/HOX8/HOX9/HOX10/MEF2D/MEF2L/MAP3K1/MEOX1/MEOX2/MEF2/MTL1/NUD1/NEEDD9/NFYB/NMBR/NOV/NTF3/PALM/ARHGEF3/LEF1/DDX47/CEND1/ANGPT4/PDE4C/PDE7A/PGRAM2/PKC3G/IL20RB/RIPK4/CTTL1/POMC/ZD/HHC13/ROBO4/BNC2/PTIP1/SGP3/SMPD3/CNOT11/SYB1/LIMS2/VAC14/PRKD1/BIN3/MAS1/PSMB4/PTPC7/LPAB5/ACTB38/MEIT1L1/CCAR2/PXN/RASGR2/S100A4/S100A6/CCL17/SFRP2/CXCR5/TRA2B/SGK1/MICAL1/SOX9/STK10/VAMP2/TAFA48/TBP/TCEA1/ACTC1/TPM3/TLE3/TLR5/TRAPEL2/TNMB/TRAFA1/PHLDA2/TWIST1/VARS/YWHAG/ZNF124/ZNF177/PTP441/CACNB2/PAX8/CXCR4/FZD5/TMEM204/NLRX1/ZH314/ZNF606/RAB11FP1/COL18A1/JUNC93B1/CAPS/COLO/SH3BGR1/SCRIPT1/HIST1H3A/SLAZ/PAARD6B/ALI10/SPINK7/KDM2B/LOXL3/IMGARP/CBX2/GAS7/FADD/LIMD1/MA7/ZFAND2/ILDB2/ZREBP6/ARHGAP29/LY86/RA/B3D/H2AFY/SMAD5-AS1/MTLS/ARHGEF10/ULK2/USP6NL/TELO2
GO:0009653	anatomical structure morphogenesis	80/311	2579/17046	6.92E-07	0.0002	0.00016	11/CHRNA5/ZBED9/CIDEA/ALPK2/CLCA1/ANKRD9/FRMD6/C15orf27/SC38A10/APOA1BP/COL11A1/SCNT1/ZFP42/TRPM6/ADCC1/CTGF/CYB561/ADRB3/ITIM1/ADAL/TRPV3/ZNF709/ZNF781/CITED4/WBP2NL/RNF168/COCH/NLRP6/DNAH8/DNMT3A/DRD4/DSG3/ECE1/EGFR/EGFR3/PATL2/TMEM17/EMIL1/UNC13D/DNAH12/EPHA3/EPHA4/ALAS1/RNF182/S/P8/ARN2/RASA3/PPM1E/VASH1/ACINI/LUMCH1/FOXO1/SPG20/FILN/ATP1/LARP1/MTOR/GABBR1/GAK/TENM1/ITN1/RS22/FBXO2/GAPDH5/SDCBP2/DK3/GLS2/VPS4A/GPR162/GNAS/GPER1/DOCK7/ZBTB44/GSTP1/GTF2B/BRF1/NME7/GZMA/ANXA2/SERPIND1/KCNIP2/NRG1/ANXA6/HLA-B/HLA-E/HLA-F/HILX/HMGAI/HPCA/APBA2/HOXB3/HOX5/HOX6/HOX7/HOX8/HOX9/HOX10/MEF2D/MEF2L/MAP3K1/MEOX1/MEOX2/MEF2/MTL1/NUD1/NEEDD9/NFYB/NMBR/NOV/NTF3/PALM/ARHGEF3/LEF1/DDX47/CEND1/ANGPT4/PDE4C/PDE7A/PGRAM2/PKC3G/IL20RB/RIPK4/CTTL1/POMC/ZD/HHC13/ROBO4/BNC2/PTIP1/SGP3/SMPD3/CNOT11/SYB1/LIMS2/VAC14/PRKD1/BIN3/MAS1/PSMB4/PTPC7/LPAB5/ACTB38/MEIT1L1/CCAR2/PXN/RASGR2/S100A4/S100A6/CCL17/SFRP2/CXCR5/TRA2B/SGK1/MICAL1/SOX9/STK10/VAMP2/TAFA48/TBP/TCEA1/ACTC1/TPM3/TLE3/TLR5/TRAPEL2/TNMB/TRAFA1/PHLDA2/TWIST1/VARS/YWHAG/ZNF124/ZNF177/PTP441/CACNB2/PAX8/CXCR4/FZD5/TMEM204/NLRX1/ZH314/ZNF606/RAB11FP1/COL18A1/JUNC93B1/CAPS/COLO/SH3BGR1/SCRIPT1/HIST1H3A/SLAZ/PAARD6B/ALI10/SPINK7/KDM2B/LOXL3/IMGARP/CBX2/GAS7/FADD/LIMD1/MA7/ZFAND2/ILDB2/ZREBP6/ARHGAP29/LY86/RA/B3D/H2AFY/SMAD5-AS1/MTLS/ARHGEF10/ULK2/USP6NL/TELO2
GO:0048518	positive regulation of biological process	130/311	4960/17046	9.63E-07	0.00026	0.00021	11/CHRNA5/ZBED9/CIDEA/ALPK2/CLCA1/ANKRD9/FRMD6/C15orf27/SC38A10/APOA1BP/COL11A1/SCNT1/ZFP42/TRPM6/ADCC1/CTGF/CYB561/ADRB3/ITIM1/ADAL/TRPV3/ZNF709/ZNF781/CITED4/WBP2NL/RNF168/COCH/NLRP6/DNAH8/DNMT3A/DRD4/DSG3/ECE1/EGFR/EGFR3/PATL2/TMEM17/EMIL1/UNC13D/DNAH12/EPHA3/EPHA4/ALAS1/RNF182/S/P8/ARN2/RASA3/PPM1E/VASH1/ACINI/LUMCH1/FOXO1/SPG20/FILN/ATP1/LARP1/MTOR/GABBR1/GAK/TENM1/ITN1/RS22/FBXO2/GAPDH5/SDCBP2/DK3/GLS2/VPS4A/GPR162/GNAS/GPER1/DOCK7/ZBTB44/GSTP1/GTF2B/BRF1/NME7/GZMA/ANXA2/SERPIND1/KCNIP2/NRG1/ANXA6/HLA-B/HLA-E/HLA-F/HILX/HMGAI/HPCA/APBA2/HOXB3/HOX5/HOX6/HOX7/HOX8/HOX9/HOX10/MEF2D/MEF2L/MAP3K1/MEOX1/MEOX2/MEF2/MTL1/NUD1/NEEDD9/NFYB/NMBR/NOV/NTF3/PALM/ARHGEF3/LEF1/DDX47/CEND1/ANGPT4/PDE4C/PDE7A/PGRAM2/PKC3G/IL20RB/RIPK4/CTTL1/POMC/ZD/HHC13/ROBO4/BNC2/PTIP1/SGP3/SMPD3/CNOT11/SYB1/LIMS2/VAC14/PRKD1/BIN3/MAS1/PSMB4/PTPC7/LPAB5/ACTB38/MEIT1L1/CCAR2/PXN/RASGR2/S100A4/S100A6/CCL17/SFRP2/CXCR5/TRA2B/SGK1/MICAL1/SOX9/STK10/VAMP2/TAFA48/TBP/TCEA1/ACTC1/TPM3/TLE3/TLR5/TRAPEL2/TNMB/TRAFA1/PHLDA2/TWIST1/VARS/YWHAG/ZNF124/ZNF177/PTP441/CACNB2/PAX8/CXCR4/FZD5/TMEM204/NLRX1/ZH314/ZNF606/RAB11FP1/COL18A1/JUNC93B1/CAPS/COLO/SH3BGR1/SCRIPT1/HIST1H3A/SLAZ/PAARD6B/ALI10/SPINK7/KDM2B/LOXL3/IMGARP/CBX2/GAS7/FADD/LIMD1/MA7/ZFAND2/ILDB2/ZREBP6/ARHGAP29/LY86/RA/B3D/H2AFY/SMAD5-AS1/MTLS/ARHGEF10/ULK2/USP6NL/TELO2

GO:0019222	regulation of metabolic process	152/311	6084/17046	1.03E-06	0.00026	0.00021	EGR3/CDH13/MBNL2/C1D/ZBTB18/DMRT2/TBR1/NPFR2/ADCY3/PSIP1/ZBED9/CIDEA/ZFP42/CTGF/ADRB3/ZNF709/ZNF781/CITED4/RNF168/NLRP6/DNMT3A/DRD4/ECE1/EGFR/BRF1/GZMA/ANXA3/SERPIND1/NGR1/HLX/HMGAI/HPCA/HOXB3/HOXC5/HOXC6/HOXD3/ACAD10/HSP90AA1/COI28A1/IBARHL2/CYR61/IL6/ISL1/ITIH3/HILS1/LCK/LG1/LIT/B/SWAD3/MEI1/MEF2D/MAP3K1/MEOX2/MF2/NFYB/NOV/NTF3/PALM/ARHGFE3/LEF1/ANGPT4/PGAM2/PIK3CG/RIK4/CYTL1/ITIH3/ARHGFE10/PPP1CC/PPP1LCC/PIWIL2/ARHGFE10/PRMT6/ZNF532/CNOT11/VAC14/PRKD1/MASP1/PSMB4/METTL4/CCAR2/PXN/RASGRF2/CCL17/SFRP2/TRA2B/S/GK1/SOX9/STK10/TA4B8/TBP/TCEA1/ACTC1/TIMP3/TLR5/TLR6/TRA1/PHLDA2/TWIST1/VARS/YWHAG/ZNF124/ZNF177/PAX8/CXCR4/FZD5/ZC3H14/ZNF606/SHPBGR3/SCRT1/HISTH3A/SLA2/SPINK7/KDM2B/LOXL3/CBX2/GAS7/FADD/LI/ZEAND2A/LDB2/ARHGAP29/H2AF1/ARHGFE10/ULK2/USP6NL/RABGAP11
GO:0031323	regulation of cellular metabolic process	137/311	5352/17046	1.54E-06	0.00037	0.00029	CDH3/CDH13/MBNL2/C1D/ZBTB18/DMRT2/TBR1/NPFR2/ADCY3/PSIP1/ZBED9/CIDEA/ZFP42/CTGF/ADRB3/ZNF709/ZNF781/CITED4/RNF168/NLRP6/DNMT3A/DRD4/ECE1/EGFR/BRF1/PATL2/SP8/XRN2/RASAS3/PPM1E/ACIN1/FLVCR1/ANXA2/KCNIP2/NGR1/HLX/HMGAI/HPCA/HOXB3/HOXC5/HOXC6/HOXD3/ACAD10/HSP90AA1/COI28A1/IBARHL2/CYR61/IL6/ISL1/ITIH3/HILS1/LCK/LG1/LIT/B/SWAD3/MEI1/MEF2D/MAP3K1/MEOX2/MF2/NFYB/NOV/NTF3/PALM/ARHGFE3/LEF1/ANGPT4/PGAM2/PIK3CG/RIK4/CYTL1/ITIH3/ARHGFE10/PPP1CC/PPP1LCC/PIWIL2/ARHGFE10/PRMT6/ZNF532/CNOT11/VAC14/PRKD1/MASP1/PSMB4/METTL4/CCAR2/PXN/RASGRF2/CCL17/SFRP2/TRA2B/S/GK1/SOX9/STK10/TA4B8/TBP/TCEA1/ACTC1/TIMP3/TLR5/TLR6/TRA1/PHLDA2/TWIST1/VARS/YWHAG/ZNF124/ZNF177/PAX8/CXCR4/FZD5/ZC3H14/ZNF606/SHPBGR3/SCRT1/HISTH3A/SLA2/SPINK7/KDM2B/LOXL3/CBX2/GAS7/FADD/LI/ZEAND2A/LDB2/H2AF1/ULK2
GO:0006928	movement of cell or subcellular component	60/311	1789/17046	2.23E-06	0.0005	0.0004	CDH13/TBR1/ADCY3/PRMT6/APCDD1/CTGF/DNAH8/EGFR/EGR3/EPHA3/EPHB4/VASH1/GAPDH5/GPER1/NRNG1/HSP90AA1/IBARHL2/CYR61/IL6/ISL1/LCK/S/MAO3/MAP3K1/NOV/NTF3/PALM/LEF1/CENDF1/ANGPT4/PIK3CG/SP17/ROB04/PRKD1/BIN3/PSMB4/TRPC7/RASGRF2/CCL17/SFRP2/CXCR3/SGK1/SOX9/STK10/ACTC1/TRPC4/PHLDA2/TWIST1/PTP4A1/CACNB2/CXCR4/COI18A1/SHPBGR3/SCRT1/PARD6B/MIGARP/FADD/LI/MD1
GO:0030154	cell differentiation	97/311	3469/17046	3.55E-06	0.00076	0.00061	CDH3/ZBTB18/TBR1/FRMD6/COI18A1/SC11/ZFP42/APCDD1/CTGF/ADRB3/DNMT3A/EGFR/EGR3/EMIL1/UNC13D/EPHA3/EPHB4/RASAS3/ACIN1/FOXO1/SPG20/FLNB/MTOR/TENM4/GAPDH5/GNAS/GPER1/FLVCR1/ANXA2/KCNIP2/NGR1/HLA-B/HLX/HOXB3/HOXD3/HSP90AA1/FMN1/IBARHL2/CYR61/IL6/ISL1/HILS1/INSC/LCK/ILG1/SMAD3/MEF2D/MAP3K1/MEOX1/MF12/NOV/NTF3/PALM/LEF1/CYTL1/MOV10L1/ROB04/PPP1CC/PIWIL2/SMAD3/PRKD1/BIN3/PSMB4/TPC7/PXN/RASGRF2/S100A6/CCL17/SFRP2/SGK1/SOX9/TA4B8/TCEA1/ACTC1/TRPC4/TWIST1/YWHAG/CACNB2/PAX8/CXCR4/FZD5/PPP1CC/PPP1LCC/PIWIL2/ARHGFE10/ULK2
GO:0048870	cell motility	44/311	1187/17046	5.41E-06	0.00105	0.00084	CDH13/ADCY3/APCDD1/CTGF/DNAH8/EGFR/EGR3/EPHA3/EPHB4/VASH1/GAPDH5/GPER1/NGR1/HLX/HILS1/LCK/SMAD3/MAP3K1/NOV/NTF3/LEF1/CEND1/ANGPT4/PIK3CG/ROB04/PRKD1/BIN3/CCL17/SFRP2/SGK1/SOX9/STK10/PHLDA2/TWIST1/PTP4A1/CXCR4/COI18A1/SHPBGR3/SCRT1/PARD6B/FADD/LI/MD1
GO:0051674	localization of cell	44/311	1187/17046	5.41E-06	0.00105	0.00084	CDH13/ADCY3/APCDD1/CTGF/DNAH8/EGFR/EGR3/EPHA3/EPHB4/VASH1/GAPDH5/GPER1/NGR1/HLX/HILS1/LCK/SMAD3/MAP3K1/NOV/NTF3/LEF1/CEND1/ANGPT4/PIK3CG/ROB04/PRKD1/BIN3/CCL17/SFRP2/SGK1/SOX9/STK10/PHLDA2/TWIST1/PTP4A1/CXCR4/COI18A1/SHPBGR3/SCRT1/PARD6B/FADD/LI/MD1
GO:0080990	regulation of primary metabolic process	133/311	5271/17046	5.85E-06	0.00109	0.00087	CDH13/MBNL2/C1D/ZBTB18/DMRT2/TBR1/NPFR2/ADCY3/PSIP1/ZBED9/CIDEA/ZFP42/CTGF/ADRB3/ZNF709/ZNF781/CITED4/RNF168/NLRP6/DNMT3A/DRD4/ECE1/EGFR/EGFR3/PATL2/SP8/XRN2/RASAS3/PPM1E/ACIN1/FLVCR1/ANXA2/KCNIP2/NGR1/HLX/HMGAI/HPCA/HOXB3/HOXC5/HOXC6/HOXD3/ACAD10/HSP90AA1/COI28A1/IBARHL2/CYR61/IL6/ISL1/ITIH3/HILS1/LCK/LG1/LIT/B/SWAD3/MEI1/MEF2D/MAP3K1/MEOX2/MF2/NFYB/NOV/NTF3/PALM/ARHGFE3/LEF1/ANGPT4/PGAM2/PIK3CG/RIK4/CYTL1/ITIH3/ARHGFE10/PPP1CC/PPP1LCC/PIWIL2/ARHGFE10/PRMT6/ZNF532/CNOT11/VAC14/PRKD1/MASP1/PSMB4/METTL4/CCAR2/PXN/RASGRF2/CCL17/SFRP2/TRA2B/S/GK1/SOX9/STK10/TA4B8/TBP/TCEA1/ACTC1/TIMP3/TLR5/TLR6/TRA1/PHLDA2/TWIST1/VARS/YWHAG/ZNF124/ZNF177/PAX8/CXCR4/FZD5/ZC3H14/ZNF606/SCRT1/HISTH3A/SLA2/SPINK7/KDM2B/LOXL3/CBX2/GAS7/FADD/LI/ZEAND2A/LDB2/H2AF1
GO:0060255	regulation of macromolecule metabolic process	132/311	5249/17046	7.92E-06	0.0014	0.00112	CDH3/CDH13/MBNL2/C1D/ZBTB18/DMRT2/TBR1/NPFR2/ADCY3/PSIP1/ZBED9/CIDEA/ZFP42/CTGF/ADRB3/ZNF709/ZNF781/CITED4/RNF168/NLRP6/DNMT3A/DRD4/ECE1/EGFR/BRF1/HLX/HMGAI/APBA2/HOXB3/HOXC5/COI28A1/IBARHL2/CYR61/IL6/ISL1/ITIH3/HILS1/LCK/LG1/LIT/B/SWAD3/MEI1/MEF2D/MAP3K1/MEOX1/MEOX2/MF12/LEF1/ANGPT4/PGAM2/PIK3CG/RIK4/CYTL1/ITIH3/ARHGFE10/PPP1CC/PPP1LCC/PIWIL2/ARHGFE10/PRMT6/ZNF532/CNOT11/VAC14/PRKD1/MASP1/PSMB4/METTL4/CCAR2/PXN/RASGRF2/TRA2B/S/GK1/SOX9/STK10/TA4B8/TBP/TCEA1/ACTC1/TIMP3/TLR5/TLR6/TRA1/PHLDA2/TWIST1/VARS/YWHAG/ZNF124/ZNF177/PAX8/CXCR4/FZD5/ZC3H14/ZNF606/SCRT1/HISTH3A/SLA2/SPINK7/KDM2B/LOXL3/CBX2/GAS7/FADD/LI/ZEAND2A/LDB2/H2AF1
GO:0051239	regulation of multicellular organismal process	70/311	2298/17046	8.18E-06	0.0014	0.00112	CDH3/KCNMB2/DMRT2/CELF2/TBR1/CIDEA/CTGF/ADRB3/TPR3/NLRP6/GNAS/GPER1/FLVCR1/ANXA2/KCNIP2/NGR1/ANXA6/HLA-B/HLA-E/HLX/HOXB3/HOXD3/IBARHL2/CYR61/IL6/ISL1/LCK/LITB/SMAD3/NOV/NTF3/PALM/LEF1/CEND1/ANGPT4/PIK3CG/LDB2/PRKD1/SFRP2/SGK1/SOX9/TLR5/PHLDA2/TWIST1/YWHAG/PAX8/CXCR4/FZD5/LNXX1/RAB11FP1/VASH1/ARHGFE3/SCRT1/FADD/LI/MD1/H2AF1/ULK2
GO:0016477	cell migration	41/311	1095/17046	9.25E-06	0.00152	0.00122	CDH13/APCDD1/CTGF/EGFR/EGR3/EPHA3/EPHB4/VASH1/GAPDH5/GPER1/NGR1/HLX/HILS1/LCK/SMAD3/MAP3K1/NOV/NTF3/LEF1/CEND1/ANGPT4/PIK3CG/ROB04/PRKD1/BIN3/CCL17/SFRP2/SGK1/SOX9/STK10/PHLDA2/TWIST1/PTP4A1/CXCR4/COI18A1/SHPBGR3/SCRT1/PARD6B/FADD/LI/MD1

GO:0044763	single-organism cellular process	241/311	11314/17046	1.03E-05	0.00163	0.0013	CDH3/TPAN5/CDH13/KCNMB2/BCKDK/TCIRG1/ABC94/C1D7/ZBTB18/TBR1/SEPT9/HCS2/NIPFR2/ADC3/SLC27A2/HIBADH/B4GALT7/PTH2/CHRNA5/CIDEA/C1CA1/ANKRD9/FRM D6/C15orf27/SLC38A10/APOA1BP/COL11A1/SLC11/EP42/TRPM6/APCDD1/CTGF/CYB5E1/ADRB3/FTM1/ADAL/TRPV3/WBP2/NJ/RNF168/COCH/NLRP6/DNAH8/DNMT3A/DRD4/D S63/EGFR/EGFR3/TMEM17/EMIL1/UNC13D/DNAH12/EPH4/ALAS1/XR1R/RSAS3/PPM1E/VASH1/ACINI/LIMCH1/FOXO1/SPG20/FLNB/ATP11A/LARP1/MTOR/GABRR1/GAK /TENM4/RGS22/FBXO2/GAPDH5/GJA3/GBZ2/AMPD2/SLC27A2/DK3/GLS2/VPS4A/GPRL62/GNAS/PIGW/IZUMIO4/GPER1/FLVCR1/GSTP1/NNIE7/GZMA/ANXA2/KCNIP2/NRG1/ANX A6/HLA-B/HLA-E/HLA-F/HIX/HMG3/HPCA/APBAZ/HOXB3/HOXD3/ACADL/HS90AA1/HTR5A/COL28A1/FMNI1/BARHL2/CYR61/L6/ISL1/HILS1/ATP9B/ACAT1/KRT15/INSC/SLC6A17/LCK/LGL1/LOX/ITB /LTPJ/SMAD3/MEI1/MEF2D/MAP3K1/MEOX1/MEOX2/MIF2/NUDT1/NEDD9/NNBR/NOV/NTF3/PALM/ARHGFE3/LEF1/DDX47/CEND1/ANGPT4/PDE4C/PDE7A/GALNT1/PGAM2/P IC/G/PIK3CG/SPA17/PIEC/IL20RB/CYTL1/POMC/PON1/MOV10L1/ZDHHC13/ROBO4/PCAT2/PPP1CC/PWILZ/ARHGFE10L/PRMT6/WDR33/SMIP3/CNOT11/SYBU/LIMS2/VACL4/PR K01/BIN3/PSMB4/TRPC7/LPAR5/ACTR3B/CCAR2/PXN/RASGRF2/EXOC4/RPL18/RPL29/S100A6/S100A7/CLL17/SFRP2/CXCR5/SGK1/AMICAL1/CERK/SOX9/STK10/NAIMP2/TAF4B/TBP/ TCEA1/ACTC1/TLR3/TLR5/TRAAPC10/TNXB/TRAFA1/TRPC4/PHLDA2/TWIST1/UPP1/VARS/YWHAG/PTP441/CACNB2/PAX8/CXCR4/FZD5/PPDPF/TMEM204/NLRX1/EPHX3/RAB11FIP 1/COL18A1/JUNC93B1/CAPS/COLQ/SHBBGR13/SCRT1/HST1H3A/SLA2/PARD6B/IL1F10/KOM2B/LOX3/MGAR/CEB2/GAS7/FADD/LIMD1/MAP7/SMO1T1/ARHGAP29/LY86/RAB3D/ H2AFY/SMAD5-AS1/MTL5/ARHGFE10/ULK2/TELO
GO:0001525	angiogenesis	21/311	398/17046	1.43E-05	0.00218	0.00174	CDH13/CTGF/EGR3/EPH4/VASH1/ANXA2/HOXB3/CYR61/L6/ISL1/MEOX2/NOV/LEF1/ANGPT4/PIK3CG/ROBO4/PRKDI1/SFRP2/TWIST1/FZD5/COL18A1
GO:0072358	cardiovascular system development	34/311	861/17046	1.96E-05	0.0028	0.00223	CDH13/COL11A1/CTGF/ECCE1/EGR3/EPH4/WASH1/FOXO1/MTOR/TENM4/FLVCR1/ANXA2/NRG1/HOXB3/CYR61/L6/ISL1/LOX/SMAD3/MEF2D/MEOX2/NOV/LEF1/ANGPT4/PIK3C G/ROBO4/PRKDI1/SFRP2/SOX9/ACTC1/TWIST1/FZD5/TMEM204/COL18A1
GO:0072359	circulatory system development	34/311	861/17046	1.96E-05	0.0028	0.00223	CDH13/COL11A1/CTGF/ECCE1/EGR3/EPH4/WASH1/FOXO1/MTOR/TENM4/FLVCR1/ANXA2/NRG1/HOXB3/CYR61/L6/ISL1/LOX/SMAD3/MEF2D/MEOX2/NOV/LEF1/ANGPT4/PIK3C G/ROBO4/PRKDI1/SFRP2/SOX9/ACTC1/TWIST1/FZD5/TMEM204/COL18A1
GO:0040011	locomotion	54/311	1666/17046	2.09E-05	0.00289	0.00231	CDH13/TBR1/ADCY3/APCDD1/CTGF/DNAH8/EGFR/EGR3/EPH43/EPH4/RASA3/WASH1/GAPDH5/GPER1/SFRP1/ND1/NRG1/HS90AA1/BARHL2/CYR61/L6/ISL1/LCK/SMAD3/MAP3 K1/NOV/NTF3/LEF1/CEND1/ANGPT4/PIK3CG/ROBO4/PRKDI1/BIN3/PSMB4/TRPC7/RASGRF2/CCL17/SFRP2/CXCR5/SGK1/SOX9/STK10/TRPC4/PHLDA2/TWIST1/PTP441/CACNB2/C XCR4/COL18A1/SH3BGRL3/SCRT1/PARD6B/FADD/LIMD1
GO:0048869	cellular developmental process	99/311	3716/17046	2.25E-05	0.00301	0.0024	NB/MTOR/TENM4/GAPDH5/GNAS/GPER1/FLVCR1/ANXA2/KCNIP2/NRG1/HLA-B/HIX/HOXB3/HOXD3/HS90AA1/FMNI1/BARHL2/CYR61/L6/ISL1/HILS1/INSC1/CK/LGL1/SMAD3/MEF2D/MAP3K1/MEOX1/MIF2/NOV/NTF3/PALM/LEF1/CEND1/CYTL1/MOV10L 1/ROBO4/PPP1CC/PWILZ/SMIP3/PRKDI1/BIN3/PSMB4/TRPC7/PXN/RASGRF2/S100A6/CCL17/SFRP2/SGK1/SOX9/TAFA4B/TCEA1/ACTC1/TRPC4/TWIST1/YWHAG/CACNB2/ PAX8/CXCR4/FZD5/PPDPF/TMEM204/COL18A1/SCRT1/PARD6B/LOX3/CB2/GAS7/FADD/LIMD1/H2AFY/NTL5/ARHGFE10/ULK2
GO:0072132	mescnyme morphogenesis	6/311	33/17046	2.57E-05	0.00333	0.00266	ISL1/SMAD3/LEF1/SOX9/ACTC1/TWIST1
GO:0031348	negative regulation of defense response	11/311	130/17046	2.64E-05	0.00333	0.00266	NLRP6/GPER1/GSTP1/HLA-B/HLA-E/ISL1/SMAD3/NOV/IL20RB/PSMB4/NLRX1
GO:0009888	tissue development	54/311	1684/17046	2.82E-05	0.00345	0.00275	CDH3/ZBTB18/DMRT2/FRMD6/COL11A1/APCDD1/CTGF/DRD4/EGFR/EPH43/SPG20/FLNB/TENM4/GBZ2/GNAS/NRG1/HLX/HPCA/HOXB3/HOXD3/FMNI1/BARHL2/CYR61/L6/ISL1/ ACAT1/KRT15/INSC/SMAD3/MEF2D/MAP3K1/MEOX1/MEOX2/NOV/NTF3/LEF1/RIPK4/CYTL1/BNC2/BIN3/PXN/S100A4/SFRP2/SOX9/ACTC1/TIMP3/TWIST1/PAX8/FZD5/COL18A1/ KDM2B/LOX3/LDB2/H2AFY
GO:0051171	regulation of nitrogen compound metabolic process	102/311	3889/17046	3.08E-05	0.00347	0.00277	CDH13/MBNL1/C1D7/ZBTB18/DMRT2/TBR1/NIPFR2/PSIP1/ZBED9/CIDEA/ZFP42/ADRB3/ZNF709/ZNF781/CITED4/RNF168/DNMT3A/DRD4/EGFR/EGR3/PATL2/SP8/XRN2/ACINI/F OXO1/SPG20/LARP1/MTOR/GABBR1/GAPDH5/DK3/GNAS/GPER1/ZBTB44/GTF2B/BRF1/GZMA/NRGL1/HIX/HMGA1/HPCA/HOXB3/HOXC5/HOXC6/HOXD3/HS90AA1/BARHL2/CY R61/L6/ISL1/HILS1/SMAD3/MEI1/MEF2D/MEOX1/MEOX2/NFYB/NTF3/PALM/LEF1/PGAM2/RIPK4/CYTL1/POMC/BNC2/PWILZ/PRMT6/ZNF533/CNOT11/PRKDI1/PSMB4/METTL4/ CCAR2/SFRP2/TRA2B/SGK1/SOX9/TAFA4B/TBP/TCEA1/TLR3/TLR5/TRAFA1/TWIST1/VARS/ZNF124/ZNF177/PAX8/FZD5/ZC9H14/ZNF606/SCRT1/HIST1H3A/SLA2/KDM2B/LOX3/CB2 /GAS7/FADD/LIMD1/LDB2/H2AFY
GO:0040012	regulation of locomotion	28/311	659/17046	3.09E-05	0.00347	0.00277	CDH13/TBR1/EGFR/VASH1/GPER1/CYR61/L6/ISL1/SMAD3/MAP3K1/NOV/NTF3/LEF1/ANGPT4/ROBO4/PRKDI1/SFRP2/SGK1/SOX9/STK10/PHLDA2/TWIST1/PTP441/CXCR4/COL18A1/S H3BGRL3/SCRT1/PARD6B/FADD
GO:0048513	organ development	80/311	2848/17046	3.14E-05	0.00347	0.00277	CDH3/ZBTB18/TBR1/SLC38A10/COL11A1/ZFP42/APCDD1/CTGF/DRD4/EGFR/EGR3/EML1/EPH43/EPH4/RASA3/EGFR/EGR3/FLNB/MTOR/TENM4/GBZ2/DK3/GNAS/FLVC R1/NNIE7/ANXA2/NRG1/HLA-B/HIX/HPCA/HOXB3/HOXD3/HS17B2/HTR5A/FMNI1/BARHL2/CYR61/L6/ISL1/ACAT1/INSC/SLC6A17/LCK/LOX/ITB/SMAD3/MEF2D/MAP3K1/MEOX1/MEOX2/NOV/NTF3/LEF1/CE ND1/CYTL1/BNC2/SMIP3/LIMS2/IMP3/BIN3/S100A4/SFRP2/CXCR5/TRA2B/SOX9/RASA3/TCEA1/ACTC1/TLR3/TLR5/PHLDA2/TWIST1/PAX8/FZD5/PPDPF/COL18A1/KDM2B/LOX3/FAOD/IDB2/ H2AFY

GO:0000904	cell morphogenesis involved in differentiation	36/311	958/17046	3.16E-05	0.00347	0.00277	TBR1/FRMD6/EGFR/UNC13D/EPHA3/EPH4/RASA3/SPG20/FLNB/NRG1/HSP90AA1/FMN1/BARHL2/SL1/LGGL1/SMAD3/MAP3K1/MFR2/NTF3/LEF1/PSMB4/TRPC7/PXN/RASGRF2/S100A4/S100A6/SFRP2/SOX9/TRPC4/TWIST1/CACNB2/PAX8/COL18A1/PARD6B/LOXL3/ULK2	36
GO:0007399	nervous system development	65/311	2174/17046	3.39E-05	0.00359	0.00286	ZBTB18/TBR1/SCLT1/APCDD1/DNMT3A/EGFR/EGR3/EMIL1/EPHA3/EPH4/RASA3/SPG20/MTOR/TENM4/SDCBP2/GPER1/GSTP1/NME7/KCNP2/NGR1/HLX/HPCA/APBA2/HOXB3/HOXD3/HSP90AA1/HTRSA/FMN1/BARHL2/IL6/IL5/IL3/ACAT1/INSC/SLCGA17/LGGL1/MEF2D/NTF3/PALM/LEF1/CEND1/PPP1CC/PRKD1/PSMB4/TRPC7/RASGRF2/S100A6/SFRP2/TRA2B/S/GSK3/SOX9/TIMP3/TRPC4/TWIST1/YWHAG/CACNB2/PAX8/CXCR4/FZD5/COLO/SCRT1/PARD6B/KDM2B/GAST/ARHGFE10/ULK2	65
GO:0001944	vasculature development	25/311	557/17046	3.43E-05	0.00359	0.00286	CDH13/CTGF/EGR3/EPH4/VASH1/FOXO1/FLVCR1/ANXA2/HOXB3/CYR61/IL6/IL5/IL3/LOX/MEOX2/NOV/LEF1/ANGPT4/PIK3CG/ROBO4/PRKD1/SFRP2/TWIST1/FZD5/TNEM204/COL18A1	25
GO:0003002	regionalization	18/311	332/17046	4.13E-05	0.00411	0.00327	DMRT2/TBR1/SP8/NME7/HOXB3/HOXG6/HOXD3/SL1/SMAD3/MEOX1/MEOX2/LEF1/SFRP2/TRA2B/PAX8/FZD5/KDM2B	18
GO:2000145	regulation of cell motility	26/311	599/17046	4.19E-05	0.00411	0.00327	CDH13/EGFR/VASH1/GPER1/CYR61/IL6/SMAD3/MAP3K1/NOV/NTF3/LEF1/ANGPT4/ROBO4/PRKD1/SFRP2/S/GK1/SOX9/STK10/PHLDA2/TWIST1/PTP4A1/COL18A1/SH3BGR/L3/SCR26/T1/PARD6B/FADD	26
GO:0050728	negative regulation of inflammatory response	9/311	91/17046	4.21E-05	0.00411	0.00327	NLRP6/GPER1/GSTP1/SL1/SMAD3/NOV/IL20RB/PSMB4/NLRX1	9
GO:0030334	regulation of cell migration	25/311	568/17046	4.72E-05	0.00449	0.00358	CDH13/EGFR/VASH1/GPER1/CYR61/IL6/SMAD3/MAP3K1/NOV/NTF3/LEF1/ANGPT4/ROBO4/PRKD1/SFRP2/S/GK1/SOX9/STK10/PHLDA2/PTP4A1/COL18A1/SH3BGR/L3/SCR26/6B/FADD	25
GO:0001568	blood vessel development	24/311	536/17046	5.12E-05	0.00477	0.00381	CDH13/CTGF/EGR3/EPH4/VASH1/FOXO1/FLVCR1/ANXA2/HOXB3/CYR61/IL6/IL5/IL3/LOX/MEOX2/NOV/LEF1/ANGPT4/PIK3CG/ROBO4/PRKD1/SFRP2/TWIST1/FZD5/COL18A1	24
GO:0048522	positive regulation of cellular process	109/311	4283/17046	5.33E-05	0.00486	0.00388	CDH3/TPAN5/CDH13/TCIRG1/DMRT2/TBR1/HGST/ADCY3/PSIP1/CTGF/ADRB3/TRPV3/CITED4/RNF168/DNMT3A/DRD4/ECE1/EGFR/EGR3/UNC13D/EPHA3/RASA3/PPM1E/ACIN1/FOXO1/LARP1/MTOR/TENM4/GAPDH/SLG3/VPS4A/GNAS/GPER1/DOK7/GSTP1/BRF1/GZMA/ANXA2/NGR1/HLA-E/HLX/HMGA1/HPCA/HOXD3/HSP90AA1/FMN1/BARHL2/CYR61/IL6/IL5/IL3/LK/LTB/S/MAD3/MEF2D/MAP3K1/MEOX1/MEOX2/MFIZ/NFIB/NOV/NTF3/PALM/ARHGFE3/LEF1/ANGP T4/PIK3CG/RIPK4/CYTL1/POMIC/ZDHHC13/PWWL2/SMPD3/LIMS2/PRKD1/PSMB4/ACTR3B/CCAR2/PXN/RASGRF2/S100A4/S100A6/CCL17/SFRP2/CXCR5/TRA2B/SOX9/STK10/VAMP2/TBP/TCEA1/TLES/TRAF1/TWIST1/YWHAG/PTP4A1/PAX8/CXCR4/FZD5/COL18A1/SLA2/MGARP/FADD/LIMD1/ZFNAND2/LDB2/L186B/ABSD/HZAFY/ARHGFE10	109
GO:0032989	cellular component	47/311	1432/17046	5.76E-05	0.00514	0.0041	TBR1/FRMD6/SCLT1/COCH/EGFR/TNEM17/UNC13D/EPHA3/EPH4/RASA3/SPG20/FLNB/TENM4/NGR1/HSP90AA1/FMN1/BARHL2/IL6/IL5/IL3/LGGL1/LGGL1/SMAD3/MAP3K1/MFR2/NTF3/PALM/LEF1/BIN3/PSMB4/TRPC7/PXN/RASGRF2/S100A4/S100A6/SFRP2/S/GK1/SOX9/ACTC1/TRPC4/TWIST1/CACNB2/PAX8/COL18A1/PARD6B/LOXL3/GAS7/LIMD1/ULK2	47
GO:0000902	regulation of cell morphogenesis	45/311	1352/17046	6.08E-05	0.00532	0.00424	TBR1/FRMD6/SCLT1/COCH/EGFR/TNEM17/UNC13D/EPHA3/EPH4/RASA3/SPG20/FLNB/NGR1/HSP90AA1/FMN1/BARHL2/IL6/IL5/IL3/LGGL1/SMAD3/MAP3K1/MFR2/NTF3/PALM/LEF1/BIN3/PSMB4/TRPC7/PXN/RASGRF2/S100A4/S100A6/SFRP2/S/GK1/SOX9/TRPC4/TWIST1/CACNB2/PAX8/COL18A1/PARD6B/LOXL3/GAS7/LIMD1/ULK2	45
GO:0045761	regulation of adenylylate cyclase activity	8/311	75/17046	6.55E-05	0.00556	0.00443	NPFRR2/ADRB3/DRD4/GABRI1/GNAS/GPER1/HPCA/PALM	8
GO:0061448	connective tissue development	14/311	224/17046	6.62E-05	0.00556	0.00443	COL11A1/CTGF/SPG20/GNAS/HOXB3/HOXD3/CYR61/ACAT1/SMAD3/MEF2D/NOV/CYTL1/SFRP2/SOX9	14
GO:0010468	regulation of gene expression	99/311	3819/17046	6.97E-05	0.00575	0.00458	CDH3/CDH13/MBNL2/C1D/ZBTB18/DMRT2/TBR1/PSIP1/ZBED9/GIDEA/ZFP42/CTGF/ZNF709/ZNF781/CTEDA/RNF168/DNMT3A/EGFR/EGR3/PATL2/SP8/XRN2/ACIN1/FOXO1/SPG20/LARP1/MTOR/DKK3/GNAS/GPER1/ZBTB44/GT2B/BRF1/NGR1/HLX/HMGA1/APBA2/HOXB3/HOXG5/HOXG6/HOXD3/BARHL2/CYR61/IL6/IL5/IL3/LCK/SMAD3/MEF2D/MEOX1/MEOX2/MFIZ/NFIB/NOV/NTF3/LEF1/RIPK4/CYTL1/POMIC/BNC2/PPP1CC/PWWL2/PRMT6/ZNF532/CNOT11/PRKD1/MASBP1/METTL14/CCAR2/SFRP2/TRA2B/S/GK1/SOX9/STK10/VAMP2/TBP/TCEA1/ACTC1/TLES/TRAF1/PHLDA2/TWIST1/VARS/ZNF124/ZNF177/PAX8/FZD5/ZC3H14/ZNF606/SCRT1/HIST1H3A/SLA2/KOM2B/LOXL3/CBX2/GAS7/FADD/LIMD1/LDB2/HZAF Y	99
GO:0051179	localization	126/311	5173/17046	7.73E-05	0.00625	0.00498	CDH3/TPAN5/CDH13/KCNMB2/TCIRG1/ABCA9/TBR1/ADCY3/SLC27A2/CHRNA5/CIDEA/CUCA/FRMD6/C15orf27/SLC38A10/TRPM6/APCDD1/CTGF/CYB5E1/PTM1/TRPV3/NLRP6/DNAH8/DRD4/EGFR/EGR3/UNC13D/EPHA3/EPH4/RASA3/VASH1/FLNB/ATP11A/MTOR/GAPDH/GIA3/GJB2/SDCBP2/SLG3/VPS4A/GNAS/CACR2B/PIGW/GPER1/FLVCR1/GSTP1/NME7/ANXA2/KCNP2/NGR1/ANXA6/HLA-E/HPCA/APBA2/HSP90AA1/BARHL2/CYR61/IL6/IL5/IL3/LGGL1/ATP9B/INSC/TOMM201/SLCGA17/LCK/ILG1/LTB/PSMB4/3/MAP3K1/MFR2/NOV/NTF3/PALM/LEF1/CEND1/ANGPT4/PDE4C/PIK3CG/POMIC/PON1/ZDHHC13/ROBO4/SMPD3/PRKD1/BIN3/MASBP1/TRPC7/RASGRF2/EXO4/RPL8/RPL29/S100A6/CCL17/SFRP2/S/GK1/SOX9/STK10/VAMP2/TRAPPC10/TRPCA/PHLDA2/TWIST1/YWHAG/PTP4A1/CACNB2/PAX8/CXCR4/FZD5/ROB1/FIP1/COL18A1/UNC93B1/COLO/SH3BGR/L3/SCR26/T1/PARD6B/LOXL3/MGARP/FADD/LIMD1/MAP7/SMDT1/REEP6/RAB3D/HZAF/USP6N1/RABGAP1L	126

GO:0032879	regulation of localization	63/311	2151/17046	8.49E-05	0.00661	0.00527	CDH3/CDH13/TBR1/CIDEA/FITM1/TRPV3/NLRP6/DRD4/EGFR/UNC13D/VASH1/MTOR/GLS2/VPS4A/GNAS/CRACR2B/GPER1/ANXA2/KCNP2/NRG1/HLA-E/HPCA/CYR61/IL6/ISL1/LCK/ILG1/SMAD3/MAP3K1/NOV/NTF3/LEF1/ANGPT4/PDE4C/PIK3CG/POMC/PON1/ROBO4/SMPD3/SYBU/PRKDJ/RASGRF2/SFRP2/SGK1/SOX9/STK10/VAMP2/PHLDA2/TWIST1/YWHAG/PTP4A1/CACNB2/PAX8/FZD5/RAB11FIP1/COL18A1/SH3BGL3/SCRT1/PARD6B/FADD/REEP6/RAB3D/RABGAP1L	63
GO:0050790	regulation of catalytic activity	63/311	2151/17046	8.49E-05	0.00661	0.00527	CDH3/NPFRR2/ADCY3/CTGF/ADRB3/DRD4/EGFR/EPHA3/RASA3/PPM1E/TBC1D9B/MTOR/GABBR1/RGS22/GNAS/GPER1/DOK7/GSTP1/GZMA/ANXA2/SERPIND1/NRG1/HPCA/HSP90AA1/COL28A1/CYR61/IL6/ITIH3/LCK/ILG1/SMAD3/MAP3K1/NTF3/PALM/ARHGEF3/LEF1/ANGPT4/PIK3CG/ARHGEF10L/VAC14/PRKDI/PSMB4/CCAR2/PXN/RASGRF2/CCL17/SF	63
GO:0043009	chordate embryonic development	25/311	593/17046	9.38E-05	0.00718	0.00573	RFP2/SGK1/STK10/TCEA1/TIMP3/TNX8/YWHAG/CXCR4/FZD5/SH3BGL3/SPINK7/FADD/ARHGAP29/H2AF1/ARHGEF10/USP6N/RABGAP1L	
GO:0046058	cAMP metabolic process	11/311	150/17046	9.81E-05	0.00738	0.00588	ZBTB18/DMRT2/COL11A1/ZFP42/ECEL1/EGFR/GNAS/FLVCR1/APBA2/HOXB3/HOXC5/HOXC6/HOXD3/HSD17B2/CYR61/ISL1/RESP18/SMAD3/MEOX1/MEOX2/LEF1/SFRP2/TWIST1/FZD5/KDM2B	25
GO:0019219	regulation of nucleobase-containing compound metabolic process	94/311	3617/17046	0.00011	0.00771	0.00615	NPFRR2/ADCY3/ADRB3/DRD4/GABBR1/GNAS/GPER1/HPCA/PALM/PDE4C/PDE7A	11
GO:0009792	embryo development ending in birth or egg hatching	25/311	598/17046	0.00011	0.00771	0.00615	CDH13/MBNL2/C1D/ZBTB18/DMRT2/TBR1/NPFRR2/PSIP1/ZBED9/CIDEA/ZFP42/ADRB3/ZNF709/ZNF781/CITED4/RNF168/DNMT3A/DRD4/EGFR/EGR3/SP8/XRN2/ACIN1/FOXO1/S	94
GO:0060485	mesenchyme development	13/311	206/17046	0.00011	0.00771	0.00615	PG20/MTOR/GABBR1/GAPDH5/DK3/GNAS/GPER1/ZBTB44/GTF2B/BRF1/GZMA/NRG1/HLX/HMGAL1/HPCA/HOXB3/HOXC5/HOXC6/HOXD3/BAH2/CYR61/IL6/ISL1/HLS1/SMAD3/MEI1/MEF2D/MEOX1/MEOX2/NFYB/NTF3/PALM/LEF1/PGAM2/RIPK4/CYTL1/POMC/BNC2/PRMT6/ZNF532/CNOT11/PRKDI/CCAR2/SFRP2/TRA2B/SGK1/SOX9/TAF4B/TBP/TCEA1/TLE3/TRAF1/TWIST1/ZNF124/ZNF177/PAX8/FZD5/ZG3H14/ZNF606/SCRT1/HIST1H3A/SLAZ/KDM2B/LOX3/CBX2/GAS7/FADD/LIMD1/LDB2/H2AFY	
GO:0051270	regulation of cellular component movement	27/311	672/17046	0.00011	0.00771	0.00615	ZBTB18/DMRT2/COL11A1/ZFP42/ECEL1/EGFR/GNAS/FLVCR1/APBA2/HOXB3/HOXC5/HOXC6/HOXD3/HSD17B2/CYR61/ISL1/RESP18/SMAD3/MEOX1/MEOX2/LEF1/SFRP2/TWIST1/FZD5/KDM2B	25
GO:0051216	cartilage development	12/311	179/17046	0.00011	0.00781	0.00623	COL11A1/CTGF/GNAS/HOXB3/HOXD3/CYR61/SMAD3/MEF2D/NOV/CYTL1/SFRP2/SOX9	12
GO:0065009	regulation of molecular function	72/311	2588/17046	0.00012	0.00825	0.00658	CDH3/NPFRR2/ADCY3/CTGF/ADRB3/DRD4/EGFR/EPHA3/RASA3/PPM1E/TBC1D9B/MTOR/GABBR1/RGS22/GNAS/GPER1/DOK7/GSTP1/GZMA/ANXA2/SERPIND1/KCNP2/NRG1/HP	72
GO:0048706	embryonic skeletal system development	10/311	129/17046	0.00013	0.00858	0.00684	CA/HSP90AA1/COL28A1/CYR61/IL6/ISL1/ITIH3/LCK/ILG1/SMAD3/MAP3K1/NTF3/PALM/ARHGEF3/LEF1/ANGPT4/PIK3CG/RIPK4/CYTL1/PON1/ARHGEF10/VAC14/PRKDI/PSMB4/CCAR2/PXN/RASGRF2/CCL17/SFRP2/SGK1/STK10/VAMP2/TCEA1/TIMP3/TNX8/TRAF1/TWIST1/YWHAG/CACNB2/CXCR4/FZD5/SH3BGL3/SPINK7/FADD/ARHGAP29/H2AFY/ARHGEF10/USP6N/RABGAP1L	
GO:0009605	response to external stimulus	67/311	2366/17046	0.00013	0.00876	0.00698	DMRT2/COL11A1/GNAS/FLVCR1/HOXB3/HOXC6/HOXD3/SMAD3/TWIST1	10
GO:0009889	regulation of biosynthetic process	98/311	3834/17046	0.00013	0.00876	0.00699	CDH13/TBR1/COL11A1/ADRB3/COCH/NLRP6/DNMT3A/EGFR/EGR3/UNC13D/EPHA3/EPHB4/RASA3/ACIN1/FOXO1/LARP1/MTOR/GPER1/GSTP1/ANXA2/SERPIND1/NRG1/HLA-B/HLA-E/HMGAL1/HSP90AA1/CYR61/IL6/ISL1/ACAT1/KRT15/LCK/SMAD3/MAP3K1/NUDT1/NOV/NTF3/LEF1/PIK3CG/IL20RB/POMC/PON1/PPP1CC/PRKDI/MASBP1/PSMB4/TRPC7/RASGRF2/DEFB134/CCL17/SFRP2/CXCR3/SOX9/TIMP3/TLR5/TRPC4/UPP1/CACNB2/CXCR4/FZD5/NLRX1/UNC93B1/CAPS/HIST1H3A/FADD/LY86/ULK2	67
GO:1901362	organic cyclic compound biosynthetic process	102/311	4032/17046	0.00014	0.00881	0.00702	CDH3/CDH13/C1D/ZBTB18/DMRT2/TBR1/NPFRR2/PSIP1/ZBED9/CIDEA/ZFP42/CTGF/ADRB3/ZNF709/ZNF781/CITE4/RNF168/DNMT3A/DRD4/EGFR/EGR3/PATL2/SP8/XRN2/FOXO1/SPG20/LARP1/MTOR/GABBR1/DK3/GNAS/GPER1/ZBTB44/GSTP1/GTF2B/BRF1/NRG1/HLX/HMGAL1/HPCA/HOXB3/HOXC5/HOXC6/HOXD3/ACAD/HSP90AA1/BAH2/CYR61/IL6/ISL1/HLS1/LTB/SMAD3/MEF2D/MEOX1/MEOX2/NFYB/NTF3/PALM/LEF1/RIPK4/CYTL1/POMC/BNC2/PRMT6/ZNF532/CNOT11/PRKDI/METTL14/CCAR2/SFRP2/SGK1/SO	98
							OX9/TAF4B/TBP/TCEA1/TLE3/TUBS/TRAF1/TWIST1/VARS/ZNF124/ZNF177/PAX8/FZD5/ZNF606/SCRT1/HIST1H3A/SLAZ/KDM2B/LOX3/CBX2/GAS7/FADD/LIMD1/LDB2/H2AFY	
							CDH3/CDH13/TCIRG1/C1D/ZBTB18/DMRT2/TBR1/NPFRR2/ADCY3/CTGF/PSIP1/ZBED9/CIDEA/ZFP42/CTGF/ADRB3/ADAM/ZNF709/ZNF781/CITE4/RNF168/DNMT3A/DRD4/EGFR/EGR3/ALAS1/SP8/XRN2/FOXO1/MTOR/GABBR1/AMPD2/DK3/GS2/GNAS/GPER1/ZBTB44/GTF2B/BRF1/NME7/HLX/HMGAL1/HPCA/HOXB3/HOXC5/HOXC6/HOXD3/HSD17B2/BAH2/CYR61/IL6/ISL1/HLS1/SMAD3/MEI1/MEF2D/MEOX1/MEOX2/NFYB/NTF3/PALM/LEF1/RIPK4/CYTL1/POMC/BNC2/PRMT6/ZNF532/CNOT11/PRKDI/CCAR2/RPL8/RPL29/SFRP2/SGK1/SOX9/TAF4B/TBP/TCEA1/TLE3/TRAF1/TWIST1/JUPP1/YWHAG/ZNF124/ZNF177/PAX8/FZD5/ZNF606/SCRT1/HIST1H3A/SLAZ/KDM2B/LOX3/CBX2/GAS7/FADD/LIMD1/LDB2/SDR42E1/H2AFY	102

GO:0065008	regulation of biological quality	85/311	3225/17046	0.00016	0.01034	0.00825	K3/GLSZ/GNAS/GPER1/FLVCR1/GSTP1/BRF1/ANXA2/SERPIND1/KGNC1/COCH/NLRP6/DRD4/ECE1/ACIN1/FOXO1/SPG20/FLNB/ATP11A/MTOR/AMPD2/DK3/PT4/PDE4C/PK3CG/IL20RB8/CYTL1/POMC/SMPD3/SYBU/PRKD1/TRPC7/ACTR3B/METT11/4/CCAR2/PXN/RASGRF2/SGK1/SOX9/VAMP2/TCEA1/TRPC4/VARS/YWHAG/PAX8/CXCR4/ZC3H14/RAB11FP1/CO1Q/SH3BGR3/HIST1H3A/GAS7/FADD/LIMD1/LDB2/SMD1/RAB3D/MTL5/ULK2	85
GO:0048705	skeletal system morphogenesis	13/311	215/17046	0.00017	0.01037	0.00827	COL11A1/CTGF/GNAS/FLVCR1/HOX8/HOXD3/FMN1/SMAD3/MEF2D/BNC2/SFRP2/SOX9/TWIST1	13
GO:0048514	blood vessel morphogenesis	21/311	475/17046	0.00018	0.01091	0.0087	CDH13/CTGF/EGR3/EPH4/VASH1/ANXA2/HOXB3/CYR61/IL6/SLI/MEOX2/NOV/LEF1/ANGPT4/PK3CG/ROBO4/PRKD1/SFRP2/TWIST1/FZD5/COL18A1	21
GO:0006796	phosphate-containing compound metabolic process	76/311	2808/17046	0.00018	0.01091	0.0087	BCKDK/TCIRG1/HCS1/NPFR2/ADCY3/ALPK2/APOA1BP/TRPM6/CTGF/ADRB3/FITM1/ADAL/NLRP6/DRD4/EGRF/EPHA3/EPH84/RASA3/PPM1E/FOXO1/MTOR/GABRR1/GAK/GAP/HS/AMPD2/GNAS/PIGW/GPER1/DOK7/GSTP1/NAME1/ANXA2/NR31/HPCA/CYR61/IL6/SLI/LCK/SMAD3/MEI/IMAP3K1/NUDT1/NTF3/PALM/ANGPT4/PDE4C/PDE7A/PGAM2/PIGC/PK3CG/RIPK4/PON1/LPCAT2/PPP1CC/SMPD3/VACL1/PRKD1/PSMB4/PXN/RASGRF2/CCL17/SFRP2/SGK1/CERK/SOX9/STK10/TNX8/TWIST1/UPP1/YWHAG/PTP4A1/CXCR4/FZD5/LIMD1/H2AFY/ULK2	76
GO:0019438	aromatic compound biosynthetic process	99/311	3915/17046	0.00019	0.01107	0.00882	CDH3/CDH13/TCIRG1/C1D/ZBTB18/DMRT2/TBR1/NPFR2/ADCY3/PSIP1/ZBED9/CIDEA/ZFP42/CTGF/ADRB3/ADA/ZNF709/ZNF781/CITED4/RNF168/DNMT3A/DRD4/EGRF/EGR3/ALAS1/SP8/XRN2/FOXO1/MTOR/GABRR1/AMPD2/DK3/GLSZ/GNAS/GPER1/ZBTB44/GTF2B/BRF1/NAME7/NR61/HLX/HMGA1/HPCA/HOX3/HOX5/HOX6/HOXD3/BARHL2/CYR61/IL6/SLI/HLS1/SMAD3/ME1/MEF2D/MEOX1/MEOX2/NFYB/NTF3/PALM/LEF1/RIPK4/CYTL1/POMC/BNC2/PRMT6/ZNF533/CNOT11/PRKD1/CCAR2/RPLB/RPL29/SFRP2/SGK1/SOX9/TAF4B/TBP/TCBA1/TLE3/TRAF1/TWIST1/UPP1/YWHAG/ZNF124/ZNF177/PAX8/FZD5/ZNF606/SCRIPT1/HIST1H3A/SLA2/KDM2B/LOXL3/CBX2/GAS7/FADD/LIMD1/LDB2/H2AFY/DMRT2/SLC38A10/CO11A1/CTGF/GNAS/FLVCR1/ANXA2/HOXB3/HOX5/HOX6/HOXD3/FMN1/CYR61/SMAD3/MEF2D/NOV/CYTL1/BNC2/SFRP2/SOX9/TWIST1	99
GO:0001501	skeletal system development	21/311	478/17046	0.0002	0.01148	0.00915	DMRT2/SLC38A10/CO11A1/CTGF/GNAS/FLVCR1/ANXA2/HOXB3/HOX5/HOX6/HOXD3/FMN1/CYR61/SMAD3/MEF2D/NOV/CYTL1/BNC2/SFRP2/SOX9/TWIST1	21
GO:0048646	anatomical structure formation involved in morphogenesis	37/311	1090/17046	0.0002	0.01148	0.00915	CDH13/DMRT2/TBR1/COL11A1/SLC11/CTGF/EGR3/TMEM17/UNC13D/EPH4/VASH1/TENM4/GNAS/ANXA2/HOXB3/FMN1/CYR61/IL6/SLI/SMAD3/MEOX1/MEOX2/NOV/LEF1/CE1/ND1/ANGPT4/PK3CG/ROBO4/PRKD1/SFRP2/SOX9/ACTL1/TWIST1/PAX8/FZD5/COL18A1/KDM2B	37
GO:0009187	cyclic nucleotide metabolic process	12/311	191/17046	0.00021	0.01188	0.00947	NPFR2/ADCY3/ADRB3/DRD4/GABRR1/AMPD2/GNAS/GPER1/HPCA/PALM/PDE4C/PDE7A	12
GO:0007155	cell adhesion	43/311	1343/17046	0.00021	0.01199	0.00956	CDH3/CDH13/CTGF/DSG3/EGRF/EGR3/UNC13D/EPH4/EPH84/MTOR/GNAS/ZUMO1/NR61/HLA-E/HLX/HOXD3/COL28A1/FMN1/CYR61/IL6/CDHR4/LCK/SMAD3/MF12/NEDD9/NOV/LEF1/PK3CG/IL20RB8/LIMS2/PCDHGC4/PCDHGB7/PCDHGA11/PXN/SFRP2/SOX9/STK10/TNX8/FZD5/COL18A1/SLA2/FADD/IL32	43
GO:0031279	regulation of cyclase activity	8/311	89/17046	0.00022	0.0121	0.00965	NPFR2/ADRB3/DRD4/GABRR1/GNAS/GPER1/HPCA/PALM	8
GO:0023051	regulation of signaling	73/311	2685/17046	0.00022	0.0121	0.00965	CDH3/TSAN5/CDH13/HCS1/NPFR2/CIDEA/APCDD1/CTGF/ADRB3/NLRP6/DRD4/ECE1/EGRF/RASA3/FOXO1/SPG20/MTOR/RGS22/DK3/GNAS/GPER1/GSTP1/ANXA2/NR61/CYR61/IL6/SLI/LG11/TBP1/SMAD3/MAP3K1/NOV/NTF3/PALM/ARHGEF3/LEF1/PK3CG/ZDHHC13/PPP1CC/ARHGEF10/LIMS2/PRKD1/PSMB4/CCAR2/PXN/RASGRF2/S100A4/CCL17/SFRP2/SOX9/VAMP2/TURS/TNX8/TRAF1/TWIST1/YWHAG/PAX8/CXCR4/FZD5/TMEM204/NLRX1/RAB11FP1/SLA2/FADD/LIMD1/ARHGAP29/LY86/ARHGFE10/TELO2	73
GO:0022610	biological adhesion	43/311	1348/17046	0.00023	0.01246	0.00993	CDH3/CDH13/CTGF/DSG3/EGRF/EGR3/UNC13D/EPH4/EPH84/MTOR/GNAS/ZUMO1/NR61/HLA-E/HLX/HOXD3/COL28A1/FMN1/CYR61/IL6/CDHR4/LCK/SMAD3/MF12/NEDD9/NOV/LEF1/PK3CG/IL20RB8/LIMS2/PCDHGC4/PCDHGB7/PCDHGA11/PXN/SFRP2/SOX9/STK10/TNX8/FZD5/COL18A1/SLA2/FADD/IL32	43
GO:0009966	regulation of signal transduction	66/311	2366/17046	0.00023	0.01246	0.00993	CDH3/TSAN5/CDH13/HCS1/NPFR2/CIDEA/APCDD1/CTGF/ADRB3/NLRP6/DRD4/EGRF/RASA3/FOXO1/SPG20/MTOR/RGS22/DK3/GNAS/GPER1/GSTP1/ANXA2/NR61/CYR61/IL6/SLI/LG11/TBP1/SMAD3/MAP3K1/NOV/NTF3/PALM/ARHGEF3/LEF1/PK3CG/ZDHHC13/PPP1CC/ARHGEF10/LIMS2/PRKD1/PSMB4/CCAR2/PXN/RASGRF2/S100A4/CCL17/SFRP2/SOX9/TURS/TNX8/TRAF1/TWIST1/YWHAG/CXCR4/FZD5/TMEM204/NLRX1/SLA2/FADD/LIMD1/ARHGAP29/LY86/ARHGFE10/TELO2	66
GO:0031326	regulation of cellular biosynthetic process	96/311	3792/17046	0.00024	0.01246	0.00993	CDH3/CDH13/C1D/ZBTB18/DMRT2/TBR1/NPFR2/PSIP1/ZBED9/CIDEA/ZFP42/CTGF/ADRB3/ADA/ZNF709/ZNF781/CITED4/RNF168/DNMT3A/DRD4/EGRF/EGR3/PATL2/SP8/XRN2/FOXO1/SPG20/LARP1/MTOR/GABRR1/DK3/GNAS/GPER1/ZBTB44/GTF2B/BRF1/NR61/HLX/HMGA1/HPCA/HOX3/HOX5/HOX6/HOXD3/ACAD1/HSP90AA1/BARHL2/CYR61/IL6/SLI/HLS1/LTB/SMAD3/MEF2D/MEOX1/MEOX2/NFYB/NTF3/PALM/LEF1/RIPK4/CYTL1/POMC/BNC2/PIWI12/PRMT6/ZNF533/CNOT11/PRKD1/METTL4/CCAR2/SFRP2/SGK1/SOX9/TAF4B/TBP/TCBA1/TLE3/TRAF1/TWIST1/UPP1/YWHAG/ZNF124/ZNF177/PAX8/FZD5/ZNF606/SCRIPT1/HIST1H3A/SLA2/KDM2B/LOXL3/CBX2/GAS7/FADD/LIMD1/LDB2/H2AFY/DMRT2/SLC38A10/CO11A1/CTGF/GNAS/FLVCR1/ANXA2/HOXB3/HOX5/HOX6/HOXD3/FMN1/CYR61/SMAD3/MEF2D/NOV/CYTL1/BNC2/SFRP2/SOX9/TWIST1	96
GO:1902531	regulation of intracellular signal transduction	46/311	1479/17046	0.00024	0.01267	0.0101	CDH13/HCS1/NPFR2/CTGF/ADRB3/NLRP6/DRD4/EGRF/RASA3/FOXO1/MTOR/GNAS/GPER1/GSTP1/NR61/IL6/SLI/LCK/MAP3K1/NOV/NTF3/ARHGEF3/PK3CG/ZDHHC13/ARHGEF10/PRKD1/PSMB4/CCAR2/PXN/RASGRF2/S100A4/CCL17/SFRP2/SOX9/TNX8/TWIST1/CXCR4/FZD5/NLRX1/SLA2/FADD/LIMD1/ARHGAP29/ARHGFE10/TELO2	46

GO:0034654	nucleobase-containing compound biosynthetic process	97/311	3846/17046	0.00025	0.01276	0.01018	CDH13/TCIRG1/C1D/ZBTB18/DMRT2/TBR1/NPFR2/ADCY3/PSIP1/ZBED9/CIDEA/ZFP42/CTGF/ADRB3/ADAL/ZNF781/CTTED4/RNF168/DNMT3A/DRD4/EGFR/EGR3/SP8/RR/N2/FOXO1/MTOR/GABBR1/AMPD2/DKK3/GLS2/GNAS/GPER1/ZBTB44/GTF2B/BRF1/NME7/NRG1/HLX/HMG1A/HPCA/HOXB3/HOXC5/HOXC6/HOXD3/BAHR12/CYR61/IL6/IL6/SL1/HL/S1/SMAD3/MEI/MEF2D/MEOX1/MEOX2/NFYB/NTF3/PALM/LEF1/RIPK4/CYTL1/POMC/BNC2/PRMT6/ZNF533/CNOT11/PRKD1/CCAR2/RPL8/RPL29/SFRP2/SGK1/SOX9/TA4B/TBP/TCEA1/TFE3/TRAFA1/TWIST1/UPP1/YWHAG/ZNF124/ZNF177/PAX8/FZD5/ZNF606/SCRIPT1/HIST1H3A/SLA2/KDM2B/LOXL3/CBX2/GAS7/FADD/UMD1/LDB2/H2AFY
GO:0051339	regulation of lysase activity	8/311	91/17046	0.00026	0.01299	0.01036	NPFR2/ADRB3/DRD4/GABBR1/GNAS/GPER1/HPCA/PALM
GO:0006915	apoptotic process	51/311	1700/17046	0.00026	0.01299	0.01036	C1D/CIDEA/ANKRD9/CTGF/DNMT3A/DSG3/EGFR/EGR3/ACIN1/FOXO1/GLS2/GPER1/GSTP1/GZMA/NRG1/ANXA6/CYR61/IL6/IL6/SL1/LCK/SMAD3/MEF2D/MAP3K1/NTF3/ARHGFB3/LEF1/JDDX47/ANGPT4/PIK3CG/PLEC/LIMS2/PRKD1/PSMB4/CCAR2/RASGRF2/SFRP2/SGK1/SOX9/STK10/ACTC1/TRAFA1/PHLDA2/TWIST1/YWHAG/PAX8/CXCR4/FZD5/COL18A1/KDM2B/FADD/LV86
GO:0006816	calcium ion transport	17/311	352/17046	0.00027	0.01331	0.01062	CLCA1/C15orf27/TRPM6/CTGF/TRPV3/DRD4/RASA3/CRACR2B/GPER1/ANXA6/LCK/PIK3CG/PRKD1/TRPC4/CACNB2/SMDT1
GO:0030878	thyroid gland development	4/311	18/17046	0.00027	0.01331	0.01062	HOXB3/HOXD3/SMAD3/PAX8
GO:0048519	negative regulation of biological process	103/311	4153/17046	0.00027	0.01331	0.01062	CDH3/CDH13/C1D/ZBTB18/B4GAL1/CIDEA/ANKRD9/APCDD1/CTGF/ADRB3/TRPV3/RNF168/NLRP6/DNMT3A/DRD4/EGFR/EGR3/PATL2/RASA3/PPM1E/VASH1/ACIN1/FOXO1/SPG20/MTOR/GABBR1/RGS22/FBXO2/DKK3/VPSAA/GNAS/GPER1/GSTP1/GZMA/ANXA2/SERPIND1/NRG1/HLA-B/HLA-E/HLX/HMG1A/HPCA/HOXB3/HOXCG/ACAD1/COL28A1/CYR61/ILE/ISL1/TH3/HLIS1/LCK/LTBR1/SMAD3/MEF2/MT3A/NOV/NTF3/PALM/LEF1/CEND1/ANGPT4/PDE4C/PIK3CG/IL20/RB/POMC/PPP1CC/PIWIL2/PRMT6/CNOT11/LIMS2/PRKD1/MASP1/PSMB4/METTL4/CCAR2/CCL17/SFRP2/SOX9/TBP/ACTC1/TIMP3/TWIST1/YWHAG/ZNF177/PAX8/FZD5/NLRX1/ZC3H14/RAB11FP1/COL18A1/SCRIPT1/HIST1H3A/SLA2/SPINK7/KDM2B/LOXL3/CBX2/GAS7/FADD/UMD1/H2AFY/ULK2
GO:0009952	anterior/posterior pattern specification	12/311	197/17046	0.00028	0.01331	0.01062	DMRT2/HOXB3/HOXC5/HOXG6/HOXD3/SMAD3/MEOX1/MEOX2/LEF1/SFRP2/FZD5/KDM2B
GO:0018130	heterocycle biosynthetic process	98/311	3911/17046	0.00029	0.01372	0.01094	CDH13/TCIRG1/C1D/ZBTB18/DMRT2/TBR1/NPFR2/ADCY3/PSIP1/ZBED9/CIDEA/ZFP42/CTGF/ADRB3/ADAL/ZNF781/CTTED4/RNF168/DNMT3A/DRD4/EGFR/EGR3/ALAS1/SP8/XRN2/FOXO1/MTOR/GABBR1/AMPD2/DKK3/GLS2/GNAS/GPER1/ZBTB44/GTF2B/BRF1/NME7/NRG1/HLX/HMG1A/HPCA/HOXB3/HOXC5/HOXD3/BAHR12/CYR61/IL6/IL6/SL1/HLIS1/SMAD3/MEI/MEF2D/MEOX1/MEOX2/NFYB/NTF3/PALM/LEF1/RIPK4/CYTL1/POMC/BNC2/PRMT6/ZNF533/CNOT11/PRKD1/CCAR2/RPL8/RPL29/SFRP2/SGK1/SOX9/TA4B/TBP/TCEA1/TFE3/TRAFA1/TWIST1/UPP1/YWHAG/ZNF124/ZNF177/PAX8/FZD5/ZNF606/SCRIPT1/HIST1H3A/SLA2/KDM2B/LOXL3/CBX2/GAS7/FADD/UMD1/LDB2/H2AFY
GO:0006793	phosphorus metabolic process	76/311	2851/17046	0.00029	0.01373	0.01095	BCKDK/TCIRG1/HCS1/NPFR2/ADCY3/ALPK2/APOA1BP/TRPM6/CTGF/ADRB3/ITIM1/ADAL/NLRP6/DRD4/EGFR/EPAH3/EPH4/ASA3/PPM1E/FOXO1/MTOR/GABBR1/GAK/GAPD/HS/AMPD2/GNAS/PIGW/GPER1/DOK7/GSTP1/NME7/ANXA2/NRG1/HPCA/CYR61/IL6/ISL1/LCK/SMAD3/MEI/MAP3K1/NUDT1/NTF3/PALM/ANGPT4/PDE4C/PDE7A/PGAM2/PIGC/PIK3CG/RIPK4/PON1/LPCAT2/PPP1CC/SMPD3/VAC14/PRKD1/PSMB4/PKN/RASGRF2/CCL17/SFRP2/SGK1/CERK1/SOX9/STK10/TNXB/TWIST1/UPP1/YWHAG/PTP4A1/CXCR4/FZD5/LMD1/H2AFY/ULK2
GO:0007267	cell-cell signaling	38/311	1154/17046	0.0003	0.01373	0.01095	KCNMB2/NPFR2/ADCY3/CHRNAS5/CTGF/ADRB3/DRD4/EGR3/GABBR1/GIA3/GIB2/GLS2/GNAS/GPER1/KCNIP2/APBA2/CYR61/IL6/ISL1/LTB/NOV/NTF3/PDE4C/POMC/SMPD3/SYB3/U/RASGRF2/CCL17/SFRP2/SOX9/VAMP2/YWHAG/CACNB2/PAX8/FZD5/RAB11FP1/COLO/RAB39
GO:0002062	chondrocyte differentiation	8/311	93/17046	0.0003	0.01373	0.01095	COL11A1/CTGF/SMAD3/MEF2D/NOV/CYTL1/SFRP2/SOX9
GO:0014031	mesenchymal cell development	10/311	144/17046	0.00031	0.01435	0.01145	EPAH3/NRG1/ISL1/SMAD3/LEF1/S100A4/SFRP2/SOX9/TWIST1/LOXL3
GO:0012501	programmed cell death	51/311	1718/17046	0.00033	0.01493	0.01191	C1D/CIDEA/ANKRD9/CTGF/DNMT3A/DSG3/EGFR/EGR3/ACIN1/FOXO1/GLS2/GPER1/GSTP1/GZMA/NRG1/ANXA6/CYR61/IL6/ISL1/LCK/SMAD3/MEF2D/MAP3K1/NTF3/ARHGFB3/LEF1/JDDX47/ANGPT4/PIK3CG/PLEC/LIMS2/PRKD1/PSMB4/CCAR2/RASGRF2/SFRP2/SGK1/SOX9/STK10/ACTC1/TRAFA1/PHLDA2/TWIST1/YWHAG/PAX8/CXCR4/FZD5/COL18A1/KDM2B/FADD/LV86
GO:0009790	embryo development	33/311	958/17046	0.00034	0.01535	0.01224	ZBTB18/DMRT2/COL11A1/ZFP42/DNMT3A/VEE1/EGFR/SP8/TENM4/GNAS/FLVCR1/NRG1/HLX/APBA2/HOXB3/HOXC5/HOXD3/HSDD1/7B2/CYR61/ISL1/RESP18/SMAD3/MEI/OX1/MEOX2/LEF1/SFRP2/SOX9/PHLDA2/TWIST1/PAX8/FZD5/KDM2B
GO:0016049	cell growth	19/311	429/17046	0.00036	0.01574	0.01255	CDH13/CTGF/ARXZ/SPG20/MTOR/NRG1/BAHR12/CYR61/IL6/SMAD3/NOV/LEF1/PRMT6/BN3/CCAR2/SFRP2/SGK1/SOX9/ULK2
GO:0010646	regulation of cell communication	73/311	2731/17046	0.00037	0.0158	0.0126	CDH3/TPAN5/CDH13/HCS1/NPFR2/CIDEA/APCDD1/CTGF/ADRB3/NLRP6/DRD4/EGFR/RASA3/FOXO1/SPG20/LARP1/MTOR/RGS22/DKK3/GNAS/GPER1/GSTP1/ANXA2/NRG1/CYR61/IL6/ISL1/LCK/LG/L1/TLTBP1/SMAD3/MAP3K1/NOV/NTF3/PALM/ARHGFB3/LEF1/PDE4C/PIK3CG/POMC/ZDHHC3/PPP1CC/ARHGFE10/SYBU/LIMS2/PRKD1/PSMB4/CCAR2/PXN/RASGRF2/S100A4/CCL17/SFRP2/SOX9/VAMP2/TLR5/TNXB/TRAFA1/TWIST1/YWHAG/PAX8/CXCR4/FZD5/TWEM204/NLRX1/RAB11FP1/SLA2/FADD/UMD1/ARHGAP29/LY86/ARHGEF10/TELO2

GO:1903035	negative regulation of response to wounding	10/311	147/17046	0.00037	0.0158	0.0126	NLRP6/GPER1/GSTP1/ANXA2/ISL1/SMAD3/NOV/IL20RB/PSMB4/NLRX1	10
GO:0071840	cellular component organization or biogenesis	133/311	5713/17046	0.00038	0.0158	0.0126	CDH3/TSPAN5/CDH13/CTG1/CID1/TBRI/SEPT9/ADCC3/PSIP1/BAG4/LIT/IDEA/FRMD6/APOA1B/COL11A1/SLC11/2/FR42/CTGF/HTMI1/WBP2NL1/RNF168/COCH/DNMT3A/DSG3/EGFR/PATL2/TMEM47/EMIL1/UNC13D/EPH3A/EPH4/ALAS1/RASA3/PPM1E/ACIN1/LIMCH1/SPG20/FLNB/ATP11A/MTOR/TENM4/GBB2/SL2/VP54/PIGW1/ZUOM1/GPER1/NME7/ANXA2/KCNP2/NRG1/ANXA6/HMGAI/COI28A1/FMN1/BARHL2/CYR61/IL6/ISL1/HLS1/ATP9B/ACAT1/KRT15/INSC/LGL1/LOX/ITBP1/SMAD3/MEI1/MAP3K1/HR23/NEED9/NOV/NTF3/PALM/LEF1/DDX47/ANGPT4/PLEC/LPCAT2/PIWIL2/PRMT6/LIMS2/PRKDI/BIN3/PSMB4/TRPC7/ACTR3B/CCAR2/PXN/RASGRF2/EXOC4/RPL8/RPL2/9/S100A4/S100A6/SFRP2/SGK1/MICAL1/SOX9/VAMP2/ACTC1/TNXB1/TRAJ1/TRPC4/TWIST1/YWHAG/CACNB2/PAX8/CXCR4/FZD5/COL18A1/CANP5/COL10/HIST1H2BM/SH3BGR1.3/HIST1H3A/PARD6B/KDM2B/LOXL3/MGARP/CBX2/GAS7/FADD/LIMD1/MAF7/LDB2/H2AFY/ARHGEF10/ULK2/USP6N1	53
GO:0008219	cell death	53/311	1816/17046	0.00038	0.0158	0.0126	CID/IDEA/ANKRD9/CTGF/DNMT3A/DSG3/EGFR/EGR3/ACIN1/FOXO1/GI52/GPER1/GSTP1/GZMA/NGR1/ANXA6/CYR61/IL6/ISL1/LCK/SMAD3/MEF2D/MAP3K1/MEOX2/NOV/NTF3/ARHGEF3/LEF1/DDX47/ANGPT4/PIK3CG/PLEC/LIMS2/PRKDI/PSMB4/CCAR2/RASGRF2/SFRP2/SGK1/SOX9/STK10/ACTC1/TRAJ1/PHLDA2/TWIST1/YWHAG/PAX8/CXCR4/FZD5/C	53
GO:0016265	death	53/311	1816/17046	0.00038	0.0158	0.0126	CID/IDEA/ANKRD9/CTGF/DNMT3A/DSG3/EGFR/EGR3/ACIN1/FOXO1/GI52/GPER1/GSTP1/GZMA/NGR1/ANXA6/CYR61/IL6/ISL1/LCK/SMAD3/MEF2D/MAP3K1/MEOX2/NOV/NTF3/ARHGEF3/LEF1/DDX47/ANGPT4/PIK3CG/PLEC/LIMS2/PRKDI/PSMB4/CCAR2/RASGRF2/SFRP2/SGK1/SOX9/STK10/ACTC1/TRAJ1/PHLDA2/TWIST1/YWHAG/PAX8/CXCR4/FZD5/C	53
GO:0048864	stem cell development	10/311	148/17046	0.00039	0.01631	0.013	EPHA3/NRG1/ISL1/SMAD3/LEF1/S100A4/SFRP2/SOX9/TWIST1/LOXL3	10
GO:0050896	response to stimulus	169/311	7634/17046	0.0004	0.01654	0.01319	CDH3/TSPAN5/CDH13/KCNMB2/CTG1/TBRI/HCT1/NPFR2/ADCC3/PSIP1/PTH2/CHRNA5/CIDEA/COL11A1/TRPM6/APCDD1/CTGF/ADRB3/TRPV3/CITEB4/RNF168/COCH/NLRP6/DNMT3A/DRD4/EGFR/EGR3/TMEM17/UNC13D/EPHA3/EPH4/RASA3/PPM1E/VASH1/ACIN1/FOXO1/SPG20/FLNB/LARP1/MTOR/GABBR1/TENM4/RGS22/FBXO2/GIA3/GB2/SDC2/BP2/DKK3/GPR162/GNAS/GPER1/GSTP1/NME7/GZMA/ANXA2/SERPIND1/KCNP2/NRG1/ANXA6/HLA-B/HLA-E/HLA-F/HLX/HMGAI/HPCA/HOX3/HS1/7B2/HSP90AA1/HTSA/CTR61/IL6/ISL1/ACAT1/KRT15/LCK/LGL1/LOX/ITBP1/SMAD3/MEI1/MAP3K1/MTT1/NUDT1/NEED9/NMBR/NOV/NTF3/PALM/ARHGEF3/LEF1/DDX47/ANGPT4/PDE4C/PDE7A/PGAM2/PIK3CG/IL20RB/CYTL1/POZM1/PON1/ZDHHC13/PPP1CC/ARHGEF10/PRMT6/WDR33/SYBU/LIMS2/VAC14/PRKDI/BIN3/MASP1/PSMB4/TRPC7/HPAR5/CCAR2/PTPRAP/PXN/RASGRF2/DEFB134/S100A4/S100A6/CCL17/SFRP2/CXCR5/SGK1/SYNDIG1L/MICAL1/SOX9/STK10/VAMP2/TCEA1/ACTC1/TIMP3/TLE3/TLR5/TNXB1/TRAJ1/TRPC4/TWIST1/UPP1/YWHAG/CACNB2/PAX8/CXCR4/FZD5/TMEM204/NLRX1/COL18A1/UNC5BB1/CANP5/HIST1H3A/SLA2/IL1F10/MGARP/FA	18
GO:0070838	divalent metal ion transport	18/311	399/17046	0.00041	0.01655	0.0132	CLCA1/CL5orf27/TRPM6/CTGF/TRPV3/DRD4/RASA3/CRACR2B/GPER1/ANXA6/LCK/PIK3CG/ZDHHC13/PRKDI/TRPC7/TRPC4/CACNB2/SMDT1	18
GO:0040007	growth	31/311	887/17046	0.00041	0.01655	0.0132	CDH13/CTGF/ADRB3/ARN2/SPG20/MTOR/TENM4/GNAS/FLVCR1/NRG1/HLX/APBA2/FMN1/BARHL2/CYR61/IL6/SMAD3/MTT1/NEED9/NOV/LEF1/BNC2/PRMT6/BIN3/CCAR2/SFRP2/SGK1/SOX9/TIMP3/COL10/ULK2	31
GO:0006171	cAMP biosynthetic process	9/311	123/17046	0.00043	0.01706	0.0136	NPFR2/ADCC3/ADRB3/DRD4/GABBR1/GNAS/GPER1/HPCA/PALM	9
GO:0072511	divalent inorganic cation transport	18/311	402/17046	0.00045	0.01769	0.0141	CLCA1/CL5orf27/TRPM6/CTGF/TRPV3/DRD4/RASA3/CRACR2B/GPER1/ANXA6/LCK/PIK3CG/ZDHHC13/PRKDI/TRPC4/CACNB2/SMDT1	18
GO:0002480	antigen processing and presentation of exogenous peptide antigen via MHC class I, TAP-independent	3/311	9/17046	0.00047	0.01814	0.01447	HLA-B/HLA-E/HLA-F	3
GO:0002862	negative regulation of inflammatory response to antigenic stimulus	3/311	9/17046	0.00047	0.01814	0.01447	NLRP6/IL20RB/PSMB4	3

GO:0019220	regulation of phosphate metabolic process	47/311	1568/17046	0.00047	0.01823	0.01454	NPFFR2/ADCY3/CTGF/ADRB3/NLRP6/DRD4/EGFR/RASA3/PPM1E/FOXO1/MTOR/GABBR1/GAPDH5/GNAS/GPER1/DOK7/GSTP1/ANXA2/NRG1/HPCA/CYR61/IL6/ISL1/LCK/SMAD3/ME1/MAAP3K1/NTF3/PALM/ANGPT4/PAM2/PIK3CG/VAC14/PRK01/PSMB4/PXN/RASGRF2/CCL17/SFRP2/SOX9/STK10/TNXB/TWIST1/YWHAG/CXCR4/FZD5/H2AFY	47
GO:0052652	cyclic purine nucleotide metabolic process	10/311	152/17046	0.00048	0.01838	0.01466	NPFFR2/ADCY3/ADRB3/DRD4/GABBR1/AMPD2/GNAS/GPER1/HPCA/PALM	10
GO:0001837	epithelial to mesenchymal transition	8/311	100/17046	0.00049	0.01838	0.01466	EPHA3/SMAD3/LEF1/S100A4/SFRP2/SOX9/TWIST1/LOXL3	8
GO:0048583	regulation of response to stimulus	84/311	3283/17046	0.00049	0.01838	0.01466	CDH3/TSPAN5/CDH13/TBR1/HCST/NPFFR2/GIDEA/PCDD1/CTGF/ADRB3/RNF168/COCH/NLRP6/DRD4/EGFR/UNC13D/RASA3/VASH1/ACIN1/FOXO1/SPG20/LARP1/MTOR/RGS22/DKK3/GNAS/GPER1/GSTP1/ANXA2/NRG1/HLA-B/HLA-E/HLA-F/HXL/HMGA1/HSP90AA1/CYR61/IL6/ISL1/LCK/LGL1/LTBP1/SMAD3/MAAP3K1/NOV/NTF3/PALM/ARHGFEF3/LEF1/PIK3CG/IL20RB/ZDHC13/PPP1CC/ARHGFEF10L/SYBU/LIMS2/PRKD1/MAAP1/PSMB4/CCAR2/PXN/RASGRF2/S100A4/CCL17/SFRP2/SOX9/TLR5/TNXB/TRAFF1/TWIST1/YWHAG/CXCR4/FZD5/TMEM204/NLRX1/UNC93B1/HIST1H3A/SLA2/FADD/LIMD1/ARHGAP29/LY86/ARHGFEF10/TELO2	84
GO:0019932	second-messenger-mediated signaling	12/311	210/17046	0.00049	0.01838	0.01466	CDH13/ADCY3/DRD4/EGFR/GNAS/NRG1/HPCA/HTRA5/PDE7A/SOX9/CXCR4/SLA2	12
GO:0016043	cellular component organization	130/311	5594/17046	0.00051	0.01865	0.01487	CDH3/TSPAN5/CDH13/TBR1/SEPT9/ADCY3/PSIP1/B4GAL7/CIDEA/FRMD6/APOA1BP/COL11A1/SCLL1/ZFP42/CTGF/FTM1/WBP2NL/RNF168/COCH/DNMT3A/DSG3/EGFR/PATL2/TMEM17/EML1/UNC13D/EPHA3/EPHA4/ALAS1/RASA3/PPM1E/ACIN1/LUMCH1/SPG20/FLNB/ATP11A/MTOR/TENM4/GIB2/GIS2/VPS4A/PIGW/ZUMO1/GPER1/NME7/ANXA2/KCNP2/NRG1/ANXA6/HMGA1/HPCA/ACAD/HSP90AA1/COL28A1/ARHL2/CYR61/IL6/ISL1/HLS1/ATP9B/ACAT1/KRT15/INSC/LG1/LOX/LTBP1/SMAD3/ME1/MAAP3K1/MAF2/NEDD9/NOV/NTF3/PALM/LEF1/ANGPT4/PLEC/LPCAT2/PIWIL2/PRMT6/LIMS2/PRK01/BN3/PSMB4/TRPC7/ACTR3B/CCAR2/PXN/RASGRF2/EXO4/RPL8/RPL29/S100A4/S100A6/SFRP2/SGK1/MICAL1/SOX9/VAMP2/ACTC1/TNXB/TRAFF1/TRPC4/TWIST1/YWHAG/CACNB2/PAX8/CXCR4/FZD5/COL18A1/CNPS/COLO/HIST1H2BM/SH3BGRL3/HIST1H3A/PA/RB6B/KDM2B/LOXL3/MGARP/CBX2/GAS7/FADD/LIMD1/MAAP7/H2AFY/ARHGFEF10/ULK2/USP6N1	130
GO:0009190	cyclic nucleotide biosynthetic process	10/311	153/17046	0.00051	0.01865	0.01487	NPFFR2/ADCY3/ADRB3/DRD4/GABBR1/AMPD2/GNAS/GPER1/HPCA/PALM	10
GO:006468	protein phosphorylation	49/311	1662/17046	0.00051	0.01865	0.01487	BCKDK/HCST/NPFFR2/ADCY3/ALPK2/TRPM6/CTGF/ADRB3/NLRP6/DRD4/EGFR/EPHA3/EPHA4/EPHA3/PRM1E/FOXO1/MTOR/GAK/GPER1/DOK7/GSTP1/ANXA2/NRG1/CYR61/IL6/ISL1/LCK/SMAD3/MAAP3K1/NTF3/ANGPT4/PIK3CG/RIPK4/PRK01/PSMB4/PXN/RASGRF2/CCL17/SFRP2/SGK1/SOX9/STK10/TNXB/TWIST1/YWHAG/CXCR4/FZD5/H2AFY/ULK2	49
GO:0051174	regulation of phosphorus metabolic process	47/311	1579/17046	0.00055	0.01981	0.0158	NPFFR2/ADCY3/CTGF/ADRB3/NLRP6/DRD4/EGFR/RASA3/PPM1E/FOXO1/MTOR/GABBR1/GAPDH5/GNAS/GPER1/DOK7/GSTP1/ANXA2/NRG1/HPCA/CYR61/IL6/ISL1/LCK/SMAD3/ME1/MAAP3K1/NTF3/PALM/ANGPT4/PAM2/PIK3CG/VAC14/PRK01/PSMB4/PXN/RASGRF2/CCL17/SFRP2/SOX9/STK10/TNXB/TWIST1/YWHAG/CXCR4/FZD5/H2AFY	47
GO:0044093	positive regulation of molecular function	49/311	1672/17046	0.00059	0.02091	0.01668	CDH3/ADCY3/CTGF/ADRB3/DRD4/EGFR/RASA3/TBC1D9B/RGS22/GNAS/GPER1/DOK7/ANXA2/NRG1/HPCA/CYR61/IL6/ISL1/LCK/LG1/SMAD3/MAAP3K1/NTF3/ARHGFE3/ANGPT4/PIK3CG/CYTL1/PON1/ARHGFEF10L/PRK01/PSMB4/PXN/RASGRF2/CCL17/SFRP2/SGK1/STK10/TCEA1/TRAFF1/TWIST1/CXCR4/FZD5/SH3BGRL3/FAOD/ARHGAP29/ARHGFEF10/SP6N1/RABGAP11	49
GO:0048762	mesenchymal cell differentiation	10/311	156/17046	0.00059	0.02091	0.01668	EPHA3/NRG1/ISL1/SMAD3/LEF1/S100A4/SFRP2/SOX9/TWIST1/LOXL3	10
GO:0009628	response to abiotic stimulus	35/311	1071/17046	0.0006	0.02091	0.01668	NPFFR2/PSIP1/COL11A1/CTGF/ADRB3/TRPV3/RNF168/DNMT3A/DRD4/EGFR/FOXO1/MTOR/GJA3/HPCA/HSP90AA1/IL6/LCK/SMAD3/MAAP3K1/PALM/ANGPT4/PPP1CC/CCAR2/SFRP2/SOX9/TIMP3/TLR5/TWIST1/CXCR4/COL18A1/MGARP/FAOD/LIMD1/MAAP7/RCS1	35
GO:0022008	neurogenesis	46/311	1548/17046	0.00066	0.02289	0.01825	ZBTB18/TBR1/SCLL1/APCDD1/DNMT3A/EPHA3/EPHA4/RASA3/SPG20/TENM4/GPER1/KCNP2/NRG1/HOXB3/HOXD3/HSP90AA1/FMNI1/BARHL2/IL6/ISL1/LG1/NTF3/PALM/LEF1/CENPL/PPP1CC/PRK01/PSMB4/TRPC7/ACTR3B/CCAR2/EXO4/RPL8/RPL29/S100A4/S100A6/SGK1/MGARP/CBX2/GAS7/FADD/LIMD1/MAAP7/H2AFY/ARHGFEF10/ULK2	46
GO:0045667	regulation of osteoblast differentiation	8/311	105/17046	0.00068	0.02304	0.01838	GNAS/CYR61/IL6/SMAD3/PRK01/SFRP2/TWIST1/LIMD1	8

GO:0030199	collagen fibril organization	5/311	39/17046	0.00068	0.02304	0.01838	COL11A1/ANXA2/LOX/SFRP2/TNX8	5
GO:0051496	positive regulation of stress fiber assembly	5/311	39/17046	0.00068	0.02304	0.01838	CTGF/PPM1E/MTOR/SMAD3/ARHGGEF10	5
GO:0050793	regulation of developmental process	55/311	1953/17046	0.00068	0.02304	0.01838	CDH3/DMRT2/TBR1/CTGF/ADRB3/COCH/EGR3/UNC13D/EPHA3/VASH1/ACIN1/FOXO1/SPG20/MTOR/TENM4/GNAS/GPER1/FLVCR1/NRG1/HLA-B/HLX/HMGA1/HOXB3/HOXD3/BARHL2/CYR61/IL6/ISL1/LCK/SMAD3/MF12/NOV/NTF3/PALM/LEF1/CEND1/ANGPT4/LIMS2/PRKD1/PXN/CCL17/SFRP2/SOX9/PHLDA2/TWIST1/YWHAQ/PAX8/CXCR4/COLOQ/SCRT1/GAS7/FADD/LIMD1/H2AFY/ULK2	55
GO:0010638	positive regulation of organelle organization	20/311	489/17046	0.00069	0.02304	0.01838	CTGF/PPM1E/MTOR/GLS2/VPS4A/GPER1/ANXA2/NRG1/FMN1/ISL1/SMAD3/MAP3K1/NTF3/PIWIL2/PRKD1/ACTR3B/YWHAG/FZD5/MGARP/ARHGGEF10	20
GO:0035270	endocrine system development	9/311	132/17046	0.00071	0.02357	0.0188	FOXO1/DKK3/HOXB3/HOXD3/IL6/ISL1/SMAD3/SOX9/PAX8	9
GO:0051336	regulation of hydrolase activity	37/311	1166/17046	0.00071	0.02357	0.0188	ADCY3/CTGF/EGFR/EPHA3/RASA3/TBC1D9B/MTOR/RGS2/GNAS/GPER1/GZMA/SERPIND1/HPCA/COL28A1/CYR61/IL6/ITIH3/LCK/LIGL1/SMAD3/NTF3/ARHGGEF3/LEF1/ARHGGEF10/L/PRKD1/RASGRF2/CCL17/SFRP2/TCEA1/TIMP3/SH3BGR13/SPINK7/FADD/ARHGAP29/ARHGGEF10/USP6N/RABGAP1L	37
GO:0044271	cellular nitrogen compound biosynthetic process	105/311	4363/17046	0.00073	0.02391	0.01907	CDH13/TCIRG1/CD1/ZBTB18/DMRT2/TBR1/NIPFR2/ADCY3/PSIP1/ZBED9/CIDEA/ZFP42/CTGF/ADRB3/ADAL/ZNF709/ZNF781/CTEDA/RNF168/DNMT3A/DRD4/EGFR/EGR3/PATL2/ALAS1/SP8/XRN2/FOXO1/LARP1/MTOR/GABBR1/AMPD2/DKK3/GLS2/GNAS/GPER1/ZBTB44/GTF2B/BRF1/NNME7/NRG1/HLX/HMGA1/HPCA/HOXB3/HOX5/HOX6/HOXD3/HSP90AA1/BARHL2/CYR61/IL6/ISL1/HLS1/SMAD3/ME1/MEF2D/MEOX1/MEOX2/NFYB/NTF3/PALM/LEF1/RIPK4/CYTL1/POMC/BNC2/PIWIL2/PRMT6/ZNF532/CNOT11/PRKD1/METTL4/CCAR2/RPL8/RPL29/SFRP2/SGK1/SOX9/TAF4B/TBP/TCEA1/TLE3/TLR5/TRAFA1/TWIST1/UPP1/VARS/YWHAG/ZNF124/ZNF177/PAX8/FZD5/ZNF606/SCRT1/HIST1H3A/SLA2/KDM2B/LOXL3/CBX2/GAS7/FADD/LIMD1/LDB2/H2AFY	105
GO:0009260	ribonucleotide biosynthetic process	13/311	251/17046	0.00074	0.02391	0.01907	TCIRG1/NIPFR2/ADCY3/ADRB3/DRD4/GABBR1/AMPD2/GNAS/GPER1/NNME7/HPCA/PALM/UPP1	13
GO:0048699	generation of neurons	44/311	1471/17046	0.00076	0.0244	0.01946	ZBTB18/TBR1/ISL1/DNMT3A/EGFR/EMIL1/EPHA3/EPH4/RASA3/SPG20/TENM4/GPER1/KCNIP2/NRG1/HOXB3/HOXD3/HSP90AA1/FMN1/BARHL2/IL6/ISL1/LGL1/NTF3/PALM/LEF1/CEND1/PPP1CC/PRKD1/PSMB4/TRPC7/RASGRF2/S100A6/SGK1/SOX9/TRPC4/TWIST1/YWHAG/CACNB2/CXCR4/FZD5/SCRT1/PARD6B/GAS7/ULK2	44
GO:0042325	regulation of phosphorylation	41/311	1341/17046	0.00076	0.0244	0.01946	NIPFR2/ADCY3/CTGF/ADRB3/NLRP6/DRD4/EGFR/RASA3/PPM1E/FOXO1/MTOR/GAPDH5/GPER1/DOCK7/GSTP1/ANXA2/NRG1/CYR61/IL6/ISL1/LCK/SMAD3/MAP3K1/NTF3/ANGPT4/PIK3CG/VACL4/PRKD1/PSMB4/PXN/RASGRF2/CCL17/SFRP2/SOX9/STK10/TNX8/TWIST1/YWHAG/CXCR4/FZD5/H2AFY	41
GO:0016310	phosphorylation	55/311	1964/17046	0.00078	0.02474	0.01973	BCKDK/HCT8/NIPFR2/ADCY3/ALPK2/TRPM6/CTGF/ADRB3/NLRP6/DRD4/EGFR/EPHA3/EPH4/RASA3/PPM1E/FOXO1/MTOR/GAK/GAPDH5/GPER1/DOCK7/GSTP1/NNME7/ANXA2/NRG1/CYR61/IL6/ISL1/LCK/SMAD3/MAP3K1/NTF3/ANGPT4/PGANM2/PIK3CG/RIPK4/VACL4/PRKD1/PSMB4/PXN/RASGRF2/CCL17/SFRP2/SGK1/CERK/SOX9/STK10/TNX8/TWIST1/YWHAQ/CXCR4/FZD5/LIMD1/H2AFY/ULK2	55
GO:0002460	adaptive immune response based on somatic recombination of immune receptors built from immunoglobulin superfamily domains	11/311	191/17046	0.00079	0.02474	0.01973	RNF168/UNC13D/HLA-B/HLA-E/HLX/IL6/LEF1/IL20RB/FZD5/SLA2/FADD	11
GO:0046390	ribose phosphate biosynthetic process	13/311	253/17046	0.00079	0.02474	0.01973	TCIRG1/NIPFR2/ADCY3/ADRB3/DRD4/GABBR1/AMPD2/GNAS/GPER1/NNME7/HPCA/PALM/UPP1	13

GO:0001932	regulation of protein phosphorylation	39/311	1258/17046	0.0008	0.02474	0.01973	NPFRR2/ADCY3/CTGF/ADRB3/NLRP6/DRD4/EGFR/RASA3/PPM1E/FOXO1/MTOR/GPER1/DOCK7/GSTP1/ANXA2/NRG1/CYR61/IL6/ISL1/LCK/SMAD3/MAP3K1/NTF3/ANGPT4/PIK3CG/PRKD1/PSMB4/PXN/RASGRF2/CCL17/SFRP2/SOX9/STK10/TNXB/TWIST1/YWHAG/CXCR4/FZD5/H2AFY	39
GO:0007389	specification process	18/311	423/17046	0.00081	0.02486	0.01982	DMRT2/TBR1/SP8/NME7/HOXB3/HOXC5/HOXC6/HOXC3/ISL1/SMAD3/MEOX1/MEOX2/LEF1/SFRP2/TXA2B/PAX8/FZD5/KDM2B	18
GO:0009887	organ morphogenesis	30/311	884/17046	0.00082	0.02501	0.01994	TBR1/CO11A1/CTGF/EGFR/EPHB4/GNAS/FLVCR1/NRG1/HLX/HOXB3/HOXB3/FMN1/CYR61/IL6/ISL1/SMAD3/MIEF2/D/LEF1/BNC2/LIMS2/SFRP2/SOX9/ACTC1/TLE3/PHLDA2/TWIST1/PXAB8/FZD5/COL18A1/KDM2B	30
GO:0085029	extracellular matrix assembly	4/311	24/17046	0.00087	0.02631	0.02098	LOX/SMAD3/SOX9/TNXB	4
GO:0010941	regulation of cell death	42/311	1395/17046	0.00089	0.02668	0.02128	CIDEA/ANKRD9/CTGF/DNMT3A/EGFR/EGR3/ACIN1/FOXO1/GLS2/GPER1/GSTP1/GZMA/NRG1/CYR61/IL6/ISL1/LCK/SMAD3/MAP3K1/NOV/NTF3/ARHGFB3/LEF1/ANGPT4/PIK3CG/LIMS2/PRKD1/PSMB4/CCAR2/RASGRF2/SFRP2/SGK1/SOX9/STK10/ACTC1/TRAFF1/TWIST1/YWHAG/PAX8/COL18A1/KDM2B/FADD	42
GO:0035413	positive regulation of catenin import into nucleus	3/311	11/17046	0.00089	0.02668	0.02128	EGFR/SMAD3/SFRP2	3
GO:0045595	regulation of cell differentiation	41/311	1356/17046	0.00095	0.02819	0.02248	TBR1/CTGF/EGR3/UNC13D/EPHA3/ACIN1/FOXO1/SPG20/MTOR/TENM4/GNAS/GPER1/NRG1/HLA-B/HLX/HOXB3/HOXB3/BARHL2/CYR61/IL6/ISL1/LCK/SMAD3/MF12/NOV/NTF3/PALM1/LEF1/PRKD1/CCL17/SFRP2/SOX9/TWIST1/YWHAG/PAX8/CXCR4/SCRT1/FADD/LIMD1/H2AFY/ULK2	41
GO:0044700	single organism signaling	129/311	5624/17046	0.00096	0.02844	0.02268	CDH3/TSPAN5/CDH13/KCNMB2/TCIRG1/HCS1/NPFFR2/ADCY3/PTH2/CHRNA5/CIDEA/APCDD1/CTGF/ADRB3/NLRP6/DRD4/ECE1/EGFR/EGR3/TMEM17/EPHA3/EPHB4/RASA3/FOXO1/SPG20/FLNBLARP1/MTOR/GABBR1/TENM4/RGS22/GIA3/GBR2/SDCBP2/DKK3/GLS2/GPR162/GNAS/GPER1/GSTP1/ANXA2/KCNP2/NRG1/ANXA6/HLA-B/HLA-E/HLA-F/HPCA/APBA2/HOXB3/HSP90AA1/HTR5A/CYR61/IL6/ISL1/LCK/LGL1/LTB1/TBP1/SMAD3/MAP3K1/NEEDS9/NMBR/NOV/NTF3/PALM/ARHGFB3/LEF1/DDX47/ANGPT4/PDE4C/PDE7A/PGAM2/PIK3CG/IL20RB/CYTL1/POMC/ZDHHC13/PPP1CC/ARHGEF10/SMIPD3/SYB1/LIMS2/VAC14/PRKD1/PSMB4/EPAR5/CCAR2/PXN/RASGRF2/S100A4/S100A6/CCL17/SFRP2/CXCR5/SGK1/MICAL1/SOX9/STK10/VAMP2/TLE3/TLRS/TNXB/TRAFF1/TWIST1/YWHAG/CACNB2/PAX8/CXCR4/FZD5/TMEM204/NLRX1/RAB11FIP1/UNC93B1/CAPS/COLO/HIST1H3/A/SLA2/ILF10/FADD/LIMD1/ARHGAP29/LY86/RAB3D/SMAD5/AS1/ARHGFE10/ULK2/TELO2	129
GO:0050777	negative regulation of immune response	8/311	111/17046	0.00097	0.02857	0.02278	NLRP6/HLA-B/HLA-E/HLX/IL20RB/MASP1/PSMB4/NLRX1	8
GO:0072522	purine-containing compound biosynthetic process	13/311	259/17046	0.00098	0.02857	0.02278	TCIRG1/NPFFR2/ADCY3/ADRB3/ADAL/DRD4/GABBR1/AMPD2/GNAS/GPER1/NME7/HPCA/PALM	13
GO:0001756	somitogenesis	6/311	63/17046	0.001	0.02857	0.02278	DMRT2/SMAD3/MEOX1/MEOX2/LEF1/SFRP2	6
GO:0048584	positive regulation of response to stimulus	52/311	1848/17046	0.001	0.02857	0.02278	CDH3/TSPAN5/CDH13/HCS1/NPFFR2/ADCY3/PTH2/CHRNA5/CIDEA/APCDD1/CTGF/ADRB3/NLRP6/DRD4/EGFR/RASA3/LARP1/MTOR/GNAS/GPER1/NRG1/HLA-B/HLA-E/HLX/HMGA1/HSP90AA1/CYR61/IL6/ISL1/LCK/SMAD3/MAP3K1/NOV/NTF3/PIK3CG/ZDHHC13/LIMS2/PRKD1/MASP1/PSMB4/CCAR2/PXN/RASGRF2/S100A4/CCL17/SFRP2/SOX9/TLRS/YWHAG/CXCR4/FZD5/NLRX1/UNC93B1/SLA2/FADD/LY86	52
GO:0023052	signaling	129/311	5629/17046	0.001	0.02857	0.02278	CDH3/TSPAN5/CDH13/KCNMB2/TCIRG1/HCS1/NPFFR2/ADCY3/PTH2/CHRNA5/CIDEA/APCDD1/CTGF/ADRB3/NLRP6/DRD4/ECE1/EGFR/EGR3/TMEM17/EPHA3/EPHB4/RASA3/FOXO1/SPG20/FLNBLARP1/MTOR/GABBR1/TENM4/RGS22/GIA3/GBR2/SDCBP2/DKK3/GLS2/GPR162/GNAS/GPER1/GSTP1/ANXA2/KCNP2/NRG1/ANXA6/HLA-B/HLA-E/HLA-F/HPCA/APBA2/HOXB3/HSP90AA1/HTR5A/CYR61/IL6/ISL1/LCK/LGL1/LTB1/TBP1/SMAD3/MAP3K1/NEEDS9/NMBR/NOV/NTF3/PALM/ARHGFB3/LEF1/DDX47/ANGPT4/PDE4C/PDE7A/PGAM2/PIK3CG/IL20RB/CYTL1/POMC/ZDHHC13/PPP1CC/ARHGEF10/SMIPD3/SYB1/LIMS2/VAC14/PRKD1/PSMB4/EPAR5/CCAR2/PXN/RASGRF2/S100A4/S100A6/CCL17/SFRP2/CXCR5/SGK1/MICAL1/SOX9/STK10/VAMP2/TLE3/TLRS/TNXB/TRAFF1/TWIST1/YWHAG/CACNB2/PAX8/CXCR4/FZD5/TMEM204/NLRX1/RAB11FIP1/UNC93B1/CAPS/COLO/HIST1H3/A/SLA2/ILF10/FADD/LIMD1/ARHGAP29/LY86/RAB3D/SMAD5/AS1/ARHGFE10/ULK2/TELO2	129
GO:0007015	actin filament organization	14/311	293/17046	0.00102	0.02892	0.02306	CTGF/PPM1E/MTOR/FMN1/SMAD3/MAP3K1/NEEDS9/BIN3/ACTR3B/MICAL1/ACTC1/SH3BGRL3/GAS7/ARHGFE10	14
GO:0098609	cell-cell adhesion	28/311	816/17046	0.00103	0.02892	0.02306	CDH3/CDH13/DSG3/EGFR/EGR3/MTOR/GNAS/HLA-E/HLX/CYR61/IL6/CDHR4/LCK/SMAD3/NOV/LEF1/PIK3CG/IL20RB/LIMS2/PCDHGC4/PCDHGB7/PCDHGA11/SOX9/STK10/TNXB/FZD5/SLA2/FADD	28

GO:0010033	response to organic substance	70/311	2687/17046	0.00103	0.02892	0.02306	CDH13/TCIRG1/NPFR2/ADCY3/CHRNA5/CIDEA/CTGF/CITED4/DNMT3A/DRD4/EGFR/EGR3/EPHA3/RASA3/FOXO1/SPG20/FLNB/MTOR/FBXO2/GIB2/GNAS/GPER1/GSTP1/NRG1/HLA-B/HLA-E/HLA-F/HPCA/HSD17B2/HSP90AA1/HTRA5/CYR61/IL6/SLI/ACATI1/LCK/LOX/LTB/LTBP1/SMAD3/MEI1/MAP3K1/ARHGFE3/LEF1/PIK3CG/IL20RB/PON1/PPP1CC/SYBU/PRKD1/PSMBA/PXN/RASGRF2/CCL17/SFRP2/CXCR5/SOX9/VAMP2/ACT1/TIMP3/TLRS/TWIST1/PAX8/CXCR4/FZD5/TMEM204/IL11/10/MGARP/FADD/LY86	70
GO:0030317	regulation of cAMP biosynthetic process	8/311	113/17046	0.00109	0.03021	0.02409	NPFR2/ADRB3/DRD4/GABBR1/GNAS/GPER1/HPCA/PALM	8
GO:0048736	appendage development	10/311	169/17046	0.0011	0.03021	0.02409	ECE1/SP8/GNAS/FLVCR1/FMNI1/MEOX2/LEF1/SFRP2/SOX9/TWIST1	10
GO:0060173	limb development	10/311	169/17046	0.0011	0.03021	0.02409	ECE1/SP8/GNAS/FLVCR1/FMNI1/MEOX2/LEF1/SFRP2/SOX9/TWIST1	10
GO:0051345	positive regulation of hydrolase activity	27/311	781/17046	0.00114	0.03103	0.02475	ADCY3/CTGF/EGFR/RASA3/TBCLD9B/RGS22/GNAS/GPER1/HPCA/CYR61/LCK/LLGL1/SMAD3/NTF3/ARHGFE3/ARHGFE10/PRKD1/RASGRF2/CCL17/SFRP2/TCEA1/SH3BGRL3/FADD/ARHGAP29/ARHGFE10/USP6NL/RABGAP1L	27
GO:0009893	positive regulation of metabolic process	82/311	3277/17046	0.00117	0.03131	0.02496	CDH3/CDH13/DMRT2/TBR1/ADCY3/PSIP1/CTGF/ADRB3/CITED4/RNF168/DRD4/ECE1/EGFR/RASA3/TBC1D9B/FOXO1/LARP1/MTOR/RGS22/GAPDH5/GNAS/GPER1/DOCK7/GSTP1/BRF1/ANXA2/NRG1/HMGA1/HPCA/HOXD3/HSP90AA1/BARHL2/CYR61/IL6/SLI/LCK/LLGL1/TB/SMAD3/MEF2/MAP3K1/MEOX1/MEOX2/MEF2/NFYB/NTF3/ARHGFE3/LEF1/ANGPT4/PIK3CG/RIPK4/CYTL1/POMC/PWIL2/ARHGFE10/PRKD1/PSMBA/PXN/RASGRF2/CCL17/SFRP2/TTRA2B/SOX9/STK10/TB9/TCEA1/ACTC1/TLRS/TRAJ1/TWIST1/PAX8/CXCR4/FZD5/SH3BGRL3/FADD/ZFAND2A/LDB2/ARHGAP29/HZAFY/ARHGFE10/USP6NL/RABGAP1L	82
GO:0043534	blood vessel endothelial cell migration	6/311	65/17046	0.00118	0.03131	0.02496	EGR3/EPHA4/WASH1/ANGPT4/PRKD1/SH3BGR13	6
GO:0030036	actin cytoskeleton organization	20/311	511/17046	0.00118	0.03131	0.02496	CTGF/EPHA3/PPM1E/LIMCH1/FLNB/MTOR/FMNI1/LLGL1/SMAD3/MAP3K1/NEDD9/NTF3/BINS3/ACTR3B/MICAL1/ACTC1/TNXB/SH3BGRL3/GAS7/ARHGFE10	20
GO:0007166	cell surface receptor signaling pathway	66/311	2511/17046	0.00118	0.03131	0.02496	CDH3/TSPAN5/CDH13/TCIRG1/ADCY3/GIDEA/APCDD1/CTGF/EGFR/TMEM17/EPHA3/EPHBA/RASA3/FOXO1/SPG20/FLNB/MTOR/DKK3/GPER1/GSTP1/NME7/NRG1/HLA-B/HLA-E/HLA-F/HOXD3/HSP90AA1/CYR61/IL6/SLI/LCK/LLGL1/TB/LTBP1/SMAD3/MAP3K1/NEDD9/NOV/NTF3/ARHGFE3/LEF1/DDX47/ANGPT4/PGAM2/IL20RB/PPP1CC/LIMS2/PRKD1/PSMBA/CCAR2/PXN/RASGRF2/CCL17/SFRP2/CXCR5/SOX9/TLE3/TRAJ1/CXCR4/FZD5/TMEM204/SLA2/IL11/10/FADD/LIMD1/LY86	66
GO:0060561	apoptotic process involved in morphogenesis	4/311	26/17046	0.00118	0.03131	0.02496	CYR61/LEF1/PAX8/FZD5	4
GO:0098602	single organism cell adhesion	25/311	704/17046	0.00119	0.03141	0.02505	CDH3/EGFR/EGR3/JUNC130/MTOR/GNAS/HLA-E/HLX/CYR61/IL6/LCK/SMAD3/MEF2/NOV/LEF1/PIK3CG/IL20RB/LIMS2/PXN/SOX9/STK10/TNXB/FZD5/SLA2/FADD	25
GO:0050678	regulation of epithelial cell proliferation	13/311	265/17046	0.00121	0.03162	0.02521	CDH3/CDH13/EGFR/EGR3/WASH1/MTOR/IL6/SMAD3/LIMS2/PRKD1/SFRP2/SOX9/TWIST1	13
GO:2000026	regulation of multicellular organismal development	43/311	1465/17046	0.00127	0.03297	0.02629	CDH3/DMRT2/TBR1/CTGF/EGR3/EPHA3/WASH1/ACINI1/SPG20/MTOR/TENM4/GNAS/GPER1/NRG1/HLA-B/HLX/HOXB3/HOXD3/BARHL2/CYR61/IL6/SLI/LCK/SMAD3/NTF3/PALM/LEF1/CEND1/ANGPT4/LIMS2/PRKD1/SFRP2/SOX9/PHLDA2/TWIST1/YWHAG/PAX8/CXCR4/COLOQ/SCRT1/FADD/HZAFY/ULK2	43
GO:0009967	positive regulation of signal transduction	40/311	1334/17046	0.00128	0.03297	0.02629	CDH3/TSPAN5/CDH13/HCS1/CTGF/ADRB3/DRD4/EGFR/RASA3/MTOR/GNAS/GPER1/NRG1/CYR61/IL6/SLI/LCK/SMAD3/MEF2/NOV/NTF3/ARHGFE3/LEF1/DDX47/ANGPT4/PGAM2/IL20RB/PPP1CC/LIMS2/PRKD1/PSMBA/CCAR2/PXN/RASGRF2/S100A4/CCL17/SFRP2/SOX9/TLRS/YWHAG/CXCR4/FZD5/SLA2/FADD/LY86	40

GO:0006140	regulation of nucleotide metabolic process	11/311	203/17046	0.00129	0.03297	0.02629	NPFPR2/ADR83/DRD4/GABBR1/GAPDH5/GNAS/GPER1/HPCA/MEI/PALM/PGAM2	11
GO:0051252	regulation of RNA metabolic process	83/311	3337/17046	0.00129	0.03297	0.02629	CDH13/MBNL2/CLD/DBTBL18/DMRT2/TBR1/PSIP1/ZBED9/CIDEA/ZFR42/ZNF709/ZNF781/CTED4/RNF168/DNMT3A/EGFR/EGR3/SR8/XRN2/ACIN1/FOXO1/SPG20/MTOR/DKK3/GP ER1/ZBTB44/GTF2B/BRF1/NRG1/HLX/HMGAI/HOX8/HOX5/HOX6/HOX9/BARHL2/CRY61/IL6/ISL1/HLS1/SMAD3/MEF2D/MEOX1/MEOX2/NFYB/NTF3/LEF1/RIPK4/CYTL1/PO MC/BN2/PRMT6/ZNF532/CNOT11/PRKD1/CCAR2/SFRP2/TRA28/SGK1/SOX9/TAFA4B/TBP/TCEA1/TLE3/TRA71/TWIST1/ZNF124/ZNF177/PAX8/FZDS/ZC3H14/ZNF606/SCRIPT1/HIST1 H3A/SLA2/KDM2B/LOXL3/CBX2/GAS7/FADD/LIMD1/LDB2/H2AFY	83
GO:0048523	negative regulation of cellular process	93/311	3831/17046	0.00131	0.03297	0.02629	CDH13/CTD/ZBTB18/B4GAL17/CIDEA/ANKRD9/APCDD1/CTGF/RNF168/NLRP6/DNMT3A/DRD4/EGFR/EGR3/PATL2/RASA3/PPM1E/VASH1/ACIN1/FOXO1/SPG20/MTOR/GABBR1/R GS2/ZFXO2/DKK3/VPSA4/GPER1/GSTP1/GZMA/ANXA2/SERPIND1/NRG1/HLX/HMGAI/HPCA/HOX83/HOX6/ACADI/COI28A3/CYR61/IL6/ISL1/THH3/HLS1/LCK/LTBP1/SMAD3/ MF2/NOV/NTF3/PALM/LEF1/CEND1/ANGPT4/PDE4C/PIK3CG/IL20RB/PPP1CC/PRMT6/LIMS2/PRKD1/MASBP1/PSMB4/METTL4/CCAR2/CCL17/SFRP2/SOX9/TBP/ACTC1/TIMP3/T WIST1/YWHAG/ZNF177/PAX8/FZDS/NLRX1/ZC3H14/RAB11FIP1/COI18A1/SCRIPT1/HIST1H3A/SLA2/SPINK7/KDM2B/LOXL3/CBX2/GAS7/FADD/LIMD1/H2AFY/ULK2	93
GO:0002709	regulation of T cell mediated immunity	5/311	45/17046	0.00132	0.03297	0.02629	HLA-B/HLA-E/IL20RB/FZD5/FADD	5
GO:0032233	positive regulation of actin filament bundle assembly	5/311	45/17046	0.00132	0.03297	0.02629	CTGF/PPM1E/MTOR/SMAD3/ARHGFE10	5
GO:0061061	muscle structure development	21/311	554/17046	0.00133	0.03311	0.02641	ZBTB18/COI11A1/EGR3/FLNB/MTOR/NRG1/HLX/IL6/ISL1/SMAD3/MEF2D/MEOX2/NOV/NTF3/LEF1/BIN3/CCL17/SOX9/ACTC1/TWIST1/TMEM204	21
GO:0032880	regulation of tumor necrosis factor production	7/311	91/17046	0.00138	0.03388	0.02702	CIDEA/GSTP1/HLA-E/ISL1/POMC/TWIST1/FADD	7
GO:0035282	segmentation	7/311	91/17046	0.00138	0.03388	0.02702	DMRT2/SMAD3/MEOX1/MEOX2/LEF1/SFRP2/FZD5	7
GO:0051046	regulation of secretion	23/311	633/17046	0.00139	0.03392	0.02705	CIDEA/NLRP6/DRD4/UNC13D/VPSA4/GNAS/GPER1/NRG1/HLA-E/IL6/ISL1/LGL1/NOV/PDE4C/POMC/SMPP3/SYBU/SGK1/VAMP2/TWIST1/PAX8/RAB11FIP1/RAB3D	23
GO:0007517	muscle organ development	15/311	337/17046	0.00139	0.03392	0.02705	ZBTB18/COI11A1/EGR3/FLNB/NRG1/HLX/IL6/ISL1/SMAD3/MEF2D/MEOX2/LEF1/BIN3/ACTC1/TWIST1	15
GO:0007154	cell communication	132/311	5832/17046	0.00142	0.03427	0.02733	CDH3/TSPAN5/CDH13/KCNMB2/JCIRG1/HCS1/NPFFR2/ADCY3/PTH2/CHRNA5/CIDEA/APCDD1/CTGF/ADRB3/NLRP6/DRD4/EGFR/EGR3/TMEM17/EPHA3/EPHB4/RASA3/ACIN1/FO XO1/SPG20/FLNB/LARP1/MTOR/GABBR1/TEENM4/RGS22/GIA3/GIB2/SDCBP2/DKK3/GLS2/GPR162/GNAS/GPER1/GSTP1/NME7/ANXA2/KCNIP2/MME7/ANXA6/HLA-B/HLA-E/HLA- H/PCPA/APBA2/HOXD3/HSP90AA1/HTR5A/CYR61/IL6/ISL1/KRT15/LCK/LGL1/LTBP1/SMAD3/MAP3K1/NUDT1/NEDD9/NIMBR/NOV/NTF3/PALM/ARHGFE3/LEF1/DDX47/ANG PT4/PDE4C/PDE7A/PGAM2/PIK3CG/IL20RB/CYTL1/POWCZDHHC13/PPP1CC/ARHGFE10/SMPP3/SYBU/LIMS2/VAC14/PRKD1/PSMB4/LPARS/CCAR2/PXN/RASGRF2/S100A4/S100 A6/CCL17/SFRP2/CXCR5/SGK1/MICAL1/SOX9/STK10/VAMP2/TLE3/TLRS/ITNB/TRA71/TWIST1/UPP1/YWHAG/CACNB2/PAX8/CXCR4/FZDS/TMEM204/NLRX1/RAB11FIP1/UNC93B 1/CAPS/COLQ/HIST1H3A/SLA2/LLF10/FADD/LIMD1/ARHGAP29/LY86/RAB3D/SMAD5-AS1/ARHGFE10/ULK2/TELO2	132
GO:0060537	muscle tissue development	15/311	338/17046	0.00143	0.03453	0.02754	ZBTB18/COI11A1/FLNB/TEENM4/NRG1/HLX/ISL1/SMAD3/MEF2D/MEOX2/LEF1/BIN3/SOX9/ACTC1/TWIST1	15
GO:0010628	positive regulation of gene expression	46/311	1608/17046	0.00144	0.03459	0.02759	CDH3/CDH13/DMRT2/TBR1/PSIP1/CTGF/CTED4/EGFR/FOXO1/LARP1/MTOR/GPER1/BRF1/HMGAI/HOXD3/BARHL2/CRY61/IL6/ISL1/LCK/SMAD3/MEF2D/MEOX1/MEOX2/MF2/N FYB/NTF3/LEF1/RIPK4/CYTL1/POMC/PWIL2/PRKD1/SFRP2/TRA2B/SOX9/TBP/TCEA1/ACTC1/TRA71/TWIST1/PAX8/FZDS/FADD/LDB2/H2AFY	46
GO:0060548	negative regulation of cell death	28/311	835/17046	0.00145	0.03461	0.0276	CIDEA/ANKRD9/CTGF/EGFR/EGR3/FOXO1/GSTP1/NRG1/CYR61/IL6/ISL1/SMAD3/NOV/NTF3/LEF1/ANGPT4/PIK3CG/LIMS2/PRKD1/PSMB4/CCAR2/SFRP2/SOX9/ACTC1/TWIST1/PA X8/KDM2B/FADD	28
GO:0048863	stem cell differentiation	12/311	238/17046	0.00147	0.03473	0.02769	EPHA3/NRG1/ISL1/SMAD3/MEOX1/LEF1/S100A4/SFRP2/SOX9/TWIST1/PAX8/LOXL3	12
GO:0060935	chemotaxis	27/311	796/17046	0.0015	0.03506	0.02796	CDH13/TBR1/EGFR/EGR3/EPHA3/EPHB4/RASA3/SERPIND1/NRG1/HSP90AAA1/CYR61/IL6/ISL1/SMAD3/NOV/NTF3/LEF1/PIK3CG/PRKD1/PSMB4/TRPC7/RASGRF2/CCL17/CXCR5/TR PC4/CACNB2/CXCR4	27
GO:0042330	taxis	27/311	796/17046	0.0015	0.03506	0.02796	CDH13/TBR1/EGFR/EGR3/EPHA3/EPHB4/RASA3/SERPIND1/NRG1/HSP90AAA1/CYR61/IL6/ISL1/SMAD3/NOV/NTF3/LEF1/PIK3CG/PRKD1/PSMB4/TRPC7/RASGRF2/CCL17/CXCR5/TR PC4/CACNB2/CXCR4	27

GO:0030029	actin filament-based process	21/311	561/17046	0.00155	0.03588	0.02862	FRMD6/CTGF/EPHA3/PPM1E/LIMCH1/FLNB/MTOR/FMN1/LLGL1/SMAD3/MAP3K1/NEDD9/NTF3/BIN3/ACTR3B/MICAL1/ACTC1/TNXB/SH3BGR13/GAS7/ARHGGEF10	21
GO:0032640	tumor necrosis factor production	7/311	93/17046	0.00156	0.03588	0.02862	CIDEA/GSTP1/HLA-E/ISL1/POMC/TWIST1/FADD	7
GO:2000147	positive regulation of cell motility	15/311	341/17046	0.00156	0.03588	0.02862	CDH13/EGFR/GPER1/CYR61/IL6/SMAD3/NTF3/LEF1/ANGPT4/PRKD1/SOX9/TWIST1/PTP4A1/COL18A1/FADD	15
GO:0042981	regulation of apoptotic process	39/311	1305/17046	0.00157	0.03588	0.02862	CIDEA/ANKRD9/CTGF/EGFR/EGR3/ACIN1/FOXO1/GLS2/GPER1/GSTP1/GZMA/NRG1/CYR61/IL6/ISL1/LCK/SMAD3/MAP3K1/NTF3/ARHGGEF3/LEF1/ANGPT4/PIK3CG/LIMS2/PSMB4/CCAR2/RASGRF2/SFRP2/SGK1/SOX9/STK10/ACTC1/TRAF1/TWIST1/NWHAG/PAX8/COL18A1/KOM2B/FADD	39
GO:0009152	purine ribonucleotide biosynthetic process	12/311	240/17046	0.00157	0.03588	0.02862	TCIRG1/NPFFR2/ADCY3/ADRB3/DRD4/GABBR1/AMPD2/GNAS/GPER1/NNME7/HPCA/PALM	12
GO:0035107	appendage morphogenesis	9/311	148/17046	0.0016	0.03603	0.02874	ECE1/SP8/GNAS/FLVCR1/FMN1/LEF1/SFRP2/SOX9/TWIST1	9
GO:0035108	limb morphogenesis	9/311	148/17046	0.0016	0.03603	0.02874	ECE1/SP8/GNAS/FLVCR1/FMN1/LEF1/SFRP2/SOX9/TWIST1	9
GO:0045785	positive regulation of cell adhesion	15/311	343/17046	0.00166	0.03707	0.02956	CDH13/EGR3/UNC13D/MTOR/NRG1/HLA-E/HLX/FMN1/CYR61/IL6/LCK/SMAD3/LEF1/SFRP2/FADD	15
GO:1903555	regulation of tumor necrosis factor superfamily cytokine production	7/311	94/17046	0.00166	0.03707	0.02956	CIDEA/GSTP1/HLA-E/ISL1/POMC/TWIST1/FADD	7
GO:0031325	positive regulation of cellular metabolic process	69/311	2688/17046	0.00167	0.03714	0.02962	CDH3/CDH13/DMRT2/TBR1/ADCY3/PSIP1/CTGF/ADRB3/CITED4/RNF168/DRD4/ECE1/EGFR/RASA3/FOXO1/LARP1/MTOR/GAPDH5/GNAS/GPER1/DOK7/GSTP1/BRF1/ANXA2/NRG1/HMGA1/HPCA/HSP90AA1/BAHR12/CYR61/IL6/ISL1/LCK/ITB/SMAD3/MEF2D/MAP3K1/MEOX1/MEOX2/MF12/NFYB/NTF3/LEF1/ANGPT4/PIK3CG/RIK4/CYTL1/POMC/PWIL2/PRKD1/PSMB4/PXN/RASGRF2/CCL17/SFRP2/TRA2B/SOX9/STK10/TBP/TCEA1/TLK5/TRAF1/TWIST1/PAX8/CXCR4/FZD5/FADD/ZF-AND2A/LDB2	69
GO:0006955	immune response	43/311	1487/17046	0.0017	0.03752	0.02992	HCST/ADCY3/RNF168/COCH/NLRP6/EGFR/UNC13D/RASA3/FOXO1/MTOR/GPER1/GZMA/NRG1/HLA-B/HLA-E/HLA-F/HLX/HSP90AA1/IL6/LCK/ITB/SMAD3/MAP3K1/LEF1/PIK3CG/IL20RB/PRKD1/MASP1/PSMB4/RASGRF2/DEFB134/CCL17/CXCR5/WAMP2/TLK5/FZD5/NLRX1/UNC93B1/SLA2/IL1F1/0/FADD/IL32/ILY86	43
GO:0050679	positive regulation of epithelial cell proliferation	9/311	150/17046	0.00175	0.03852	0.03072	CDH3/CDH13/EGFR/EGR3/MTOR/IL6/PRKD1/SOX9/TWIST1	9
GO:0043067	regulation of programmed cell death	39/311	1314/17046	0.00177	0.03879	0.03093	CIDEA/ANKRD9/CTGF/EGFR/EGR3/ACIN1/FOXO1/GLS2/GPER1/GSTP1/GZMA/NRG1/CYR61/IL6/ISL1/LCK/SMAD3/MAP3K1/NTF3/ARHGGEF3/LEF1/ANGPT4/PIK3CG/LIMS2/PSMB4/CCAR2/RASGRF2/SFRP2/SGK1/SOX9/STK10/ACTC1/TRAF1/TWIST1/NWHAG/PAX8/COL18A1/KOM2B/FADD	39
GO:1902107	positive regulation of leukocyte differentiation	8/311	122/17046	0.00179	0.03879	0.03093	EGR3/ACIN1/GNAS/HLX/IL6/LCK/LEF1/FADD	8

GO:0002711	positive regulation of T cell mediated immunity	4/311	29/17046	0.0018	0.03879	0.03093	HLA-B/HLA-E/FZD5/FADD	4
GO:0031280	negative regulation of immunity	4/311	29/17046	0.0018	0.03879	0.03093	DRD4/GABBR1/HPCA/PALM	4
GO:0071822	protein complex subunit organization	46/311	1629/17046	0.00187	0.03948	0.03149	TCIRG1/SEPT9/APOA1BP/COLL1A1/CTGF/EMIL1/PPM1E/MTOR/VPS4A/ANXA2/NRG1/ANXA6/HMGA1/ACAD/HSP90AA1/FMN1/HILS1/ACATI/LLGL1/LOX/SMAD3/ME1/MAP3K1/NEDD9/ANGPT4/BIN3/ACTR3B/PXN/RPL8/RPL29/SFRP2/MICAL1/SOX9/VAMP2/ACTC1/TNXB/TRAF1/TWIST1/HIST1H2BM/SH3BGR13/HIST1H3A/PARD6B/GAS7/FADD/H2AFY/ARHGEF10	46
GO:0045597	positive regulation of cell differentiation	26/311	768/17046	0.00187	0.03948	0.03149	CTGF/EGFR3/UNC13D/EPHA3/ACIN1/MTOR/TENM4/GNAS/GPER1/NRG1/HLX/HOXD3/CYR61/IL6/LCK/SMAD3/PALM/LEF1/PRKDI/SFRP2/SOX9/TWIST1/PAX8/CXCR4/FADD/H2AFY	26
GO:0048704	embryonic skeletal system morphogenesis	7/311	96/17046	0.00188	0.03948	0.03149	COL11A1/GNAS/FLVCR1/HOXB3/HOXD3/SMAD3/TWIST1	7
GO:0021781	glial cell fate commitment	3/311	14/17046	0.00189	0.03948	0.03149	NRG1/NTF3/SOX9	3
GO:0048871	multicellular organismal homeostasis	14/311	313/17046	0.0019	0.03948	0.03149	CDH3/ADCY3/CIDEA/ZG16B/CTGF/ADRB3/FOXO1/ANPD2/GNAS/ACAD/IL20RB/CYTL1/SOX9/LDB2	14
GO:0030001	metal ion transport	26/311	769/17046	0.00191	0.03948	0.03149	KCNMB2/TCIRG1/CLCA1/C15orf27/SLC38A10/TRPM6/CTGF/TRPV3/DRD4/RASA3/CRACR2B/GPER1/KCNIP2/ANXA6/LCK/NIF2/PIK3CG/ZDHHC13/PRKDI/TRPC7/SGK1/VAMP2/TRAAPC10/TRPC4/CACNB2/SMDT1	26
GO:0022604	regulation of cell morphogenesis	18/311	457/17046	0.00191	0.03948	0.03149	TBR1/COCH/UNC13D/EPHA3/SPG20/BARHL2/IL6/SMAD3/MF2/PALM/LEF1/PXN/SFRP2/TWIST1/PAX8/GAS7/LIMD1/ULK2	18
GO:0070588	calcium ion transmembrane transport	10/311	182/17046	0.00191	0.03948	0.03149	C15orf27/TRPM6/TRPV3/DRD4/RASA3/PIK3CG/TRPC7/TRPC4/CACNB2/SMDT1	10
GO:1901564	organonitrogen compound metabolic process	54/311	1996/17046	0.00192	0.03948	0.03149	BCKDK/TCIRG1/NPFFR2/ADCY3/HIBADH/BAGAL1/APOA1BP/ADRB3/ADAL/DNMT3A/DRD4/ECEL1/PATL2/ALAS1/LARP1/MTOR/FUCA1/GABBR1/GAPDH5/AMPD2/GLS2/GNAS/GPE1/GSTP1/NMIE7/HPCA/ACADJ/BARHL2/CYR61/IL6/ITH3/ACATI/MEI/NUDT1/PALM/PDEAC/PDE7A/PGAM2/CYTL1/POMC/PON1/PCAT2/PWIL2/SMPD3/CNOT11/PRKDI/PSMB4/METTL4/RPL8/RPL29/CERK1/UPP1/VARS/PAX8	54
GO:0014032	neural crest cell development	5/311	49/17046	0.00193	0.03948	0.03149	NRG1/SL1/LEF1/SOX9/TWIST1	5
GO:0006164	purine nucleotide biosynthetic process	12/311	246/17046	0.00194	0.03948	0.03149	TCIRG1/NPFFR2/ADCY3/ADRB3/DRD4/GABBR1/AMPD2/GNAS/GPER1/NMIE7/HPCA/PALM	12
GO:0051272	positive regulation of cellular component movement	15/311	349/17046	0.00196	0.03948	0.03149	CDH13/EGFR/GPER1/CYR61/IL6/SMAD3/NTF3/LEF1/ANGPT4/PRKDI/SOX9/TWIST1/PTP4A1/COL18A1/FADD	15
GO:0010562	positive regulation of phosphorus metabolic process	33/311	1062/17046	0.00196	0.03948	0.03149	ADCY3/CTGF/ADRB3/DRD4/EGFR/RASA3/MTOR/GAPDH5/GNAS/GPER1/DOK7/ANXA2/NRG1/IL6/SL1/LCK/SMAD3/MAP3K1/NTF3/ANGPT4/PIK3CG/PRKDI/PSMB4/PXN/RASGRF2/CCL17/SFRP2/SOX9/STK10/CXCR4/FZD5	33

GO:0045937	positive regulation of phosphate metabolic process	33/311	1062/17046	0.00196	0.03948	0.03224	ADCY3/CTGF/ADRB3/DRD4/EGFR/RASA3/MTOR/GAPDH5/GNAS/GPER1/DOK7/ANXA2/NRG1/HPCA/CYR61/IL6/ISL1/LCK/SMAD3/MAP3K1/NITF3/ANGPT4/PIK3CG/PRKD1/PSMB4/PXN/RASGRF2/CCL17/SFRP2/SOX9/STK10/CXCR4/FZD5	33
GO:0009165	nucleotide biosynthetic process	14/311	315/17046	0.00202	0.04003	0.03224	TCIRG1/NPFFR2/ADCY3/ADRB3/DRD4/GABBR1/AMPD2/GNAS/GPER1/NME7/HPCA/ME1/PALM/UPP1	14
GO:0044085	cellular component biogenesis	61/311	2329/17046	0.00205	0.04087	0.03259	CDH3/CDH13/TCIRG1/CD/SEPT9/PSIP1/APOA1BP/SCLT1/CTGF/WBP2NL/PATL2/TMEM17/EPHA3/PPM1E/MTOR/TENM4/GIB2/VPS4A/ANXA2/NRG1/ANXA6/HMG1/ACAD1/HSP90A1/FMN1/HILS1/ACAT1/LLGL1/LOX/SMAD3/ME1/MAP3K1/NEDD9/PALM/DDX47/ANGPT4/PLEC/LIMS2/BIN3/ACTR3B/PXN/SOX9/VAMP2/ACTC1/TNXB/TRAFA1/TWIST1/FZD5/COLQ/HIST1H2BM/HIST1H3A/PARD6B/GAS7/FADD/LIMD1/LDB2/H2AFY/ARHGFE10/ULK2/USP6NL	61
GO:0071706	tumor necrosis factor superfamily cytokine production	7/311	98/17046	0.00211	0.04188	0.0334	CIDEA/GSTP1/HLA-E/ISL1/POM1C/TWIST1/FADD	7
GO:0034329	cell junction assembly	11/311	217/17046	0.00219	0.04315	0.03441	CDH3/CDH13/EPHA3/GIB2/FMN1/SMAD3/PLEC/LIMS2/PXN/FZD5/PARD6B	11
GO:0010467	gene expression	111/311	4805/17046	0.0022	0.04315	0.03441	CDH3/TSPAN5/CDH13/MBNL2/CLD/IBTB18/DMRT2/CELF2/TBR1/PSIP1/ZEBD9/GIDEA/ZFP42/CTGF/ZNF709/ZNF781/CTEAD4/RNF168/DNMT3A/ECE1/EGFR/EGR3/PATL2/SP8/XRN1/2/ACIN1/FOXO1/LARP1/MTOR/DKK3/GS2/GNAS/GPER1/ZBTB44/GTF2B/BRF1/NRG1/HIX/HMG1/APB2/HOX3/HOX5/HOX6/HOX3/FMN1/BARHL2/CYR61/IL6/ISL1/HLS1/LCK/LTB/SMAD3/MEF2D/MEOX1/MEOX2/MFI2/NFYB/NOV/NITF3/LEF1/DDX47/RIPK4/CYTL4/POMC/MOVL0L1/BNCC2/PPP1CC/PWIL2/PRMT6/ZNF532/WDR33/CNOT11/PRKDI/MASP1/PSMB4/ME1/TLL14/CCAR2/RPL8/RPL29/SFRP2/TRA2B/SGK1/SOX9/TF48/TBP/TCEA1/ACTC1/TLE3/TRAFA1/PHLDA2/TWIST1/VARS/YWHAG/ZNF124/ZNF177/PAX8/FZD5/ZC3H14/ZNF606/SCRT1/HIST1H3A/SLA2/KDM2B/LOXL3/CBX2/GAS7/FADD/LIMD1/LDB2/H2AFY	111
GO:0009725	response to hormone	31/311	985/17046	0.00221	0.04315	0.03441	TCIRG1/NPFFR2/ADCY3/CTGF/CTEAD4/DNMT3A/DRD4/EGFR/EGR3/RASA3/FOXO1/MTOR/GIB2/GNAS/GPER1/NRG1/HTFSA/IL6/ISL1/ACAT1/LCK/LOX/ME1/LEF1/PSMB4/PXN/RAS	31
GO:0001101	response to acid chemical	13/311	284/17046	0.00224	0.04315	0.03441	GRF2/VAMP2/TIMP3/PAX8/MGARP CTGF/DNMT3A/EGFR/EPHA3/MTOR/GNAS/HPCA/HSD17B2/IL6/PONI/SOX9/TIMP3/COL18A1	13
GO:1901293	nucleoside phosphate biosynthetic process	14/311	319/17046	0.00227	0.04315	0.03441	TCIRG1/NPFFR2/ADCY3/ADRB3/DRD4/GABBR1/AMPD2/GNAS/GPER1/NME7/HPCA/ME1/PALM/UPP1	14
GO:0050727	regulation of inflammatory response	12/311	251/17046	0.00229	0.04315	0.03441	NLRP6/GPER1/GSTP1/IL6/ISL1/SMAD3/NOV/PIK3CG/IL20RB/MASP1/PSMB4/NLRX1	12
GO:0022607	cellular component assembly	57/311	2152/17046	0.00229	0.04315	0.03441	CDH3/CDH13/TCIRG1/SEPT9/PSIP1/APOA1BP/SCLT1/CTGF/WBP2NL/PATL2/TMEM17/EPHA3/PPM1E/MTOR/TENM4/GIB2/VPS4A/ANXA2/NRG1/ANXA6/HMG1/ACAD1/HSP90A1/FMN1/HILS1/ACAT1/LLGL1/LOX/SMAD3/ME1/MAP3K1/NEDD9/PALM/ANGPT4/PLEC/LIMS2/BIN3/ACTR3B/PXN/SOX9/VAMP2/ACTC1/TNXB/TRAFA1/TWIST1/FZD5/COLQ/HIST1H2BM/HIST1H3A/PARD6B/GAS7/FADD/LIMD1/H2AFY/ARHGFE10/ULK2/USP6NL	57
GO:0030814	regulation of cAMP metabolic process	8/311	127/17046	0.0023	0.04315	0.03441	NPFFR2/ADRB3/DRD4/GABBR1/GNAS/GPER1/HPCA/PALM	8
GO:0060284	regulation of cell development	25/311	739/17046	0.00231	0.04315	0.03441	TBR1/JUNC13D/EPHA3/SPG20/TENM4/GPER1/HOX83/HOXD3/BARHL2/IL6/ISL1/SMAD3/MFZ2/NITF3/PALM/LEF1/PRKD1/SFRP2/SOX9/TWIST1/YWHAG/PAX8/CXCR4/SCRT1/ULK2	25
GO:0003382	epithelial cell morphogenesis	5/311	51/17046	0.00231	0.04315	0.03441	FRMD6/FLNB/MAP3K1/PAX8/COL18A1	5
GO:0051350	negative regulation of lyase activity	4/311	31/17046	0.00232	0.04315	0.03441	DRD4/GABBR1/HPCA/PALM	4
GO:1902742	apoptotic process involved in development	4/311	31/17046	0.00232	0.04315	0.03441	CYR61/LEF1/PAX8/FZD5	4

GO:0023056	positive regulation of signaling	42/311	1467/17046	0.00232	0.04315	0.03441	CDH3/TPAN5/CDH13/HCS1/CTGF/ADRB3/DRD4/ECE1/EGFR/RASA3/MTOR/GNAS/GPER1/NRG1/CYR61/IL6/ISL1/LCK/SMAD3/MAP3K1/NOV/NTF3/PIK3CG/ZDHHC13/LIMS2/PRKD1/PSMB4/CCAR2/PXN/RASGRF2/S100A4/CCL17/SFRP2/SOX9/VAMP2/TLB5/YWHAG/CXR4/FZD5/SLA2/FADD/LY86	42
GO:0042327	positive regulation of phosphorylation	30/311	946/17046	0.00232	0.04315	0.03441	ADCY3/CTGF/ADRB3/DRD4/EGFR/RASA3/MTOR/GAPDH5/GPER1/DOK7/ANX2/NRG1/CYR61/IL6/ISL1/LCK/MAP3K1/NTF3/ANGPT4/PIK3CG/PRKD1/PSMB4/PXN/RASGRF2/CCL17/SFRP2/SOX9/STK10/CXR4/FZD5	30
GO:1903055	positive regulation of extracellular matrix organization	3/311	15/17046	0.00233	0.04315	0.03441	SMAD3/MF12/SOX9	3
GO:0031324	negative regulation of cellular metabolic process	57/311	2154/17046	0.00234	0.04318	0.03443	C1D/ZBTB18/RNF168/NLRP6/DNMT3A/DRD4/PAT12/PPM1E/ACIN1/FOXO1/MTOR/GABBR1/DKK3/GPER1/GSTP1/GZMA/ANX2/SERPIND1/NRG1/HMGA1/HPCA/HOXB3/HOXC6/ACADL/COL28A1/IL6/ISL1/TH3/HLS1/SMAD3/NTF3/PALM/LEF1/PIK3CG/PRMT6/MASP1/PSMB4/METTL14/CCAR2/SFRP2/SOX9/TBP/TIMP3/TWIST1/YWHAG/ZNF177/ZC3H14/SCRT1/HIST1H3A/SLA2/SPINK7/KDM2B/LOX13/CBX2/FADD/LIMD1/H2AFY	57
GO:0051960	regulation of nervous system development	23/311	660/17046	0.00237	0.04348	0.03468	TBR1/EPHA3/SPG20/MTOR/TENM4/GPER1/NRG1/HOXB3/HOXD3/BARHL2/IL6/ISL1/NTF3/PALM/CEND1/PRKD1/SFRP2/SOX9/YWHAG/CXCR4/COLQ/SCRT1/ULK2	23
GO:0006355	regulation of transcription, DNA-templated	79/311	3210/17046	0.00237	0.04348	0.03468	CDH13/C1D/ZBTB18/DWMT2/TBR1/PSIP1/ZBED9/CIDEA/ZFP42/ZNF781/CITED4/RNF168/DNMT3A/EGFR/EGR3/SP8/XRN2/FOXO1/SPG20/MTOR/DKK3/GPER1/ZBTB44/GT F2B/BRF1/NRG1/HLX/HMGA1/HOXB3/HOXC5/HOXC6/HOXD3/BARHL2/CYR61/IL6/ISL1/HLS1/SMAD3/MEF2D/MEOX1/MEOX2/NFYB/NTF3/LEF1/RIPK4/CYTL1/POW/BNC2/PRMT 6/ZNF532/CNOT11/PRKD1/CCAR2/SFRP2/SGK1/SOX9/TAF4B/TBP/TCEA1/TLE3/TRAF1/TWIST1/ZNF124/ZNF177/PAX8/FZD5/ZNF606/SCRT1/HIST1H3A/SLA2/KDM2B/LOX13/CBX2/GAS7/FADD/LIMD1/LDB2/H2AFY	79
GO:0040017	positive regulation of locomotion	15/311	357/17046	0.00243	0.0444	0.03541	CDH13/EGFR/GPER1/CYR61/IL6/SMAD3/NTF3/LEF1/ANGPT4/PRKD1/SOX9/TWIST1/PTP4A3/COL18A1/FADD	15
GO:0051241	negative regulation of multicellular organismal process	29/311	908/17046	0.00247	0.04475	0.03568	CDH3/CIDEA/ADRB3/TRPV3/VASHT1/SPG20/GNAS/GSTP1/ANX2/HLX/IL6/ISL1/SMAD3/NOV/LEF1/CEND1/ANGPT4/PIK3CG/IL20RB/POMC/LIMS2/SFRP2/SOX9/TWIST1/PAX8/NLR X1/RAB11FIP1/LIMD1/ULK2	29
GO:0051128	regulation of cellular component organization	52/311	1928/17046	0.0025	0.04475	0.03568	CDH13/TBR1/CIDEA/CTGF/COCH/PATL2/UNC13D/EPHA3/PPM1E/SPG20/MTOR/GLSZ/NPS4A/GPER1/ANX2/NRG1/HMGA1/HPCA/FMN1/BARHL2/CYR61/IL6/ISL1/SMAD3/MAP3K1/PSMB4/CCAR2/PXN/RASGRF2/S100A4/CCL17/SFRP2/SOX9/VAMP2/TLB5/YWHAG/CXR4/FZD5/SLA2/FADD/LY86	52
GO:0042303	molting cycle	7/311	101/17046	0.00251	0.04475	0.03568	CDH3/APCDD1/TRPV3/EGFR/GNAS/SOX9/LDB2	7
GO:0042633	hair cycle	7/311	101/17046	0.00251	0.04475	0.03568	CDH3/APCDD1/TRPV3/EGFR/GNAS/SOX9/LDB2	7
GO:0043200	response to amino acid	7/311	101/17046	0.00251	0.04475	0.03568	CTGF/DNMT3A/EGFR/MTOR/HPCA/IL6/TIMP3	7
GO:0060828	regulation of canonical Wnt signaling pathway	11/311	221/17046	0.00252	0.0449	0.0358	FOXO1/DKK3/ISL1/SMAD3/LEF1/PSMB4/CCAR2/SFRP2/SOX9/FZD5/LIMD1	11
GO:0050673	epithelial cell proliferation	14/311	323/17046	0.00254	0.04496	0.03585	CDH3/CDH13/EGFR/EGR3/YASH1/MTOR/IL6/SMAD3/NOV/LIMS2/PRKD1/SFRP2/SOX9/TWIST1	14
GO:0060429	epithelium development	32/311	1037/17046	0.00255	0.04505	0.03592	CDH3/DWMT2/FRMD6/APCDD1/CTGF/EGFR/FLNB/GNAS/NRG1/FMN1/CYR61/IL6/ACAT1/KRT15/INSC/SMAD3/MAP3K1/MEOX1/MEOX2/NTF3/LEF1/RIPK4/PXN/SFRP2/SOX9/TWIST1/PAX8/FZD5/COL18A1/KDM2B/LDB2/H2AFY	32
GO:0014706	striated muscle tissue development	14/311	324/17046	0.00261	0.04585	0.03656	ZBTB18/COL11A1/FLNB/TENM4/NRG1/HLX/ISL1/SMAD3/MEF2D/MEOX2/LEF1/BIN3/ACTC1/TWIST1	14

GO:0048015	phosphatidylinositol-mediated signaling	10/311	190/17046	0.00262	0.04585	0.03656	HCST/EGFR/FOXO1/MTOR/GPER1/NRG1/LCK/PIK3CG/SOX9/TWIST1	10
GO:0001934	positive regulation of protein phosphorylation	29/311	913/17046	0.00268	0.04663	0.03718	ADCY3/CTGF/ADRB3/DRD4/EGFR/RASA3/MTOR/GPER1/DOX7/ANXA2/NRG1/CYR61/IL6/ISL1/LCK/MAP3K1/NITF3/ANGPT4/PIK3CG/PRKD1/PSMB4/PXN/RASGRF2/CCL17/SFRP2/SOX9/STK10/CXCR4/FZD5	29
GO:0010556	regulation of macromolecule biosynthetic process	87/311	3621/17046	0.00272	0.04727	0.03769	CDH13/C1D/ZBTB18/DMRT2/TBR1/PSIP1/ZBED9/CIDEA/ZFP42/CTGF/ZNF709/ZNF781/CTEDA4/RNF168/DNMT3A/EGFR/EGR3/PATL2/SP8/XRN2/FOXO1/SPG20/LARP1/MTOR/DKK3/GPER1/ZBTB44/GSTP1/GTF2B/BRF1/NRG1/HLX/HMGAI1/HOXB3/HOXC5/HOXC6/HOXD3/BAHRH2/CYR61/IL6/ISL1/LTB/SMAD3/MEF2D/MEOX1/MEOX2/NFYB/NITF3/LEF1/RIPK4/CYTL1/POMC/BNC2/PIWIL2/PRMT6/ZNF532/CNOT11/PRKD1/METTL4/CCAR2/SFRP2/SK1/SOX9/TAFA4B/TBP/TCEA1/TLE3/TRAFA1/VAES/ZNF124/ZNF177/PAX8/FZD5/ZNF606/SCRT1/HIST1H3A/SLA2/KDM2B/LOXL3/CBX2/GAS7/FADD/LIMD1/LDB2/HZAFY	87
GO:1903506	regulation of nucleic acid-templated transcription	79/311	3227/17046	0.00275	0.04749	0.03787	CDH13/C1D/ZBTB18/DMRT2/TBR1/PSIP1/ZBED9/CIDEA/ZFP42/ZNF709/ZNF781/CTEDA4/RNF168/DNMT3A/EGFR/EGR3/SP8/XRN2/FOXO1/SPG20/MTOR/DKK3/GPER1/ZBTB44/GT F2B/BRF1/NRG1/HLX/HMGAI1/HOXB3/HOXC5/HOXC6/HOXD3/BAHRH2/CYR61/IL6/ISL1/HLS1/SMAD3/MEF2D/MEOX1/MEOX2/NFYB/NITF3/LEF1/RIPK4/CYTL1/POMC/BNC2/PRMT6/ZNF532/CNOT11/PRKD1/CCAR2/SFRP2/SK1/SOX9/TAFA4B/TBP/TCEA1/TLE3/TRAFA1/TWIST1/ZNF124/ZNF177/PAX8/FZD5/ZNF606/SCRT1/HIST1H3A/SLA2/KDM2B/LOXL3/CBX2/GAS7/FADD/LIMD1/LDB2/HZAFY	79
GO:0001916	positive regulation of T cell mediated cytotoxicity	3/311	16/17046	0.00282	0.04861	0.03876	HLA-B/HLA-E/FADD	3
GO:0051093	negative regulation of developmental process	24/311	710/17046	0.00284	0.04861	0.03876	CDH3/ADRB3/VASH1/FOXO1/SPG20/GNAS/GPER1/HLX/IL6/ISL1/SMAD3/MEF2/NOV/LEF1/CEND1/ANGPT4/LIMS2/CCL17/SFRP2/SOX9/TWIST1/PAX8/LIMD1/ULK2	24
GO:0010647	regulation of cell communication	42/311	1485/17046	0.0029	0.04948	0.03946	CDH3/TSPAN5/CDH13/HCS1/CTGF/ADRB3/DRD4/EGFR/RASA3/LARP1/MTOR/GNAS/GPER1/NRG1/CYR61/IL6/ISL1/LCK/SMAD3/MAP3K1/NOV/NITF3/PIK3CG/ZDHC13/LIMS2/PRK4/D1/PSMB4/CCAR2/PXN/RASGRF2/S100A4/CCL17/SFRP2/SOX9/VAMP2/TLR5/YWHAG/CXCR4/FZD5/SLA2/FADD/LY86	42
GO:0009892	negative regulation of metabolic process	62/311	2412/17046	0.00292	0.04965	0.03959	C1D/ZBTB18/CIDEA/CTGF/RNF168/NLRP6/DNMT3A/DRD4/EGFR/PATL2/PPM1E/ACIN1/FOXO1/MTOR/GABRR1/DKK3/GPER1/GSTP1/GZMA/ANXA2/SFRPIND1/NRG1/HMGAI1/HPC4/HOXB3/HOXC6/ACADU/COL28A1/IL6/ISL1/ITIH3/HLX/SMAD3/NITF3/PALM/LEF1/PIK3CG/PIWIL2/PRMT6/CNOT11/MASP1/PSMB4/METTL4/CCAR2/SFRP2/SOX9/TBP/TIMP3/TWIST1/YWHAG/ZNF177/ZG3H14/SCRT1/HIST1H3A/SLA2/SPINK7/KDM2B/LOXL3/CBX2/FADD/FAD/LIMD1/HZAFY	62
GO:0048017	inositol lipid-mediated signaling	10/311	193/17046	0.00293	0.04971	0.03964	HCST/EGFR/FOXO1/MTOR/GPER1/NRG1/LCK/PIK3CG/SOX9/TWIST1	10
GO:0006139	nucleobase-containing compound metabolic process	116/311	5102/17046	0.00295	0.04974	0.03966	CDH13/MBNL2/TCIRG1/C1D/ZBTB18/DMRT2/CELF2/TBR1/NPFFR2/ADCY3/PSIP1/ZBED9/CIDEA/APOALBP/ZFP42/CTGF/ADRB3/ADAL/ZNF709/ZNF781/CTEDA4/RNF168/DNMT3A/DRD4/EGFR/EGR3/PATL2/SP8/XRN2/ACIN1/FOXO1/MTOR/GABRR1/GAPDH5/AMPD2/DKK3/SL52/GNAS/GPER1/ZBTB44/GTF2B/BRF1/NME7/GZMA/NRG1/HLX/HMGAI1/HPCA/HOXB3/HOXC5/HOXC6/HOXD3/BAHRH2/CYR61/IL6/ISL1/HLS1/SMAD3/MEI/MEF2D/MEOX1/MEOX2/NUDT1/NFYB/NITF3/PALM/LEF1/DDX47/PDE4C/PDE7A/PGAM2/RIPK4/CYTL1/POMC/MOV10L1/BNC2/PIWIL2/PRMT6/ZNF532/WDR33/CNO11/PRKD1/METTL4/CCAR2/RPL8/RPL29/SFRP2/TRA2B/SGK1/SOX9/TAFA4B/TBP/TCEA1/TLE3/TRAFA1/TWIST1/UPP1/VAES/YWHAG/ZNF124/ZNF177/PAX8/FZD5/ZG3H14/ZNF606/SCRT1/HIST1H3A/SLA2/KDM2B/LOXL3/CBX2/GAS7/FADD/LIMD1/LDB2/HZAFY	116
Hypermethylated DMC, Cellular Component								
	Description	GeneRatio	BgRatio	pvalue	p.adjust	qvalue	geneId	Count

cellular_compone nt	GO:000575	16277/17046	2.63E-07	0.00013	0.01154	0.00011	CDH3/CCDC180/TSPAN5/CDH13/MBNL2/KCNMB2/BCKDK/TCIRG1/ABCA9/C1D/ZBTB18/DMRT2/CELF2/TBR1/SEPT9/HCST/NPFFR2/ADCY3/SLC27A2/HIBADH/PSIP1/PXMP4/BAGAL1/TTPH2/CHRNA5/CIDEA/ALPK2/CLCA1/FRMD6/C15orf27/ZG168/SLC38A10/KRT40/APOA1BP/COL11A1/VYP068/GALNT1/ZFP42/CPD/TRPM6/LYSMD4/APCDD1/CTGF/IRRCS4/CV8561/ADRB3/FITM1/ADAL/TRPV3/ZNF709/ZNF781/CITED4/WBP2NL/RNF168/COCH/NLRP6/DNAH8/DNAH9/DRD4/DSG3/ECE1/EGFR/EGR3/PATL2/TMEM17/EML1/UNC13D/DNAH12/EPHA3/EPHB4/ALAS1/RNF182/SP8/XRN2/RASA3/PPM1E/VASH1/ACIN1/TBC1D9B/FOXO1/SPG20/FLN1/SEI113/ATP11A/LARP1/MTOR/FUCA1/WDR37/GABRR1/NUPT1/DSCR9/GAK/TEENM4/FAM169A/RGS22/FBXO2/GAPDH5/GIAB3/GIB2/AMPD2/SDCBP2/DK3/SL2/VPS44/GPR162/GNAS/CACR2B/P/IGW/ZUIM01/GPER1/DOCK7/DCBLD1/FLVCR1/ZBTB44/GSTP1/GTF2B/BRF1/CCDC106/NMIE7/GZMA/ANXA2/SERPIND1/KCNIP2/NRNG1/ANXA6/HLA-B/HLA-E/HLA-F/HLX/HMGA1/HPCA/APBA2/HOXB3/HOXC5/HOXC6/HOXD3/HSD17B2/ACAD11/HTSA/COL28A1/MS4A10/FMN1/BARHL2/CYR61/IL6/ISL1/ITIH3/HLS1/ATP9B/KCF/ACAT1/KRT17/KRT15/INSC/TOMM20/SLCGA17/RESF18/CDHR4/LCK/LGL1/LOX/ITBP1/TBP1/SMAD3/MEI1/MEF2D/MAP3K1/MEOX1/MEOX2/MR2/MTLA/NUDT1/NEED9/NFYB/NMBR/NOV/NTF3/WRAP73/DEF6/PALM/ARHGFE3/LEF1/DXK47/CEND1/ANGPT4/PDE4C/PDE7A/GALNT1/PAGM2/PIGC/PIK3CG/SPA17/PLEC/IL20RB/RIPK4/CYTL1/POMC/PONI/MOV10/L1/ZDHHC13/ROBO4/BNC2/LPCAT2/FAM118A/PPP1CC/PIWIL2/ARHGFE10/PRMT6/ZNF532/WDR33/SMPD3/CNOT11/SYBU/UMS2/VAC14/PRKD1/BN3/PCDHGC4/PCD/HGB7/PCD/HGA11/MASP1/PSMB4/TRPCT/IPAR5/ACTR3B/METTL4/CCAR2/PTPRCA/PXN/RASGRF2/EXOC4/RPL8/DEFB134/CTNNA3/RPL29/S100A6/S100A5/S100A6/CCL17/C19orf33/SFRP2/CXCR5/TRAZB/SGK1/SYNDIG1/MICAL1/CERK/SOX9/STK10/VAMP2/TA4B/TBP1/ACT1/TIMP3/TEI3/LR5/TRAPP10/TNXB1/TRAFC1/TRPC4/PHLDA2/TWIST1/UPP1/VARS/YWHAG/ZNF124/ZNF177/PTPA41/CACNB2/PAX8/CXCR4/FZD5/GDPD3/TMEM204/NLRX1/ZMYM1/EPHX3/ZC3H14/ZNF606/RAB11/FIP1/RNF39/COL18A1/UNC93B1/CAPS/CO1Q/HIST1H2BM/SH3BGRL3/GSG1/SCR11/HIST1H3A/SLAZ/PTARD68/IL1F10/SPINK7/KDM2B/LOXL3/MGARP/CBX2/GAS7/FADD/LIMD1/MAP7/ZFAND2A/LDB2/SMDT1/RCSDI/IL32/R/EP6/SDR42E1/TBC1D31/ARHGAP29/LR86/RAB3D/H2AFY/MTLS/ARHGFE10/ULK2/USP6N/TELO2/RABGAP1/TMCC2
GO:0005769	early endosome	266/17046	5.44E-05	0.0133	0.01154	0.00011	ECE1/EGFR/EPHA3/ATP11A/VPS4A/GPER1/ANXA2/HLA-B/HLA-E/HLA-F/ILG1/VAC14/PTPA41/CXCR4/FZD5/RABGAP1
GO:0031931	TORC1 complex	16/17046	0.00013	0.02145	0.01861	0.00011	LARP1/MTOR/TELO2
GO:0030054	cell junction	1073/17046	0.00035	0.04268	0.03702	0.00011	CDH3/CDH13/CHRNA5/FRMD6/DSG3/EGFR/FLNB/GABBR1/GAK/GIAB3/GIB2/GPER1/DOCK7/ANXA6/HMGA1/HOXC5/FMN1/SLCGA17/LCK/NEED9/NOV/PLEC/PPP1CC/UMS2/PRKD1/PXN/RPL8/VAMP2/ACT1/TRPC4/YWHAG/CXCR4/FZD5/TMEM204/COL1Q/PARD6B/LIMD1
Hypermethylated DMC Molecular Function							
GO:0003674	Description molecular_function	GeneRatio 15274/17046	pvalue 9.59E-16	p.adjust 6.31E-13	qvalue 5.71E-13	Count 312	geneID CDH3/TSPAN5/CDH13/MBNL2/KCNMB2/BCKDK/TCIRG1/ABCA9/C1D/ZBTB18/DMRT2/CELF2/TBR1/SEPT9/HCST/NPFFR2/ADCY3/SLC27A2/HIBADH/PSIP1/PXMP4/BAGAL1/ADPRHL1/CHRNA5/ZBED9/PWMP2A/CIDEA/ALPK2/CLCA1/FRMD6/C15orf27/ZG168/SLC38A10/KRT40/APOA1BP/COL11A1/GALM/SLC11/ZFP42/CPD/TRPM6/APCDD1/CTGF/IRRCS4/CYB561/ADRB3/FITM1/ADAL/TRPV3/ZNF709/ZNF781/CITED4/WBP2NL/RNF168/COCH/NLRP6/DNAH8/DNAH9/DRD4/DSG3/ECE1/EGFR/EGR3/PATL2/EML1/UNC13D/ZBTB7C/DNAH12/EPHA3/EPHB4/ALAS1/RNF182/SP8/XRN2/RASA3/PPM1E/VASH1/ACIN1/TBC1D9B/FOXO1/SPG20/FLN1A/SEI113/ATP11A/LARP1/MTOR/FUCA1/WDR37/GABBR1/NUPT1/DSCR9/GAK/TEENM4/ITNL1/RGS22/FBXO2/GAPDH5/GIAB3/GIB2/AMPD2/SDCBP2/GLS2/VPS44/GPR162/GNAS/CACR2B/P/IGW/ZUIM01/GPER1/DOCK7/DCBLD1/FLVCR1/ZBTB44/GSTP1/GTF2B/BRF1/CCDC106/NMIE7/GZMA/ANXA2/SERPIND1/KCNIP2/NRNG1/ANXA6/HLA-B/HLA-E/HLA-F/HLX/HMGA1/HPCA/APBA2/HOXB3/HOXC5/HOXC6/HOXD3/HSD17B2/ACAD11/HTSA/COL28A1/MS4A10/FMN1/BARHL2/CYR61/IL6/ISL1/ITIH3/HLS1/ATP9B/ACAT1/KRT17/KRT15/INSC/TOMM20/SLCGA17/RESF18/CDHR4/LCK/LGL1/LOX/ITBP1/TBP1/SMAD3/MEI1/MEF2D/MAP3K1/MEOX1/MEOX2/MR2/MTLA/NUDT1/NEED9/NFYB/NMBR/NOV/NTF3/DEF6/PALM/ARHGFE3/LEF1/DDX47/ANGPT4/PDE4C/PDE7A/GALNT1/PAGM2/PIGC/PIK3CG/SPA17/PLEC/IL20RB/RIPK4/CYTL1/POMC/PONI/MOV10/L1/ZDHHC13/ROBO4/BNC2/LPCAT2/FAM118A/PPP1CC/PIWIL2/ARHGFE10/PRMT6/ZNF532/WDR33/SMPD3/CNOT11/SYBU/UMS2/VAC14/PRKD1/BN3/PCDHGC4/PCD/HGB7/PCD/HGA11/MASP1/PSMB4/TRPCT/IPAR5/ACTR3B/METTL4/CCAR2/PTPRCA/PXN/RASGRF2/EXOC4/RPL8/RPL29/S100A4/S100A5/S100A6/CCL17/SFRP2/CXCR5/TRAZB/SGK1/MICAL1/CERK/SOX9/STK10/VAMP2/TA4B/TBP1/ACT1/ACTC1/TIMP3/TEI3/LR5/TRAPP10/TNXB1/TRAFC1/TRPC4/PHLDA2/TWIST1/UPP1/VARS/ZNF124/ZNF177/PTPA41/CACNB2/PAX8/CXCR4/FZD5/GDPD3/TMEM204/NLRX1/ZMYM1/EPHX3/ZC3H14/ZNF606/RAB11/FIP1/RNF39/COL18A1/UNC93B1/CAPS/CO1Q/HIST1H2BM/SH3BGRL3/GSG1/SCR11/HIST1H3A/SLAZ/PTARD68/IL1F10/SPINK7/KDM2B/LOXL3/MGARP/CBX2/GAS7/FADD/LIMD1/THAP3/MAP7/ZFAND2A/LDB2/RCSDI/IL32/REPE6/SDR42E1/LR86/RAB3D/H2AFY/MTLS/ARHGFE10/ULK2/USP6N/TELO2/RABGAP1/TMCC2

APPENDIX B: ABSTRACTS PRESENTED/PUBLISHED

B1: The effect of androgen receptor expression in fibroblasts co-cultured with prostate cancer cells.

Oral presentation: The Australian Society for Medical Research South Australian Scientific Meeting, Adelaide, SA, June 4, 2014.

Helen Palethorpe¹, Damien Leach¹, Eleanor Need¹, Paul Drew^{1,2}, Eric Smith¹

¹*Discipline of Surgery, Basil Hetzel Institute for Translational Health Research, The University of Adelaide*

²*School of Nursing and Midwifery, Flinders University*

Background: The interaction between stromal and epithelial cells is important in the initiation and progression of prostate cancer. Normal prostate fibroblasts express the androgen receptor (AR), which is required for appropriate prostate development. A poor prognostic indicator in prostate cancer is the loss of AR expression in a subset of cancer associated fibroblasts (CAFs). The role of AR in CAFs, and the effect of its loss, is uncertain. This study compares the effect of AR expression in fibroblasts in direct or indirect co-cultures with prostate cancer cells.

Methods: The androgen independent prostate cancer cell line PC3 and the immortalised prostate myofibroblast lines PshTert (AR-negative) and PshTertAR (PshTert stably transduced with AR; AR-positive) were used. The fibroblasts were stably transduced with red fluorescent protein, the PC3 cells with green fluorescent protein. The cells were grown in direct (cells added together to the culture plate) or indirect (transwell) co-culture. The AR ligand DHT, the anti-androgen bicalutamide, or vehicle was added to the culture medium. Fluorescence images were captured to monitor changes in cell morphology and number during co-culture, and cells were counted after 6 days of co-culture.

Results: Compared to the AR-negative fibroblasts, AR-positive fibroblasts significantly reduced PC3 cell numbers in both direct and indirect co-culture. DHT attenuated this reduction, whilst bicalutamide blocked the effect of DHT. In direct co-culture PC3 cells induced progressive morphological changes, followed by clearance, of AR-negative fibroblasts. PC3 cells did not induce morphological changes or clearance of AR-positive fibroblasts. The effects on AR-negative fibroblasts were not observed in indirect co-cultures.

Conclusions: Prostate myofibroblasts expressing AR reduced the numbers of PC3 prostate

cancer cells, in both direct and indirect co-culture. DHT attenuated these effects. Direct but not indirect co-culture resulted in local loss of AR-negative but not AR-positive fibroblasts. These results suggest that both soluble mediators and direct cell-cell contact may play important roles in the development and progression of prostate cancer.

B2: Myofibroblast androgen receptor expression regulates direct and indirect interactions between myofibroblast and prostate cancer cells *in vitro*

Poster presentation: Florey Postgraduate Research Conference, Adelaide, SA, September 25, 2014.

Helen Palethorpe¹, Damien Leach¹, Eleanor Need¹, Paul Drew^{1,2}, Eric Smith¹

¹*Discipline of Surgery, Basil Hetzel Institute for Translational Health Research, The University of Adelaide*

²*School of Nursing and Midwifery, Flinders University*

Background and Aims: Expression of the androgen receptor (AR) in prostate fibroblasts is required for normal prostate development and progression of prostate cancer. Whilst loss of AR expression in activated fibroblasts, referred to as myofibroblasts, is a poor prognostic indicator in prostate cancer, the mechanisms behind this are poorly understood. In this study, we compared the effect of AR-positive and AR-negative prostate myofibroblasts on direct and indirect interactions with prostate cancer cells *in vitro*.

Methodology: The androgen-independent prostate cancer cell line, PC3, was transduced with a green fluorescent protein. A red fluorescent protein was used to differentiate immortalised prostate myofibroblast lines, PShTert-Ctrl (AR-negative) and PShTert-AR (PShTert stably transduced with AR; AR-positive), from PC3 cells. Myofibroblasts and PC3 cells were co-cultured either directly in a plate (direct) or in a transwell system, which precluded direct cell-cell contact (indirect). Phenol red-free medium was supplemented with hormone-stripped fetal bovine serum, and either the AR ligand 5 α -dihydrotestosterone (DHT) or vehicle, with or without the anti-androgen bicalutamide. Fluorescence images were captured to monitor changes in cell morphology and to determine cell numbers. Proliferation was determined using CellTrace Violet. Cell cycle was analysed using propidium iodide.

Results: PC3 cell morphology was altered following direct and indirect co-culture with myofibroblasts. AR-negative myofibroblasts induced PC3 cell enlargement and a dense accumulation of large perinuclear granules. In contrast, PC3 cells exposed to AR-positive myofibroblasts formed long cytoplasmic extensions with narrowing of the cell body, followed by a progressive decrease in cell size from days 3 to 6 of co-culture with cell fragmentation

and disintegration. In direct co-culture, PC3 cells formed cohesive aggregates, expanding in size over time, in the presence of AR-negative myofibroblasts, in contrast to single cells or discohesive clusters with AR-positive myofibroblasts.

AR-positive myofibroblasts significantly reduced PC3 cell numbers in both direct and indirect co-culture compared to the AR-negative myofibroblast ($P < 0.0001$). DHT mitigated this reduction ($P = 0.007$), and the effects of DHT were blocked by bicalutamide.

Proliferation and cell cycle analyses indicated that soluble factors from both myofibroblasts induced PC3 cell death, displacing PC3 cells out of the cell cycle into the sub-G1 region. A reduction in proliferation was observed ($P < 0.0001$), and death most notably enhanced, by soluble factors from the AR-positive myofibroblast. DHT had no effect on PC3 cells exposed to soluble factors from AR-negative myofibroblasts ($P > 0.5$), however slowed proliferation ($P = 0.0002$), reduced progression to sub-G1, and attenuated the death of PC3 cells exposed to myofibroblasts expressing AR.

Direct co-culture of PC3 cells progressively destroyed and cleared adjacent AR-negative myofibroblasts, with an inverse correlation between the number of PC3 cells seeded and the number of AR-negative myofibroblasts recovered ($P = 0.0002$). The absence of the effect in indirect co-culture suggests a requirement for direct cell-cell contact. Cell cycle analysis revealed an increase in the percentage of sub-G1 AR-negative myofibroblasts. PC3 cells had no obvious effect on AR-positive myofibroblasts.

Conclusions: Myofibroblast AR expression was a key determinant of PC3 cell behaviour.

Whilst both AR-negative and AR-positive myofibroblasts produced soluble factors that induced PC3 cell death, the magnitude of cell death was enhanced by myofibroblasts expressing AR. DHT reduced the inhibition of proliferation and level of cell death observed in the presence of soluble factors from AR-positive myofibroblasts. Additionally, we have first-time evidence that PC3 cells mediate the death of AR-negative myofibroblasts via direct cell-cell contact. Our findings suggest that both indirect and direct cell interactions may play important roles in the development and progression of prostate cancer.

B3: Fibroblast androgen receptor expression regulates fibroblast and prostate cancer cell interactions *in vitro*

Poster presentation: The Queen Elizabeth Hospital Research Day, The Basil Hetzel Institute for Translational Health Research, Adelaide, SA, October 17, 2014.

Helen Palethorpe^{*}, Damien Leach^{*}, Eleanor Need^{*}, Paul Drew^{*#}, Eric Smith^{*}

^{*}*Discipline of Surgery, Basil Hetzel Institute for Translational Health Research, The University of Adelaide*

[#]*School of Nursing and Midwifery, Flinders University*

Introduction: Androgen receptor (AR) expression in prostate fibroblasts is required for prostate carcinogenesis. Conversely, loss of fibroblast AR is a poor prognostic indicator in prostate cancer. We investigated the prostate cancer cell-fibroblast interaction in relation to fibroblast AR expression.

Research question and hypothesis: The AR status of prostatic fibroblasts differentially affects interactions with prostate cancer cells *in vitro*.

Research methods: The prostate cancer cell line, PC3, was transduced with a green fluorescent protein, differentiating from AR-negative and AR-positive fibroblasts transduced with a red-fluorescent protein. Fibroblasts and PC3 cells were co-cultured either directly, allowing cell contact, or indirectly. Medium was supplemented with the AR ligand 5 α -dihydrotestosterone (DHT) or vehicle. Fluorescence images were captured and cell counts performed.

Results: Morphological changes were induced in PC3 cells depending on fibroblast AR status. AR-positive, in contrast to AR-negative fibroblasts, significantly reduced PC3 numbers ($P < 0.0001$). DHT mitigated this reduction ($P = 0.007$). Direct co-culture of PC3 cells destroyed adjacent AR-negative fibroblasts, with an inverse correlation between PC3 seeding number and the number of AR-negative fibroblasts recovered ($P = 0.0002$). The effect was absent in indirect co-culture suggesting a requirement for direct cell contact.

Conclusions: Fibroblast AR expression modifies PC3 cell behaviour. Further research is required to determine the mechanisms involved.

B4: Expression of androgen receptor and the androgen receptor responsive gene FKBP5 in oesophageal adenocarcinoma

Poster presentation: 7th Australian Medical and Health Research Congress, Melbourne, Victoria, November 16-19, 2014.

Eric Smith¹, Helen Palethorpe¹, Andrew Ruszkiewicz², Damien Leach², Eleanor Need², Paul Drew^{1,3}.

¹*Discipline of Surgery, Basil Hetzel Institute for Translational Health Research, The University of Adelaide,* ²*Gastroenterology Research Laboratory, SA Pathology,* ³*School of Nursing and Midwifery, Flinders University.*

Introduction: Oesophageal adenocarcinoma (EAC) is a male dominant disease. The role of androgen signalling mediated by the androgen receptor (AR) is unknown in this cancer.

Aims: To determine the expression and clinical correlates of AR, and the AR-responsive gene FKBP5, in EAC.

Methods: Immunohistochemistry for AR and FKBP5 was performed on 77 cases of EAC. The EAC cell line OE33, which is AR negative, was stably transduced with AR (OE33-AR). The effect of androgen (dihydrotestosterone, DHT) on the expression of AR and FKBP5 was measured in OE33 and OE33-AR by Western blot and qRT-PCR.

Results: AR staining was observed in 75 of 77 cases of EAC (97%). Staining was both nuclear and cytoplasmic in 63 (82%) cases, nuclear only in seven (9%), and cytoplasmic only in five (6%). FKBP5 staining was observed in 49 cases (64%), and all of these also had nuclear localisation of AR. Of the 28 cases that did not express FKBP5, 21 had nuclear localisation of AR and 7 did not. There was a significant association between FKBP5 expression and AR nuclear localisation ($p=0.0005$). Clinicopathological data were available for 76 cases. Nuclear localisation of AR and FKBP5 expression was associated with decreased median survival (451 vs 2800 days). There were no significant differences in gender, T- or N-stage, grade, vascular or perineural-invasion between the FKBP5-negative and positive cases. AR and FKBP5 protein were not detectable in OE33. DHT induced a time-dependent increase in FKBP5 expression in OE33-AR, but not in the AR-negative untransduced OE33.

Conclusions: These data suggest that AR is expressed frequently in EAC, and that nuclear localisation of AR may be necessary, but not sufficient, for FKBP5 expression. Furthermore,

expression of the AR dependent gene FKBP5 is associated with decreased patient survival.

B5: Androgen receptor pathway as a prognostic indicator in esophageal adenocarcinoma

Poster presentation: Digestive Diseases Week, Washington, May 16-19, 2015.

Published: Gastroenterology, Volume 148, Issue 4, Supplement 1, April 2015, Page S-356

Eric Smith, Helen M. Palethorpe, Andrew Ruszkiewicz, Damien Leach, Eleanor Need, Paul Drew

Background: Esophageal adenocarcinoma (EAC) is a male dominant disease. The role of male sex steroid hormones (androgens) in the biology of EAC is unknown. Androgens activate the androgen receptor (AR), thereby altering the expression of AR-responsive genes, eg. FK506 binding protein 5 (FKBP5), cyclin B1 (CCNB1) and vascular endothelial growth factor A (VEGFA). The role of androgen signalling mediated by AR is unknown in this cancer.

Methods: Immunohistochemistry for AR and FKBP5 was performed on 77 cases of EAC. Expression of AR and FKBP5 in cell lines was determined by Western blot, and functional AR by transactivation assays. The AR-negative EAC cell line OE33 was stably transduced with AR (OE33-AR). Expression of FKBP5, CCNB1, VEGFA, E2F transcription factor 1 (E2F1) and cyclin D1 (CCND1) was measured by qRT-PCR in cell lines treated with 0 nM or 10 nM of the androgen dihydrotestosterone (DHT).

Results: AR staining was observed in 75 of 77 cases of EAC (97%). Staining was both nuclear and cytoplasmic in 63 (82%) cases, nuclear only in seven (9%), and cytoplasmic only in five (6%). FKBP5 staining was observed in 49 cases (64%), and all of these also had nuclear localisation of AR. Of the 28 cases that did not express FKBP5, 21 had nuclear localisation of AR and 7 did not. There was a significant association between FKBP5 expression and AR nuclear localisation ($p=0.0005$). Clinicopathological data were available for 76 cases. FKBP5 expression was associated with decreased median overall survival (451 vs 1338 days) and 5-year survival (32 vs 44%). By multivariable Cox Proportional Hazard Models analysis, FKBP5 expression (HR 3.043, 95% CI 1.417-6.531), T- and N-stage, but not patient age nor the presence of Barrett's esophagus were associated with decreased survival. Functional AR expression was not detected in the EAC cell lines OE33, OE19, JH-EsoAd1 or FLO-1. DHT induced a time-dependent increase in FKBP5 expression in OE33-AR, but not in the AR- negative EAC cell lines. DHT induced a dose-dependent inhibition of

cell proliferation of OE33-AR, but not OE33. This inhibition of cell proliferation was associated with an increased number of cells in the G0/G1 phase of the cell cycle, reduced expression of CCNB1 ($p < 0.0001$) and E2F1 ($p < 0.0001$), and increased expression of cyclin D1 ($p = 0.0006$). There was no significant difference in p16 expression. DHT inhibited cell migration of OE33-AR. Expression of VEGFA, a potent angiogenic factor which enhances metastasis, was increased 3-fold in response to DHT in OE33-AR ($p < 0.0001$), but not in OE33.

Conclusions: AR was expressed frequently in EAC, and expression of the AR-responsive gene FKBP5 was associated with decreased patient survival. These data suggest that androgen receptor mediated signalling may play a significant role in the biology of EAC, and have implications for new therapeutic interventions.

B6: Myofibroblast androgen receptor expression modifies direct and indirect interactions between myofibroblasts and prostate cancer cells *in vitro*

Oral presentation: The Australian Society for Medical Research South Australian Scientific Meeting, Adelaide, SA, June 3, 2015.

Helen Palethorpe¹, Damien Leach¹, Eleanor Need¹, Paul Drew^{1,2}, Eric Smith¹

¹*Discipline of Surgery, Basil Hetzel Institute for Translational Health Research, The University of Adelaide*

²*School of Nursing and Midwifery, Flinders University*

Background: Prostate fibroblasts express the androgen receptor (AR) in the normal prostate and during cancer development. Loss of AR expression in activated cancer-associated fibroblasts is a poor prognostic indicator in prostate cancer. Why this loss is associated with poor outcome is unknown. We therefore investigated the interactions between immortalised AR-positive (PShTert-AR) or AR-negative (PShTert-Ctrl) myofibroblasts, models of activated fibroblasts, and the prostate cancer cell line, PC3, in direct or indirect co-culture *in vitro*.

Methods: Myofibroblasts were transduced with a red fluorescent protein to differentiate them from the prostate cancer cell line, PC3, transduced with a green fluorescent protein. PC3 cells were either co-cultured with myofibroblasts together (direct co-culture), or separately in a transwell system (indirect co-culture), or were grown in conditioned culture medium (CCM) prepared from myofibroblast monocultures. Cultures were supplemented with the AR ligand, 5 α -dihydrotestosterone (DHT), or vehicle, with or without anti-androgen bicalutamide, to determine AR-mediated effects. Cell morphology and cell counts were assessed by fluorescence microscopy over six days. Proliferation was measured by CellTrace Violet and apoptosis determined by CellEvent caspase-3/7 green detection reagent.

Results: PShTert-AR myofibroblasts reduced PC3 cell counts following direct and indirect co-culture compared to PShTert-Ctrl myofibroblasts ($P < 0.0001$). DHT decreased PShTert-AR numbers in monoculture and co-culture and minimised the loss of PC3 cells with the PShTert-AR myofibroblast ($P < 0.0001$). PShTert-AR CCM slowed PC3 cell proliferation and caused PC3 cell loss, from days three to six of treatment, whilst PShTert-Ctrl CCM increased PC3 cell proliferation. Apoptosis was detected in 68% of PC3 cells within 96 hours of PShTert-AR CCM treatment compared to 11% with PShTert-Ctrl CCM. PShTert-Ctrl

myofibroblast counts were reduced by PC3 cells when in direct co-culture ($P = 0.006$), with morphological changes and apoptosis detected exclusively in PShTert-Ctrl myofibroblasts in contact with PC3 cells.

Conclusions: The outcome of the myofibroblast-PC3 cell interaction was dependent on myofibroblast AR expression. This is the first evidence that PC3 cells destroy PShTert-Ctrl myofibroblasts by direct contact and is consistent with the clinical observation of poorer prognosis with reduced stromal AR. Determining the underlying mechanisms may lead to novel treatments.

B7: Expression of androgen receptor and the androgen-responsive gene FKBP5 are independent prognostic indicators for oesophageal adenocarcinoma

Oral presentation (Eric Smith): South Australian Men's Health Research Symposium, Adelaide, SA, June 18, 2015.

Eric Smith^{1*#}, Helen M Palethorpe^{1#}, Andrew R Ruskiewicz², Suzanne Edwards³, Damien A Leach⁴, Tim J Underwood⁵, Eleanor F Need⁶, Paul A Drew^{1,7}.

1 Solid Cancer Regulation Group, The University of Adelaide, Discipline of Surgery, Basil Hetzel Institute for Translational Health Research, The Queen Elizabeth Hospital, 28 Woodville Rd, Woodville South, SA 5011, Australia.

2 Gastroenterology Research Laboratory, SA Pathology, Frome Road, Adelaide, SA 5000, Australia.

3 Data Management and Analysis Centre, The University of Adelaide, Royal Adelaide Hospital, North Terrace, Adelaide, SA 5005, Australia.

4 Cancer Biology Group, The University of Adelaide, Discipline of Surgery, Basil Hetzel Institute for Translational Health Research, The Queen Elizabeth Hospital, 28 Woodville Rd, Woodville South, SA 5011, Australia.

5 Cancer Sciences Unit, Somers Cancer Research Building, University of Southampton, Southampton General Hospital, Tremona Road, Southampton, SO16 6YD, UK.

6 Breast Biology and Cancer Unit, The University of Adelaide, Discipline of Surgery, Basil Hetzel Institute for Translational Health Research, The Queen Elizabeth Hospital, 28 Woodville Rd, Woodville South, SA 5011, Australia.

7 School of Nursing and Midwifery, Flinders University, PO Box 2100, Adelaide, SA 5001, Australia.

Background: Oesophageal adenocarcinoma (OAC) is a male dominant disease, but the role of androgens is unclear. This study examined the expression and clinical correlates of the androgen receptor (AR) and the androgen-responsive gene, FKBP5, in OAC.

Methods: Expression of AR and FKBP5 was determined by immunohistochemistry. The effect of the AR ligand 5 α -dihydrotestosterone (DHT) on the expression of a panel of androgen-responsive genes was measured in AR-positive and AR-negative OAC cell lines. Correlations in expression between androgen-responsive genes were analysed in an independent cohort of OAC tissues.

Results: There was AR staining in 75 of 77 cases (97%), and FKBP5 staining in 49 (64%), all of which had nuclear AR. Nuclear AR with FKBP5 expression was associated with decreased median survival (451 versus 2800 days), and was an independent prognostic indicator (HR 2.894, 95% CI 1.396 to 6.002, *P*-value = 0.0043) in multivariable Cox proportional hazards models. DHT induced a significant increase in expression of the androgen-responsive genes FKBP5, HMOX1, FBXO32, VEGFA, WNT5A and KLK3 only in AR-positive cells. Significant correlations in expression were observed between these androgen-responsive genes in an independent cohort of OAC tissues.

Conclusion: Nuclear AR and expression of FKBP5 is associated with decreased survival in OAC.

B8: Myofibroblast androgen receptor expression modifies direct and indirect interactions between myofibroblasts and prostate cancer cells *in vitro*

Poster presentation: South Australian Men's Health Research Symposium, Adelaide, SA, June 18, 2015.

Helen Palethorpe¹, Damien Leach¹, Eleanor Need¹, Paul Drew^{1,2}, Eric Smith¹

¹*Discipline of Surgery, Basil Hetzel Institute for Translational Health Research, The University of Adelaide*

²*School of Nursing and Midwifery, Flinders University*

Background: Prostate fibroblasts express the androgen receptor (AR) in the normal prostate and during cancer development. Loss of AR expression in activated cancer-associated fibroblasts is a poor prognostic indicator in prostate cancer. Why this loss is associated with poor outcome is unknown. We therefore investigated the interactions between immortalised AR-positive (PShTert-AR) or AR-negative (PShTert-Ctrl) myofibroblasts, models of activated fibroblasts, and the prostate cancer cell line, PC3, in direct or indirect co-culture *in vitro*.

Methods: Myofibroblasts were transduced with a red fluorescent protein to differentiate them from the prostate cancer cell line, PC3, transduced with a green fluorescent protein. PC3 cells were either co-cultured with myofibroblasts together (direct co-culture), or separately in a transwell system (indirect co-culture), or were grown in conditioned culture medium (CCM) prepared from myofibroblast monocultures. Cultures were supplemented with the AR ligand, 5 α -dihydrotestosterone (DHT), or vehicle, with or without anti-androgen bicalutamide, to determine AR-mediated effects. Cell morphology and cell counts were assessed by fluorescence microscopy over six days. Proliferation was measured by CellTrace Violet and apoptosis determined by CellEvent caspase-3/7 green detection reagent.

Results: PShTert-AR myofibroblasts reduced PC3 cell counts following direct and indirect co-culture compared to PShTert-Ctrl myofibroblasts ($P < 0.0001$). DHT decreased PShTert-AR numbers in monoculture and co-culture and minimised the loss of PC3 cells with the PShTert-AR myofibroblast ($P < 0.0001$). PShTert-AR CCM slowed PC3 cell proliferation and caused PC3 cell loss, from days three to six of treatment, whilst PShTert-Ctrl CCM increased PC3 cell proliferation. Apoptosis was detected in 68% of PC3 cells within 96 hours of PShTert-AR CCM treatment compared to 11% with PShTert-Ctrl CCM. PShTert-Ctrl

myofibroblast counts were reduced by PC3 cells when in direct co-culture ($P = 0.006$), with morphological changes and apoptosis detected exclusively in PShTert-Ctrl myofibroblasts in contact with PC3 cells.

Conclusions: The outcome of the myofibroblast-PC3 cell interaction was dependent on myofibroblast AR expression. This is the first evidence that PC3 cells destroy PShTert-Ctrl myofibroblasts by direct contact and is consistent with the clinical observation of poorer prognosis with reduced stromal AR. Determining the underlying mechanisms may lead to novel treatments.

B9: Myofibroblast androgen receptor expression modifies direct and indirect interactions between myofibroblasts and prostate cancer cells *in vitro*

Poster presentation: 2015 Florey Postgraduate Research Conference, Adelaide, SA, September 24, 2015.

Helen Palethorpe¹, Damien Leach¹, Eleanor Need¹, Paul Drew^{1,2}, Eric Smith¹

¹*Discipline of Surgery, Basil Hetzel Institute for Translational Health Research, The University of Adelaide*

²*School of Nursing and Midwifery, Flinders University*

Background: Prostate fibroblasts express the androgen receptor (AR) in the normal prostate and during cancer development. Loss of AR expression in activated cancer-associated fibroblasts is a poor prognostic indicator in prostate cancer. Why this loss is associated with poor outcome is unknown. We therefore investigated the interactions between immortalised AR-positive (PShTert-AR) or AR-negative (PShTert-Ctrl) myofibroblasts, models of activated fibroblasts, and the prostate cancer cell line, PC3, in direct or indirect co-culture *in vitro*.

Methods: Myofibroblasts were transduced with a red fluorescent protein to differentiate them from the prostate cancer cell line, PC3, transduced with a green fluorescent protein. PC3 cells were either co-cultured with myofibroblasts together (direct co-culture), or separately in a transwell system (indirect co-culture), or were grown in conditioned culture medium (CCM) prepared from myofibroblast monocultures. Cultures were supplemented with the AR ligand, 5 α -dihydrotestosterone (DHT), or vehicle, with or without anti-androgen bicalutamide, to determine AR-mediated effects. Cell morphology and cell counts were assessed by fluorescence microscopy over six days. Proliferation was measured by CellTrace Violet and apoptosis determined by CellEvent caspase-3/7 green detection reagent.

Results: PShTert-AR myofibroblasts reduced PC3 cell counts following direct and indirect co-culture compared to PShTert-Ctrl myofibroblasts ($P < 0.0001$). DHT decreased PShTert-AR numbers in monoculture and co-culture and minimised the loss of PC3 cells with the PShTert-AR myofibroblast ($P < 0.0001$). PShTert-AR CCM slowed PC3 cell proliferation and caused PC3 cell loss, from days three to six of treatment, whilst PShTert-Ctrl CCM increased PC3 cell proliferation. Apoptosis was detected in 68% of PC3 cells within 96 hours of PShTert-AR CCM treatment compared to 11% with PShTert-Ctrl CCM. PShTert-Ctrl

myofibroblast counts were reduced by PC3 cells when in direct co-culture ($P = 0.006$), with morphological changes and apoptosis detected exclusively in PShTert-Ctrl myofibroblasts in contact with PC3 cells.

Conclusions: The outcome of the myofibroblast-PC3 cell interaction was dependent on myofibroblast AR expression. This is the first evidence that PC3 cells destroy PShTert-Ctrl myofibroblasts by direct contact and is consistent with the clinical observation of poorer prognosis with reduced stromal AR. Determining the underlying mechanisms may lead to novel treatments.

B10: Developing an *in vitro* model to investigate the role of androgen signalling in oesophageal adenocarcinoma

Poster presentation: 2016 Florey Postgraduate Research Conference, Adelaide, SA, September 29, 2016.

Helen Palethorpe¹, Eric Smith^{1,2}, Paul Drew^{1,3}

¹*Adelaide Medical School, Faculty of Health Sciences, The University of Adelaide*

²*Department of Haematology and Oncology, The Queen Elizabeth Hospital*

³*School of Nursing and Midwifery, Flinders University*

Background: We have previously shown that nuclear localisation of the androgen receptor (AR) or expression of the androgen responsive gene FKBP5 were associated with decreased survival in oesophageal adenocarcinoma (OAC), suggesting a possible role for androgens in this cancer. Here we investigated the effect of androgen signalling on the behaviour *in vitro* of AR expressing OAC cell lines.

Methods: Three AR-negative OAC cell lines, OE33, JH-EsoAd1 and OE19, were stably transduced with AR and green fluorescent protein (GFP). The effect of the AR ligand 5 α -dihydrotestosterone (DHT) was determined by measuring proliferation by CellTrace Violet dilution, migration by scratch wound assay and the expression of androgen-responsive genes by quantitative real-time reverse-transcription PCR.

Results: At higher concentrations, including those typically used in androgen studies, DHT inhibited cell proliferation in all AR expressing cell lines with the IC₅₀ different for each. The lack of growth at higher DHT concentrations was accompanied by an increase in the percentage of cells in G₀/G₁, a reduction in cell division and an increase in senescence-associated beta-galactosidase (SA- β -gal) staining. The baseline expression and response to DHT of androgen-responsive genes varied between the cell lines, with FKBP5 the most responsive to androgen signalling. For OE33-AR-GFP there was an approximate 3-fold increase in FKBP5 expression at the IC₅₀ ($p = 0.049$), whilst at the higher concentration of DHT, at which proliferation was inhibited, the increase was 12-fold above baseline ($p = 0.0003$). DHT reduced migration for OE33-AR-GFP ($p \leq 0.006$) and JH-AR-GFP ($p \leq 0.0002$), and increased migration for OE19-AR-GFP ($p \leq 0.0004$).

Conclusion: These are the first studies to investigate the functional effect of androgen signalling in OAC cell lines. DHT concentration and cell line type were important determinants of androgen responsiveness and cell behaviour. This study provides a

foundation to investigate the molecular basis for the role of androgen signalling in the biology of this lethal cancer.

B11: The effect of fibroblasts on androgen signalling in oesophageal adenocarcinoma cell lines *in vitro*

Oral presentation: The Queen Elizabeth Hospital Research Day, The Basil Hetzel Institute for Translational Health Research, Adelaide, SA, October 21, 2016.

Helen Palethorpe^{*}, Eric Smith^{*,#}, Paul Drew^{1,**}

^{*}*Adelaide Medical School, Faculty of Health Sciences, The University of Adelaide*

[#]*Department of Haematology and Oncology, The Queen Elizabeth Hospital*

^{**}*School of Nursing and Midwifery, Flinders University*

Background: Nuclear localisation of androgen receptor (AR) and expression of androgen responsive gene FKBP5 in oesophageal adenocarcinoma (OAC) suggest AR is functional and are associated with decreased survival, yet AR expressing OAC cell lines failed to grow in monoculture with concentrations of androgen typically used *in vitro*. We therefore investigated whether fibroblasts could modify growth and androgen signalling in OAC.

Methods: The AR-negative OAC cell line, OE33 was stably transduced with AR and green fluorescent protein (GFP) then grown, with or without 10 nM of AR ligand 5 α -dihydrotestosterone (DHT), in monoculture or direct co-culture with different fibroblasts; neonatal foreskin (NFF), mammary (MF), nasal from chronic rhinosinusitis with nasal polyp (CRSwNP) and PShTert myofibroblasts from benign prostatic hyperplasia (PShTert). Cell growth was measured by cell counts, nuclear translocation by immunocytochemistry, and the expression of androgen-responsive genes by quantitative real-time reverse-transcription PCR.

Results: In monoculture, and direct co-culture with NFFs, MFs, or CRSwNP, DHT inhibited the growth of OE33-AR cells ($P < 0.0001$). AR translocated completely to the nucleus with downregulation of cyclin B1 (CCNB1) and upregulation of FKBP5. In contrast, PShTert myofibroblasts permitted growth. AR was localised to the cytoplasm and nucleus. FKBP5 was upregulated with no downregulation of CCNB1, suggesting either differential regulation of androgen signalling by PShTert or the ability of PShTert to override the typical effect of CCNB1 following its response to androgen.

Conclusion: This is the first study to investigate whether fibroblasts alter the response of an OAC cell line to androgen. The PShTert myofibroblast produced a differential response to androgen in OE33-AR cells with results consistent with clinical findings. This suggests certain fibroblasts can modify response to androgen in OAC.

APPENDIX C: PRESENTATIONS & AWARDS

Conference & community presentations

- The Australian Society for Medical Research South Australian Scientific Meeting, Adelaide, SA, June 4, 2014. The effect of androgen receptor expression in fibroblasts co-cultured with prostate cancer cells, **Helen Palethorpe**, Damien Leach, Eleanor Need, Paul Drew, Eric Smith. ORAL PRESENTATION.
- Florey Postgraduate Research Conference, Adelaide, SA, September 25, 2014. Myofibroblast androgen receptor expression regulates direct and indirect interactions between myofibroblast and prostate cancer cells *in vitro*, **Helen Palethorpe**, Damien Leach, Eleanor Need, Paul Drew, Eric Smith. POSTER PRESENTATION.
- The Queen Elizabeth Hospital Research Day, Adelaide, SA, October 17, 2014. Fibroblast androgen receptor expression regulates fibroblast and prostate cancer cell interactions *in vitro*, **Helen Palethorpe**, Damien Leach, Eleanor Need, Paul Drew, Eric Smith. POSTER PRESENTATION.
- The Australian Society for Medical Research South Australian Scientific Meeting, Adelaide, SA, June 3, 2015. Myofibroblast androgen receptor expression modifies direct and indirect interactions between myofibroblasts and prostate cancer cells *in vitro*, **Helen Palethorpe**, Damien Leach, Eleanor Need, Paul Drew, Eric Smith. ORAL PRESENTATION.
- South Australian Men's Health Research Symposium, Adelaide, SA, June 18, 2015. Myofibroblast androgen receptor expression modifies direct and indirect interactions between myofibroblasts and prostate cancer cells *in vitro*, **Helen Palethorpe**, Damien Leach, Eleanor Need, Paul Drew, Eric Smith. POSTER PRESENTATION.
- 2015 Florey Postgraduate Research Conference, Adelaide, SA, September 24, 2015. Myofibroblast androgen receptor expression modifies direct and indirect interactions between myofibroblasts and prostate cancer cells *in vitro*, **Helen Palethorpe**, Damien Leach, Eleanor Need, Paul Drew, Eric Smith. POSTER PRESENTATION.
- University of the Third Age Flinders Incorporated community presentation, Active Elder Association Hall, Ascot Park, Adelaide, SA, September 1, 2016. Prostate Cancer: It's more than the cancer cell, **Helen Palethorpe**. ORAL PRESENTATION.
- 2016 Florey Postgraduate Research Conference, Adelaide, SA, September 29, 2016. Developing an *in vitro* model to investigate the role of androgen signalling in oesophageal adenocarcinoma, **Helen Palethorpe**, Eric Smith, Paul Drew. POSTER PRESENTATION.
- The Queen Elizabeth Hospital Research Day, Adelaide, SA, October 21, 2016. The

effect of fibroblasts on androgen signalling in oesophageal adenocarcinoma cell lines *in vitro*, **Helen Palethorpe**, Eric Smith, Paul Drew. ORAL PRESENTATION.

Awards

- Shortlisted for the Adelaide Research and Innovation Pty Ltd (ARI) Prize for the project with the most commercial potential, 2014 Florey Postgraduate Research Conference, Adelaide, SA, September 25, 2014.
- Poster presentation award, The Queen Elizabeth Hospital Research Day, Adelaide, SA, October 17, 2014.
- Poster presentation award, South Australian Men's Health Research Symposium, Adelaide, SA, June 18, 2015.

REFERENCES

- Adany, R, Heimer, R, Caterson, B, Sorrell, JM & Iozzo, RV 1990, 'Altered expression of chondroitin sulfate proteoglycan in the stroma of human colon carcinoma. Hypomethylation of PG-40 gene correlates with increased PG-40 content and mRNA levels', *J Biol Chem*, 265, 11389-96.
- Adany, R & Iozzo, RV 1990, 'Altered methylation of versican proteoglycan gene in human colon carcinoma', *Biochem Biophys Res Commun*, 171, 1402-13.
- Adany, R & Iozzo, RV 1991, 'Hypomethylation of the decorin proteoglycan gene in human colon cancer', *Biochem J*, 276 (Pt 2), 301-6.
- Akgun, H, Lechago, J & Younes, M 2002, 'Estrogen receptor-beta is expressed in Barrett's metaplasia and associated adenocarcinoma of the esophagus', *Anticancer Res*, 22, 1459-61.
- Albregues, J, Bertero, T, Grasset, E, Bonan, S, Maiel, M, Bourget, I, Philippe, C, Herraiz Serrano, C, Benamar, S, Croce, O, Sanz-Moreno, V, Meneguzzi, G, Feral, CC, Cristofari, G & Gaggioli, C 2015, 'Epigenetic switch drives the conversion of fibroblasts into proinvasive cancer-associated fibroblasts', *Nat Commun*, 6, 10204.
- Allen, M & Louise Jones, J 2011, 'Jekyll and Hyde: the role of the microenvironment on the progression of cancer', *J Pathol*, 223, 162-76.
- Amos-Landgraf, JM, Heijmans, J, Wielenga, MC, Dunkin, E, Krentz, KJ, Clipson, L, Ederveen, AG, Groothuis, PG, Mosselman, S, Muncan, V, Hommes, DW, Shedlovsky, A, Dove, WF & Van Den Brink, GR 2014, 'Sex disparity in colonic adenomagenesis involves promotion by male hormones, not protection by female hormones', *Proc Natl Acad Sci U S A*, 111, 16514-9.
- Anderson, LA, Watson, RG, Murphy, SJ, Johnston, BT, Comber, H, Mc Guigan, J, Reynolds, JV & Murray, LJ 2007, 'Risk factors for Barrett's oesophagus and oesophageal adenocarcinoma: results from the FINBAR study', *World J Gastroenterol*, 13, 1585-94.
- Andersson, M, Storm, HH & Mouridsen, HT 1991, 'Incidence of new primary cancers after adjuvant tamoxifen therapy and radiotherapy for early breast cancer', *J Natl Cancer Inst*, 83, 1013-7.
- Awan, AK, Iftikhar, SY, Morris, TM, Clarke, PA, Grabowska, AM, Waraich, N & Watson, SA 2007, 'Androgen receptors may act in a paracrine manner to regulate oesophageal adenocarcinoma growth', *Eur J Surg Oncol*, 33, 561-8.
- Bacac, M, Provero, P, Mayran, N, Stehle, JC, Fusco, C & Stamenkovic, I 2006, 'A mouse stromal response to tumor invasion predicts prostate and breast cancer patient

- survival', *PLoS One*, 1, e32.
- Balkwill, FR, Capasso, M & Hagemann, T 2012, 'The tumor microenvironment at a glance', *J Cell Sci*, 125, 5591-6.
- Bennett, NC, Gardiner, RA, Hooper, JD, Johnson, DW & Gobe, GC 2010, 'Molecular cell biology of androgen receptor signalling', *Int J Biochem Cell Biol*, 42, 813-27.
- Bergamaschi, A, Tagliabue, E, Sorlie, T, Naume, B, Triulzi, T, Orlandi, R, Russnes, HG, Nesland, JM, Tammi, R, Auvinen, P, Kosma, VM, Menard, S & Borresen-Dale, AL 2008, 'Extracellular matrix signature identifies breast cancer subgroups with different clinical outcome', *J Pathol*, 214, 357-67.
- Blanchere, M, Berthaut, I, Portois, MC, Mestayer, C & Mowszowicz, I 1998, 'Hormonal regulation of the androgen receptor expression in human prostatic cells in culture', *J Steroid Biochem Mol Biol*, 66, 319-26.
- Bodelon, C, Anderson, GL, Rossing, MA, Chlebowski, RT, Ochs-Balcom, HM & Vaughan, TL 2011, 'Hormonal factors and risks of esophageal squamous cell carcinoma and adenocarcinoma in postmenopausal women', *Cancer Prev Res (Phila)*, 4, 840-50.
- Bonnans, C, Chou, J & Werb, Z 2014, 'Remodelling the extracellular matrix in development and disease', *Nat Rev Mol Cell Biol*, 15, 786-801.
- Calon, A, Espinet, E, Palomo-Ponce, S, Tauriello, DV, Iglesias, M, Cespedes, MV, Sevillano, M, Nadal, C, Jung, P, Zhang, XH, Byrom, D, Riera, A, Rossell, D, Mangués, R, Massague, J, Sancho, E & Batlle, E 2012, 'Dependency of colorectal cancer on a TGF-beta-driven program in stromal cells for metastasis initiation', *Cancer Cell*, 22, 571-84.
- Camp, JT, Elloumi, F, Roman-Perez, E, Rein, J, Stewart, DA, Harrell, JC, Perou, CM & Troester, MA 2011, 'Interactions with fibroblasts are distinct in Basal-like and luminal breast cancers', *Mol Cancer Res*, 9, 3-13.
- Cano, P, Godoy, A, Escamilla, R, Dhir, R & Onate, SA 2007, 'Stromal-epithelial cell interactions and androgen receptor-coregulator recruitment is altered in the tissue microenvironment of prostate cancer', *Cancer Res*, 67, 511-9.
- Castoria, G, Lombardi, M, Barone, MV, Bilancio, A, Di Domenico, M, Bottero, D, Vitale, F, Migliaccio, A & Auricchio, F 2003, 'Androgen-stimulated DNA synthesis and cytoskeletal changes in fibroblasts by a nontranscriptional receptor action', *J Cell Biol*, 161, 547-56.
- Chai, J & Jamal, MM 2012, 'Esophageal malignancy: a growing concern', *World J Gastroenterol*, 18, 6521-6.
- Chandanos, E & Lagergren, J 2009, 'The mystery of male dominance in oesophageal cancer

- and the potential protective role of oestrogen', *Eur J Cancer*, 45, 3149-55.
- Chandanos, E, Lindblad, M, Jia, C, Rubio, CA, Ye, W & Lagergren, J 2006, 'Tamoxifen exposure and risk of oesophageal and gastric adenocarcinoma: a population-based cohort study of breast cancer patients in Sweden', *Br J Cancer*, 95, 118-22.
- Chang, C, Lee, SO, Yeh, S & Chang, TM 2013, 'Androgen receptor (AR) differential roles in hormone-related tumors including prostate, bladder, kidney, lung, breast and liver', *Oncogene*.
- Chang, C, Lee, SO, Yeh, S & Chang, TM 2014, 'Androgen receptor (AR) differential roles in hormone-related tumors including prostate, bladder, kidney, lung, breast and liver', *Oncogene*, 33, 3225-34.
- Chen, F, Zhuang, X, Lin, L, Yu, P, Wang, Y, Shi, Y, Hu, G & Sun, Y 2015, 'New horizons in tumor microenvironment biology: challenges and opportunities', *BMC Med*, 13, 45.
- Chen, Q, Zhuang, H & Liu, Y 2012, 'The association between obesity factor and esophageal cancer', *J Gastrointest Oncol*, 3, 226-31.
- Choe, C, Shin, YS, Kim, SH, Jeon, MJ, Choi, SJ, Lee, J & Kim, J 2013, 'Tumor-stromal interactions with direct cell contacts enhance motility of non-small cell lung cancer cells through the hedgehog signaling pathway', *Anticancer Res*, 33, 3715-23.
- Compagno, D, Merle, C, Morin, A, Gilbert, C, Mathieu, JR, Bozec, A, Mauduit, C, Benahmed, M & Cabon, F 2007, 'siRNA-directed in vivo silencing of androgen receptor inhibits the growth of castration-resistant prostate carcinomas', *PLoS One*, 2, e1006.
- Cook, MB, Wood, SN, Cash, BD, Young, P, Acosta, RD, Falk, RT, Pfeiffer, RM, Hu, N, Su, H, Wang, L, Wang, C, Gherman, B, Giffen, C, Dykes, C, Turcotte, V, Caron, P, Guillemette, C, Dawsey, SM, Abnet, CC, Hyland, PL & Taylor, PR 2015a, 'Association between circulating levels of sex steroid hormones and Barrett's esophagus in men: a case-control analysis', *Clin Gastroenterol Hepatol*, 13, 673-82.
- Cook, MB, Wood, SN, Cash, BD, Young, P, Acosta, RD, Falk, RT, Pfeiffer, RM, Hu, N, Su, H, Wang, L, Wang, C, Gherman, B, Giffen, C, Dykes, C, Turcotte, V, Caron, P, Guillemette, C, Dawsey, SM, Abnet, CC, Hyland, PL & Taylor, PR 2015b, 'Association Between Circulating Levels of Sex Steroid Hormones and Barrett's Esophagus in Men: A Case-Control Analysis', *Clinical Gastroenterology and Hepatology*, 13, 673-682.
- Cooper, SC, Croft, S, Day, R, Thomson, CS & Trudgill, NJ 2009, 'Patients with prostate cancer are less likely to develop oesophageal adenocarcinoma: could androgens have a role in the aetiology of oesophageal adenocarcinoma?', *Cancer Causes Control*, 20,

1363-8.

- Cooper, SC & Trudgill, NJ 2012, 'Subjects with prostate cancer are less likely to develop esophageal cancer: analysis of SEER 9 registries database', *Cancer Causes Control*, 23, 819-25.
- Corley, DA, Kubo, A & Zhao, W 2008, 'Abdominal obesity and the risk of esophageal and gastric cardia carcinomas', *Cancer Epidemiol Biomarkers Prev*, 17, 352-8.
- Cox, TR & Ertel, JT 2011, 'Remodeling and homeostasis of the extracellular matrix: implications for fibrotic diseases and cancer', *Dis Model Mech*, 4, 165-78.
- Culig, Z, Hobisch, A, Cronauer, MV, Radmayr, C, Trapman, J, Hittmair, A, Bartsch, G & Klocker, H 1994, 'Androgen receptor activation in prostatic tumor cell lines by insulin-like growth factor-I, keratinocyte growth factor, and epidermal growth factor', *Cancer Res*, 54, 5474-8.
- Cunha, GR 1994, 'Role of mesenchymal-epithelial interactions in normal and abnormal development of the mammary gland and prostate', *Cancer*, 74, 1030-44.
- Cunha, GR, Hayward, SW, Wang, YZ & Ricke, WA 2003, 'Role of the stromal microenvironment in carcinogenesis of the prostate', *Int J Cancer*, 107, 1-10.
- Cunha, GR, Ricke, W, Thomson, A, Marker, PC, Risbridger, G, Hayward, SW, Wang, YZ, Donjacour, AA & Kurita, T 2004, 'Hormonal, cellular, and molecular regulation of normal and neoplastic prostatic development', *J Steroid Biochem Mol Biol*, 92, 221-36.
- Curtis, RE, Boice, JD, Jr., Shriner, DA, Hankey, BF & Fraumeni, JF, Jr. 1996, 'Second cancers after adjuvant tamoxifen therapy for breast cancer', *J Natl Cancer Inst*, 88, 832-4.
- Davey, RA & Grossmann, M 2016, 'Androgen Receptor Structure, Function and Biology: From Bench to Bedside', *Clin Biochem Rev*, 37, 3-15.
- Dawson, MA & Kouzarides, T 2012, 'Cancer epigenetics: from mechanism to therapy', *Cell*, 150, 12-27.
- De Wever, O, Van Bockstal, M, Mareel, M, Hendrix, A & Bracke, M 2014, 'Carcinoma-associated fibroblasts provide operational flexibility in metastasis', *Seminars in Cancer Biology*, 25, 33-46.
- Derakhshan, MH, Liptrot, S, Paul, J, Brown, IL, Morrison, D & Mccoll, KE 2009, 'Oesophageal and gastric intestinal-type adenocarcinomas show the same male predominance due to a 17 year delayed development in females', *Gut*, 58, 16-23.
- Dimairo, MA, Kwok, S, Montgomery, KD, Lowe, AW & Pai, RK 2012, 'Immunohistochemical panel for distinguishing esophageal adenocarcinoma from

- squamous cell carcinoma: a combination of p63, cytokeratin 5/6, MUC5AC, and anterior gradient homolog 2 allows optimal subtyping', *Hum Pathol*, 43, 1799-807.
- Domper Arnal, MJ, Ferrandez Arenas, A & Lanas Arbeloa, A 2015, 'Esophageal cancer: Risk factors, screening and endoscopic treatment in Western and Eastern countries', *World J Gastroenterol*, 21, 7933-43.
- Dumont, N, Liu, B, Defilippis, RA, Chang, H, Rabban, JT, Karnezis, AN, Tjoe, JA, Marx, J, Parvin, B & Tlsty, TD 2013, 'Breast fibroblasts modulate early dissemination, tumorigenesis, and metastasis through alteration of extracellular matrix characteristics', *Neoplasia*, 15, 249-62.
- Eder, IE, Culig, Z, Ramoner, R, Thurnher, M, Putz, T, Nessler-Menardi, C, Tiefenthaler, M, Bartsch, G & Klocker, H 2000, 'Inhibition of Lncap prostate cancer cells by means of androgen receptor antisense oligonucleotides', *Cancer Gene Ther*, 7, 997-1007.
- Eder, T, Weber, A, Neuwirt, H, Grunbacher, G, Ploner, C, Klocker, H, Sampson, N & Eder, IE 2016, 'Cancer-Associated Fibroblasts Modify the Response of Prostate Cancer Cells to Androgen and Anti-Androgens in Three-Dimensional Spheroid Culture', *Int J Mol Sci*, 17.
- Edgren, G, Adami, HO, Weiderpass, E & Nyren, O 2013, 'A global assessment of the oesophageal adenocarcinoma epidemic', *Gut*, 62, 1406-14.
- Egeblad, M, Nakasone, ES & Werb, Z 2010, 'Tumors as organs: complex tissues that interface with the entire organism', *Dev Cell*, 18, 884-901.
- Erler, JT & Giaccia, AJ 2006, 'Lysyl oxidase mediates hypoxic control of metastasis', *Cancer Res*, 66, 10238-41.
- Fang, H & Declerck, YA 2013, 'Targeting the tumor microenvironment: from understanding pathways to effective clinical trials', *Cancer Res*, 73, 4965-77.
- Flavell, SJ, Hou, TZ, Lax, S, Filer, AD, Salmon, M & Buckley, CD 2008, 'Fibroblasts as novel therapeutic targets in chronic inflammation', *Br J Pharmacol*, 153 Suppl 1, S241-6.
- Franco, OE, Shaw, AK, Strand, DW & Hayward, SW 2010, 'Cancer associated fibroblasts in cancer pathogenesis', *Semin Cell Dev Biol*, 21, 33-9.
- Frantz, C, Stewart, KM & Weaver, VM 2010, 'The extracellular matrix at a glance', *J Cell Sci*, 123, 4195-200.
- Gaggioli, C, Hooper, S, Hidalgo-Carcedo, C, Grosse, R, Marshall, JF, Harrington, K & Sahai, E 2007, 'Fibroblast-led collective invasion of carcinoma cells with differing roles for RhoGTPases in leading and following cells', *Nat Cell Biol*, 9, 1392-400.
- Gao, W, Bohl, CE & Dalton, JT 2005, 'Chemistry and structural biology of androgen

- receptor', *Chem Rev*, 105, 3352-70.
- Garcia-Arenas, R, Lin, FF, Lin, D, Jin, LP, Shih, CC, Chang, C & Lin, MF 1995, 'The expression of prostatic acid phosphatase is transcriptionally regulated in human prostate carcinoma cells', *Mol Cell Endocrinol*, 111, 29-37.
- Gascard, P & Tlsty, TD 2016, 'Carcinoma-associated fibroblasts: orchestrating the composition of malignancy', *Genes Dev*, 30, 1002-19.
- Giannoni, E, Bianchini, F, Calorini, L & Chiarugi, P 2011, 'Cancer associated fibroblasts exploit reactive oxygen species through a proinflammatory signature leading to epithelial mesenchymal transition and stemness', *Antioxid Redox Signal*, 14, 2361-71.
- Gingrich, JR, Barrios, RJ, Kattan, MW, Nahm, HS, Finegold, MJ & Greenberg, NM 1997, 'Androgen-independent prostate cancer progression in the TRAMP model', *Cancer Res*, 57, 4687-91.
- Goetz, JG, Minguet, S, Navarro-Lerida, I, Lazcano, JJ, Samaniego, R, Calvo, E, Tello, M, Osteso-Ibanez, T, Pellinen, T, Echarri, A, Cerezo, A, Klein-Szanto, AJ, Garcia, R, Keely, PJ, Sanchez-Mateos, P, Cukierman, E & Del Pozo, MA 2011, 'Biomechanical remodeling of the microenvironment by stromal caveolin-1 favors tumor invasion and metastasis', *Cell*, 146, 148-63.
- Gonda, TA, Varro, A, Wang, TC & Tycko, B 2010, 'Molecular biology of cancer-associated fibroblasts: can these cells be targeted in anti-cancer therapy?', *Semin Cell Dev Biol*, 21, 2-10.
- Green, J, Czanner, G, Reeves, G, Watson, J, Wise, L, Roddam, A & Beral, V 2012a, 'Menopausal hormone therapy and risk of gastrointestinal cancer: nested case-control study within a prospective cohort, and meta-analysis', *Int J Cancer*, 130, 2387-96.
- Green, J, Roddam, A, Pirie, K, Kirichek, O, Reeves, G, Beral, V & Million Women Study, C 2012b, 'Reproductive factors and risk of oesophageal and gastric cancer in the Million Women Study cohort', *Br J Cancer*, 106, 210-6.
- Gregson, EM, Bornschein, J & Fitzgerald, RC 2016, 'Genetic progression of Barrett's oesophagus to oesophageal adenocarcinoma', *Br J Cancer*, 115, 403-10.
- Grimm, M, Lazariotou, M, Kircher, S, Stuermer, L, Reiber, C, Hofelmayr, A, Gattenlohner, S, Otto, C, Germer, CT & Von Rahden, BH 2010, 'MMP-1 is a (pre-)invasive factor in Barrett-associated esophageal adenocarcinomas and is associated with positive lymph node status', *J Transl Med*, 8, 99.
- Gu, ZD, Li, JY, Li, M, Gu, J, Shi, XT, Ke, Y & Chen, KN 2005, 'Matrix metalloproteinases expression correlates with survival in patients with esophageal squamous cell carcinoma', *Am J Gastroenterol*, 100, 1835-43.

- Han, G, Buchanan, G, Ittmann, M, Harris, JM, Yu, X, Demayo, FJ, Tilley, W & Greenberg, NM 2005, 'Mutation of the androgen receptor causes oncogenic transformation of the prostate', *Proc Natl Acad Sci U S A*, 102, 1151-6.
- Hanson, JA, Gillespie, JW, Grover, A, Tangrea, MA, Chuaqui, RF, Emmert-Buck, MR, Tangrea, JA, Libutti, SK, Linehan, WM & Woodson, KG 2006, 'Gene promoter methylation in prostate tumor-associated stromal cells', *J Natl Cancer Inst*, 98, 255-61.
- Hayden, AL, Derouet, MF, Noble, F, Primrose, JN, Blaydes, JP, Thomas, G & Underwood, TJ 2012, 'OC-121 Fibroblast activation in the tumour microenvironment promotes tumour cell invasion and resistance to chemotherapy in oesophageal adenocarcinoma', *Gut*, 61, 52-53.
- Hayward, SW, Rosen, MA & Cunha, GR 1997, 'Stromal-epithelial interactions in the normal and neoplastic prostate', *Br J Urol*, 79 Suppl 2, 18-26.
- Heisler, LE, Evangelou, A, Lew, AM, Trachtenberg, J, Elsholtz, HP & Brown, TJ 1997, 'Androgen-dependent cell cycle arrest and apoptotic death in PC-3 prostatic cell cultures expressing a full-length human androgen receptor', *Mol Cell Endocrinol*, 126, 59-73.
- Henry, LR, Lee, HO, Lee, JS, Klein-Szanto, A, Watts, P, Ross, EA, Chen, WT & Cheng, JD 2007, 'Clinical implications of fibroblast activation protein in patients with colon cancer', *Clin Cancer Res*, 13, 1736-41.
- Henshall, SM, Quinn, DI, Lee, CS, Head, DR, Golovsky, D, Brenner, PC, Delprado, W, Stricker, PD, Grygiel, JJ & Sutherland, RL 2001, 'Altered expression of androgen receptor in the malignant epithelium and adjacent stroma is associated with early relapse in prostate cancer', *Cancer Res*, 61, 423-7.
- Horstman, AM, Dillon, EL, Urban, RJ & Sheffield-Moore, M 2012, 'The role of androgens and estrogens on healthy aging and longevity', *J Gerontol A Biol Sci Med Sci*, 67, 1140-52.
- Hsu, JW, Hsu, I, Xu, D, Miyamoto, H, Liang, L, Wu, XR, Shyr, CR & Chang, C 2013, 'Decreased tumorigenesis and mortality from bladder cancer in mice lacking urothelial androgen receptor', *Am J Pathol*, 182, 1811-20.
- Hu, M, Yao, J, Cai, L, Bachman, KE, Van Den Brule, F, Velculescu, V & Polyak, K 2005, 'Distinct epigenetic changes in the stromal cells of breast cancers', *Nat Genet*, 37, 899-905.
- Hubmacher, D & Apte, SS 2013, 'The biology of the extracellular matrix: novel insights', *Curr Opin Rheumatol*, 25, 65-70.

- Hur, C, Miller, M, Kong, CY, Dowling, EC, Nattinger, KJ, Dunn, M & Feuer, EJ 2013, 'Trends in esophageal adenocarcinoma incidence and mortality', *Cancer*, 119, 1149-58.
- Iacopino, F, Angelucci, C & Sica, G 2012, 'Interactions between normal human fibroblasts and human prostate cancer cells in a co-culture system', *Anticancer Res*, 32, 1579-88.
- Jiang, L, Gonda, TA, Gamble, MV, Salas, M, Seshan, V, Tu, S, Twaddell, WS, Hegyi, P, Lazar, G, Steele, I, Varro, A, Wang, TC & Tycko, B 2008, 'Global hypomethylation of genomic DNA in cancer-associated myofibroblasts', *Cancer Res*, 68, 9900-8.
- Jones, PA & Takai, D 2001, 'The role of DNA methylation in mammalian epigenetics', *Science*, 293, 1068-70.
- Jordana, M, Särnstrand, B, Sime, PJ & Ramis, I 1994, 'Immune-inflammatory functions of fibroblasts', *European Respiratory Journal*, 7, 2212-2222.
- Takehi, Y, Hirao, Y, Kim, WJ, Ozono, S, Masumori, N, Miyanaga, N, Nasu, Y & Yokomizo, A 2010, 'Bladder Cancer Working Group report', *Jpn J Clin Oncol*, 40 Suppl 1, i57-64.
- Kalayarasan, R, Ananthakrishnan, N, Kate, V & Basu, D 2008, 'Estrogen and progesterone receptors in esophageal carcinoma', *Dis Esophagus*, 21, 298-303.
- Kalluri, R 2016, 'The biology and function of fibroblasts in cancer', *Nat Rev Cancer*, 16, 582-98.
- Karnoub, AE, Dash, AB, Vo, AP, Sullivan, A, Brooks, MW, Bell, GW, Richardson, AL, Polyak, K, Tubo, R & Weinberg, RA 2007, 'Mesenchymal stem cells within tumour stroma promote breast cancer metastasis', *Nature*, 449, 557-63.
- Kendall, BJ, Macdonald, GA, Hayward, NK, Prins, JB, O'brien, S, Whiteman, DC & Study of Digestive, H 2013, 'The risk of Barrett's esophagus associated with abdominal obesity in males and females', *Int J Cancer*, 132, 2192-9.
- Kim, CJ, Sakamoto, K, Tambe, Y & Inoue, H 2011, 'Opposite regulation of epithelial-to-mesenchymal transition and cell invasiveness by periostin between prostate and bladder cancer cells', *Int J Oncol*, 38, 1759-66.
- Kim, SM, Park, YY, Park, ES, Cho, JY, Izzo, JG, Zhang, D, Kim, SB, Lee, JH, Bhutani, MS, Swisher, SG, Wu, X, Coombes, KR, Maru, D, Wang, KK, Buttar, NS, Ajani, JA & Lee, JS 2010, 'Prognostic biomarkers for esophageal adenocarcinoma identified by analysis of tumor transcriptome', *PLoS One*, 5, e15074.
- Kinugasa, Y, Matsui, T & Takakura, N 2014, 'CD44 expressed on cancer-associated fibroblasts is a functional molecule supporting the stemness and drug resistance of malignant cancer cells in the tumor microenvironment', *Stem Cells*, 32, 145-56.

- Klemm, F & Joyce, JA 2015, 'Microenvironmental regulation of therapeutic response in cancer', *Trends Cell Biol*, 25, 198-213.
- Kobayashi, K 1985, '[Effect of sex hormone on the experimental induction of esophageal cancer]', *Nihon Geka Gakkai Zasshi*, 86, 280-9.
- Kokontis, JM, Hay, N & Liao, S 1998, 'Progression of LNCaP prostate tumor cells during androgen deprivation: hormone-independent growth, repression of proliferation by androgen, and role for p27Kip1 in androgen-induced cell cycle arrest', *Mol Endocrinol*, 12, 941-53.
- Krtolica, A, Parrinello, S, Lockett, S, Desprez, PY & Campisi, J 2001, 'Senescent fibroblasts promote epithelial cell growth and tumorigenesis: a link between cancer and aging', *Proc Natl Acad Sci U S A*, 98, 12072-7.
- Lagergren, J 2011, 'Influence of obesity on the risk of esophageal disorders', *Nat Rev Gastroenterol Hepatol*, 8, 340-7.
- Lagergren, J, Bergstrom, R, Lindgren, A & Nyren, O 1999, 'Symptomatic gastroesophageal reflux as a risk factor for esophageal adenocarcinoma', *N Engl J Med*, 340, 825-31.
- Lagergren, J & Jansson, C 2005, 'Sex hormones and oesophageal adenocarcinoma: influence of childbearing?', *Br J Cancer*, 93, 859-61.
- Lagergren, J & Lagergren, P 2013, 'Recent developments in esophageal adenocarcinoma', *CA Cancer J Clin*, 63, 232-48.
- Lagergren, J & Nyren, O 1998, 'Do sex hormones play a role in the etiology of esophageal adenocarcinoma? A new hypothesis tested in a population-based cohort of prostate cancer patients', *Cancer Epidemiol Biomarkers Prev*, 7, 913-5.
- Lagergren, K, Lagergren, J & Brusselaers, N 2014, 'Hormone replacement therapy and oral contraceptives and risk of oesophageal adenocarcinoma: a systematic review and meta-analysis', *Int J Cancer*, 135, 2183-90.
- Lai, KP, Yamashita, S, Huang, CK, Yeh, S & Chang, C 2012, 'Loss of stromal androgen receptor leads to suppressed prostate tumourigenesis via modulation of pro-inflammatory cytokines/chemokines', *EMBO Mol Med*, 4, 791-807.
- Leach, DA & Buchanan, G 2017, 'Stromal Androgen Receptor in Prostate Cancer Development and Progression', *Cancers (Basel)*, 9.
- Leach, DA, Need, EF, Toivanen, R, Trotta, AP, Palenthorpe, HM, Tamblyn, DJ, Kopsaftis, T, England, GM, Smith, E, Drew, PA, Pinnock, CB, Lee, P, Holst, J, Risbridger, GP, Chopra, S, Defranco, DB, Taylor, RA & Buchanan, G 2015, 'Stromal androgen receptor regulates the composition of the microenvironment to influence prostate cancer outcome', *Oncotarget*, 6, 16135-50.

- Leach, DA, Trotta, AP, Need, EF, Risbridger, GP, Taylor, RA & Buchanan, G 2017, 'The prognostic value of stromal FK506-binding protein 1 and androgen receptor in prostate cancer outcome', *Prostate*, 77, 185-195.
- Lepage, C, Drouillard, A, Jouve, JL & Faivre, J 2013, 'Epidemiology and risk factors for oesophageal adenocarcinoma', *Dig Liver Dis*, 45, 625-9.
- Lerut, T, Naftoux, P, Moons, J, Coosemans, W, Decker, G, De Leyn, P, Van Raemdonck, D & Ectors, N 2004, 'Three-field lymphadenectomy for carcinoma of the esophagus and gastroesophageal junction in 174 R0 resections: impact on staging, disease-free survival, and outcome: a plea for adaptation of TNM classification in upper-half esophageal carcinoma', *Ann Surg*, 240, 962-72; discussion 972-4.
- Li, L, Lou, Z & Wang, L 2011, 'The role of FKBP5 in cancer aetiology and chemoresistance', *Br J Cancer*, 104, 19-23.
- Li, P, Chen, J & Miyamoto, H 2017, 'Androgen Receptor Signaling in Bladder Cancer', *Cancers (Basel)*, 9.
- Li, R, Wheeler, T, Dai, H, Frolov, A, Thompson, T & Ayala, G 2004, 'High level of androgen receptor is associated with aggressive clinicopathologic features and decreased biochemical recurrence-free survival in prostate: cancer patients treated with radical prostatectomy', *Am J Surg Pathol*, 28, 928-34.
- Li, Y, Li, CX, Ye, H, Chen, F, Melamed, J, Peng, Y, Liu, J, Wang, Z, Tsou, HC, Wei, J, Walden, P, Garabedian, MJ & Lee, P 2008, 'Decrease in stromal androgen receptor associates with androgen-independent disease and promotes prostate cancer cell proliferation and invasion', *J Cell Mol Med*, 12, 2790-8.
- Lim, DHK & Maher, ER 2010, 'SAC Review - DNA methylation: a form of epigenetic control of gene expression', *The Obstetrician & Gynaecologist*, 12, 37-42.
- Lin, EW, Karakasheva, TA, Hicks, PD, Bass, AJ & Rustgi, AK 2016, 'The tumor microenvironment in esophageal cancer', *Oncogene*, 35, 5337-5349.
- Lindblad, M, Garcia Rodriguez, LA, Chandanos, E & Lagergren, J 2006, 'Hormone replacement therapy and risks of oesophageal and gastric adenocarcinomas', *Br J Cancer*, 94, 136-41.
- Litvinov, IV, Antony, L, Dalrymple, SL, Becker, R, Cheng, L & Isaacs, JT 2006, 'PC3, but not DU145, human prostate cancer cells retain the coregulators required for tumor suppressor ability of androgen receptor', *Prostate*, 66, 1329-38.
- Litvinov, IV, Antony, L & Isaacs, JT 2004, 'Molecular characterization of an improved vector for evaluation of the tumor suppressor versus oncogene abilities of the androgen receptor', *Prostate*, 61, 299-304.

- Liu, L, Chirala, M & Younes, M 2004, 'Expression of estrogen receptor-beta isoforms in Barrett's metaplasia, dysplasia and esophageal adenocarcinoma', *Anticancer Res*, 24, 2919-24.
- Lonergan, PE & Tindall, DJ 2011, 'Androgen receptor signaling in prostate cancer development and progression', *Journal of Carcinogenesis*, 10, 20.
- Lu, P, Takai, K, Weaver, VM & Werb, Z 2011, 'Extracellular matrix degradation and remodeling in development and disease', *Cold Spring Harb Perspect Biol*, 3.
- Lu, P, Weaver, VM & Werb, Z 2012, 'The extracellular matrix: a dynamic niche in cancer progression', *J Cell Biol*, 196, 395-406.
- Lu, Y & Lagergren, J 2012, 'Reproductive factors and risk of oesophageal cancer, a population-based nested case-control study in Sweden', *Br J Cancer*, 107, 564-9.
- Ma, WL, Hsu, CL, Wu, MH, Wu, CT, Wu, CC, Lai, JJ, Jou, YS, Chen, CW, Yeh, S & Chang, C 2008, 'Androgen receptor is a new potential therapeutic target for the treatment of hepatocellular carcinoma', *Gastroenterology*, 135, 947-55, 955 e1-5.
- Madar, S, Goldstein, I & Rotter, V 2013, 'Cancer associated fibroblasts'--more than meets the eye', *Trends Mol Med*, 19, 447-53.
- Majek, O, Gondos, A, Jansen, L, Emrich, K, Holleczeck, B, Katalinic, A, Nennecke, A, Eberle, A, Brenner, H & Group, GCSW 2013, 'Sex differences in colorectal cancer survival: population-based analysis of 164,996 colorectal cancer patients in Germany', *PLoS One*, 8, e68077.
- Mao, Y, Keller, ET, Garfield, DH, Shen, K & Wang, J 2013, 'Stromal cells in tumor microenvironment and breast cancer', *Cancer Metastasis Rev*, 32, 303-15.
- Marques, RB, Erkens-Schulze, S, De Ridder, CM, Hermans, KG, Waltering, K, Visakorpi, T, Trapman, J, Romijn, JC, Van Weerden, WM & Jenster, G 2005, 'Androgen receptor modifications in prostate cancer cells upon long-term androgen ablation and antiandrogen treatment', *Int J Cancer*, 117, 221-9.
- Marsh, D, Suchak, K, Moutasim, KA, Vallath, S, Hopper, C, Jerjes, W, Upile, T, Kalavrezos, N, Violette, SM, Weinreb, PH, Chester, KA, Chana, JS, Marshall, JF, Hart, IR, Hackshaw, AK, Piper, K & Thomas, GJ 2011, 'Stromal features are predictive of disease mortality in oral cancer patients', *J Pathol*, 223, 470-81.
- Mathieu, LN, Kanarek, NF, Tsai, HL, Rudin, CM & Brock, MV 2014, 'Age and sex differences in the incidence of esophageal adenocarcinoma: results from the Surveillance, Epidemiology, and End Results (SEER) Registry (1973-2008)', *Dis Esophagus*, 27, 757-63.
- Matsumoto, T, Sakari, M, Okada, M, Yokoyama, A, Takahashi, S, Kouzmenko, A & Kato, S

- 2013, 'The androgen receptor in health and disease', *Annu Rev Physiol*, 75, 201-24.
- Matsuoka, H, Sugimachi, K, Ueo, H, Kuwano, H, Nakano, S & Nakayama, M 1987, 'Sex hormone response of a newly established squamous cell line derived from clinical esophageal carcinoma', *Cancer Res*, 47, 4134-40.
- Matsuyama, Y, Tominaga, T, Nomura, Y, Koyama, H, Kimura, M, Sano, M, Miura, S, Takashima, S, Mitsuyama, S, Ueo, H & Ohashi, Y 2000, 'Second cancers after adjuvant tamoxifen therapy for breast cancer in Japan', *Ann Oncol*, 11, 1537-43.
- Matsuzawa, Y 2008, 'The role of fat topology in the risk of disease', *Int J Obes (Lond)*, 32 Suppl 7, S83-92.
- Mbeunkui, F & Johann, DJ, Jr. 2009, 'Cancer and the tumor microenvironment: a review of an essential relationship', *Cancer Chemother Pharmacol*, 63, 571-82.
- Menon, S, Nightingale, P & Trudgill, N 2014, 'Is hormone replacement therapy in post-menopausal women associated with a reduced risk of oesophageal cancer?', *United European Gastroenterol J*, 2, 374-82.
- Miki, Y, Ono, K, Hata, S, Suzuki, T, Kumamoto, H & Sasano, H 2012, 'The advantages of co-culture over mono cell culture in simulating in vivo environment', *J Steroid Biochem Mol Biol*, 131, 68-75.
- Minamiguchi, K, Kawada, M, Someno, T & Ishizuka, M 2003, 'Androgen-independent prostate cancer DU145 cells suppress androgen-dependent growth of prostate stromal cells through production of inhibitory factors for androgen responsiveness', *Biochem Biophys Res Commun*, 306, 629-36.
- Miyamoto, H, Yang, Z, Chen, YT, Ishiguro, H, Uemura, H, Kubota, Y, Nagashima, Y, Chang, YJ, Hu, YC, Tsai, MY, Yeh, S, Messing, EM & Chang, C 2007, 'Promotion of bladder cancer development and progression by androgen receptor signals', *J Natl Cancer Inst*, 99, 558-68.
- Mohler, JL, Chen, Y, Hamil, K, Hall, SH, Cidlowski, JA, Wilson, EM, French, FS & Sar, M 1996, 'Androgen and glucocorticoid receptors in the stroma and epithelium of prostatic hyperplasia and carcinoma', *Clin Cancer Res*, 2, 889-95.
- Morley, JE 2001, 'Androgens and aging', *Maturitas*, 38, 61-71; discussion 71-3.
- Morley, JE & Perry, HM, 3rd 2003, 'Androgens and women at the menopause and beyond', *J Gerontol A Biol Sci Med Sci*, 58, M409-16.
- Mrazek, AA, Carmical, JR, Wood, TG, Hellmich, MR, Eltorkey, M, Bohanon, FJ & Chao, C 2014, 'Colorectal Cancer-Associated Fibroblasts are Genotypically Distinct', *Curr Cancer Ther Rev*, 10, 97-218.
- Muller, M, Den Tonkelaar, I, Thijssen, JH, Grobbee, DE & Van Der Schouw, YT 2003a,

- ‘Endogenous sex hormones in men aged 40-80 years’, *Eur J Endocrinol*, 149, 583-9.
- Muller, M, Van Der Schouw, YT, Thijssen, JH & Grobbee, DE 2003b, ‘Endogenous sex hormones and cardiovascular disease in men’, *J Clin Endocrinol Metab*, 88, 5076-86.
- Munoz, J, Wheler, JJ & Kurzrock, R 2015, ‘Androgen receptors beyond prostate cancer: an old marker as a new target’, *Oncotarget*, 6, 592-603.
- Narunsky, L, Oren, R, Bochner, F & Neeman, M 2014, ‘Imaging aspects of the tumor stroma with therapeutic implications’, *Pharmacol Ther*, 141, 192-208.
- Nie, L, Lyros, O, Medda, R, Jovanovic, N, Schmidt, JL, Otterson, MF, Johnson, CP, Behmaram, B, Shaker, R & Rafiee, P 2014, ‘Endothelial-mesenchymal transition in normal human esophageal endothelial cells cocultured with esophageal adenocarcinoma cells: role of IL-1beta and TGF-beta2’, *Am J Physiol Cell Physiol*, 307, C859-77.
- Niu, Y, Altuwajjri, S, Lai, KP, Wu, CT, Ricke, WA, Messing, EM, Yao, J, Yeh, S & Chang, C 2008a, ‘Androgen receptor is a tumor suppressor and proliferator in prostate cancer’, *Proc Natl Acad Sci U S A*, 105, 12182-7.
- Niu, Y, Altuwajjri, S, Yeh, S, Lai, KP, Yu, S, Chuang, KH, Huang, SP, Lardy, H & Chang, C 2008b, ‘Targeting the stromal androgen receptor in primary prostate tumors at earlier stages’, *Proc Natl Acad Sci U S A*, 105, 12188-93.
- Niu, Y, Chang, TM, Yeh, S, Ma, WL, Wang, YZ & Chang, C 2010, ‘Differential androgen receptor signals in different cells explain why androgen-deprivation therapy of prostate cancer fails’, *Oncogene*, 29, 3593-604.
- Nordenstedt, H, White, DL & El-Serag, HB 2010, ‘The changing pattern of epidemiology in hepatocellular carcinoma’, *Dig Liver Dis*, 42 Suppl 3, S206-14.
- Nordenstedt, H, Younes, M & El-Serag, HB 2012, ‘Expression of androgen receptors in Barrett esophagus’, *J Clin Gastroenterol*, 46, 251-2.
- O'doherty, MG, Freedman, ND, Hollenbeck, AR, Schatzkin, A & Abnet, CC 2012, ‘A prospective cohort study of obesity and risk of oesophageal and gastric adenocarcinoma in the NIH-AARP Diet and Health Study’, *Gut*, 61, 1261-8.
- Ohlund, D, Elyada, E & Tuveson, D 2014, ‘Fibroblast heterogeneity in the cancer wound’, *J Exp Med*, 211, 1503-23.
- Olapade-Olaopa, EO, Mackay, EH, Taub, NA, Sandhu, DP, Terry, TR & Habib, FK 1999, ‘Malignant transformation of human prostatic epithelium is associated with the loss of androgen receptor immunoreactivity in the surrounding stroma’, *Clin Cancer Res*, 5, 569-76.
- Olea, N, Sakabe, K, Soto, AM & Sonnenschein, C 1990, ‘The proliferative effect of "anti-

- androgens" on the androgen-sensitive human prostate tumor cell line LNCaP', *Endocrinology*, 126, 1457-63.
- Olumi, AF, Grossfeld, GD, Hayward, SW, Carroll, PR, Tlsty, TD & Cunha, GR 1999, 'Carcinoma-associated fibroblasts direct tumor progression of initiated human prostatic epithelium', *Cancer Res*, 59, 5002-11.
- Orimo, A, Gupta, PB, Sgroi, DC, Arenzana-Seisdedos, F, Delaunay, T, Naeem, R, Carey, VJ, Richardson, AL & Weinberg, RA 2005, 'Stromal fibroblasts present in invasive human breast carcinomas promote tumor growth and angiogenesis through elevated SDF-1/CXCL12 secretion', *Cell*, 121, 335-48.
- Otomo, R, Otsubo, C, Matsushima-Hibiya, Y, Miyazaki, M, Tashiro, F, Ichikawa, H, Kohno, T, Ochiya, T, Yokota, J, Nakagama, H, Taya, Y & Enari, M 2014, 'TSPAN12 is a critical factor for cancer-fibroblast cell contact-mediated cancer invasion', *Proc Natl Acad Sci U S A*, 111, 18691-6.
- Ozdemir, BC, Pentcheva-Hoang, T, Carstens, JL, Zheng, X, Wu, CC, Simpson, TR, Laklai, H, Sugimoto, H, Kahlert, C, Novitskiy, SV, De Jesus-Acosta, A, Sharma, P, Heidari, P, Mahmood, U, Chin, L, Moses, HL, Weaver, VM, Maitra, A, Allison, JP, Lebleu, VS & Kalluri, R 2014, 'Depletion of carcinoma-associated fibroblasts and fibrosis induces immunosuppression and accelerates pancreas cancer with reduced survival', *Cancer Cell*, 25, 719-34.
- Page, ST, Lin, DW, Mostaghel, EA, Marck, BT, Wright, JL, Wu, J, Amory, JK, Nelson, PS & Matsumoto, AM 2011, 'Dihydrotestosterone administration does not increase intraprostatic androgen concentrations or alter prostate androgen action in healthy men: a randomized-controlled trial', *J Clin Endocrinol Metab*, 96, 430-7.
- Peddareddigari, VG, Wang, D & Dubois, RN 2010, 'The tumor microenvironment in colorectal carcinogenesis', *Cancer Microenviron*, 3, 149-66.
- Pei, H, Li, L, Fridley, BL, Jenkins, GD, Kalari, KR, Lingle, W, Petersen, G, Lou, Z & Wang, L 2009, 'FKBP51 affects cancer cell response to chemotherapy by negatively regulating Akt', *Cancer Cell*, 16, 259-66.
- Phan, SH 2008, 'Biology of fibroblasts and myofibroblasts', *Proc Am Thorac Soc*, 5, 334-7.
- Purim, O, Gordon, N & Brenner, B 2013, 'Cancer of the colon and rectum: potential effects of sex-age interactions on incidence and outcome', *Med Sci Monit*, 19, 203-9.
- Quail, DF & Joyce, JA 2013, 'Microenvironmental regulation of tumor progression and metastasis', *Nat Med*, 19, 1423-37.
- Rhim, AD, Oberstein, PE, Thomas, DH, Mirek, ET, Palermo, CF, Sastra, SA, Dekleva, EN, Saunders, T, Becerra, CP, Tattersall, IW, Westphalen, CB, Kitajewski, J, Fernandez-

- Barrena, MG, Fernandez-Zapico, ME, Iacobuzio-Donahue, C, Olive, KP & Stanger, BZ 2014, 'Stromal elements act to restrain, rather than support, pancreatic ductal adenocarcinoma', *Cancer Cell*, 25, 735-47.
- Ricciardelli, C, Choong, CS, Buchanan, G, Vivekanandan, S, Neufing, P, Stahl, J, Marshall, VR, Horsfall, DJ & Tilley, WD 2005, 'Androgen receptor levels in prostate cancer epithelial and peritumoral stromal cells identify non-organ confined disease', *Prostate*, 63, 19-28.
- Ricke, EA, Williams, K, Lee, YF, Couto, S, Wang, Y, Hayward, SW, Cunha, GR & Ricke, WA 2012, 'Androgen hormone action in prostatic carcinogenesis: stromal androgen receptors mediate prostate cancer progression, malignant transformation and metastasis', *Carcinogenesis*, 33, 1391-8.
- Rieder, F, Biancani, P, Harnett, K, Yerian, L & Falk, GW 2010, 'Inflammatory mediators in gastroesophageal reflux disease: impact on esophageal motility, fibrosis, and carcinogenesis', *Am J Physiol Gastrointest Liver Physiol*, 298, G571-81.
- Rubashkin, MG, Ou, G & Weaver, VM 2014, 'Deconstructing signaling in three dimensions', *Biochemistry*, 53, 2078-90.
- Rutegard, M, Lagergren, P, Nordenstedt, H & Lagergren, J 2011, 'Oesophageal adenocarcinoma: the new epidemic in men?', *Maturitas*, 69, 244-8.
- Salmela, MT, Karjalainen-Lindsberg, ML, Puolakkainen, P & Saarialho-Kere, U 2001, 'Upregulation and differential expression of matrilysin (MMP-7) and metalloelastase (MMP-12) and their inhibitors TIMP-1 and TIMP-3 in Barrett's oesophageal adenocarcinoma', *Br J Cancer*, 85, 383-92.
- Sanz-Moreno, V, Gaggioli, C, Yeo, M, Albregues, J, Wallberg, F, Viros, A, Hooper, S, Mitter, R, Feral, CC, Cook, M, Larkin, J, Marais, R, Meneguzzi, G, Sahai, E & Marshall, CJ 2011, 'ROCK and JAK1 signaling cooperate to control actomyosin contractility in tumor cells and stroma', *Cancer Cell*, 20, 229-45.
- Semba, S, Kodama, Y, Ohnuma, K, Mizuuchi, E, Masuda, R, Yashiro, M, Hirakawa, K & Yokozaki, H 2009, 'Direct cancer-stromal interaction increases fibroblast proliferation and enhances invasive properties of scirrhous-type gastric carcinoma cells', *Br J Cancer*, 101, 1365-73.
- Sever, R & Brugge, JS 2015, 'Signal transduction in cancer', *Cold Spring Harb Perspect Med*, 5.
- Sharma, S, Kelly, TK & Jones, PA 2010, 'Epigenetics in cancer', *Carcinogenesis*, 31, 27-36.
- Shukla, GC, Plaga, AR, Shankar, E & Gupta, S 2016, 'Androgen receptor-related diseases: what do we know?', *Andrology*, 4, 366-81.

- Siegel, RL, Miller, KD, Fedewa, SA, Ahnen, DJ, Meester, RG, Barzi, A & Jemal, A 2017a, 'Colorectal cancer statistics, 2017', *CA Cancer J Clin*.
- Siegel, RL, Miller, KD & Jemal, A 2017b, 'Cancer Statistics, 2017', *CA Cancer J Clin*, 67, 7-30.
- Singh, M, Jha, R, Melamed, J, Shapiro, E, Hayward, SW & Lee, P 2014, 'Stromal androgen receptor in prostate development and cancer', *Am J Pathol*, 184, 2598-607.
- Singh, M & Lee, P 2013, 'Expression and Function of Stromal Androgen Receptor in Prostate Cancer'.
- Smith, DF & Toft, DO 2008, 'Minireview: the intersection of steroid receptors with molecular chaperones: observations and questions', *Mol Endocrinol*, 22, 2229-40.
- Spechler, SJ & Souza, RF 2014, 'Barrett's esophagus', *N Engl J Med*, 371, 836-45.
- Sukocheva, OA, Li, B, Due, SL, Hussey, DJ & Watson, DI 2015, 'Androgens and esophageal cancer: What do we know?', *World J Gastroenterol*, 21, 6146-56.
- Taddei, A, Fabbroni, V, Pini, A, Lucarini, L, Ringressi, MN, Fantappie, O, Bani, D, Messerini, L, Masini, E & Bechi, P 2014, 'Cyclooxygenase-2 and inflammation mediators have a crucial role in reflux-related esophageal histological changes and Barrett's esophagus', *Dig Dis Sci*, 59, 949-57.
- Tan, MH, Li, J, Xu, HE, Melcher, K & Yong, EL 2015, 'Androgen receptor: structure, role in prostate cancer and drug discovery', *Acta Pharmacol Sin*, 36, 3-23.
- Tanner, MJ, Welliver, RC, Jr., Chen, M, Shtutman, M, Godoy, A, Smith, G, Mian, BM & Buttyan, R 2011, 'Effects of androgen receptor and androgen on gene expression in prostate stromal fibroblasts and paracrine signaling to prostate cancer cells', *PLoS One*, 6, e16027.
- Tchernof, A & Despres, JP 2013, 'Pathophysiology of human visceral obesity: an update', *Physiol Rev*, 93, 359-404.
- Thornton, JW & Kelley, DB 1998, 'Evolution of the androgen receptor: structure-function implications', *Bioessays*, 20, 860-9.
- Thrift, AP & Whiteman, DC 2012, 'The incidence of esophageal adenocarcinoma continues to rise: analysis of period and birth cohort effects on recent trends', *Ann Oncol*, 23, 3155-62.
- Tiffin, N, Suvarna, SK, Trudgill, NJ & Riley, SA 2003, 'Sex hormone receptor immunohistochemistry staining in Barrett's oesophagus and adenocarcinoma', *Histopathology*, 42, 95-6.
- Tihan, T, Harmon, JW, Wan, X, Younes, Z, Nass, P, Duncan, KL & Duncan, MD 2001, 'Evidence of androgen receptor expression in squamous and adenocarcinoma of the

- esophagus', *Anticancer Res*, 21, 3107-14.
- Torre, LA, Bray, F, Siegel, RL, Ferlay, J, Lortet-Tieulent, J & Jemal, A 2015, 'Global cancer statistics, 2012', *CA Cancer J Clin*, 65, 87-108.
- Torre, LA, Siegel, RL, Ward, EM & Jemal, A 2016, 'Global Cancer Incidence and Mortality Rates and Trends--An Update', *Cancer Epidemiol Biomarkers Prev*, 25, 16-27.
- Tsujino, T, Seshimo, I, Yamamoto, H, Ngan, CY, Ezumi, K, Takemasa, I, Ikeda, M, Sekimoto, M, Matsuura, N & Monden, M 2007, 'Stromal myofibroblasts predict disease recurrence for colorectal cancer', *Clin Cancer Res*, 13, 2082-90.
- Turley, SJ, Cremasco, V & Astarita, JL 2015, 'Immunological hallmarks of stromal cells in the tumour microenvironment', *Nat Rev Immunol*, 15, 669-82.
- Ueo, H, Matsuoka, H, Sugimachi, K, Kuwano, H, Mori, M & Akiyoshi, T 1990, 'Inhibitory effects of estrogen on the growth of a human esophageal carcinoma cell line', *Cancer Res*, 50, 7212-5.
- Underwood, TJ, Hayden, AL, Derouet, M, Garcia, E, Noble, F, White, MJ, Thirdborough, S, Mead, A, Clemons, N, Mellone, M, Uzoho, C, Primrose, JN, Blaydes, JP & Thomas, GJ 2015, 'Cancer-associated fibroblasts predict poor outcome and promote periostin-dependent invasion in oesophageal adenocarcinoma', *J Pathol*, 235, 466-77.
- Verbeek, RE, Siersema, PD, Ten Kate, FJ, Fluiter, K, Souza, RF, Vleggaar, FP, Bus, P & Van Baal, JW 2014, 'Toll-like receptor 4 activation in Barrett's esophagus results in a strong increase in COX-2 expression', *J Gastroenterol*, 49, 1121-34.
- Vizoso, M, Puig, M, Carmona, FJ, Maqueda, M, Velasquez, A, Gomez, A, Labernadie, A, Lugo, R, Gabasa, M, Rigat-Brugarolas, LG, Trepas, X, Ramirez, J, Moran, S, Vidal, E, Reguart, N, Perera, A, Esteller, M & Alcaraz, J 2015, 'Aberrant DNA methylation in non-small cell lung cancer-associated fibroblasts', *Carcinogenesis*, 36, 1453-63.
- Wagner, JR, Busche, S, Ge, B, Kwan, T, Pastinen, T & Blanchette, M 2014, 'The relationship between DNA methylation, genetic and expression inter-individual variation in untransformed human fibroblasts', *Genome Biol*, 15, R37.
- Wang, J, Zhang, G, Wang, J, Wang, L, Huang, X & Cheng, Y 2016, 'The role of cancer-associated fibroblasts in esophageal cancer', *J Transl Med*, 14, 30.
- Wen, S, Chang, HC, Tian, J, Shang, Z, Niu, Y & Chang, C 2015, 'Stromal androgen receptor roles in the development of normal prostate, benign prostate hyperplasia, and prostate cancer', *Am J Pathol*, 185, 293-301.
- Whiteman, DC, Sadeghi, S, Pandeya, N, Smithers, BM, Gotley, DC, Bain, CJ, Webb, PM, Green, AC & Australian Cancer, S 2008, 'Combined effects of obesity, acid reflux and smoking on the risk of adenocarcinomas of the oesophagus', *Gut*, 57, 173-80.

- Wikstrom, P, Marusic, J, Stattin, P & Bergh, A 2009, 'Low stroma androgen receptor level in normal and tumor prostate tissue is related to poor outcome in prostate cancer patients', *Prostate*, 69, 799-809.
- Worthley, DL, Giraud, AS & Wang, TC 2010, 'Stromal fibroblasts in digestive cancer', *Cancer Microenviron*, 3, 117-25.
- Xie, SH & Lagergren, J 2016a, 'A global assessment of the male predominance in esophageal adenocarcinoma', *Oncotarget*, 7, 38876-38883.
- Xie, SH & Lagergren, J 2016b, 'The Male Predominance in Esophageal Adenocarcinoma', *Clin Gastroenterol Hepatol*, 14, 338-347 e1.
- Yamaguchi, H, Yoshida, N, Takanashi, M, Ito, Y, Fukami, K, Yanagihara, K, Yashiro, M & Sakai, R 2014, 'Stromal fibroblasts mediate extracellular matrix remodeling and invasion of scirrhous gastric carcinoma cells', *PLoS One*, 9, e85485.
- Yamashita, K, Miyashiro, Y, Maekubo, H, Okuyama, M, Honma, S, Takahashi, M & Numazawa, M 2009, 'Development of highly sensitive quantification method for testosterone and dihydrotestosterone in human serum and prostate tissue by liquid chromatography-electrospray ionization tandem mass spectrometry', *Steroids*, 74, 920-6.
- Yamashita, M, Ogawa, T, Zhang, X, Hanamura, N, Kashikura, Y, Takamura, M, Yoneda, M & Shiraishi, T 2012, 'Role of stromal myofibroblasts in invasive breast cancer: stromal expression of alpha-smooth muscle actin correlates with worse clinical outcome', *Breast Cancer*, 19, 170-6.
- Yamashita, Y, Hirai, T, Mukaida, H, Kawano, K, Toge, T, Niimoto, M & Hattori, T 1989, 'Detection of androgen receptors in human esophageal cancer', *Jpn J Surg*, 19, 195-202.
- Yassin, AA & Saad, F 2007, 'Plasma levels of dihydrotestosterone remain in the normal range in men treated with long-acting parenteral testosterone undecanoate', *Andrologia*, 39, 181-4.
- Yialamas, MA & Hayes, FJ 2003, 'Androgens and the ageing male and female', *Best Pract Res Clin Endocrinol Metab*, 17, 223-36.
- Yu, S, Xia, S, Yang, D, Wang, K, Yeh, S, Gao, Z & Chang, C 2013, 'Androgen receptor in human prostate cancer-associated fibroblasts promotes prostate cancer epithelial cell growth and invasion', *Med Oncol*, 30, 674.
- Yu, S, Yeh, CR, Niu, Y, Chang, HC, Tsai, YC, Moses, HL, Shyr, CR, Chang, C & Yeh, S 2012, 'Altered prostate epithelial development in mice lacking the androgen receptor in stromal fibroblasts', *Prostate*, 72, 437-49.

- Zeisberg, EM & Zeisberg, M 2013, 'The role of promoter hypermethylation in fibroblast activation and fibrogenesis', *J Pathol*, 229, 264-73.
- Zhang, Y, Wang, Q, Ma, A, Li, Y, Li, R & Wang, Y 2014, 'Functional expression of TLR9 in esophageal cancer', *Oncol Rep*, 31, 2298-304.
- Zhu, C, Luong, R, Zhuo, M, Johnson, DT, Mckenney, JK, Cunha, GR & Sun, Z 2011, 'Conditional expression of the androgen receptor induces oncogenic transformation of the mouse prostate', *J Biol Chem*, 286, 33478-88.